INFORMATION TO USERS

The most advanced technology has been used to photograph and reproduce this manuscript from the microfilm master. UMI films the text directly from the original or copy submitted. Thus, some thesis and dissertation copies are in typewriter face, while others may be from any type of computer printer.

The quality of this reproduction is dependent upon the quality of the copy submitted. Broken or indistinct print, colored or poor quality illustrations and photographs, print bleedthrough, substandard margins, and improper alignment can adversely affect reproduction.

In the unlikely event that the author did not send UMI a complete manuscript and there are missing pages, these will be noted. Also, if unauthorized copyright material had to be removed, a note will indicate the deletion.

Oversize materials (e.g., maps, drawings, charts) are reproduced by sectioning the original, beginning at the upper left-hand corner and continuing from left to right in equal sections with small overlaps. Each original is also photographed in one exposure and is included in reduced form at the back of the book.

Photographs included in the original manuscript have been reproduced xerographically in this copy. Higher quality 6" x 9" black and white photographic prints are available for any photographs or illustrations appearing in this copy for an additional charge. Contact UMI directly to order.

U·M·I

University Microfilms International
A Bell & Howell Information Company
300 North Zeeb Road, Ann Arbor, MI 48106-1346 USA
313/761-4700 800/521-0600

Order Number 9108172

Part I. Evaluation of silver as a reductive amperometric detector electrode for HPLC and FIA. Part II. Evaluation of supercritical fluid extraction (SFE) as a sample preparation technique. Part III. Development and validation of HPLC methods using supercritical fluid extraction and reversed-phase HPLC with electrochemical detection (LCEC)

Schneiderman, Martin Alan, Ph.D.

City University of New York, 1990

U·M·I
300 N. Zeeb Rd.
Ann Arbor, MI 48106

A

Part I. Evaluation of Silver as a Reductive Amperometric Detector Electrode for HPLC and FIA.

Part II. Evaluation of Supercritical Fluid Extraction (SFE) as a Sample Preparation Technique.

Part III. Development and Validation of HPLC Methods using Supercritical Fluid Extraction and Reversed-Phase HPLC with Electrochemical Detection (LCEC).

by

Martin Alan Schneiderman

A dissertation submitted to the Graduate Faculty in Chemistry in partial fulfillment of the requirements for the degree of Doctor of Philosophy, The City University of New York.

1990

This manuscript has been read and accepted for the Graduate Faculty in Chemistry in satisfaction of the dissertation requirement for the degree of Doctor of Philosophy.

27 Sept. 90
Date

David C. Lorde
Chairman of Examining Committee

9/27/90
Date

Executive Officer

Ronald F Borne

Joshua Leo
Supervisory Committee

The City University of New York

Abstract

Part I. Evaluation of Silver as a Reductive Amperometric Detector Electrode for HPLC and FIA.

Part II. Evaluation of Supercritical Fluid Extraction (SFE) as a Sample Preparation Technique.

Part III. Development and Validation of HPLC Methods using Supercritical Fluid Extraction and Reversed-Phase HPLC with Electrochemical Detection (LCEC).

by

Martin Alan Schneiderman

Advisor: Professor David C. Locke

The design, characterization and application of two complimentary analytical tools useful in the analysis of electroactive substances of pharmaceutical, environmental and industrial significance is described. The first, detailed in part I, is concerned with the evaluation of silver as a reductive amperometric detector electrode for HPLC. Three detector variants have been developed, utilizing silver in the form of a continuous silver disc, a segmented silver oxide grid assembly and in a differential arrangement. The dynamic properties of the three cells, i.e., the linear dynamic range, the reproducibility, and dependence on flow rate and electrode area were tested using a series of quinones and nitro-aromatics as model substances. The electrochemical detector (ECD) with the continuous electrode has a wide linear dynamic range, high sensitivity and an extremely rapid response time for analytes reduced at potentials anodic of -1.2V versus SCE. The analytical superiority and versatility of the silver oxide grid design at potentials cathodic of -1.2V versus SCE with respect to reproducibility and dynamic range is illustrated through the determination of mercaptobenzotriazole in cooling waters.

Part II is concerned with the use of supercritical fluid extraction (SFE) for sample preparation. A simple laboratory-constructed system is described which allows quantitative and selective recovery of quinones and nitro-aromatics from complex matrices. Parameters such as temperature, pressure, modifier type and amount were examined to optimize conditions for maximum recoveries. The operation of the system was validated with carbon black samples spiked with a series of quinones. For these compounds, quantitative recovery was maintained down to 1-5 μg/g. Experimental results demonstrating the performance of the system with respect to reproducibility and selectivity in the fractionation of samples containing both polar and non-polar polycyclicaromatic hydrocarbons are presented and discussed.

In part III, the two tools are linked together through the general theme of the development and validation of HPLC methods incorporating SFE sample preparation with ECD. This approach has been utilized for the determination of anthraquinone in wood and paper pulp, nitrosoamines in powdered milk and ground coffee, vitamin K_1 in baby formula, retinyl palmitate in ready-to-eat breakfast cereals, menadione in animal feed, Diazepam in tablets, 1-nitropyrene in diesel exhaust, and parathion in oil seeds and grains. The advantages and liabilities of these methods with regard to simplicity, speed, sensitivity, matrix interactions, and selectivity are discussed and are compared to their counterpart compendial methodologies.

Acknowledgements

I am indebted to my mentor, David C. Locke, who has helped guide my thinking through years of interactions in which he shared with me his accute insights into separations chemistry through all phases of my graduate training and dissertation research. This thesis reflects his advice, help, encouragement, last minute readings and much care. It would be impossible to thank him sufficiently for the time and faith he has invested in me. I would also like to formally thank Johna Leddy and Ronald Birke for serving on my thesis advisory committee and helping me to develop this project..

Last, I would like to thank my parents for encouraging me throughout my training. They shared with me each joy and crisis, and I feel that this degree should belong, in part, to them.

TABLE OF CONTENTS

LIST OF TABLES

PART I

PART II

PART III

Chapter 1

Chapter 2

Chapter 3

Chapter 4

Chapter 5

Chapter 6

Chapter 7

Chapter 8

Chapter 9

LIST OF FIGURES

PART III

Chapter 1

Chapter 2

Chapter 3

Chapter 4

Chapter 5

Chapter 6

Chapter 7

Chapter 8

Chapter 9

Part I

Evaluation of Silver as a Reductive Detector Electrode for HPLC and FIA

High pressure liquid chromatography (HPLC) is today's predominant method of separation analysis (1). Fundamental advances in column technology for HPLC have occurred at a greater pace than the methods for detecting the small amounts of analytes present in such separations. The usual HPLC detection systems based on spectrophotometry and refractive index (1,2) are often nonselective, and simultaneously eluting species often produce analytical interferences. For chemical systems in which the complete resolution of species may be hindered by similiar retention times, such nonselective detectors yield serious analytical difficulties. In addition, for compounds that have typical UV extinction coefficients, detection is limited to a few tenths of a microgram (3).

In recent years, there has evolved significant interest on the part of analytical chemists in the possible interfacing and applications of electrochemical detectors (EC's) for both chromatographic and flow injection analysis (FIA) detection. This detection scheme offers several inherent advantages over spectroscopic techniques in terms of selectivity, sensitivity, linear dynamic range, response time, cost and versatility. This has resulted in the commercial development and marketing of various EC's for HPLC as well as a significant number of useful scientific and technical publications in the areas of industrial process control, biomedical analysis and environmental research. The basics of the technique are covered in several excellent general reviews (4-12) and early work regarding the marriage of electrochemistry and HPLC for the quantitation of various organic compounds are included in a bibliography (13). Recent developments regarding amperometric detection hardware and innovative schemes have been described by Johnson and Bond (14). Weber and Purdy (15) have described detector design and optimization from a mass transfer viewpoint. In-depth details on the design and operation of electrochemical detectors can be found in several papers (16-26).

In principle, such devices can be operated in various modes depending upon the electrochemical characterisitics of the analytes under investigation and the variability of the perturbation signal. In fact, in most cases the instrumentation used in applying the excitation function and measuring the current response is identical. The two main categories are the oxidative and reductive mode electrochemical detectors. However, in practice the design and application of reductive cells presents some special problems; these have not achieved the same degree of popularity as oxidative

amperometric detectors. Consequently, the majority of applications has been for the measurement of oxidizable organic compounds, whereas little work has been done with reducible species. The applicability of the electrochemical technique could be extended considerably, if the reductive mode of detection could be satisfactorily developed. This goal has not yet been fully realized.

The reason for this secondary position for reductive detectors is multifaceted. First, the mere association of reductive amperometry with the classical dropping mercury electrode (DME) has frightened away many potential users. Accordingly, atomic absorption spectroscopy has replaced classical polarography as the method of choice for the determination of heavy metals. Second, concurrent development of a large number of variants on classical voltammetry, involving different potential waveforms, forced convection, numerous electrode shapes, and a variety of signal processing approaches has consumed valuable research time and money. Furthermore, matrix interference effects diminish the reproducibility of the results of analysis. Such effects include dissolved oxygen, trace metals, and hydrogen ions. The former influences the background and noise level and the latter factor dictates which analytes can be detected. Finally, few working electrodes have been systematically characterized in terms of working range, sensitivity and reproducibility.

Efforts to improve the detection capabilities of this method have been primarily directed toward either the need to exclude dissolved oxygen from the flow system or to discriminate against its effects. In 0.1 M KCl, oxygen is easily reduced; the reaction proceeds in two steps:

$$O_2 + 2H^+ + 2e^- \longrightarrow H_2O_2 \qquad E_{1/2} = -0.05 \text{ V vs SCE}$$

$$H_2O_2 + 2H^+ + 2e^- \longrightarrow 2H_2O \qquad E_{1/2} = -1.0 \text{ V vs SCE}$$

The presence of oxygen in the mobile phase, about 0.5 mM in air-saturated aqueous solutions, therefore results in a high reductive background current. Also, hydrogen peroxide, an intermediate in the reduction process, may chemically react with components in the mobile phase.

Several methods of removing oxygen have been reported. Sparging with an inert gas, either by direct means (27) or assisted by heating (28-32) or vacuum (33) is probably the most frequently used method for oxygen removal. However, for trace LC work this approach is not always adequate. Alternatively, various chemical and mechanical devices have been proposed to circumvent this problem, including a high pressure electrochemical cell (34), the use of gas permeable tubing housed in either a vaccum shell (35-38) or in a chemical zinc oxygen scrubber (39) and catalytic reduction of mobile phase oxygen with alcoholic mobile phases (40,41). Although these devices (42) have met with some success, they are difficult to construct, increase the dead volume of the detector and are susceptible to rupture. Methods of discriminating against the effects of dissolved oxygen have also been reported including reverse pulse amperometry and dual electrode detection (43-45).

While the problem of dissolved oxygen has received considerable attention, the impact of the working electrode has been virtually overlooked. Despite the large number of publications on Liquid Chromatography/Electrochemistry (LCEC), to our knowledge, no one has addressed this issue in detail. Some workers have briefly mentioned the parameters involved, and general comparisons of electrode materials have been made (46); however, their efforts fall far short of a comprehensive treatise. In fact, the lack of systematic studies has led to the inappropiate use of electrodes designed for oxidative work and has further fueled the debate over the utility of these detectors (41). Despite this pessimistic attitude, some promising reports on reductive mode electrochemical detection have dealt with the analysis of nitro compounds (47-70), quinones (71-75), organomercury compounds (76,77), peroxides (78,79), inorganic ions (80,81), nitrosamines (82-84) and benzodiazepines (85). A comprehensive bibliography listing analytes of biological, industrial and environmental interest which are good candidates for detection by reductive mode LCEC has been published by Smyth (86-88). This early work clearly demonstrated the feasibility and power of the technique as well as the areas that needed improvement.

Several factors must be considered when selecting the electrode material for use in analytical reductions, the most important being the oxygen and hydrogen overpotentials. The operating range of an electrode material is usually limited on the negative side by the reduction of hydrogen ions and residual oxygen, both of which can be influenced by the presence of metals. In addition to having a wide operating

range, the ideal material should possess freedom from transition metal poisoning, have a small background current, and have a response relatively independent of pH over a large region. Furthermore, it should be compatible with a variety of solvents, easy to fabricate and operate and be reproducible. Finally, it should be readily polarizable, i.e., supply or accept electrons, yield a predictable response, and undergo a fast and reversible reaction with the depolarizer.

Historically, mercury has been the electrode material of choice for reduction by virtue of its high hydrogen overvoltage and, thus, wide cathodic potential range. Additional electrochemical advantages of mercury include a small and reproducible residual current and the possibility for surface renewal. Furthermore, a wealth of literature already exists concerning organic reductions at mercury, and, it is generally recognized that such reductions are rapid and reversible (89).

Several different approaches at incorporating mercury electrodes into reductively based flow cells have been presented (90-126). The application of the classical DME for use as a continuous analytical sensor seems to have been contempleted first by Drake (90) but a practical version of the transducer was first described by Kemula (91). In his initial system, a vertical DME was mounted in the central port of a glass tee. Analytes in the flowing eluent, which entered from an inclined side port, were partially reduced as they they passed the DME and the resulting signal was related to the analyte concentration. Blaedel and Todd (92) also described a primitive reductive flow-cell equipped with a deaeration device for the continuous measurement of column effluent from an ion-exchange column. The separation of species having similar half-wave potentials prior to reduction greatly enhanced the selectivity and utility of classical polarography for the determination of components in complex mixtures. Newer models designed by Fleet and Little (93) and Hanekamp et al. (94,95) for use with efficient HPLC columns are machined from plastic bodies containing narrow tapered channels and compartments. The column effluent usually impinges immediately on a conically ground horizontal mercury capillary before passing an inclined wick of a reference electrode and exiting the cell. The close proximity of the three electrodes results in both a sensitive and rapid response to the separated components. Concurrently, various types of on-line sensors (96-110) incorporating the vertical DME, have been developed for monitoring metals in industrial effluents. Although these early systems were crude, these detectors were characterized by good

reproducibility, wide dynamic range, modest detection limits, and freedom from most matrix interferences. In fact, figures of merit for these devices, i.e., minimum detectable limit (MDL) and linear dynamic range (LDR) were comparable to or better than the corresponding values obtained from classical benchmark methods.

Unfortunately, several problems also arise when a conventical vertical DME capillary is used in flowing streams. First, these electrodes are prone to mechanical faults such as clogging as well as problems associated with the handling of liquid mercury such as toxic spills. Second, the continuously changing area of the drop results in large capacitive currents. Third, the analytical signal is dependent on many parameters, such as drop size, mercury height and drop rate, which are very hard to control and reproduce. Furthermore, the size of the capillary restricts the miniaturization of the cell volume. Finally, the electrodes are cumbersome and difficult to use. Thus, the use of the DME in flowing cells remains as the single most limiting factor in the transition of reductive LCEC from a laboratory curiosity to a routine tool.

The desire to increase the utility of the DME for routine analysis has stimulated research on methods which reduce faradaic background and charging current and increase the reliability of operation. The literature is concerned with two such methods. In the first, the capillary is configured in a horizontal rather than the vertical orientation. Such an electrode was earlier shown by Tyler and Karchmer (111), Smoler (112), as well as by Florence (113) to have one quarter the drop time of a vertical capillary in static solutions. Subsequently, Scarano et al. (114) reported on the functional characteristics of the rapidly dropping electrode for use in flowing streams. Wasa and Musha (115) also successfully used a horizontal DME capillary with the column effluent approaching the drop at a right angle which seems to eliminate some of the mechanical problems. Rapid drop times of less than one second enable the measurement of small currents from the reduction of analytes such as nitropyridine in the presence of a high background signal. Hence, most figures of merit such as sensitivity level can be extended. In addition, the influence of the signal on external parameters such as flow rate and drop height is greatly reduced. Ma and Stillman (116) reported on the construction of a complete HPLC system equipped with a modern miniature polarographic detector. The body of the detector was fabricated from a Teflon bar containing a narrow central channel and two side ports. An inclined horizontally based dropping mercury electrode was press-fitted into the upper port. A

pulse-free mobile phase stream delivered from a compression vessel impinged perpendicularly onto the drop and radially passed a reference electrode located in the lower port. This effective arrangement was used to monitor inexpensively nanogram levels of various pesticides and vitamins.

The second type involves the use of a mechanical piston to slow the growth of the mercury drop and, thus, minimize charging currents due to variations in drop area. Hartmann and Budan (117) as well as Mairanovski et al. (118), demonstrated that current oscillations can be reduced by the application of uniform pressure with a glass plate or spatula. Michel and Zalka (119) utilized this principle by installing a moveable piston in their flow-cell. By pushing the piston pin toward the mercury capillary outlet, expansion of the mercury drop is hindered and a shorter, more controllable drop rate is obtained. In this manner, capacitive currents due to loss of electric contact with the mercury drop can be greatly attenuated. The gap distance can be finely tuned to give the optimum drop time and signal-to-noise ratio (S/N). Frei et al. (49,50) extensively evaluated a similar cell for actual chromatographic separations. This detector, which contained an adjustable drop-dampening mechanism, retained the wide cathodic range and surface renewal properties of mercury and also permitted the reduction of cell volume to a thin layer. Once the effects and interactions of mercury height, piston gap and flow rate on response were optimized, the performance and price compared favorably with UV detectors. This method is applicable to small volumes and good results have been reported. However, the technique requires careful control of mercury height, piston gap and flow rate and is not yet useful with high flow rates. Despite this large research effort, spanning several decades, reductive amperometry using the DME remains a difficult venture.

The resulting need for a mercury electrode which is reliable and easy to operate has been partially solved by the introduction of constant area mercury electrodes. In general, two approaches have been developed. The use of hanging stationary drop or automated hanging drop electrodes, such as those developed by EG&G (120) and Metrohm (121) are especially promising though older ideas such as mercury pools are of interest. Rabenstein and Saetre (122-125) constructed a detector based on a stationary mercury pool held in an inverted glass U tube. The cell was evaluated by determining amino acids through their specific interactions with mercury. When the pool was used in conjunction with high flow rates, several electrochemical problems

arise. For example, vibration and edge effects due to creeping of solution between the mercury and its container resulted in excessive noise levels. In addition, there was a poor tolerance for rapid movement of the solution. Considering the high noise levels and the lack of renewal of the mercury surface, the utility of this design is very limited.

Second generation mercury pool detectors have now appeared. One model, developed by Trojanek (70,126) offers excellent detection limits, rapid response time (a quarter of a second), and is capable of reliable operation with little manual intervention. In this cell, the analyte is injected through a porous ceramic cone which contacts a sealed mercury reservoir. Analytes are reduced on a thin layer of mercury at the tip of the cone facing the mercury supply. After each injection, turbulence causes the tip of the cone to be replenished with fresh mercury maintaining a reproducible surface. An additional feature of this cell is that contact with the mercury supply is never broken, keeping capacitive currents very low. While this device represents an improvement over previous designs, the cone is reported to become frequently blocked, so a number of expensive replacements must be kept on hand. In addition, this cell has not yet been fully evaluated by many workers since fabrication requires many sophisticated machine operations and specialized skills.

In the other approach, cells employing capillaries on which a mercury drop hangs have been developed and characterized (127-139). The analytical performance of the static mercury drop electrode has been described by Bond and Jones (127). In particular, Bond emphasized the considerable improvements in faradaic current-to-capacitive current ratios resulting from the stationary nature of the drop at the time of the measurement. One of the most elegant examples was described by Lloyd (138) who miniaturized a polarographic detector by employing a disposible pipet as a capillary support for the drop. The effluent inlet is arranged only 0.4 mm from the cone of the drop so that the total effective volume of the cell can be reduced to as little as 0.2 μL. An extremely small noise level of 200 pA superimposed on a 1 nA background current was obtained for this cell operated at - 1.0 V vs SCE using a phosphate (pH 3.0) mobile phase. A minimum detectable quantity of 265 pg for m-dinitrobenzene is easily obtained with this design. Although this detector design affords adequate detector limits and selectivity, problems with reproducibility have plagued this design.

Construction problems have been coped with very ingeniously in the design of the

Princeton Applied Research commercial detector (120). The mobile phase is directed normally from a lower vertical jet onto an upper hanging mercury drop or in some cases a DME. The analyte undergoes reduction at the mercury-inlet interface so that the effective working volume is very small. The reference and auxiliary electrodes surround the DME in a relatively large vessel, maintaining a small uncompensated resistance. An additional feature of this cell is that it can be used for non-aqueous work or in gradient solvent mixtures since the bulk of the solution does not interfere with the working interface. Furthermore, the lack of cross contamination eliminates the need for frequent dismantling and cleaning. There has always been a certain amount of black magic associated with this design, as no two cells perform alike in terms of sensitivity, drift and lifetime. In fact, some cells would never produce a signal at all. This is compounded by the expense of the replacement capillaries.

Naturally, attention has focused on the development of alternative approaches, usually involving the use of mercury film type electrodes or the use of glassy carbon. The first strategy, initially proposed by Durst (76,139,140) utilizes the face of either a gold, platinum, or silver rod mounted in a cube as a substrate for a thin film of mercury. Later, Bratin and Kissinger (21,47) applied mercury-plated precious metal electrodes to the determination of numerous reducible groups.

Amalgamated thin film electrodes were found to retain many of the desirable characteristics of liquid mercury, with only a small sacrifice in available potential window. In comparison with dropping mercury detectors, amalgam thin-layer detectors offer subnanogram detection limits and care-free routine operation. In addition, the thin-layer design offers the possibility of adding a second amalgam electrode to the same cell volume (141-146). The resultant dual cell configuration can be used to increase selectivity or sensitivity or both. For example, operated in the series mode, a reactive intermediate species formed at the first electrode can be selectively monitored at low potentials at the second electrode. This mode can also give qualitative information about the analyte from the ratio of the responses collected at each electrode. Operated in the adjacent mode, a differential cell can easily be formed. A blank chromatogram can be used to nullify those factors which cause baseline noise and drift, i.e., effects of impurities, temperature, and flow fluctuations. Furthermore, these cells are easy and inexpensive to construct, can be miniaturized, and need less knowledge of electrochemistry to operate properly. However, not

withstanding these advantages, the extensive use of film electrodes has been hindered by difficulties: on the one hand, interferences from impurities and complex surface reactions leading to passivation, and on the other hand, the difficulty in obtaining a flat, uniform and reproducible surface for any length of time. Moreover, the support material for the mercury film should be easily wetted by mercury yet its solubility in mercury should at the same time be very low. In practice, it is almost impossible to combine these two features. In spite of problems arising from surface inhomogenity and the need to fabricate a new electrode each time it deteriorates, mercury film electrodes have found wide electroanalytical application in anodic stripping voltammetry (147-155), and spectroelectrochemistry (156-160). In addition, applications of mercury-film electrodes to trace determinations in conjunction with FIA and HPLC have been described (161-178).

Glassy carbon possesses a modest cathodic window in addition to its wide anodic range, making it a target for further cathodic studies. However, the bug-a-boo hindering the widespread use of carbon as a reductive indicating electrode is its variability in performance, a consequence of the occurrence of carbon-oxygen functionalities on the surface free-valence carbon sites and variations in surface area and manufacturing procedures (237,238). These charge transfer mediators can serve to enhance as well as hinder redox reactions. Even after glassy carbon has been polished and electrochemically pre-treated, electron transfer remains slow and only quasi-reversible. The high overpotential for most organic compounds at glassy carbon restricts detection to mainly the multi nitro-aromatic group. Also, the attainment of long-term reproducibility is a problem.

Nevertheless, Kissinger (28) turned the disadvantage of a high overpotential and slow kinetics for oxygen reduction at glassy carbon into an advantage for discriminating against its effects on the background current during the determination of readily-reducible nitro compounds Since oxygen is reduced at a much higher potential than the analytes of interest on glassy carbon, the residual current remains low, favoring lower detection limits. In another notable reductive application, Gunasingham, Tay and Ang (167) employed a glassy carbon electrode as a substrate for a thin-layer of mercury. The thin-layer of mercury is continually plated and stripped via microprocessor control from a glassy carbon electrode located in an elaborate wall-jet cell. The objective behind this configuration was to present a fresh mercury surface to

each analyte, analgous to the traditional dropping mercury electrode. However, several problems related to the uniformity of the film were encountered. Although glassy carbon is inert, the mercury deposit does not wet the substrate and, thus, forms a collection of droplets, making the surface inhomogeneous. Consequently, reproducibility was poor and kinetics were slow. In addition, the "wash-out" time of this cell is limited by the plating/stripping stages which takes more than two seconds. Many of the problems associated with the construction of a polarographic detector have been solved, although widespread use will always be limited to investigators with golden hands.

Characterization of Silver as a Working Reductive Electrode for HPLC and FIA

The desire to quantitate quinones and nitro-aromatics isolated by supercritical fluid extraction in trace amounts from complex materials such as foodstuffs and environmental samples provided the impetus for the development of a suitable HPLC detector. The major limitation to the use of UV spectrophotometric detectors in these separations is their sensitivity to all co-extracted components which may have absorptivities two or more orders of magnitude larger than those of the analytes to be analyzed. In addition, due to the modest absorptivities of quinones and nitro compounds, acceptable sensitivity by use of UV spectroscopy can be achieved only after preliminary derivatization processes. Despite the problems associated with reductive electrochemical detectors, as mentioned above, there are several good reasons to pursue the development of a reductive detector for these analytes. First, as few other reducible functionalities are likely to be found in these samples, such a detector offers the potential for simplified separations in terms of time and peak resolution. Second, the favorable electrochemical characteristics of these analytes such as their low reduction overpotential, good reversibility and lack of adsorption phenomena promotes the attainment of low detection limits without time consuming derivatizations.

Quinones are of interest because of their use in modern wood pulping processes (179), as oxidation products of polycyclic aromatic hydrocarbons in the environment (67), and as important biogenic compounds found in electron transport systems of plants, bacteria, and animals (180). Ubiquinones are vital to photosynthesis in plants and

bacteria, as well as for blood clotting in animals (43). Other less widely distributed quinones are found in plants, where they serve roles including that of allelochemicals for protection against predation.

Nitro aromatics represent an important family of organics whose widespread use and application makes their detection a problem of considerable analytical interest. Many nitro compounds are used as drugs, veterinary products, cosmetic ingredients, perfumes and fragrances, explosives and propellents, agricultural chemicals, industrial raw materials and intermediates, bactericides and other consumer/industrial products. Moreover, many derivatives display varying degrees of mutagenicity and carcinogenicity (67).

A suitable working electrode for such an application should be robust like glassy carbon, yet be inexpensive, easy to fabricate and more reproducible from electrode to electrode. These latter attributes are often associated with microelectrodes (181-183). Of the electrode materials we investigated, silver fulfilled many early expectations. Silver possesses several favorable electrochemical, and mechanical properties which facilitates its use as an reductive sensor. Chief among these advantages is a surface that is uniformly wetted and exhibits a high degree of flatness which enables the attainment of a steady capacity and a reproducible surface area. In addition, the surface is impervious to most organic and aqueous solutions. Zojek (172,173) demonstrated that the response time following a potential step or pulse is rapid and the surface is not readily susceptible to passivation from trace metals so prevalent in a stainless steel HPLC system. On the contrary, these metals can, in some circumstances, catalyze the redox reaction. Moreover, silver has a high electroactivity and a wide cathodic range with a short equilibration time. These features of silver have been used to advantage in applications such as a substrate in surface-enhanced Raman scattering studies (SERS) (156-160) and elimination of edge effects in capacitive measurements (184,185) and in chronoamperometric measurements (186,187).

Another attractive feature of silver involves the ease with which it can be machined with ordinary metal working tools. Silver electrodes of various shapes and sizes can be prepared to effect different conversion efficiencies. Packed beds containing silver powder or silver mesh have been successively used for energy generation and storage,

bulk coulometric conversion, and on-the-fly electrosynthetic preparations of specific organic compounds (168,176,177). At the other extreme, Petersen (188) fabricated and evaluated a composite electrode containing silver particles dispersed in a Kel-F matrix for use as an reductive LC detector. Even though the importance of silver as a selective oxidant and electrode has long been recognized, its application to organic trace analysis remains relatively unexplored (188-195).

In one of the few works on the analytical applications of a silver disc, Miles and Fine (188-190) showed by cyclic voltammetric studies that trace quantities of nitro-esters exhibit a reversible reduction wave on silver. However, this work was applied only to static systems. Recently, an amperometric detector fabricated from silver was successfully applied for the determination of cyanide in industrial effluents (191-195). Preliminary reports also discussed the reversibility of the response of various nitrobenzenes at conventional and micro-silver electrodes (189,190,196-198).

The objective of the experiments presented in this chapter is to demonstrate the suitability of silver as an extremely versatile electrode for reductive LC detection. For these purposes, the design, construction, and use of amperometric thin-layer detectors based on a conventional silver disc, a dual pair of silver discs, and a silver oxide grid array in conjunction with HPLC and FIA are presented.

The thin-layer approach involves passing the chromatographic effluent through a narrow cavity in a spacer that is sandwiched between two blocks. This technique allows the electrolysis of a thin layer solution to be achieved in a very short time period. This approach offers an attractive strategy for delineating the basic dependency of the response on various experimental parameters. The effects of applied potential on background and analytical signal, effects of flow on response and influence of pH and various interferences are investigated and compared with those values at an amalgam electrode. In addition, the efficiency, linear dynamic range, sensitivities and detection limits for various quinones and nitro compounds were determined.

In an attempt to assess the effect of electrode surface area on signal amplitude for silver, a differential configuration was employed. To implement this design, a second cell chamber was machined adjacent to the first slot in the Teflon gasket.

In this chamber, a second electrode of similar size was inserted to serve as a reference. To determine the effect of size on signal for a given electrode material, the diameter of the pair was varied while the corresponding responses were measured under the same potential for an electroactive analyte and for supporting electrolyte. In this way, the resulting common mode difference signal is relatively free from errors due to capacitance changes, enabling an accurate comparison.

To ascertain the efficacy of silver at extreme potentials or in nonaqueous solutions, a partially blocked microarray electrode was assembled. Such a configuration possesses several advantages relative to solid electrodes of the same geometric dimensions. The small size of each electrode relative to a large sea of non-or semi-conducting area results in a decrease in capacitive current as well as an increase in faradaic current density due to nonplanar diffusion of material to the electrode surface. This capability has promise for minimizing interferences from surface redox reactions. In addition, the electrochemical cell incorporating a microarray ensemble has a small RC time constant and a small iR dependency (199-209).

Typically, these composite electrodes are fabricated by suspending a powdered conductor in a polymeric matrix. These include composites fabricated from epoxies and graphite (210), Teflon® and graphite (211), polyethylene and graphite (212), Kel-F® and graphite (213-219) and Kel-F® and silver (188). Alternatively, a porous conductor can be impregnated with an insulating polymer. This approach has produced electrodes encapsulated with wax or epoxy-resin (220-226). While these fabrication approaches yield the desired effects, they suffer from practical difficulties that limit the ease with which the resulting electrodes can be routinely prepared, used and renewed for subsequent reuse.

On the contrary, a solid silver electrode can conveniently be fashioned into an ensemble by selectively controlling the growth of silver oxide semi-conducting sites by means of a nylon screen. Applying the insulating sites to the areas outlined by the screen pores provides a simple alternative to the multistep fabrication procedure usually associated with composite electrodes. The utilization of such a procedure follows a rapidly growing literature of exploiting lithographic tactics for chemical sensors. An early amperometric application was described by Wightman (183) who used a lithographically-defined gold array coated with electroactive polymers to

fabricate molecular diode and transistor structures. Problems associated with bleeding and flaking of the electrode coating prevented common usage as an amperometric sensor. The kinetics, mechanism, and products from partial oxidations of organics at passivated silver in bulk solutions have been studied by Hampson et al. (187-189). There is, however, no prior description of a continually-renewable self-contained lithographically-defined silver oxide electrode designed for reductive applications. Such a microelectrode can be readily and simply fabricated from a silver substrate and offers a high success rate. In fact, the ensemble used herein can be constructed in approximately ten minutes. Once made, such assemblies can be easily cleaned by immersing in cleaning solution, prior to a plating bath. In addition, since the thickness of the sites can be accurately controlled, the resulting electrode surface is flat enough to be incorporated into a thin-layer cell containing a thin gasket. Moreover, the sites bind strongly to the silver substrate, providing carefree operation for an entire day. Using this assembly, we show that compared with a continuous silver electrode, the grid design is superior in regard to reproducibility, detection limits, cathodic range and minimization of passivation for the determination of hard-to-reduce analytes. The capabilities of the grid electrode at extreme potentials are illustrated by the determination of mercaptobenzotriazole (MBT) in cooling waters.

EXPERIMENTAL

Detector Design

The principal requirements for the design and use of thin-layer transducers have been recently reviewed (227-230). In general, the cell should fulfill the following six requirements: 1, simplicity of design; 2, easy access to the working electrode to allow its mechanical polishing and surface inspection; 3, as small a dead volume as possible; 4, minimization of cellular impedance; 5, compatibility with non-aqueous and aqueous solutions; and 6, a very rapid response time.

Several prototype cells fabricated only from Kel-F®, Delrin®or nylon containing inlaid metallic electrodes were built and tested but proved to be either unreliable in operation due to leakage, or difficult to construct and maintain. The advantages and disadvantages of various materials used in the fabrication of thin-layer cells have been discussed in detail by several workers (231-252).

Construction problems were solved by using stainless steel in conjunction with Kel-F® to form the cell chamber. A chamber made partially of stainless steel can be readily drilled and tapped to accept compression fittings. In addition, the stainless steel body can replace an expensive and leaky platinum button as an auxiliary electrode. Kel-F® was chosen as the insulating material for the silver electrode by virtue of its ease of machining, resistance to all LC solvents and oxygen impermeability. Also, Kel-F® can be readily polished to a mirror-like finish, permitting fabrication of a planar surface with the silver electrode.

Construction of Various Detectors

Single Electrode Cell

A modified version of the flow-cell of Kissinger (19) is used most often in the present investigation. The construction of this detector is illustrated in Figure 1. A major feature in this design is the position of the reference and auxiliary electrodes. The auxiliary electrode is directy opposite to the working electrode and is separated only by flowing solution stream in the thin-layer channel. This minimizes the problem of contamination and provides a symmetrical electrical field in the neighborhood of the working electrode. By positioning the reference electrode in a chamber connected to the cell by a wide bore channel, the iR potential drop between the working electrode and the sensing point is minimized. The thin layer cavity was constructed of two 1 in. x 1 in. x 3/8 in. (LxWxH) square blocks. The top block (E), made of 316 stainless steel had two tapped holes to provide the detector with an inlet and outlet port. The inlet port was machined to accept 1/16 in. O.D. x 0.002 in. I.D. narrow bore Teflon tubing, secured with a 10-32 male tapered finger-tightened Kel-F fitting (Upchurch). The other end of the tubing was connected to the column with a 10-32 Waters compression fitting and a 30° tapered stainless steel ferrule. The column-to-detector tubing was coated with a layer of epoxy to form a jacket, which is impermeable to oxygen. The outlet port was tapped 1/4-28 and bottomed to receive the extended arm of the reference compartment. A flat Kel-F washer 7/32 in. in diameter seated in the bottom of the port formed a seal with the reference compartment.

The bottom block (A) contained a central hole reamed to 1/8 in. The hole at the lower surface of the block was enlarged and recessed to about 7/32 in. in diameter and 1/16 in. deep. A silver disc 0.125 ± 0.001 in. in diameter and 1/2 in. in length was pressed

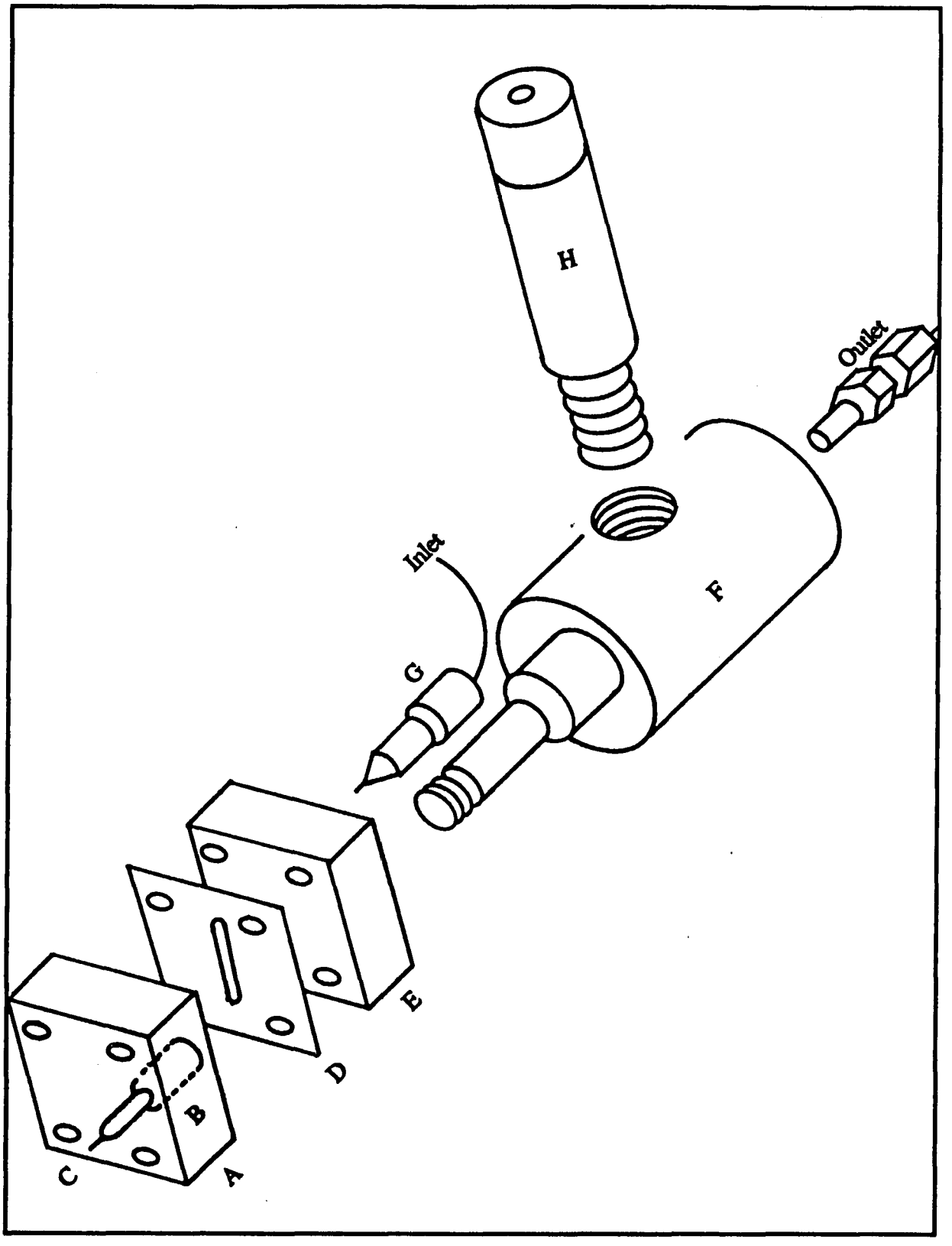

Figure 1. Silver-based electrochemical detector cell. A, Kel-F working electrode block; B, silver electrode; C, pinjack connector; D, Teflon spacer; E, stainless steel auxiliary block; F, reference electrode cavity; G, inlet from HPLC column; H, calomel reference electrode housing; I, Swagelok bulkhead fitting outlet.

into the Kel-F block after it was heated to temperature of 100°C with heating tape. Electrical contact to the silver electrode was made with a miniature pin-jack (Concord Electronics). The recess in the block surrounding the pin-jack was filled with epoxy cement flush with the lower surface of the block. The exact position of the silver electrode is not critical; however, it should be slightly downstream of the point where the inlet tube emerges from the opposite block. For comparison studies, a second interchangeable lower block assembly was made containing either a gold or carbon disc electrode. A 1/8 in. diameter high purity gold rod was pressed into a central under-sized well and then polished sequentially with 800 grit silicon paper and 0.25 μm diamond paste. A layer of mercury was applied to the highly polished gold surface by floating the electrode block in a pool of instrument-grade mercury for 5 minutes and then wiping off the excess adhering mercury with an index card. The amalgam electrode was electrochemically pre-treated by cycling between 0 and -1.5 V *vs.* SCE several times prior to use.

For the carbon block, a 3.2 mm glassy carbon electrode (type GC-30, Tokai Carbon Co., Ltd., Tokyo, Japan), 5/16 in. in length was coated length-wise with epoxy and cast into a central 1/8 in. well. Pressure was applied to the electrode assembly during curing with a C-clamp and a Teflon plate (the epoxy did not adhere to the Teflon) to ensure a uniform bond. After curing, the excess epoxy in the hole was milled away, exposing the carbon into which a small dimple was cut with a carbide tapered bit. A brass pin-jack was cemented into the dimple with conducting silver epoxy and secured with Epo-Tek 349 epoxy to provide electrical contact with the carbon.

The auxiliary block and the working block were arranged opposite one another when the two blocks were assembled. The electrode faces were separated by a thin 0.005 in. Teflon gasket cut from commercial sheet Teflon (AIN Plastics). A central slot, 5/32 in. wide by 3/4 in. long cut in the gasket extended from the inlet hole to the outlet hole and defined the cell volume and electrode area. The spacer thickness determined the inter-electrode distance. To avoid trapping gas bubbles at the entrance and exit ports, the slot in the spacer was brought to a sharp point at each end. After the absence of pits on the final surfaces was assured, the assembly was clamped together with four #4-40 machine screws at each corner. In this arrangement, effluent from the column enters through the upper half, impinging a few millimeters in front of the silver working electrode and then flows across the working electrode surface as thin film

between the auxiliary and working electrodes. The bolted cubes were further insulated from the environment in an air tight cylindrical Kel-F enclosure, 2 in. x 1-1/8 in., which is also used for mounting of the cell to a stand.

A calomel reference electrode was used for all measurements and consisted of a discarded inner element of a commercial SCE (Fisher Scientific) potted in a 3/8-24 threaded Delrin stem (Almac Plastics). A BNC connector soldered to the inner element and secured in place with epoxy was used for electrical connection with the potentiostat. The element was housed in a reference cell made from a bored-out nylon rod, 5/8 in. in diameter and 3 in. long. The top end of the rod was tapped 3/8-24 to accept the element bushing, whilst the lower tip was turned down and threaded 3/8-24 to fit into the reference compartment. A porous ceramic plug ground to a 1/16 in. rod was pressed through a rubber septum located in the tip of the cell. The plug affords electrolytic connection of the reference cell with the flowing stream. The cell was filled with 3 M NaCl solution through a bicycle valve located in the side wall of the nylon rod.

The flow-through reference compartment was fabricated from a cylindrical Kel-F rod, 1-1/8 x 2 in. terminating in a turned-down arm 1/4 in. in diameter and 1 in. in length. The arm was threaded 1/4-28 to connect the reference compartment with the outlet port in the stainless steel. A 0.040 in. axial hole was drilled on a lathe to allow unimpeded flow through the compartment. A central well was bored into the compartment and tapped 3/8-24 to accomodate the tip from the reference cell. A groove surrounding the well was fitted with a 1/2 in. O.D. Kelraz O-ring to ensure watertightness. The outlet end of the compartment was machined to receive a 1/16 in. Swagelok 10-32 union. The outlet was connected to the waste vessel via a 2 in. length of 1/16 in. O.D. x 0.010 in. I.D. stainless steel tubing. In this design, the effects of high uncompensated resistance on dynamic range caused by placing the reference electrode downstream were not manifested because of the close proximity of the working electrode to the auxiliary electrode.

Differential Cell

The flow-cell of the differential detector consisted of two working electrodes in two identical thin-layer chambers, which were in contact with a common reference compartment. Fabrication of matching chambers is critical for the proper operation of this configuration; however, the optimization of such parameters as detector volume is not absolutely necessary. An exploded view of each chamber in the flow-cell can be seen in Figure 2. The detector body consisted of two cyclindrical plates, 1-1/2 in. in diameter and 1/2 in. thick. The two blocks were separated by a rather thick (0.025 in.) circular Teflon gasket cut with a sharpened metal compass from sheet Teflon. The gasket contained two milled channels, 3/32 in. wide by 3/8 in. long, located along the central axis, which separated the cell halves and accurately defined the volume for each chamber. The top plate, made of type 304 stainless steel serves as the auxiliary electrode as well as the chamber cover. It contained four 0.040 in. drill bores to provide an inlet and outlet port for each chamber. The inlet holes were drilled out and machined to accept standard 1/16 in. O.D. stainless steel tubing held in place by a 30^{o} tapered ferrule and a Waters 10-32 compression fitting. The two 0.040 in. outlet passageways located on the liquid face of the plate were drilled to a depth of 1/4 in., where they joined a common central outlet port. The outlet port was drilled out, bottomed, and tapped 3/8-24 to receive the reference compartment. The connection of the compartment with the block was sealed by a Kelraz O-ring held in the bottom of the port. This simple arrangement of inlet and outlet ports routed incoming effluent through the individual channels before exiting the cell body. Electrical contact with the potentiostat was made by means of a threaded (#6-32) brass post. Following machining, the surface of the stainless steel plate was ground using 600 grit carborundum powder on a flat glass plate followed by polishing on a Microcloth (Buehler) cloth with a 0.05 μm alumina (Fisher) slurry.

The opposite plate made of Kel-F contained two holes, 1/8 in. in diameter and symmetrically spaced along the center line 1/2 in. apart to accept the working electrodes. Two high purity (4N) silver discs (Handy and Harman), 1/8 in. in diameter by 1/2 in. in length, were pressed-fit into their respective holes in the Kel-F plate while the assembly was warmed with heating tape. The holes at the lower surface of the block were enlarged and recessed to about 5/32 in. in diameter and 1/16 in. in depth to provide clearance holes for miniature pin-jacks (Concord Electronics), which afford electrical connection with the potentiostat. After the pin-jacks were inserted into

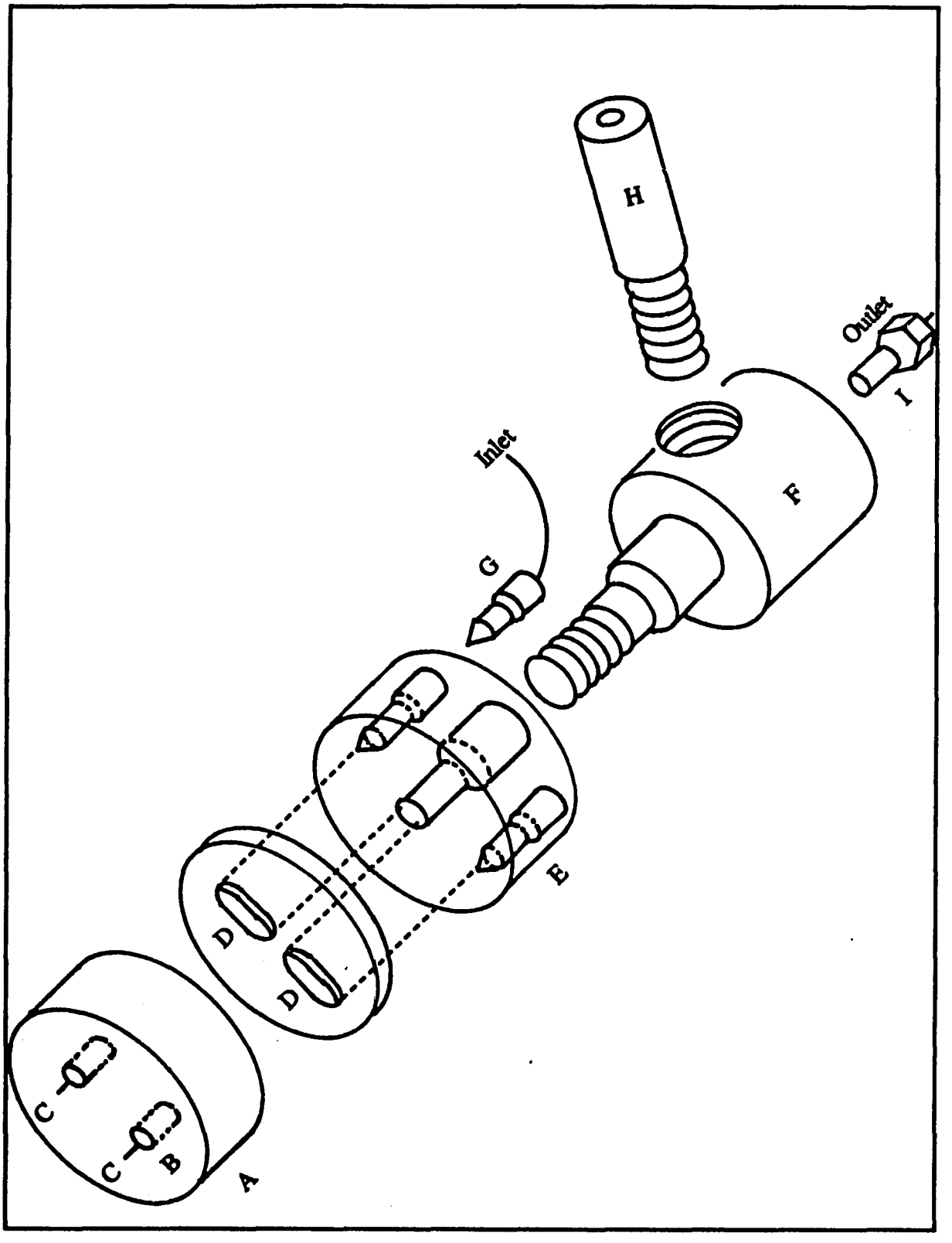

Figure 2. Differential electrochemical flow-cell schematic: A, dual lower Kel-F block; B, silver working electrodes 1 and 2 ; C, electrical contacts; D, dual flow channels in Teflon spacer; E, common upper stainless steel auxiliary electrode block; F, reference electrode cavity; G, mobile phase inlets; H, calomel reference electrode housing; I, common Swagelok bulkhead fitting outlet.

the silver discs, both recesses in the block were packed flush to the surface with Epo-Tek 349 epoxy (Epoxy Technology Inc.). The silver electrodes mounted in the Kel-F plate were polished first with 800 grit silicon carbide powder, then with a 0.05 μm alumina slurry and, finally, with 0.2 μm diamond paste on a velvet cloth to a mirror-like finish. Three additional interchangeable lower blocks containing 1/32 in., 1/16 in., and 3/32 in. silver disc pairs were constructed to probe the dependency of electrode area on signal amplitude. Four drill holes symmetrically located around the perimeter of the plates and gasket allowed the unit to be aligned and tightly sandwiched together with 4- #4-40 machine screws.

The reference electrode here was of the silver-silver chloride type immersed in 3M sodium chloride solution saturated with silver chloride contained in a reference cell (bridge). The reference electrode was fabricated from a dental grade silver rod, 0.10 in. in diameter and 2-1/2 long, anodized in chloride media with silver chloride. The silver rod was pressed into the stem of a 10-32 type banana plug. The stem was insulated from the filling solution by a 3/8-24 threaded nylon bushing, which also served as a removable electrode holder. The bushing was sealed in the reference cell (bridge) by a 1/2 in. O.D. O-ring made of Kelraz.

The reference cell was made from 5/8 in. diameter nylon rod (Almac Plastics) drilled and tapped to take the silver reference electrode bushing at the top end and turned down and threaded 3/8-24 at the bottom to fit into the reference compartment. Electrolytic connection of the cell with the flowing stream was provided by a Vycor #7930 disk sealed in the tip of the cell with a rubber septum. The completed reference electrode was housed in a downstream compartment, fabricated from a cylindrical Kel-F rod, 1-1/8 by 2-1/2 in. long. The main axis was drilled out to 1/8 in. for continuous liquid flow. A central well was milled perpendicular to the face to connect with the main axial passageway. The well was tapped 3/8-24 to accept the reference cell (bridge) and sealed by a lower Kelraz O-ring. One end of the cylindrical compartment was turned down to 3/8 in. and threaded by means of a lathe to mate with the common 3/8-24 outlet port in the stainless steel block. The other end was drilled out to accept a 1/16 in. Swagelok bulkhead union, which was connected via a 1/16 in. O.D. stainless steel tube to a waste vessel. The assembled detector was then attached to the HPLC system which contained two liquid streams. One stream was pumped by a high pressure syringe pump through an injection valve and the column to the sample

cell of the differential detector. The other by-pass stream was pumped through a column packed with glass beads to the reference chamber. The difference in electrochemical response between the sample and the reference cells was measured and registered on a chart recorder. In this way, the signal was continuously compensated for the background current. In addition, if both silver electrodes were different in size or composition, the effects of such parameters on the signal could readily be examined.

Silver Grid Array

In principle and construction, the silver oxide grid cell is similar to that described earlier for the single thin-layer cell. The main differences are as follows: 1, The inter-cellular distance was greatly reduced by using a thinner gasket, thereby keeping current paths short and independent; 2, Junction potentials were reduced by using a reference electrode designed for non-aqueous media, so accurate potential could be maintained at the electrode during an electrochemical reaction. A schematic diagram of the silver grid cell is shown in Figure 3.

The substrate for the silver grid electrode was a 3/8 in. x 0.125 in. silver rod (4N pure, Handy & Harmon) force-fit into a 1/8 in. hole drilled into a 1 in. x 1 in. x 3/8 in. Kel-F bottom block. Electrical connection to the silver was made with a 0.040 in. Ag-or Au-plated pinjack (Concord Electronics) forced into a hole drilled lengthwise into the center of the silver rod.

The same stainless steel top block assembly used in the single cell was also compatible with the grid design. However, the inlet connection to the top block was modified by inserting a 2 in. length of 1/16 in. O.D. x 0.002 in. I.D. stainless steel tubing contained in two Kel-F male 10-32 endfittings between the column and the stainless steel top. By isolating the inlet tube from the power line, the cell was found to be less susceptible to environmental magnetic and electrical fields. The two blocks were pressed together between a 0.002 in. Teflon film (Dielectrix Corp.) containing a 3/32 in. x 3/4 in. channel, which defined the cell volume. The downstream end of the channel was enlarged to 1/4 in. with a leather punch to reduce the uncompensated resistance. Column effluent flowed into the cell through a 0.025 in. hole in the top block and out to the reference electrode compartment through a 0.043 in. hole in the

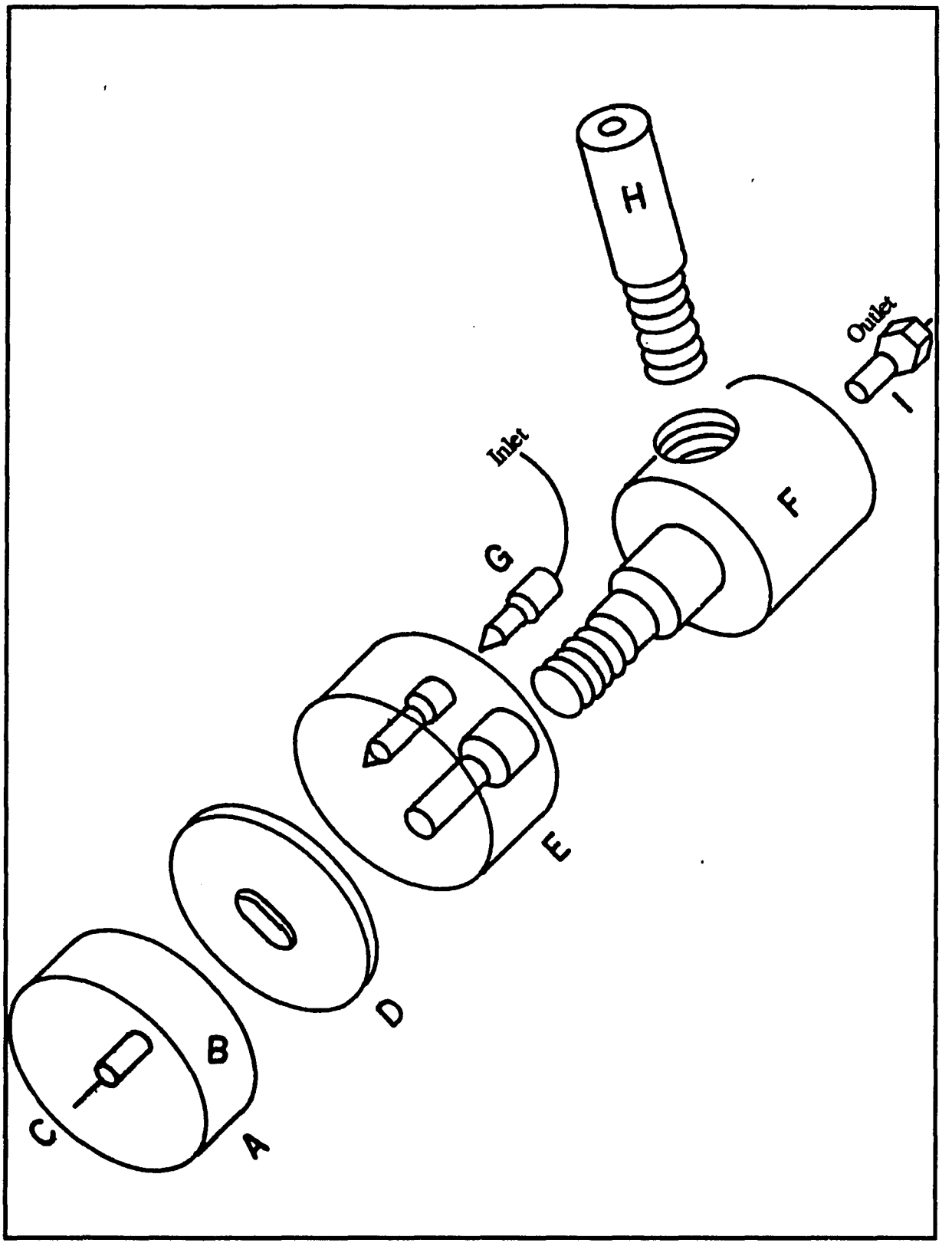

Figure 3. Silver oxide grid electrochemical flow-cell schematic: A, working electrode Kel-F block; B, cavity for silver grid electrode; C, electrical contact; D, Teflon spacer; E, auxiliary electrode upper stainless steel block; F, reference electrode cavity; G, mobile phase inlet ; H, calomel reference electrode housing; I, Swagelok bulkhead fitting outlet.

same block. To keep the detector body fastened, the blocks were held together by a retaining plate with four #4-40 screws.

The reference electrode was a Ag-Ag^+ ClO_4^- electrode. It was fabricated from 22 - gauge silver wire (Carlo Erba) sealed in a Teflon stopper and mounted in a glass chamber. The wire was polished with emery paper No. 800 and washed with acetone and distilled water. After being placed for eight hours in concentrated ammonium hydroxide solution, the wire was rinsed and kept in distilled water until use. The chamber was filled with a saturated solution of silver perchlorate in acetonitrile-water (90+10, v/v) and closed by a Vycor plug sealed with a piece of heat-shrinkable tubing. The reference electrode potential was checked daily versus a saturated calomel electrode and was found to be on the average 350 ± 10 mV more positive. The chamber was fitted after being heated to 150^{0}C with heating tape into a drilled out 1/4-28 plastic connector. Epoxy applied around the neck of the chamber helped to prevent leakage. The chamber screwed into the central well of a 1-1/2 in. long x 1-1/8 in. diameter nylon rod machined to produce a union-tee. To make connection to the electrochemical cell, one end of the tee was turned down on a lathe to 1/4 in. O.D. and threaded 1/4-28 to fit the stainless steel block. The other end was drilled and tapped to accept a 1/16 in. Swagelok fitting, which was drilled out to 1/16 in. I.D. along the main axis to accept the stainless steel waste tube.

Circuit Design of Bipotentiostat

A laboratory-built potentiostat based on a standard inverting configuration was used to control the potential applied and to measure the responses from the working electrodes. Several circuits employed in the control of rotating ring-disc electrodes (253-255) and single and dual thin-layer electrochemical detectors (256-272) were considered and some of the best features were incorporated into a design which gives stable control of the dual set of electrodes, high current sensitivity with high background current offset capability, and ease of operation.

Electrical Components

High quality components were used throughout the construction of the potentiostat because lower quality devices, especially in the applied circuit and current-to-voltage converters, produced unacceptable noise levels when low levels of current noise were being measured. All operational amplifiers were 52K modules (Analog Devices,

Norwood, MA) These amplifiers have extremely low current and voltage specifications and were wired according to Analog Devices Application Notes to optimize performance.

All resistors were 1% metal film precision resistors (Dale) and all capacitors were polystyrene (TRW, 5% tolerance). Bournes 10-K Ω precision potentiometers were used to select the applied potential and Bournes 10-K Ω "knobpots" model 3610 10-turn precision potentiometers were used to control the offset current.

The manual switches were constructed as single pole, double throw switches make-before-break switches with berylithium copper contacts which are isolated on Teflon® stand-offs. These switches were patterned after the zero adjust switch of a Keithly Model 602 solid state electrometer. (Keithly Instruments, Cleveland, Ohio). The open contact resistance of these swtches were measured and found to be greater than 10^{14} Ω. An Analog Device power supply and manifold model No. 801 was used to supply the ± 15 V DC at 100 mA required to operate the potentiostat. All electrical connections were made with a point-to-point technique with Alpha Teflon® coated 22 gauge stranded wire. Shielded cable (Belden RG174/U) was used in conjunction with BNC connectors to carry the current from the electrochemical cell.

Circuit Layout

All individual resistor-capacitor feedback loops were efficiently arranged in close proximity to their respective op-amps, so as to keep wire length and crossover to a minimum. These circuits were mounted on solid Teflon® boards, 6 in. x 6 in. x 1/8 in., on which silver-plated forks and posts were arranged to accept the resistors and capacitors. Potentiometers and switches were mounted directly on the board, in close proximity to their function, in specially-designed Kel-F® fixtures. Input/output connections with the electrochemical cell were accomplished with BNC connectors mounted in recessed brass holders on the board. The circuit was completed by soldering all resistors and making all interconnections as shown in Figures 4 - 6. The completed PC boards were mounted on the detector housing walls to minimize the distance between cell components and electronic controllers.

Circuit Operation

Figures 4-6 show the schematic of the circuits needed to independently control the

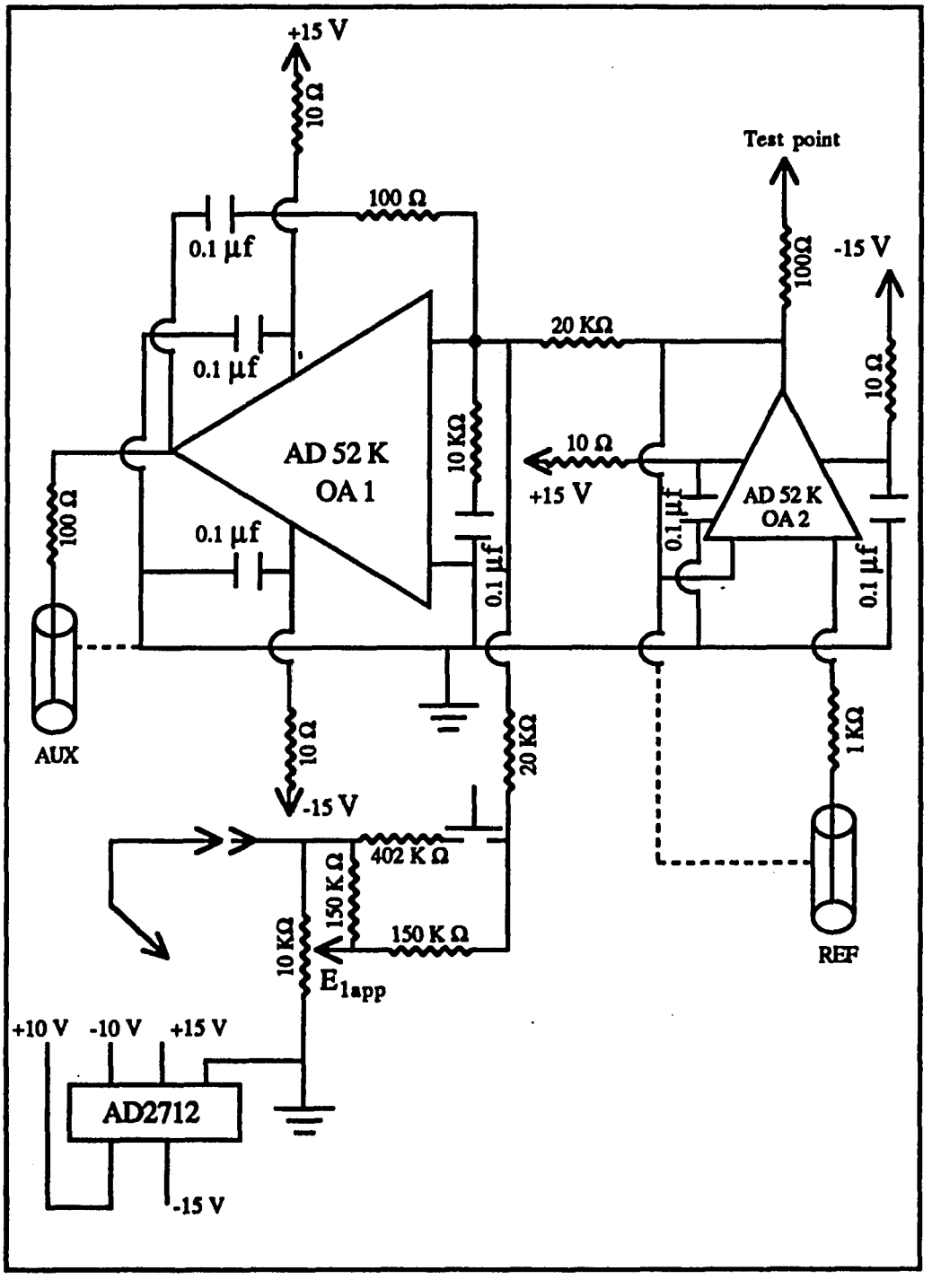

Figure 4. Schematic diagram of the potential control section of the potentiostat. Components: all resistors, 1 % metal film as labelled; all capacitors, 5 % polystyrene as labelled, all switches rotary make-before-break; inputs/outputs, BNC 3/8-32 connectors; cable, shielded RG/174U

potential of the twin working electrodes. The circuit is divided into two modules according to function for ease of understanding and fabrication. The input connections are labelled as follows: W_1 and W_2 are the working electrodes, AUX is the auxiliary electrode and REF is the reference electrode.

The circuitry for potentiostatic control of W_1 consists of the controller amplifier (OA_1), the reference voltage follower (OA_2) and the current-to-voltage converter (OA_3). The main or controlling op-amp (OA_1) is arranged in the inverting configuration and contains the reference voltage follower (OA_2) and auxiliary path in the feedback loop. The potential is selected from a 10 turn precision potentiometer and applied to the inverting (summing) input. The function of this op-amp is to compare continually the impressed voltage with the voltage measured by the reference electrode. When a deviation is detected, for example, from a faradaic or charging process, the output of OA_1 connected to the auxiliary electrode emits the necessary current signal to make the reference and applied signals once again equal. In practice, the potential at the output of OA_2 is equal in magnitude but opposite in sign to that applied; E(applied) = -E(ref). Because the potential of W_1 is maintained at virtual ground by means of the feedback loop of the current-to-voltage converter (OA_3), $E(W_1)$ - E(ref) = E(applied).

The current-to-voltage converter (OA_3) shown in Figure 5, is provided with a series of feedback resistors to give a sensitivity range of 0.1 to 500 nA/volt. Each resistor is provided with a capacitor which allows the signal to be filtered with a time constant of 0.1 seconds. The current flowing into OA_3 is represented by the output voltage of OA_3, $= -I_1R_f$, which also feeds a Linear Instruments model 1700 strip-chart recorder.

A precision voltage source connected to an adjustable 5-K Ω potentiometer provides an offset voltage to buck out any residual current. The offset voltage is connected to a voltage follower (OA_4) in order to prevent interactions with the incoming signal current, which, in most cases, is much smaller in magnitude. The output of the voltage follower (OA_4) is fed through either a 500-K Ω, 1-M Ω, or 10-M Ω resistor, providing an offset current range of 1 nA to 20 nA at the inverting input of the current-to-voltage converter (OA_3).

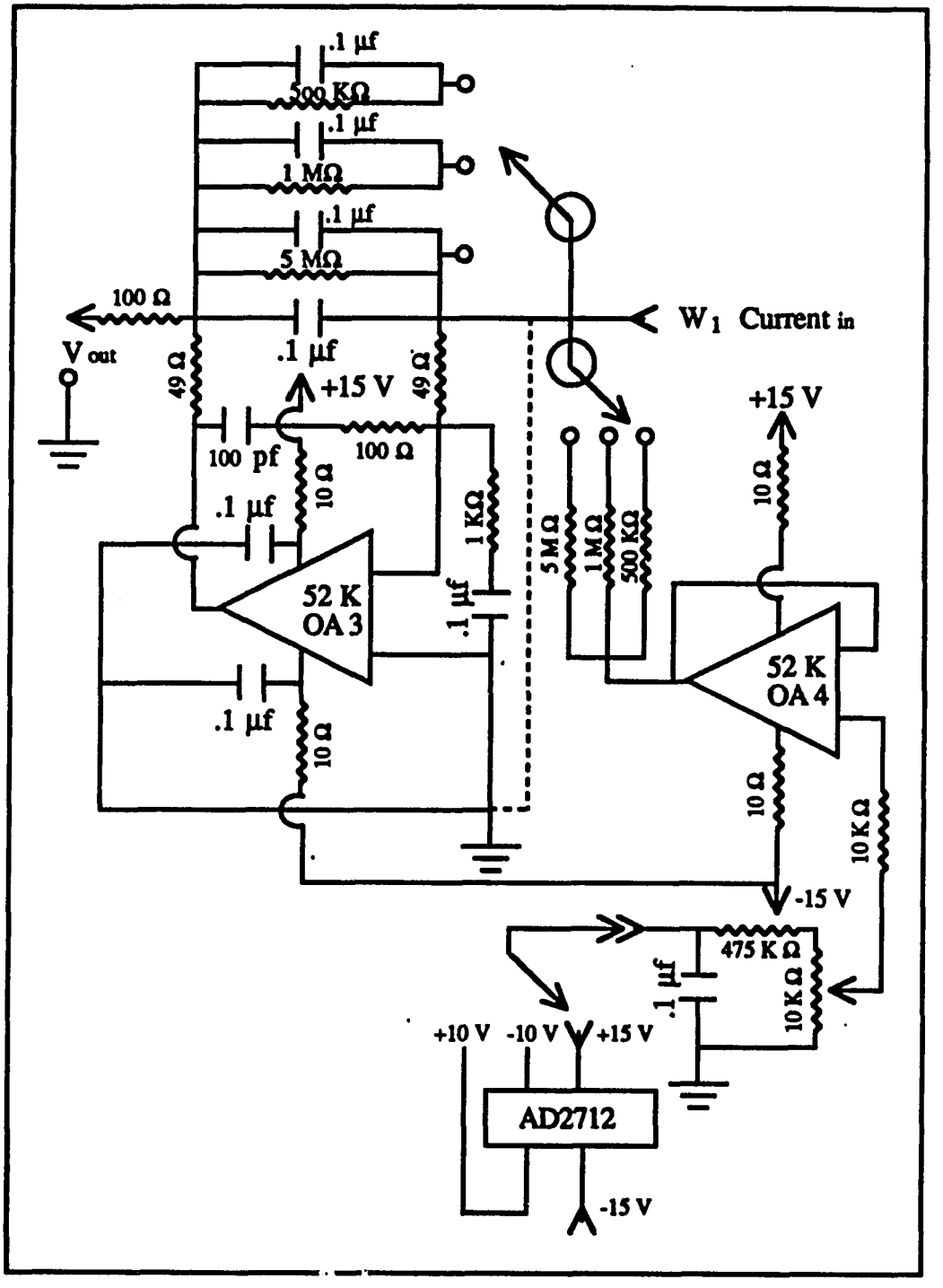

Figure 5. Schematic diagram of electrometer connected to electrode 1. Components: all resistors, 1 % metal film as labelled; all capacitors, 5 % polystyrene as labelled, all switches rotary make-before-break; inputs/outputs, BNC 3/8-32 connectors; cable, shielded RG/174U.

The circuitry required for potentiostatic control of the second working electrode, consists of a basic current-to-voltage converter (C-V) section with two additional op-amps for signal inversion and manipulation, labelled OA_5, OA_6, OA_7, and OA_8, respectively. A schematic of the second current-to-voltage converter is shown in Figure 6. The second current-to-voltage converter section is designed to measure the current from an electrode not held at ground potential. In this case, the noninverting input of OA_5 is provided with a voltage offset, E_{offset}, equal to the difference between the desired W_2 potential level (E_2) and the preset W_1 potential level (E_{1app}). Because E_{1app} is equal to $-E_{ref}$, W_2 is thus maintained at a potential E_2 with respect to the reference electrode. Operational amplifier 6 (OA_6) provides an adjustable background compensation source at the inverting input of OA_5, if required. Operational amplifier 7 (OA_7) takes the output of the C-V converter, $(-I_2R_f + E_{offset})$, and inverts it with unity gain so that V_{out} is equal to $I_2R_f - E_{offset}$. This voltage, along with E_{offset} itself, is then summed and inverted by OA_8 so that the output of OA_8 represents only I_2 following in W_2. This arrangement obviously necessitates the setting of the W_1 (SCE) potential prior to that of W_2 (SCE). However, the very small number of times this is actually done in practice precludes the need for any further sophistication.

Operation of Potentiostat

It should be noted that extreme care should be taken to ensure that the high impedance part of the circuit is not touched with bare hands. A slight contamination of the Teflon® board or switches may drastically affect the performance.

Peak Detector Circuit Description

To obtain a more accurate representation of the peak currrent response than that rendered by a strip chart recorder, a peak detector was constructed. A schematic for the peak detector, which is based in part on circuits described by Curran (273) and Crouch (274) is shown in Figure 7. The basic operation of the peak detector is as follows. When Sw_1, the re-set switch, is closed the circuit acts as a voltage follower with a gain of one. In this state, the peak detector can be zeroed. With Sw_1 open, as the voltage at the input, V_{in}, from detector increases, the capacitor C follows the signal and is charged up to the peak voltage. Operational amplifier OA_1 with diodes D_1 and

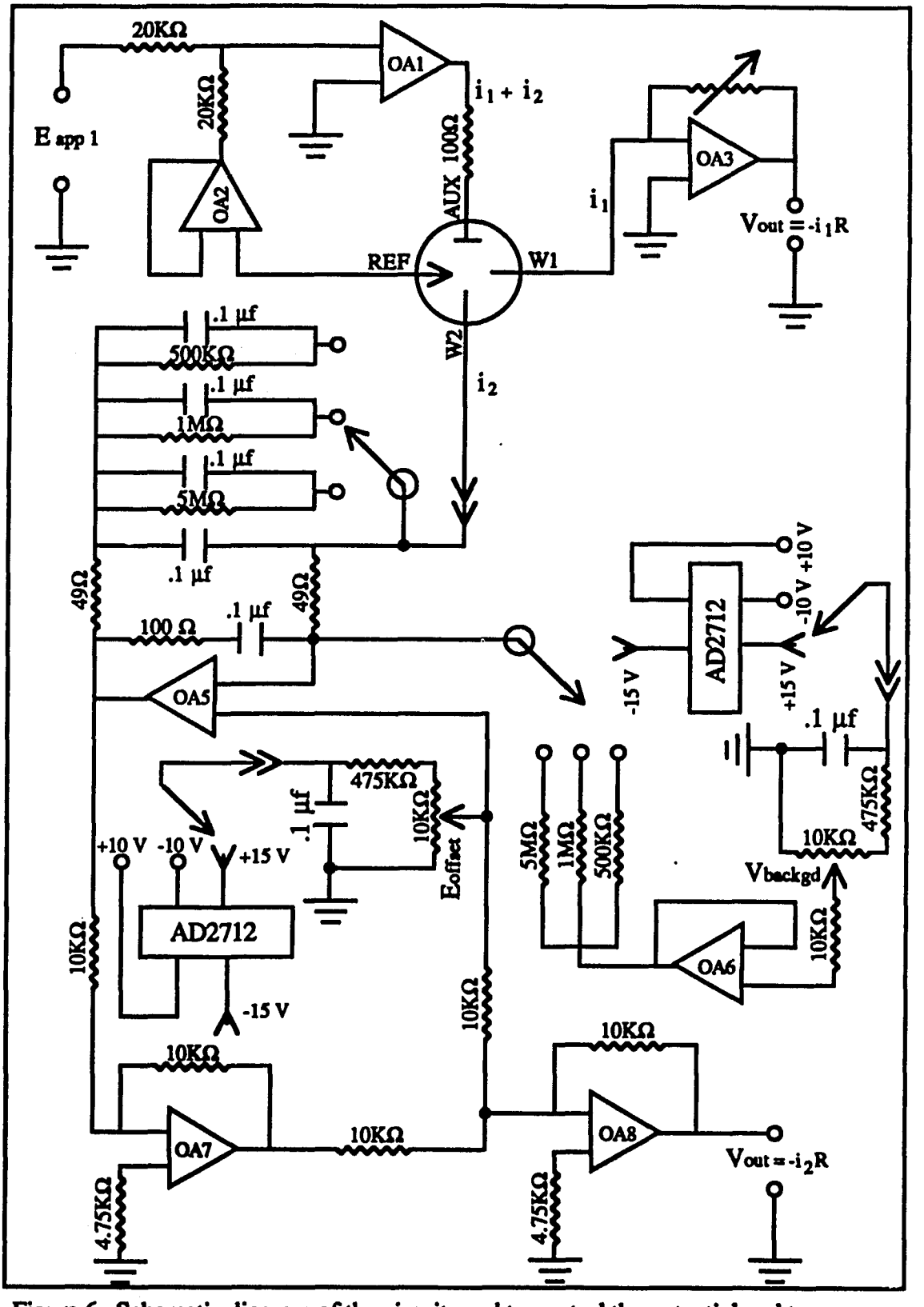

Figure 6. Schematic diagram of the circuit used to control the potential and to measure the current at electrode 2. Components: all resistors, 1 % metal film as labelled; all capacitors, 5 % polystyrene as labelled, all switches rotary make-before-break; inputs/outputs, BNC 3/8-32 connectors; cable, shielded RG/174U.

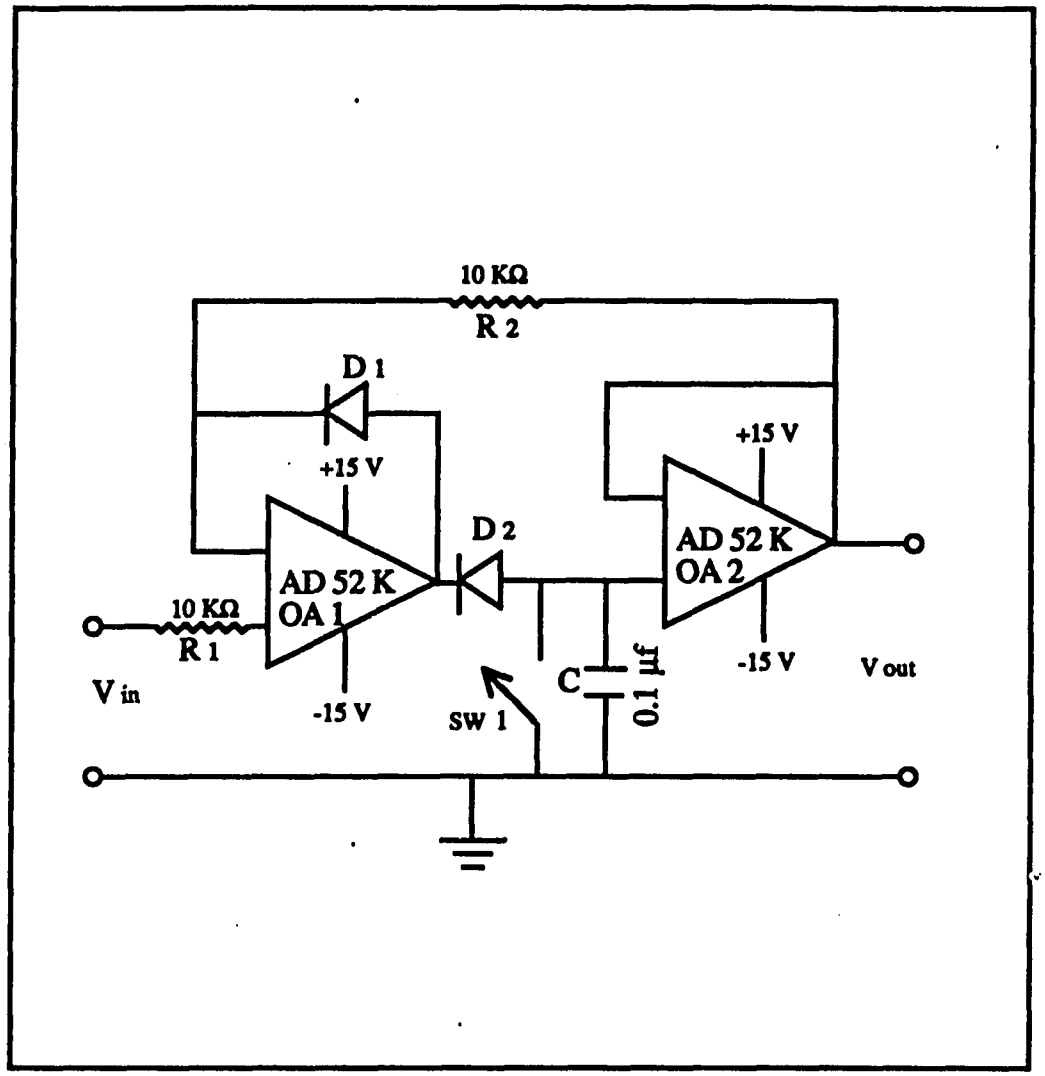

Figure 7. Peak height detector circuitry. Components: operational amplifiers (OA 1 and OA2), Analog Devices 52 K; diodes (D1 and D2), IN 914; bias resistors (R1and R2), 10 KΩ (1 % metal film); storage capacitor (C), 0.1 µf (5 % polystyrene); switch (sw 1), manual reset push button. Inputs/outputs: Vin= detector signal input; Vout= meter display.

D_2, and resistor R_2 acts as a half-wave rectifier so only negative input voltages are tracked. If the voltage is positive, feedback is through D_1, and if negative, through D_2, A_2, and R_2. When the voltage is received and the voltage begins to decay, the capacitor should theoretically remain at the peak voltage indefinitely. The 10000 pF polystyrene capacitor was chosen for its small leakage rate. Its discharge is further slowed by the bias of D_2 and the high impedance of operational amplifier follower OA_2. The voltage of OA_2 is outputted to the input of a Keithley Model 179 DVM for display. The op-amps are BiFet devices because of their high input resistance and low bias current.

Operating Procedure for Peak Detector

First, the baseline is established with switch 1 (sw_1). At this time, any baseline irregularities (e.g., due to air bubbles) may be observed and, if possible, corrected. A steady baseline will be seen as a stable meter reading, which is to be noted. At this point, the detector offset may be altered to adjust the output voltage to some convenient value (e.g. 1V). Then, the sample is injected and, after the solvent peak elutes, switch 1 (sw_1) is manually opened. As the peak maximum is reached and passed, the meter holds a steady reading which indicates the maximum peak height. This value is then noted. The peak height is the difference between the noted values. This should be followed by reestablishment of a steady baseline. The next experiment may then be carried out. The system, as constructed, is operated manually. It could be completely automated, but at additional expense and complexity.

Construction of the Pneumatic Filling Device

Deoxygenation and sample delivery was accomplished in a modified 3 mL Reacti-Vial® connected directly to the injection valve. The top of a Reacti-Vial® was fitted with a stainless steel 304 flanged insert containing two ports located along the central axis. The seal between the vial and the insert was effected by a 1/2 in. O.D. O-ring held in a lower groove of the insert. A 1/16 in. stainless steel dip tube 4 in. in length was inserted through the side port so that the lower part touched the conical tip, while the upper part was connected to port #6 of a model 7125 injection valve (Rheodyne, Cotati, CA). A 1/8 in. to 1/16 in. adaptor (Swagelok), brazed into the central port, is used for venting the vessel during degassing as well as a fitting for pressurization of the vial during sample delivery.

Operation of Filling Device

In the inject position of the injection valve, a fine stream of nitrogen from a 22-gauge hypodermic needle is inserted through the adaptor purges the contents at ca. 1 mL/min. After 2-3 min, the nitrogen stream is removed and the adaptor is connected to a 35 psi source of nitrogen. Subsequently, the sample loop is washed and filled with deoxygenated sample by toggling the injection valve between the injection and load position while applying gentle pressure with a tissue against the front needle port.

Fabrication of Silver Grid Electrode

The block containing the silver substrate was initially ground flush to a coarse matte finish on an optical flat using a slurry of 600 grit SiC powder (Buehler). The electrode assembly was then held perpendicular to a lab-constructed polishing wheel covered with a SiC slurry on a Texmet pad (Buehler). A stream of distilled water was directed at the electrode to reduce frictional heating. The assembly was rotated 45^0 in a figure eight configuration until a fine matte finish is obtained. The SiC grinding done upon initial preparation of the electrode was generally not repeated. The next series of operations involved polishing the block assembly to a glossy finish using a v-type motion toward and away from the center of a texmet wheel covered with a 0.5 μm alumina slurry (Buehler). Finally, the electrode was rinsed with distilled water and polished on a wet Microcloth (Buehler) wheel covered with a 0.05 μm alumina (Fisher). To produce the grid design, an additional gasket containing a 1/2 in. diameter nylon screen (100-500 μm pore size) was superimposed on top of the regular spacer while the silver substrate was electrochemically etched by alternate one minute cycles of oxidation at +0.6 V *vs* (Ag/AgCl) followed by dissolution in 3 M HCl. After 5 minutes, the screen was removed and the applied potential was adjusted to the desired cathodic level enabling measurements to begin. In this manner, the pores of the screen act as templates for the elements of the microelectrode ensemble. Furthermore, the pore density defines the element density. This procedure results in ensembles which are composed of 350 μm silver oxide size discs surrounded by a symmetrical 150 μm wide silver grid. Examination of the electrode with a loupe revealed no pitting.

Chemicals

Quinone samples were obtained from Aldrich Chemicals, Sigma, Eastman and Pfaltz and Bauer. Nitroaromatics were purchased from Aldrich Chemicals. These were used as received after checking purity by HPLC with EC and UV detection.

HPLC Apparatus

An HPLC was assembled from a Varian 8500 syringe pump, a Rheodyne Model 7125 sampling valve with a pneumatic sample degasser and loading device and a 20-μL sample loop, and a lab-built electrochemical detector. Separations were done on a 150 mm x 3.9 mm I.D. column, packed with 10 μm diameter particle size μ-Bondapak C-18 (Waters Assoc., Milford, MA).

In order to accomodate deoxygenation with helium, several modifications were made to the model 8500 pump. First, the molded cap on the solvent reservoir was replaced with one machined from nylon pressed-fitted into a brass cylindrical housing. The brass housing was necessary to accept threads for fittings as well as to act as a substrate for silver solder joints from plumbing lines. Three holes were drilled along the central axis of the cap assembly. A dip tube, 1/8 in. O.D. x 8 in. long, was inserted through the central hole and brazed in place so that the tip of the tube just touched the bottom of the solvent bottle. The other end of the tube was connected to the inlet check valve of the pump head cylinder. A degassing tube terminating in a 316 stainless steel diffuser was silver soldered into one of the side holes. The other side hole was tapped to accept a 1/8 in. pipe-to-tube 1/8 in. adaptor. This fitting was connected to either a source of nitrogen or served as an atmospheric vent depending upon the operational mode of the pump. Second, two additional on/off-vent gas solenoids were added to the electronic board controlling the drive mechanism of the pump cylinder. The electrical leads of solenoids 1 and 2 were connected to ports 1 and 2 and ports 3 and 4, respectively, located at the front of the board. It is important to note that both solenoids were controlled in such a manner that neither solenoid was turned on at the same time. When the pump was in the off position, solenoid 1 provided a source of nitrogen to the degassing tube. During degassing the nitrogen was directed through the mobile phase and out through the vent port of solenoid 2 to the atmosphere. After a degassing period of 10 min, the fill button was depressed, which simultaneously activated solenoid 2 and closed solenoid 1. Gas pressure from the solenoid 2 displaced mobile phase from the glass reservoir bottle into the cavity of the syringe cylinder until the 250 mL capacity limit was reached. Following fill-up, the back pressure provided by the plunger of the pump prevented re-entry of oxygen. In this fashion, the contents of the bottle could be degassed directly in the bottle prior to fill-up without exposing the degassed contents to atmospheric oxygen.

RESULTS

Evaluation of Potentiostat

For this experiment, both electrode inputs were connected through 100-K Ω resistors to the reference follower (OA_2) input which in turn was connected through a 50-K Ω resistor to the auxiliary input. To test the circuit, a 0.5 V signal from the offset potentiometer was applied to both working inputs and the output of the reference follower was monitored for several days. Within that time period no drift in the voltage was detected. The rest of the circuit was tested by applying a 10-nA current produced by the output of the offset operational amplifier (OA_7), to the working electrode(s). Most of this current was offset and the remaining current (50 nA) was amplified on the 0.1 nA/volt scale and followed on a Linear Model 1200 strip-chart recorder. The peak-to-peak noise was less than 1 pA and drift over a 10-hour period produced less than a 2% change in the 50-pA current being monitored. These noise levels are well below those encountered in electrochemical cells and, therefore, would make minor contribution to the total noise found in these systems.

Performance of Peak Detector

The peak circuit operation was verified using a triangular wave which has an amplitude of 5.0 V at a frequency of 10 Hz to simulate a chromatographic peak. The results are shown in Table 1, where the peak detector output voltage is listed as a function the calculated slope of the input waveform. The peak detector appears to be capable of capturing the peak to within a few parts per thousand relative to signals changing as rapidly as 100-300 V/s. The error is no worse than 3 % relative up to 5000 V/s. It is estimated that the slopes of the experimental current-time curves were less than 1000 V/s.

Evaluation of Pneumatically Controlled Degassing and Filling Device

Oxygen present in sample solutions poses several problems for reductive electrochemical trace work. When a sample containing oxygen is injected into an HPLC system containing a C_{18} column, the oxygen does not come out in the void as might be expected but rather elutes as a broad tailing band which can obscure significant portions of the chromatogram. The elution behavior of oxygen is largely

independent of mobile phase composition so little flexibility exists in manipulating its elution position (275).

To lessen the effects of dissolved oxygen in these studies, the samples to be analyzed are deoxygenated in a modified Reacti-Vial® connected directly to the injection valve which is then used to pneumatically fill the injection loop. Figure 8 compares chromatograms of a mixture of nitrobenzenes, obtained under identical conditions, utilizing the described device (a) and by syringe injection following off-line degassing (b). Although the contents were degassed prior to syringe injection, the three peaks for the nitrobenzene derivatives are completely obscured by the high oxygen reduction current. Only the massive amperometric response due to oxygen is seen. After this injection, the baseline required over 30 min to stabilize. In contrast, using the described device, an oxygen-free solution enters the detector, and well-defined peaks for the three nitrobenzenes free from oxygen interference are observed. Note, also, the disappearance of the large peak due to a pressure surge when the valve position is changed. The same sensitivity setting was used for each chromatogram. Table 2 compares the efficiency of the described device in terms of reproducibility with that obtained by conventional syringe injection with an initial nitrogen purge. Similar background and peak currents are observed, and the only difference is the slightly better precision when the pneumatic device is employed. The effectiveness of this device in maintaining the high precision and accuracy of the injection valve can be attributed to the repetitive delivery of an excess of 3 loop volumes per injection, as recommended by its manufacturer (276). The peak heights of 8 replicate injections of 0.54 ng amounts of m-dinitrobenzene in 20-μL of solvent had a coefficient of variation of 0.5 %. For small samples, this device is particularly valuable because the loss of sample due to entrainment in the deoxygenation assembly and its associated pipe-work is minimized. In addition, it maintains the accuracy and precision specifications of the manufacturer. Furthermore, it can be useful in studies requiring multiple injections of the same sample, such as in the construction of an hydrodynamic voltammogram (HDV) curve. Finally, such a device can easily be constructed by a person unskilled in machine operations. Except for chromatograms in Figure 8a, this device was used for collecting all chromatograms presented in this work.

Table 1. Response of the Peak Detector to a Simulated Peak.

Slopes (v/s)	Peak Voltage (V) *	% Accuracy
± 7.0	4.98	99.7
± 35	5.00	100
± 70	5.05	101
± 350	4.99	99.7
± 700	4.89	97.8
± 3500	4.85	97.0

* True peak voltage =5.00 V

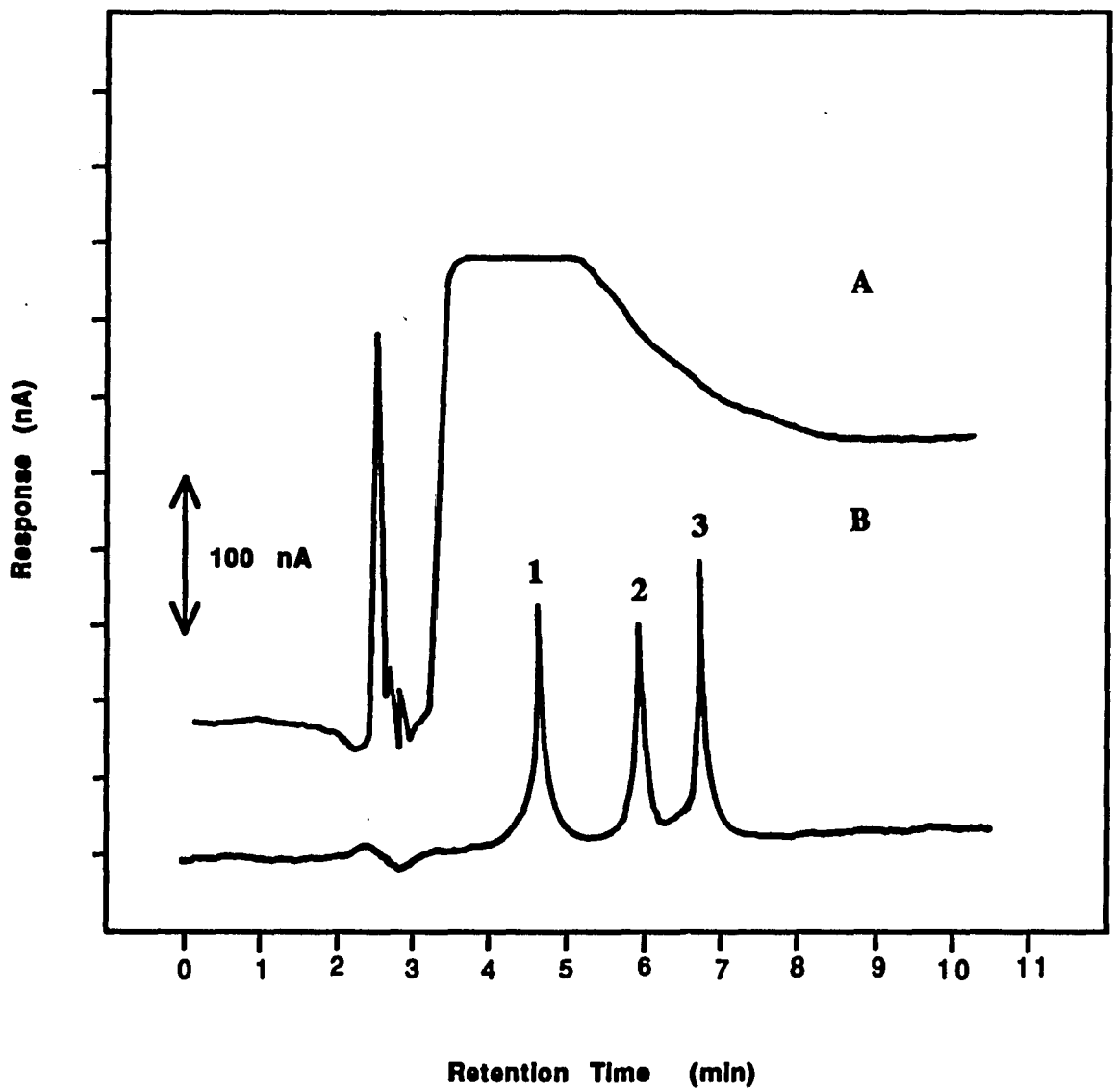

Figure 8. Amperometric chromatograms of a mixture of m-dinitrobenzene, o-nitrotoluene, and 1-chloro-3-nitrobenzene in 20 µL acetonitrile obtained by loading the injection valve with (A) a gas-tight syringe and (B) with the described pneumatic device. Separation conditions: column, 150 x 3.9 mm ID µBondapak C-18 column; mobile phase, acetonitrile-aq 0.05 M sodium perchlorate (55+45, v/v); flow rate, 2.0 mL/min; applied potential, -1.1 V vs SCE. Peak identities: 1, m-dinitrobenzene (31 ng); 2, o-nitrotoluene (27 ng); 3, 1-chloro-3-nitrobenzene (45 ng).

Table 2. Efficiency of Pneumatic Degassing and Loading Device.

Trial	Peak Current (nA) *	
	Syringe Injection	Pneumatic Device
1	4.74	4.54
2	4.56	4.52
3	4.42	4.55
4	4.45	4.57
5	4.44	4.53
6	4.53	4.51
7	4.68	4.56
8	4.59	4.50
Average	4.55	4.54
RSD (n=8)	2.5 %	0.5_4 %

* Peak heights represent currents from an on-column injection of 0.54 ng of m-dinitrobenzene.

Performance of Detector

During the initial phases of testing, cell parameters such as the "effective volume", uncompensated resistance and response time of the three silver-based thin-layer reductive detectors were measured. At this stage, the performance of the detectors was evaluated by injecting benzoquinone or nitrobenzene onto a column containing an inert packing of glass beads or directly into the detector through a short stainless capillary (FIA mode). After the efficacy of the basic cell design was assured, the performance of the silver working electrode, either the conventional continuous disc or the grid oxide design was evaluated in terms of residual current, accessible potential range, equilibration time, noise levels, sensitivity, reproducibility, linear dynamic range, detection limits, and influence of flow rate. For the sake of comparison, the critical electrode characteristics were compared with the corresponding values obtained with a mercury film amalgam or in some cases a carbon electrode. For gathering analytical data, an actual chromatographic system was used in conjunction with a C_{18} column to separate a series of quinones and nitro-aromatics.

Detector Volume

One of the most fundamental requirements of a flow cell for HPLC is a small detector volume with no dead volume. Of the various HPLC components, the detector flow cell makes the largest contribution to extracolumn band broadening, whose effects on the efficiency of the separation can diminish over-all resolution. In addition to the volume of the electrochemical cell, its flow characteristics determine the mass transport behavior and, thus, the electrochemical response. In a reductive detector in which the current signal is determined by the rate of mass transport of a substance being reduced at the electrode surface, the geometric volume of the detection passage does not unequivocally determine the solution volume in which the detection occurs.

The effective volume can be easily determined by measuring the "wash time", the time necessary to electrolyze 95 % of the electroactive species following a step change in concentration. Experimentally, two syringe pumps are needed to gauge this parameter. One of the pumps was filled with mobile phase composed of 0.05 M phosphate buffer (pH 6.8) and the other with $1x10^{-5}$ M benzoquinone. The pumps were connected to the detector through a six position rotary valve, which facilitated changeover of solution without changing its flow rate. As the valve was toggled

from buffer to electroactive species, the time needed for a 95% drop in limiting current was recorded for a plateau potential of -0.5 V vs. SCE. The measured "wash time" intervals (ΔT) are tabulated as a function of flow rate for the different cell designs in Table 3. The corresponding "wash out" volumes, calculated from the product of the time interval and flow rate data in Table 3, are plotted against flow rate in Figure 9. Extrapolation of these curves back to F=0 mL/min yields an effective detector volume of 10, 17, and 25 μL for the silver disc, silver oxide grid and differential design, respectively. For the sake of comparison, the geometrical detector volumes for the silver disc, silver oxide grid, and differential designs are 9.6, 15.2, and 20.4 μL, respectively. The experimentally determined values are somewhat greater than the geometrical volume of the cells, indicating that diffusion plays a role in the over-all hydrodynamics of the systems.

The strong signal dependence on cell volume at constant flow rate is demonstrated in Figure 10. A sudden increase in response is seen when the cell volume is reduced below 9 μL. The increased current response can be attributed to the increased importance of deviations of the cell walls and the electrode surface from planarity on diffusion which can lead to additional sources of mass transport such as edge effects.

Response Time

A good detector must follow a chromatographic solute elution profile accurately. In other words, peak distortion caused by the detector must be small compared with that of the column. Using the approach developed by Stulik (128) and Hanekamp (94), we determined the time constants of the various cell designs at various flow rates by measuring the time needed to reach 63.2 % of the maximum signal following a stepwise change in benzoquinone concentration. Under these conditions, the time-current relationship of the output signal is the familiar $S=S_{max}[1-\exp(-t/\tau)]$, where S is the signal amplitude at t, S_{max} is the maximum signal amplitude and τ is the response time of the cell. At a fraction 0.632 of the maximum signal amplitude, the measured time is equal to the cell time constant. These values, corrected for system dead time, are listed in Table 4. In the flow rate range of 1-2 mL/min, the time constant for any cell design is no worse than 1.1 sec, which is sufficiently fast for accurate quantitation.

Table 3. Effect of Flow Rate on Wash Time for Different Cell Designs.

Flow Rate (mL/min)	Wash Time [(Δ) T], sec		
	Silver Grid	Oxide	Differential
0.5	1.32	2.16	3.24
1.0	0.78	1.26	1.74
1.5	0.60	0.96	1.32
2.0	0.51	0.78	1.14
2.5	0.45	0.72	1.04
3.0	0.44	0.68	0.98
3.5	0.44	0.65	0.98
4.0	0.45	0.68	0.98
4.5	0.49	0.70	----

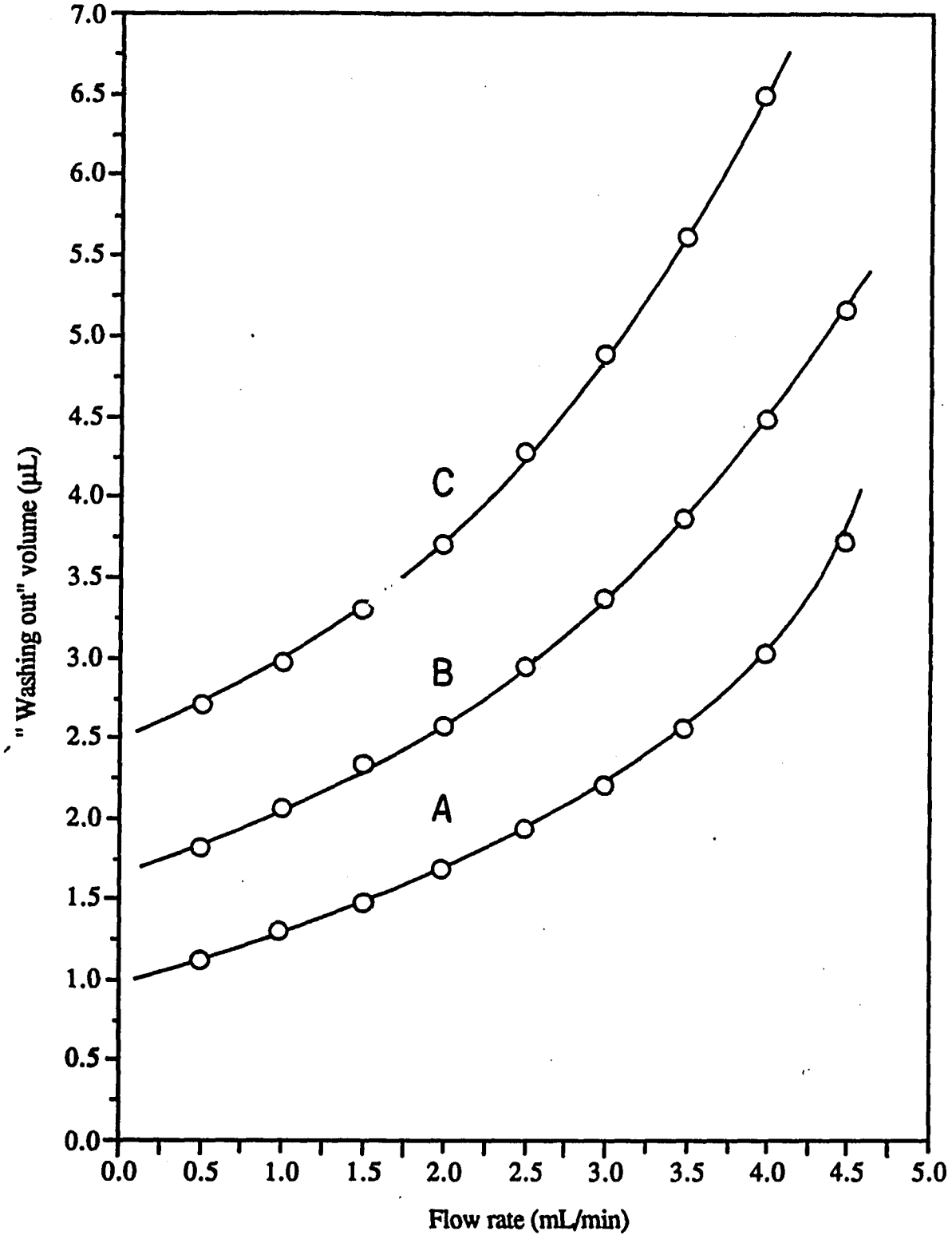

Figure 9. Dependence of the "washing out" volume on the flow rate. Flow injection analysis conditions: sample, 20 µL of 1x 10^{-5}M benzoquinone; wash solvent, 0.05M phosphate buffer, pH 6.8; applied potential, -0.50 V *vs* SCE; flow rate, 1.0 mL/min. Cell configurations: A, silver-based thin layer; B, silver oxide grid design; C, differential design.

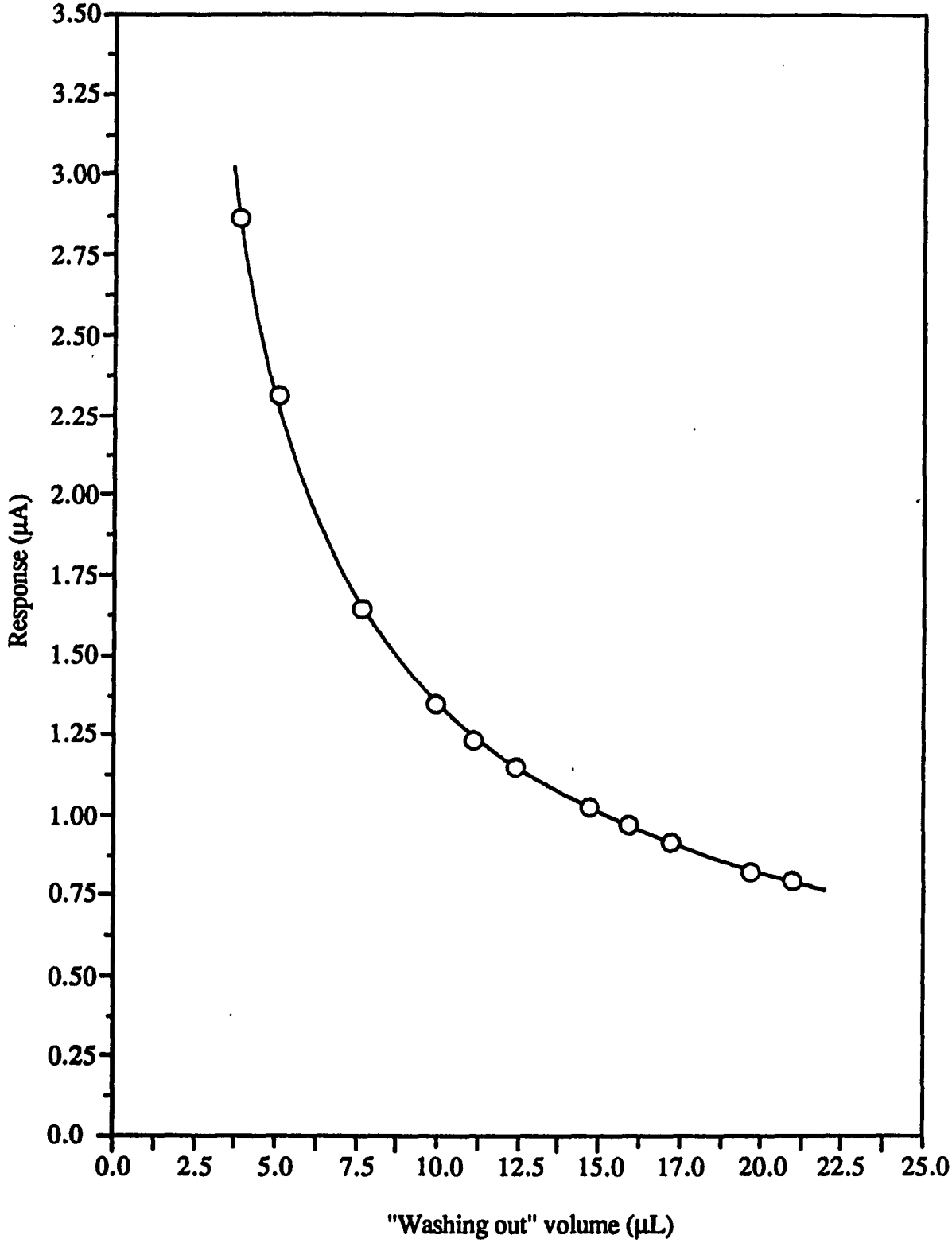

Figure 10. Response of silver-based thin-layer detector design as a function of "washing out " volume. Flow injection analysis conditions: sample, 20 µL of 1x 10^{-5}M benzoquinone; wash solvent, 0.05 M phosphate buffer, pH 6.8; applied potential, -0.50 V vs SCE; flow rate, 1.0 mL/min.

Table 4. Response Times of Various Silver-Based Electrochemical Cells as a Function of Flow Rate.

	Response Time, τ, (sec) [1]			
Cell Design	0.5 mL/min	1.0 mL/min	1.5 mL/min	2.0 mL/min
Thin-Layer Cell	1.25	0.60	0.45	0.38
Differential Cell	2.15	1.10	0.70	0.67
Silver Oxide Grid Cell	1.00	0.45	0.35	0.32

[1] Time required to reach 63.2 % of the maximum signal amplitude following a 100 µL injection containing 1×10^{-5} M benzoquinone.

The effect of response time on sensitivity for the silver disc design was investigated by installing an adjustable set screw in a central well located in the top plate. By adjusting the relative position of the screw in the well, the response time of the cell can be varied from 0.5 to 5.0 sec without changing the linear flow rate. In practice, the screw was adjusted in increments of 0.004 in. with the aid of a feeler gauge, which in turn resulted in a 8.3 μL incremental change in the response volume. Using the procedure of Stulik (128), we determined this change in response volume corresponded to a response time change of 0.5 sec under the present flow rate conditions of 1.0 mL/min. After each geometrical volume rearrangement, the steady-state signal from a stream of benzoquinone in acetonitrile-aq 0.05 M phosphate buffer, pH 6.8 (50+50, v/v) was allowed to equilibrate and was measured. The influence of response time on response can be seen in Figure 11. As might be expected, the current response decreases with increasing time constant, however, it decreases more rapidly than expected for time constants greater than 1 sec. For longer time constants, the electrochemical detector is no longer able to accurately track the elution profile produced by the column. Under these conditions, the peaks appear distorted as its peak width increases at the expense of its peak height. It is obvious from Figure 12 that the signal-to-noise ratio is significantly improved by decreasing the response time for this design. Thus, for benzoquinone in acetonitrile-aq phosphate buffer, pH 6.8 (50+50, v/v), the signal-to-noise ratio increases linearly with a slope of 0.95 from 1.8 to 0.65 sec, and at about a 8-fold higher rate from 0.45 to 0.27 sec. When the response time was reduced below 0.25 sec, spurious signals occured due to phase changes within the feedback loop of the controlling amplifier in the potentiostat. To maximize response signal but avoid electronic problems, we used cells having response times of 0.5-1.0 sec.

In order to study the effect of depolarizer concentration on response time, the detector cell was connected directly to a syringe pump from which various concentrations of benzoquinone were introduced at a flow rate of 2.0 mL/min and the currents were measured. Figure 13 shows the relationship between concentration and current response for the three different designs. Of the three designs, only the time constant of the silver oxide grid-based cell exhibited any dependence on concentration. This suggests that the effective surface area of this electrode is dependent upon the current density involved in the reduction. The increasing current response with increasing concentration of benzoquinone results in a decreased effective electrode surface area and, thus, leads to a decrease in the volume in which the detection takes place.

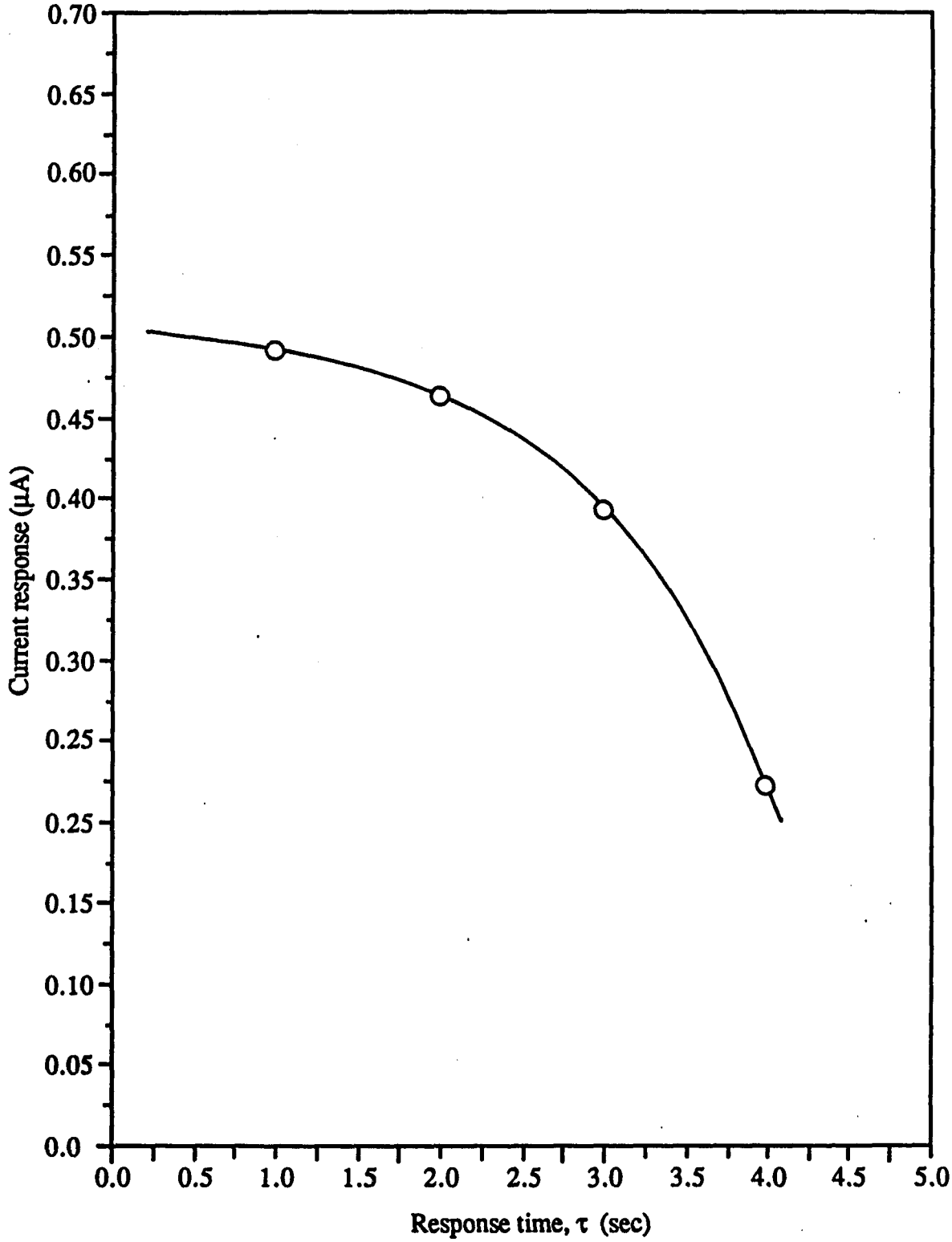

Figure 11. Effect of response time on detector response for the silver-based thin-layer variation. Chromatographic conditions: column, 150 x 3.9 mm ID μBondapak C-18 column; mobile phase, acetonitrile-aq 0.05 M phosphate buffer, pH 6.8 (50+50, v/v); flow rate, 2.0 mL/min; sample, 20 μL of 4.0 μg/mL m-dinitrobenzene in mobile phase.

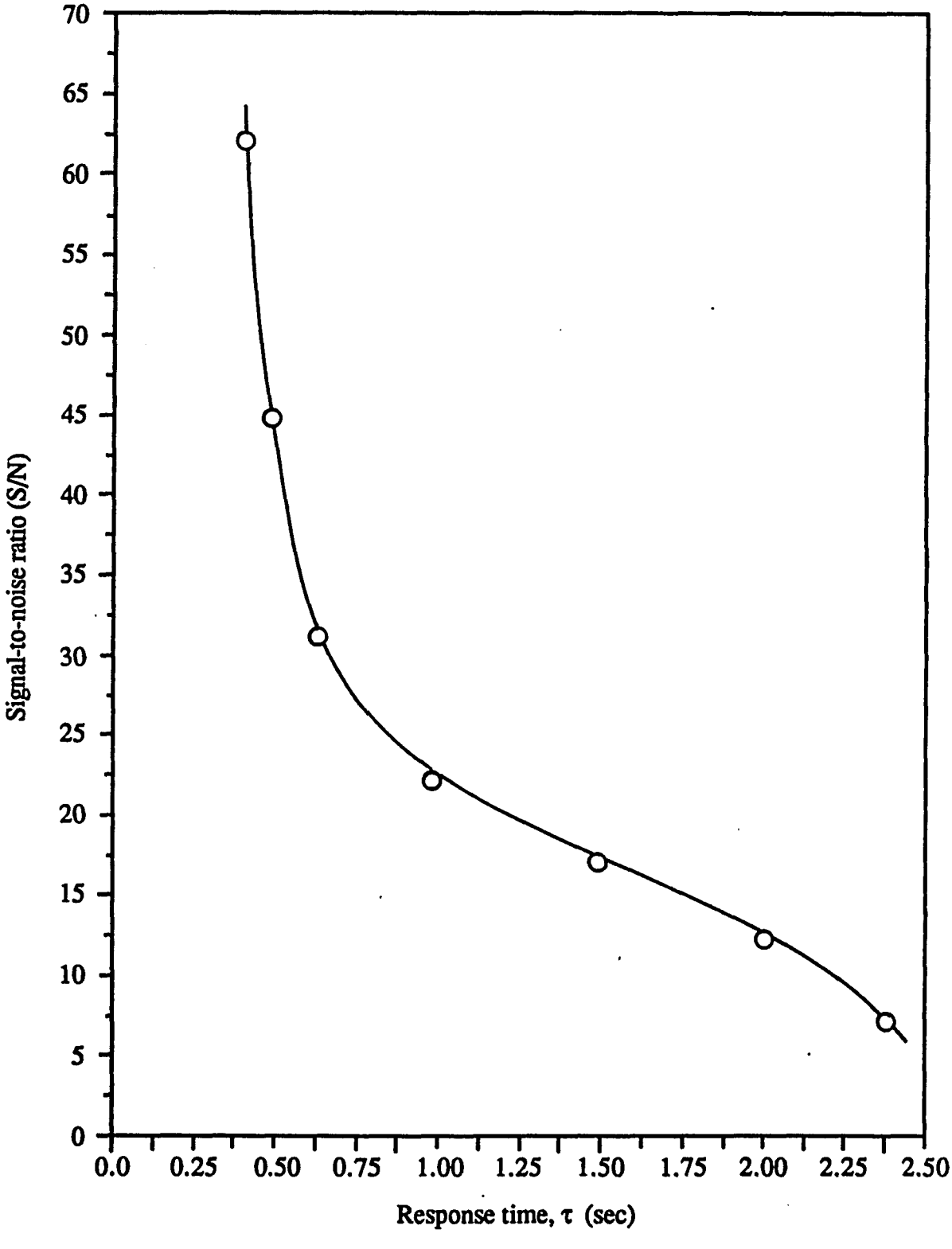

Figure 12. Dependence of signal-to-noise ratio upon response time of the silver-based thin-layer cell design. Flow injection analysis conditions: supporting electrolyte, acetonitrile-aq 0.05M phosphate buffer, pH 6.8 (50+50, v/v); flow rate, 0.5 mL/min; applied potential, -1.0 V *vs* SCE; sample, consecutive 20 μL injections of 3.5×10^{-5} M benzoquinone.

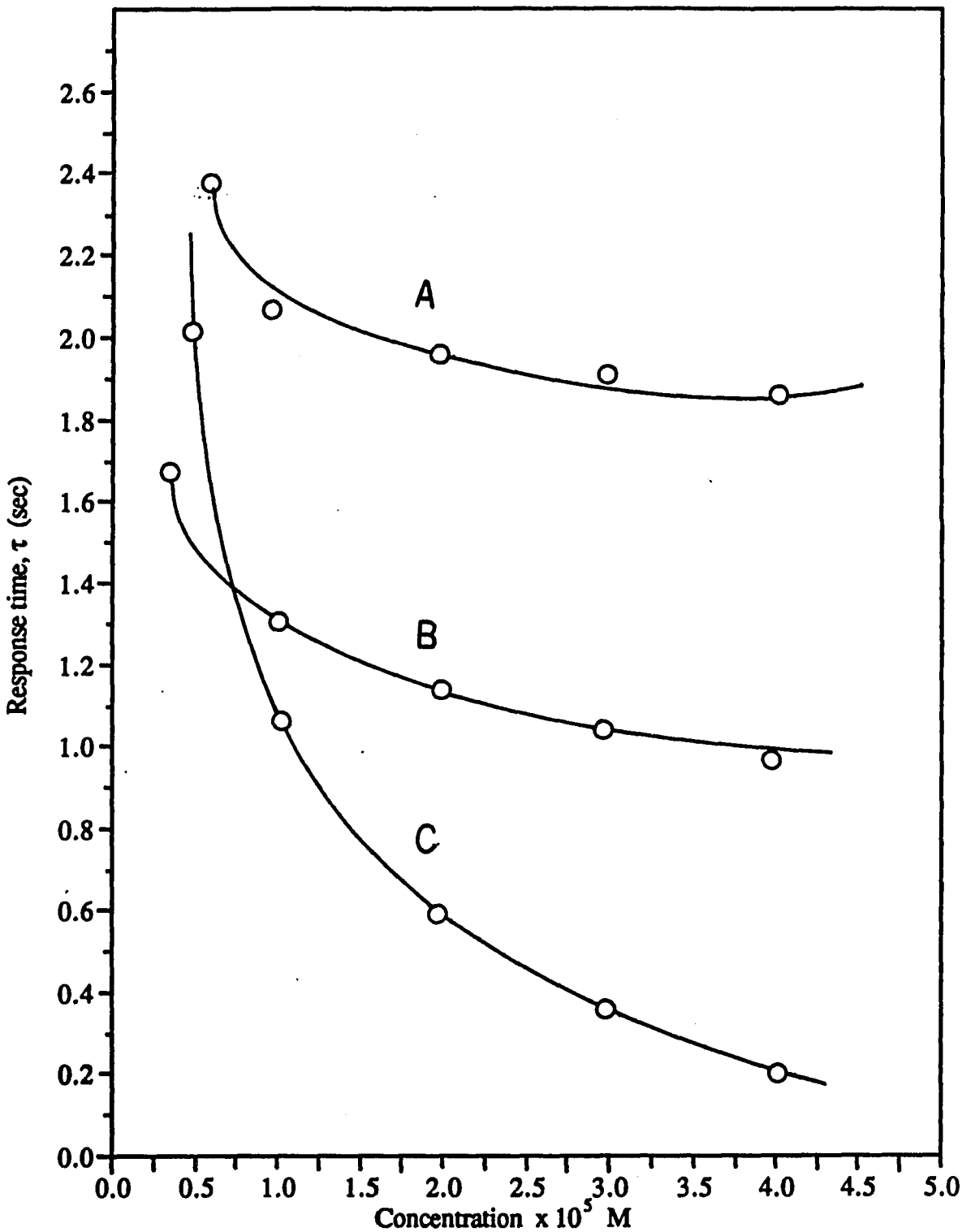

Figure 13. Dependence of the response time curve on the concentration of depolarizer. Flow injection analysis conditions: supporting electrolyte, acetonitrile-aq 0.05 M phosphate buffer, pH 6.8 (50+50, v/v); flow rate, 0.5 mL/min; applied potential, -0.5 V vs SCE reference; sample, consecutive 20 µL injections of benzoquinone in supporting electrolyte. Cell configurations: A, silver-based thin-layer; B, differential; C, silver oxide grid design.

Uncompensated Resistance

It is desirable for several reasons to design a cell which has a low ohmic resistance. For example, under a high resistance the cell acts as an antenna for static charge which increases the noise level and decreases the sensitivity. In some cases, a high resistance can cause phase changes within the fragile auxiliary-reference feedback loop resulting in the complete loss of potentiostatic control. In such a case, equivalent performance can be obtained from a classical two electrode configuration. In addition, uncompensated cell resistance reduces the linear dynamic range, interfering with accurate quantitation at higher concentration levels.

In order to evaluate the uncompensated resistance, R_u, of each cell configuration, small pulses of approximately 50 mV in amplitude were superimposed on a small standing potential of -150 mV vs. SCE. Because faradaic processes are not significant in this potential vicinity and assuming the capacity remains constant, the output current follows a simple decay expression given by $I = (E/R_u) \exp(-t/R_u)$. The determination of R_u using this expression can be further simplified by extrapolating the transient current-time plot to t=0, Because at t=0, $R_u = E/I$. Table 5 lists the uncompensated cell resistances for the various cell configurations studied. These values ranged from 55.5-K Ω to 71.4-K Ω for the various thin-layer cells. These values are of the same order of magnitude as those predicted by Kissinger (18) from simulation studies for thin-layer cells equipped with a downstream reference electrode. In these studies, various time-dependent signals were imposed on a dummy cell represented by the parallel combination of the faradaic resistance (R_f) and double layer capacitance (C_{dl}) in series with a resistor corresponding to the uncompensated resistance (R_u) between the downstream reference electrode and the working electrode. The resulting I-V curves were plotted and their slope was used to determine the value of R_u.

Table 5. Uncompensated Cell Resistance for Different Configurations.

Cell Design	I_c (μA) [1]	R_u (K Ω) [2]
Single Thin-Layer Cell	0.9	55.5
Differential Cell	2.1	24.0
Grid Oxide Cell	0.7	71.4

Flow injection analysis (FIA) conditions: supporting electrolyte, acetonitrile-0.05M phosphate buffer, pH 6.8 (50+50, v/v); flow rate, 2.0 mL/min; standing applied potential, 150 mV; pulse height, 50 mV.

[1] Current obtained by extrapolating charging curve back to t=0.

[2] R_u obtained from $\Delta E / I_c$, where ΔE is equal to 50 mV.

Short Term Noise

Noise can be broadly defined as the variation of the detector output signal which cannot be attributed to the solute itself passing through the cell. Noise is superimposed on the standing current and tends to increase the height of the baseline. Several noise sources have been identified (269,277-280). The seven main sources which contribute to the noise level include incomplete wetting of electrode surface, fluctuations in flow rate, impurities, double-layer changes due to non-potentiostatic conditions (turbulence), variations in temperature, electrode surface processes, and amplifier noise. The impact of these individual sources on the noise level is difficult to predict and are dependent on such parameters as signal size, magnitude of the background current, surface quality, electrode pretreatment, and pumping system.

To assess the order of magnitude of the static noise, peak-to-peak deviations were measured for a constant buffer concentration under various experimental conditions. These values are tabulated in Table 6. The noise level falls slightly with a reduction in potential and an increase in pH. However, the employment of the pulseless solvent delivery system allows the noise level to be relatively independent of rapid flow fluctuations. These observations are typical of low frequency noise, which is regular in nature. The average total current noise amounts to 202 pA (peak-to-peak). For benzoquinone, this corresponds to 36 pg per 20 μL injection.

The electronic noise of the detector was measured with a simple inactive electronic dummy cell inserted in place of the actual flow-cell and was only 28 pA. Based on this evidence, we can assume that the major portion of the noise arises from variations within the cell, i.e., residual oxygen and fluctuations in temperature or flow rate. At the present stage of development of quality op-amps, only a small proportion of the noise is introduced by the electronic components or from voltage line surges.

Drift

Drift is the steady movement of the baseline in the same direction (up or down scale) over long periods of time. During a 12-hour stability test, run with mobile phase flowing through the cell at a rate of about 1.0 mL/min, drift was about 5nA/hr. Drift in any one-hour period was less than the detector noise at maximum sensitivity. This is caused predominantly by variations in the surface composition of the silver electrode.

Table 6. Effect of Various Experimental Parameters on the Peak-to-Peak Noise Level.

Potential (V)	pH	Flow Rate (mL/min)	Noise Level (pA)
1.0	3	1.0	245
0.5	3	1.0	192
1.0	3	2.0	250
0.5	3	2.0	198
1.0	6.8	1.0	230
0.5	6.8	1.0	172
1.0	6.8	2.0	245
0.5	6.8	2.0	180
1.0	8.0	1.0	200
0.5	8.0	1.0	145
1.0	8.0	1.0	215
0.5	8.0	2.0	152

Effect of Electrode Area on Signal-to-Noise Ratio

Several sizes of silver disc electrodes were investigated in order to determine the effect of electrode area on the sensitivity of the electrochemical detector and, thus, optimize its signal-to-noise ratio. The accurate estimation of this ratio is complicated by the interdependencies between signal and noise levels and differences in double-layer capacitance values. To circumvent these problems, a differential cell composed of two independent cells featuring identical electrode pairs was employed. The signal component of the ratio for various electrodes possessing surface areas of 2.0 mm^2, 4.5 mm^2, and 8.0 mm^2 was obtained from its current response at -0.5 V vs SCE toward benzoquinone. At the same time, the second electrode, also poised at -0.5 V vs SCE, was subjected to an electrolyte blank. The noise component of the ratio was measured at the second electrode, following background correction, by registering short term peak-to-peak baseline fluctuations. In this way, the signal-to-noise ratio can be measured simultaneously under the same solution conditions. The linear flow rate of the mobile phase was 1.0 mL/min. A plot of signal-to-noise ratio against surface area is shown in Figure 14. For comparison, similar plots for gold amalgam and glassy carbon are also shown. As can be seen for the glassy carbon electrode, the signal-to-noise ratio steadily decreased over the range of areas from 2 to 8 mm^2. In contrast, the signal-to-noise ratio at the pre-treated silver and gold amalgam electrodes initially increased until a maximum was reached for an electrode area of 7 mm^2. The differences in behavior exhibited by the various electrodes can be explained by an analysis of the relationship between noise and "electrochemical surface area" and the factors which cause it to deviate from the geometric area. A linear relationship between geometric area and noise was obtained for glassy carbon, suggesting its "electrochemical area" is equivalent to its geometric surface area. These findings are in agreement with those of Lankelma and Poppe (269,270), for an electrode with a geometrical area proportional to its capacitance. In contrast, for amalgam film and silver electrodes, the rate of noise increase for smaller electrodes was less than that expected based solely on geometrical considerations. This behavior is indicative of a surface whose cross-sectional geometric area does not unequivocally determine its "electrochemical area". Significant deviations from equality of both areas can be caused by the adsorption of contaminants typically present in mobile phase supporting electrolytes such as chloride ions, the extent of which is dependent upon the charge passed, applied potential, geometric area, and the concentration of adsorbate (281).

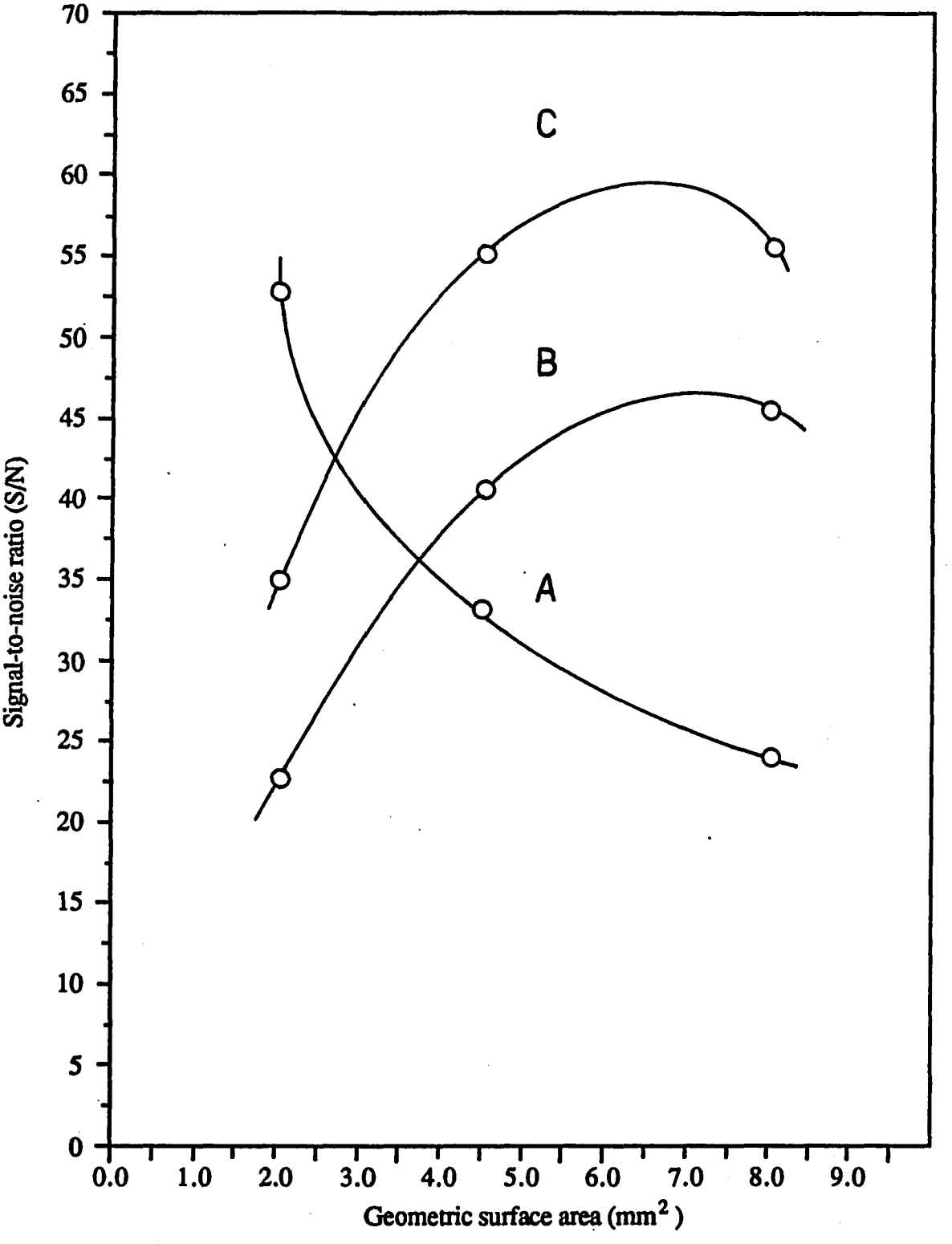

Figure 14. Influence of surface area on response of (A) glassy carbon, (B) gold amalgam, and (C) pretreated silver for 20 µL injections of 10^{-5}M benzoquinone. Flow injection analysis conditions: supporting electrolyte, acetonitrile-aq 0.05 M sodium perchlorate (50/50, v/v); flow rate, 1.0 mL/min; applied potential -0.5 V vs SCE.

As the surface area electrode increases, the prominence of a reduced "electrochemical area" due to adsorption was decreased and the noise level rose in accordance with geometrical calculations. As might be expected based on a linear diffusion model (103), the faradaic signal increased slowly and uniformly over the 2 to 8 mm^2 area range. Thus, to minimize noise arising from the capacitance of the electrode and yet maintain high sensitivity, a silver disc with a surface area of 8 mm^2 was used in all subsequent quantitative studies.

Pretreatment Procedure

The electrochemical behavior of silver is significantly affected by the condition of the electrode surface. The surface of silver has been studied as to the types of surface functionalities present and their importance in effecting electron-transfer. Typically, prior to using silver as a cathodic working electrode, the silver is initially activated by a potential cycling treatment to expose the maximum number of silver sites. The increased activity following pretreatment has been predominantly ascribed to the formation of Pyramidal Ag_4^+ surface groups stabilized by co-adsorbed Cl^- ions which may act as electron transfer mediators (282,283). The exposure of fresh silver edges, microparticulates and defect sites may also provide additional sites for selective electron-transfer (284-289).

The most classical pretreatment method for silver involves oxidation-reduction cycling (ORC) (282-289). This procedure consists of first anodizing the surface to generate a silver chloride layer, followed by its reduction, presumably to yield a reformed layer of pure silver. The mechanism by which this reformation process occurs may be summarized by the following sequence of dissolution, complexation, transport and deposition (286).

$$Ag \rightleftharpoons Ag^+ + e \qquad \text{(dissolution)}$$

$$Ag^+ + (n+1)\,Cl^- \rightleftharpoons AgCl_{(n+1)}^{-n} \qquad \text{(complex formation)}$$

$$AgCl_{(n+1)}^{-n}\,(a) \rightleftharpoons AgCl_{(n+1)}^{-n}\,(b) \qquad \text{(solution transport from position a to position b)}$$

$$AgCl_{(n+1)}^{-n} \rightleftharpoons AgCl\,(s) + nCl^- \qquad \text{(deposition and growth)}$$

Chronoamperometric curves were generated in a supporting electrolyte of 0.05 M phosphate buffer (pH 6.8) containing no electroactive species to gain insight into the surface processes that occur during pretreatment.

The electrochemical behavior of a freshly polished silver electrode differs from that of a "reformed" or cycled electrode. Figures 15 and 16 show chronoamperometric charging curves for both a freshly polished and a pre-treated or "reformed" electrode, respectively. The current-time relationship obtained for the polished silver electrode after the application of a potential step from 0.0 V to -1.0 V versus SCE does not reach the initial level within the period of observation. Also, the plot of ln [I] versus time, shown in Figure 17 does not yield a straight line as predicted for an electrode surface undergoing only a double-layer charging process (290). These findings strongly indicate the occurrence of one or more faradaic surface processes. As a mechanically polished silver electrode is very susceptible to oxide coverage (291-293), a plausible process in this potential region is the partial reduction of the oxide layer. These findings are in accord with those of Droog et al. (294) for the reduction of silver oxides. Accordingly, a mechanically polished silver electrode without pretreatment suffers from changes in surface composition and differential capacity and poor reproducibility. After the silver electrode is subjected to numerous oxidation-reduction cycles between +1.0 V and -1.0 V vs SCE, an essentially feature-less charging curve shown in Figure 16 is obtained. This charging pattern is indicative of the lack of faradaic surface processes. We can conclude that the reformation process yields a surface composed of a highly purified form of silver which lacks easily reducible contaminants. In addition, following a cycling period of 5 minutes, repetitive application of potential steps of -1.0 V vs SCE resulted in identically-shaped curves which indicated surface nucleation and growth processes such as the conversion of residual AgCl into Ag clusters have reached a steady-state.

Residual Current

In general, a chromatographic detector produces an output signal when the mobile phase alone is flowing through the detector. The residual current for a reductive detector arises primarily from the reduction of trace levels of metals, oxygen, and hydronium ions in the mobile phase. The impact of these species on the magnitude of the residual current is dependent upon such variables as the mobile phase composition, surface pretreatment procedure and applied potential. The absolute value of the background is important because some fluctuation in the value is expected, for example, due to minor flow variations. If the background current is high enough, even a very small variation may create enough noise to limit the level of detection.

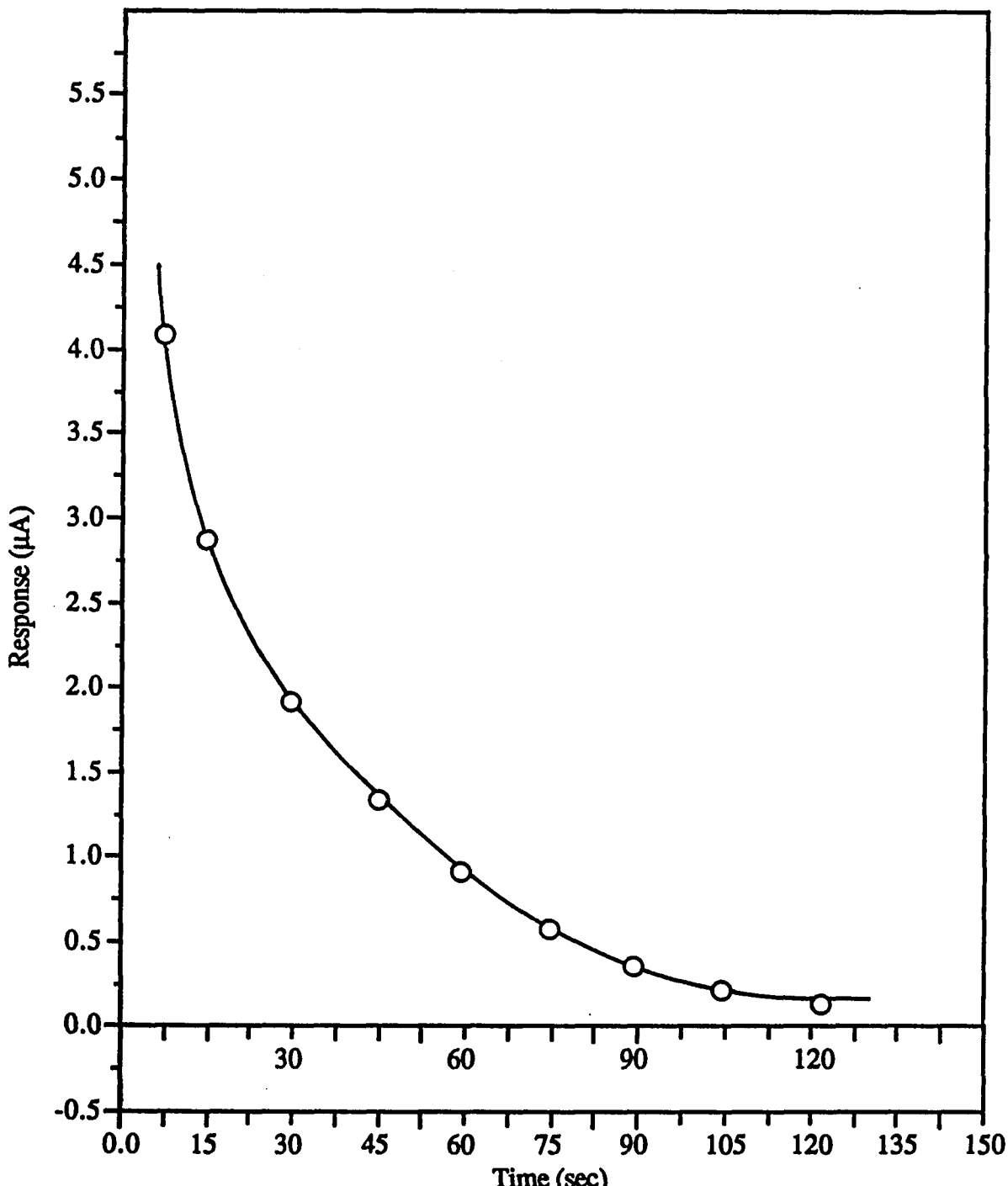

Figure 15. Current-time relationship after application of a potential step at a freshly prepared silver electrode from 0 to -1.0 V *vs* SCE. Flow injection analysis conditions: supporting electrolyte, acetonitrile-aq 0.05 M phosphate buffer, pH 6.8; flow rate 2.0 mL/min. Data shown for each time setting is the average of four experiments on a single electrode with no polishing between runs. Background response was offset prior to the initiation of the step.

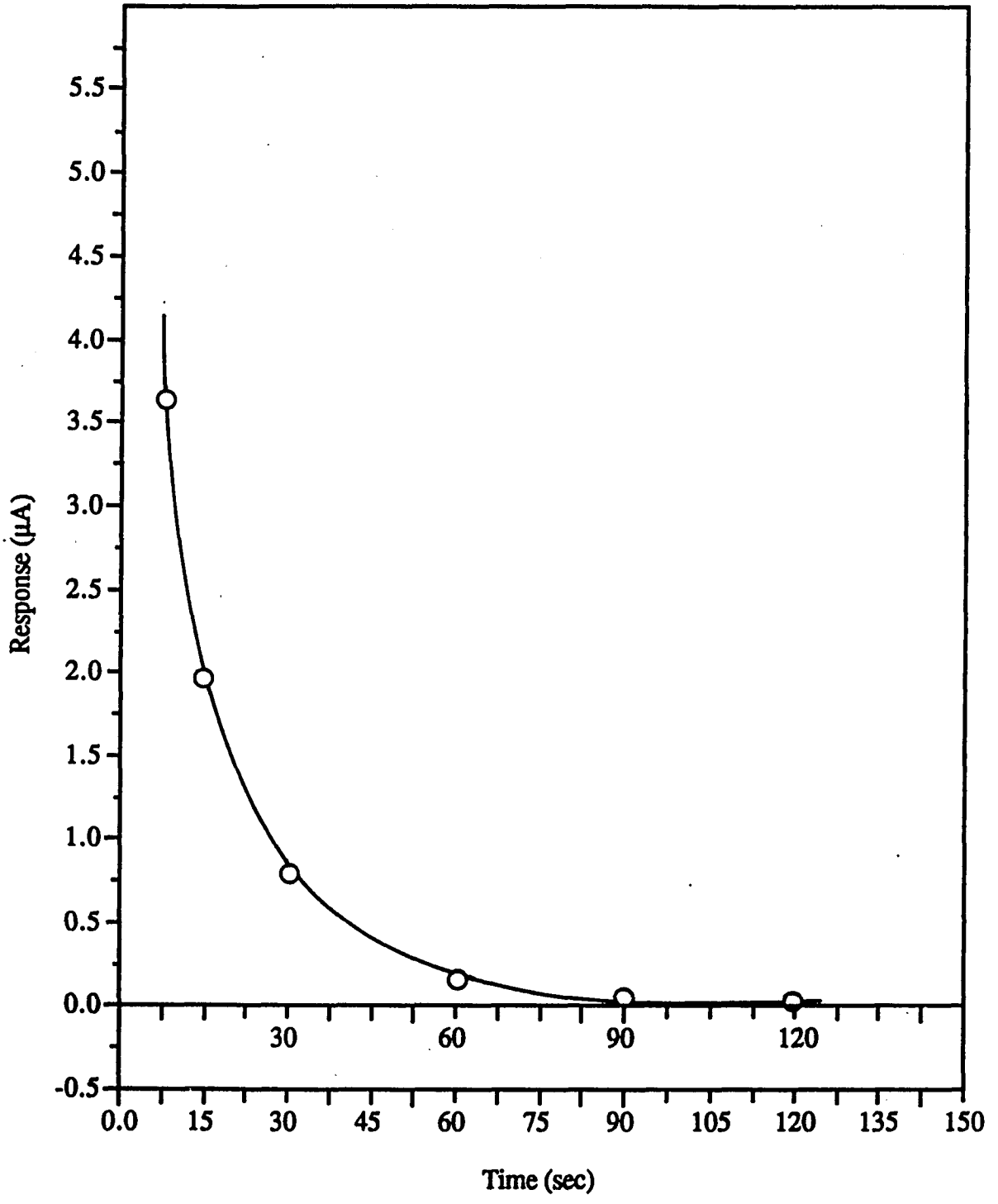

Figure 16. Current-time relationship after application of a potential step at a reformed or pre-treated silver electrode from 0 to -1.0 V *vs* SCE. Flow injection analysis conditions: supporting electrolyte, acetonitrile-aq 0.05 M phosphate buffer, pH 6.8; flow rate, 2.0 mL/min. Background current response was offset prior to the initiation of the step.

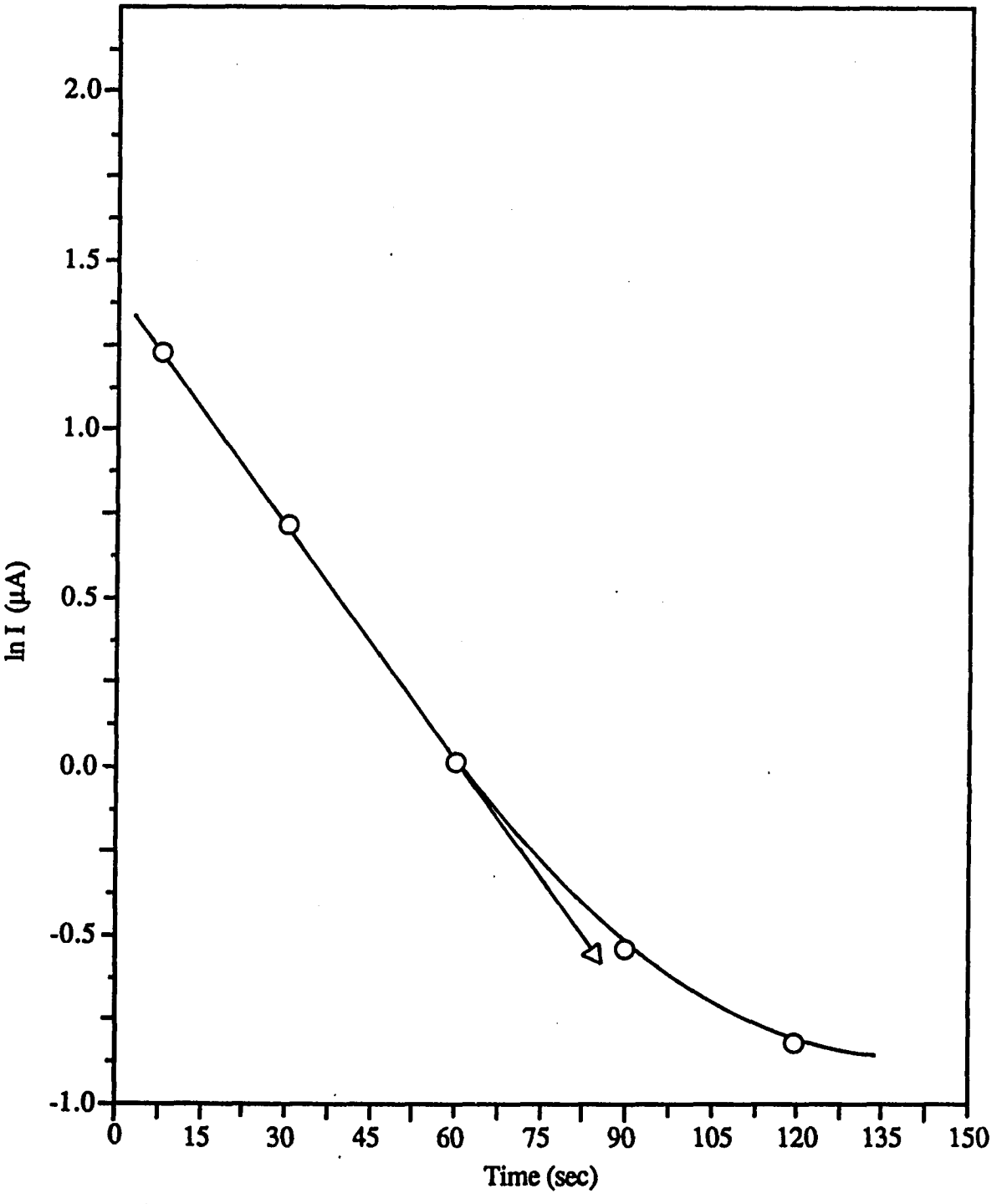

Figure 17. Plot of ln I as a function of time following a potential step from 0 to -1.0 V *vs* SCE at a freshly prepared silver electrode. Flow injection analysis conditions: supporting electrolyte, acetonitrile-aq 0.05 M phosphate buffer, pH 6.8; flow rate, 2.0 mL/min. The data shown is the average of four experiments on a single electrode with no polishing between runs.

The nature and relative magnitudes of the residual current for various solid electrodes were compared using both a potential step function and a manual potential scan. A series of potential steps ranging in value from -100 mV to -400 mV were consecutively applied to each electrode biased at -50 mV vs. SCE. The residual current for each step was sampled after approximately 60 msec. The residual current-potential step curves shown in Figure 18 clearly illustrate that gold and platinum are not suitable for cathodic use. Even a very small step of 25 mV results in an unmanageable residual current. The residual current for a reformed silver electrode increases linearly at a slow rate with increasing pulse amplitude. This feature makes silver ideally suited for measuring the small currents typically encountered in amperometric detection of trace analytes. This decay pattern exhibited by reformed silver is similar to that of a properly prepared mercury film electrode.

The effect of pretreatment on residual current as a function of potential for a mechanically polished silver electrode and a pretreated electrode is shown in Figure 19 A and B, respectively. The background curve obtained at a freshly polished silver electrode is characterized by a steeply rising portion which begins at -0.85 V vs SCE. Following the ORC reformation process, the potential at which the background current begins to rise is cathodically shifted to -1.25 V vs SCE under the same solution conditions. In the absence of other possible reduction processes which occur at this potential, such as the reduction of oxygen and metals, this shift of some 400 mV indicated that the activation energy for hydrogen evolution on the reformed surface is significantly increased compared to that on a mechanically polished electrode. The rate of hydrogen evolution at silver has been shown by Gerischer and Mehl (295) to be controlled by the recombination of hydrogen atoms on the silver surface. While on a mechanically clean silver surface adsorbed hydrogen atoms can move about from site to site, following reformation the deposited silver atoms hinder the recombination of hydrogen atoms which reduces the rate of hydrogen evolution (296,297).

Several gold amalgam film electrodes made from substrates of different surface quality were investigated in order to illustrate the dependency of residual current on polishing. As can be seen from Figure 20, the residual current of amalgam films made from substrates containing surface imperfections is quite high. The high residual current undoubtedly results from incomplete or non-uniform mercury surface coverage. In addition, film electrodes were found to be very sensitive to the passage of the high

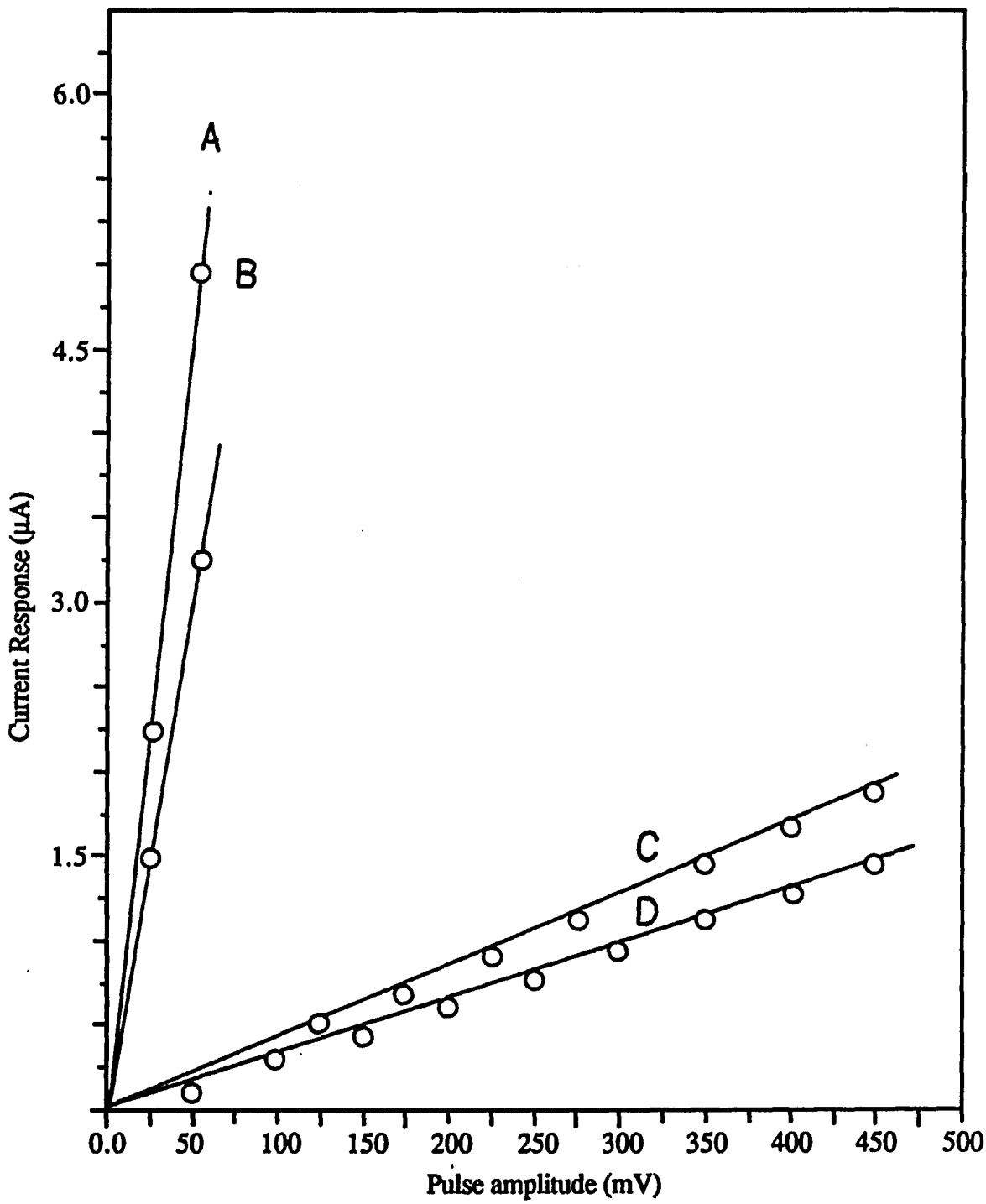

Figure 18. Dependence of steady-state residual current upon pulse amplitude for (A) Au, (B) Pt, (C) Au/ Hg film and (D) pre-treated silver electrodes. Flow injection analysis conditions: supporting electrolyte, acetonitrile-aq 0.05 M phosphate buffer, pH 6.8; flow rate, 2.0 mL/min.
* Steady-state current measured 5 sec after onset of a 2-sec pulse.

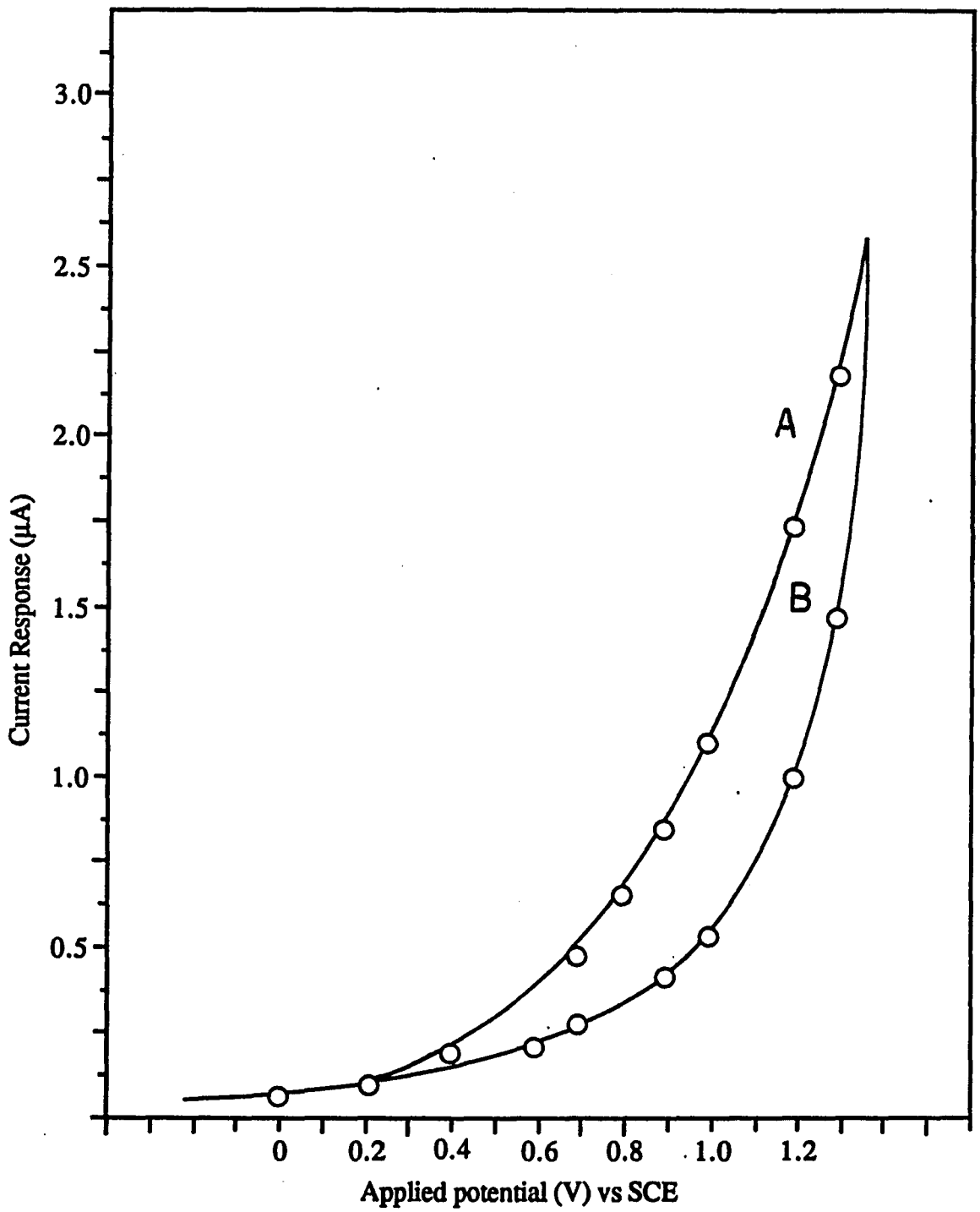

Figure 19. Background current response obtained from a silver electrode which was (A) mechanically polished and (B) electrochemically pretreated in KCl. Flow injection analysis conditions: supporting electrolyte, acetonitrile-aq 0.05 M phosphate buffer, pH 6.8; flow rate, 2.0 mL/min.

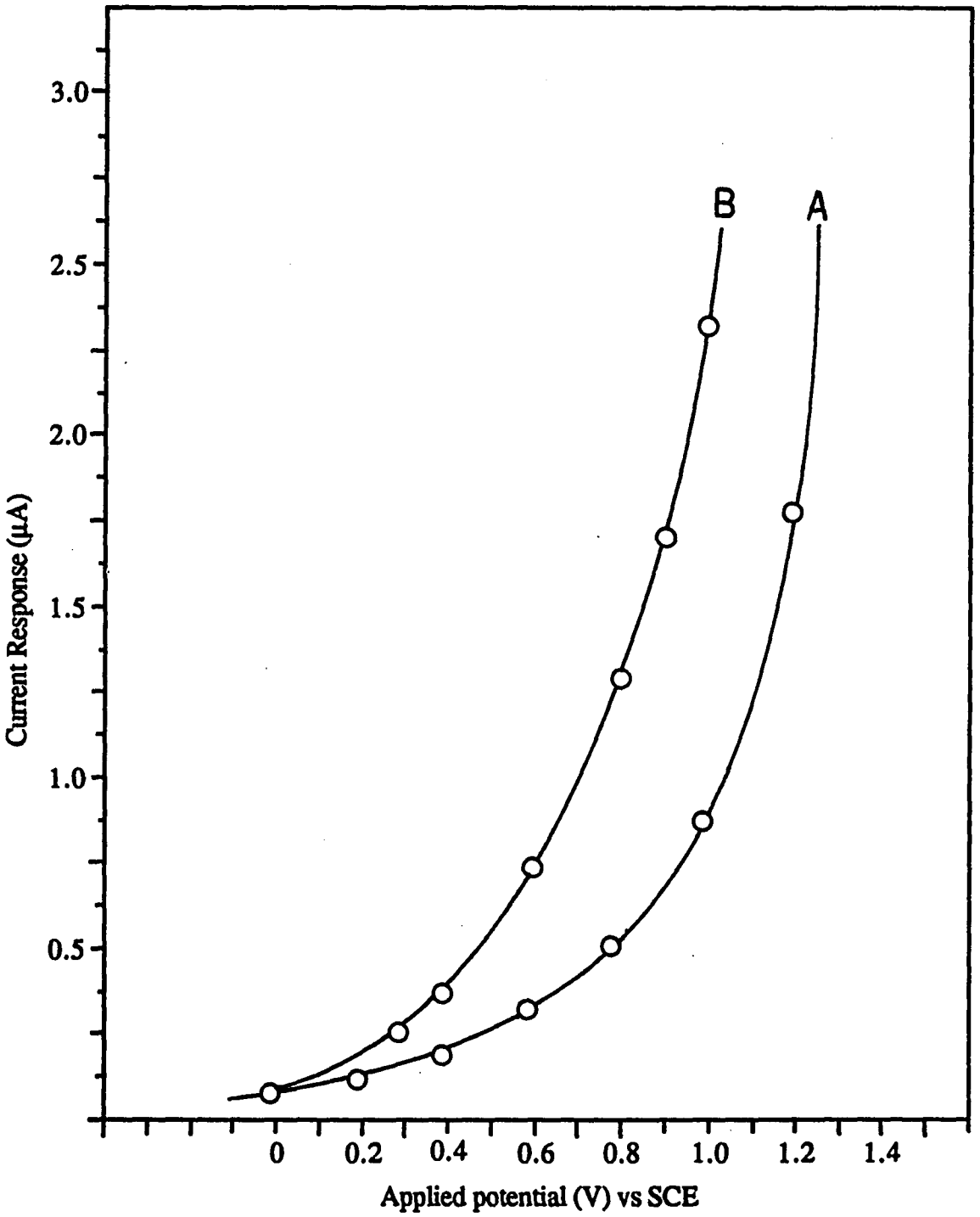

Figure 20. Background current of an amalgamated gold electrode prepared from (A) a well polished substrate and (B) a poorly polished substrate. Flow injection analysis conditions: supporting electrolyte, acetonitrile-aq 0.05 M phosphate buffer, pH 6.8; flow rate, 2.0 mL/min.

currents typically encountered during start up or during system malfunction. Several scattered gold bald patches on the film surface were revealed by visual inspection of the damaged electrode. As a result, the residual current is at least five times higher after such damage and is similar in nature and magnitude with that of a pure gold electrode. Background scans are shown in Figure 21 for (A) a well polished silver electrode and (B) a poorly polished but pre-treated silver disc electrode as a function of potential in a 0.05 M phosphate (pH 6.8) mobile phase. In contrast to mercury film electrodes, the residual current at higher potentials at a reformed silver electrodes does not appear to be very sensitive to minor scratches. This is evidenced by the similarity of the potentials at which hydrogen evolution commences. Using SEM micrographs and capacitive measurements, Larken et al. (298) illustrated that minor scratches do not impede the transport of silver chloride complexes formed during the oxidation portion of the pretreatment procedure. As a result, silver clusters formed during reduction were more or less uniformly distributed on both well and poorly polished surfaces. For both electrodes, the background current changes very slowly with potential over the range of 0.05 V to -1.25 V vs SCE. The attainment of a low and reproducible background current with a fast and simple polishing and electrochemical pretreatment by potential cycling facilitates its use in applications requiring high throughput such as in quality control laboratories.

A manual potential scan can readily show the effects of pH and the influence of eluent composition on the residual current. The pH affects the background current most significantly at potentials more negative than -1.0 V vs SCE. For an applied potential of -1.0 V, the background is about 800 nA at pH 3, while at pH 7 the background is about 400 nA. The steady decrease in residual current for a reformed silver electrode as a function of increasing pH, shown in Figure 22, can be attributed to a change in spacing between surface groups. As the pH increases from 2 to 8, the nodular silver deposits tend to exhibit a more closed-packed structure (286). As a result of the geometrical condensation, surface patches of silver nodules exhibit improved discrimination against surface processes involving adsorption such as oxygen reduction and hydrogen evolution. For a mercury film electrode, such a pH dependency is not evident. The decrease in residual current observed for both as a result of gradually changing the eluent composition from pure water to 100% acetonitrile, shown in Figure 23, can readily be explained by the increase in dielectric constant and by increased overpotential for hydrogen evolution.

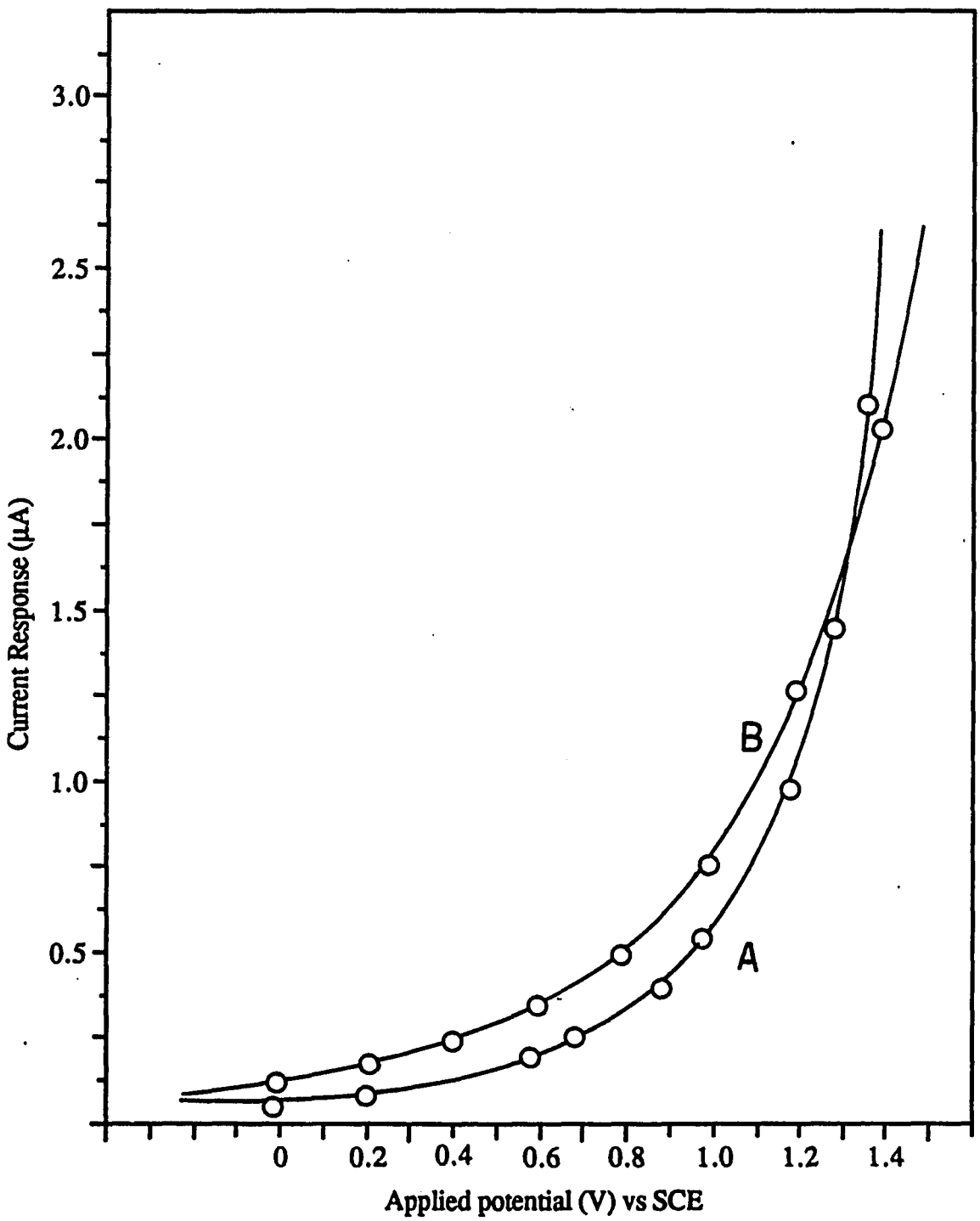

Figure 21. Background current of a silver electrode prepared from (A) a well polished pretreated substrate and (B) a poorly polished pretreated substrate. Flow injection analysis conditions: supporting electrolyte, acetonitrile-aq 0.05 M phosphate buffer, pH 6.8; flow rate, 2.0 mL/min.

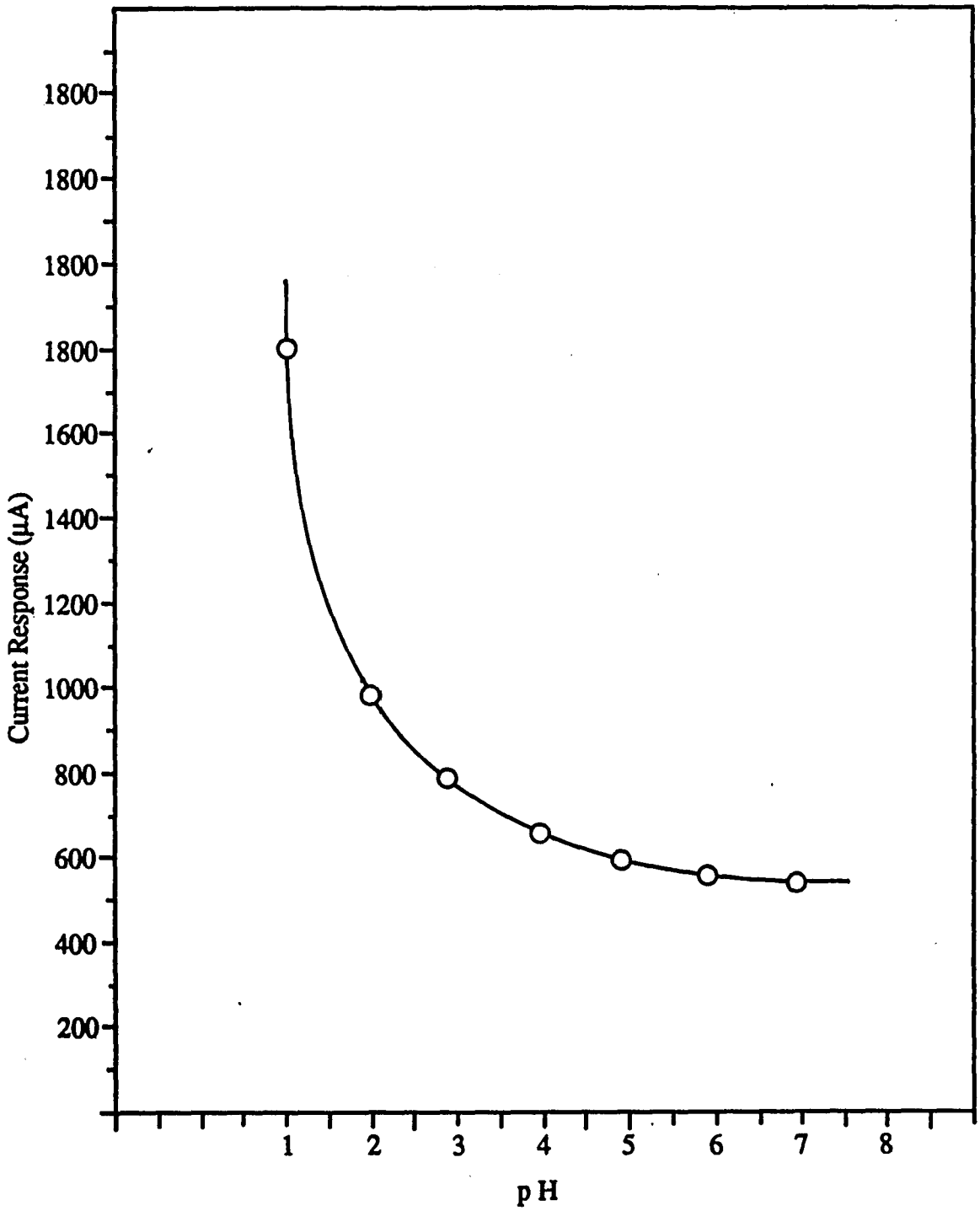

Figure 22. Effect of pH on residual current. Flow injection analysis conditions: supporting electrolyte, acetonitrile-aq 0.05 M phosphate buffer, pH 6.8; flow rate, 2.0 mL/min; applied potential, -0.5 V vs SCE reference.

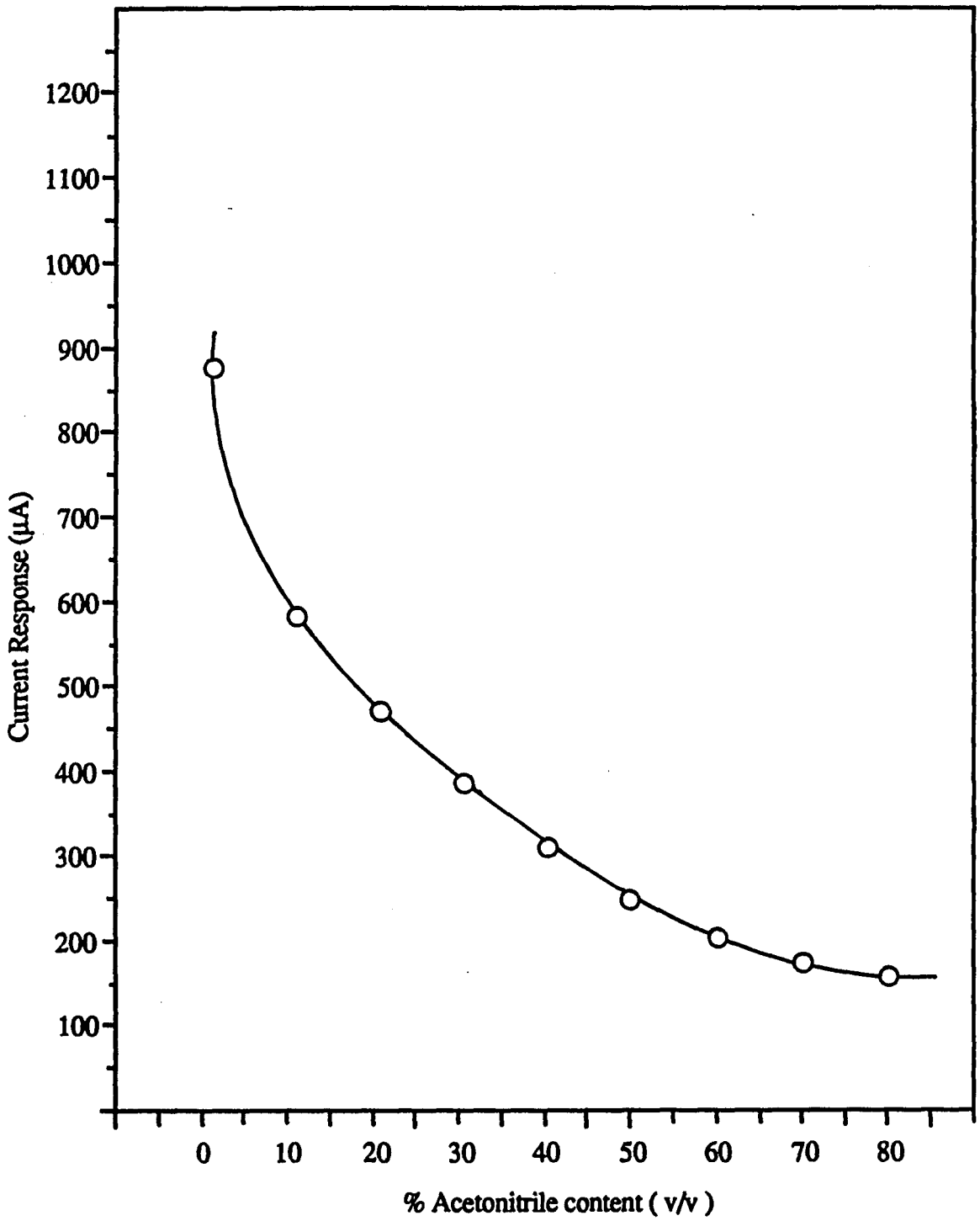

Figure 23. Background current response of silver-based thin layer cell as a function of acetonitrile content. Flow injection analysis conditions: supporting electrolyte, acetonitrile-aq 0.05 M phosphate buffer, pH 6.8; flow rate, 2.0 mL/min; applied potential, -0.5 V vs SCE reference.

Accessible Potential Range

The potential region in which an electrode can operate is governed by the solvent-electrolyte breakdown potentials which depend upon a variety of factors including proneness of the electrode material to electrochemical breakdown, and, in aqueous solutions, hydrogen and oxygen evolution overvoltages. In practice, however, the anodic and cathodic limits depend on an acceptable background current level and this, in turn, depends on the sensitivity required. The results of the potential window studies for silver, silver oxide grid, mercury film and carbon in different media are presented in Table 7. The compilation of various values was determined by scanning the potential at 5 mV/sec and by manually stepping the potential in 50 mV intervals until a 2 μA residual current cut-off point is reached. A typical plot used in the determination of the working range of silver is shown in Figure 21. It is apparent from the Figure that the silver electrode has a wide working range, extending from 0.0 to -1.25 V vs SCE before the peak current exceeds the 2 μA criterion advocated by Linquist (299,300). In this range, the background current changes slowly with potential at a rate of about 450 nA/V. As can be seen from Table 7, the ranges obtained for silver compare quite favorably with a mercury amalgam electrode and a glassy carbon electrode. This indicates, as one might expect, generally consistent characteristics for hydrogen and oxygen overvoltages and solvent decomposition at silver, mercury film and carbon in the given electrolytes. This interpretation is in accordance with similar "inner sphere" adsorption mechanisms given by Jüttner (301) for the reduction of oxygen and evolution of hydrogen at these electrodes. The wide cathodic range at the silver oxide grid electrode seems to compare most closely to mercury at both ends of the potential range spectrum. The increased potential range for the silver oxide grid electrode arises primarily from its ability to discriminate against reactions controlled solely by electron transfer such as hydronium ion reduction or other surface related phenomena (double-layer charging, adsorption-desorption, or chemical changes of the electrode surface).

Equilibration Time

In amperometric detection, the application of a potential to the working electrode generates a large transient or charging current, which ideally decays rapidly. The faradaic steady-state current has two components. First, the residual current arises from redox reactions of surface functionalities. The second component is a result of reduction of traces of electroactive impurities in the solution.

Table 7. Working Potential (Window) Range for Various Solid Electrode Materials in Different Flowing Media.

	Aqueous Mobile Phase Component [1]		
Electrode Material	0.01 M $HClO_4$ (pH 2)	Sodium Acetate (pH 4.5)	Sodium Phosphate (pH 6.8)
Silver	0-0.45 V	0-0.75 V	0-1.25 V
Gold amalgam	0-0.55 V	0-0.80 V	0-1.30 V
Silver oxide grid	0-1.15 V	0-1.45 V	0-1.50 V
Glassy Carbon	+1.1-0.35 V	+1.0-0.60 V	+1.0-1.00 V

[1] Each HPLC mobile phase composed of 50 % (v/v) aqueous electrolyte and 50 % (v/v) acetonitrile.

[2] Potentials obtained by extrapolating the steeply increasing part of the residual current curve to 2 μA.

Equilibration curves for silver and amalgamated gold electrodes at a flow rate of 1.0 mL/min are shown in Figure 24. Analysis of the curves indicate that the current at the silver electrode decays to a stable baseline value within 20-30 min after potential adjustment, enabling use of a low current scale and an increase in detector sensitivity. However, a freshly prepared gold amalgam electrode may require 60 minutes, or sometimes as long as 4 hours, before the background current reaches a steady-state. The slow attainment of a steady-state current response is most probably the result of the slow conversion of residual mercury into amalgam.

Morphology of Signal

The shape of the hydrodynamic voltammogram can be used as a simple diagnostic tool in the evaluation of an electrochemical detector. Faulty location of the electrodes in the cell can result in deformed and prolonged shapes of the voltammogram, which increases the value of the limiting current (i_l) usually employed for quantatitive measurements, and also results in higher noise levels and poorer selectivity. In addition, the rising portion of the wave can be used as an indicator of the degree of reversibility of the detector toward a given reduction process. To evaluate the detector from this viewpoint it is important to make a correct choice of the test solute. We have found that best results are obtained with quinone solutions. Regardless of the method used to obtain the hydrodynamic voltammograms, such as consecutive sample injections or a continuous flow of the substance through the detector, for a reversible reduction the equation for the hydrodynamic voltammogram is described by (13)

$$E = E_{1/2} + (RT/n\mathcal{F}) \{\ln [(i / (i_l - i)]\} \qquad (1)$$

Equation 1 has the same form as that for classical polarography and the larger n is, the steeper the wave. A hydrodynamic voltammogram (HDV) corrected for background for benzoquinone is shown in Figure 25. This curve was constructed by plotting the measured peak current against applied voltage, point by point every 5 mV in the range from 370-470 mV *vs* SCE for 20-µL aliquots of 9.1×10^{-3} M benzoquinone. At each potential setting, the currents were measured after waiting 10 s for the charging current to decay. A plot of $\ln [i / (i_l - i)]$ vs. E for benzoquinone is shown in Figure 26. The x-intercept of 409 mV vs SCE corresponds to the half-wave potential and the slope yielded an n value of 1.66 which is in satisfactory agreement the theoretical value of 2.00. HDV's for benz[a]anthracenequinone, 5,12-naphthacenequinone, phenanthracequinone, 9-fluorenone, and acenaphthenequinone are shown in Figure

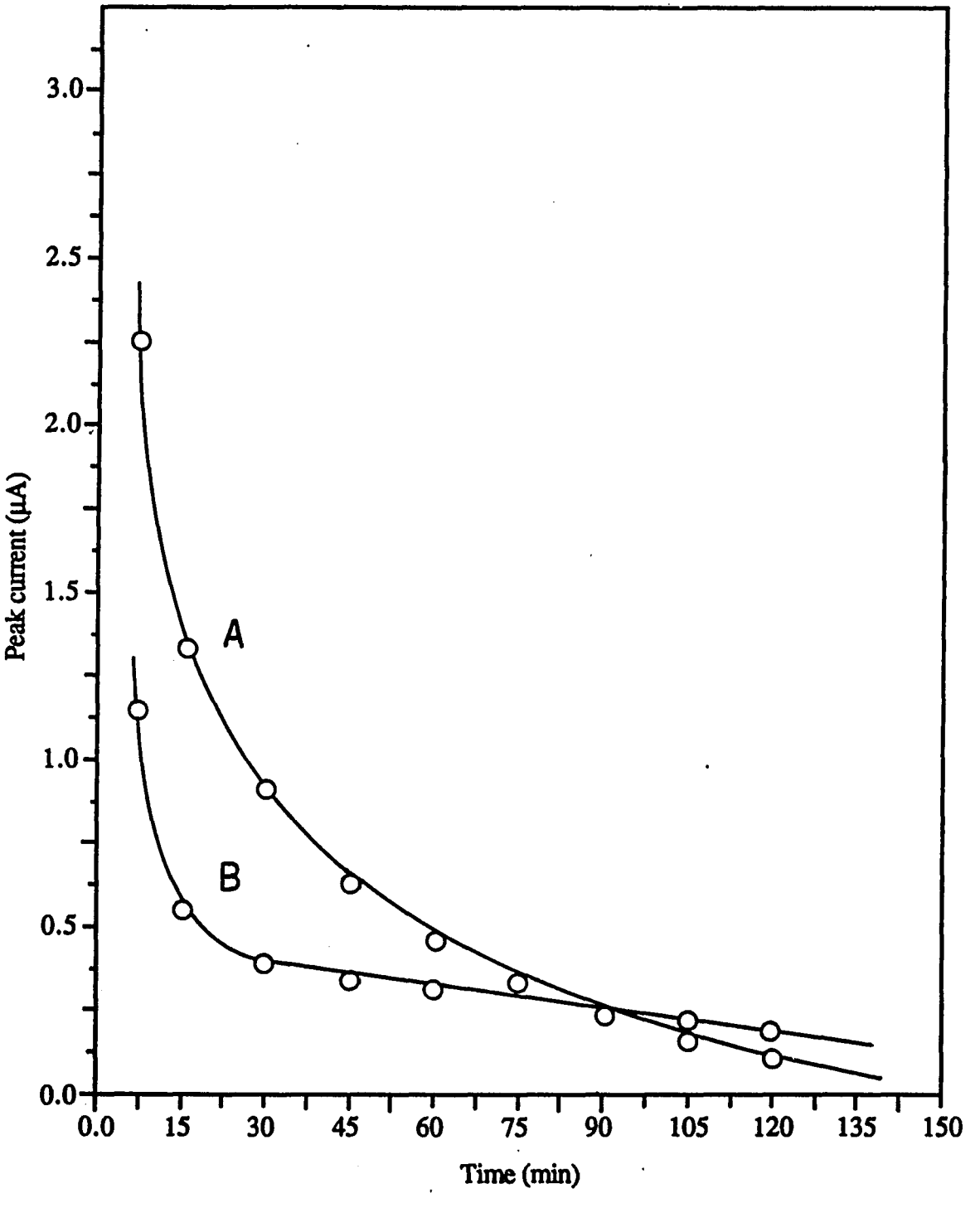

Figure 24. Response of (A) Hg/Au film and (B) electrochemically pretreated silver electrode during equilibration. Flow injection analysis conditions: supporting electrolyte, acetonitrile-aq 0.05 M phosphate buffer, pH 6.8; flow rate, 1.0 mL/min; applied potential, -0.5 V vs SCE reference; sample, 200 ng injections of benzoquinone.

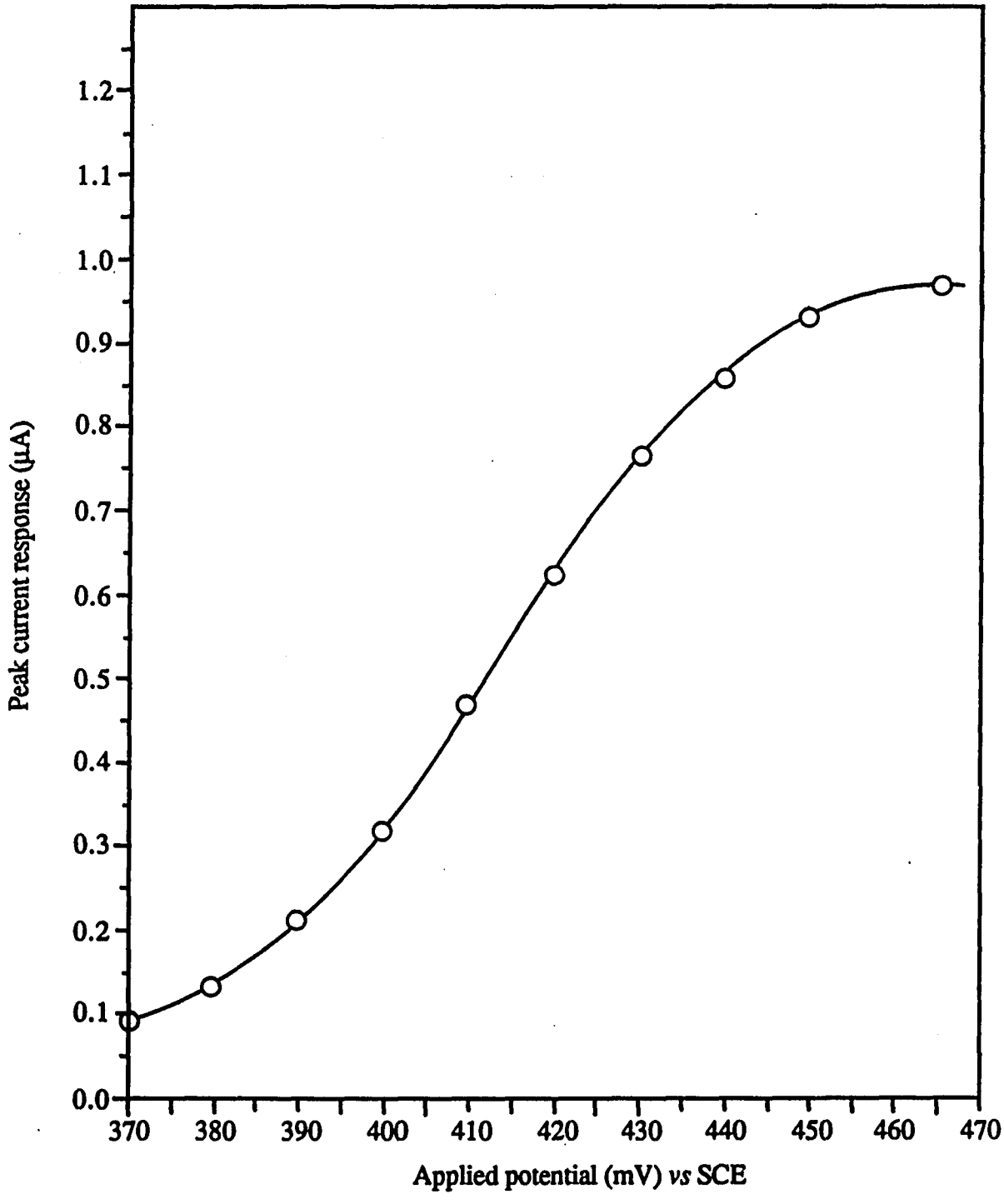

Figure 25. Relationship between peak current and applied potential for benzoquinone. HPLC conditions: column, 150 x 3.9 mm ID μBondapak C-18; mobile phase, acetonitrile-aq 0.05 M phosphate buffer, pH 6.8; flow rate, 2.0 mL/min; sample, 181 ng benzoquinone in mobile phase injected at each potential setting.

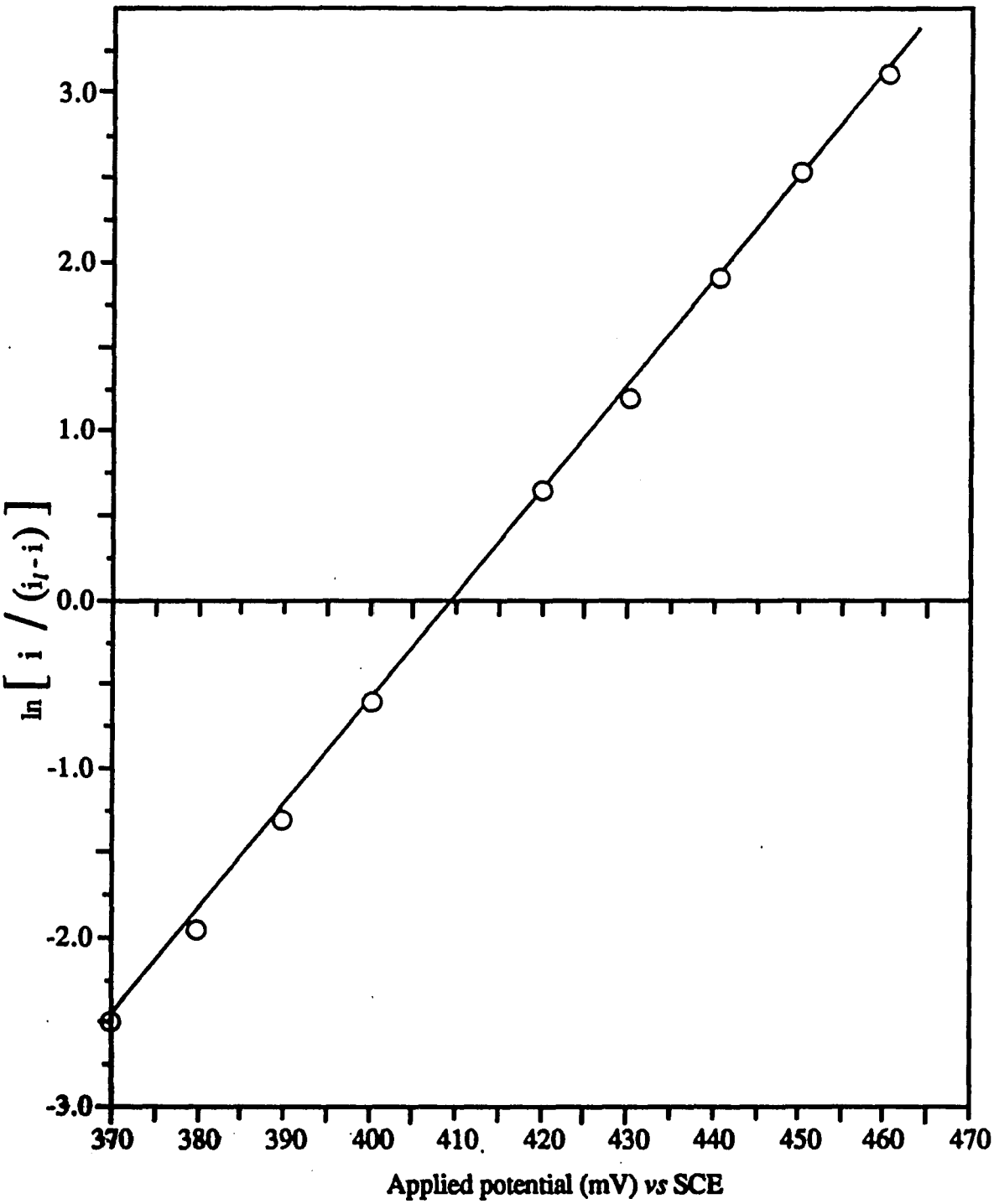

Figure 26. Plot of $\ln \left[i / (i_l - i) \right]$ *vs* applied potential. HPLC conditions: column, 150 x 3.9 mm ID μBondapak C-18; mobile phase, acetonitrile-aq 0.05 M phosphate buffer, pH 6.8 (50+50, v/v); flow rate, 2.0 mL/min; sample, 20 μg benzoquinone in mobile phase injected at each potential setting. The slope of the plot is 63.9 V^{-1} and the x-intercept ($E_{1/2}$) is 409 mV.

27. The ln [i /(i_l - i)] vs. E plots for these compounds deviated substantially from linearity. Another way to characterize these plots is by the application of Tomes criterion (302) for wave-shape reversibility, which is given by the relationship

$$| E_{3/4}-E_{1/4} | = RT/nF \ln[9]= 58.4/n \text{ mV at } 25.0^0C \qquad (2)$$

where, $E_{3/4}$-$E_{1/4}$ are the potentials at which i=0.25 i_l and i=0.75 i_l, respectively. According to Equation 2, for a reversible 2-electron transfer, ΔE=29.2 mV. Based on the experimental ΔE values for the group of quinones in Table 8, their reductions at silver can be considered quasi-reversible under the chosen conditions.

The electrocatalytic effect of a potential cycling-type of pretreatment (between +1.0 and -1.0 V vs SCE) on the electrochemical behavior of phenanthracenequinone at silver is shown in Figure 28. Curve A is the HDV obtained following pretreatment; curve B is the HDV obtained at a bare silver electrode. The shape of the wave obtained at a bare silver electrode was quite broad and application of Tomes criterion gave a value of 45 mV for $E_{3/4}$-$E_{1/4}$. This value is significantly higher than the theoretical value and indicates that the species is poorly catalyzed on this surface. The reason for the low activity may result from the lack of functional groups on the surface; however, there are other possible explanations. These possibilities include the presence of impurities on the surface that hinders the reduction process. Impurities may come from the polishing step or the initial fabrication of the silver rod. Evans et al. (288) reported that the surface of a mechanically polished silver electrode was contaminated with various sulfur and oxygen moieties which might inhibit a reduction process.

Following pretreatment, the value of $E_{3/4}$-$E_{1/4}$ from the HDV for the reduction of phenanthracenequinone was reduced to 27 mV. This value is in agreement, within experimental error, with the theoretical value of 29.2 mV for a reversible two electron transfer. The increased reversibility for quinone reduction at silver following pretreatment can be explained by considering the role of reformed silver clusters in decreasing the susceptibility of the surface to oxide coverage. Vetter et al. (303) showed that the reduction mechanism for phenanthracenequinone at silver is based on a "outer sphere" process. In general, for an "outer sphere" process, an enhanced electrochemical reaction rate for an analyte arises primarily from improved electron-transfer at the electrode surface rather than from a particular chemical interaction with the functional groups on its surface (304). The electron-transfer rate

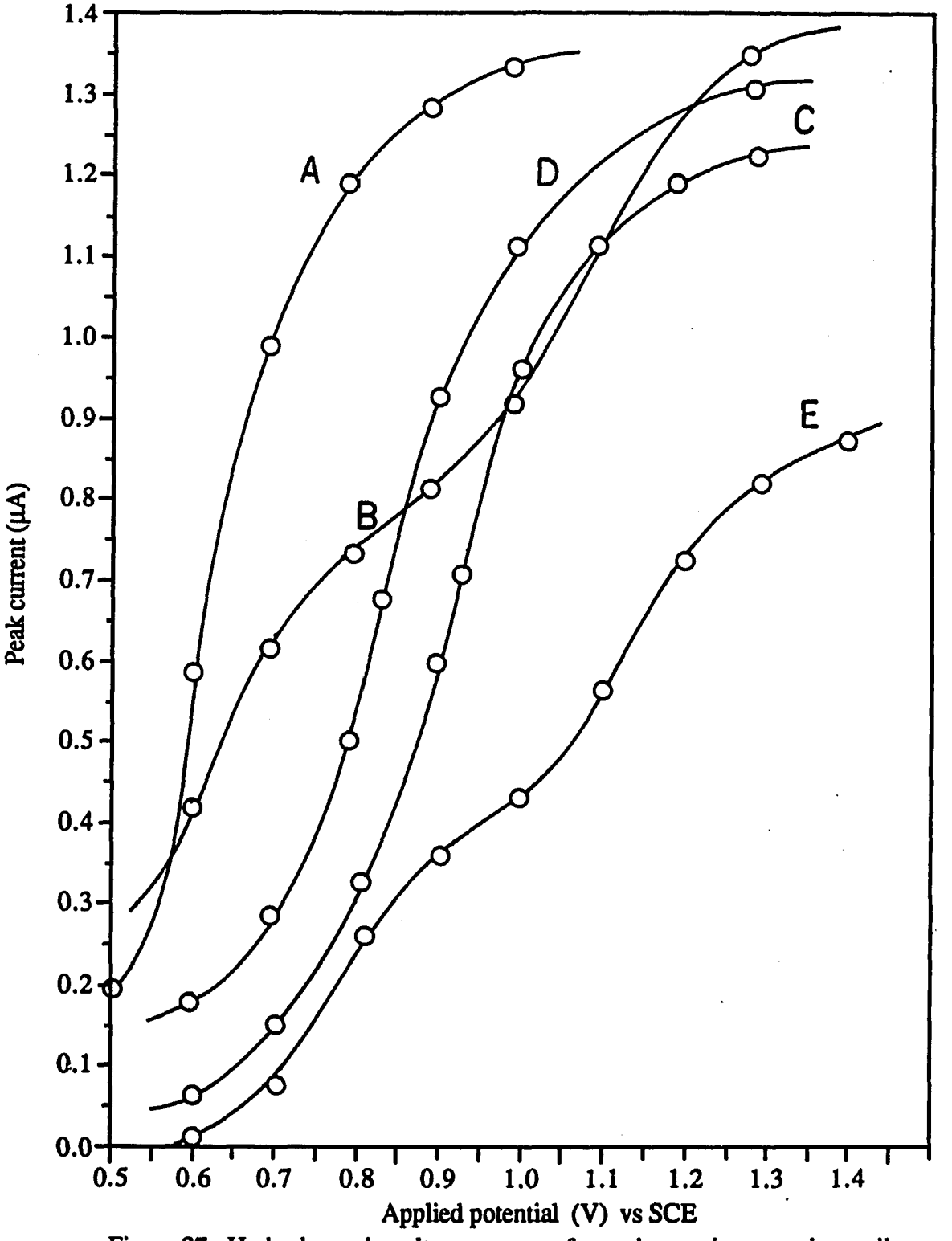

Figure 27. Hydrodynamic voltammograms for various quinones using a silver electrode and a mobile phase containing acetonitrile-aq 0.05 M phosphate buffer, pH 6.8 (50+50, v/v). Potentials in volts versus SCE-3.0 M NaCl. Wave identities: (A), phenanthracenequinone (540 ng); (B), 5,12 naphthacenequinone (820 ng); (C), fluorenone (600 ng); (D), benz[a]anthracenequinone (870 ng); and (E), acenenaphthacenequinone (313 ng).

Table 8. Selectivity of a Silver Cathode Toward Various Quinones.

Compound	ΔE (mV) [1]
Acenaphthenequinone [2]	37
Phenantheacenequinone	20
9-Fluorenone	20
5,12-Naphthacenequinone	45
Benz[a]anthracenequinone	23
Benzoquinone	29
Nitroanthraquinone	35

[1] Expressed by the width of the steeply rising portion of HDV curve between the $I_{3/4}$ - $I_{1/4}$ fraction of the maximum peak current.

[2] Only first wave used in the calculation of curve width.

HDV conditions: column, 150 mm x 3.9 mm I.D. μ-Bondapak C-18; mobile phase, acetonitrile-aq 0.05M $NaClO_4$ (50+50, v/v); flow rate, 2.0 mL/min; sample size, 20-μL injected at each potential setting; cathodic scan range, 0-1.2 V *vs* SCE reference.

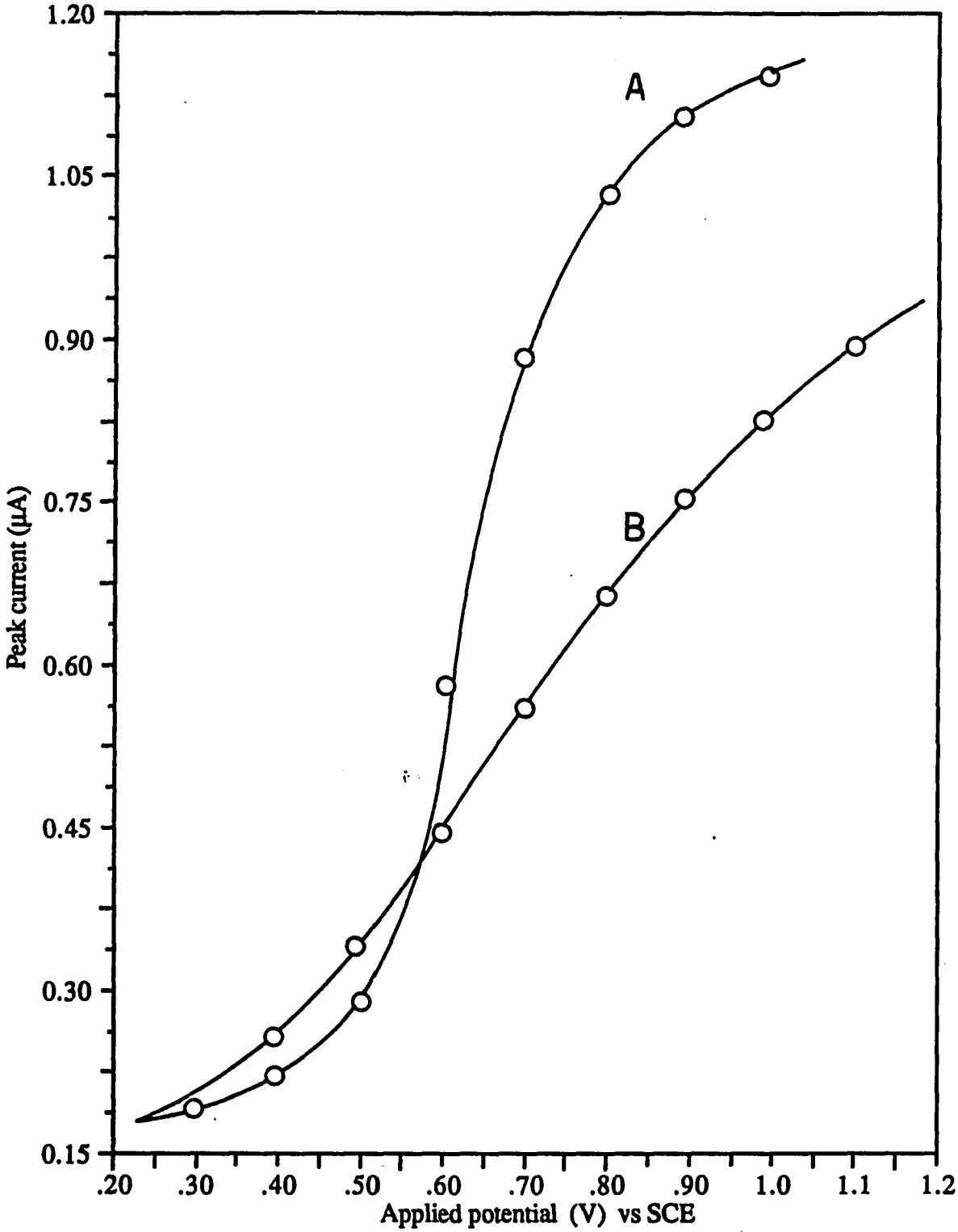

Figure 28. Influence of electrochemical pre-treatment on the shape (reversibility) of the reduction wave of phenanthracenequinone at a silver cathode. HPLC conditions: separation column, 150 x 3.9 mm ID μBondapak C-18; flow rate, 2.0 mL/min; mobile phase, acetonitrile-aq 0.05 M phosphate buffer, pH 6.8 (50+50, v/v). Potentials in volts versus SCE-3.0 M NaCl; sample, 200 ng of phenanthracenequinone in mobile phase injected at each potential setting. Electrode preparation: A, pre-treated by potential cycling in KCl; B, freshly prepared silver electrode.

on precious metal electrodes is generally limited by the semiconducting properties of oxide layers which can reduce the rate by several orders of magnitude (305-307). Although, the formation of an oxide layer is thermodynamically favored on a bare silver electrode (304), even in the presence of oxygen, any AgCl formed on a pretreated surface from the interaction with residual Cl ions adsorbed during pretreatment is uniformly redeposited as conducting silver clusters on the cathodically poised electrode (308). The results of this experiment point out the significance of the chloride stabilized surface functionalities on reduction processes occuring at silver. The same group that inhibits hydrogen evolution actually activates the silver surface with respect to phenanthracenequinone reduction.

Conversion Efficiency

The conversion efficiency for an electrochemical cell is dependent on parameters such as the surface area and the porosity of working electrode, cell dimensions, cell response time and flow rate. Electrochemical cells with efficiency values greater than 0.95 are typically called coulometric, while those with values less than 0.05 are called amperometric (18). Each type of cell has its advantages and liabilities. Coulometric cells are mass sensitive, produce a predictable current response and do not require external calibration. However, signal-to-noise ratios can rarely be optimized for coulometric detectors since they are often fabricated from electrodes with large areas and thus susceptible to adsorption problems and high noise levels. On the other hand, amperometric detectors are concentration sensitive and their signal-to-noise ratios for a particular analyte can usually be optimized by adjusting such parameters as the electrode surface area, mobile phase pH, mobile phase composition and mobile phase flow rate. However, its current response is usually difficult to predict.

The conversion efficiency of each design was determined by pumping a solution of supporting electrolyte containing a fixed concentration of benzoquinone through the cell and measuring the steady-state limiting current. For quantitative conversion, the theoretical steady-state current $(i_{ss})_{\mathcal{F}}$ is given by Faraday's law :

$$(i_{ss})_{\mathcal{F}} = nFC_iV_f \qquad (3)$$

where C_i is the inlet concentration and V_f is the volume flow rate. The conversion efficiency is the ratio of the measured steady-state current to that given by Faraday's law :

$$\% \ R_{eff} = (i_{ss})_{meas} / (i_{ss})_{\mathcal{F}} \times 100 \qquad (4)$$

The conversion efficiency is plotted as a function of flow rate in Figure 29 for the silver disc design. At a flow rate of 50 mL/hr, the electrolysis efficiency was 1.0 %; as the flow rate increased from 50 to 100 mL/hr this value was reduced by a factor of three. The sudden decline in electrolysis efficiency over this flow rate range was observed because the effects of flow rate on each of the current components in Equation 4 is different. At low flow rates, the limiting diffusion current from the amperometric reduction of an analyte varies with the cube root of flow rate (103), whereas, the current from its quantitative conversion is expected to increase linearly with respect to flow rate. Although both current components of the fraction increase over this flow rate range, the greater increase of that expected for quantitative conversion at low flow rates tends to diminish the fraction. As the flow rate is increased, the conversion fraction reaches a plateau as deviations from quantitative conversion creep in due to kinetic and size limitations.

Effects of Metals

Metals present in the mobile phase pose several problems for reductive electrochemical trace work. Their facile reduction at applied potentials necessary for the reduction of most organic moieties can increase the background current to an unmanageable level. In addition, their adsorption on solid electrodes can change the reproducibility of the electrode response as well as the reduction mechanism observed for the analyte under investigation.

To elucidate the effect of metallic contamination on the background current and response at silver and amalgamated gold, 20-µL aliquots of deaerated phosphate mobile phase containing 50 µg/mL of copper nitrate were injected into the LC system and the background current was registered. The process was repeated every two minutes for a 15 minute period at an applied potential of -1.0 V vs SCE. Figure 30 shows the effect of these metals on the background current at a gold amalgam electrode and at a silver electrode. Initially, the background current at the gold amalgam electrode steadily decreased and then abruptly rose after 1.5 hours. At this time, the cell was dismantled and the electrode examined. It showed a rather thick amalgam coating which formed a short circuit with the auxiliary electrode. Subsequently, the contaminated amalgam electrode yielded a response for benzoquinone which was diminished by as much as 35 %. In addition, large spikes upon the injection of quinone analytes were obtained and stability was restored only

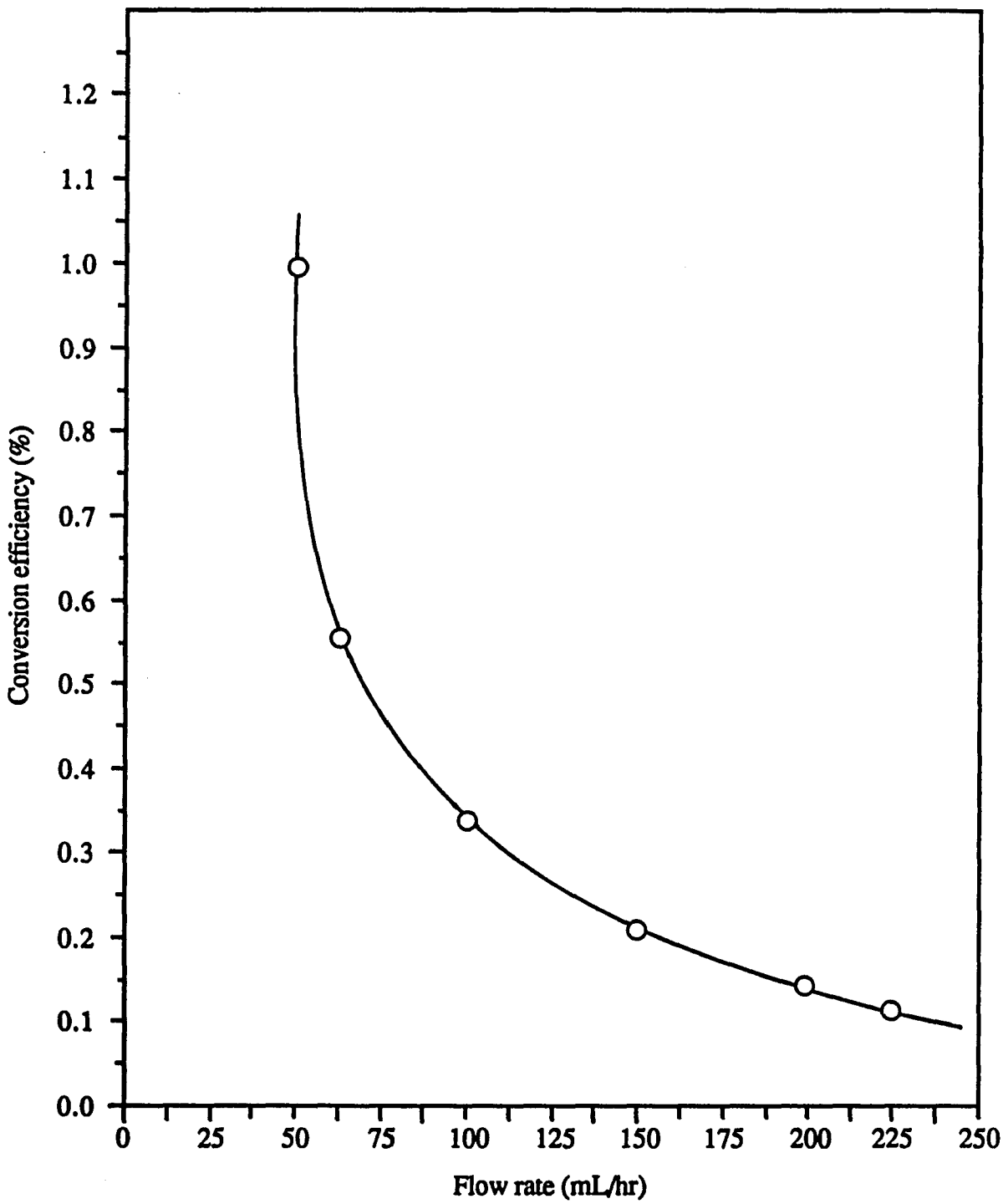

Figure 29. Dependence of the degree of electrolytic conversion upon volume flow rate. HPLC conditions: column, 150 x 3.9 mm ID μBondapak C-18; mobile phase, acetonitrile-aq 0.05 M phosphate buffer, pH 6.8; applied potential, -1.0 v vs SCE reference in NaCl; sample, 181 ng of benzoquinone in mobile phase injected at each flow rate setting.

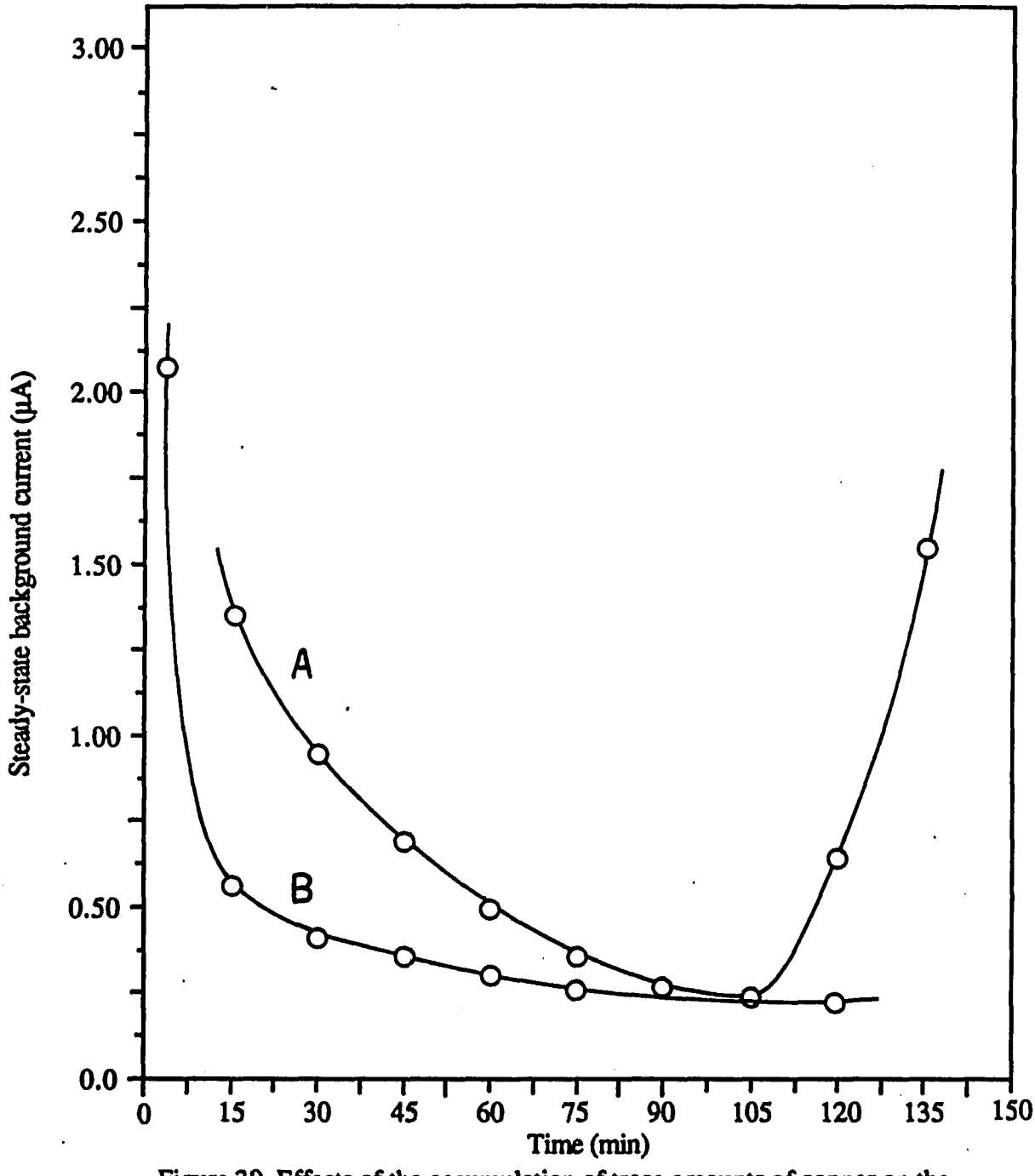

Figure 30. Effects of the accumulation of trace amounts of copper on the steady-state background current of (A) gold amalgamated electrode and (B) pre-treated silver electrode. HPLC conditions: separation column, 150 x 3.9 mm ID μBondapak C-18; flow rate, 2.0 mL/min; mobile phase, acetonitrile-aq 0.05 M phosphate buffer, pH 6.8 (50+50, v/v); sample, 20 μL of mobile phase containing 50 μg/mL copper nitrate injected at intervals of 7.5 min.

slowly after each injection of sample. The influence of dissolved metals such as copper, cadmium, and zinc on amalgam film electrodes have been discussed in studies of anodic stripping voltammetry (136-139), where it has been observed that intermetallic bonds formed among various metals in the amalgam can shield the film from further reductive activity. A much reduced effect of metal adsorption was observed on the silver electrode. Although, small injection spikes were seen for quinone analytes on low current ranges, the baseline was restored quickly and the response toward the quinones remained relatively unchanged. Inspection of the working electrode cube with a loupe revealed a creamy-white uniform surface without any isolated patches of heavy metallic growth following metallic contamination. The uniform deposition of the foreign metal has been shown by Bort et al. (309) and Schmidt et al. (310) to be caused by the formation of a chloro-metallic complex with residual chloride ions, which thereby enhances the mobility of the metal across the silver surface. Following transportation, reconstitution of the silver surface rather than three dimensional growth occurs through lateral diffusion of the foreign metal atoms until defect sites are uniformly filled (311). As reconstitution proceeds, the density of the surface changes but extensive nucleation at a single site does not occur to the extent to which a short circuit is formed with the auxiliary top block. Moreover, since the reduction mechanism for most quinones does not involve a strong chemical interaction with silver surface functionalities (304), its current response remains relatively unperturbed by minor surface changes as long as the surface remains conducting.

Dependence of Electrochemical Response on Flow Rate at a Silver Disc Electrode

Many workers (312-322), have attempted to use hydrodynamic equations based on heat theory to predict the behavior of electrochemical detectors, but obtained contradictory results. In a nutshell, the response of an amperometric detector was predicted to depend only upon analyte concentration, fluid velocity, cell geometry, electrode area and analyte diffusion coefficient. However, whether limiting current (i_l) is proportional to $F^{1/2}$ or to $F^{1/3}$ (linear flow rate) for channel electrodes, has been a matter of discussion for almost 30 years (312). A number of factors have been given by Moldoveanu and Anderson (320-322) for the inconsistency in the values determined for the flow rate exponent in the current expression. These include deviations from laminar flow, adsorption, passivation, effect of very small cell volume

on diffusion layer, inequality of steady-state currents with peak currents for chromatographic peaks, low coulombic efficiency level and uncertainity in diffusion coefficients and other empirical constants.

However, to apply this concept in practice for chromatography, both $F^{1/2}$ and $F^{1/3}$ dependencies have the same meaning, i.e., peak current increases as flow rate increases. Here, the electrochemical responses of the thin-layer cell containing a 3.2 mm silver electrode for various quinones were studied as a function of flow rate. As shown in Figure 31, the peak current in each case tended to increase gradually with increasing flow rate, which reflects both effects based on nonequilibration of the sample in the separation column and the change of electrolytic efficiency in the electrochemical cell with flow rate. A linear relationship was found between I_l and $F^{1/3}$ in the range of $0.5 < F < 1.5$ mL/min, the usual flow rate range for electrochemical detectors. At flow rates higher than 1.5 mL/min, however, a plateau was reached. The increasing current helps to compensate for the decrease in coulometric efficiency and provides an advantage over optical detectors such as UV and refractometric types, for which the response is inversely proportional to the flow rate of the mobile phase. The noise level did not change significantly between 0.5 and 1.5 mL/min, but showed a gradual increase when the flow rate exceeded 2.0 mL/min. In addition, the chromatographic efficiency decreases at higher flow rates. Thus, a flow rate of 2.0 mL/min was accepted as the best compromise for all further studies. These results are in good agreement with those obtained by Moldoveanu and Anderson (320,322) for thin-layer cells having thin diffusion layers.

The cube root dependency of flow rate on current clearly indicated that the response from the silver-based thin-layer detector arises solely from diffusion processes parallel (planar) to the electrode surface. Moreover, laminar flow conditions were well respected over the range of flow rates examined. Under these conditions, the diffusion limiting current arising at a disc-shaped electrode is given by the relationship (317)

$$I_{ss} = 1.47\, n\mathcal{F}C\,(DA/b)^{2/3}\,F^{1/3} \qquad (5)$$

where C is the bulk concentration of the electroactive species, D is the diffusion coefficient of the electroactive species, A is the electrode area, b is the channel height, F is the volume flow rate, and the other terms having their usual meaning. For the silver disc electrochemical detector used here, A is 0.080 cm^2, b is 0.025 cm, D for

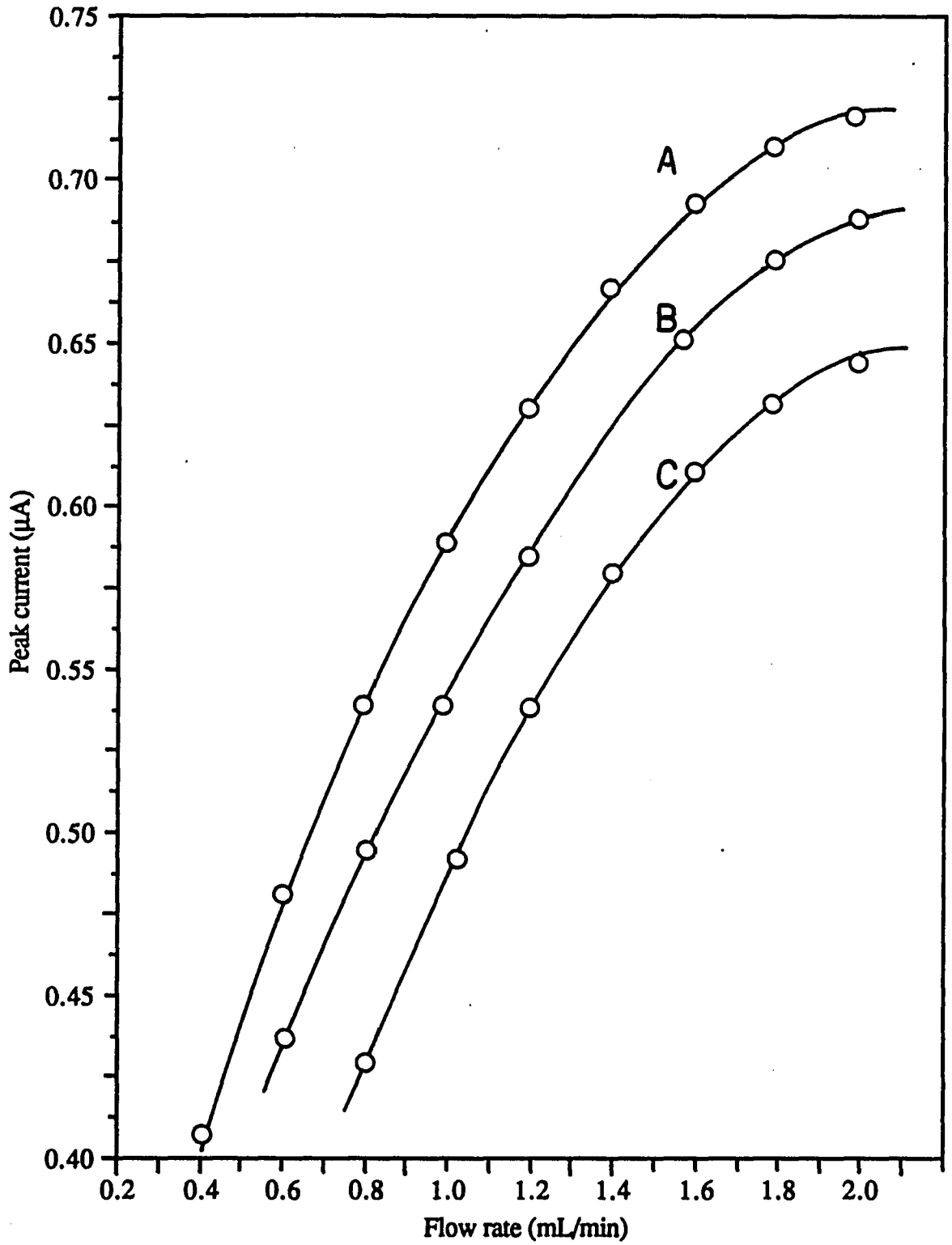

Figure 31. Relationship between peak current and flow rate for (A) benzoquinone, (B) phenanthracenequinone, (C) benz[a]anthracenequinone at a pre-treated silver cathode. HPLC conditions: separation column, 150 x 3.9 mm ID μBondapak C-18; mobile phase, acetonitrile-aq 0.05 M phosphate buffer, pH 6.8; applied potential, -1.1 V vs SCE; sample size, 130 ng, 270 ng, and 415 ng of benzoquinone, phenanthracenequinone, and benz[a]anthracenequinone, respectively, injected at each flow rate setting.

benzoquinone is 8.8 x 10^{-6} cm^2/sec (303), C is 1.5 x 10^{-6}M, and the flow rate is 2.0 mL/min. Using the above equation, i_{ss} works out to be 0.53 μA which compares well with the experimental value of 0.42 μA.

To further demonstrate the impact of cell geometry on detector performance, the influence of spacer thickness (duct height) and position of the entrance port on the the current response were examined. In order to study the effect of spacer thickness, the detector was connected directly to a syringe pump containing 1x10^{-5} M benzoquinone in mobile phase, and the limiting currents were measured as a function of flow rate for various duct heights ranging 0.005 to 0.089 cm. Following each run, the effective duct height was adjusted by inserting an additional spacer of appropriate thickness. Table 9 lists the corresponding exponential dependence on flow rate for the various duct heights. Three tendencies are shown in Table 9. Only for spacers smaller than 0.025 cm, is the common thin-layer 1/3rd order response observed. For spacers betweeen 0.038 and 0.076 cm, the exponential dependence on flow rate was observed to be 1/2. Weber and Purdy (313) showed that such a dependency is characteristic of a thin-layer cell in which the flow is not yet well developed. For thick spacers, the order of the exponential dependence on flow rate increased to 0.75. Such a dependency has been shown by Gunasingham et al. (323) to be characteristic of a stream which impinges normal to the electrode surface. Unfortunately, the increased sensitivity resulting from decreasing spacer thickness can rarely be exploited in quantitation because the noise level increases at an equal or greater rate. In addition, the increased impedance between the working and auxiliary electrodes results in deviations from the linear response of the detector. Furthermore, a very thin cell places greater demands on the quality of electrode polishing due to the increased possibility for short circuiting betweeen electrode blocks.

To study the influence of inlet port position on response, the top block of the cell was modified so that the effluent impinged normally on the leading edge of the silver electrode. Figure 32 shows the relationship between I_l and flow rate for benzoquinone in a thin-layer cell in which the inlet port is located just in front of the electrode face and has a gasket thickness of 0.013 cm. The slope of the Log $I_l = f$ (Log F) plot is 0.55 with a correlation coefficient of 0.997. In comparison, the corresponding slope for a cell which contains an up stream inlet port and gasket thickness of 0.013 cm is

Table 9. Influence of Spacer (Duct) Thickness on the Current Flow Rate Dependency for a Silver-Based Thin-Layer Cell.

Spacer Thickness (cm)	Flow Rate Exponential
0.005	0.33
0.013	0.35
0.025	0.35
0.038	0.45
0.051	0.50
0.064	0.50
0.076	0.55
0.089	0.70

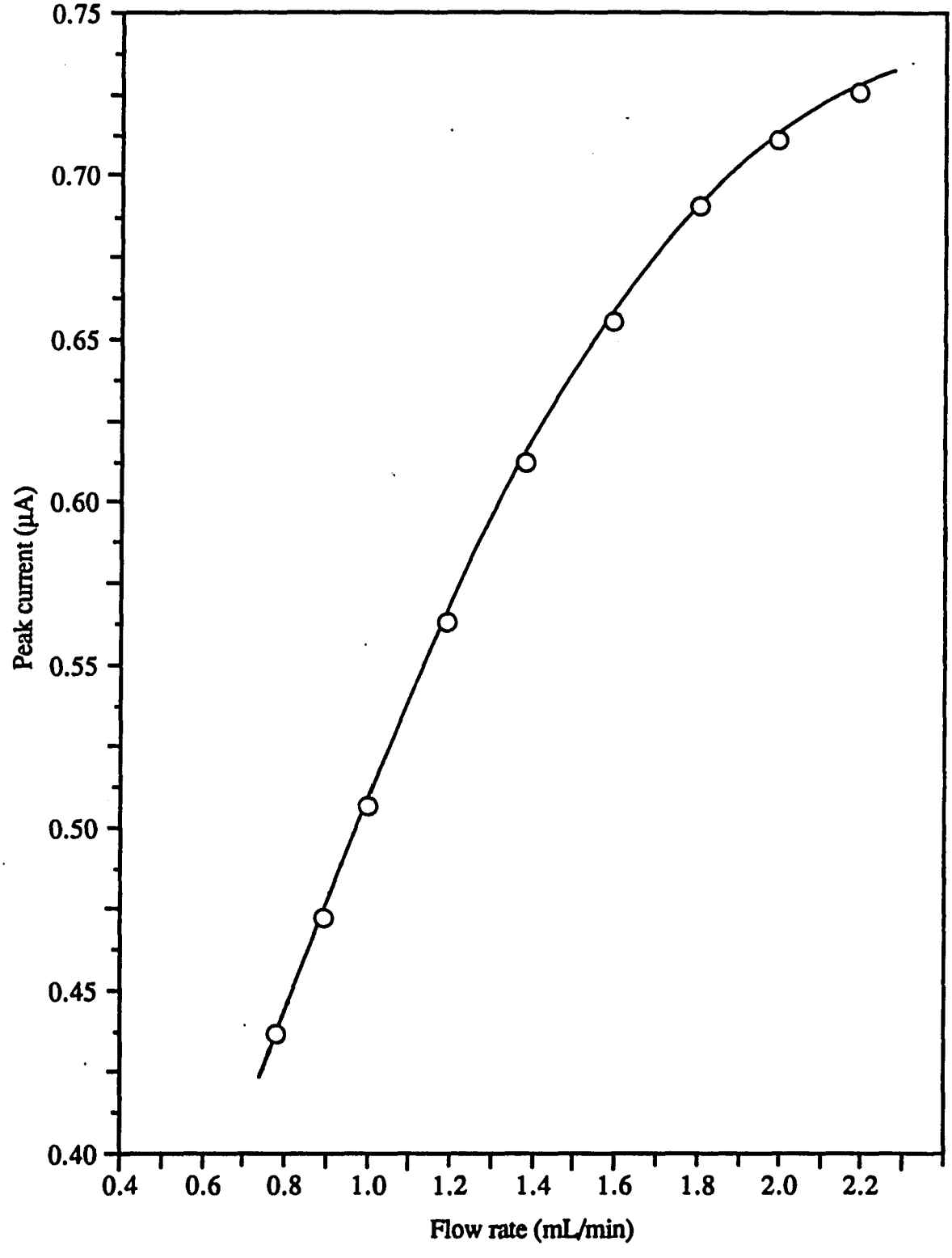

Figure 32. Relationship between peak current response and flow rate for benzoquinone from a silver-based thin layer cell in which the inlet port is located just in front of the electrode surface. HPLC conditions: separation column, 150 x 3.9 mm ID μBondapak C-18; mobile phase, acetonitrile-aq 0.05 M phosphate buffer, pH 6.8; applied potential, -1.1 V vs SCE; sample, 130 ng of benzoquinone injected at each flow rate setting.

0.337, which is indicative of well developed thin-layer behavior. The dependency on flow rate is magnified as the inlet port is moved toward the electrode surface because the current response arises from diffusion processes which are parallel as well as normal to the electrode surface. These findings support the claims by Weber and Purdy (312,313), namely, the same cell can show different hydrodynamic characteristics depending upon the distance traveled by the mobile phase before the flow becomes laminar (developed).

Effect of Grid Size on Response of Silver Oxide Grid Electrode

An unique feature of the silver oxide grid electrode is the ability to optimize the analytical sensitivity and background noise by controlling the pore size of the screen used in the initial fabrication. The sensitivity and background noise of the silver oxide grid electrode as a function of the diameter of the silver islands is summarized in Table 10. Analytical sensitivity diminishes with decreasing active silver site size, but significantly less rapidly than expected based on a linear diffusion model for analyte transport which predicts I_l to be proportional to $A^{2/3}$ (103).

When an electrode surface is partially covered with an electroinactive substance the diffusion of electroactive analytes to and from the active regions of the electrode surface may no longer be regarded as linear even if the electrode surface is flat. This blocking effect on the transport of electroactive substances to partially passivated electrode surfaces has been treated theoretically by Caprani et al. (324) and Gueshi et al. (325,326), based on a model for radial diffusion to a surface composed of a number of parallel semi-infinite cylindrical unit cells. For a single unit cell, the equation describing the limiting current is given by (327-330)

$$I_l = n\mathcal{F}ADC \{(2/r) / [\ln (4\phi)]\} \qquad (6)$$

where, ϕ is equal to Dt/r^2, r is the radius of an active site, and the other terms have their usual meaning. The relative insensitivity of the faradaic response of the silver oxide electrode to grid size can be explained by its logarithmic dependence of the current on the radius. For example, the diffusion controlled total current at a 10 μm site is predicted to be only 1/2 that at a 1000 μm site. It should be emphasized that no attempt was made to relate the measured total limiting current to that yielded by an individual site because the currents at individual sites may not be independent of each other and the exact number of sites was unknown.

Table 10. Background Current, Sensitivity for Nitroglycerin, and Noise of Silver Oxide Grid Electrode as a Function of Silver Site Size.

Diameter of Active Site (μm)	Background Current (μA)	Sensitivity (μA/μg)	Peak-to-Peak Noise (pA)
750	315	8.4	405
500	280	8.0	115
375	270	7.9	103
250	250	7.9	90
100	225	6.2	75

Separation Conditions: column, 150 mm x 3.9 mm I.D. μ-Bondapak C-18; mobile phase, acetonitrile-water (70+30, v/v); applied potential, -1.35 V *vs* SCE; flow rate, 2.0 mL/min; sample size, 20-μL aliquot containing 1.0 ng nitroglycerin.

A rather dramatic decrease in noise is observed as the size of the active silver sites on the electrode is reduced. The noise reported in Table 10 appears to be related to the number of inactive sites as well as the topology of the active ones. The noise decreases from 405 to 75 pA as the size of the active sites decreases from 750 to 100 μm. In addition, the pattern of the noise varied from periodic non-random high-frequency baseline fluctuations at 500 μm to predominantly random low-frequency noise at 100 μm. The increased number of inactive sites formed on electrodes possessing smaller active silver sites offers greater inhibition to surface processes involving hydrogen evolution or oxygen reduction. The regularity of the noise at particle sizes larger than 400 μm suggests that surface clefts and pits may be responsible for nonuniform flow patterns which can cause additional noise. On the other hand as the active silver particle size is reduced, surface contributions to the over-all noise level become less important and the noise reached a lower limit of 75 pA. Background current appears to be relatively independent of silver content for particle sizes in the range of 500-250 μm.

Effect of Flow Rate on Response of Silver Grid Oxide Electrode

To examine the dependence of peak current upon flow rate at the silver oxide grid electrode, chromatographic peaks for nitrophenol were recorded at different flow rates ranging from 0.5 to 2.0 mL/min. Figure 33 A shows the straight line obtained when the logarithm of the response from the silver oxide grid electrode is plotted against the logarithm of the flow rate. Also shown in Figure 33 is the corresponding peak current versus flow rate dependence obtained using a silver electrode with a diameter of 3.2 mm (B). The peak current at the silver oxide grid electrode increases only slightly over the entire range of flow rates employed. In contrast and as expected, an increase in peak current is obtained at the continuous electrode upon increasing the flow rate. Slopes of 0.05 and 0.34 were obtained for the silver oxide grid and continuous electrode, respectively. The value obtained for the grid electrode represents a significant decrease in flow rate dependence. This behavior is attributed to nonlinear diffusion to individual silver sites on the assembly and overlap of the diffusion regimes of adjacent silver sites (225). It should be emphasized that flow rate-independence was obtained without increasing the dead volume of the detector. A 0.013 cm spacer thickness was used to obtain these data. In contrast, a spacer thickness of 0.13 cm was required to exhibit similar flow rate-independence using composite electrodes composed of carbon fibers (222) or Kel-F (225).

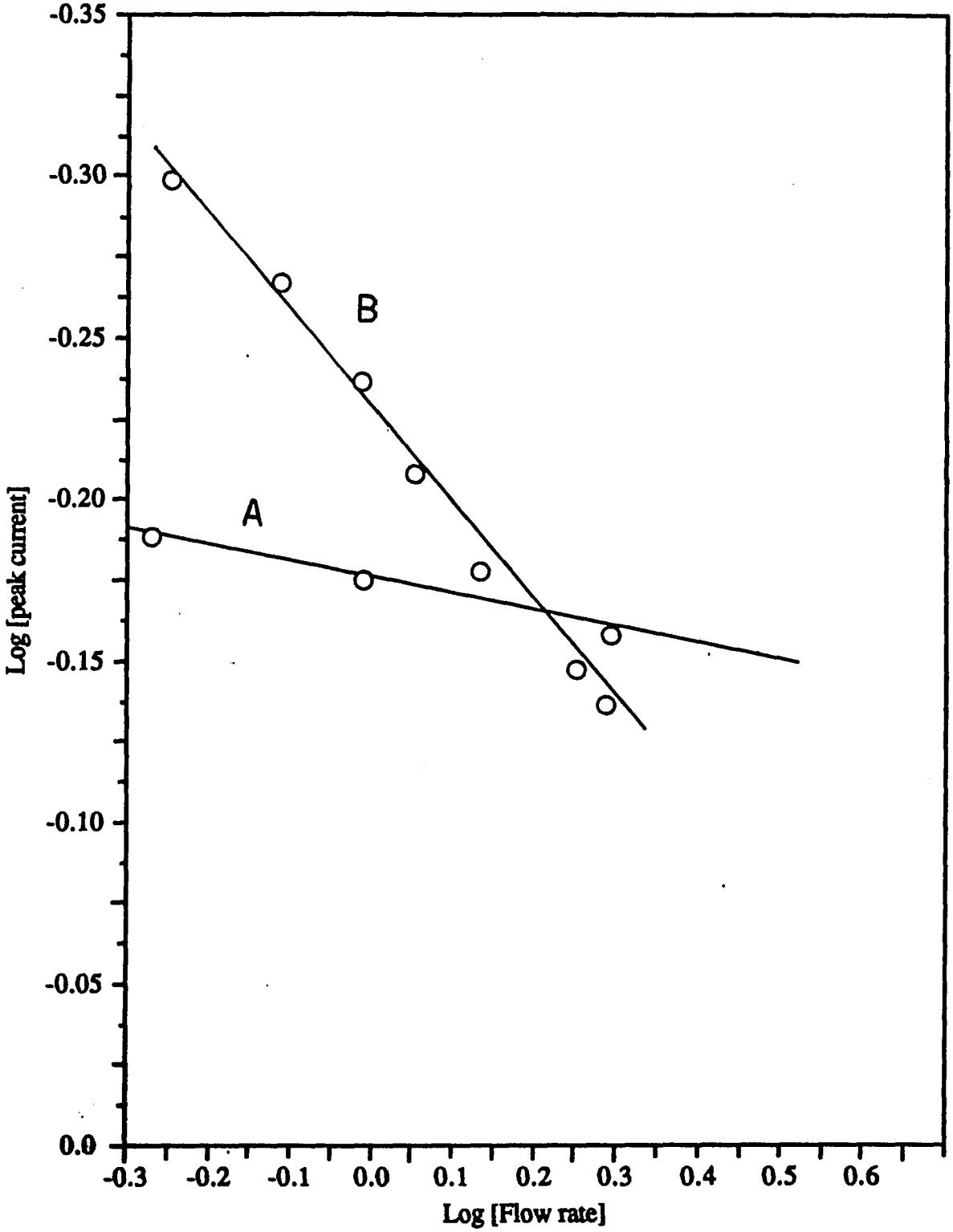

Figure 33. Logarithmic dependence of peak current (μA) upon flow rate (mL/min) for (A) silver oxide grid electrode and (B) continuous silver electrode. HPLC conditions: separation column, 150 x 3.9 mm ID μBondapak C-18; mobile phase, acetonitrile-aq 0.05 M phosphate buffer, pH 6.8 (60+40, v/v); applied potential, -1.2 V*vs* SCE; sample, 20 μL aliquots of 110 ng of nitrophenol injected at each flow rate setting. The slopes of curves A and B are 0.05 and 0.34, respectively.

This improvement in the flow rate independent behavior may be attributed to larger separation between the individual active sites. Because one of the noise sources in a flow system arises from fluctuations in flow rate, (316) the reduced flow rate dependence leads to a reduction in noise.

Analytical Considerations

The sensitivity of the chromatographic/electrochemical system fitted with macro and micro silver electrodes was investigated by monitoring the reduction of a series of quinones and nitro-aromatics over the millimolar to sub-millimolar concentration range. To minimize background interference and maximize analyte response, flow injection hydrodynamic voltammograms (HDV's) were used to select an applied potential at which current reaches the limiting-current plateau of the particular analyte. The flow rate in these studies was 2.0 mL/min. Table 11 summarizes the applied potential used for the various analytes. The location and number of nitro groups and other substituents on the benzene ring affected the applied potentials required for reduction. The 2,4-dinitro substituted compounds produced two well-defined reduction waves which were shifted 200 mV positive to those for mononitro-substituted compounds. The mononitro-substituted compounds required applied potential ranging from -0.70 V vs SCE for nitrobenzene to -1.10 V vs SCE for 4-chloro-2-nitroaniline. Also, as indicated by the data, a large negative potential is required to monitor all organonitrochloro compounds eluted from a chromatographic column. This range of reduction potentials could be used to advantage in providing added detection selectivity. In general, use of a less negative applied potential resulted in loss of sensitivity, whereas a more negative applied potential lead to detector drift and increased background current and noise. A summary of the results of the response studies is given in Tables 12-18.

Linear Dynamic Range

The linear dynamic range can be defined as the range of sample weights from the minimum detectable quantity (MDQ) to the weight injected at which an arbitary e.g. 5 % deviation from linearity is observed in the plot with unit slope of log peak current versus log solute weight (1,2). In all instances the mobile phase was acetonitrile - aq 0.01 M sodium perchlorate (60/40, v/v). Figure 34 shows the relationship between the peak current and the amount injected for benzoquinone, 9-fluorenone and nitrobenzene. The correlation coefficients, and linear response ranges for the various

Table 11. Applied Potentials Used in the Generation of Analytical Data.

Compound	- Applied Potential (V) *vs* SCE
Benzoquinone	0.50
Acenaphthenequinone	1.10
Phenanthracenequinone	0.85
9-Fluorenone	1.30
5,12 naphthacenequinone	1.00
Benz[a]anthracenequinone	1.10
Nitroglycerin	0.85
Nitrobenzene	0.70
Nitrophenol	1.20
p-Nitroaniline	0.90
1-Chloro-3-nitrobenzene	0.75
1-Chloro-2-nitrobenzene	0.80
1-Chloro-4-nitrobenzene	1.00
o-Nitrotoluene	0.85
1,4 Dichloro-5-nitrobenzene	0.90
2,4 Dinitroaniline	0.75
2,4 Dinitrophenol	0.75
m-Dinitrobenzene	0.95
4-Chloro-2-nitroaniline	1.10

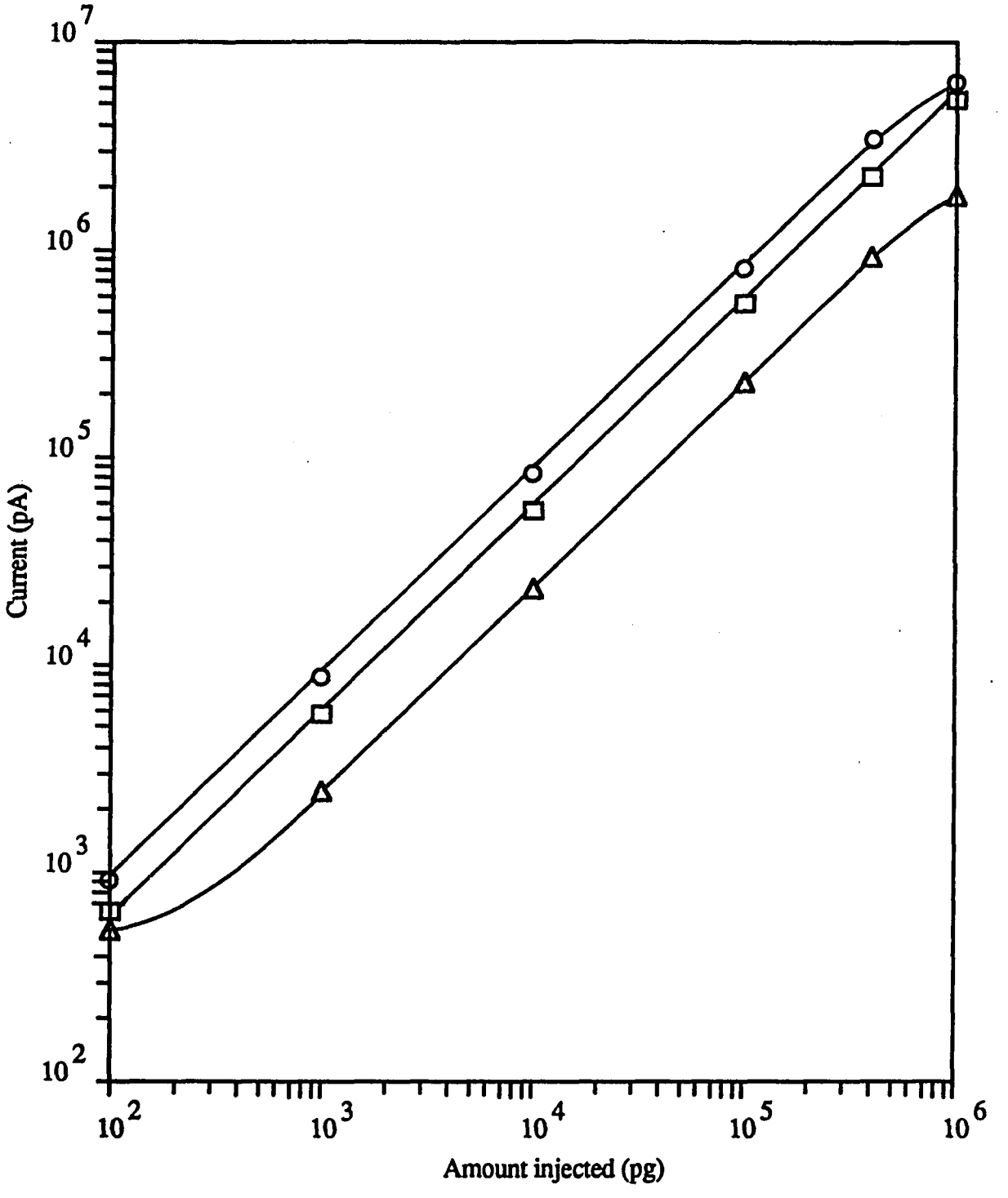

Figure 34. Calibration curves obtained with a continuous silver electrode from 20 µL injections of benzoquinone, m-dinitrobenzene and 9-fluorenone. HPLC conditions: separation column, 150 x 3.9 mm I.D. µ-Bondapak C-18; mobile phase, acetonitrile-aq 0.05 M sodium perchlorate; flow rate, 2.0 mL/min; applied potential, -1.2 V *vs* SCE. Correlation coefficients, 0.9978 for m-dinitrobenzene (○), 0.9998 for benzoquinone (□), and 0.9985 for 9-fluorenone (△).

analytes examined are given in Table 12. Of particular significance are the correlation coefficients for the calibration curves. These values are a clear indication of the linearity and high reproducibility of this technique. In all instances, linearity was maintained over at least a 10^3-fold concentration range. The upper concentration limit of the linear response is determined by the sensitivity of the circuitry in the potentiostat. Of the various compounds studied, benzoquinone showed the widest concentration range (2.6×10^{-8} to 4.2×10^{-4} M). Its calibration curve clearly indicates that there was no observable deviation from linearity over this concentration range.

A major factor which controls the linearity of response of electrochemical detectors is the geometrical relationship between the counter and working electrodes. The effect of uncompensated cell resistance on calibration curves obtained for m-dinitrobenzene using a silver electrode potential poised at -0.95 V versus SCE is shown in Figures 35 A and 35 B. These data were obtained for a concentration range centered about 3.5×10^{-5} M in a pH 6.8 phosphate mobile phase. With the described thin-layer detector, the uncompensated resistance was 55-K Ω and the linear calibration curve in Figure 35 A was obtained. When the calomel reference electrode was moved far downstream into the overflow flask, the uncompensated cell resistance increased to about 4-M Ω and the nonlinear calibration curve in Figure 35 B was obtained. This nonlinearity is due to a shift in the positive direction of the effective working electrode potential when the current increases cathodically. This causes the signal current response to decrease according to the voltammetric behavior of the analyte at the lower potential. The upper limit of linearity can be extended by increasing the applied potential or by decreasing the size of the injection loop.

To compare the linear dynamic range obtainable at the silver oxide grid electrode with that of a conventional electrode, calibration curves were constructed for nitroglycerin covering the concentration range of 2.2×10^{-3} - 2.2×10^{-8} M at each electrode. The mobile phase was composed of 30 % (v/v) acetonitrile in aqueous 0.005M sodium perchlorate. The potentiostat controlled the potential at -1.25 V vs SCE. The flow rate was 2.0 mL/min. Figure 36 shows the calibration curves for nitroglycerin obtained at each electrode. The cell with the grid electrode yielded a highly linear calibration curve of at least 5 orders of magnitude (correlation coefficient = 0.998). The upper limit of this interval was given by the operational range of the potentiostat, which attained

Table 12. Linearity of Response of Silver-Based Flow-Through Detector for Various Quinones and Nitro-aromatics.

Compound	Linear Range (mg/mL)	Correlation Coefficient
Benzoquinone	2.75×10^{-6} - 4.51×10^{-2}	0.999_8
Acenaphthenequinone	11.0×10^{-6} - 1.82×10^{-2}	0.999_6
Phenanthracenequinone	12.5×10^{-6} - 2.00×10^{-2}	0.999_4
9-Fluorenone	24.0×10^{-6} - 2.23×10^{-2}	0.998_5
5,12 Napthacenequinone	12.5×10^{-6} - 3.00×10^{-2}	0.998_9
Benz[a]anthracenequinone	21.0×10^{-6} - 3.23×10^{-2}	0.9992
Nitroglycerin	3.25×10^{-6} - 4.68×10^{-3}	0.999_1
Nitrobenzene	4.75×10^{-6} - 2.01×10^{-2}	0.988_4
m-Dinitrobenzene	4.34×10^{-6} - 2.15×10^{-2}	0.997_8
p-Nitrophenol	5.00×10^{-6} - 3.72×10^{-2}	0.999_6
Nitroaniline	9.00×10^{-6} - 6.65×10^{-2}	0.995_8
1-Chloro-3-nitrobenzene	10.0×10^{-6} - 6.74×10^{-2}	0.996_9
1-Chloro-2-nitrobenzene	11.3×10^{-6} - 7.20×10^{-2}	0.997_4
1-Chloro-4-nitrobenzene	11.6×10^{-6} - 7.00×10^{-2}	0.994_5
o-Nitrotoluene	11.5×10^{-6} - 6.84×10^{-2}	0.996_5
1,4 Dichloro-5-nitrobenzene	9.00×10^{-6} - 5.00×10^{-2}	0.978_9
2,4 Dinitroaniline	7.00×10^{-6} - 5.00×10^{-2}	0.999_3

HPLC conditions: separation column, 150 mm x 3.9 mm I.D. μ-Bondapak C-18; mobile phase, acetonitrile-aq 0.01M sodium perchlorate (60/40, v/v); flow rate, 2.0 mL/min; injection volume, 20-μL.

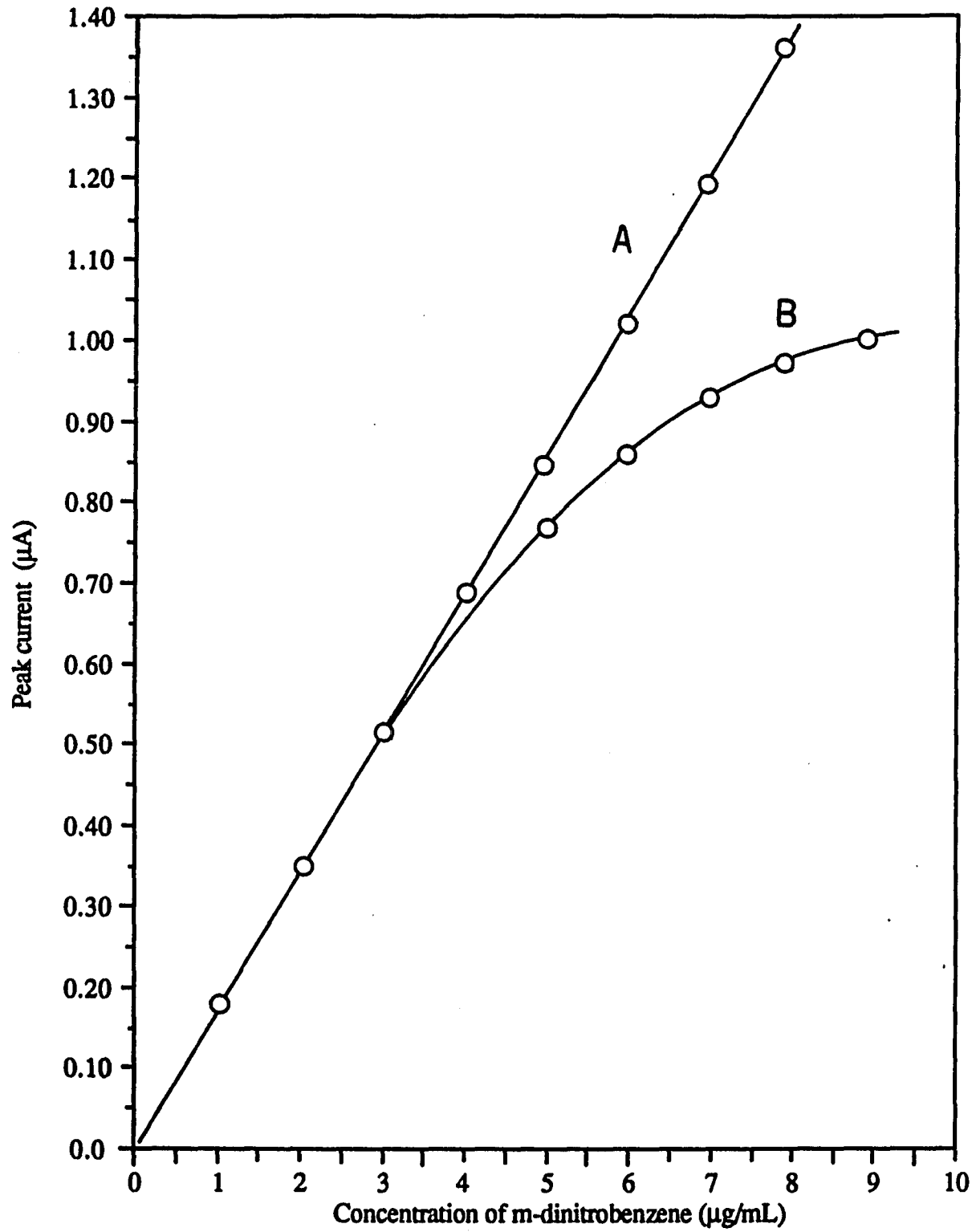

Figure 35. Influence of uncompensated resistance on the linearity of the calibration curve obtained for m-dinitrobenzene using a silver electrode. HPLC conditions: separation column, 150 x 3.9 mm ID μ-Bondapak C-18; mobile phase, acetonitrile-aq 0.05 M phosphate buffer, pH 6.8 (60/40, v/v); flow rate, 2.0 mL/min; applied potential, -0.95 V *vs* SCE. Electrode arrangements: A, working and auxiliary electrodes opposite each other and in close proximity to reference electrode; B, working and auxiliary electrodes opposite each other and reference electrode located downstream.

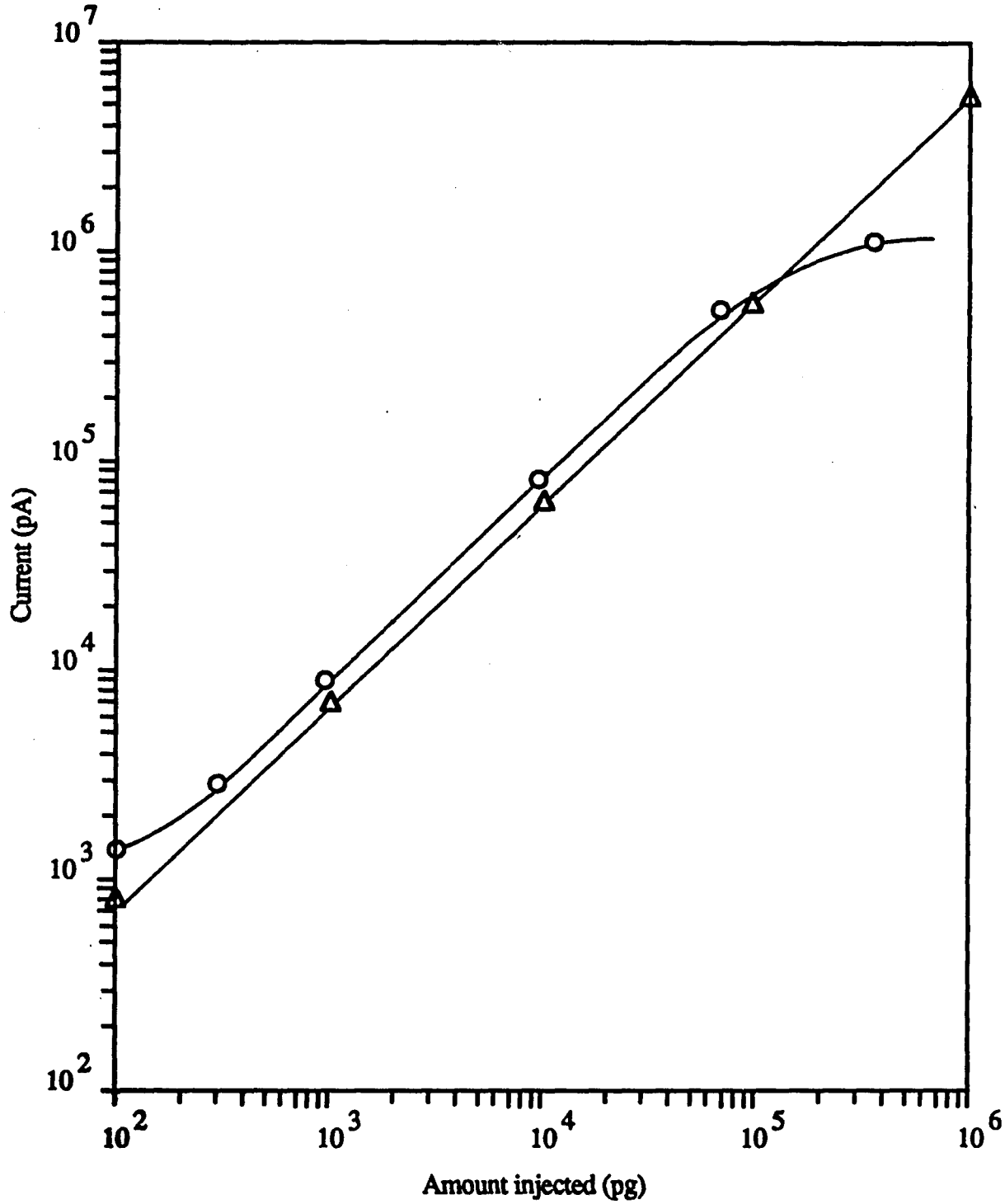

Figure 36. Linearity of the detector response obtained with (O) a continuous silver electrode and (Δ) a silver oxide grid electrode from 20-μL injections of nitroglycerin onto a 150 x 3.9 mm ID μBondapak C-18 column with a mobile phase of acetonitrile-aq sodium perchlorate delivered at a flow rate of 2.0 mL/min. Applied potential was - 1.25 V vs SCE. Other chromatographic conditions same as in Figure 35.

saturation voltage at a current of ca. 15 μA. At a conventional electrode, a non-linear plot leveling-off at concentrations higher than 2.2×10^{-5} M was observed for this same range. Moreover, particularly with dilute electrolyte, very large injection spikes were obtained with the conventional disk electrode and baseline stability was restored only very slowly after each injection of sample. This made the measurement of small peaks difficult. The extension of linear range in situations where a non-linear response is observed at a conventional electrode enabled the grid electrode to be used for quantitation in non-aqueous solutions with dilute concentrations of supporting electrolyte.

Minimum Detection Limits

The detection limit can be expressed in various ways. It is most commonly defined as that quantity of solute introduced into the detector which produces a peak current three times the noise level. In these experiments, the noise was measured as the full peak-to-peak variation in the baseline, recorded over a minimum of 20 time constants. Under conditions of a flow rate of 2.0 mL/min and an applied potential of -1.2 V vs. SCE, the noise levels were 275 pA and 150 pA for the silver disc and silver oxide grid assemblies, respectively, with negligible drift. The amount of analyte corresponding to the detection limit was calculated through linear regression and extrapolation of the respective linear dynamic curves. The minimum detectable quantities for various quinones and nitro-aromatic solutes are listed in Table 13. It is seen that the minimum detectable quantity at the lower part of the linear range is in general on the order of 100-350 pg for each component. Only slight differences exist for compounds which have similar diffusion coefficients, which contain similar functional groups and display similar electrochemical behavior. The detection limits reported here for the continuous silver disc are comparable to those reported with amalgam working electrodes. One disadvantage of operating with the silver oxide grid electrode for compounds such as benzoquinone, p-nitroaniline, 1-chloro-2-nitrobenzene, o-nitrotoluene, and 2,4-dinitroaniline, which undergo reduction at potentials anodic of -1.0 V vs SCE is the higher detection limit relative to that encountered with the continuous silver disc electrode. This effect is the result of the lower information gathering area employed with the grid electrode. The magnitude of this effect will be dependent on the system at a hand; however, a 1.2 -1.5 fold increase in the detection limit appears to be common. However, the potential for increased selectivity associated with the grid electrode can more than compensate for this difference.

Table 13. Detection Limits for Various Test Analytes Obtained Using a Continuous Silver Disc Electrode and a Silver Oxide Grid Electrode.

Compound	Detection Limit (pg) [1] Continuous Silver Disc	Silver Oxide Grid
Benzoquinone	55	82
Acenaphthenequinone	250	300
Phenanthracenequinone	300	330
9-Fluorenone	500	450
5,12 Naphthacenequinone	345	440
Benz[a]anthracenequinone	680	610
Nitroglycerin	90	95
Nitrobenzene	71	85
Nitrophenol	100	125
Nitroaniline	154	205
1-Chloro-3-nitrobenzene	220	265
1-Chloro-2-nitrobenzene	235	305
1-Chloro-4-nitrobenzene	230	290
o-Nitrotoluene	235	285
1,4-Dichloro-5-nitrobenzene	185	240
2,4 Dinitrobenzene	145	235

[1] Amount of analyte which yields a signal-to-noise ratio of 3; on-column detection limits under the following HPLC conditions: column, 150 mm x 3.9 mm I.D. μ-Bondapak C-18; applied potential, -1.2 V vs SCE; mobile phase, acetonitrile-aq. 0.05 M $NaClO_4$ (60/40, v/v) delivered at 2.0 mL/min.

Sensitivity

The sensitivity of the electrochemical technique depends on the chromatographic conditions, the detector design and the electrochemical behavior of the compounds in question. For a given set of experimental conditions, the chromatographic peak heights depend on the retention time and the mechanism of the respective electrochemical reactions.

The sensitivity (i.e., peak current per microgram) of silver and silver oxide grid electrodes was studied by injecting 20-μL samples of various quinones and nitro-compounds at 11 different concentrations ranging from 5×10^{-4} M to 2.5×10^{-7} M. The data taken from thirty injections over a period of nearly 7 hours are summarized in Table 14.

The advantageous feature of using the silver oxide grid electrode over a continuous silver electrode at high potentials is readily seen from Figure 37. Although the sensitivity at the grid electrode is lower than at the continuous silver electrode at low potentials, its signal-to-noise ratio remains almost steady throughout the cathodic potential range examined (0.5 - 1.3 V *vs.* SCE) while that of the continuous silver electrode rapidly deteriorates beyond - 0.85 V *vs.* SCE. Indeed, it is expected that this is the potential region where a composite amperometric detector should give improved signal-to-noise ratios because of its ability to discriminate against noise sources arising from surface processes occurring at elevated cathodic potentials. The virtual independence of sensitivity from applied potential should simplify routine analytical procedures by eliminating the need for frequent standardization.

Reproducibility

The detector reproducibility can be considered in terms of the coefficient of variation, σ / x, where σ is the standard deviation and x is the mean value. The reproducibility of the detector was determined by making 12 repeat injections each of 20 μl aliquots of the quinones and nitro-aromatics at three concentration levels equivalent to an on-column injection of 500 ng, 100 ng and 20 ng The peak heights were calculated as mentioned above and the variance of the data obtained. The results are given in Table 15.

Table 14. Sensitivities Obtained for Various Test Analytes at a Continuous Silver Disc Electrode and at a Silver Oxide Grid Electrode.

	Sensitivity (μA/μg)	
Compound	Continuous Silver Disc	Silver Oxide Grid
Benzoquinone	5.50	5.00
Acenaphthenequinone	2.75	1.83
Phenanthracenequinone	2.50	1.85
9-Fluorenone	2.25	1.75
5,12 Naphthacenequinone	1.65	1.45
Benz[a]anthracenequinone	1.55	1.41
Nitroglycerin	9.50	8.15
Nitrobenzene	8.50	8.62
Nitrophenol	6.75	7.23
Nitroaniline	3.80	3.95
1-Chloro-3-nitrobenzene	3.75	3.60
1-Chloro-2-nitrobenzene	3.45	3.55
1-Chloro-4-nitrobenzene	3.50	3.40
o-Nitrotoluene	4.75	3.60
1,4 Dichloro-5-nitrobenzene	4.75	5.00
2,4 Dinitrobenzene	4.85	4.90
2,4-Dinitrophenol	4.35	4.55
4-Chloro-2-nitroaniline	4.80	4.88

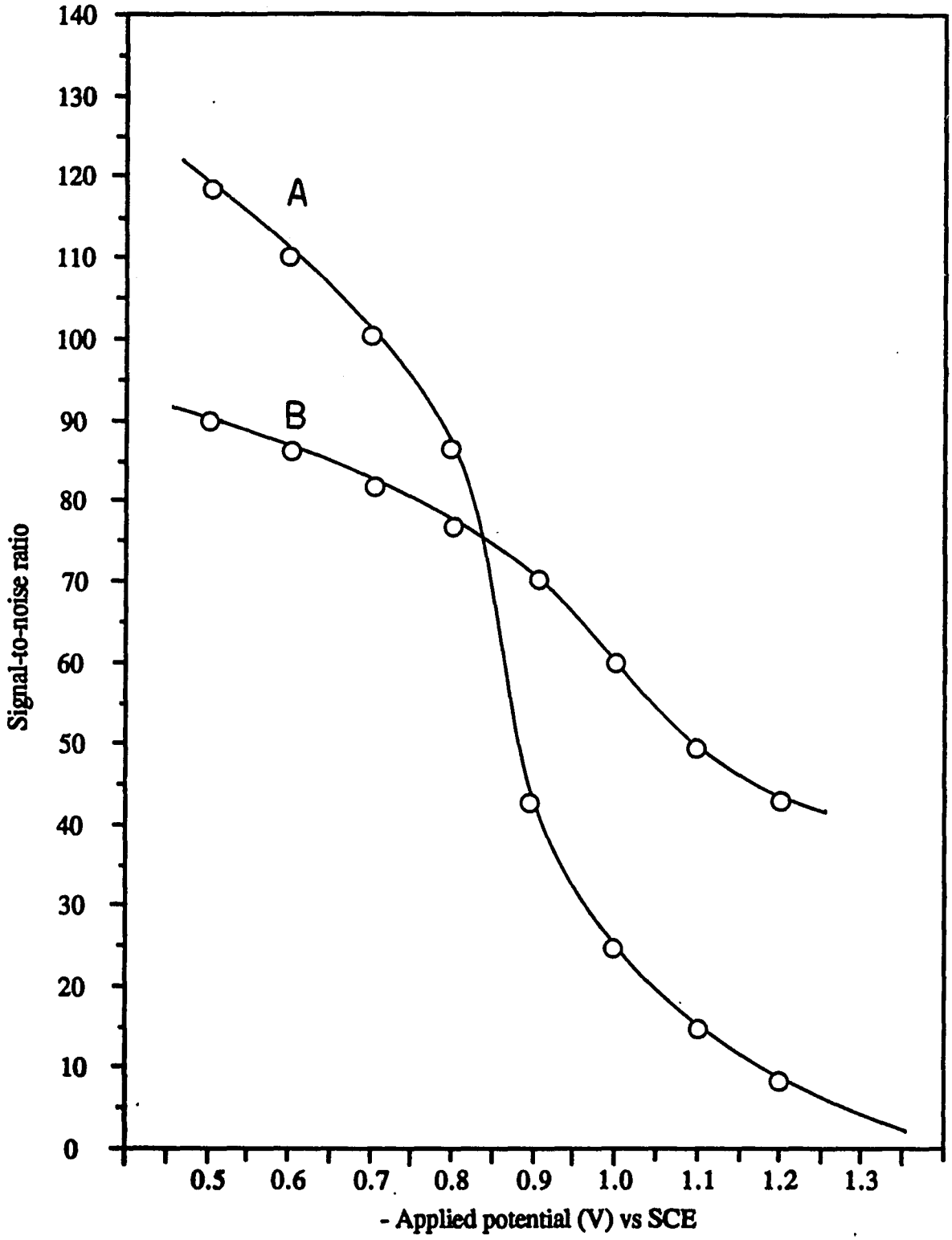

Figure 37. Effect of applied potential on signal-to-noise ratio for (A) continuous silver electrode and (B) silver oxide grid electrode. HPLC conditions: separation column, 150 x 3.9 mm ID μBondapak C-18; mobile phase, acetonitrile-aq 0.05 M phosphate buffer, pH 6.8; flow rate, 2.0 mL/min. Signal measured for 20 μL injections of 1 x 10^{-6} mol/L nitrophenol at each potential setting. Noise was measured as peak-to-peak with an added time constant of 0.3 sec.

Table 15. Within-Day Reproducibility of Continuous Silver Disc Electrode Toward Various Analytes.

	% RSD (n=12)		
Compound	500 ng	100 ng	20 ng
Benzoquinone	1.0	1.8	4.6
Acenaphthenequinone	1.2	2.6	7.2
Phenanthracenequinone	1.6	3.2	5.5
9-Fluorenone	1.8	3.6	4.4
5,12 Naphthacenequinone	1.7	3.1	5.2
Benz[a]anthracenequinone	1.5	2.9	6.3
Nitroglycerin	1.2	2.8	6.7
Nitrobenzene	1.3	2.3	3.5
Nitrophenol	1.8	2.1	4.3
Nitroaniline	1.6	2.5	4.9

Typical values of the relative standard deviations for the test compounds were 1 %, 3 %, and 5 % for 500 ng, 100 ng, and 20 ng, respectively.

The adsorption of electrolysis products and the formation of polymer films can cause the electrode surface to become passive and lose activity. The inherent ability of mercaptobenzotriazole (MBT) to cause electrode fouling upon reduction has been utilized for the estimation of fouling at the continuous silver electrode and the silver oxide grid electrode. The results of the study for consecutive injections at levels of 1 µg and 500 ng in various mixtures of acetonitrile and water are summarized in terms of reproducibility in Tables 16-18. An injection rate of 10 samples per hour was employed. At a conventional continuous silver electrode, the peak currents decrease rapidly in the first 10 min and continue to decrease thereafter at a slower rate. Following 8 repetitive injections of samples, more than 90 % loss of activity is observed at the 1 µg level. A decrease in % RSD at both levels irrespective of solvent type was observed at the continuous silver disc electrode, although passivation was greatly reduced in acetonitrile mixtures. Evidently this loss of sensitivity is due to the irreversible adsorption of MBT on the the silver surface. The decreased passivation in acetonitrile mixtures could be attributed both to an increased solubility of the analyte under investigation in the organic solvent and to a reduction of polymer film formation caused by the interaction with the solvent.

On the other hand, the silver oxide grid electrode shows minimal decrease in the observed sensitivity for MBT following 25 injections at both concentration levels. Even at the 1.0 µg level, variations in peak heights measured from repetitive injections on a single grid surface were highly reproducible, typically with relative standard deviations no worse than 3 %. The limiting current for two different grid surfaces prepared from the same silver substrate agreed to within 5 %. A similar improvement in the reproducibility has been described by Tallman (188) for a silver / Kel-F composite electrode. Comparable reproducibilities were observed for a single electrode from one day to the next, with chromatograph and potentiostat shut down overnight. Between cells, the day-to-day reproducibility was found to vary by less than 5 %. The ability of the grid electrode to resist fouling affords a means of diminishing (though not eliminating) the adsorption problem. One reason for this is that the strong chemical interactions formed between the adsorbed anion of MBT and the silver surface can be decomposed by the surface oxide sites (331-333).

Table 16. Reproducibility of Continous Silver-Based Detector Response Toward Mercaptobenzotriazole (MBT) in Acetonitrile-Water (10+90, v/v).

	1.0 µg	0.5 µg
Injection No.	Peak Height (µA)	Peak Height (µA)
1	5.25	2.6
2	2.7	1.3
3	2.4	1.2
4	2.1	1.1
5	1.6	0.6
6	1.1	0.40
7	0.22	0.35
8	0.50	0.30
9	0.45	0.25
10	0.41	0.22
11	0.36	0.20
12	0.32	0.17

Table 17. Reproducibility of Continous Silver-Based Detector Toward Mercaptobenzotriazole (MBT) in Acetonitrile-Water (80+20, v/v).

	1.0 µg	0.5 µg
Injection No.	Peak Height (µA)	Peak Height (µA)
1	5.15 µA	2.65 µA
2	4.35	1.90
3	3.90	1.90
4	3.25	1.80
5	2.85	1.85
6	2.71	1.75
7	2.65	1.65
8	2.41	1.52
9	2.38	1.45
10	2.36	1.43
Average	3.2 ± 30 %	1.8 ± 19 %

Table 18. Reproducibility of Silver Grid-Based Detector Toward Mercaptobenzotriazole (MBT) in Acetonitrile-Water (10+90, v/v).

	1.0 μg	0.5 μg
Injection No.	Peak Height (μA)	Peak Height (μA)
1	4.75	2.38
2	4.81	2.43
3	4.79	2.41
4	4.69	2.35
5	4.73	2.29
6	4.78	2.41
7	4.71	2.40
8	4.67	2.36
9	4.69	2.35
Average	4.74 μA ± 1.1 %	2.38 μA ± 4.3 %

Peak currents were measured in the flow injection mode by injecting various amounts of MBT at 6 min intervals. The silver oxide grid electrode was held at - 1.25 V *vs* SCE reference. Flow rate was 2.0 mL/min.

Application to Cooling Waters

To illustrate the analytical utility of the silver oxide grid electrode, an ethylene glycol-based automobile antifreeze formulation containing 2-mercaptobenzotriazole (MBT) was analyzed. 2-Mercaptobenzotriazole (MBT) is used frequently as an additive in such samples to eliminate the corrosive effects of oxygen on copper and its alloys. Monitoring of MBT is currently of importance for water-pollution control because of its occasional escape from cooling hardware. Most frequently it is determined spectrometrically or indirectly by gravimetry using batch procedures (334,335). These methods are time-consuming and not compatible with automation. Although the electrochemical behavior of MBT at the dropping mercury electrode (DME) has been well established in static solutions (336), their applicability to continuous on-line transducers incorporating solid electrodes has been severely limited by the presence of excessive amounts of deactivating excipients such as ethylene glycol.

The potential of the silver oxide grid electrode for continuous monitoring of MBT in ethylene glycol based solutions is demonstrated by the precision obtained during an unbroken 3-hr period of operation. A series of 12 determinations were performed by injecting 100 ng, 500 ng, 750 ng of standard MBT made up in ethylene glycol-water (15/85, v/v); the mean peak currents found were 0.48 μA, 2.43 μA and 3.55 μA, respectively; and the relative standard deviations (RSD) for 4 determinations at each level were 1.4 %, 2.3 %, and 3.8 %, respectively. Between-day RSD values were all less than 2.5 %.

The linear dynamic range of the response was also measured for the chromatographic system by injecting various amounts of standard MBT in the range of 1 μg to 100 pg made up in ethylene glycol-water (15/85,v/v) and measuring the peak height. A calibration curve is shown in Figure 38; the slope was 4.75 μA/μg and the correlation coefficient was 0.998. The lower and upper limits of this linear range corresponded to concentrations of 5.0 pg/μL and 50 ng/mL, respectively. An amount of 200 pg of the substance yields a chromatographic peak whose height equals three times the peak-to-peak noise amplitude. For the detector with a solid silver electrode, a substantially narrower linear dynamic range was obtained with the same flow rate, namely, from 0.035 to 25 μg/mL. The calibration curve obtained at the continuous silver electrode for four experimental points had a regression coefficient of 0.987 and a slope of 4.9 μA/μg.

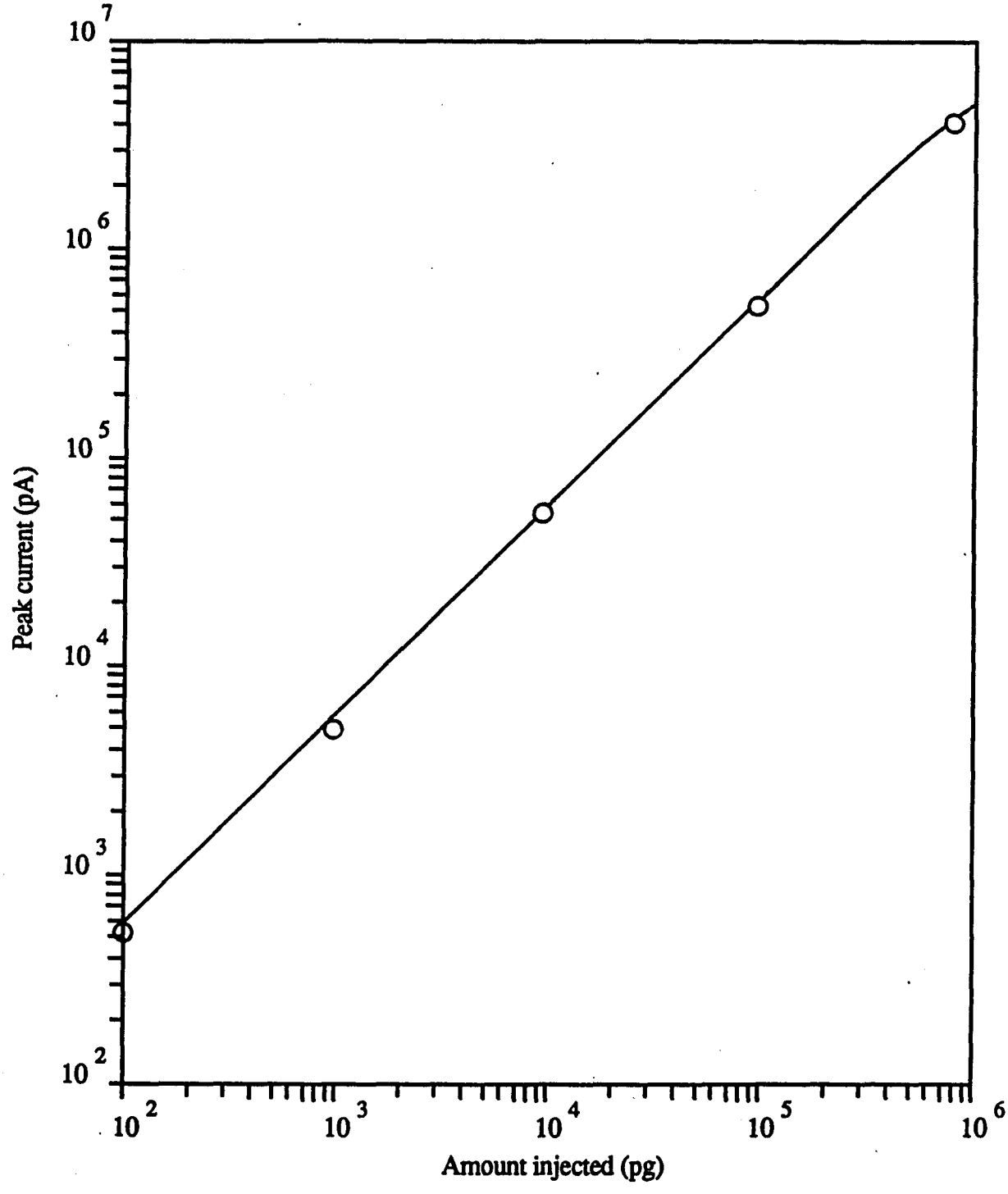

Figure 38. Linearity of silver oxide grid electrode response to 20 µL injections of MBT in glycol-water (15/85, v/v). Chromatographic conditions: column, 150 x 3.9 mm µBondapak C-18; mobile phase, acetonitrile-aq 0.05 M sodium perchlorate (10/90, v/v); flow rate, 2.0 mL/min; applied potential, -1.25 V *vs* SCE.

Table 19 presents the results of the analysis of synthetic blends of mercaptobenzotriazole in glycol mixtures of varying composition. It would appear that for solutions with up to 20% (v/v) ethylene glycol, differences in composition of the mixtures examined had no appreciable effect on the percentage recovery of mercaptobenzotriazole. In this range, the average recovery is 96.7 %. Samples containing as little as 35 ppm MBT were analyzed with good recovery.

The effects of various trace amounts of metals such as copper, zinc and iron on the analytical method are summarized in Table 20, which were found not to interfere in the determination of benzotriazole. However, zinc would cause serious interference when present in concentrations greater then 25 ppm, but such a concentration would rarely be met in practice. The results obtained from a similiar study employing a gold amalgamated electrode are presented in Table 21. The presence of heavy metals in the samples is reflected in a gradual change in the detector response with each injection. The decrease in detector response is due to the accumulation of the metal in the amalgam.

Figure 39 shows a chromatogram of a commercial automobile antifreeze formulation after being diluted 10^5:1 with distilled water to prevent the major components from saturating the detector. No sample pretreatment other than filtering was performed prior to injection. As can be seen, the silver oxide grid electrode detector is sensitive enough to permit direct quantitation of the additive in water samples. The early eluting peaks in the chromatogram most probably represent species which are derived from both the water and reagents. Using the calibration curve shown in Figure 38, the concentration of MBT present in the sample prior to dilution was 2.5 % (w/v) with a RSD of 1.98 % (n=3). When the same sample was re-analyzed using a conventional silver or gold amalgam film electrode, irreproducible results were obtained presumably caused by the deactivating effect of ethylene glycol. This example clearly demonstrates the superior performance of the silver oxide grid design as an LCEC detector for the determination of analytes found in a matrix containing notorious electrode deactivating agents. We attribute this performance to the simple and elegant fabrication process which gave a uniform surface. Moreover, the grid design needs no polishing after the initial polishing treatment.

Table 19. Recovery of Mercaptobenzotriazole from Mixtures of Varying Composition.

Glycol % (v/v)	Water % (v/v)	MBT Added (µg)	Percentage recovery
2.5	97.5	5.00	91
12.5	87.5	50.0	97
12.5	87.5	500	102
25	75	100	88
25	75	250	74

Table 20. Response of Silver Oxide Grid Electrode Toward Mercapto-benzotriazole in the Presence of Metal Ions.

MBT (μg/mL)	Metal	Added (μg/g)	i_p (μA)
5	Blank	0	0.478
5	Copper	25	0.482
5	Zinc	25	0.473
5	Iron	25	0.481
5	Zinc	45	0.350

Table 21. Effect of Gradual Accumulation of Heavy Metals on the Response of Mercaptobenzotriazole at an Amalgam Electrode.

Order of Sample Injection[2]	I / I_0[1]		
	Cu	Pb	Cd
1	0.88	0.94	1.02
2	0.70	0.84	0.94
3	0.53	0.76	0.87
4	0.43	0.69	0.84
5	0.33	0.64	0.85

[1] Ratio of the currents of the amalgam electrode in the presence and absence of interfering metal.

[2] Subsequent injection of 20 µL of 1 x 10^{-2} mg/mL m-dinitrobenzene containing 25 ppm interfering metal.

HPLC conditions: column, 150 mm x 3.9 mm I.D. µ-Bondapak C-18; mobile phase, acetonitrile-0.01M aq $NaClO_4$ (20/80, v/v); flow rate, 2.0 mL/min; applied potential, - 1.35 V *vs* SCE reference electrode.

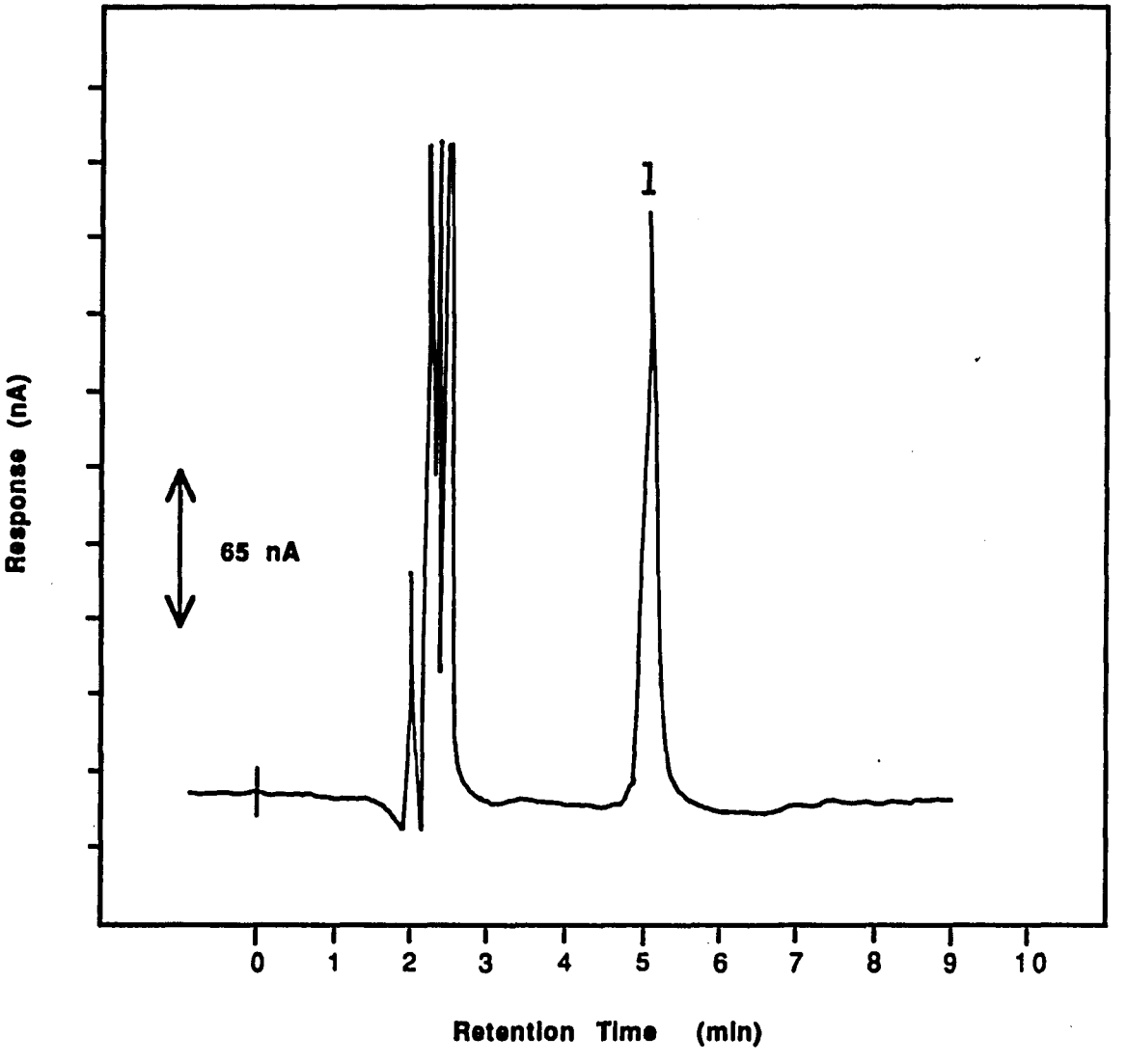

Figure 39. Chromatogram of a commercial automobile water pump conditioner formulation. Chromatographic conditions: column, 150 x 3.9 mm I.D. μBondapak C-18; mobile phase, acetonitrile-aq 0.05 M sodium perchlorate (10+90, v/v); flow rate, 2.0 mL/min; applied potential, -1.35 V *vs* SCE; sample, 20 μL aliquot of 10^{-5}-fold dilution of sample injected. Peak identity: 1, MBT.

The silver oxide grid flow cell was in use for several weeks at a time without any irreversible deterioration of performance. Deactivation, however, can occur if the polarity of the cell is inadvertantly reversed. When this occurs, the stainless steel block becomes corroded and a deposit of iron is found on the silver. The cell is easily restored to its original condition by dismantling and repolishing the silver and stainless steel surfaces.

Conclusions

On the basis of this work, silver is competitive in terms of cost and performance with other available state-of-the-art solid electrodes for use in reductive amperometric detection. The electrode is superior in many respects to gold amalgamated electrodes, the most commonly used reductive detector. The electrode is easier to prepare than gold amalgam, and exhibits superior reproducibility and a much shorter equilibration time when pretreated by alternate potential cycling. Like gold amalgam, it exhibits a wide linear dynamic range, high sensitivity levels and low detection limits. These favorable characteristics are best shown at potentials more cathodic than -1.2 V vs SCE because background current and noise levels in this potential range are more reproducible than at carbon or gold amalgam. Edge effects and spike noise common to amalgamated gold electrodes, caused by a non-uniform surface, were not observed with silver electrodes. Although slightly lower sensitivity levels were obtained for some analytes, silver is more convenient to use on a routine basis.

There are other advantages of using silver as a reductive amperometric detector. Silver can be readily be converted into a composite oxide electrode without cumbersome fabrication procedures associated with array electrodes. The electrode surface design is easy to fabricate and can be readily resurfaced when it becomes fouled. In addition, the electrode is compatible with most mobile phases and is mechanically strong. Like other array sensors, the grid electrode exhibits adjustable signal-to-noise characteristics, flow-rate independence and high precision. Consequently, grid electrodes typically exhibit better detection limits at high applied potentials than attained at solid electrodes under otherwise identical conditions. Unlike previously described composite electrodes, the grid electrode has a substantially longer lifetime, has a larger surface area, does not need to be regularly polished, and does not suffer from the problems caused by a very small current or imperfections of the active surface.

For analytical applications, silver provides a unique flexibility involving a trade-off between sensitivity and enhanced signal-to-noise ratio. A continuous silver disc can be used for maximum sensitivity with relatively "clean" systems where the analytes undergo facile reduction. However, when a matrix is complex and composed of hard-to-reduce analytes, freedom from passivation and large operating range are of paramount importance; operating the detector with a grid type array may simplify the analysis. The only drawback encountered with the use of silver oxide grid electrode was slightly lower sensitivity levels for compounds which are reduced under -0.5 V vs SCE. This, however, is not a major problem since most electroactive analytes of biological and industrial significance usually undergo reduction beyond -1.0 V vs SCE.

Operationally, the silver based detectors are equivalvent to a 10 μL UV cell in terms of band broadening and their response times are quite adequate for flow injection analysis or fast kinetic studies. In addition, these cells do not require frequent dismantling or cleaning, even when the investigated system is changed. Finally, the construction of the various silver designs is simple and operation of the cells does not require special electrochemical knowledge. With regard to over-all performance with standards or with analytes contained within a simple matrix, the continuous silver transducer described is comparable to solid mercury-based detectors. For a complex matrix where surface passivation problems exist or where high potentials are required, the silver oxide grid design is superior to its mercury counterpart.

We think that silver can make a perceptible contribution to the progress of reductive electrochemical detection and constitutes a valuable alternative to the conventional types of mercury electrodes commonly used in reductive amperometry detection.

Part II

Evaluation of Supercritical Fluid Extraction (SFE) as a Sample Preparation Technique

Introduction

Historically, methods for sample preparation have received little attention, although they are critical and often limiting steps in analysis schemes used to quantitate trace analytes. In addition, this step maybe more time-consuming than the actual quantitation procedure. Indeed, advances in the sensitivity and precision of analytical instruments have consistently outstripped development of sample preparation procedures necessary to capitalize on the advances.

Traditionally, off-line techniques such as liquid-liquid extraction (L-L) using either sonication, a separatory funnel or a Soxhlet apparatus, and solid-liquid extraction employing an open adsorption column or more recently solid-phase cartridges, have been used to prepare complex samples for subsequent chromatographic analysis. Although valuable, these techniques are labor intensive and require relatively large volumes of ultrapure solvent. Without a doubt, the most serious drawback associated with liquid extractions concerns the multiple evaporations and dilutions prior to analysis. During these processes, the isolated species is prone both to degradation or transformation caused by heat and to loss caused by several multistep manipulations. In addition, impurities found in common solvents are concentrated and may appear as artifacts in analytical chromatograms.

To overcome problems associated with industrial-scale extractions, such as increased scrutiny under pollution-control laws, increased awareness of solvent toxicity, and increased energy costs of solvent removal, engineers have recently investigated the use of supercritical fluids as extractants. Randall (1) prepared a thorough review on the uses and patents issued up to 1982 in the area of process supercritical fluid extraction. Groves et al. (2) reviewed the properties of supercritical fluids and their advantages for environmental waste cleanup. Two recent texts (3,4) describe both the theoretical and practical aspects of many SFE processes which deal with natural products such as spices, hops, flavors, fragrances, oils and fats or the removal of unwanted components from materials such as caffeine from coffee beans, nicotine from tobacco, polychlorinated biphenyls from transformer oils, and pesticide residues from soil.

Although the groundwork for the asessment of solubility data and fluid-phase equilibria has been established (5-14), progress in the field of analytical-scale SFE has been slow. Furthermore, until recently, instrumentation specifically designed to

implement analytical SFE was not available. There are two major reasons, perhaps, for the limited interest in SFE following its introduction. The first is the concurrent rapid development of HPLC and the second is the lack of widespread understanding of the practical or theoretical aspects of the process.

However, in principle, supercritical fluids offer a number of advantages over liquids for the preparation of samples for analysis by chromatographic and spectroscopic techniques (1-3,15). Chief among these advantages is the potential for comparable or better extraction efficiencies at more rapid rates with higher penetrating power. In addition, the solvating power of a supercritical fluid towards a particular species can easily be manipulated through pressure programming, making possible class -selective fractionations. Furthermore, the mild conditions provided by extraction with carbon dioxide can protect thermally labile analytes. Finally, analytes can be isolated from the supercritical fluid simply by decreasing its density to a subcritical value.

As a first approach to our main objective of incorporating SFE procedures into existing compendial HPLC methods for foodstuffs and pharmaceutical formulations, we report here investigations conducted to establish optimum extraction conditions for the isolation of various quinones. Following optimization studies, attention is focussed on the performance of the collection device and the suitability of this approach for the removal of quinones from solid adsorbents. Finally, the utilization of SFE for multi-step sample fractionations is successfully demonstrated.

Quinones were chosen for study because of their suspected health risk, usefulness in pharmaceutical formulations and industrial processes, and their presence in environmental samples. Furthermore, these compounds are typically encountered at such levels so as to necessitate a sample preparation step or cleanup prior to their determination. The application of SFE procedures in conjunction with LCEC methods for the analysis of pharmaceutical formulations, consumer products, industrial processes, and environmental samples will be described in subsequent chapters.

The use of analytical SFE for the recovery of organics has been investigated by Wright et al. (15), Hawthorne and co-workers (16), and Raymer and Pellizarri (17), especially in regard to environmental studies. For all matrices examined, these

authors reported comparable or higher recoveries for analytes of environmental interest in 30 to 60 min as compared with those obtained with several hours of liquid extraction using a Soxhlet apparatus. Additional work by McNally and Wheeler (18) illustrated a general flow chart for the optimization of parameters used in the extraction of polar herbicides.

Various modes of coupling SFE extraction with chromatographic analysis have also been described (19-29). Early work in this area was reported by Stahl (19) who devised a spray capillary element for directing the supercritical fluid loaded extractant onto a TLC plate. Unger and Roumeliotis (20) have designed a coupling unit for the combination of SFE with HPLC which consists of a microbore column accumulator inserted in place of the conventional loop in an HPLC injection valve. In the inject mode, the extract is eluted from the accumulator and introduced onto the analytical column. Subsequentally, Sugiyama and Saito (21) illustrated the advantages of directly coupling SFE with packed column SFC for the extraction and analysis of caffeine in coffee. McNally and Wheeler (22) reported on sample introduction techniques for SFC which were based on SFE. Systems for the direct fluid injection of supercritical fluid extracts into a mass spectrometer have been explored by Kalinoski et al. (23). Wright et al. (24) have discussed the design of a sophisticated interface composed of heated switching valves for the combination of SFE with capillary GC (24). Hawthorne et al. (25-29) streamlined the instrumentation required for coupling SFE and GC by directly collecting the SFE extract inside a capillary GC column via cryofocusing. These and other techniques for the integration of SFE with other chromatographic methods have been reviewed by Davies et al. (30).

Experimental

Chemicals

P-Benzoquinone; 1,4 naphthoquinone; anthraquinone; 9,10 phenanthracenequinone; 5,12 naphthacenequinone; benz[a]anthracene-7-12-dione; and acenaphthoquinone were obtained from Aldrich and used without further purification.

Apparatus

The SFE extractor unit was based on the design previously described by Scott (31). The laboratory-constructed instrument consisted primarily of four modular

components that included a high pressure fluid delivery system, a thermostated extraction vessel, a precision back-pressure valve and a collection device. A block diagram of this device is shown in Figure 1. An Aminco (model 46-13411) high pressure diaphram-type compressor delivered a steady stream of carbon dioxide to the extraction vessel. This model was chosen because it can compress gaseous carbon dioxide which is drawn directly from a storage cyclinder without the need for dip tubes, auxiliary pressurization sources and pumphead cooling devices. The supercritical fluid was transferred by 1/4 in. O.D. thick wall tubing to a stainless-steel four-way cross bulk union which was mounted to the wall of a drying oven (Lab-Line Instruments). The two side ports of the cross were equipped with a rupture disc type relief valve and a Bourdon pressure gauge. The relief valve, containing a rupture disc rated at 15,000 psi could rapidly vent the pump and extraction vessel should over-pressurization occur. Typically, pressures in the range of 4000 to 9000 psi were used. A stainless-steel insert (1/4 in. O.D. x 3 in. long) joined at the axial port of the cross made connection to the bottom of the extraction chamber.

The extraction vessel most commonly used in these experiments was constructed from a 6 in. length of 3/8 in. O.D. stainless steel tubing sealed with two Swagelok 3/8 in. to 1/4 in. column endfittings. This construction provided safe operation at pressures up to 10,000 psi. Two glass wool plugs were packed into the inlet and outlet ends of the extraction vessel to prevent sample movement in case of sudden pressure surges. The temperature of the fluid in the extraction chamber was maintained constant to $\pm 2^0$C by the drying oven. Extraction temperatures in the range of 45 to 65^0C were generally used.

The outlet of the extraction chamber was connected to a precision metering valve (Autoclave Engineers, P/N 20SC4071), which served to maintain supercritical pressures inside the chamber and to direct the extraction effluent onto a collection trap during depressurization. In the collection mode, the supercritical fluid effluent passed through a drilled out 1/4 in. elbow containing a frit which served to control the expansion of the effluent plume prior to depressurization across the trap. The trap, a 4 in. section of 1/4 in. O.D. tubing, was inserted into the elbow and held in place with a Swagelok 1/4 in. nut. Most frequently, the trap was dry-packed with silica gel, Celite or C-18 bonded phase (Corasil, Waters Assoc., Milford, MA) which was held in place on the low pressure end by means of a frit press-fitted into a 1/4 in. column

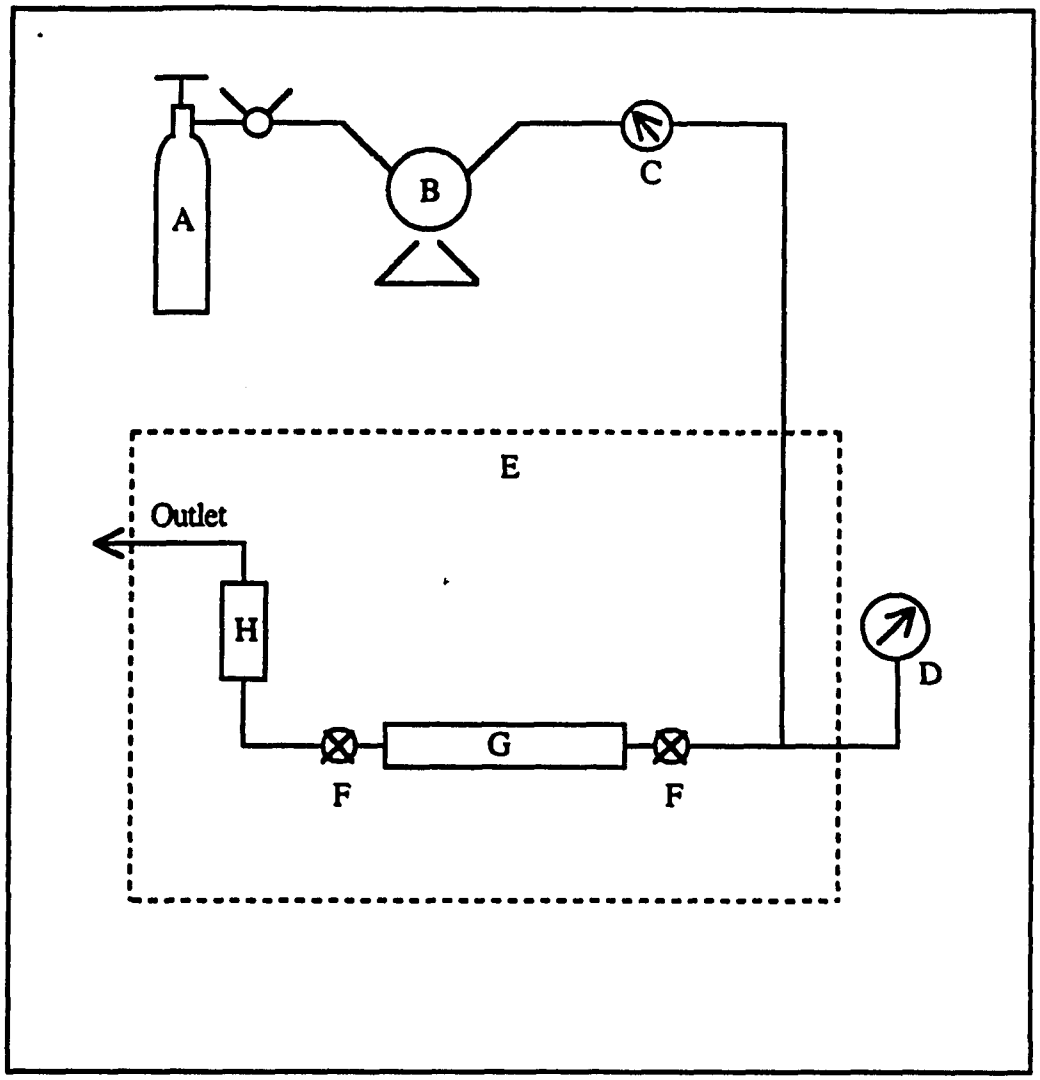

Figure 1. Supercritical fluid extractor. A=carbon dioxide cylinder with high-pressure regulator; B=diaphragm compressor; C=dome-loaded line regulator; D= pressure gauge; E=drying oven; F=metering valve; G=extraction chamber; H=collector-trap.

endfitting. Extreme care must be exercised during collection to prevent aerosol formation and dry-ice plugs which can result in losses in recovery.

Extraction Procedure

The sample to be extracted is loaded into the extraction chamber using a tap and fill manipulation and secured in place with glass wool plugs before the chamber is sealed with the two endfittings. The assembled chamber is inserted into the manifold cross housed in the oven and purged of air with carbon dioxide at a pressure of 100 psi. During this operation, the back-pressure regulator is fully open. When the apparatus has reached the desired temperature, the back-pressure valve is closed and the chamber is then pressurized with supercritical carbon dioxide at the desired pressure and the extraction is then typically allowed to proceed for 15 min. After the extraction is complete, the back-pressure valve is carefully cracked open and the extract-laden effluent was collected across the packed trap. Subsequentially, the trap is disconnected and its contents, including the adsorbent and extracted analytes, are carefully added to a disposible syringe fitted with an in-line filter. Acetone-methylene chloride (50/50,v/v) is passed through the syringe to elute any deposited analytes. The extract is evaporated to dryness in a rotary evaporator maintained at 50^0C and reconstituted in mobile phase prior to HPLC analysis.

Chromatography

HPLC analysis was accomplished with a lab-constructed HPLC with a thin layer reductive mode electrochemical detector (pp. 16-19). A mobile phase composed of acetonitrile-water containing 0.05 M sodium perchlorate (65/35,v/v) provided adequate separation with a short run-time. Based on previous studies (pg. 93), an applied potential of -1.2 V versus SCE offers excellent sensitivity for the 7 quinones. The identity of the quinones was confirmed by comparing the LC retention times with those of authentic samples by co-chromatography.

Results and Discussion

Dependence of Recovery on Pressure, Temperature and Time

In our initial studies, we investigated the effect of pressure on the recovery of benzoquinone, 1,4-naphthoquinone, phenanthracenequinone, anthraquinone,

acenaphthacenequinone, 7-H-benz[a]anthracene-7-one and 5,12-naphthacenequinone from chromatographic paper. Each sample was extracted in triplicate for 20 min with carbon dioxide over the pressure range of 5000 to 8000 psi at 45 and 60^{0}C. The influence of this parameter on the recovery of the 7 quinones is tabulated in Tables 1 and 2 for 45 and 60^{0}C, respectively. For both temperatures, as expected, the percentage recovered increased with pressure. For 6 of the 7 quinones examined, a plateau in recovery was reached near 8000 psi. This is attributed to an increase in the solubility of these quinones in carbon dioxide as its density increases under diffusion-controlled conditions.

Additional extractions were performed to determine the length of time required to yield quantitative recovery of the quinones using pure carbon dioxide and carbon dioxide modified with 5 % by volume of methanol as extractants. These extractions were performed at 8000 psi and 60^{0}C. Extracts were collected at 5 min intervals and analyzed as described in the experimental section. As shown in Table 3, the extractions for each of these quinones were essentially complete during the first 15 min using pure carbon dioxide. As shown in Table 4 for incomplete extractions, enhanced extraction rates can be obtained through the direct addition of 5 % (v/v) of methanol to the matrix prior to extraction.

Instrumental Considerations

An important instrumental consideration for analytical SFE is the collection device used during depressurization. Depending on the exact conditions, it is possible for analytes to form aerosols and be easily lost to the atmosphere. The performance of a packed-guard column as a collection device was evaluated by performing several extractions in which different packing materials were utilized for otherwise identical extractions of 100 µg of anthraquinone from chromatographic paper. The recovery results are shown in Table 5. It is clear that the recoveries and reproducibilities are independent of packing material and are satisfactory for quantitative work.

For comparison, a similar extraction was conducted with a cold trap, constructed from a crimped stainless steel hollow U tube (1/16 in. x 0.005 in. I.D.) inserted in a Dewar

Table 1. Effect of Pressure on Extraction Efficiency Using CO_2 For 20 Min at 45°C.

Quinone	Percentage Recovery [1]			
	Pressure (psi)			
	5000	6000	7000	8000
Benzoquinone	41	48	57	69
1,4-Naphthoquinone	39	44	52	65
Phenanthracenequinone	11	26	32	44
Anthraquinone	56	68	77	84
Acenaphthequinone	14	23	38	55
7H-Benz[a]anthracene-7-one	49	65	73	80
5,12-Naphthacenequinone	16	22	28	42

[1] Each recovery value represents the mean of 3 extractions and determinations at each pressure.

Table 2. Effect of Pressure on Extraction Efficiency Using CO_2 For 20 Min at 60°C.

Quinone	Percentage Recovery [1]			
	Pressure (psi)			
	5000	6000	7000	8000
Benzoquinone	56	67	83	87
1,4-Naphthoquinone	51	60	85	91
Phenanthracenequinone	27	43	71	74
Anthraquinone	54	67	92	96
Acenaphthequinone	31	45	71	80
7H-Benz[a]anthracene-7-one	46	72	90	92
5,12-Naphthacenequinone	19	42	62	77

[1] Each recovery value represents the mean of 3 extractions and determinations at each pressure.

Table 3. Effect of Equilibration Time on Extraction Efficiency Using CO_2 at 60°C and 8000 psi.

Quinone	Percentage Recovery [1]			
	Time (min)			
	5	10	15	20
Benzoquinone	57	72	80	85
1,4-Naphthoquinone	50	71	88	90
Phenanthracenquinone	43	51	69	70
Anthraquinone	60	74	90	94
Acenaphthequinone	59	72	80	84
7H-Benz[a]anthracene-7-one	62	74	80	89
5,12-Naphthacenequinone	38	53	68	74

[1] Each recovery value represents the mean of 3 extractions and determinations for each equilibration time.

Table 4. Effect of Methanol on Extraction Efficiency Using CO_2 at 60°C and 8000 psi For 5 min.

Quinone	Percentage Recovery[1]	
	Pure CO_2	CO_2 + MeOH[2]
Benzoquinone	57	77
1,4-Naphthoquinone	50	75
Phenanthracenequinone	43	67
Anthraquinone	60	84
Acenaphthequinone	59	72
7H-Benz[a]anthracene-7-one	62	81
5,12-Naphthacenequinone	38	57

[1] Each recovery value represents the mean of 3 extractions and determinations with each extractant composition.

[2] Modified carbon dioxide extractant prepared by adding 0.5 mL of methanol to extraction chamber prior to extraction

Table 5. Evaluation of a Packed Trap as a Collector.

Packing Material	Percentage Recovery [1]	RSD (n=3)
Silica	92	3.9
Alumina	87	3.3
Celite	89	2.7
C - 18	92	2.4

[1] Each recovery value represents the mean of 3 extractions and determinations using carbon dioxide at 8000 psi, 65^{0}C for 20 min with each packing material.

of liquid nitrogen. Chromatographic analysis of the trap wash showed an efficiency of only 55 %. Perhaps the efficiency of this simple trap can be improved by packing the hollow tube with stainless steel balls and thus increasing the surface area of the trap.

To further evaluate the efficiency of the packed trap, the exiting carbon dioxide was sampled in a downstream liquid trap. For these purposes, a 8 in. length of 1/16 in. O.D. x 0.010 in. stainless steel tubing, connected in series with the packed guard column trap, was inserted into a 250 mL volumetric flask containing 100 mL of methylene chloride. Following depressurization, the connecting tubing was rinsed with methylene chloride and combined with the main extract. Analysis of the combined extract showed that no breakthrough of the quinones had occurred.

Selectivity

Complex samples often require a class-fractionation step using conventional LC adsorbents following solvent extraction. The development of a single-step class-selective extraction technique offers several advantages for sample preparation, for example, the potential for decreased labor and sample loss. In addition, the possibility of lower extraction limits can be achieved because of the absence of co-extractives. The potential of supercritical fluid extraction to provide class-selective fractionations was investigated by sequentially extracting a sample composed of 200 μg of pyrene, phenanthrene, benzoquinone, 1,4-naphthoquinone and anthraquinone at low pressure and then at higher pressures. The model sample was initially extracted with carbon dioxide at 3500 psi and 60^{0}C for 5 min. The trap was removed and held for analysis by capillary GC/FID. Later, the sample was re-extracted for an additional 15 min at 8000 psi and 60^{0}C. This extract was collected and analyzed using the LCEC methodology described in the experimental section. The chromatographic results for the low and high pressure fractions are shown in Tables 6 and 7, respectively. Approximately 82 % of the PAH's were recovered in the first fraction while greater than 95 % of the quinones were retained on the paper substrate. These quinones were quantitatively isolated in the second fraction after the pressure was raised to 8000 psi. Figure 2 shows the LCEC chromatogram of the high pressure extract. The absence of the interfering components is evident. Although some overlap of components occurred in the two fractions, these results clearly demonstrate the feasibility of supercritical fluids for on-line reasonably efficient fractionations and specific-class isolations.

Table 6. Composition of Low Pressure Extract Obtained with Supercritical Carbon Dioxide at 3500 psi, 60^{0}C For 5 min.

Component	Concentration, μg/g [1]	Percentage Recovery
Pyrene	166	83
Phenanthrene	162	81
Benzoquinone	10	5
1,4-Naphthoquinone	4	2
Anthraquinone	0	0
5,12-Naphthacenequinone	0	0

[1] Analysis by Capillary GC using Hewlett Packard Model 5890 equipped with FID detector. GC conditions: 30 m x 0.025 mm I.D. DB-5 fused capillary column; temperature, 150^{0}C for 2 min, then temperature programmed at 10^{0}C/min to 250^{0}C; Carrier gas, He, 1 mL/min.

Table 7. Composition of High Pressure Extract Obtained with Supercritical Carbon Dioxide at 8000 psi, 60°C For 15 Min.

Component	Concentration, μg/g	Percentage Recovery [1]
Pyrene [2]	28	14
Phenanthrene [2]	24	12
Benzoquinone [3]	176	88
1,4-Naphthoquinone [3]	184	92
Anthraquinone [3]	186	93
5,12-Naphthacenequinone [3]	150	75

1 Each recovery value represents the mean of 3 extractions.

2 Analysis by Capillary GC using Hewlett Packard Model 5890 equipped with FID detector. GC conditions: 30 m x 0.025 mm I.D. DB-5 fused capillary column; temperature, 150°C for 2 min, then temperature programmed at 10°C/min to 250°C; Carrier gas, He, 1 mL/min.

3 Analysis by HPLC with a silver-based electrochemical detector poised at -1.2 V vs SCE.

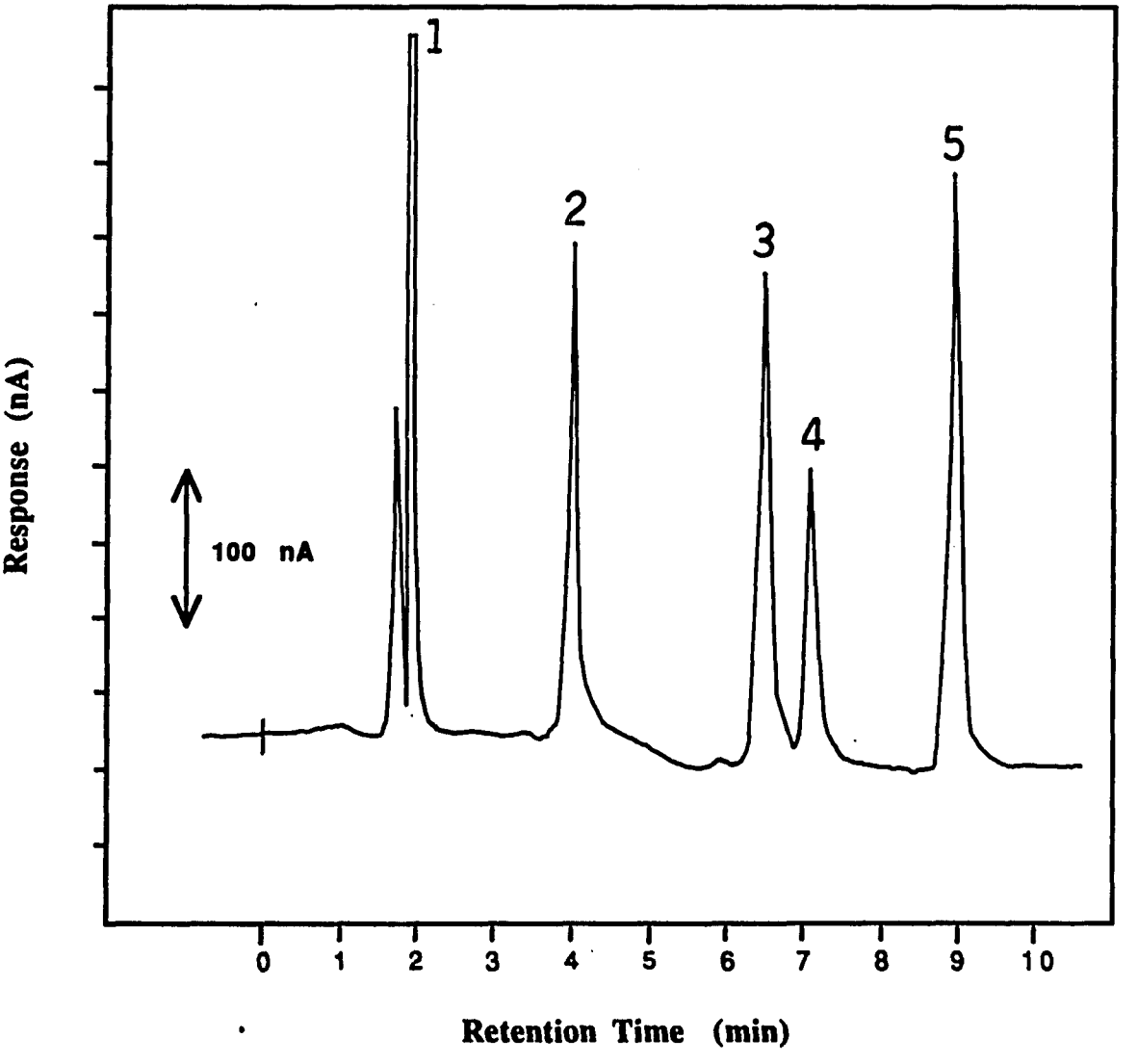

Figure 2. Chromatogram of a series of quinones. Chromatographic conditions: column, 150 x 4.6 mm I.D. Alltech C-8 (10 μm); mobile phase, acetonitrile-aq 0.05 M sodium perchlorate (65+35, v/v); flow rate, 1.5 mL/min; applied potential, -1.2 V *vs* SCE. Peak identities: 1, benzoquinone (83.6 ng); 2, 1,4-naphthoquinone (320 ng); 3, anthraquinone (260 ng); 4, phenanthracenequinone (76 ng); 5, 5,12-napthacenequinone (233 ng).

Minimum Extraction Concentration Levels

Extraction limits for various quinones were estimated by using a challenging matrix such as carbon black (Darco G-60, Fisher Scientific Co.). Two gram samples of carbon black were spiked with progressively lower amounts of the 7 quinones and extracted with carbon dioxide for 15 min at 8000 psi and 60^0C. The extracts were analyzed using LCEC, and the extraction limit for each component was estimated as the concentration level above which the recovery dropped below 75 %. These limits are summarized in Table 8. These limits suggest that SFE can be readily applied to the preparation of solid samples containing various quinones at the trace level.

Reproducibility

The ability of LCEC methods which include SFE sample preparation procedures to yield reproducible results was investigated by extracting and analyzing replicate carbon black samples containing 1,4-naphthoquinone. The coefficient of variation for 5 replicate extractions and subsequent determinations ranged from 2.3 to 4.9 % for within-day work and from 3.4 to 7.6 % for between-day studies. In general, this level of precision compares well with conventional LC methods incorporating liquid extraction techniques.

Table 8. Minimum Extraction Concentration Levels For Various Quinones.

Quinone	Extraction Limit, μg/g
Benzoquinone	5
1,4-Naphthoquinone	1
Phenanthracenequinone	20
Anthraquinone	3
Acenaphthequinone	15
7 H-Benz[a]anthracene-7-one	10
5,12-Naphthacenequinone	25

SFE conditions: 8000 psi, 65^{0}C for 20 min.

Silica trap, eluted with acetone-methylene chloride (50/50, v/v).

Quinones determined with a silver-based electrochemical detector poised at -1.2 V vs SCE.

Conclusions

The scope of sample preparation has been expanded by the sucessful demonstration of the utility of supercritical carbon dioxide in analytical extractions. SFE has been shown to be a useful method for the rapid and low temperature recovery of quinones from low moisture solid samples. The procedure is simple and provides relatively clean extracts suitable for direct chromatographic analysis within 20 min. In fact, each extraction and analysis required approximately 40 min to complete including weighing the sample, assembling the extraction train and performing the extraction and subsequent LCEC quantitation. In contrast to liquid solvent extractants, the polarity of the supercritical carbon dioxide can be altered dramatically by simply adjusting the temperature and pressure. This degree of selectivity affords the potential for analytical fractionation in conjunction with extraction. In addition, this method is well suited to small as well as large samples. Furthermore, ease of solvent removal and extract concentration provides the potential for facile interfacing with most modern chromatographic analysis schemes. Finally, carbon dioxide is non-toxic and is readily available in high purity.

The analytical value of this technique as an alternative method of sample preparation can only be manifested through its successful incorporation into routine HPLC or GC screening procedures. Possibilities include the determination of trace levels of pharmaceuticals, vitamins, pesticides, and suspected carcinogens.

Part III. Development and Validation of HPLC Methods Which Involve Supercritical Fluid Extraction Prior to Reversed-Phase HPLC with Electrochemical Detection (LCEC)

Part III Chapter 1

Determination of Anthraquinone in Paper and Wood.

Introduction

Pulping decomposes lignin (a very complex molecule consisting of more or less oxidized methoxy-rich phenylpropanoic units connected by ether and C-C linkages) to a number of phenols and other aromatic compounds. During wood pulping operations, anthraquinone is added in catalytic amounts to aid delignification, stabilize carbohydrates, and to increase pulp yield (1). Methods for the analysis of wood and paper generally require a multi-step procedure involving extraction and clean-up prior to quantitation.

In terms of instrumentation, the procedures for the quantitation of anthraquinone are diverse. High-performance liquid chromatography (HPLC) with UV spectrophotometric detection (2) or on-line post-column reduction and UV detection (3), straight electrochemistry (without HPLC) using either chemical reduction of anthraquinone and electrochemical oxidation of the product (4), or differential pulse polarography (5), or gas chromatography (GC) and GC-mass spectrometry (MS), (6, 7) have proven most popular.

Several isolation procedures involving time-consuming Soxhlet extraction or multiple solvent extractions have been reported. A commonly used procedure described by Currah (7) utilizes a 5-19 hour extraction with chloroform, followed by concentration of the extract prior to LC analysis. The non-selective nature of extraction results in a "rich extract" which prevents accurate quantitation of anthraquinone below 0.5 ppm. In another procedure developed by Bröenstad and co-workers (2), wood samples are subjected to steam distillation prior to liquid extraction with isooctane. The isooctane was subsequently evaporated in a rotary evaporator and the extract was reconstituted in methanol for measurement. However using this multi-step procedure, only about 60 % of the anthraquinone was recovered due in part to the formation of emulsions. Nelson and Cletek (8) avoided these problems by using a Waters C-18 Sep-Pak® to isolate anthraquinone from black liquor, followed by HPLC-UV. UV detection offers little selectivity, responding to anthraquinone and to other compounds co-extracted with it. The reported limit of detection is only 0.2 μg (8). All of these preparation techniques suffer from shortcomings of phase separation difficulties, transfers, evaporations, and considerable preparation time.

The extraction of anthraquinone from Kraft paper and pine plywood fortified with

anthraquinone using supercritical fluid CO_2 is reported here. Anthraquinone is determined in the extract using HPLC with electrochemical detection at a silver electrode. This method is rapid, highly selective and sensitive to subnanogram levels of anthraquinone in paper and wood.

Experimental

Chemicals

9,10-Anthraquinone (Sigma) was used without further purification since HPLC and GC-MS showed essentially one peak. Acetonitrile, methylene chloride, and acetone were HPLC grade. The HPLC eluent was 80-20 (v/v) acetonitrile-aqueous pH 6.8 buffer (0.025 M each KH_2PO_4 and Na_2HPO_4). CO_2 was bone-dry grade.

Apparatus

An HPLC chromatograph was assembled from a Varian 8500 syringe pump, a Rheodyne 7125 sampling valve with a pneumatic sample degasser and loading device and a 20-µL sample loop, and a lab-built electrochemical detector. The column was 150 mm x 3.9 mm I.D., packed with 10 µm µ-Bondapak C-18 (Waters Assoc.). The eluent was degassed by bubbling extensively with helium. The electrochemical detector was of the conventional thin-layer amperometric design (pp. 16-19) and employed a silver working electrode, stainless steel auxiliary electrode and a calomel reference electrode. To minimize movement and noise pick-up, the cell was mounted in an inner well of the chromatograph box supporting the injector and column panel. Signals from the EC detector were monitored with a peak detector (pp. 30-32) and recorded on a Linear model 1200 strip chart recorder (Linear Instruments, Irvine, CA).

Preparation of Standard Solutions

A stock anthraquinone solution was prepared weekly by dissolving 114 mg of anthraquinone in methanol in a 100 mL volumetric flask. Using a gas-tight syringe with an 18-gauge needle, calibration solutions covering the range of 11.4 to 114 µg/mL were prepared daily by appropiate serial dilution of the stock solution.

Polishing Procedure

The block containing the silver electrode was polished first on an optical flat with a 600 grit silicon carbide (Buehler) slurry using a figure-of-eight motion, until the silver appeared flush with the Kel-F. It was then lapped on a Texmet pad (Buehler) with a 600 grit silicon carbide using a back-and-forth motion until the silver acquired a mirror finish. Next it was polished on a 2-7/8 in. diameter wheel spinning at 45 rpm, with a 0.5 μm alumina (Buehler) slurry using a V-motion. Finally, the block was polished with 0.05 μm alumina on Microcloth (Buehler). The stainless-steel auxiliary electrode block was first polished with a 600 grit silicon carbide slurry, and finally with 1 μm diamond paste (Buehler) on Microcloth. Repolishing of the silver was required after about 100 injections, or about three times per week in continuous use.

Extraction Procedure

To carry out an extraction, about 6 strips (3 in. x 1/2 in., accurately weighed) of Kraft paper previously soaked and dried, or approximately 0.5 g of pine plywood sawdust were packed into a 3/8 in. O.D. by 6 in. long extraction chamber and held in place with glass wool. The paper and sawdust samples were fortified with anthraquinone deposited from a stock solution in methylene chloride and dried before being loaded into the chamber. The extraction chamber was assembled into a laboratory constructed extraction train (pp. 124-125), brought to 65^{0}C, flushed briefly with atmospheric pressure CO_2, the exit valve closed, and the sample pressurized to 8000 psi and equilibrated for 20 min. The exit valve was then carefully opened to bleed out the extract-laden CO_2, and the extract collected on the silica gel trap. The silica trap was washed with methylene chloride-acetone (50/50, v/v), the solution evaporated in a rotary evaporator to dryness, and the residue reconstituted in 10 mL of mobile phase for HPLC.

GC-MS

For comparision with the HPLC-ECD, some extracts were analyzed by GC-quadrupole MS using a Hewlett-Packard 5988 A system with a Hewlett-Packard 1000 data system. A 30 m x 0.025 mm I.D. DB-5 fused-silica capillary column (J & W Scientific) was used. The initial temperature, 150^{0}C, was held for two 2 min followed by temperature programming at 100^{0}C/min to 250^{0}C where it was held 20 min.

Results and Discussion

Chromatography

The composition of the mobile phase was optimized to effect the best separation for anthraquinone in terms of peak shape and retention time. For these studies, repeated injections of 2.28 μg were made, with the mobile phase being systematically varied through the range of 50 to 90 % acetonitrile. A comparison of the chromatograms obtained with each mobile phase composition showed the best separation characteristics were obtained with acetonitrile-water (80/20, v/v). This composition gave a sharp peak for anthraquinone with a retention time of 7.5 min. Lower percentages of acetonitrile resulted in decreased column life and extremely long retention times.

Hydrodynamic Voltammogram

Figure 1 shows the hydrodynamic voltammogram of anthraquinone on the silver electrode. The peak current reaches a plateau at about -1.1 V vs. calomel, which is the potential used in all subsequent experiments. The difference in the value of the applied potential at 75% of the plateau current and that at 25% of the plateau current is 82 mV, indicating the reduction of anthraquinone under these conditions is not fully reversible. Reversibility is inferred from a value of 28.2 mV for the potential difference at these two currents, for a convective diffusion-controlled 2-electron process (16).

Effect of Flow Rate on Response

As indicated in Figure 2, at effluent flow rates up to about 100 mL/h, the peak current increases approximately with the 1/3rd power of the flow-rate. This suggests that the reduction current is controlled by convective mass transport (17). Since the response becomes independent of flow rate at higher flows, 2 mL/min was used in subsequent experiments.

Response to Anthraquinone

A series of standards in the concentration range from 114 μg/mL to 1.2 μg/mL was used to investigate detector response. The resulting peak currents at -1.1 V vs calomel and 2 mL/min are plotted vs weight injected in Figure 3. The response, as shown in Figure 4, is a linear function of weight injected, with a slope of 1.0, over at least 4 orders of magnitude of sample weight. The noise level was 300 pA, so that at a signal-to-noise ratio of 3, the minimum detectable quantity is 210 pg.

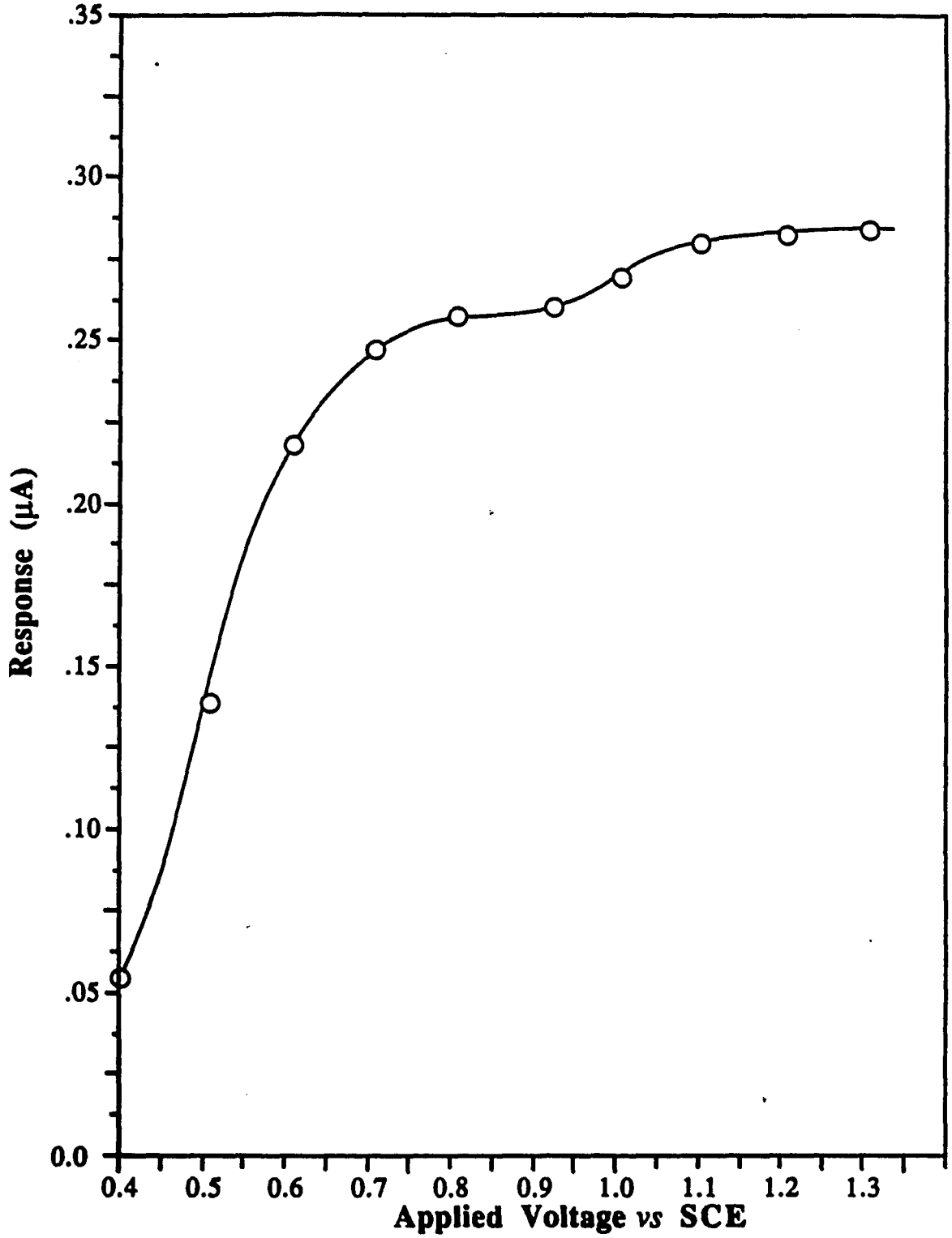

Figure 1. Hydrodynamic voltammogram of anthraquinone on silver electrode vs. SCE. Chromatographic conditions: column, 150 x 3.9 mm I.D. μ-Bondapak C-18 (10 μm); mobile phase, 80/20 (v/v) acetonitrile-aqueous 0.05 M phosphate buffer (pH 6.8); sample size, 0.44 μg anthraquinone per 20 μL mobile phase injected at each potential setting.

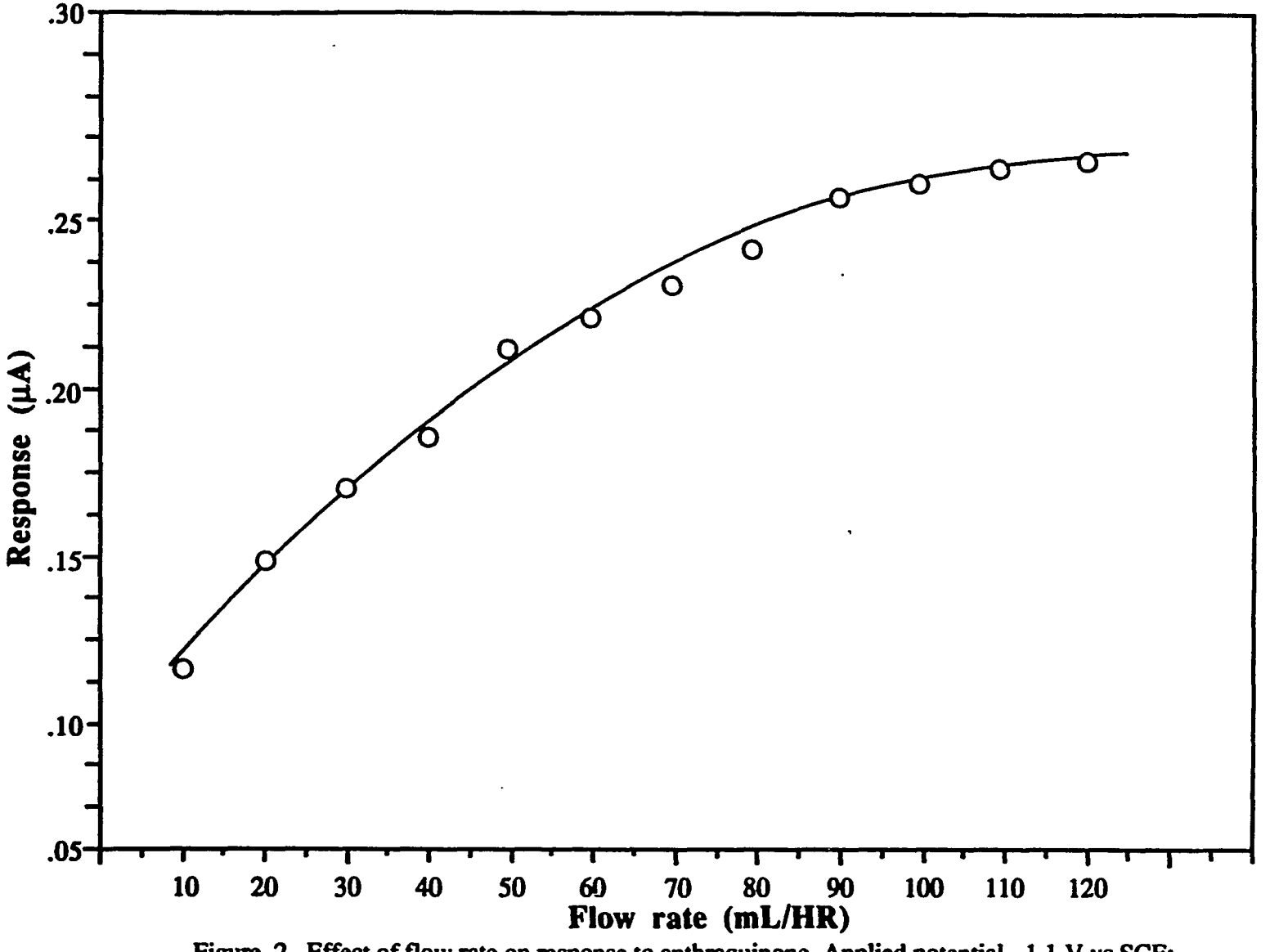

Figure 2. Effect of flow rate on response to anthraquinone. Applied potential, -1.1 V vs SCE; other chromatographic parameters as in Figure 1. Equation of the curve is $I_p = F^{0.352}$

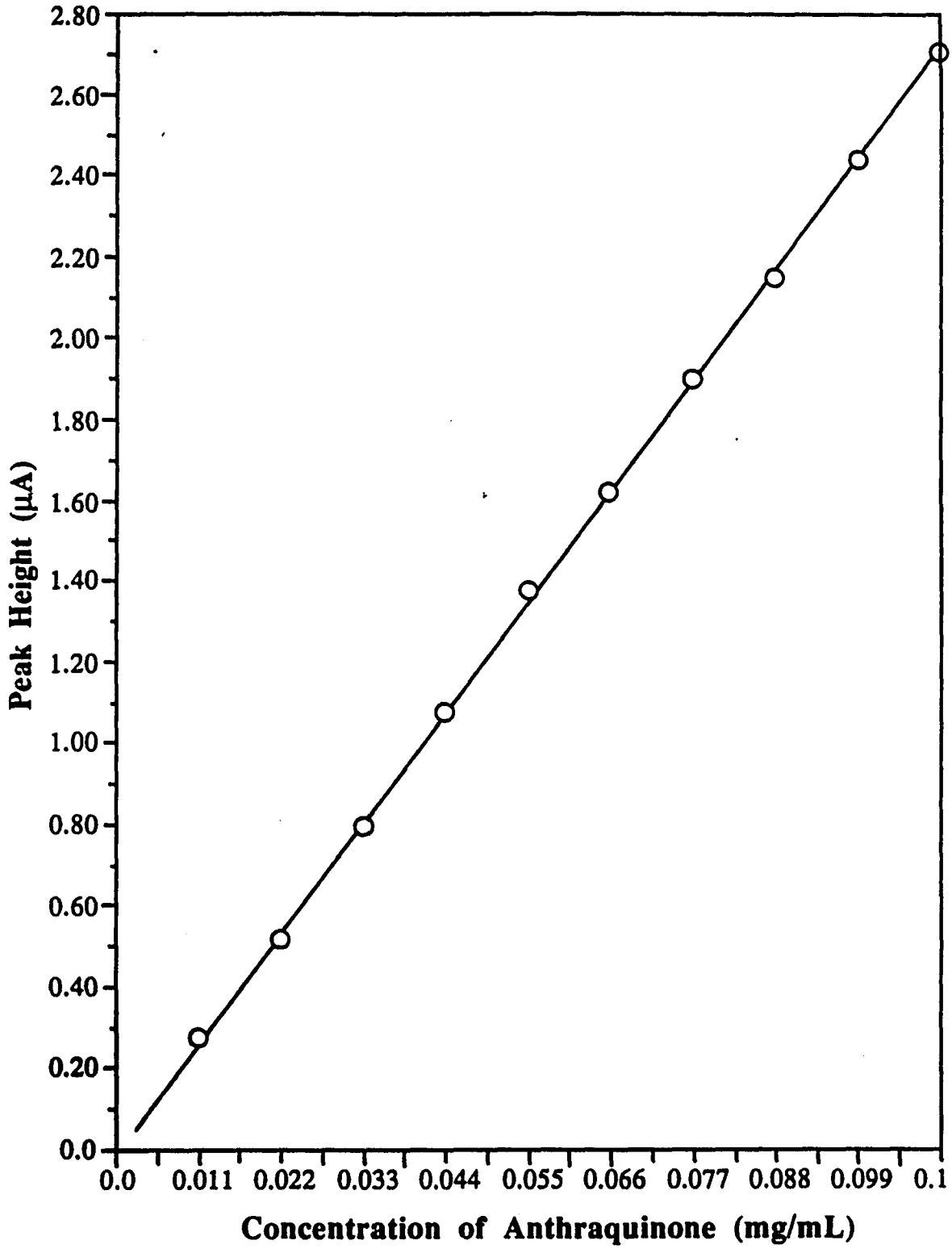

Figure 3. Calibration curve for anthraquinone obtained from 20 μL injections onto a 150 by 3.9 mm I.D. μ-Bondapak C-18 column with a acetonitrile-(pH 6.8) phosphate (80/20, v/v) mobile phase. Flow rate was 2.0 mL/min. Potential of silver working electrode was -1.1 V vs SCE.

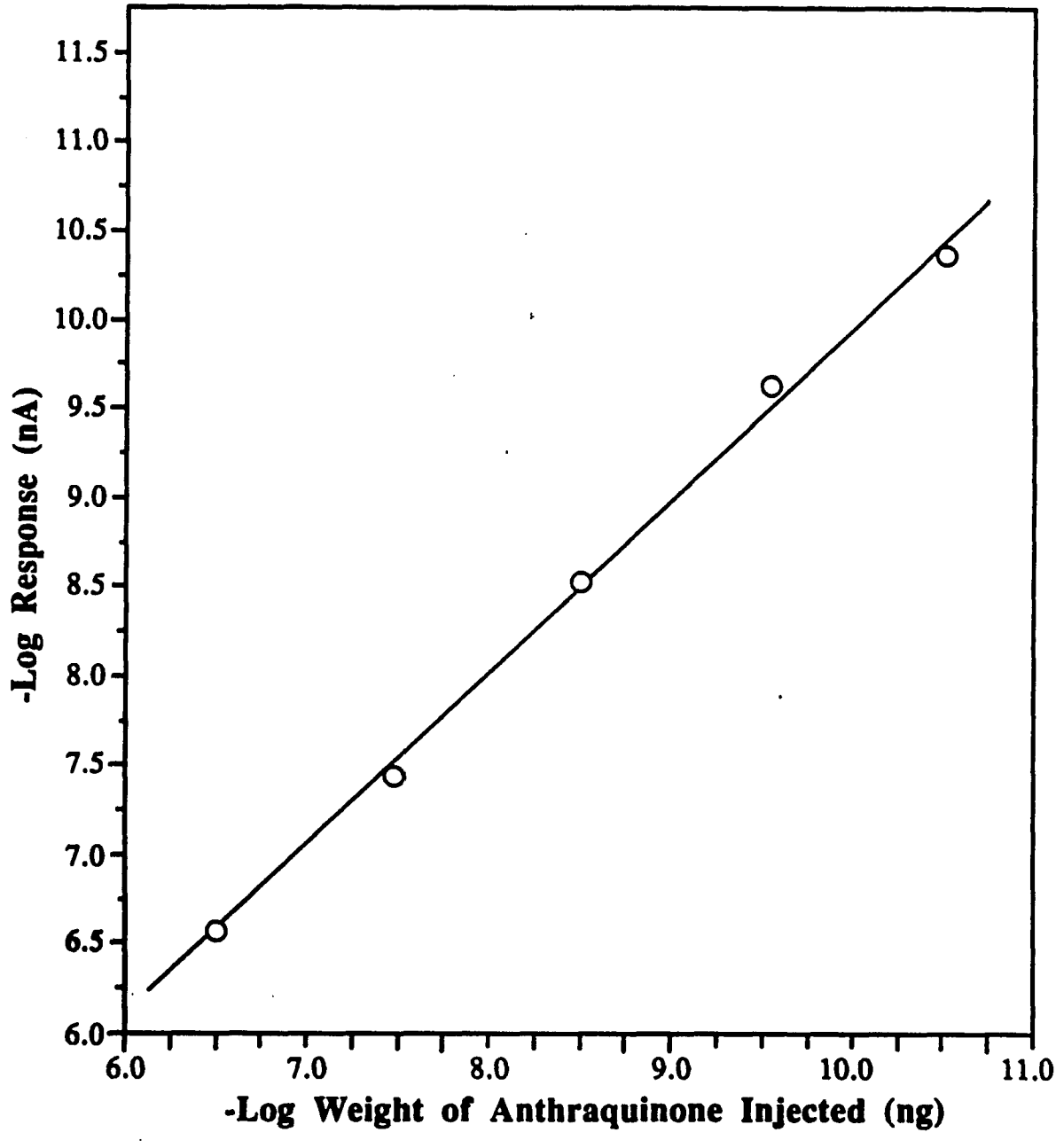

Figure 4. Linearity of detector response to amounts of anthraquinone in 20 µL samples. Chromatographic conditions: column, 150 x 3.9 mm I.D. µ-Bondapak C-18; eluent, 80/20 acetonitrile-0.05M phosphate buffer (pH 6.8); flow rate, 2.0 mL/min; applied potential of working electrode, -1.2 V *vs* SCE.

SFE Efficiency

Ability of supercritical fluid CO_2 to extract anthraquinone was assessed by spiking 300 mg of Kraft paper strips (3 in. x 1/2 in.) and 500 mg sawdust samples with levels of anthraquinone varying from 50 μg to 1 mg for the the paper and 3 μg to 500 μg for the sawdust. As shown in Table 1, good recoveries from the paper were obtained down to lowest level studied. In the case of sawdust, however, the percentage extracted under the conditions used falls off below about 10 μg anthraquinone, presumably because it is strongly adsorbed to some active site on the wood. It is clear from the data that approximately 1 μg is effectively irreversibly adsorbed, which accounts for the percentage extracted value.

To examine the effect of the extraction time for the procedure, pine samples containing 100 μg of anthraquinone were extracted for 5, 10, 15, and 20 min at 8000 psi and 60^0C. As shown in Table 2, the bulk of the anthraquinone was recovered in the first 15 min. Twenty min extractions yielded slightly more anthraquinone, and the recoveries from 30 min extractions were the same as these. Therefore an extraction time of 15 min was used for all samples.

Analytical Precision

The daily repeatability of the method was evaluated for the percentage recovery from the sawdust samples. The average precision (coefficient of variation) for the three extractions at each level of spiking was 2.2 %, which was approximately independent of the level of anthraquinone added. The day-to-day precision was determined by extracting sawdust spiked at five different levels (2 μg to 10 μg) on each of the five consecutive days. The average recovery was 93.2 % with an average coefficient of variation of 3.8 %, again almost independent of anthraquinone added.

Comparison with Soxhlet Extraction

One of the advantages of SFE is speed; a 20 min extraction gives >90% recovery. Soxhlet extraction of spiked Kraft paper samples with acetonitrile or methanol, however, required at least 4 h to reach 82% recovery. After 1 h, 16 % was extracted, after 2 h, 39 %, 3 h, 61 %, and 4 h, 83 %. In addition, there are no emulsions or other technical difficulties with supercritical fluid extraction, no light or air; and fewer impurities in CO_2 than in ordinary solvents.

Table 1. Determination of Anthraquinone in Paper and Wood.

Kraft Paper		Sawdust	
Weight added (mg)	Recovery %	Weight added (mg)	Recovery %
1.0	101	0.5	94
0.75	98	0.25	97
0.50	96	0.10	90
0.40	97	0.05	91
0.25	100	0.01	83
0.20	93	0.005	76
0.10	89	0.003	68
0.05	93		

Table 2. Optimization of equilibrium Time at 65°C and 8000 psi.

Time (min)	Percentage Recovery
5	60.0
10	75.7
15	91.0
20	92.3
30	91.7

Two gram pine samples fortified with 100 µg anthraquinone were extracted, in triplicate, for each equilibration period.

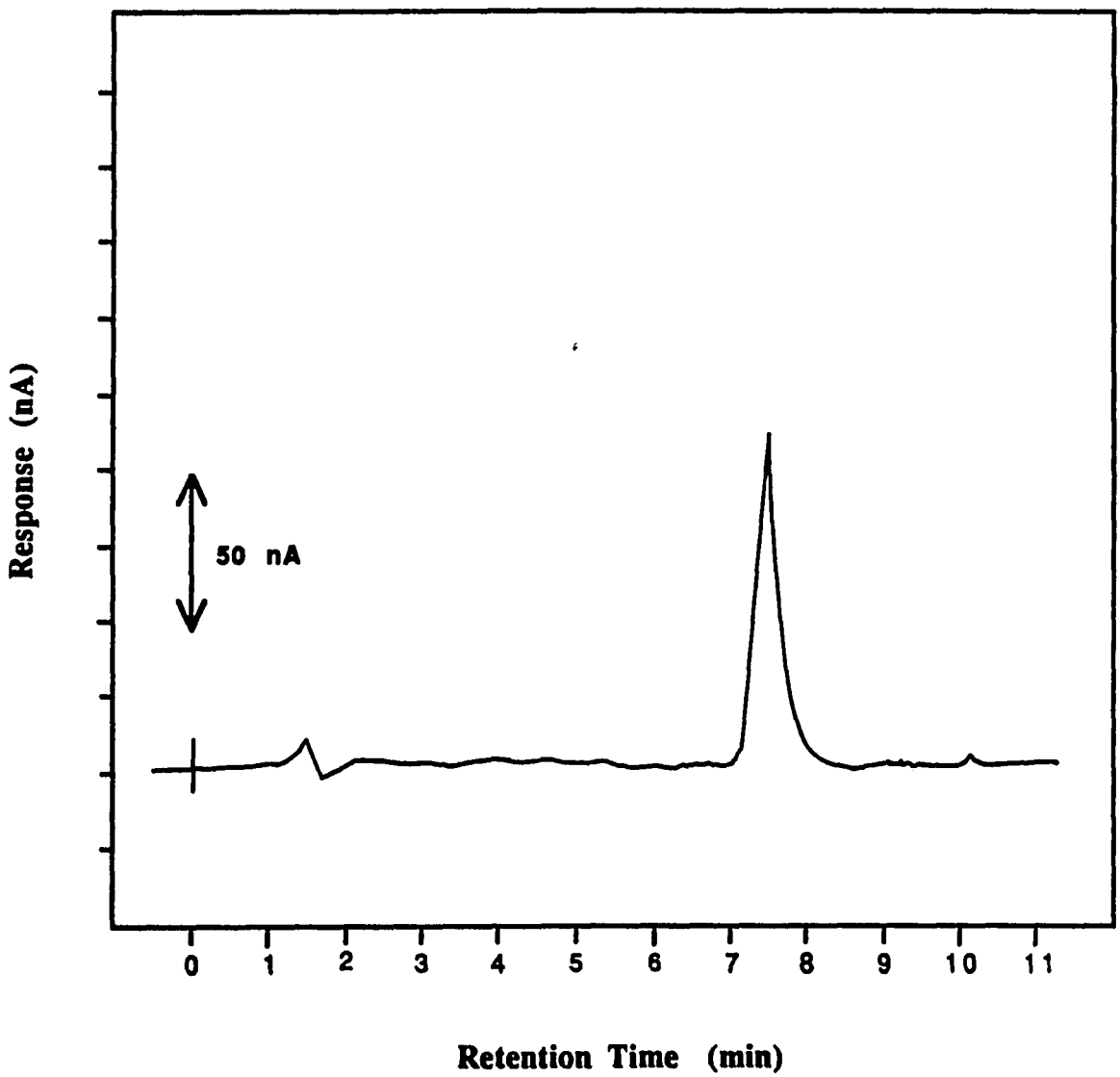

Figure 5. HPLC-ECD chromatogram of supercritical fluid extract of sawdust spiked with 44 μg anthraquinone. Chromatographic conditions as in Figure 1. Extraction conditions: SFE at 8000 psi CO_2, 65^0 C, 20 min.

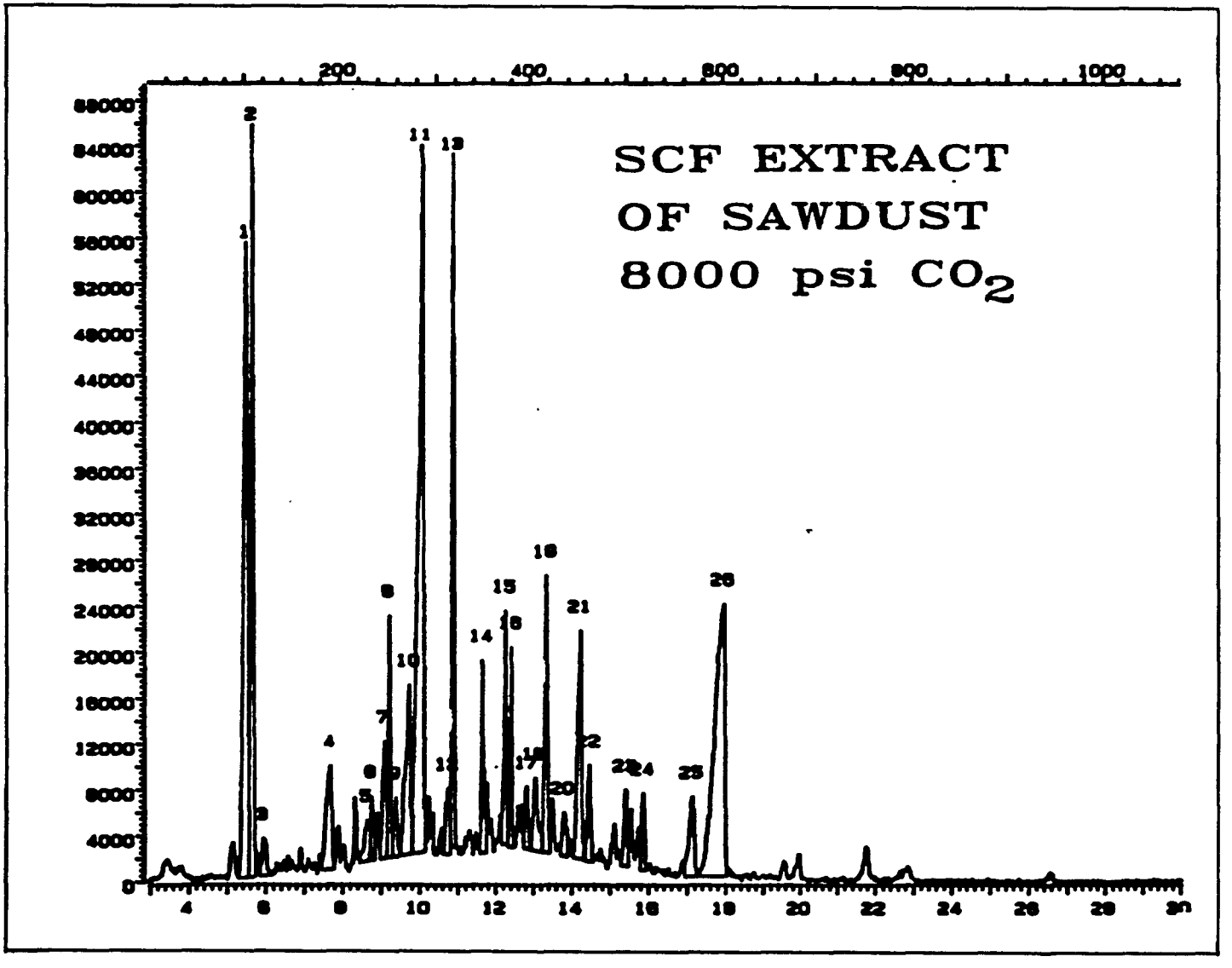

Figure 6. GC-MS chromatogram of a supercritical fluid extract of a sawdust sample spiked with 0.44 µg of anthraquinone. Extraction conditions: 8000 psi CO_2, 65^{0}C, 20 min.

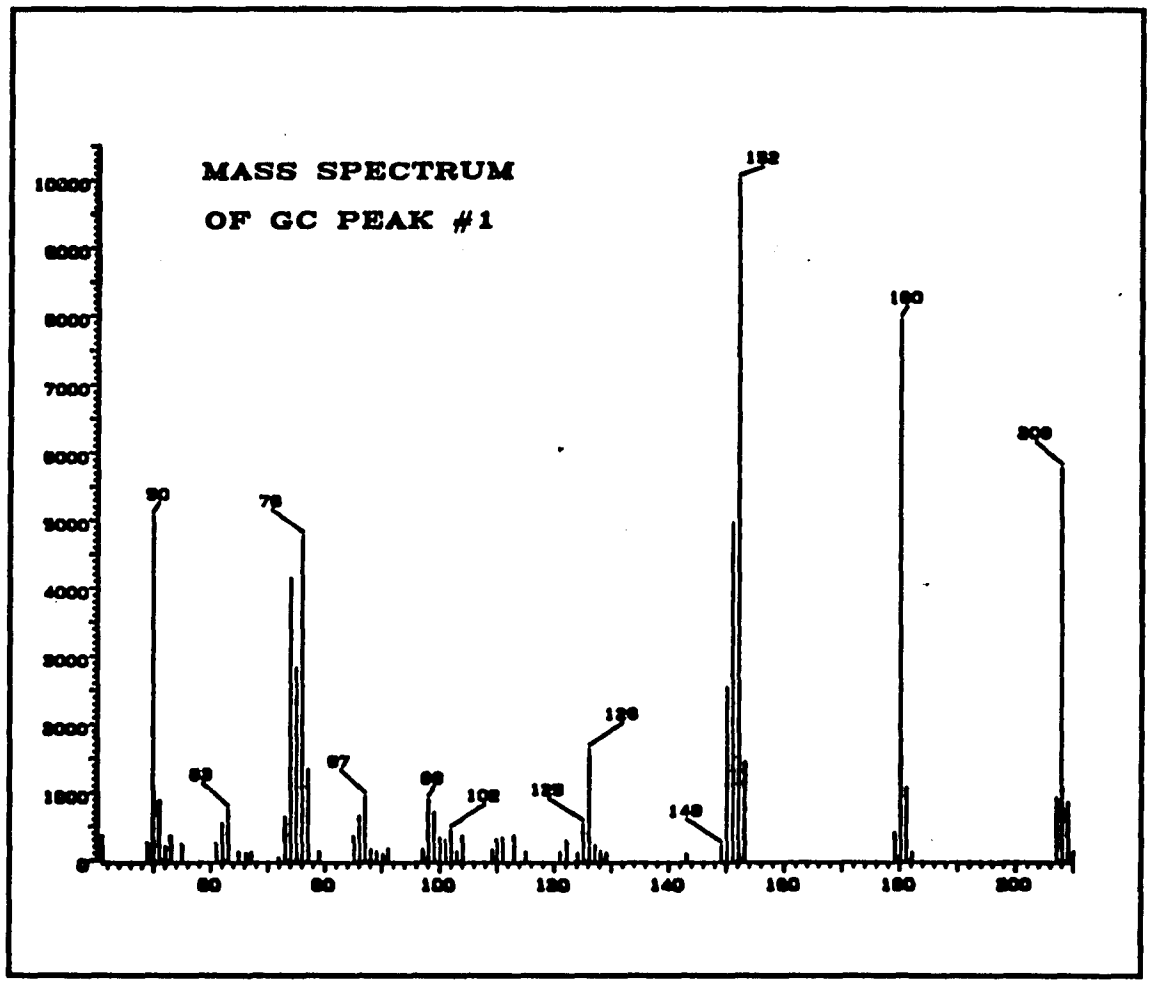

Figure 7. Mass spectrum of GC peak 1 in Figure 6. Extraction conditions: 8000 psi CO_2, 65 ^{0}C, 20 min. GC conditions: 30 m x 0.025 mm I.D. DB-5 fused-silica capillary column; temperature, 150 ^{0}C for 2 min, then temperature programmed at 10 ^{0}C /min to 250 ^{0}C; carrier gas, He, 1 mL/min.

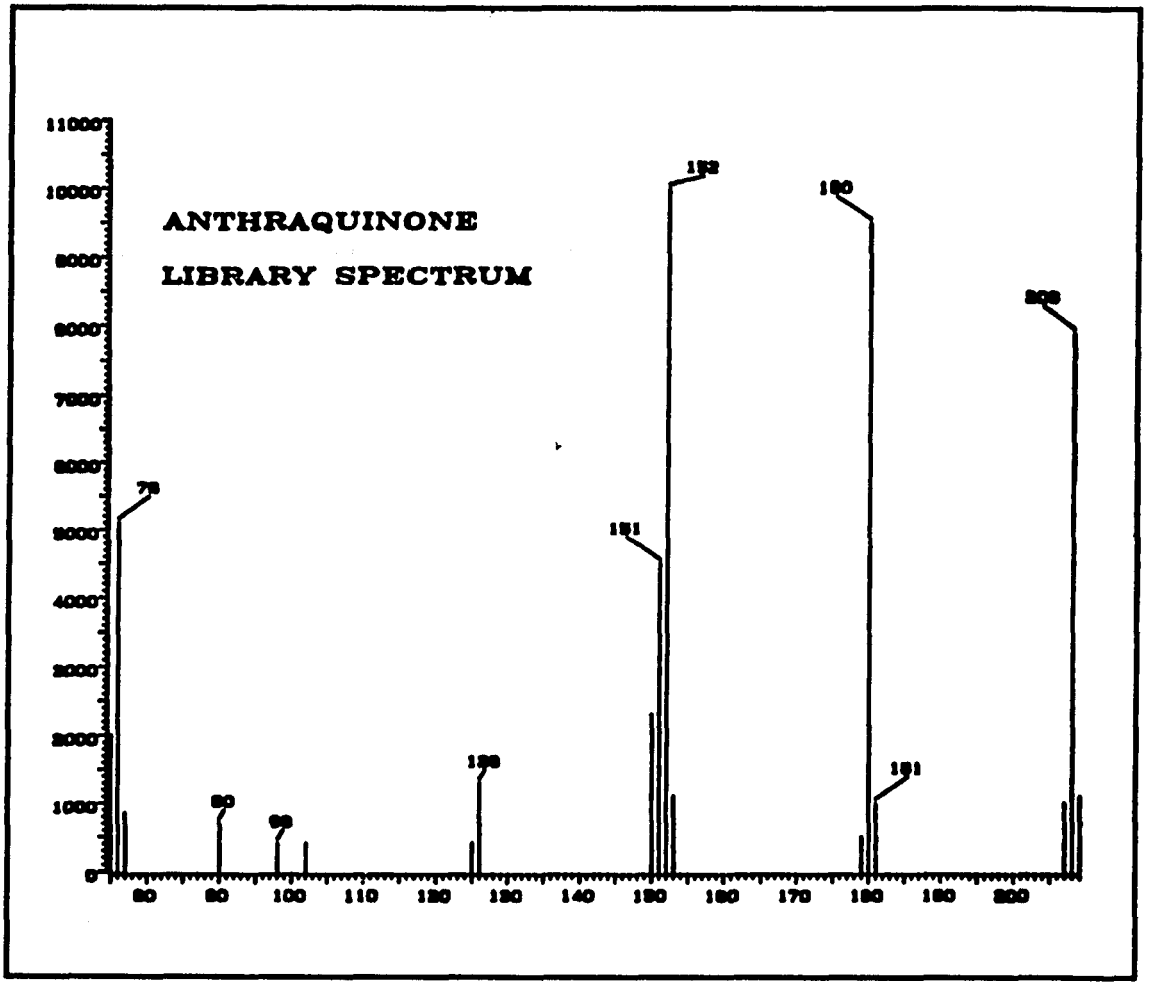

Figure 8. Library standard mass spectrum of anthraquinone. Extraction conditions: 8000 psi CO_2 , 65 ^{0}C, 20 min. GC conditions; 30 m x 0.025 mm I.D. DB-5 fused-silica capillary column; temperature, 150^{0}C for 2 min, then temperature programmed at 10^{0}C /min to 250^{0}C; carrier gas, He, 1 mL/min.

Comparison of HPLC-ECD with GC-MS

A typical HPLC-ECD chromatogram is shown in Figure 5; only one peak is observed in a de-aerated sample. On the other hand, the mass spectrometer is a universal detector, and a fairly rich chromatogram results from SFE of a spiked sawdust sample, as shown in Figure 6. The anthraquinone peak, peak 1, is clearly identifiable by its mass spectrum, shown in Figure 7, along with the Wiley-NBS MS library (supplied with the Hewlett-Packard 1000 data system) spectrum of the compound shown in Figure 8. With a column of poorer resolving power, one would have difficulty separating anthraquinone from co-extractants, and in addition one would have to wait for all the peaks to emerge before injecting another sample. By comparison, the HPLC-ECD method is highly selective, sensitive, and rapid.

Conclusions

Anthraquinone is extracted from Kraft paper and pine plywood sawdust using supercritical carbon dioxide at 8000 psi and 65^{0}C. Quantitative extraction requires only 20 min, does not lead to formation of emulsions or other phase separation problems as does solvent extraction, and is far faster than Soxhlet extraction, which requires at least 4 h to extract 82 % of the anthraquinone. The anthraquinone is determined using reversed-phase high-performance liquid chromatography with reductive electrochemical detection at a silver electrode at -1.1 V *vs* calomel. The minimum detectable quantity of anthraquinone is 210 pg and response is linear over at least 4 orders of magnitude.

Part III Chapter 2

Determination of Volatile N-Nitrosoamines in Dried Foods.

Introduction

As a class of compounds, nitrosoamines (NAs) have biological properties which have generated a great deal of interest in the field of cancer research. In addition to being potent carcinogens, NAs are acutely toxic, mutagenic and teratogenic (1, 2, 3). The biological properties (4, 5) and the chemical properties (6) of NAs have been recently reviewed.

Nitrosoamines are readily formed by the reaction of nitrite ion with secondary amines under acidic, basic or neutral conditions (7, 8, 9, 10). Judging from the wide variety of amine precursors occuring in nature, particularly in foodstuffs, a large group of naturally occurring nitrosoamines must be expected. Thus, the literature has many references (11, 12) to the presence of volatile N-nitrosoamines in various cured meats such as sausages, salami, wieners, fried bacon, and fish.

In contrast, food samples dried by hot flue gases, electric heat and circulating hot air have received much less attention even though there is evidence (13, 14) that gaseous nitrogen oxides present in the ambient air can promote nitrosoamine formation. The fact that both direct and indirect drying methods can result in the formation of detectable levels of N-nitrosodimethylamine (NDMA) in such foods as dried milk and malt (15,16,17,18) has prompted the development of routine sampling techniques which may be used to screen such commodities.

The low levels at which nitrosoamines occur in foods and the heterogeneous nature of foods have necessitated a multistep analytical procedure. This has nearly always been achieved by incorporating an isolation procedure prior to the separation and detection steps. Several methods designed for recovering nitrosoamines from dried foods have been used with varying degrees of success. For example, Sen et al. (19) directly extracted foodstuffs predigested in 3M potassium hydroxide with methylene chloride. The pooled organic phase was then centrifuged and concentrated in a Kuderna-Danish (K-D) concentrator. Eisenbrand (20) used a Soxhlet apparatus with methylene chloride for recovering nitrosoamines from dried wheat. In the procedure of Kawabata et al. (21), solid foods high in oil content were frozen before extraction with methylene chloride, subsequently the extract was cleaned-up and concentrated.

Distillation has been used by a number of workers to isolate nitrosoamines from food samples. Sen et al. (22) reported a vacuum distillation procedure based on a common rotary flash evaporator. Dried samples were digested in potassium hydroxide under reduced pressure for several hours in the modified commercial apparatus. Subsequently, the aqueous distillate was extracted in methylene chloride and concentrated in a K-D apparatus. Goodhead and Gough (23) described a versatile steam distillation procedure which is adaptable to almost any food matrix. The food sample was slurried with water and sodium chloride, and then steam distilled. The distillate was then extracted with methylene chloride, cleaned-up and concentrated. Libby et al. (17) and Harvey et al. (24) blended processed foods with oil prior to distillation. The distillate, containing all components soluble in the oil-water emulsion and more volatile then oil, was then extracted with methylene chloride and concentrated.

Soild phase extraction using Celite as a diluent as well as an adsorbent has become an accepted procedure for isolating nitrosoamines in dried milk products. In the method of Harvey et al. (16), ground dried milk was mixed with anhydrous sodium sulfate and Celite. The resulting free flowing dry mixture was then packed into a glass chromatography column and the lipid material was eluted with methylene chloride. The extract was further cleaned-up and concentrated. Hotchkiss et al. (25) adapted a similar procedure to malt beverages.

While each of these procedures appears workable, none completely suited routine needs for producing acceptable data with speed, simplicity, and efficiency from a large number of foodstuff samples. Distillations, for example, particularly with mineral oil, have been shown to be responsible for artifact formation (24) and are time consuming. In addition, excessive foaming during processing leads to severe losses. Direct extraction, while straightforward and simple requires purified solvents and reagents, and elaborate precautions are required to obtain reliable results. Even then, direct extraction offers limited sensitivity for porous food matrices. Although solid phase extraction with Celite offers high recoveries, high speeds, and reduced solvent volume, the binding process involves much manual intervention with suspected carcinogens.

Presently the technique of choice for the quantitation of nitrosoamines involves chemiluminescence using an on-line thermal energy analyzer (TEA) detector (26, 27). Undoubtedly, a TEA detector is highly selective and sensitive for N-nitrosoamine compounds; however, this device suffers from a variety of drawbacks (26) such as positive and negative false responses, complicated apparatus and high price. Of the other common GC and HPLC detectors only the electrochemical detector has received much attention for these compounds due to its selectivity, sensitivity, simplicity and low cost. Vohra and Harrington (28,29) initially described the LC separation and electrochemical detection of N-nitrosodimethylamine (NDMA), N-nitrosodiethylamine (NDEA) and N-nitrosodipropylamine (NDPA) with a crude polarographic detector. Even in its primitive state, such a system showed much promise with detection limits approaching 800 pg for analytical standards. A commercially available detector based on a static mercury drop has been promoted by its manufacturer (30) as an HPLC detector for the analysis of nitrosoamines. We have described (pp. 17-120) a silver-based thin layer cell capable of detecting 200 pg of readily reducible compounds such as quinones and nitro-compounds. Subsequent improvements in cell design, electrode materials, degassing and pumping hardware, and electronic controlling units will undoubtedly result in selectivity and detection limits comparable to the TEA detector, which approaches 15 ppb for most volatile nitrosoamines, but at a fraction of the cost.

In this chapter, supercritical fluid extraction (SFE) is used for the isolation of NDMA and NDEA from dried foodstuffs prior to their HPLC separation and electrochemical detection. We (31) and others (32-39) have recently demonstrated that SFE, a technique which combines the virtues of both distillation and solvent partition, offers a quantitative, potentially selective and rapid means of isolating a variety of hydrophobic analytes from complex matrices using simple straightforward plumbing. In addition, recoveries are comparable to conventional techniques, however, extracts are typically cleaner thereby requiring no further clean-up. In contrast to liquid partition or oil distillation, problems associated with foaming and emulsions are eliminated. Similarly, gentle extraction conditions and the lack of light or oxygen reduce artifact formation. Furthermore, not only is the time and cost of each analysis reduced, but more importantly, the handling of the putative human carcinogens is minimized. Finally, and most importantly from a detection viewpoint, there is no solvent to evaporate. This unique feature enables SFE to be compatible with a variety of detectors.

For the purposes of analytical method development, therefore, we have determined the following conditions under which the extraction of these nitrosoamines is optimized as well as made insensitive to small changes in pressure. At the same time, we have examined the effects of various separation and detection parameters such as mobile phase pH and applied potential on sensitivity. Furthermore, we have determined detection limits for these compounds extracted from dried foodstuffs under representative sets of good conditions. Finally, the advantages and possibilities of this hyphenated technique are described and are compared to others.

Experimental

Chemicals

N-nitrosodimethylamine (NDMA), N-nitrosodiethylamine (NDEA) were purchased from Aldrich (Milwaukee,WI) and used without further purification. Celite 545 was obtained from Fisher Scientific Co. (Pittsburgh, PA). Chloroacetic acid sodium salt was acquired from Kodak. HPLC-grade acetonitrile was obtained from Baker (Phillipsburg, NJ). In-house glass distilled water was used throughout this study. Linde bone-dry grade carbon dioxide (Prest-O-Sales, Long Island City, NY) was used in all experiments.

Precautions: All glassware, spatulas and mechanical tools were carefully cleaned to avoid contamination with N-nitrosoamines. Because of the potential carcinogenic hazard, all analytical work was carried out, whenever possible, under a well ventilated fume hood using protective gloves. In addition, as these compounds are photo-labile, solutions should be prepared under subdued light.

Preparation of stock solutions of NDEA and NDMA

Approximately 55 mg of each nitrosoamine, accurately weighed $\pm$ 0.1 mg, was transferred into a 100 mL volumetric flask with a glass stopper, diluted to the mark with acetonitrile and mixed well to form a final concentration of 550 µg/ml. Fresh stock solutions were prepared once a week.

Preparation of working solutions

By serial dilutions of the stock solution, working solutions were prepared in acetonitrile for each nitrosoamine at 55 µg/mL, 5.5 µg/mL, and 550 ng/mL. The dilute solutions were stored in the dark and prepared once a week.

Apparatus

All extractions were performed with a laboratory-constructed high-pressure manifold already described (pp. 124-125). In this particular case the collection device was simply an HPLC guard column (4.2 mm x 60 mm) packed with Celite located downstream of the back-pressure regulator. The utilization of Celite facilitates comparison with recommended procedures, which typically employ Celite in the form of a solid phase column.

HPLC with electrochemical detection (ECD) was used to quantify the material recovered from the supercritical extractions. HPLC-ECD analysis was accomplished with a laboratory-built chromatograph (pp. 16-36). In this system, mobile phase was pumped by a Varian 8500 syringe-pump, modified for continuous mobile phase deoxygenation. Samples, 20-μL in volume, were introduced by a pneumatically driven delivery device into a Rheodyne 7125 six port valve. Separations were performed on a 10 μm MicroBondapak C-18 column 150 mm x 3.9 mm I.D. (Waters Associates, Milford, MA). The electrochemical detector was of the conventional thin-layer amperometric design (pp. 16-19) and employed a silver working electrode, stainless steel auxiliary electrode and a calomel reference electrode. To minimize movement and noise pick-up, the cell was mounted in an inner well of the chromatograph box supporting the injector and column panel. The potentiostat and the current-follower circuits were assembled on two individual Teflon® PC boards which were mounted to the outer walls of the chromatograph box with plastic guides. All switches, potentiometers, inputs and outputs were mounted directly onto the Teflon® boards in fixtures located in close proximity to the associated electronic function. Signals from the EC detector were monitored with a peak detector (43) and recorded on a Linear model 1200 strip chart recorder (Linear Instruments, Irvine, CA).

Extraction procedure

One gram, accurately weighed, of ground material was placed in the extraction chamber and sealed with two endfittings containing glass wool. Thereafter, the chamber was inserted into the high-pressure manifold with the downstream pressure regulator opened. After the temperature was brought to 60°C, the chamber was purged twice with low pressure carbon dioxide before the regulator valve was closed. Subsequently, the chamber was pressurized to 8000 psi and equilibrated under these conditions for 15 min. Following equilibration the regulator valve was slowly opened, reducing the pressure to a sub-critical value to enable the nitrosoamines to be collected

on the Celite trap.

Desorption

With a spatula, the extract on Celite was loaded into a 10 mL glass syringe fitted with a coarse frit. The collected N-nitrosoamines were eluted with 4 x 0.5 mL of acetonitrile into a 4 mL Reacti-Vial.

Chromatographic conditions

The mobile phase contained 45 % (v/v) acetonitrile in an aqueous 0.01M chloroacetic acid (sodium salt) solution adjusted to pH 3.5 with phosphoric acid; the flow rate was 2 mL/min. The detector was set at -1.2 V versus SCE. The sensitivity was set at 100 nA/V.

Results and Discussion

Hydrodynamic Voltammogram

For characterization of the electrochemical properties of NDMA and NDEA, chromatographically-associated hydrodynamic voltammograms were generated. The HDVs for NDMA and NDEA are shown in Figures 1 and 2, respectively. The broad shape of these sigmoidal curves with a $E_{3/4}$-$E_{1/4}$ difference of approximately 100 mV is indicative of a quasireversible reaction (47). From these curves, the plateau voltage of -1.2 V *vs* SCE was selected for HPLC quantitation. These results are consistent with earlier studies by Osteryoung et al. (45,46), Pulidori et al. (47) and Chang and Harrington (48) on the reduction of alkyl N-nitrosoamines at mercury in static aqueous electrolytes.

Effect of pH on signal-to-noise ratio for NDMA

The signal-to-noise ratio for NDMA was very dependent upon pH as shown in Figure 3. This second derivative-shaped curve is the result of the interdependencies of two trends; the noise level decreases with increasing pH values while the analytical reduction signal is greatest at low pH values. Using a silver working electrode, pH values less than 3.5 lead to a decrease in signal-to-noise ratio, because the noise level rises as the potential for hydrogen evolution is decreased. The noise level increases from 300 nA to 1.5 μA as the pH decreases from 7 to 1. At higher pH values, however, the analytical signal is decreased, being reduced some 25 times as the pH increases from 1 to 7. These findings are in agreement with those of Pulidori et al.

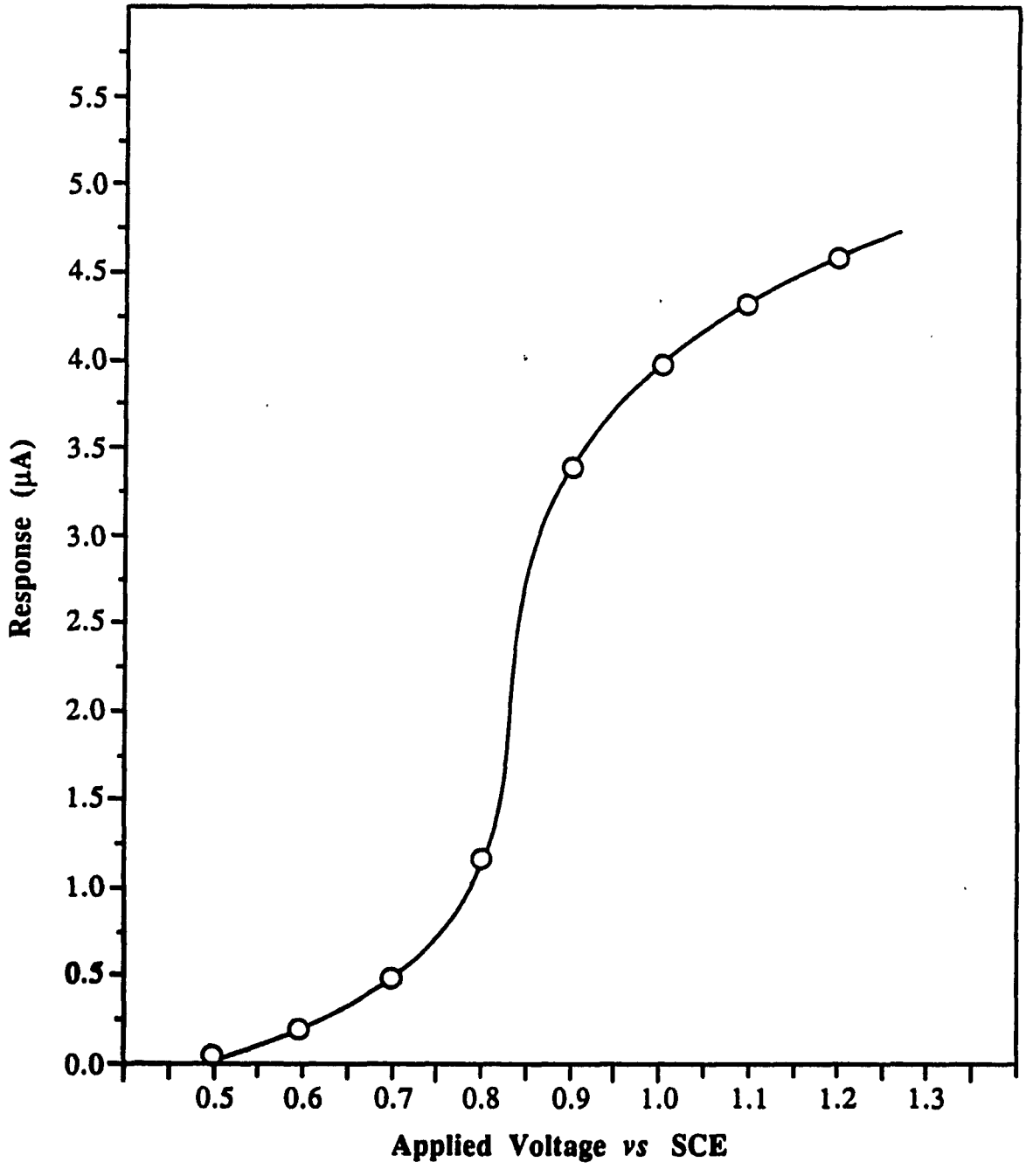

Figure 1. Hydrodynamic voltammogram of N-nitrosodimethylamine (NDMA) on a silver electrode *vs* SCE. Chromatographic conditions: column, 150 x 3.9 I.D. mm μ-Bondapak C-18 (10 μm); mobile phase, 45% v/v acetonitrile in 0.01M chloroacetic acid (pH 3.5); flow rate, 2.0 mL/min; sample size, 0.55 μg NDMA per 20 μL mobile phase injected at each potential setting.

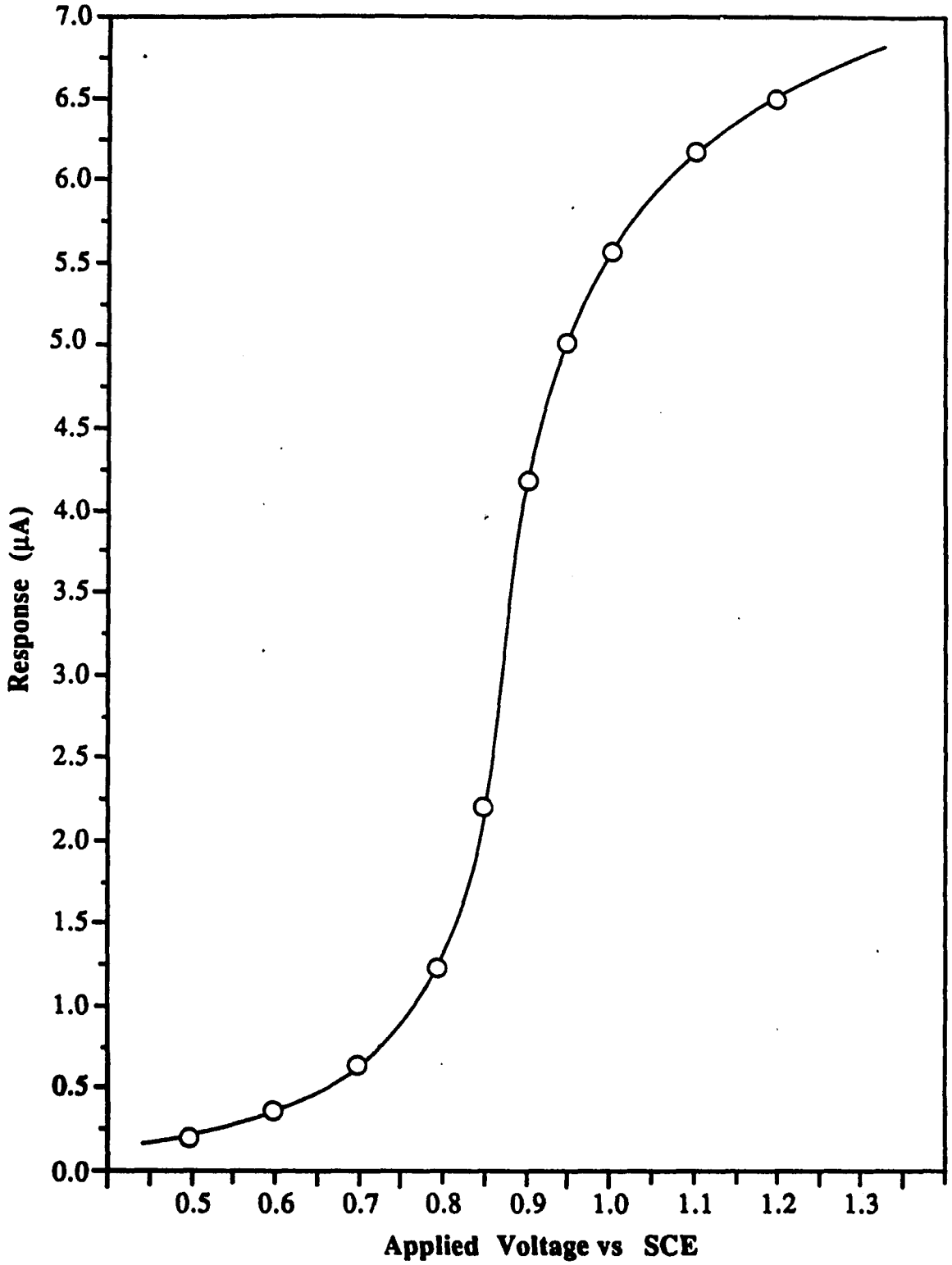

Figure 2. Hydrodynamic voltammogram of N-nitrosodiethylamine (NDEA) on a silver electrode *vs* SCE. Chromatographic conditions: column, 150 x 3.9 I.D. mm μ-Bondapak C-18 (10 μm); mobile phase, 45% v/v acetonitrile in 0.01M chloroacetic acid (pH 3.5); flow rate, 2.0 mL/min; sample size, 1.1 μg NDEA per 20 μL mobile phase injected at each potential setting.

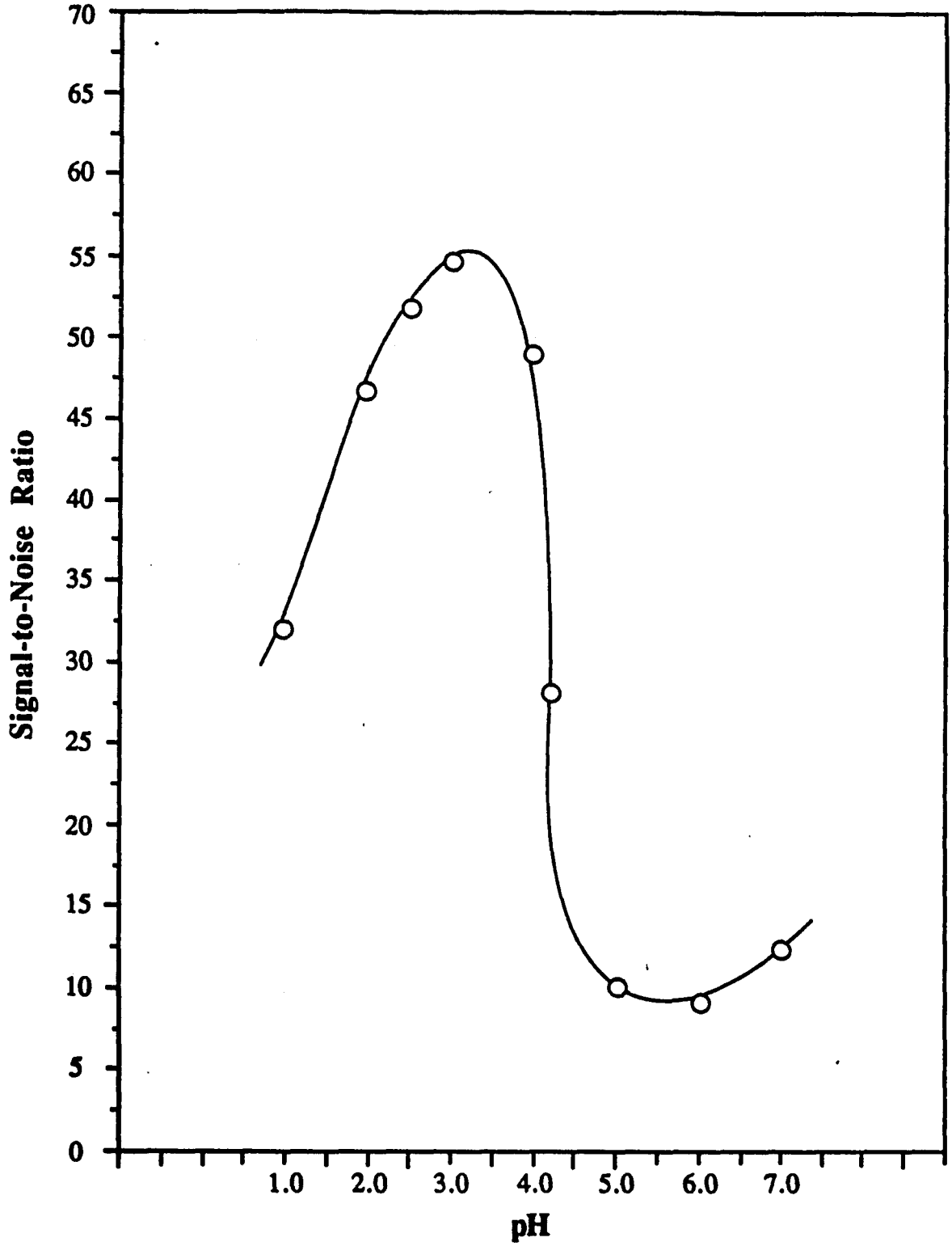

Figure 3. Influence of pH on signal-to-noise ratio for the detection of NDMA at a silver cathode. Chromatographic conditions: column, 150 x 3.9 mm I.D. μ-Bondapak C-18; mobile phase, 45 % v/v acetonitrile in chloroacetic acid (pH 3.5); flow rate, 2.0 mL/min; applied potential, -1.1 V *vs* SCE.

(47) who found evidence for the establishment of a protonation equilibrium between the alkyl-nitrosoamine and its conjugate acid prior to the occurrence of the electron transfer process in static solutions. In neutral or weakly alkaline solutions, the reductive wave was limited by the rate of the protonation reaction, whereas at lower pH values the wave was diffusion-controlled. In practice the pH was adjusted in the present study to 3.5 to maximize the signal-to-noise ratio. The same pH was used for NDEA in all subequent studies, although its pH dependency was not investigated.

HPLC Analysis

A typical chromatogram of the separation of the two nitrosoamines studied is shown in Figure 4. Under the conditions described in the experimental section, the retention times of NDMA and NDEA were 4 min and 5 min, respectively. They were well separated from each other as well as from earlier eluting impurities. These extraneous peaks were consistently present in the prepared standard solutions of nitrosoamines that have passed through the separation procedure, and are thus well defined artifacts of the method and present no major problem in the analysis. Using a log-log scale, Figure 5 shows the mean values of the responses obtained from each nitrosoamine at concentrations ranging between 55 µg/mL and 550 ng/mL. An excellent linear response as indicated by slopes of 0.903 and 0.955 nA-mL/ng were obtained for NDMA and NDEA, respectively. Figures 6 and 7 show working curves of peak current *versus* concentration in the range of 5.0 to 0.5 µg/mL for each nitrosoamine. Both curves were linear over this range with correlation coefficients of 0.996 for NDMA and 0.998, for NDEA. The precision in this range, as measured by the relative standard deviation (RSD), was less than 2.2 %. Although the response factor for each nitrosoamine is relatively high compared to quinones and nitro-compounds (pg. 104), of the order of 60 nA/ng, the minimum detectable limit for these nitrosoamines is approximately 0.5 ng for a signal-to-noise ratio of 3 to 1. The slightly elevated noise level observed in this case can be attributable to lowering of the hydrogen overpotential observed at silver in such an acidic mobile phase.

SFE Extraction

In order to establish the optimum conditions for extraction of these alkyl-nitrosoamines, one gram samples of Celite were spiked with 1 µg of NDMA and then immediately extracted at four pressures in the range of 5000-8000 psi for 15 min at 60^{0}C. The dependence of recovery on pressure and equilibration time for NDMA is

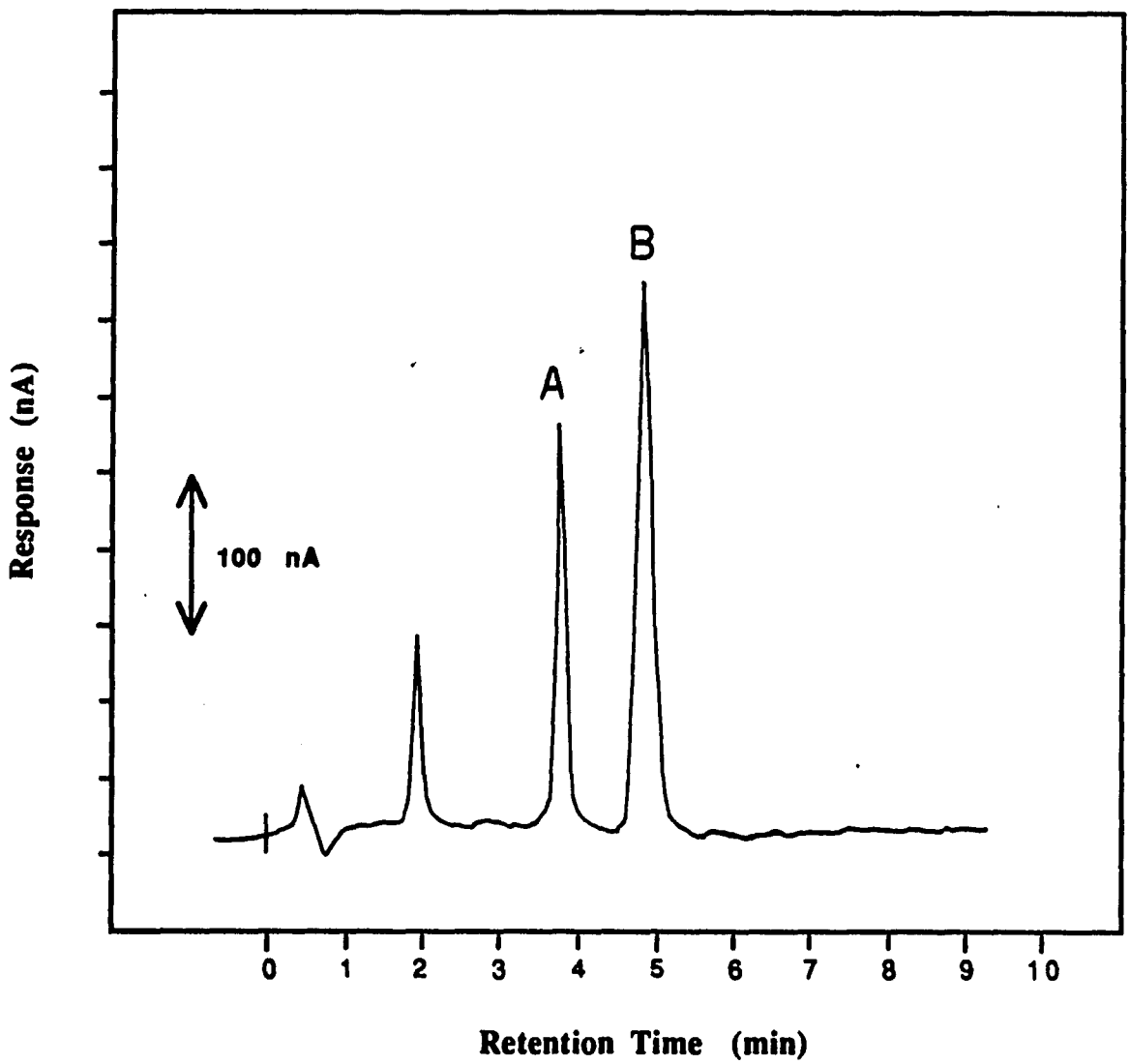

Figure 4. Separation of standard mixture of N-nitrosoamines by reversed-phase chromatography with reductive amperometric detection. Chromatographic conditions: column, 150 x 3.9 I.D. mm packed with μ-Bondapak C-18, particle diameter 10 μm; mobile phase, 45 % v/v acetonitrile in 0.01M chloroacetic acid (pH 3.5); flow rate, 2.0 mL/min; applied potential, -1.2 V *vs* SCE. Peak identities as follows: peak A, NDMA (28.8 ng); B, NDEA (55.0 ng).

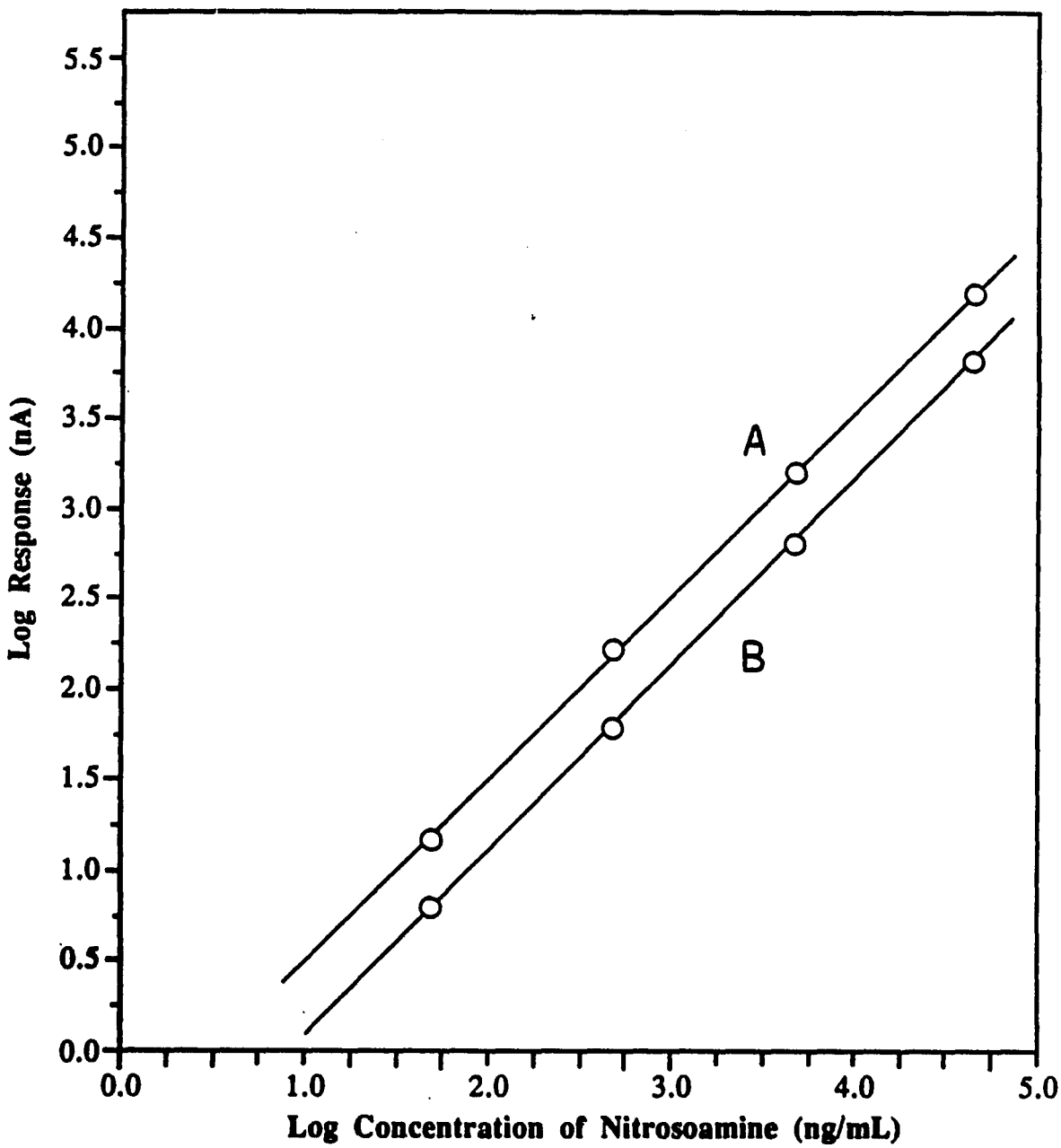

Figure 5. Linearity of detector response to amounts of (A) NDMA and (B) NDEA in 20 µL samples. Chromatographic conditions: column, 150 x 3.9 mm I.D. µ-Bondapak C-18; mobile phase, 45% v/v acetonitrile in 0.01M chloroacetic acid (pH 3.5); flow rate, 2.0 mL/min; potential of working electrode, -1.2 V *vs* SCE.

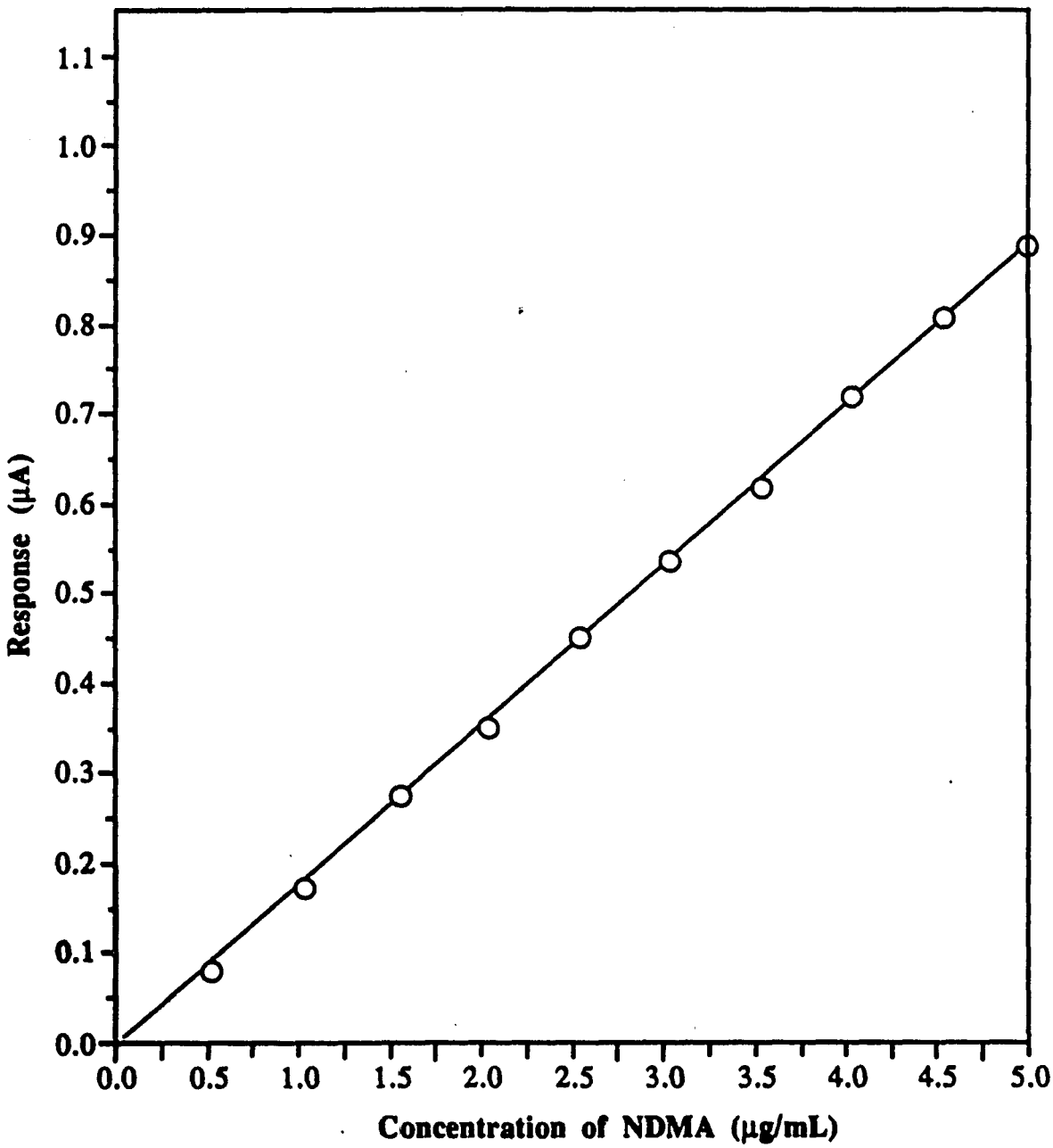

Figure 6. Calibration curve for NDMA obtained from 20 μL injections onto a 150 by 3.9 mm I.D. μ-Bondapak C-18 column with a 45% v/v acetonitrile in 0.01 M chloroacetic acid (pH 3.5) mobile phase. Flow rate, 2.0 mL/min. Potential of silver working electrode, -1.1 V vs SCE.

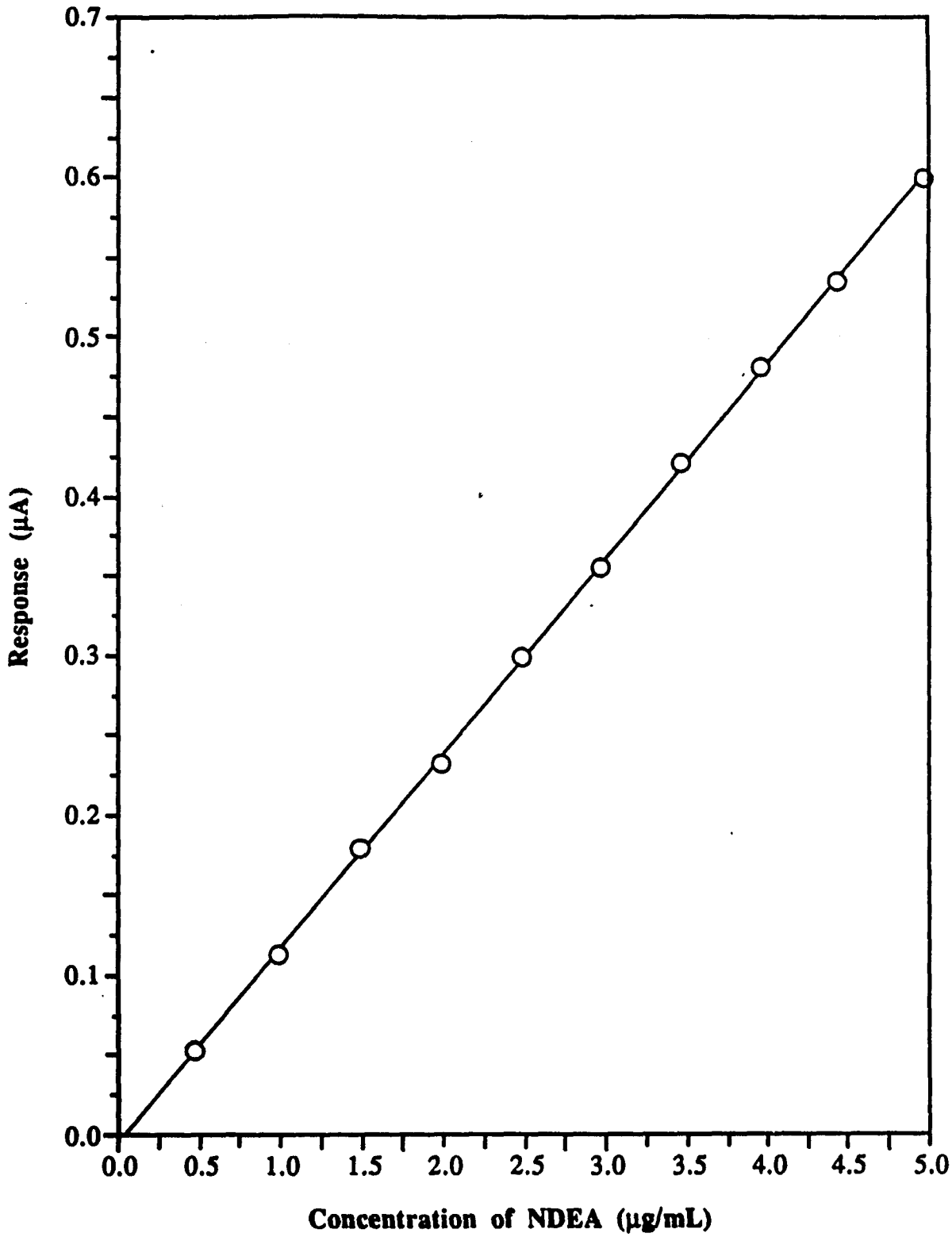

Figure 7. Calibration curve for NDEA obtained from 20 μL injections onto a 150 by 3.9 mm I.D. μ-Bondapak C-18 column with a 45% v/v acetonitrile in 0.01 M chloroacetic acid (pH 3.5) mobile phase. Flow rate, 2.0 mL/min. Potential of silver working electrode, -1.1 V vs SCE.

shown in Figures 8 and 9, respectively. As can be seen for this volatile nitrosoamine, recoveries in excess of 90 % were achieved within 20 min by extraction at 8000 psi and 60°C. To determine the efficiency of these conditions for dried milk, 500 ng and 5 μg each of NDMA and NDEA were added to a gram of various dried foodstuffs which had given a negative response for nitrosoamines. The spiked samples were analyzed by the preparation procedure outlined and the recoveries are summarized in Table 1. Typical HPLC-ECD chromatograms obtained from various commodities by this method are shown in Figures 10 and 11. The percentage recovery of NDMA and NDEA added to various samples at the two levels are satisfactory and are not significantly dependent on the matrix type. In fact, the average recovery of NDMA reported here at the 5.0 μg/g level is comparable to that obtained by using an atmospheric distillation technique (49).

Linearity of SFE Procedure

To investigate the linearity of the assay, a dried milk sample was spiked with NDMA and NDEA at 5 concentrations ranging from 550 ng/g to 55 μg/g. For each concentration level, 3 replicate injections were made and linearity plots constructed. An example is shown in Figure 12, from which it can be seen that at least up to 55 μg/g, the detector response for the recovered extracts is linear. A tail-off in response was observed for higher concentrations of nitrosoamines, which was attributed to electrode passivation. Since under normal conditions it is unlikely that concentrations of nitrosoamines over 55 μg/g will be encountered, this effect is not regarded as a disadvantage and in any case can be overcome by dilution of the sample. The minimum detection limit fot the total procedure approaches 250 ng/g for both NDMA and NDEA.

Precision

The precision of the entire procedure over a normal working day was examined by analyzing 5 replicates of a single sample of milk which was spiked with 550 ng/g NDMA. All analyses were performed by the same analyst during the same day. As illustrated in Table 2, the mean concentration recovery was 550 ng/g with a standard deviation of 5.7 ng/g for this sample of milk

Long term repeatability was followed over a period of 3 weeks and involved two determinations per day. The variation of response, 7 %, is higher but the detector will

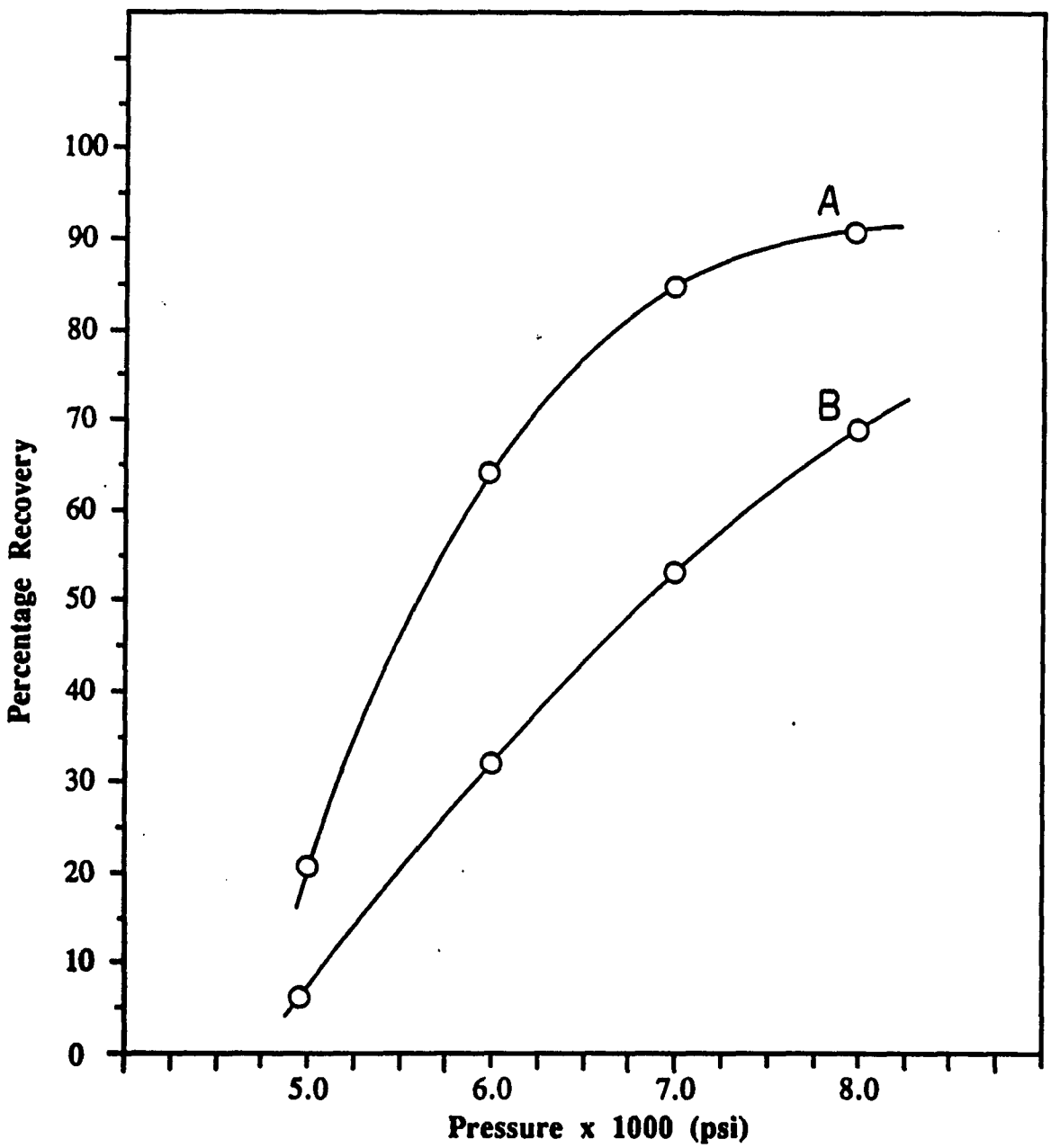

Figure 8. Effect of pressure on efficiency of SFE procedure for NDMA at (A) 60^{0}C and (B) 45^{0}C. In each case equilibration time was 20 min. One gram samples of Celite fortified with 1 µg NDMA were extracted at each pressure setting. HPLC analysis conditions as in Figure 4.

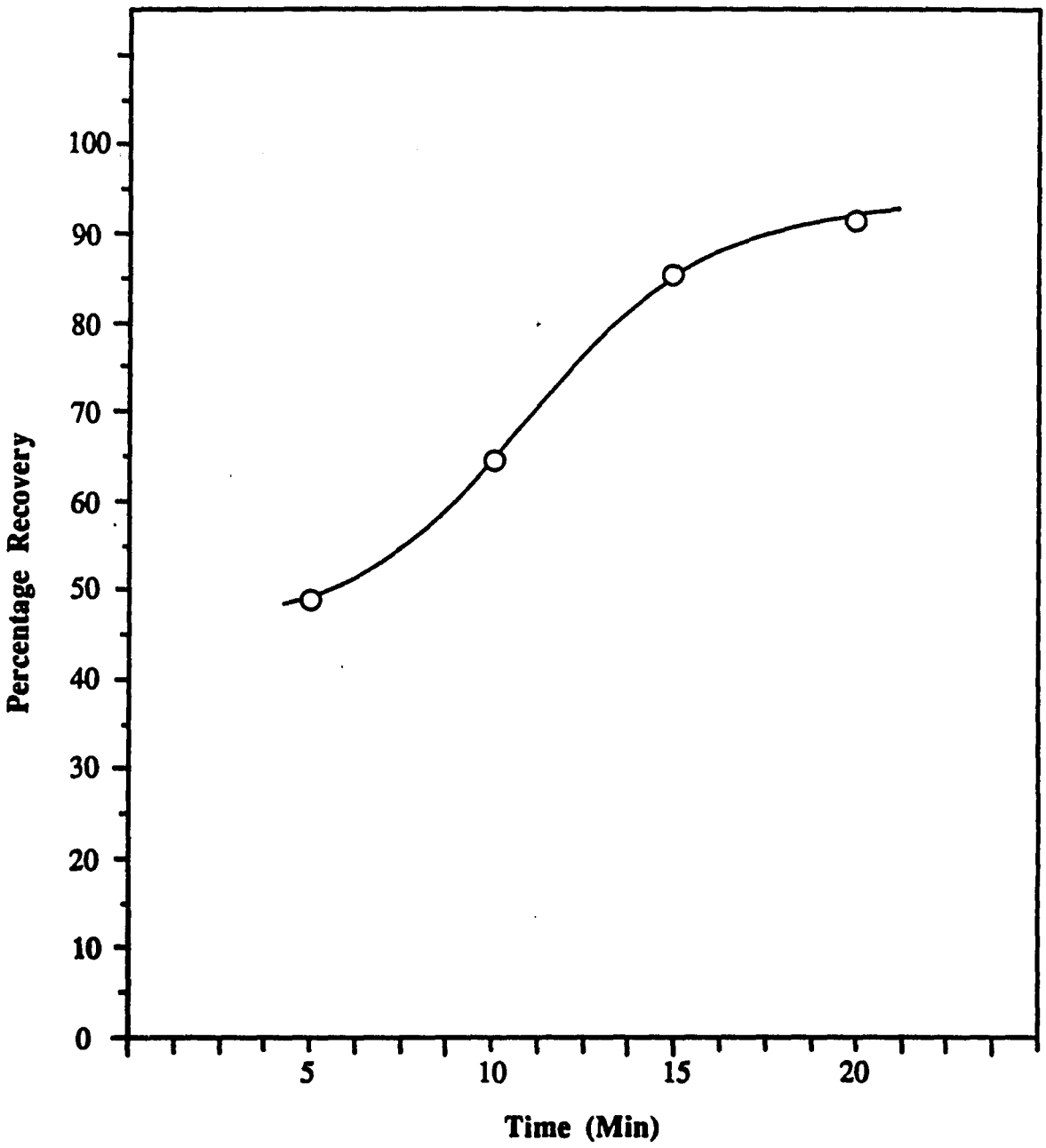

Figure 9. Effect of time on efficiency of SFE procedure for NDMA using CO_2 at 8000 psi and 60^{0}C. One gram samples of Celite fortified with 1 µg NDMA were extracted for each equilibration period. HPLC chromatographic analysis conditions as in Figure 4.

Table 1. Recovery of NDMA and NDEA from Fortified Foodstuffs.

	Percentage Recovery			
	NDMA		NDEA	
	Fortification Level (μg/g)			
Sample	0.5	5.0	0.5	5.0
Non-fat milk	89	91	90	93
Chicken soup powder	83	94	88	95
Coffee	91	93	85	87
Infant formula	86	89	92	94

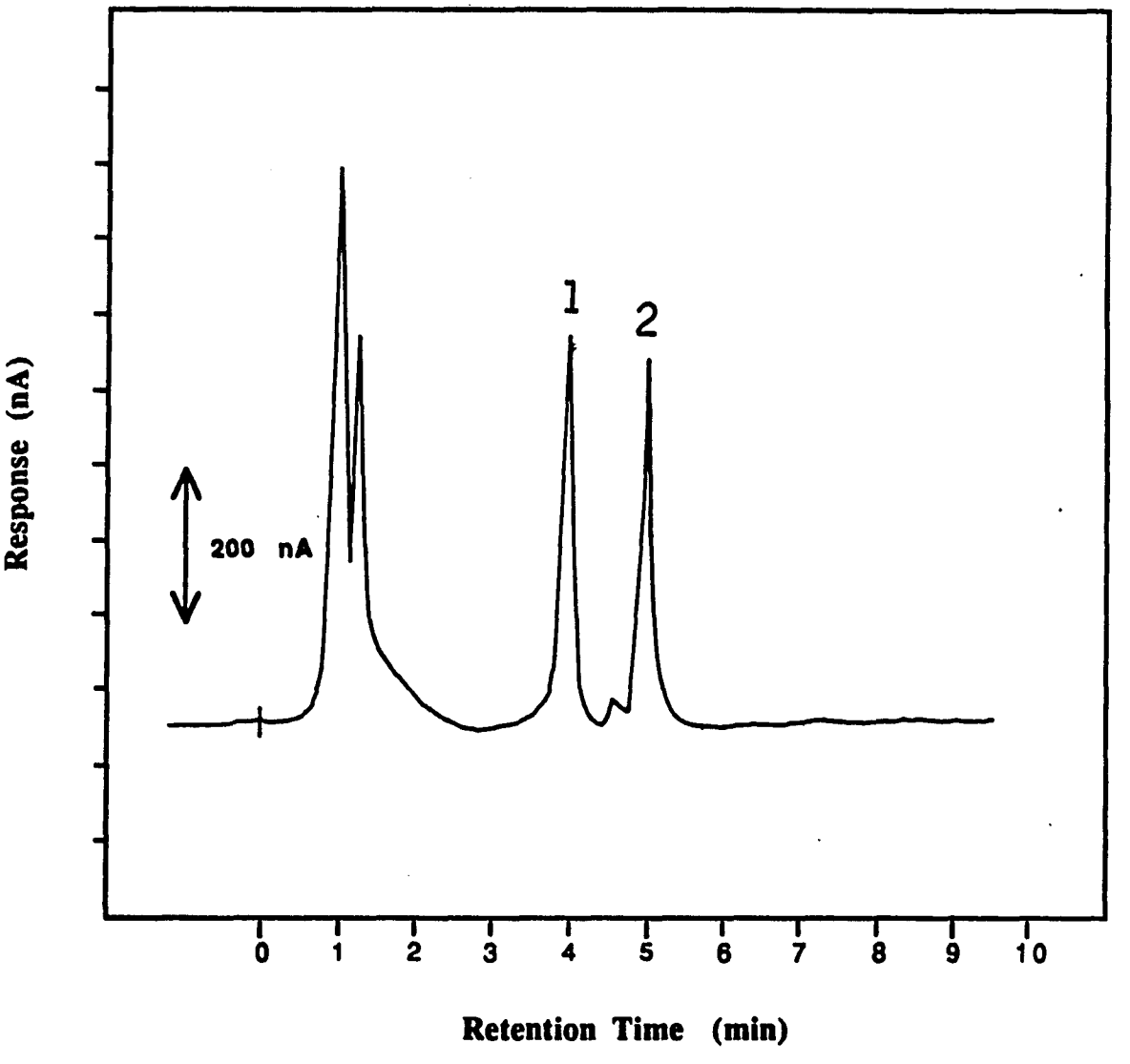

Figure 10. LCEC chromatogram of a supercritical fluid extract of a dried milk sample spiked with NDMA and NDEA. Extraction conditions: SFE with 8000 psi CO_2, 60^{0}C, 20 min. A gram aliquot of dried milk spiked with 55 μg each of NDMA and NDEA per gram of milk was subjected to the outlined procedure. HPLC-ECD conditions as in Figure 4. Peak identities as follows: 1, NDMA; 2, NDEA.

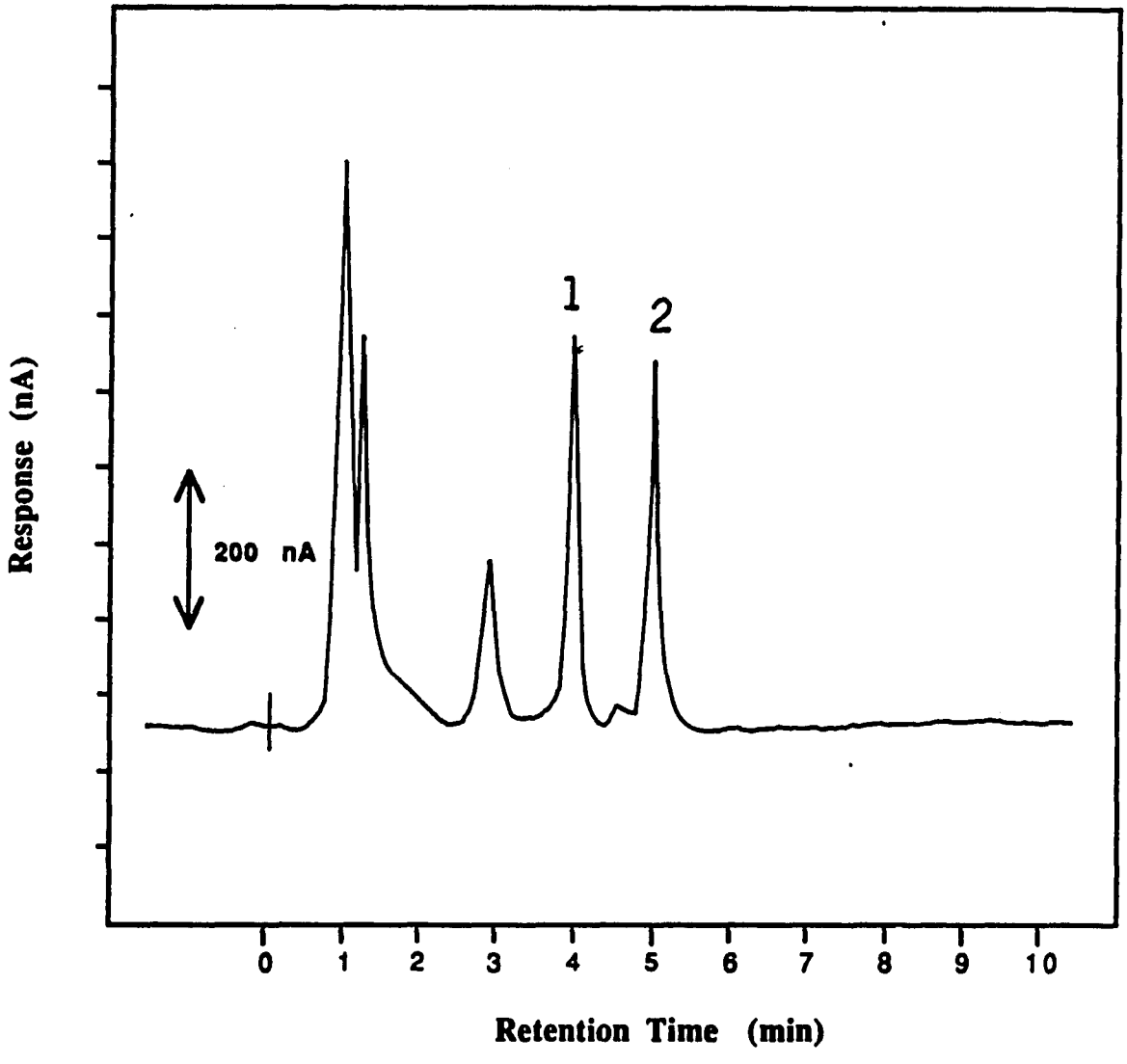

Figure 11. LCEC chromatogram of a supercritical fluid extract of a coffee sample spiked with NDMA and NDEA. Extraction conditions: SFE with 8000 psi CO_2, 60^{0}C, 20 min. A gram aliquot of coffee spiked with 55 µg each of NDMA and NDEA per gram of coffee was subjected to the outlined procedure. HPLC-ECD conditions as in Figure 4. Peak identities as follows: 1, NDMA; 2, NDEA.

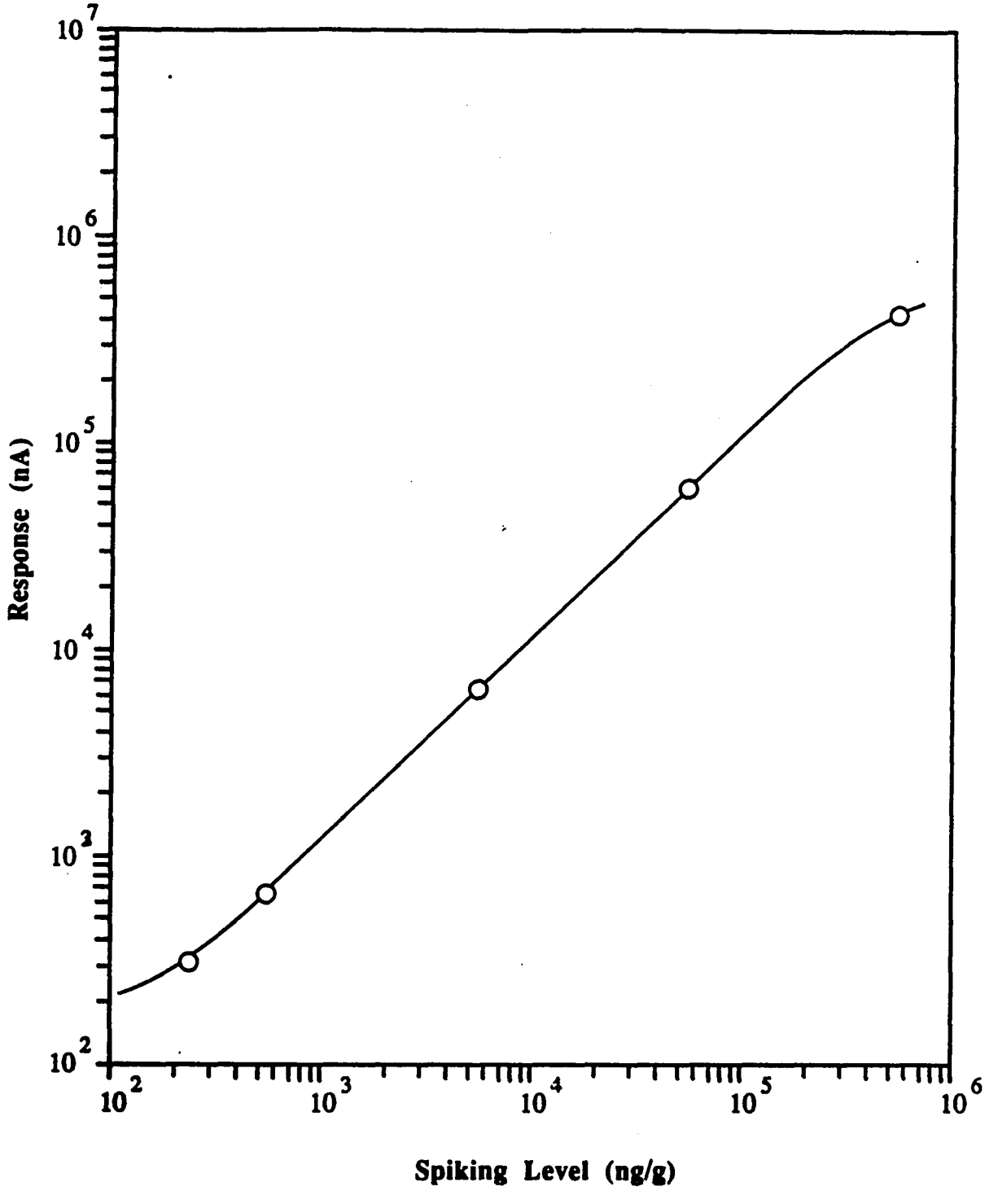

Figure 12. Linearity of SFE sample preparation and detection procedure for milk samples spiked with NDMA. Extraction conditions: carbon dioxide at 8000 psi and 60 °C for 20 min. Chromatographic conditions: column, 150 x 3.9 mm I.D. μ-Bondapak; mobile phase, 45 % v/v acetonitrile in 0.01 M chloroacetic acid (pH 3.5); flow rate, 2.0 mL/min; applied potential, -1.2 V *vs* SCE.

Table 2. Within-day Precision of Proposed Procedure For Dried Milk Fortified with NDMA.

Determination number	Analytical Result, ng/g
1	544
2	547
3	552
4	557
Range	544-557
Average	550
RSD % (n=4)	5.7

One gram samples of dried milk fortified with 550 ng NDMA prior to extraction.

SFE at 8000 psi CO_2, 60^0C for 20 min.

Celite trap, eluted with 100 % v/v acetonitrile.

NDMA determined by HPLC/ECD using the following conditions: column, 150 mm x 3.9 mm I.D. μ-Bondapak C-18 (10 μm); mobile phase, 45 % (v/v) acetonitrile in 0.01 M chloroacetic acid, pH 3.5; applied potential, -1.2 V *vs* SCE.

still function adequately at the end of this period. Provided the detector is calibrated each day with a standard nitrosoamine reference solution, as is normal with any detector, the variations over an extended period cause little trouble.

Interferences

In trace analysis, there is always the possibility of contamination or artifact formation. The potential of the SFE procedure to form nitrosoamines as artifacts was investigated by adding 50 µL of a 0.10 mg/mL solution of sodium nitrite to a milk sample that had given a negative response for the nitrosoamines and immediately analyzing the mixture. For this particular sample, no NDMA was found in the extract.

Comparison with Column Elution Method

Finally the SFE procedure was compared with a column elution method, described by Harvey et al. (16). Five samples of dried milk to which 750 ng/g of NDMA were added were immediately analyzed by the two methods on the same day by the same analyst. The average level of NDMA determined for the five samples by using the SFE method and the column elution method was 694 ng/g with a RSD of 4.3 % and 812 ng/g with a RSD of 3.9 %, respectively. Overall the two methods compare favorably.

Conclusions

In conclusion, in conjunction with a LCEC system, the SFE procedure is applicable to screening dried foodstuffs for alkyl-nitrosoamines. Using the SFE procedure, which requires a minimal amount of equipment and solvents, a single analyst in our laboratory has analyzed 8 samples in a single work day. Compared with other more harsh procedures, the more rapid SFE method is much less susceptible to artifact nitrosoamine formation, which can occur in many foodsuffs containing residual nitrite levels. The SFE method is quantitatively comparable to the lengthy multi-step procedures. The selectivity and sensitivity of the EC detector is sufficient to allow, in most cases, the analysis of samples without a further clean-up step. This minimizes the risks inherent in working with dangerous compounds, such as the N-nitrosoamines. Based on the yield-to-cost ratio of this method, it is proposed that the SFE method be further studied as a screening procedure for alkyl-nitrosoamines in dried foodstuffs.

Part III Chapter 3

Determination of Vitamin K_1 in Powdered Infant Formulas

Introduction

Despite the demands of the Infant Formula Act of 1980 (1), at present there is no standard method for determination of vitamin K_1 (phylloquinone) in these food products. Previously vitamin K_1 in infant formulas was determined by the chick bioassay (2,3), using the modifications described by Almquist (4). The chick bioassay, however, is not practical for quality control-type procedures because it is very costly, time-consuming, lacks precision and requires the maintenance of a battery of chicks.

Several existing vitamin K methods (5-18) other than the chick bioassay have been reviewed. These include the techniques of gas chromatography (5,6), thin layer reflectance densitometry (7), spectrophotometry (8,9), photochemical fluorometry (10), electrochemistry (11-13), and liquid chromatography with UV detection (14-18). Of these, the LC methods are generally superior in terms of speed, sensitivity, resolution of vitamin K_1 from other substances in the formulas, analytical precision, and procedural simplicity.

To improve the sensitivity and selectivity of quantitation following HPLC separation, electrochemical detectors have recently been used in trace level determinations of various K vitamins in rat liver tissue (19), human serum (20), and rat plasma (21-23). To our knowledge, however, reductive electrochemical detection has not been applied to the determination of this vitamin in infant formulas.

In most cases, the efficiency of the method for the analysis of fat-soluble vitamins depends on sample preparation. Published methods for the isolation of vitamin K_1 from the infant formula matrix usually describe an initial alkali or enzyme hydrolysis of interfering lipids before extraction of the phylloquinone (24). Hwang (17) simplified this procedure by first treating formula samples with ammonia and methanol, followed by extraction with a methylene chloride-isooctane solvent mixture and silica column cleanup. These sample preparation techniques typically suffer from shortcomings of phase separation difficulities, transfers, evaporations, or considerable preparation time.

In view of the need for a rapid, accurate procedure to determine the vitamin K_1 content of infant formulas, a reversed-phase HPLC method in which supercritical carbon dioxide is used to isolate vitamin K_1 from these foodstuffs has been developed. Following LC separation, quantitation of the vitamin K in the extract is accomplished with a highly sensitive and specific electrochemical detector in the reductive mode. This chapter describes the development of the method and the results of its application to various infant formulas.

EXPERIMENTAL

Chemicals

Vitamin K_1 was purchased from ICN Biochemicals (Costa Mesa, CA); purity not specified but only one LC peak was observed. HPLC grade acetonitrile, methylene chloride and acetone were obtained from J. T. Baker (Phillipsburg, NJ). In-house glass distilled water was used throughout this study. Reagent grade $NaClO_4$ was obtained from GFS Chemicals (Columbus, OH) and was used without further purification. Linde brand bone-dry grade carbon dioxide (Prest-O-Sales, Long Island City, NY) was used in all extractions

Preparation of Standards

A 0.4 mg/mL primary stock solution of vitamin K_1 was prepared by dissolving 40.0 mg of vitamin K_1 in methylene chloride in a 100 mL volumetric flask. For calibration of the chromatographic system, a series of working standard solutions were prepared at 5 concentration levels between 0.2 and 2.0 µg/mL by diluting the primary stock solution with acetonitrile-methylene chloride (95/5, v/v). An additional set of 6 solutions covering the concentration range of 400 µg/mL to 4 ng/mL were prepared at decade intervals in acetonitrile-methylene chloride for linear dynamic range characterization.

Apparatus

The liquid chromatographic system and silver based reductive amperometric detector have been described thoroughly above (pp. 16-36). All separations were performed on a MicroBondapak C-18, 150 mm x 3.9 mm I.D., 10 µm column (Waters

Associates, Milford, MA) using a mobile phase composed of acetonitrile-methylene chloride-aq 0.05 M $NaClO_4$ (90/5/5, v/v). The mobile phase was filtered through a 0.45 μm filter and then degassed with helium for 10 min before use. The output from the detector was stored by a peak detector (pp. 32-33) and recorded on a Linear model 1200 strip chart recorder (Linear Instruments, Irvine, CA).

Precautions

Sample manipulations were performed in the absence of direct sunlight to avoid degradation of vitamin K_1.

Extraction Procedure

A 1 gram sample, accurately weighed, of powdered formula was transferred to the extraction chamber and held in place between two glass plugs. The chamber was sealed and inserted into a laboratory-assembled high-pressure manifold (pp. 124-125). Initially, the system was brought to 60^0C and then purged of oxygen with ambient pressure carbon dioxide. Subsequently, the back pressure valve was closed and the system pressure was increased to an operating pressure of 8000 psi. After a 15 min equilibration period, the back pressure valve was cracked open and the extracted analytes were deposited on a guard column packed with silica (Fisher Scientific, Pittsburgh, PA). On completion, the contents of the trap were emptied into a 50 mL syringe fitted with an in-line filter (Gelman Scientific). The vitamins on the adsorbent were washed with 30 mL of methylene chloride-acetone (50/50, v/v) into a 150 mL round bottom flask, evaporated to dryness under reduced pressure in a rotary evaporator and reconstituted in 1 mL of mobile phase for HPLC analysis.

Results and Discussion

Chromatography

The composition of the mobile phase was optimized to effect sharp peaks with a short retention time for vitamin K_1 as well as to provide long term maintenance of column performance. Preliminary separations performed on a new μ-Bondapak column revealed that binary acetonitrile-water mixtures containing as much as 95 % v/v acetonitrile offered relatively poor peak shapes and non-reproducible retention times due, presumably, to the build-up of lipids and other fat soluble products on the

column. Considering these problems, we investigated the addition of small amounts of methylene chloride to increase the solubility of vitamin K_1 in binary acetonitrile-water mixtures. Repeated injections of 800 ng of vitamin K_1 were made, using a mobile phase composed of 90 % v/v in aq 0.05 M $NaClO_4$ to which the added methylene chloride was systematically varied throughout the range of 0-10 %. A comparison of the chromatograms obtained with each mobile phase composition showed that selection of a mobile phase consisting of acetonitrile-methylene choride-aq 0.05 M $NaClO_4$ (90/5/5, v/v), resulted in a sharp vitamin K_1 peak with a retention time of 8 min. Higher percentages of methylene chloride resulted in a series of negative peaks.

Electrochemical Behavior

Vitamin K_1 has been shown by Fieser (25) and Patriarche and Lingane (26) to exhibit well defined polarographic reduction waves in static alcoholic mixtures. From the analyst's point of view, the most interesting result of these investigations (25,26) is that a single wave, whose intensity is proportional to the vitamin K_1 concentration, has been observed for concentrations of vitamin K_1 less than 2×10^{-4} M. To characterize the electrochemical properties of vitamin K_1 in flowing eluents at silver, chromatographically assisted hydrodynamic voltammograms were generated by manually setting the working electrode potential at values from - 0.6 to -1.2 V at 0.05 V increments, and injecting a 20 µL aliquot of the 0.4 mg/mL vitamin K_1 standard at each potential. The resulting HDV is shown in Figure 1. As shown in Figure 1, the optimum potential for maximum response is -1.1 V *versus* SCE. The broad shape of the reduction curve with a $I_{3/4} - I_{1/4}$ difference of 130 mV is indicative of a quasireversible reaction (27).

The electrochemical response was also dependent on the mobile phase flow rate and the supporting electrolyte concentration. For flow rates less than 100 mL/h, response increases with the one-third power of the flow rate, indicating a convective mass transfer-limited current (28). Above this flow rate, response is independent of flow rate. To decrease the effects of fluctuations in flow rate on background current, the flow rate was maintained at 2 mL/min in all further studies. Similarly, increasing the supporting electrolyte concentration reduces solute retention time and solute diffusion coefficient. Shorter retention times produce narrower peaks and thus greater peak

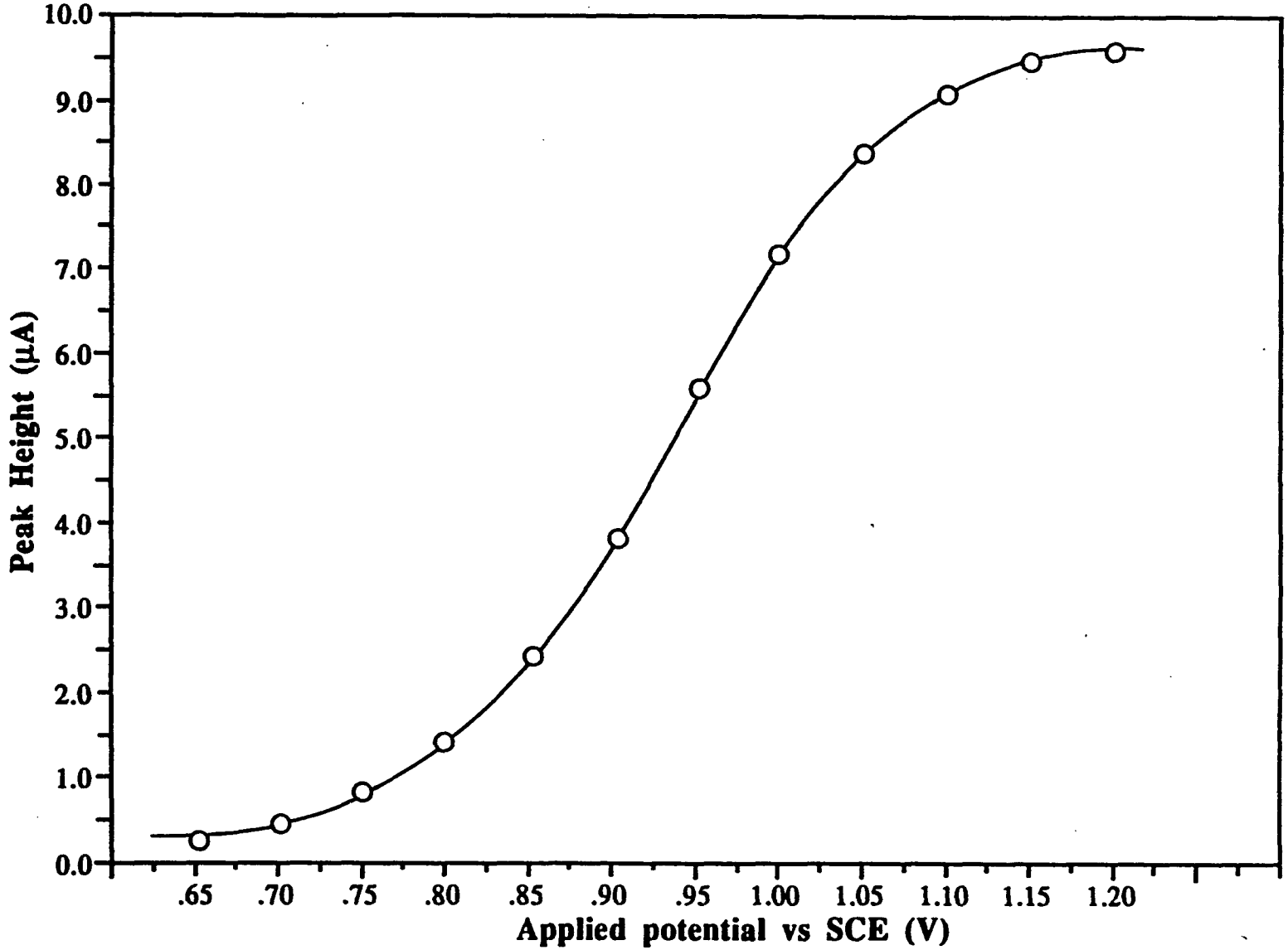

Figure 1. Hydrodynamic voltammogram of vitamin K-1 on silver electrode vs SCE. Column: 150 x 3.9 mm I.D. µ-Bondapak C-18. Mobile phase: acetonitrile-methylene chloride - aq 0.025M $NaClO_4$ (90+5+5, v/v). Sample size: 20 µg vitamin K-1 per 20 µL mobile phase injected at each potential setting.

height, whereas a slower diffusion coefficient reduces the mass transfer rate. Peak height response *versus* electrolyte concentration passes through a maximum, in this case at a $NaClO_4$ concentration of 0.025M.

Linearity and Calibration of EC Detector

The linearity of the detector response for vitamin K_1 was investigated and found to extend over 5 orders of magnitude from 8 μg to 80 pg per 20 μL injections with a correlation coefficient of 0.994. A tail-off from linearity of response was observed for concentration levels above 400 μg/mL, due to the limited solubility of vitamin K_1 in this particular mobile phase. For standard solutions, 80 pg of vitamin K_1 gave a peak which was about 3 times as intense as the noise level. Coefficients of variation for triplicate injections of standards at 8 μg, 800 ng, 80 ng, 8 ng, 800 pg and 80 pg were 6.3%, 3.8%, 2.8%, 5.2% and 7.6%, respectively.

The calibration graph shown in Figure 2 was constructed from 3 replicate measurements of 10 standards by plotting peak height against amount of vitamin K_1 injected over a range of 4 to 40 ng. The curve was rectilinear and passed through the origin. Using linear regression analysis, the resulting calibration can be expressed by the equation, y (nA)=1.208 x (ng) + 0.005.

Extraction Efficiency

In order to establish the optimum conditions for extraction of vitamin K_1, one gram samples of Chromosorb W (Alltech Associates, Deerfield, IL), were spiked with 1 μg of vitamin K_1 and extracted at four pressures in the range of 5000-8000 psi for 20 min at temperatures of 45 and 65^{0}C, respectively. The effect of pressure on recovery for 45 and 65 ^{0}C is shown by curves (A) and (B), respectively, in Figure 3. As can be seen, recoveries increase with increasing pressure at both temperatures, however, the effect is much more pronounced at 65^{0}C. The optimum extraction time was also studied. Table 1 shows that recoveries suitable for analytical work are reached within 20 min, with essentially no change up to 30 min. Under the above extraction conditions, recovery at the 1 μg/g level was 92 % with a multiple extraction precision (relative standard deviation, RSD) of 3.0 % (n=3).

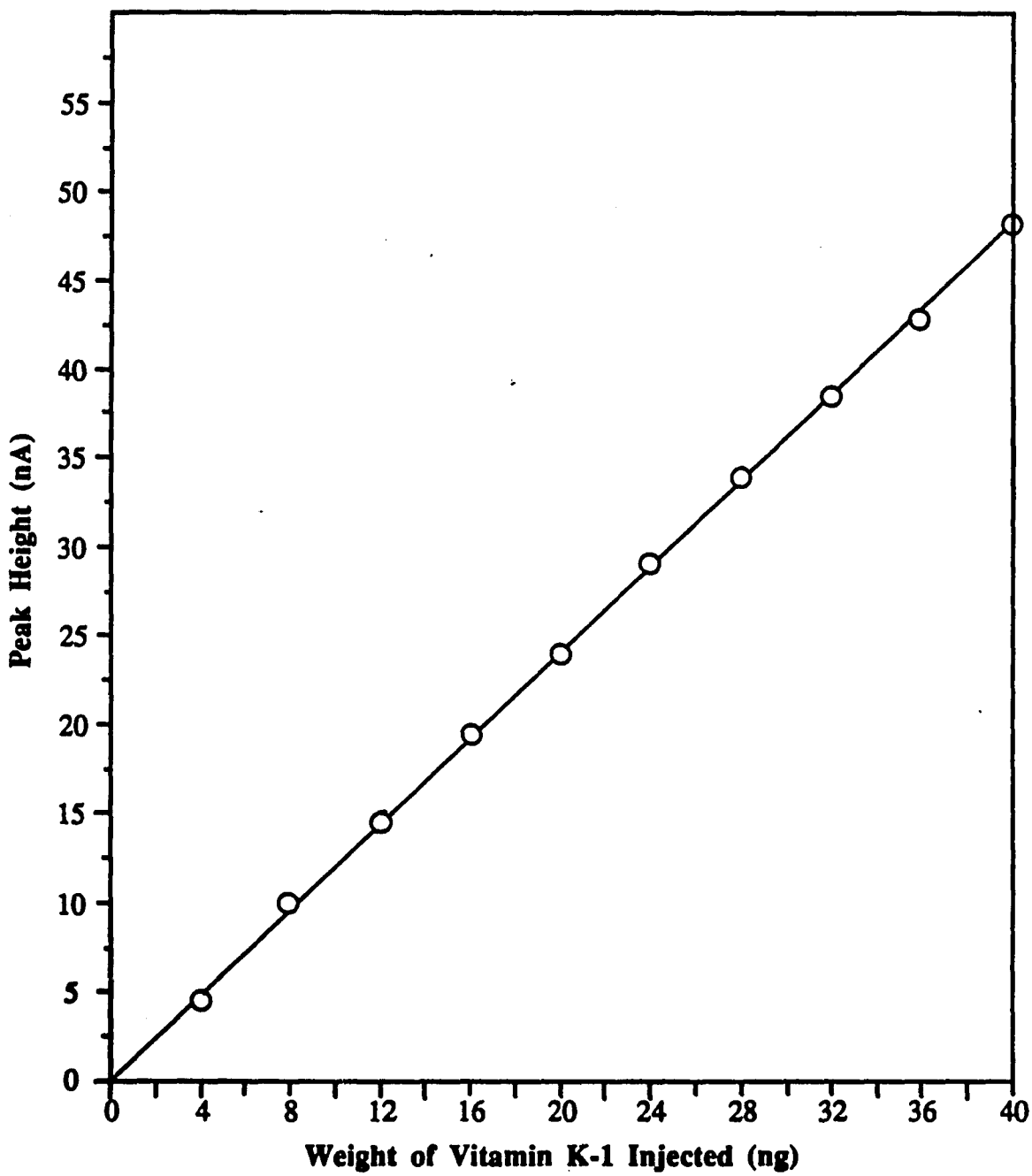

Figure 2. Calibration curve of vitamin K-1. Chromatographic analysis conditions: column, 150 x 3.9 mm I.D. μ-Bondapak C-18 (10 μm); mobile phase, acetonitrile-methylene chloride-aq 0.025M $NaClO_4$ (90+5+5, v/v); flow rate, 2.0 mL/min; applied potential, -1.1 V vs SCE.

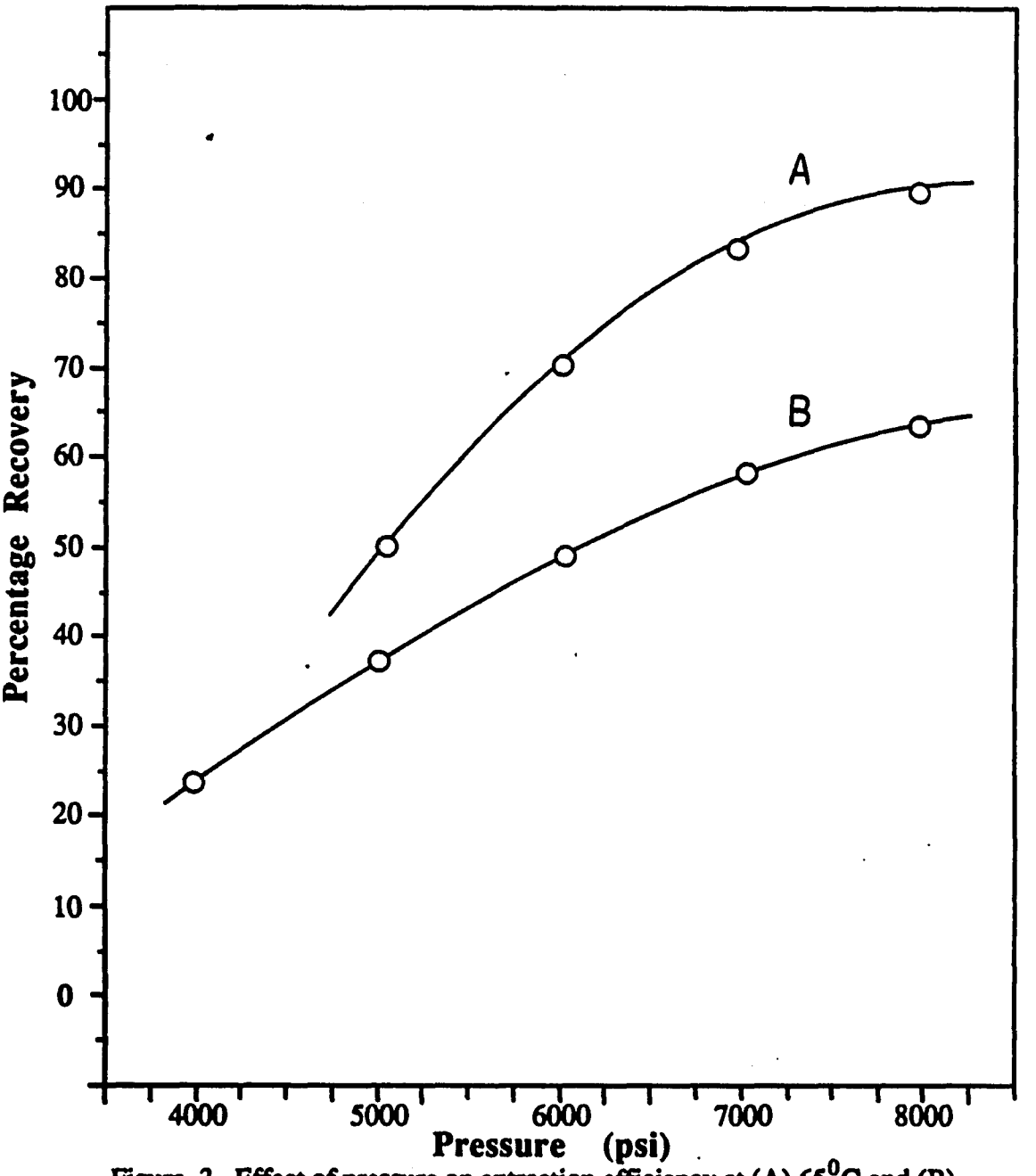

Figure 3. Effect of pressure on extraction efficiency at (A) 65^{0}C and (B) 45^{0}C. In each case, equilibration time was 20 min. Chromatographic analysis conditions: column, 150 x 3.9 mm I.D. μ-Bondapak C-18 (10 μm); mobile phase, acetonitrile-methylene chloride-aq 0.025M $NaClO_4$ (90+5+5, v/v); flow rate, 2.0 mL/min; applied potential, -1.1 V vs SCE. One gram samples of Chromosorb W spiked with 1 μg vitamin K-1 were extracted at each pressure.

Table 1. Effect of Equilibration Time on The Recovery of Vitamin K_1 From Chromosorb W at 8000 psi and 60°C.

Time, min	Recovery, %	RSD, % (n=3)
5	74	4.4
10	78	2.6
15	89	3.4
20	91	2.8
30	92	3.1

One gram samples of Chromosorb W spiked with 1 μg vitamin K-1 were extracted, in triplicate, for each equilibration period.

The efficacy of the chosen conditions for vitamin K_1 in infant formula was confirmed by spiking samples of a soy-based formula and a milk-based formula with vitamin K_1, at fortification levels ranging from 0.25 to 2.0 μg/g in 5 to 7 increments. Each of these samples was then extracted using the SFE procedure outlined in the experimental section and vitamin K_1 was determined by LC with EC detection. Figure 4 shows a typical standard addition curve for a soy-based product. Recovery was established by comparing the resulting average slope of the standard additions curve with the slope of the calibration curve obtained by injection of non-extracted standards. The average recoveries of the extraction procedure (mean ± RSD) over this concentration range were 94.4 % ± 6.5% for a soy-based formula (n=7) and 95.6 % ± 7.4 for a milk-based product (n=7), comparable to the results of Barnett et al. (15). Loss of vitamin K_1 during the complete assay was negligible.

Over-all Precision

The within-day precision of the over-all method was evaluated at four different concentration levels by triplicate assays of spiked milk-based samples on a single day. The results are shown in Table 2. The within-day coefficient of variation of these determinations varied from 8.4 % to 4.6 % at the low and high concentration limits, respectively. The average coefficient of variation of these 12 determinations was 6.4 %.

Day-to-Day Reproducibility

Day-to-day reproducibility was established for milk-based formula samples fortified with vitamin K_1 at 0.5, 1.0, 1.5, and 2.0 μg/g by carrying out three assays per day for each concentration level over a period of 3 days. The coefficients of variation are shown in Table 3. For 3 of 4 concentration levels examined, the average coefficient of variation was generally less than 6.1 %.

Analytical Results

The method was applied, in triplicate, to quantitation of the vitamin K_1 content in 2 types of commercially available formulas, each with label declarations of 0.8 μg/g. Data for the individual formulas are presented in Table 4. Vitamin K_1 levels of 0.87 and 0.95 μg/g were found for the soy-based and milk-based formulas, respectively.

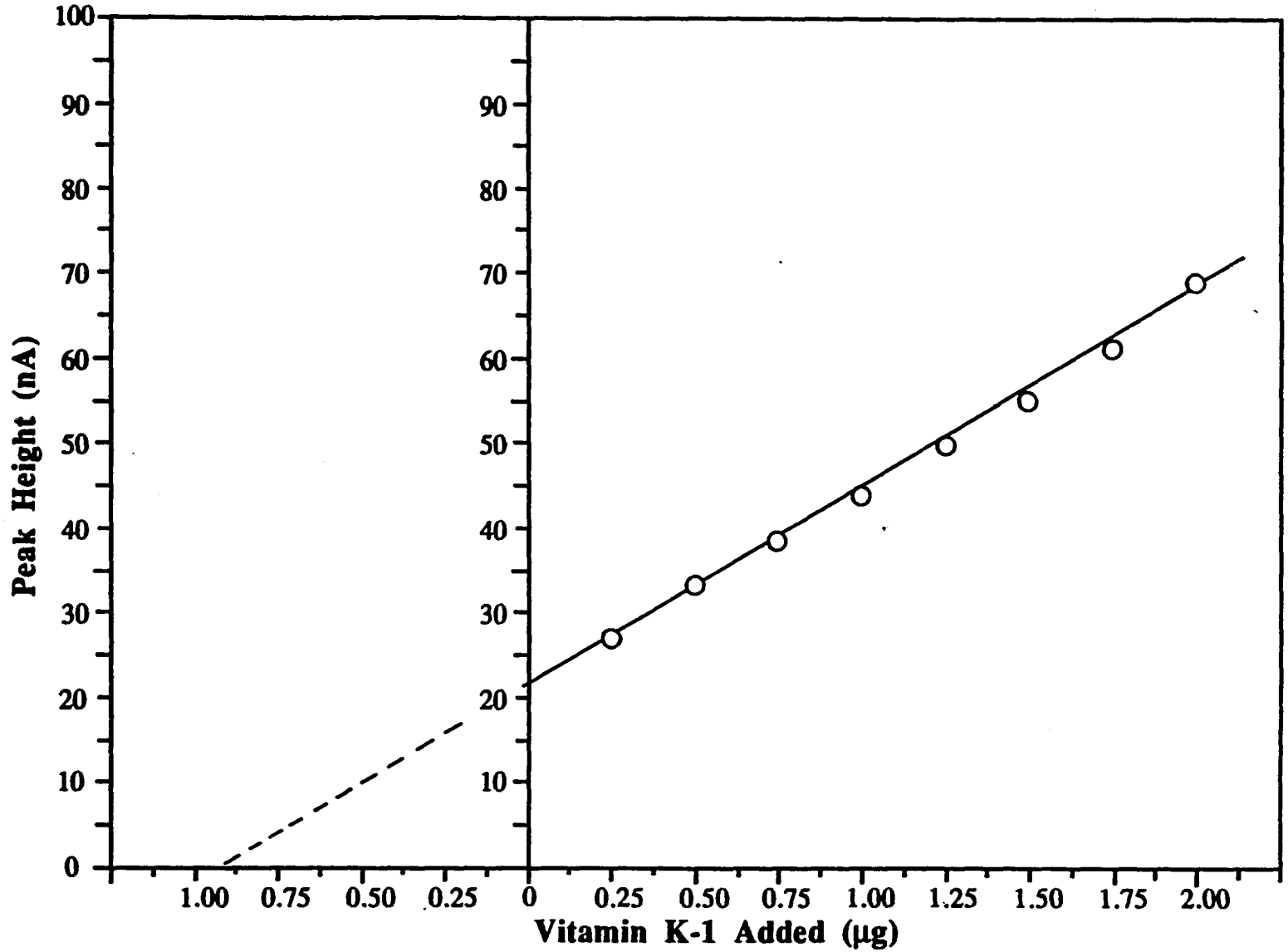

Figure 4. Linearity of SFE preparation procedure as a function of the addition of standard vitamin K-1 for a soy-based product. Extraction conditions: SFE at 8000 psi CO_2, 60^{0}C, 20 min. Chromatographic analysis conditions as in Figure 3.

Table 2. Inter-assay Precision For The Determination of Vitamin K_1 in a Milk-Based Infant Formula.

Added Conc., µg/g	Assayed Conc., µg/g	n	RSD, %
0.25	0.23	3	8.4
0.50	0.51	3	7.2
1.00	0.93	3	5.3
1.25	1.18	3	4.6

SFE Conditions: 8000 psi CO_2, 65°C for 20 min.
Silica trap, eluted with methylene chloride-acetone (50/50, v/v).

Vitamin K_1 determined by HPLC/ECD using the following conditions: column, 150 mm x 3.9 mm I.D. µ-Bondapak C-18 (10 µm); mobile phase, acetonitrile-methylene chloride-aq 0.05 M $NaClO_4$ (90+5+5, v/v/v); flow rate, 2.0 mL/min; applied potential, -1.2 V vs SCE.

Table 3. Day-to-Day Reproducibility of Proposed HPLC Method.

	Average Assayed Conc., µg/g			
Actual Conc., µg/g	Day 1	Day 2	Day 3	Mean ± RSD
0.5	0.45	0.52	0.42	0.46 ± 10.8 %
1.0	0.86	0.92	0.94	0.91 ± 4.6 %
1.5	1.34	1.41	1.25	1.33 ± 6.0 %
2.0	1.78	1.92	1.70	1.80 ± 6.1 %

Table 4. Results of LC Determination of Vitamin K_1 Extracted with Supercritical Fluid Carbon Dioxide from Two Types of Infant Formulas.

Product	K_1 found	Percentage of Declared	RSD (n=3)
Soy protein-based	0.95 μg/g	118 %	6.9 %
Milk-based	0.87 μg/g	108 %	8.2 %

SFE Conditions: 8000 psi CO_2, 65^{0}C for 20 min.
Silica trap, eluted with methylene chloride-acetone (50/50, v/v).

Vitamin K_1 determined by HPLC/ECD using the following conditions: column, 150 mm x 3.9 mm I.D. μ-Bondapak C-18 (10 μm); mobile phase, acetonitrile-methylene chloride-aq 0.05 M $NaClO_4$ (90+5+5, v/v/v); flow rate, 2.0 mL/min; applied potential, -1.2 V vs SCE.

Figure 5 presents a LC-electrochemical detector chromatogram of an extract after SFE fractionation, and Figure 6 is the same product spiked with 0.5 μg/g vitamin K_1. The high degree of resolution and freedom from exogenous interferences afforded by the electrochemical detector is evidenced by the absence of peaks near vitamin K_1. Similarly, the one peak chromatogram shown in Figure 7 was obtained from a soy-based product prepared by using the outlined preparation procedure.

For comparison, 10 g of the soy-based product spiked with 10 μg vitamin K_1/g sample was extracted using the SFE procedure, and the extract was analyzed by reversed-phase liquid chromatography with a UV detector at 248 nm. A different (and newer) C-18 column was used with mobile phase lacking the $NaClO_4$ electrolyte. The chromatogram is shown in Figure 8. The peak corresponds to approximately 5 μg vitamin K_1. The supercritical fluid CO_2 is extracting more compounds than just vitamin K_1, but the co-extracted materials are not electroactive under the chosen conditions. As almost all fat-soluble vitamins absorb to some exent at this wavelength, the analysis of multivitamin samples with UV detection can only be carried out following a good chromatographic separation. In addition to enhanced selectivity, the electrochemical detector is 4 x times more sensitive than the UV detector which is reported to be have a detection limit of 0.3 ng (17).

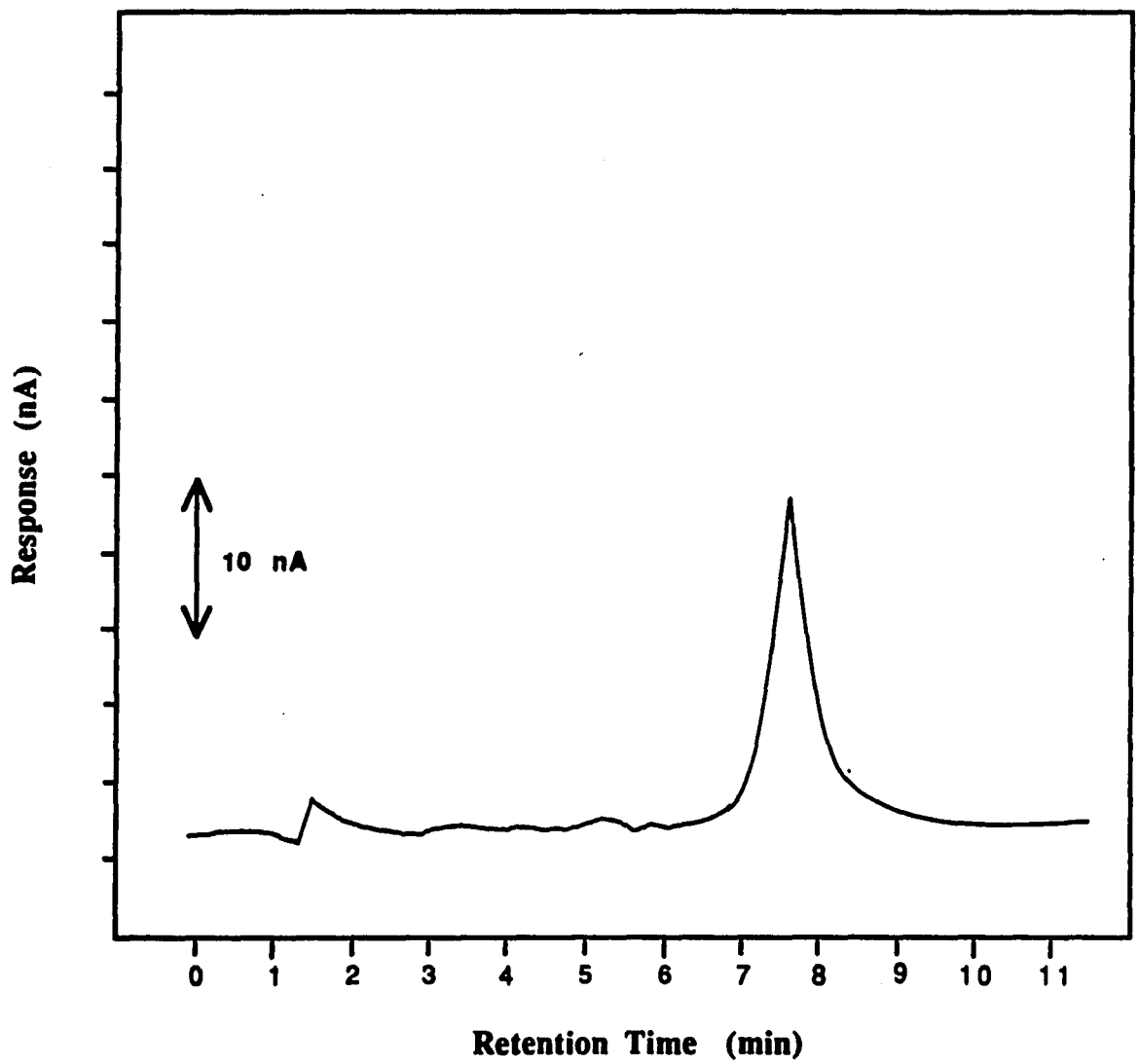

Figure 5. LC-ECD chromatogram of vitamin K-1 extracted from a commercially available milk-based fortified formula by SFE technique. Extraction conditions: SFE at 8000 psi CO_2, 60^0 C, 20 min. Chromatographic analysis conditions as in Figure 3.

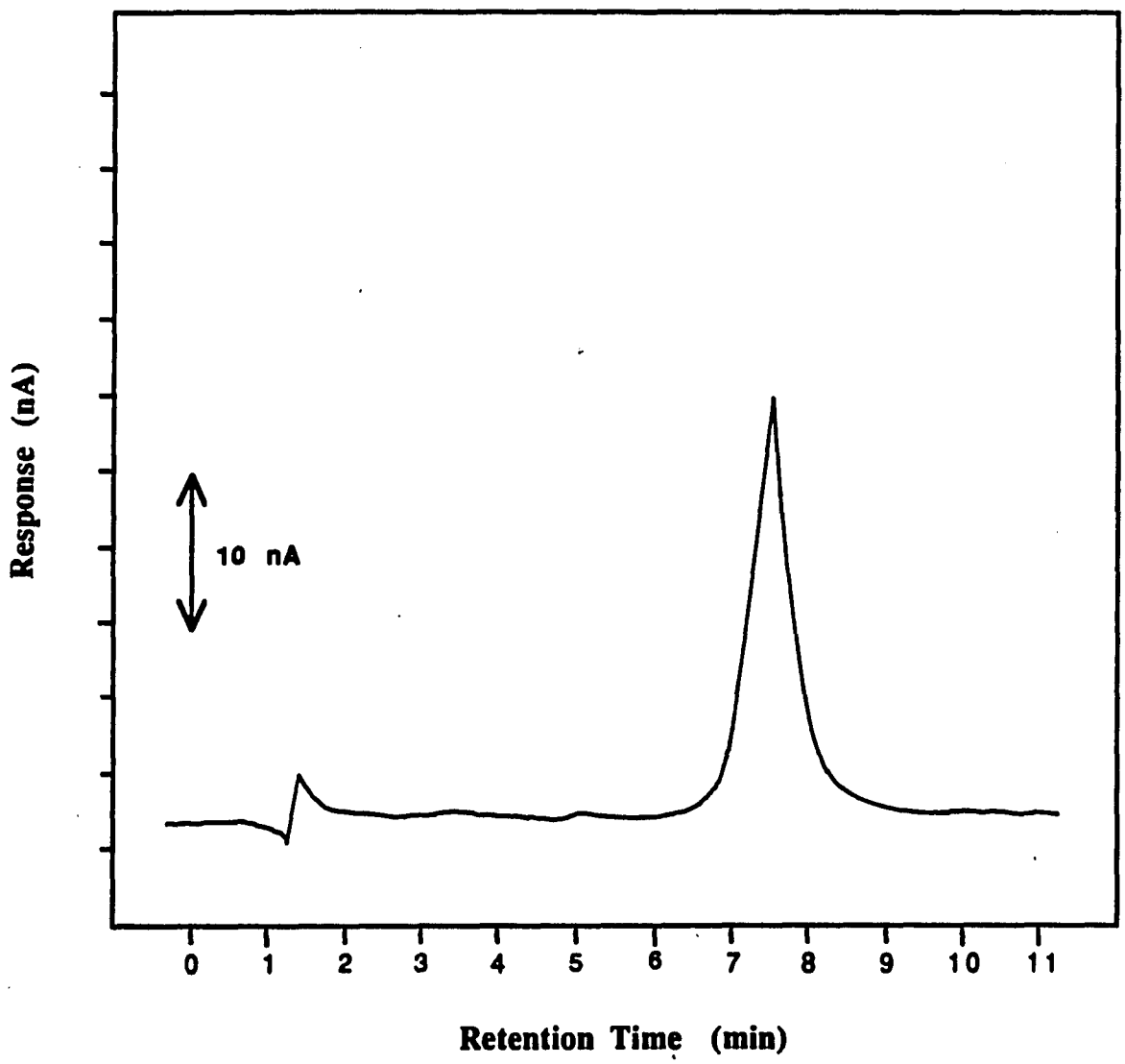

Figure 6. HPLC-ECD chromatogam of a supercritical fluid extract of a milk-based formula spiked with vitamin K-1 prior to extraction and analysis. Extraction conditions: SFE at 8000 psi CO_2, 60 ^{0} C, 20 min. Chromatographic conditions as in Figure 3. Silver applied potential at -1.1 V vs SCE. Recorder sensitivity, 10 nA/V, 1V full-scale. Sample spiked with 0.25 µg standard vitamin K-1 per gram product.

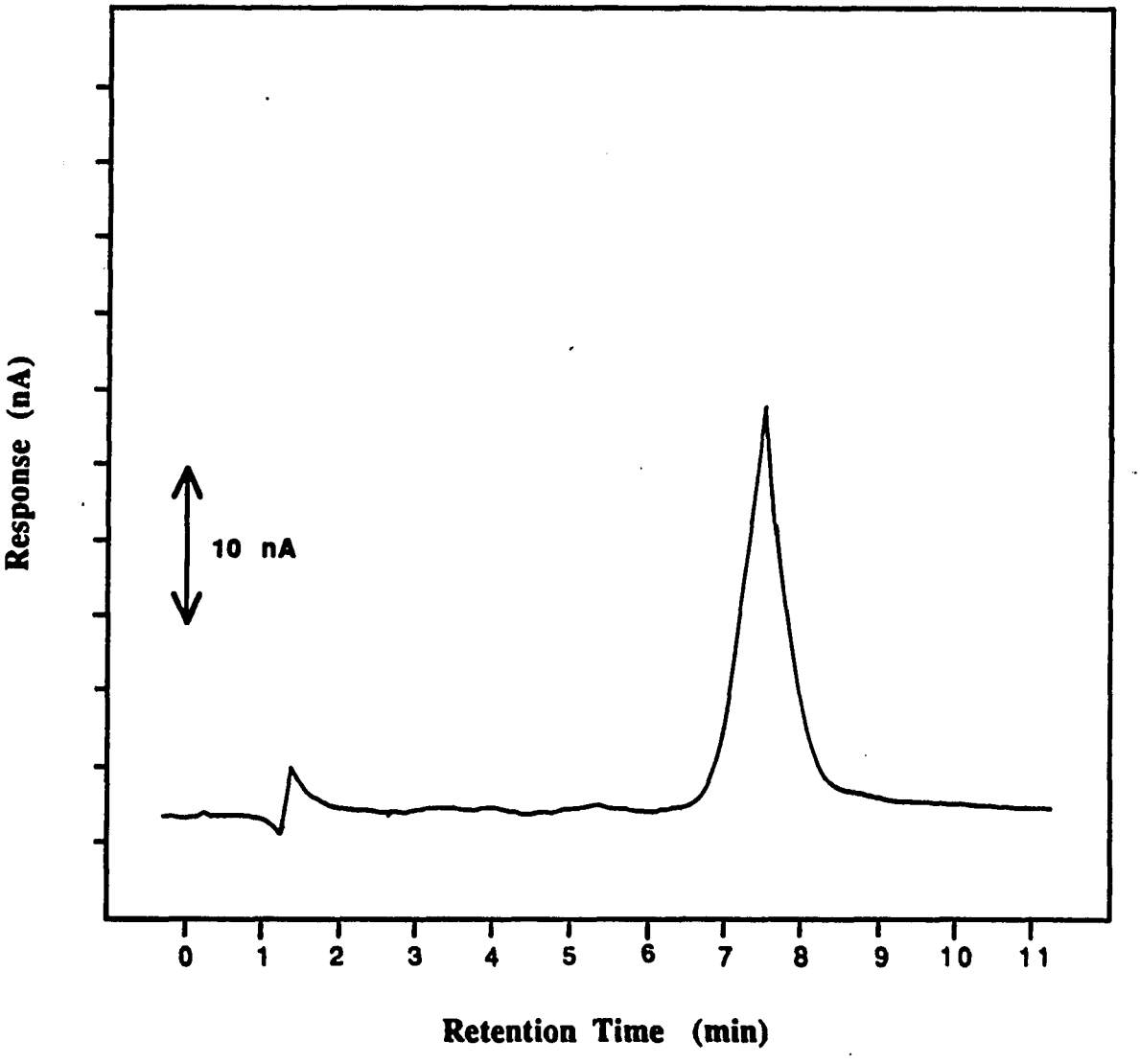

Figure 7. HPLC-ECD chromatogam of a supercritical fluid extract of a soy-based formula spiked with vitamin K-1 prior to extraction and analysis. Extraction conditions: SFE at 8000 psi CO_2, 60^0 C, 20 min. Chromatographic conditions as in Figure 3. Silver applied potential at -1.1 V vs SCE. Recorder sensitivity, 10 nA/V, 1V full-scale.

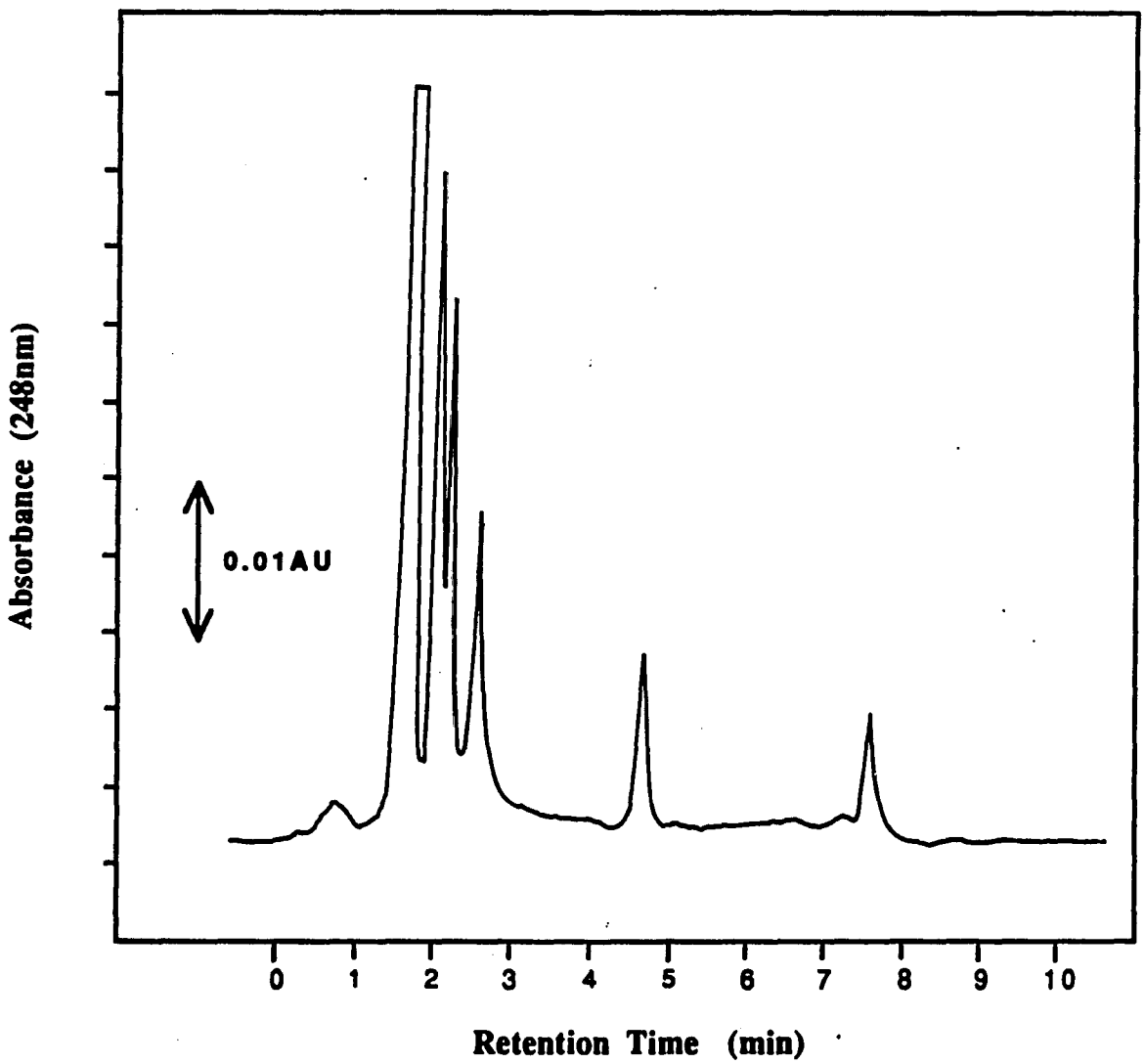

Figure 8. Liquid chromatogram with UV detection of added vitamin K-1 extracted from soy protein-based infant formula by SFE technique. Sample spiked with 10 µg vitamin K-1/g product. LC conditions: Perkin-Elmer 4000 LC system equipped with UV detector at 248 nm, 0.10 AUFS. Column, 150 mm x 4.6 mm I.D. Whatman C-18, with acetonitrile-methylene chloride-water (90+5+5, v/v) eluant.

Conclusions

The scope of HPLC method development for vitamin K_1 has been extended by the incorporation of SFE for sample preparation and ECD for quantitation. The introduction of SFE in place of saponification as a means of sample preparation provides shorter preparation times, minimal sample handling, and increased vitamin stability. Compared with a UV detector, an EC detector offers enhanced selectivity, sensitivity, simplified chromatography, and shortened analysis times. In addition, the need for a secondary cleanup step, required in most LC methods, is eliminated. The performance of the HPLC method is characterized by good reproducibility (5-8 % RSD), low detection limits (80 pg) and conditions favorable for direct detection of the analyte. Furthermore, throughout this work no column deterioration was observed and retention behavior was reproducible.

Part III Chapter 4

Determination of Vitamin A Palmitate in Ready-to-Eat Breakfast Cereals

Introduction

Ready-to-eat cereals are typically fortified with vitamin A at the 25-125 μg/g level. The retinyl palmitate form of vitamin is the one most commonly used by cereal manufacturers, since this form exhibits the greatest stability toward oxygen.

The assay of retinyl palmitate in cereals presents several problems related to sample preparation and clean-up, precision, and specificity for the vitamin chemist. Retinyl palmitate is sensitive to heat, light, and oxygen. Its selective isolation at the levels found in cereals is complicated by the presence of lipids as well as other fat-soluble vitamins such as E, K, and D. Sample preparation procedures are further complicated by matrix components such as excipients, antioxidants and emulsifiers. A good review on the measurement of vitamin A in foods was published by Parrish (1). In-depth practical details of established methods for vitamin A can be found in several books (2-4).

Historically, compendial sample preparation procedures for vitamin A in foods and feeds have involved "brute force" techniques for the removal of interfering substances such as lipids, steroids, carotenoids, vitamin A decomposition products and other fat-soluble vitamins. The general scheme recommended by the AOAC (5) includes saponification followed by liquid-liquid extraction and open-column purification prior to determination. Most of the drawbacks associated with this procedure stem from the initial saponification step. Alkaline hydrolysis, while effective in matrix removal, is an unnecessarily harsh treatment with regard to vitamin stability. This process is also carried out under conditions of heat, and light, all of which could catalyze destruction of vitamin A activity. In addition, uncontrolled conversion of retinoids to the alcohol form is accompanied by variable isomer mixtures and loss of internal precision and sensitivity. Furthermore, the subsequent extraction of the saponified fraction with an organic solvent is costly, laborious, and its efficiency is dependent on the residual moisture and fat content. The multiple transfers, evaporations and washings during the extraction can lead to unpredictable losses. Finally, the entire procedure is dependent on individual technique and is not amenable to simultaneous determination of several fat-soluble vitamins nor to automation. These problems, associated with the preparation of powdered milk, margarine and cereals, have been recently reviewed by Thompson (5).

To circumvent the problems associated with alkaline hydrolysis, a few alternate approaches to lipid removal have been investigated. Among them is an enzymatic hydrolysis method developed by Barnett et al. (6) for the simultaneous isolation of vitamins A, D_2, D_3, E, and K_1 in infant formula. In this latter method, triglycerides are converted into long chain fatty acids by lipase at ambient temperature and at neutral pH. By using enzymatic hydrolysis in place of alkaline hydrolysis, a predictable and controllable mixture of vitamin esters and alcohols is formed. However, the method is time-consuming, requires a secondary extraction prone to errors, and the final separation and the quantitation of the various isomers remains a major problem.

Following the introduction of small particle supports, high pressure gel permeation chromatography (HP-GPC) has received increased attention as a fractionation or clean-up method for fat-soluble vitamins in lipid matrices. Advantages and early applications of this technique to lipid foodstuffs have been reviewed by Vivilecchia et al. (7) and by Krishen (8). Holasiva and Blattna (9) rapidly fractionated retinol, retinyl palmitate, and carotene from other fat-soluble vitamins in fortified margarine using a single Sephadex LH-20 column. They achieved quantitative recovery of the retinyl ester without saponification and thus avoided conditions which might lead to degradation of retinyl palmitate in the sample. Simlarly, Landen and Eitenmiller (10) selectively separated retinyl palmitate and ß-carotene from the bulk lipid in a margarine sample with a μ-Styragel column. Using the same philosophy, Landen (11) investigated the use of two or more μ-Stryragel columns connected in series for the isolation of retinyl palmitate from breakfast cereals. Brown-Thomas et al. (12) more recently described a sample preparation procedure in which GPC was used to selectively isolate both retinyl acetate and ergocalciferol from the bulk of the lipid material in a coconut oil sample (SRM 1563) and a cod-liver oil sample (SRM 1588). In this method, vitamin fractionation was achieved on an semi-preparative amino or cyano column prior to fat elimination on a polystyrene/divinylbenzene gel column using a mobile phase composed of 30% methyl tert-butyl ether in methylene chloride. Although GPC is a non-destructive technique and eliminates the need for subsequent extractions, this procedure still requires too much sample handling in the form of evaporations and manual intervention for routine monitoring. The existing preparation methods, variously modified, continue in wide use despite their shortcomings. An improved method that employs newer technology is needed.

The AOAC method (13) specified for the quantitation of vitamin A in food extracts is the Carr-Price Colorimetric procedure. This procedure relies on the formation of a transient blue-colored complex produced by the interaction of vitamin A with antimony trichloride. This procedure is subject to numerous analytical problems. First, the reagent used to form the characteristic blue chromophore, antimony trichloride, is very corrosive because it picks up atmospheric moisture to form hydrochloric acid. Second, extraneous sterols in the cereal mixture can also react with this reagent, causing spuriously high vitamin A levels. Finally, rapid fading of the blue color leads to a time dependency and thus poor reproducibility. As a result, the method requires considerable skill, expense, time, and is not specific nor amenable to simultaneous determinations of isomeric forms. Other less popular colorimetric and fluorimetric methods have been reported by Neeld and Pearson (14), Dugan et al. (15), Sobotka et al. (16) and Erdman et al. (17). Similarly these methods are not specific and are subject to interferences and other analytical problems (18). It is generally recognized that a more precise and specific method is needed for the determination of vitamin A compounds in foods.

Recent advances in the HPLC of fat-soluble vitamins, including the use of high resolution small diameter packing materials and specific detectors have resulted in improved specificity, precision and speed of analysis when compared to traditional methodologies. Numerous publications (19-32) describing various LC approaches including normal phase, reversed phase and non-aqueous reversed phase for the separation of vitamin A in food materials can be found in the literature. A reversed-phase LC method was described by Thompson and Maxwell (19) for the quantitation of vitamin A in margarine, infant formulas and fortified milk using a 10 μm LiChrosorb column after saponification and hexane extraction. The HPLC results of Thompson and Maxwell agreed closely with spectrophotometric methods for vitamin A. Henderson and McLean (20) described a streamlined version of the Thompson and Maxwell method in which sample quantities were reduced permitting the elimination of a secondary clean up step. However, recovery studies were performed at levels 10 times the amount normally found in milk. Egberg et al. (21) used reversed-phase HPLC on a Vydac 10 μm ODS column to quantitate the all trans- and cis-isomers of vitamin A in foods following saponification. Cohen and Lapointe (22) utilized a μ-Bondapak C-18 column to determine simultaneously vitamins A, D, and E in animal feeds. Mankel (23) determined vitamins A, E, and D in margarine and

powdered foodstuffs by employing reversed-phase chromatography after saponification and open column purification. Ashoor and Knox (24) employed a linear gradient composed of acetonitrile, n-butanol and glacial acetic acid for the reversed-phase separation of vitamin A palmitate in fortified foods and vitamin supplements following liquid extraction with acetone-chloroform (50/50, v/v). Reversed-phase HPLC methods are not usually suitable for high throughput since they have long run times, and are tedious and not rugged, mainly because of the preliminary purification steps needed. Fat and oil droplets can easily be retained on the column surface resulting in shortened column life, occasional peak ghosting and high operating back-pressures. In addition, the steps necessary to dry and reconstitute extracts in the reversed phase eluent are accompanied by erratic losses of vitamin A.

One solution to these problems is the use of normal phase columns and mobile phases to lessen fat contamination. Normal phase LC methods containing a preliminary saponification step as well as those compatible with direct extract injection have been described (25-29). Dennison and Kirk (25) described a normal phase procedure on μ-Porasil after saponification and subsequent extraction of the sample with hexane for the analysis of vitamin A as retinol in cereal products. These authors (25) reported that the presence of carotenoids, various food additives, and vitamin A oxidation products did not interfere. Similarly Head and Gibbs (26) determined vitamin A activity in saponified food composites by HPLC on a 10 μm LiChrosorb® Si (60) with gradient elution. Thompson et al. (27) described an HPLC method in which the saponification step was replaced by a general fat extraction procedure. In this method, the ground sample is mixed with water and directly extracted with hexane. After centrifugation a 100 μL aliquot of the extract was removed for subsequent separation on a LiChrosorb® Si (60) column using ethyl ether-hexane (2+98) as the mobile phase. Widicus and Kirk (28,29) also reported on a normal phase method in which crude extracts from breakfast cereals are directly chromatographed on a μ-Porasil column, using an isocratic mobile phase of hexane-chloroform (85+15) with a flow rate of 1.5 mL/min. Although normal phase HPLC methods have eliminated column contamination problems and have shortened and simplified the sample preparation procedure, normal mobile phases are not compatible with many sensitive and selective detection schemes.

To circumvent these problems, non-aqueous reversed-phase (NARP) HPLC methods

have been described (30,31). A NARP method has been described by Parris (30) for the analysis of a variety of low moisture samples containing vitamin A palmitate. Separations were achieved with a C-18 column and an acetonitrile-methylene chloride mobile phase. Results indicated that up to 10 mg of the crude fatty extract can be injected before column deterioration occurs. Landen and Eitenmiller (31) reported on the NARP-HPLC analysis of vitamin A palmitate extracts obtained from the GPC fractionation of margarine samples. Similarly, Landen developed NARP methods for the determination of vitamin A palmitate in breakfast cereals (10) and the simultaneous determination of vitamin A palmitate and tocopherol in infant formulas (32). In each case the vitamins, selectively fractionated from the lipid matrix by GPC, were quantitated on either a Zorbax ODS or μ-Bondapak C-18 column using methylene chloride-acetonitrile-methanol (30+69.8+0.2, v/v) with an UV absorbance detector. Barnett and Frick (6) developed a sophisticated NARP scheme using a sequence of gradients to improve the separation of several fat-soluble vitamins, including vitamin A, in baby formula extracts. In general none of these methods has won wide acceptance as a method that is relatively simple, precise, accurate and versatile.

In an attempt to improve the reliability of the HPLC method, we decided to eliminate the saponification step including the associated extractions, manipulations, and determine vitamin A activity directly as retinyl palmitate. This required a rapid technique for extracting trace levels of fat-soluble vitamins with minimal handling. These difficulties were overcome by performing a single efficient extraction with supercritical carbon dioxide and subjecting the extract to HPLC separation with electrochemical detection.

Supercritical fluid extraction has been previously shown by us (pp. 181-201) to be a gentle tool for isolating trace quantities of vitamin K-1 from infant formula. SFE offers a number of advantages including it is rapid and can be conducted in a dark, oxygen-free environment. In addition, easy solvent removal provides the potential for automation and compatibility with many subsequent separation schemes.

Although the advantages of electrochemical detection following LC separation with regard to enhanced selectivity, sensitivity and reduced cost are obvious, few applications for commercial vitamin formulations have been reported. The virtues of voltammetry for the determination of standard vitamin A in static systems has been

discussed by Atuma et al. (33,34). More recently, Huang et al. (35) described the merits of amperometric detection at a glassy carbon electrode for the determination of trace levels of vitamin A in plasma. In comparison to UV detection, enhanced sensitivity and selectivity were obtained for complex clinical samples.

EXPERIMENTAL

Chemicals

Retinyl palmitate in oil was purchased from Sigma Chemical Co. (St. Louis, Mo). HPLC-grade acetonitrile and isopropanol were obtained from J. T. Baker (Phillipsburg, NJ). In-house distilled water was used throughout the study. Reagent grade $NaClO_4$ was obtained from Fisher Scientific (Pittsburgh, PA) and was used without further purification.

Laboratory precautions

All extracts and analytical standards were protected from light by storage in actinic glassware or in aluminum foil-wrapped vials.

Preparation of standards

A stock solution of retinyl palmitate was prepared in isopropanol at a concentration of 350 µg/mL. Working solutions ranging from 3.5 to 35.0 µg/mL were prepared by diluting the stock solution with mobile phase.

Apparatus

The laboratory-constructed HPLC used in the study has been thoroughly described elsewhere (pp. 16-36). It consisted sequentially of a Varian 8500 syringe-pump, a Rheodyne 7125 injector, a 150 mm x 4.6 mm I.D. Altex C-8 analytical column and an amperometric thin-layer detector equipped with a glassy carbon electrode. The working potential was set at + 1.2 V vs SCE. The electrochemical response was recorded on a Linear Model 1200 strip chart recorder. A peak detector (pp. 30-32) was used to store store individual peak heights for quantitation.

The mobile phase was comprised of methanol-acetonitrile-aq. 0.05 M $NaClO_4$

(45/45/10, v/v). Prior to use the mobile phase was filtered and thoroughly degassed with nitrogen according to procedure of Kissinger (36). The flow rate through the column was 2 mL/min and the column was maintained at ambient temperature.

Sample preparation procedure

Breakfast cereals were obtained from local retail stores. Prior to analysis, bulk composite samples were formed by mixing samples from two different lots. Typically, a two gram sample of each cereal was transferred to the extraction chamber and held in place between two glass wool plugs. The chamber was sealed and inserted into a laboratory-built high pressure extraction manifold (pp. 124-125). The samples were extracted with carbon dioxide at 8000 psi and 60^{0}C for 15 min. Following depressurization, the supercritically extracted analytes were transferred to a syringe fitted with a filter and washed with 30 mL of isopropanol. The crude extract was evaporated in a rotary evaporator maintained at 45^{0}C, reconstituted in mobile phase and a 20-μL aliquot of the resulting solution was injected onto the analytical HPLC column.

Results and Discussion

Chromatography

Vitamin A palmitate can be separated by normal-phase as well as by reversed-phase chromatography. However, in this study attention was focussed on a reversed-phase method because retention times obtained on chemically bonded reversed-phase supports are less susceptible to traces of water, and the commonly used mobile phases are readily compatible with electrochemical detectors. During preliminary studies, we investigated reversed-phase separations using a mobile phase composed of acetonitrile-water (90/10, v/v) containing 0.025 M sodium perchlorate. However, with this solvent system, poor peak shapes and long retention times were obtained for vitamin A palmitate. The addition of isopropanol to the mobile phase provided a markedly improved peak shape for vitamin A and compressed the separation of vitamin A from interferences into the smallest possible time span. The role of isopropanol, in an aqueous-acetonitrile mixture (18/82, v/v), on vitamin A retention time is shown in Figure 1. A mobile phase prepared from 45 % (v/v) isopropanol and sufficient aqueous-acetonitrile stock solution (18/82, v/v) to give a final composition of isopropanol-acetonitrile-water (45+45+10, v/v/v) offers the best results with respect

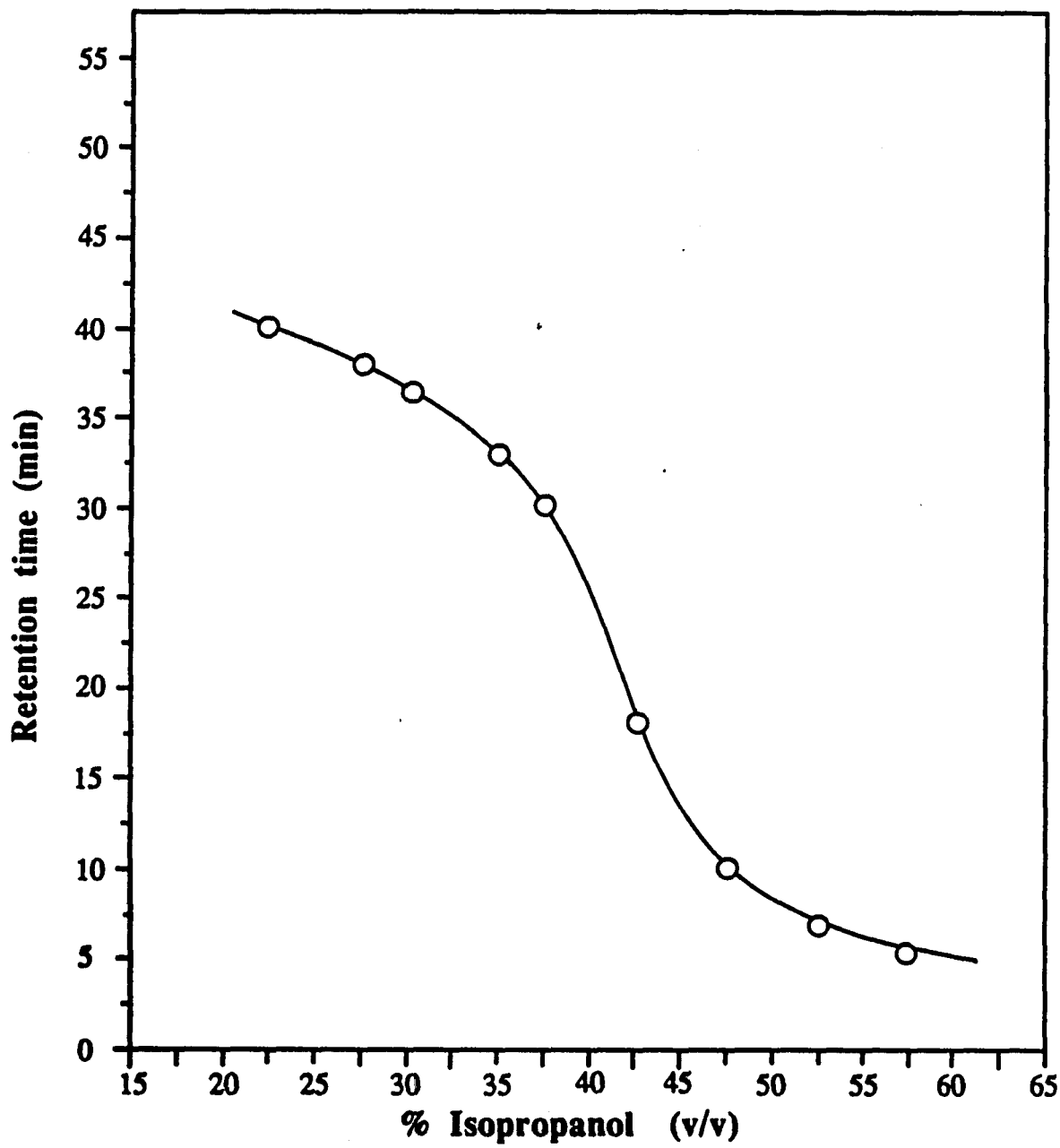

Figure 1. Dependence of vitamin A palmitate retention on isopropanol content of mobile phase. Chromatographic conditions: column, 150 x 3.9 mm I.D. μ-Bondapak C-18 (10 μm); flow rate, 2.0 mL/min, silver detector electrode potential, 1.2 V *vs* SCE; mobile phase, each mobile phase prepared by mixing appropiate volumes of pure isopropanol and a stock aqueous-acetonitrile (18/82, v/v) solution.

to retention and selectivity. Under these conditions, the retention time for vitamin A is 10 min with a capacity factor (k') of 9.0. The effect of both isopropanol and acetonitrile together is dramatic; a change in isopropanol content of only 5 % centered about the 45 % level can move the retention time of vitamin A from 9.5 min to 20 min.

Response Characteristics of Vitamin A

In order to achieve maximum selectivity and sensitivity with an electrochemical detector, the influence of such parameters as applied potential, mobile phase composition, flow rate and supporting electrolyte concentration must be established. If oxygen is not removed from the mobile phase, spurious capacitive currents, due to air bubbles, are raised to such an extent that no oxidative signals can be observed. Removal of oxygen by the procedure outlined by Kissinger (36) proved to be satisfactory.

Hydrodynamic voltammogram

The potential dependence of the detector response was evaluated by carrying out a series of experiments at constant flow rate, in which a standard vitamin A solution containing 0.55 μg was repeatedly injected into the LC at a series of increasing detector electrode potentials. Following peak elution, peak currents were recorded and plotted as a function of applied potential to obtain the so-called hydrodynamic voltammogram (HDV). A typical HDV for vitamin A at 2 mL/min is shown in Figure 2. Although interpretation of the curve is complex, it appears to exhibit the general characteristics of an irreversible oxidation controlled by an electrode reaction. The peak current increases as the potential is increased until a plateau is reached around +1.2 V *vs* SCE. In a practical sense, it is clear that the electrode should be held at a potential of 1.2 V vs SCE for maximum sensitivity. Though higher potentials did yield some increased response, this potential was selected as a compromise between maximum response and minimum residual current.

Role of mobile phase composition on electrochemical detection

Mobile phase was systematically varied to optimize analytical sensitivity and steady-state background current. The influence of mobile phase composition on background and sensitivity is shown in Figures 3 and 4, respectively. As shown in Figure 3, a rather dramatic decrease in background is observed as the isopropanol content increases. This is presumably due to the decreasing dielectric constant of the

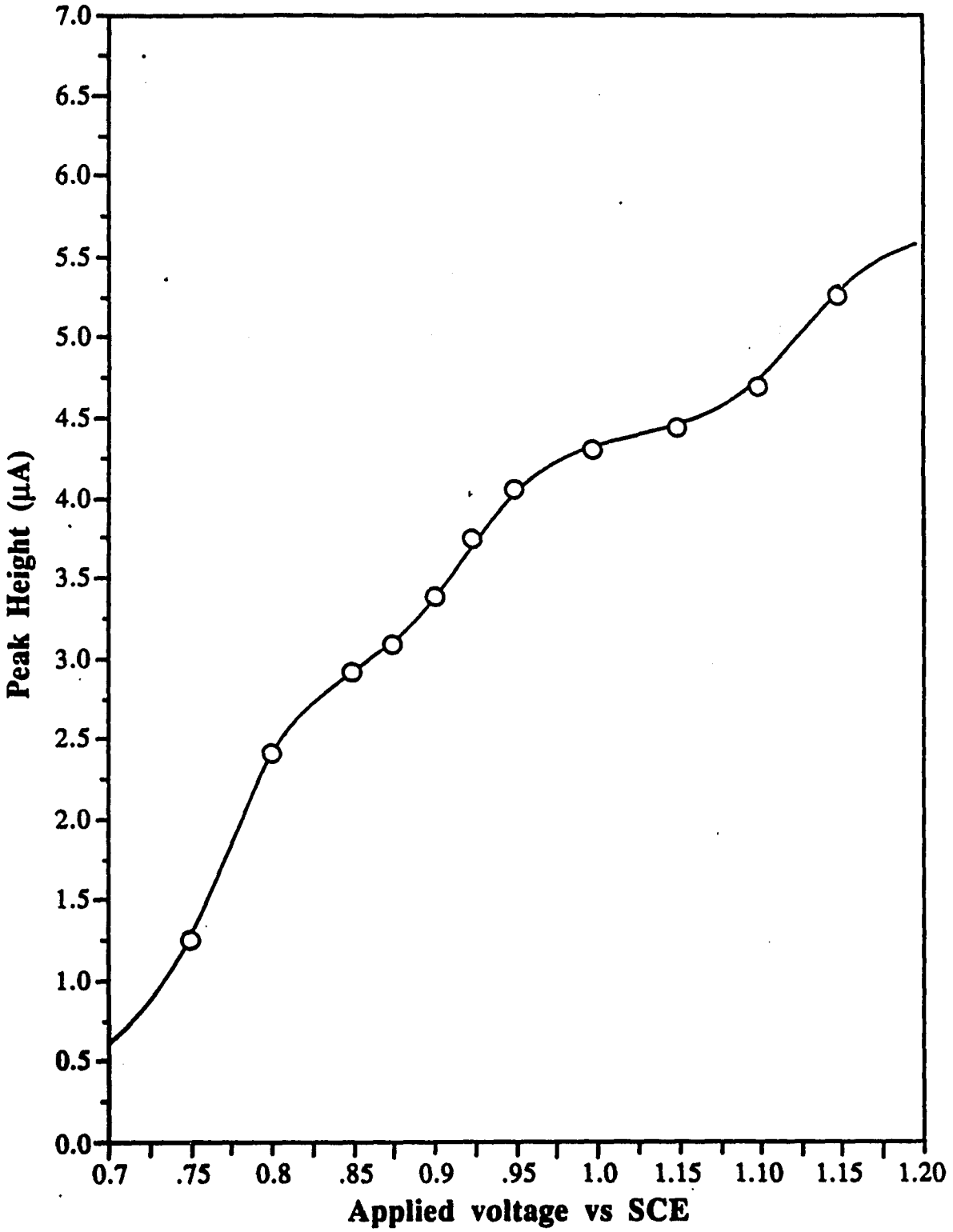

Figure 2. Hydrodynamic voltammogram of vitamin A palmitate. Chromatographic conditions: column, 150 x 3.9 mm I.D. µ-Bondapak C-18 (10 µm); mobile phase, acetonitrile-isopropanol-aq 0.025M $NaClO_4$ (45+45+10, v/v); flow rate, 2.0 mL/min; sample size, 20 µL aliquot injected of 275 µg/mL standard vitamin A palmitate in mobile phase.

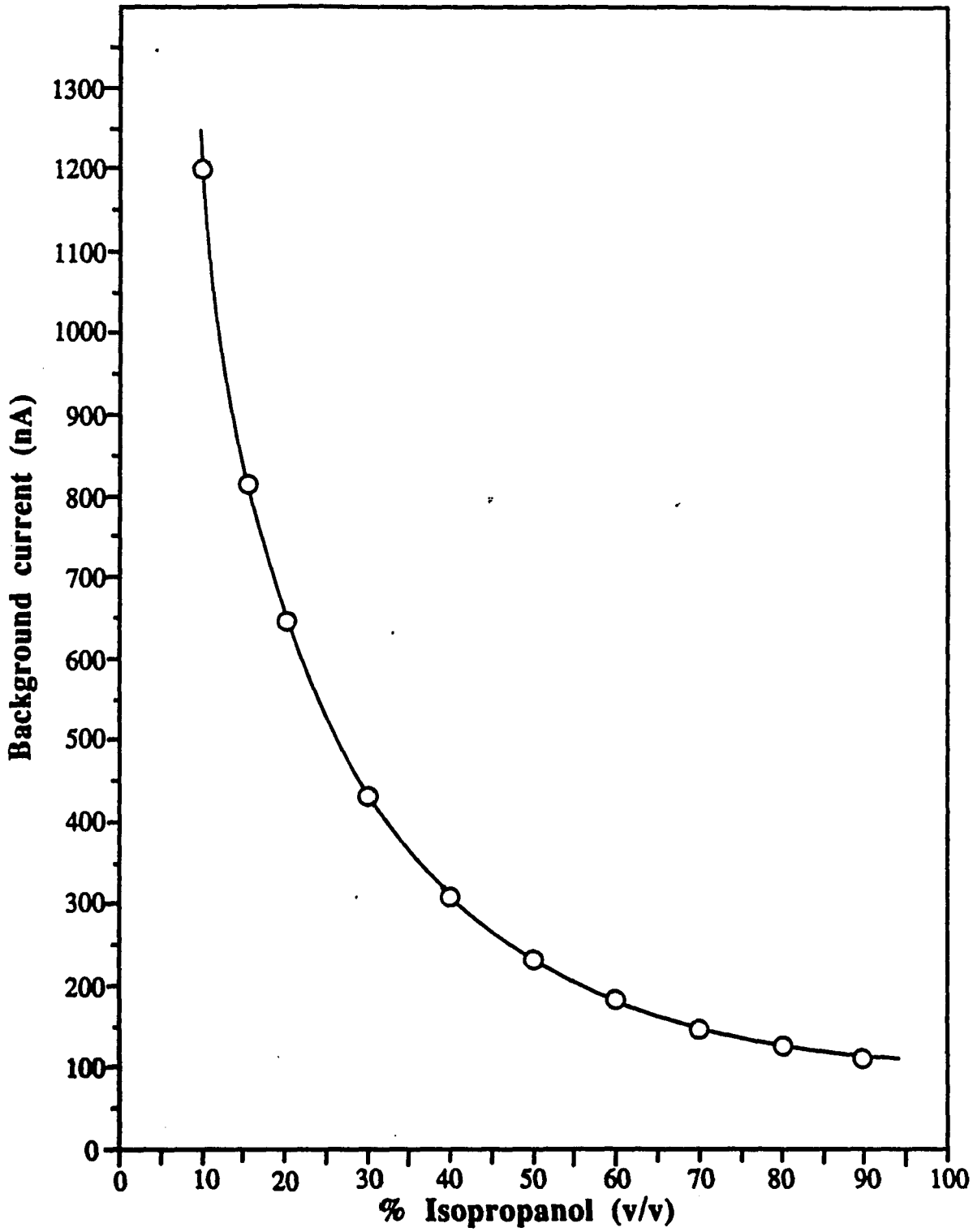

Figure 3. Background current as a function of isopropanol content of mobile phase. Chromatographic conditions: Column, 150 x 3.9 I.D. mm μ-Bondapak C-18 (10 μm); mobile phase, prepared from appropiate volumes of isopropanol and stock solution of 0.025 M $NaClO_4$-acetonitrile (18/82, v/v); flow rate, 2.0 mL/min; applied potential, 1.2 V *vs* SCE.

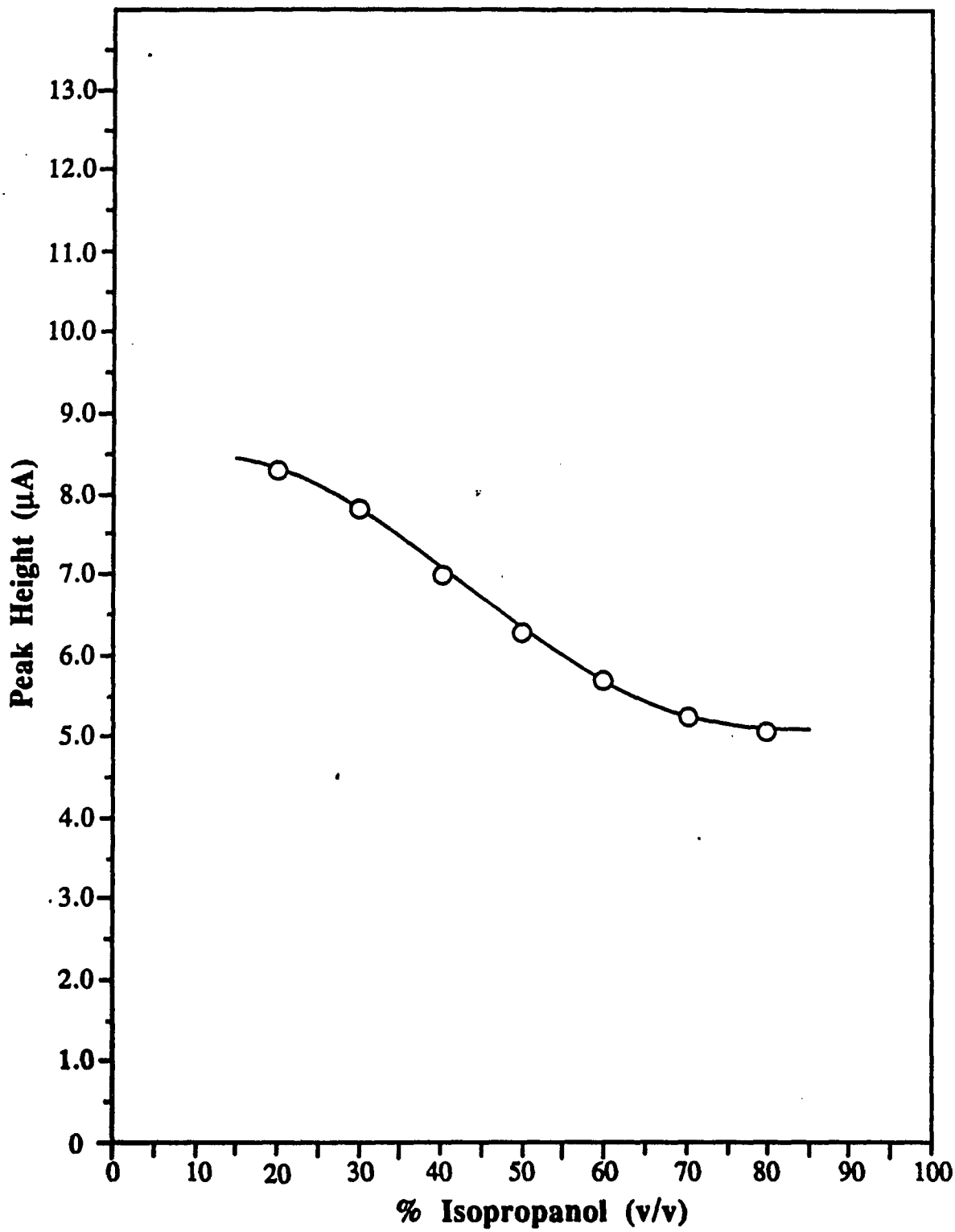

Figure 4. Effect of isopropanol content on the magnitude of the reduction signal of vitamin A palmitate. Chromatographic conditions: column, 150 x 3.9 mm I.D. μ-Bondapak C-18 (10 μm); mobile phase, prepared from appropiate volumes of isopropanol and stock solution of 0.025 M $NaClO_4$ -acetonitrile (18/82, v/v); flow rate, 2.0 mL/min; applied potential; +1.2 V *vs* SCE; sample size, 20 μL of 350 μg/mL injected at each mobile phase.

eluent mixture. On the other hand, the effect of of eluent composition on the peak height sensitivity for vitamin A is shown in Figure 4. As expected, the peak height decreased with increasing isopropanol proportion, which can be attributed in part to elongated retention times and broader peaks. The maximum isopropanol proportion that was feasible was up to 45 %, above which the selectivity dramatically decreased.

Influence of electrolyte concentration

Figure 5 illustrates the effect of concentration of electrolyte on detector response for vitamin A. Without sodium perchlorate, no response at all is obtained. At concentrations of electrolyte below 0.025M, the detector response increased with electrolyte concentration. Beyond this concentration, a plateau and even a small decrease in response is seen. A sodium perchlorate concentration of 0.025 M offers a wide linear dynamic range with a minimun amount of column deterioation.

Dependence on Flow Rate

Figure 6 shows the dependence of the peak current on the flow rate. As was shown in previous studies (37, pp. 84-90), an increase in sensitivity is obtained with increasing flow rate. As the flow rate increases, the peak current rises rapidly at first and then more slowly until a plateau is reached. When replotted on a log-log scale, the data in Figure 6 give a straight line with a slope of 0.39. This value is in good agreement with the value 0.33 reported by Weber (38) at flow rates greater than 2 mL/min. A flow rate of 2 mL/min was chosen as optimal flow rate for vitamin A in all further separation studies.

Quantitation of Vitamin A Palmitate

The response of vitamin A palmitate determined with the ECD exhibits a wide range of linearity from 5.5 µg to 550 pg. A typical working calibration curve used to determine vitamin levels is shown in Figure 7. The curve is linear in the range of 3.5 to 35 µg/mL and passes within experimental error through the origin. Based upon a signal-to-noise ratio of 3 and a background current of 90 pA, the limit of detection is approximately 275 pg. Concentrations in excess of 40 µg/mL were not studied in order to minimize the possibility of electrode fouling, although linearity typically extends substantially above this range.

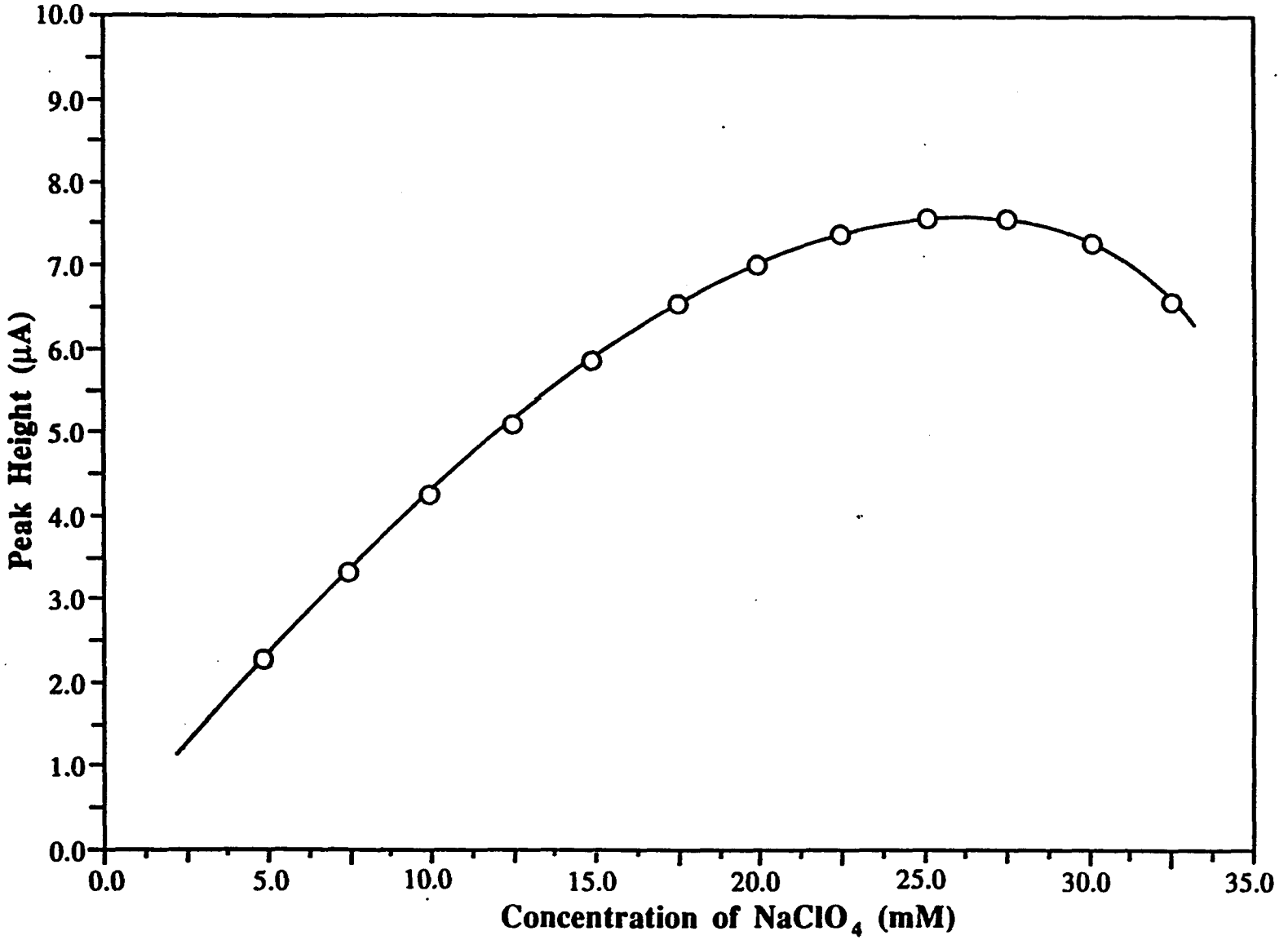

Figure 5. Influence of the concentration of $NaClO_4$ on the reduction of vitamin A palmitate. Conditions: stationary phase, μBondapak C-18 (10 μm); mobile phase, acetonitrile-isopropanol-water (45+45+10,v/v); flow rate, 2.0 mL/min; applied potential, 1.2 V *vs* SCE.

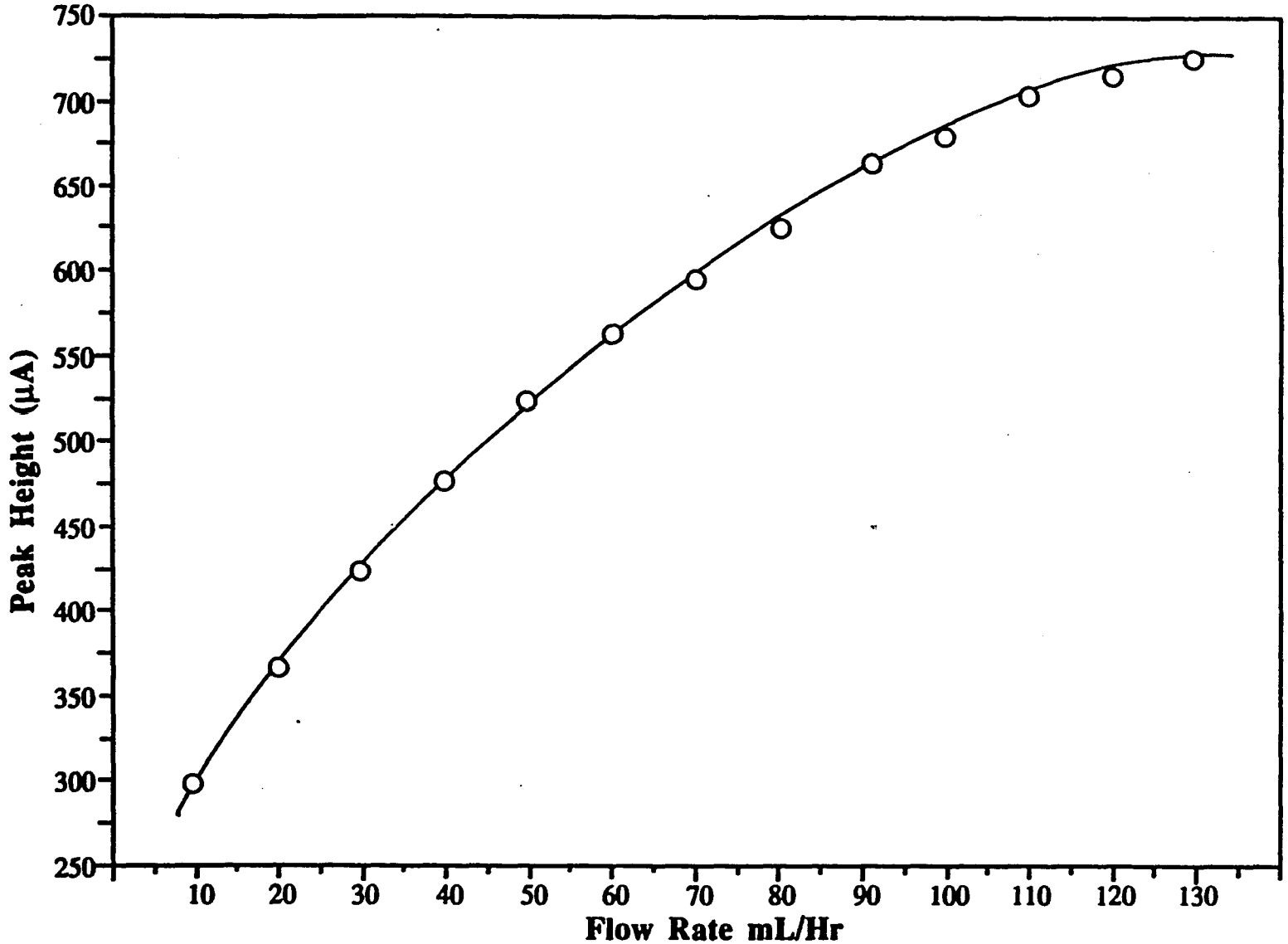

Figure 6. Dependence of peak current on flow rate. Except for flow rate, chromatographic conditions as in Figure 5.

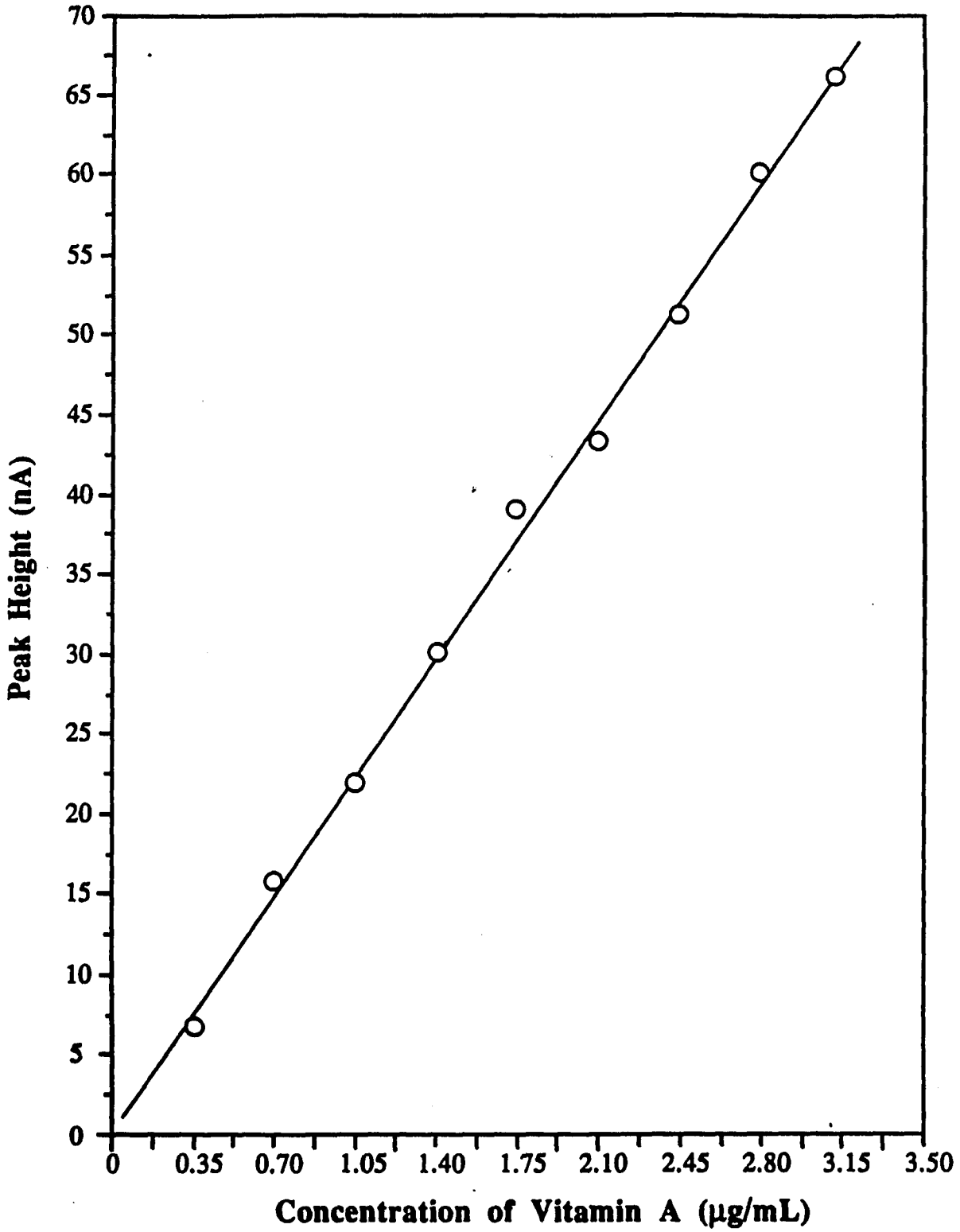

Figure 7. Detector response curve for vitamin A palmitate. Chromatographic and detector conditions: column, 150 x 3.9 mm I.D. μ-Bondapak C-18 (10 μm); mobile phase, acetonitrile-isopropanol-aq $NaClO_4$ (45+45+10,v/v); flow rate, 2.0 mL/min; applied potential, -1.1 V *vs* SCE.

Extraction Procedure

Prime objectives in the development of the sample preparation procedure were the need for the conservation of the integrity of the vitamins; the elimination of interfering substances; and the minimization of the total number of steps to reduce the expenditure of time and the possibility of error. Earlier work in our laboratory (pg. 191) involving the desorption of vitamin K_1 from adsorbent cartridges, suggested that supercritical carbon dioxide is a clean and efficient extractant for these hydrophobic analytes.

As a first approach to the development of this sample preparation procedure, it is necessary to optimize the pressure, temperature, and equilibration time. The influence of pressure on efficiency at 45^0C and 60^0C was assessed by extracting one gram samples of Chromosorb W spiked with 50 μg of vitamin A at several pressures in the range of 5000 to 8000 psi. The dependence of pressure on percentage recovery for each temperature is illustrated by the two curves in Figure 8. From curve (A) at 60^0C, it may be seen that efficiency rises steeply in the region of 5000 to 7500 psi and reaches a plateau around 8000 psi. When the temperature is lowered to 45^0C, a sigmoidal-shaped curve (B) is observed over 5000 to 7500 psi range with a limiting efficiency far below 90 %. The optimum extraction time was also studied. As shown in Table 1, the extraction is complete within 15 minutes, with essentially no change up to 90 minutes. For maximum sensitivity, an equilibration time of 15 minutes at 8000 psi and 60^0C was chosen. Under these extraction conditions, a chromatogram of an extract obtained by means of supercritical fluid desorption of a Chromosorb W cartridge spiked with 25 μg/g with vitamin A palmitate is shown in Figure 9. Chromatographic analysis shows only one peak at 10 min for vitamin A with a mean percentage recovery of 94 % and a coefficient of variation of 3.1 % (n=3).

Evaluation of the batch SCFE-HPLC-ECD procedure

In order to characterize the accuracy and precision of the method unfortified cereal bases, such as corn, wheat, and oat were spiked with vitamin A palmitate at levels ranging from 10-125 μg/g. The vitamin A was then recovered by the SFE procedure described earlier and analyzed in triplicate using a glassy carbon based electrochemical detector following reversed-phase HPLC. The recoveries for the various cereal bases fortified at 4 levels ranging from 10 to 125 μg/g are presented in Table 2. Efficiences in Table 2 represent the average of three extractions. Over all, as demonstrated in Table 2, extraction recoveries remained high over the entire range of concentrations

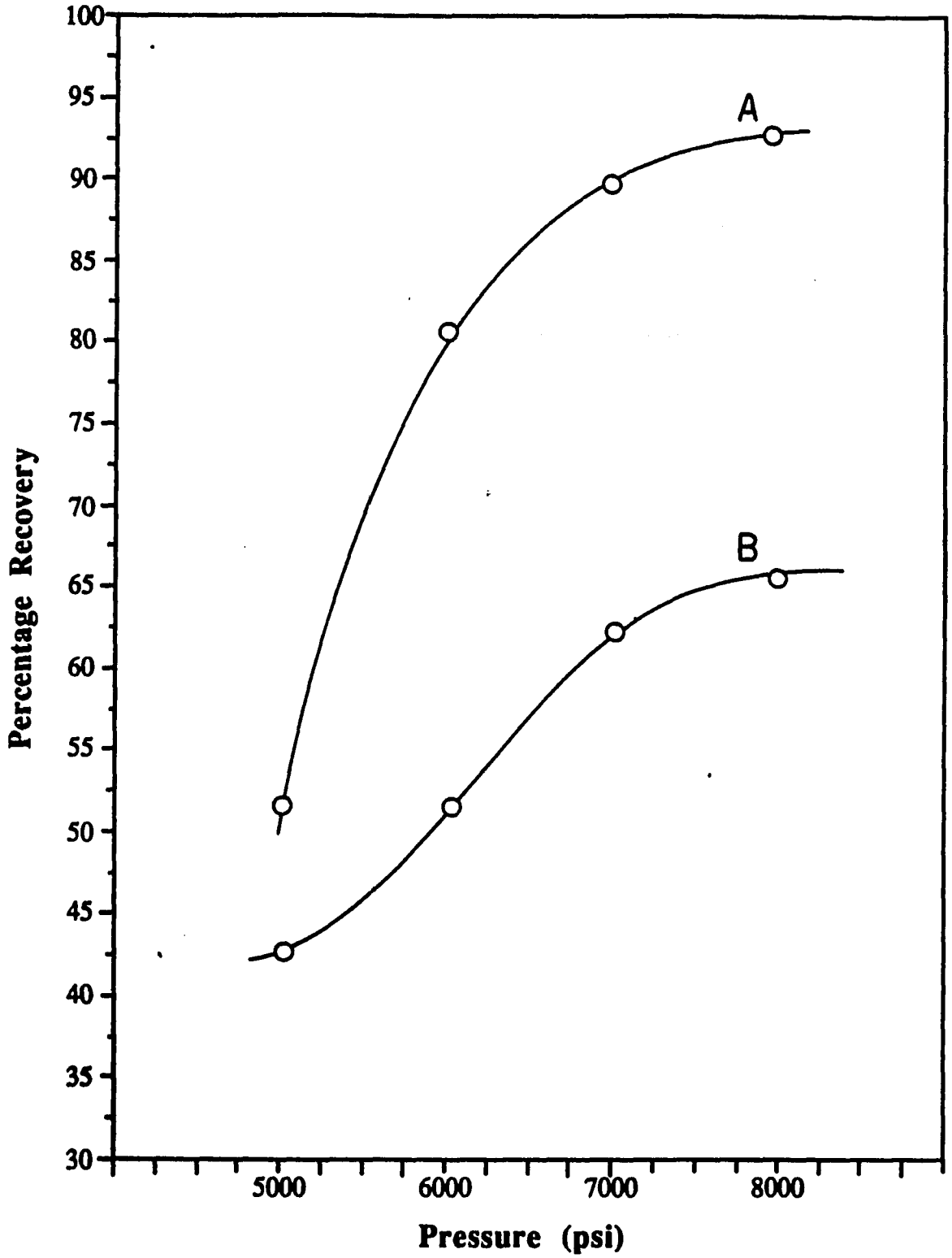

Figure 8. Effect of pressure on extraction efficiency at (A) 65 ^{0}C and (B) 45 ^{0}C. Equilibration time in each case was 20 min. Samples, one gram samples of Chromosorb W spiked with 50 µg of vitamin A palmitate were extracted at each pressure. Chromatographic analysis conditions as in Figure 2.

Table 1. Effect of equilibration time on Recovery for Vitamin A Palmitate at 8000 psi and 60°C.

Time, min	Average Recovery, %	RSD (n=3)
5	74	3.7 %
10	78	4.1 %
15	93	3.3 %
20	91	3.0 %
30	93	3.4 %

One gram samples of Chromosorb W fortified with 50 µg retinyl palmitate were extracted, in triplicate, for each equilibration period.

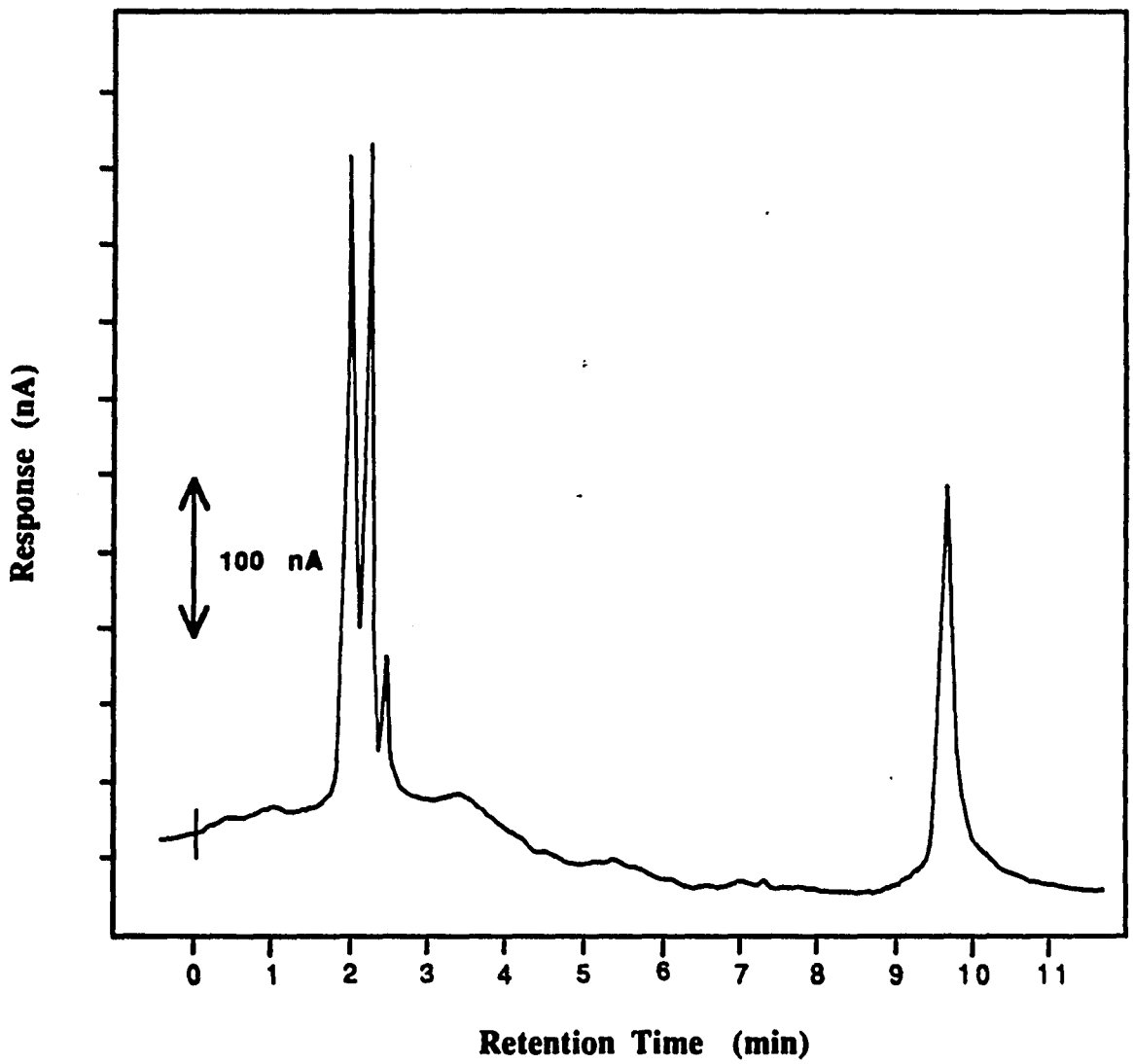

Figure 9. Typical chromatogram of vitamin A standard recovered from a solid phase cartridge by using SFE sample preparation. Column: 150 x 3.9 mm I.D. μ-Bondapak C-18 (10 μm). Mobile phase: acetonitrile-isopropanol-aq 0.025 M $NaClO_4$ (45+45+10, v/v). Detector: carbon-based working electrode, applied potential 1.2 V *vs* SCE. Sample, cartridge spiked with 50 μg vitamin A palmitate/ g Celite. SFE at 8000 psi CO_2, 60° C, 20 min.

Table 2. Application of Described Procedure to Fortified Grains.

Grain Substrate	Fortification level, µg/g	% Recovery ± RSD (n=3)
Corn	10	91 ± 6.4
	25	93 ± 6.1
	50	95 ± 5.9
	125	102 ± 5.6
Wheat	10	92 ± 3.8
	25	90 ± 3.2
	50	102 ± 3.4
	125	94 ± 2.5
Oat	10	92 ± 5.1
	25	103 ± 4.7
	50	90 ± 4.1
	125	93 ± 4.6

examined. For samples fortified with 10 μg/g, 25 μg/g, 50 μg/g, and 125 μg/g, recoveries ranged from 90.8 to 92.9 %, 89.6 to 103.1 %, 90.2 to 101.7 %, and 92.9 to 102.3 %, respectively. The average recovery of vitamin A palmitate over this entire range was 94.6 % with a relative standard deviation of (RSD) of 5.2 % (n=12). No significant differences were seen for retinyl palmitate from either corn, wheat, or oat cereals. Figure 10 is a chromatogram of a blank wheat sample taken through the entire procedure. This chromatogram clearly demonstrates that interferences contributed by natural compounds were minimal and that background vitamin A palmitate levels are far below the detectable limit. A typical chromatogram obtained from an extract of a spiked corn sample isolated by SFE is presented in Figure 11. The chromatogram illustrates the degree of resolution of vitamin A palmitate from interfering peaks encountered during this study. The single peak occurred at a retention time of less than 10 min. The identity of the vitamin A peak was verified by co-injection of the corresponding standard. The peaks at 2.5 min and 4 min were found in chromatograms from all grains fortified with standard vitamin A and appear to be related to antioxidant additives.

Effect of Lipids Load

The effect of excess lipid on the efficency and ruggedness of this procedure was examined by adding microgram amounts of vitamin A dissolved in 250 mg of vegetable oil to a series of previously analyzed corn samples fortified at 125 μg/g with vitamin A. The results are shown in Table 3. The recovery of vitamin A palmitate was not significantly affected by the presence of lipid or existing vitamin level. Throughout this work, over 50 cereal extracts were chromatographed on the same column without a change in retention time for the vitamin A peak, indicating that column deterioration as a result of lipid carry-over was not a problem.

Precision

Table 4 shows the results of precision studies performed with wheat fortified in the range of 25-100 μg/g. For within-day precision, RSD's ranged from 2.3 to 3.6 %. For day-to-day precision, the RSD's ranged from 3.8 to 8.1%.

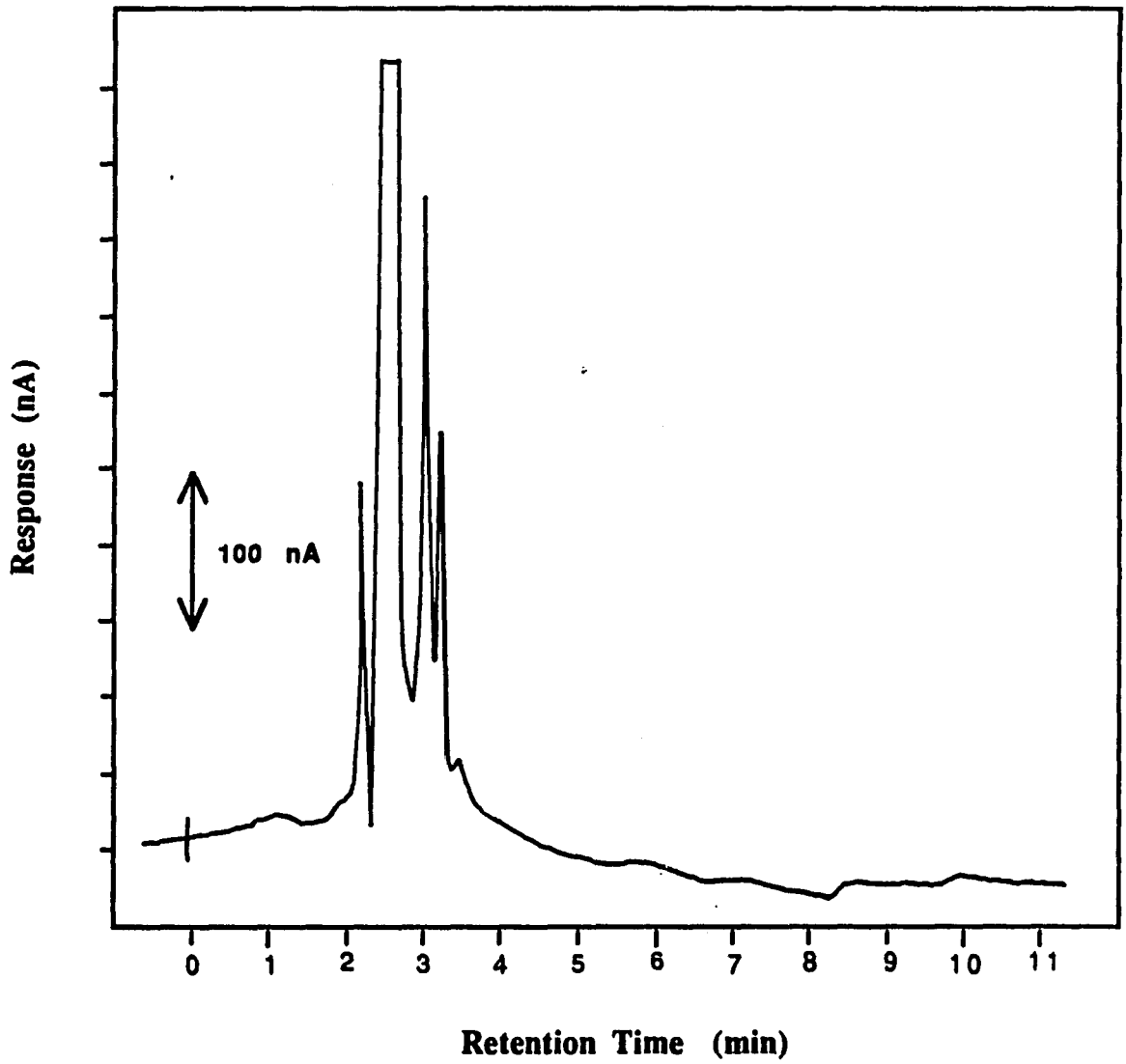

Figure 10. Typical chromatogram of a supercritical fluid extract of an unfortified wheat sample. Column: 150 x 3.9 mm I.D. μ-Bondapak C-18 (10 μm). Mobile phase: acetonitrile-isopropanol- aq 0.025 M $NaClO_4$ (45+45+10, v/v). Detector: carbon-based working electrode, applied potential 1.2 V vs SCE. SFE at 8000 psi CO_2, 60^0C, 20 min.

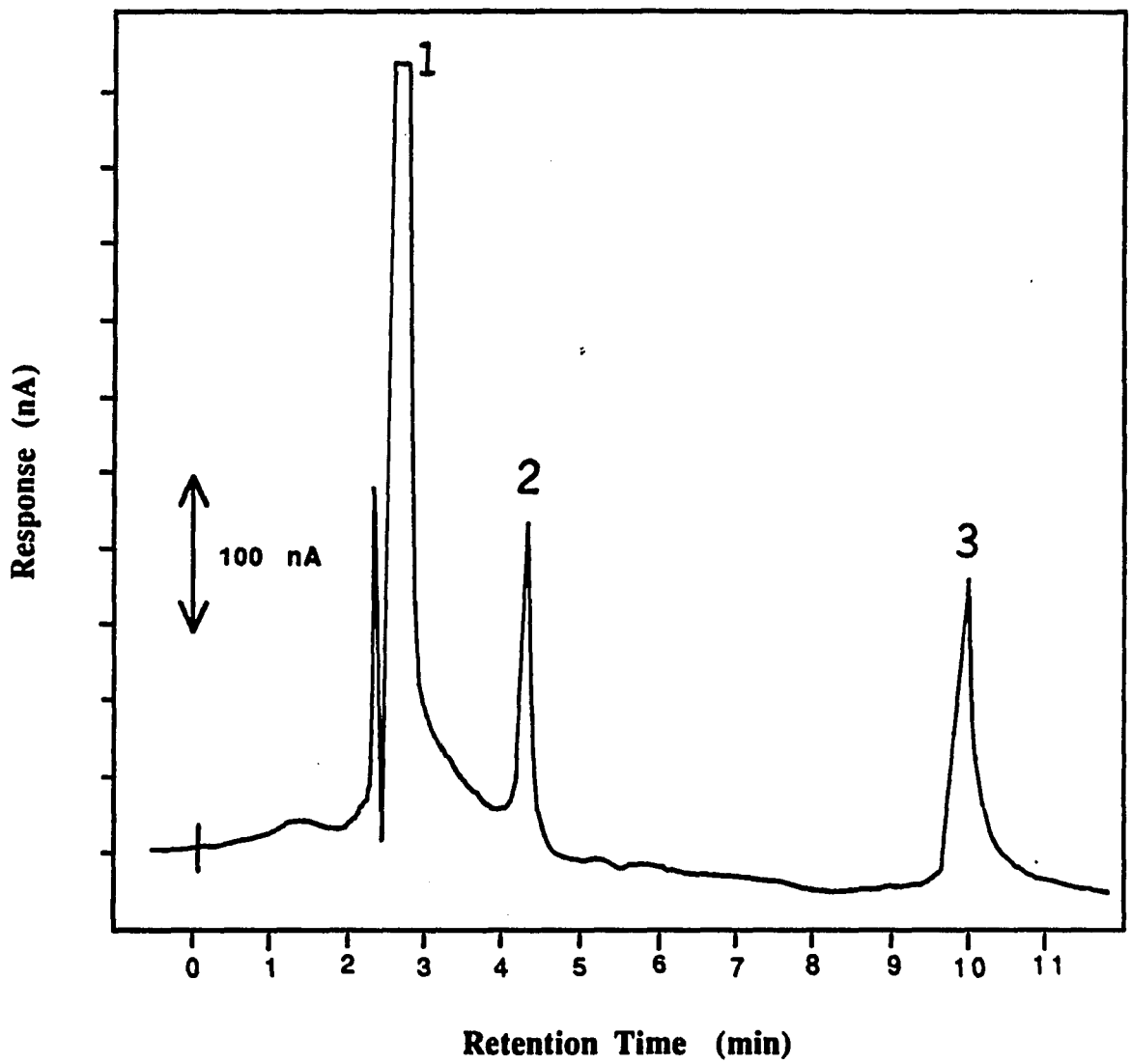

Figure 11. Typical chromatogram of a supercritical fluid extract of a corn sample fortified with vitamin A palmitate prior to sample preparation and chromatographic analysis. Column: 150 x 3.9 mm I.D. μ-Bondapak C-18 (10 μm). Mobile phase: acetonitrile-isopropanol- aq 0.025 M $NaClO_4$ (45+45+10, v/v). Flow rate was 2.0 mL/min. Detector: carbon-based working electrode, applied potential 1.2 V vs SCE. SFE at 8000 psi CO_2, 60°C, 20 min. Peak identities are as follows: (1), BHT; (2), impurity; (3), vitamin A palmitate.

Table 3. Effect of Lipid Carry-over on Efficiency of Sample Preparation Procedure.

Sample	Vitamin A Added, µg	Initial Sample, µg/g	Composite, µg/g	Recovery, %
A	10	127	135	99
B	20	129	150	101
C	30	129	149	93
D	40	129	174	103
Average				99
Range				93-103
RSD (n=4)				4.3

Table 4. Precision Results For Retinyl Palmitate Assay.

Concentration Spiked, μg/g	Mean Found, μg/g	n*	Relative Standard Deviation, (%)
	Daily		
25.0	25.8	3	3.6
50.0	48.8	3	3.0
100.0	102	3	2.3
	Between-day		
25.0	24.6	5	8.1
50.0	51.2	4	5.5
100.0	98.6	4	3.8

n* is the number of days for the between-day results and the number of samples analyzed on one day for within-day results.

Application of SCFE-HPLC-ECD Methodolgy to Commercial Breakfast Cereals.

The method outlined was applied in triplicate to the quantitation of retinyl palmitate in five fortified breakfast cereals with label declarations of 25% and 100% USRDA. Table 5 shows the results of the vitamin assay. For all samples analyzed, the vitamin A found exceeded the declared labels by 9.6% to 65%. The coefficient of variation for triplicate determinations of the same sample ranged from 1.6 to 4.8%. A typical electrochemical chromatogram of a wheat-based cereal extract prepared by SFE is depicted in Figure 12. Similarly, chromatograms of extracts from a bran and corn-based cereal are shown in Figures 13 and 14, respectively. As can be seen in all chromatograms recorded by the electrochemical detector, retinyl palmitate is well resolved from early eluting excipients with no interference from other compounds. In addition, retinyl palmitate was the only form of vitamin A detected in the cereals examined. The identity of the vitamin A peak in the sample chromatograms was verified by co-injection of standard retinyl palmitate. This resolution and the freedom from complications makes quantitation easy.

For comparison, a 10 gram sample from the rice cereal lot previously analyzed was extracted using the SFE procedure outlined and quantitated using a UV detector at 254 nm. Injection of this extract onto a Supelcosil C-18 (10 μm) column with a mobile phase of acetonitrile-isopropanol-water (45+45+10, v/v) at a flow rate of 2.0 mL/min yielded the complex chromatogram shown in Figure 15. With the UV detector, accurate quantitation of vitamin A palmitate peak, which appears on the falling edge of an impurity peak of similar amplitude, requires a more sophisticated solvent program i.e., gradient program. Although these extraneous peaks were not positively identified they are presumably due to anti-oxidants (BHT), additional isomers of retinol and other complimentary UV absorbing vitamins. Moreover, the electrochemical detector with a detection limit 5-10 times lower than a UV detector offers the potential for direct quantitation of low level samples with no concentration.

Table 5. Determination of Retinyl Palmitate in Commercially Fortified Breakfast Cereals.

Cereal	Base	% US RDA[1]	Vitamin A Content, µg/g	RSD, % (n=3)
Rice Krispies	Rice	25	33	2.1
Special K	Rice	25	39	3.3
Corn Flakes	Corn	25	30	3.2
Raisin Bran	Bran	25	41	4.8
Product 19	Bran	100	110	1.6

[1] 25% US RDA for retinyl palmitate in breakfast cereals corresponds to 24.7 µg/g.

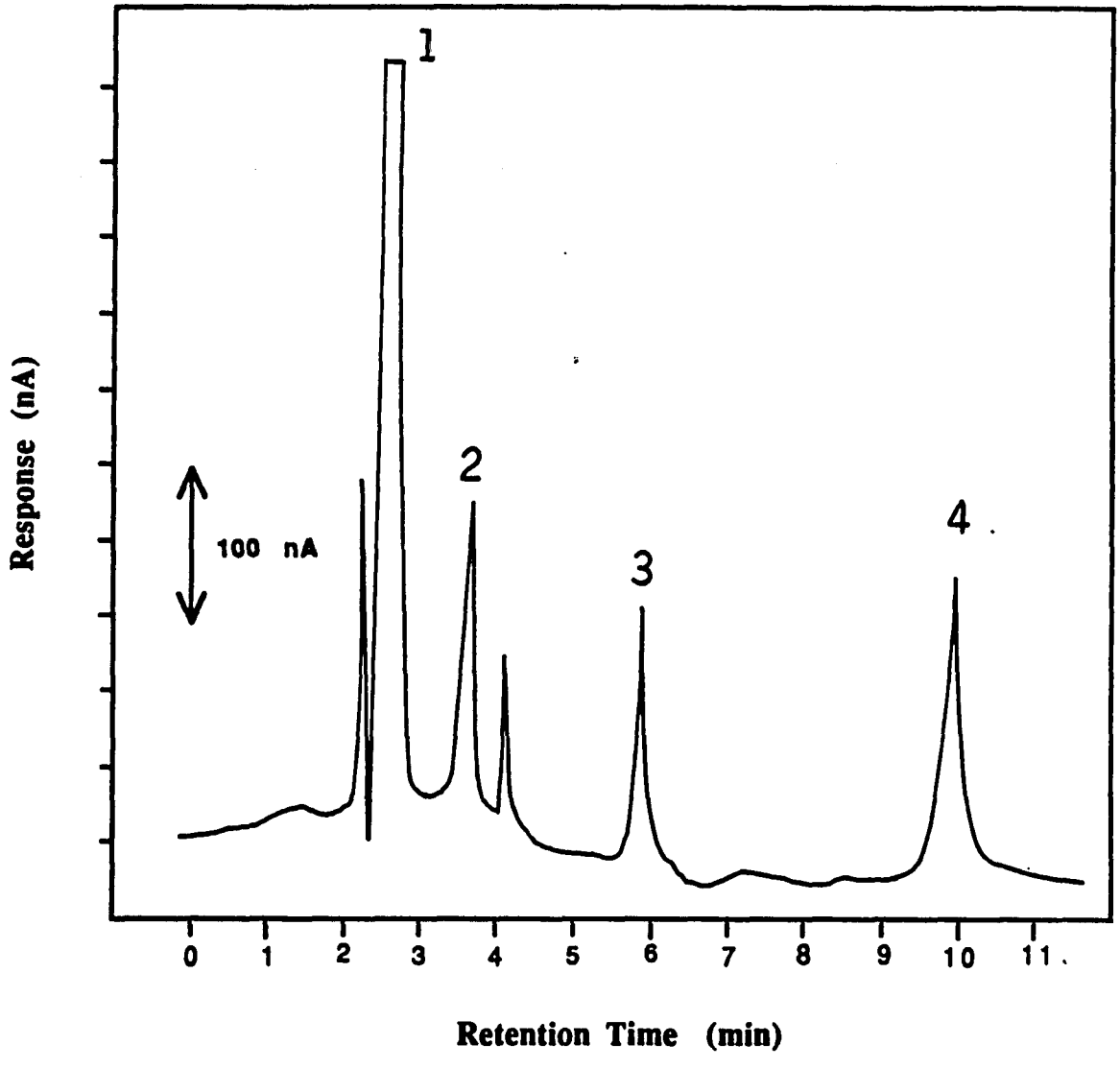

Figure 12. Typical chromatogram of a supercritical fluid extract of a wheat-based ready-to-eat breakfast cereal. Column: 150 x 3.9 mm I.D. μ-Bondapak C-18 (10 μm). Mobile phase: acetonitrile-isopropanol- aq .025 M $NaClO_4$ (45+45+10,v/v). Flow rate was 2.0 mL/min. Detector: carbon-based working electrode, applied potential 1.2 V vs SCE. SFE at 8000 psi CO_2, 60^0C, 20 min. Peak identities are as follows: (1), BHT; (2), impurity; (3), impurity; (4), vitamin A palmitate.

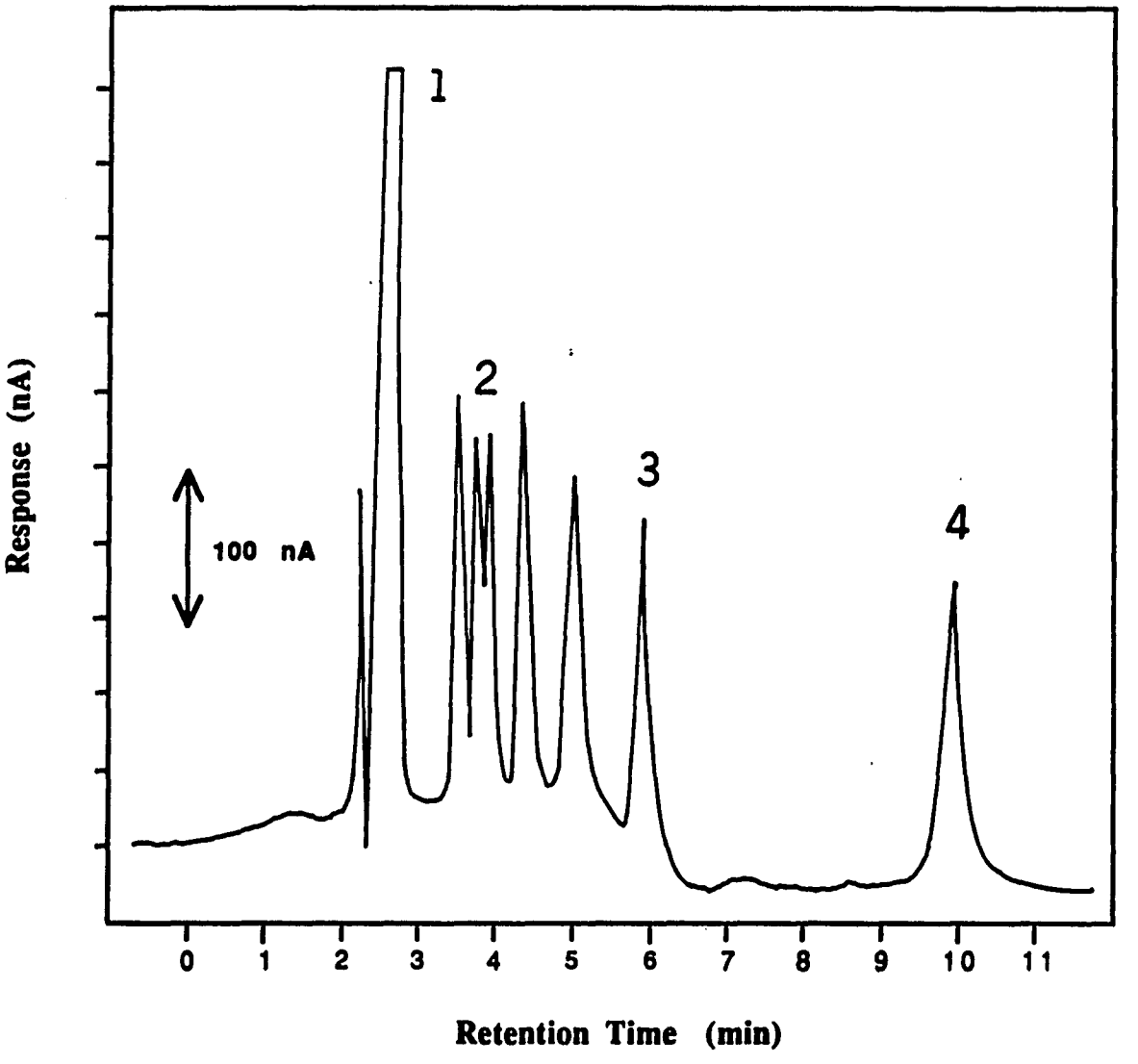

Figure 13. Typical chromatogram of a supercritical fluid extract of a bran based ready-to-eat breakfast cereal. Column: 150 x 3.9 mm I.D. μ-Bondapak C-18 (10 μm). Mobile phase: acetonitrile-isopropanol- aq .025 M $NaClO_4$ (45+45+10, v/v). Flow rate was 2.0 mL/min. Detector: carbon-based working electrode, applied potential 1.2 V vs SCE. SFE at 8000 psi CO_2, 60^0C, 20 min. Peak identities are as follows: (1), BHT; (2), impurity; (3), impurity; (4), vitamin A palmitate.

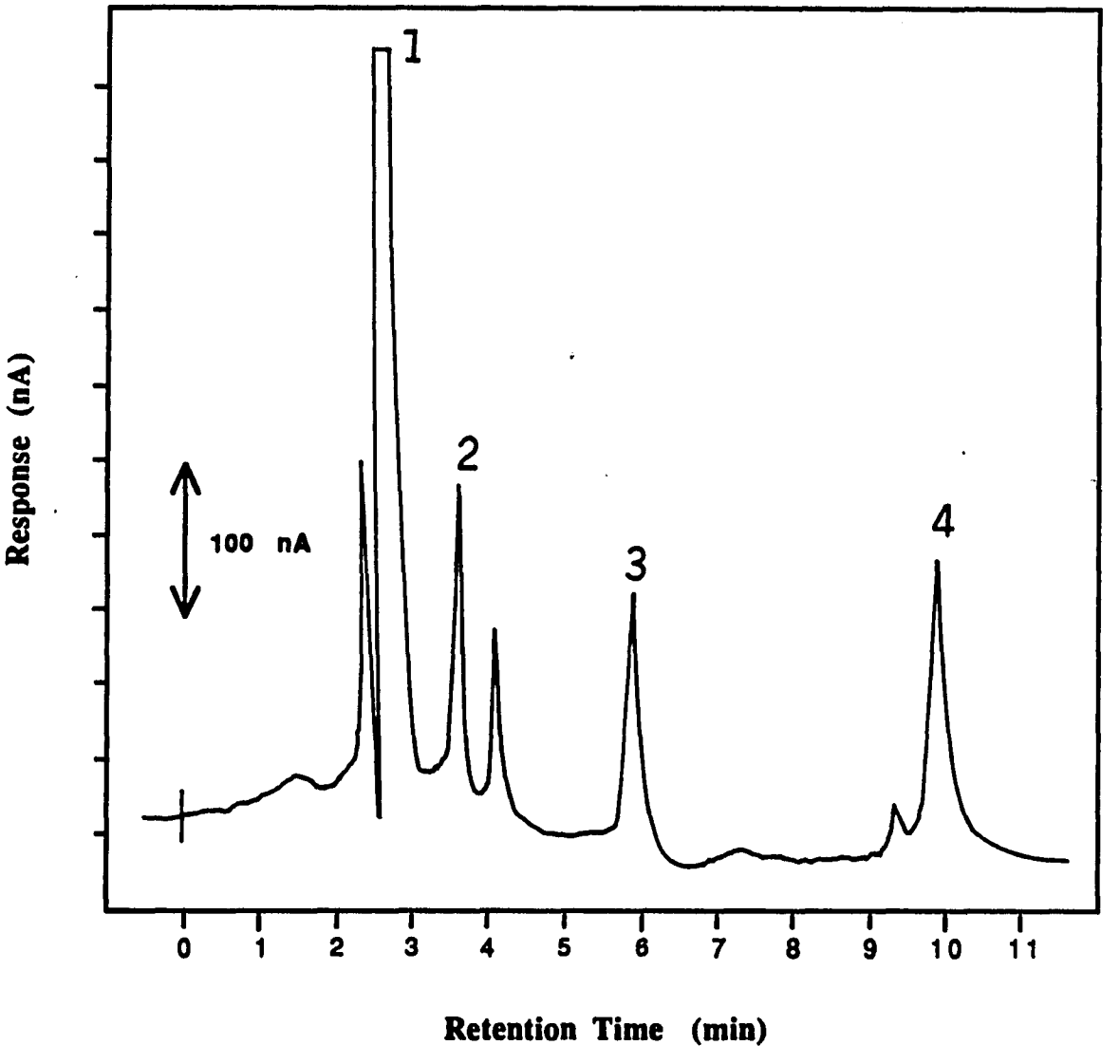

Figure 14. Typical chromatogram of a supercritical fluid extract of a corn-based ready-to-eat breakfast cereal. Column: 150 x 3.9 mm I.D. μBondapak C-18 (10 μm). Mobile phase: acetonitrile-isopropanol- aq 0.025 M $NaClO_4$ (45+45+10, v/v). Flow rate was 2.0 mL/min. Detector: carbon-based working electrode, applied potential 1.2 V vs SCE. SFE at 8000 psi CO_2, 60^{0}C, 20 min. Peak identities are as follows: (1) BHT, (2) impurity, (3) impurity,(4) vitamin A palmitate.

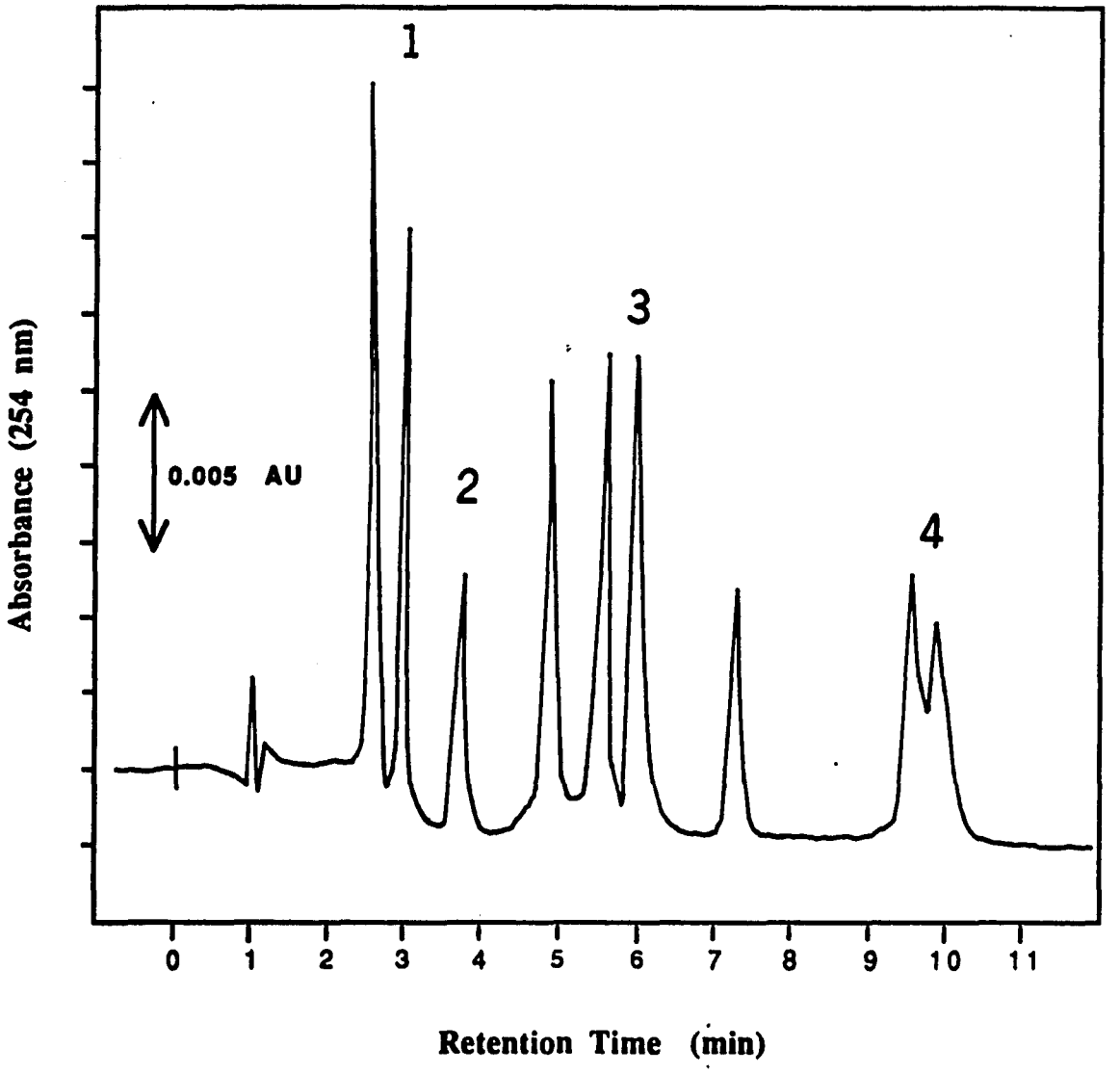

Figure 15. Typical chromatogram with UV detection of a supercritical fluid extract of a rice-based ready-to-eat breakfast cereal. Column: 150 x 4.6 mm I.D. Supelcosil C-18 (10 µm). Mobile phase: acetonitrile-isopropanol-water (45+45+10, v/v). Flow rate was 2.0 mL/min. Detector: carbon-based working electrode with an applied potential of +1.2 V vs SCE. SFE at 8000 psi CO_2, 60°C, 20 min. Peak identities are as follows: (1), BHT; (2), impurity; (3), impurity; (4), vitamin A palmitate.

Conclusions

In summary, the SFE procedure in conjunction with HPLC-ECD appears to provide a sound technique for the quantitation of retinyl palmitate in fortified ready-to-eat breakfast cereals. The advantages of the procedure include the quantification of the more stable vitamin form, non-destructive procedure requiring no saponification, sample clean-up, lengthy extractions and harsh reagents; all operations were performed at 60^0C; and total turn around time was less than 50 min per sample.

Undoubtedly, this technique can provide the high degree of resolution, reproducibility, and ease of quantitation required in the industrial quality assurance laboratory. Increased use of this new technology will greatly reduce the imprecision and inaccuracies associated with vitamin analysis. The method should also be suitable for other applications requiring the extraction of other hydrophobic organic compounds from foodstuffs.

Part III Chapter 5

Determination of Menadione in Animal Feeds

Introduction

In long-term feeding studies of chemical substances, compound adminstration to laboratory animals is accomplished by incorporating the substance into the animals' feed. Analytical methods are required to monitor dose level, to verify uniform distribution in the feed mix, and to test for stability. Laboratory animal feeds are complex mixtures of diverse susbtances; if co-extracted, these excipients may interfere in the determination of the analyte of interest. Extensive sample clean-up procedures may then be required.

The extraction of a lipophilic compound, menadione (vitamin K_3), from laboratory rat chow spiked with the compound using supercritical fluid CO_2 is reported in this chapter. The extracted menadione is quantitated using reversed phase HPLC with an electrochemical detector (ECD). No clean-up of the extract was required. Menadione (2-methyl-1,4-naphthoquinone) is a synthetic provitamin (1) which is converted into the active vitamin K_2 (menaquinone) in the liver, where it acts as a cofactor in the production of blood clotting factors (2). To combat a vitamin K deficiency in animals brought about by antibiotic or anticoagulant treatments, menadione can be adminstered by fortification of the feed (2).

Present methods for the isolation of lipophilic vitamins from feeds and related materials involve time-consuming liquid extraction and multiple evaporation steps, which introduce analytical uncertainty, and matrix interactions, and limit ability to automate such assays (3). Moreover, the solvents used are dangerous or expensive and the frequent emulsions reduce the accuracy of the results. For example, the AOAC method (4) for tocopherol in foods and feeds requires an 8 hour Soxhlet extraction in ethanol, alkaline hydrolysis of the co-extracted lipids, and a multistage liquid-liquid partition procedure.

Bourgeois et al. (3) eliminated the solvent extraction steps by initially saponifying the lipids, and then isolating retinol and α-tocopherol on commercial disposable cartridges packed with diatomaceous earth. We believe the need exists for a simpler and cleaner isolation procedure for the fat-soluble vitamins in complex matrices is met by SFE.

A variety of wet chemical and instrumental procedures are available for the determination of manadione isolated from various media. Colorimetric methods employing such reagents as piperidine and malonitrile (5) to produce colored products are time-consuming and not

suitable for high throughput. Gas chromatographic (GC) methods, reviewed some time ago by Sheppard and Hubbard (6), are not highly reproducible and have been superceded by HPLC methods (7). While most HPLC procedures use a UV detector (UVD), greater specificity and sensitivity for K vitamins have been achieved with the ECD. The ease of the 2-electron reduction of menadione and related compounds has been known for some time (8), allowing use of HPLC flow cells equipped with solid electrodes such as glassy carbon (9), porous graphite (10). HPLC-ECD has been applied to the determination of K vitamins isolated from rat liver tissue (10), human serum (9), and rat plasma (11). A dual ECD in the reduction-oxidation mode using coulometric-coulometric or coulometric-amperometric response or coulometric/fluorimetric detection, offers as expected highest sensitivity and selectivity towards plama samples (12). The detection limits of these three modes of ECD are reported (12) to be 150 pg, 280 pg, and 25 pg, respectively (12).

Experimental

Chemicals

Menadione was obtained from Sigma (St Louis, MO) and was used without further purification. HPLC-grade acetonitrile, methylene chloride, and acetone were purchased from J. T. Baker (Phillipsburg, NJ). Water was glass distilled. Carbon dioxide was Linde bone-dry grade.

Standard Preparation

For sample spiking, a stock solution of menadione was prepared by dissolving 30.0 mg in 100 mL of methylene chloride; this solution was then diluted with methylene chloride to make solutions in the range of 1.5 to 300 mg/mL.

For calibration, a 0.30 mg/mL stock solution was prepared in acetonitrile; this solution was diluted accordingly to make 20 HPLC standards in the range of 300 to 1.5 μg/mL. Solutions of menadione were protected from sunlight during storage and use.

Feed Preparation

Crushed laboratory rat chow (Ralston-Purina Co, Type 5010-C) samples (500 mg) were fortified in the range of 200 ppm to 0.3 % by adding 1 mL aliquots of methylene chloride solutions of menadione, mixing, and allowing the solvent solvent to evaporate.

Instrumentation

The liquid chromatographic system and silver based reductive amperometric detector have been described thoroughly elsewhere (pp. 16-36). All separations were performed on a MicroBondapak C-18, 150 mm x 3.9 mm I.D., 10 μm column (Waters Associates, Milford, MA) using a mobile phase composed of acetonitrile in 0.025 M aq. $NaClO_4$ (90/10, v/v). The mobile phase was filtered through a 0.45 μm filter and then degassed with helium for 10 min before use. The output from the detector was stored by a peak detector (pp. 30-32) and recorded on a linear model 1200 strip chart recorder (Linear Instruments, Irvine, CA) having a fsd of 1.0 V.

To confirm the identity of menadione isolated by SFE and that of HPLC peak, a Hewlett-Packard 5988A GC/quadrupole mass spectrometer (GC/MS) system with a Hewlett-Packard 1000 data system was used with a 30 m x 0.25-mm I.D., DB-5 cross-linked methyl silicone bonded phase fused silica capillary column (J &W Scientific). The initial temperature, 150 ^{0}C, was held for 2 min followed by temperature progamming at 100 ^{0}C/min to 250 ^{0}C. The carrier gas was He at 1 mL/min, and splitless injection was used.

Extraction Procedure

A 500 mg sample, accurately weighed, of crushed fortified feed was transferred to the extraction chamber and held in place between two glass plugs. The chamber was sealed and inserted into a laboratory-assembled high-pressure manifold (pp. 124-125). Initially, the system was brought to 60^{0}C and then purged of oxygen with ambient pressure carbon dioxide. Subsequently, the back pressure valve was closed and the system pressure was increased to an operating pressure of 8000 psi. After a 15 min equilibration period, the back pressure valve was cracked open and the extracted analytes were deposited on a guard column packed with silica (Fisher Scientific, Pittsburgh, PA). On completion, the contents of the trap were emptied into a 50 mL syringe fitted with an in-line filter (Gelman Scientific). The vitamins on the adsorbent were washed with 30 mL of methylene chloride-acetone (50/50, v/v) into a 150 mL round bottom flask, evaporated to dryness under reduced pressure in a rotary evaporator and reconstituted in 5 mL of mobile phase for HPLC analysis.

Results and Discussion

Hydrodynamic voltammogram

Figure 1 shows the hydrodynamic voltammogram on silver electrode for repetitive injections of 20 µL of a 0.33 µg/mL menadione standard. The limiting current plateau was reached at approximately -0.75 V *versus* calomel, which was the potential used in all subsequent experiments. The 2-electron reduction is evidently quasi-reversible, because the value of $E_{3/4}$-$E_{1/4}$, is approximately 100 mV, is intermediate between the values corresponding to reversibility (28.2 mV) and irreversibility (113 mV) (13).

Effect of flow rate

The variation of response with eluent flow rate is shown in Figure 2. For flows up to 1.67 mL/min, response increased with approximately one-third the power of the flow rate. According to Weber (14), this suggests the reduction current is limited by convective transport of menadione to the electrode. Because the response becomes essentially independent of flow rate at flows higher than 1.7 mL/min, a flow rate of 2 mL/min was used in subsequent experiments.

Supporting electrolyte concentration

The ECD generally requires the presence of electrolyte to reduce solution resistance, but electrolyte suppresses solute solubility in the mobile phase and increases retention. As shown in Figure 3, detector response increased sharply with the concentration of $NaClO_4$ and peaked at about 0.025 M. At higher concentrations, the peak current waned, which might be attributed to increased peak broadening resulting from increased retention time and to a decrease in the diffusion coefficient attending the increase in $NaClO_4$ concentration.

Response of ECD to Menadione

The ECD response parameters were determined by injecting 20 µL samples of standard solution of menadione in acetonitrile over the concentration range 0.03 µg/mL to 300 µg/mL. A log-log plot, shown in Figure 4, of peak current *versus* weight of menadione injected was a straight line of unit slope over the range from 600 pg to at least 6 µ g. The noise level was 0.05 nA, so that, at a signal-to-noise ratio of 3, the minimum detectable quantity (MDQ) was 125 pg. The ECD is thus about four times more sensitive than the UVD, which has a reported detection limit of 0.5 ng (9).

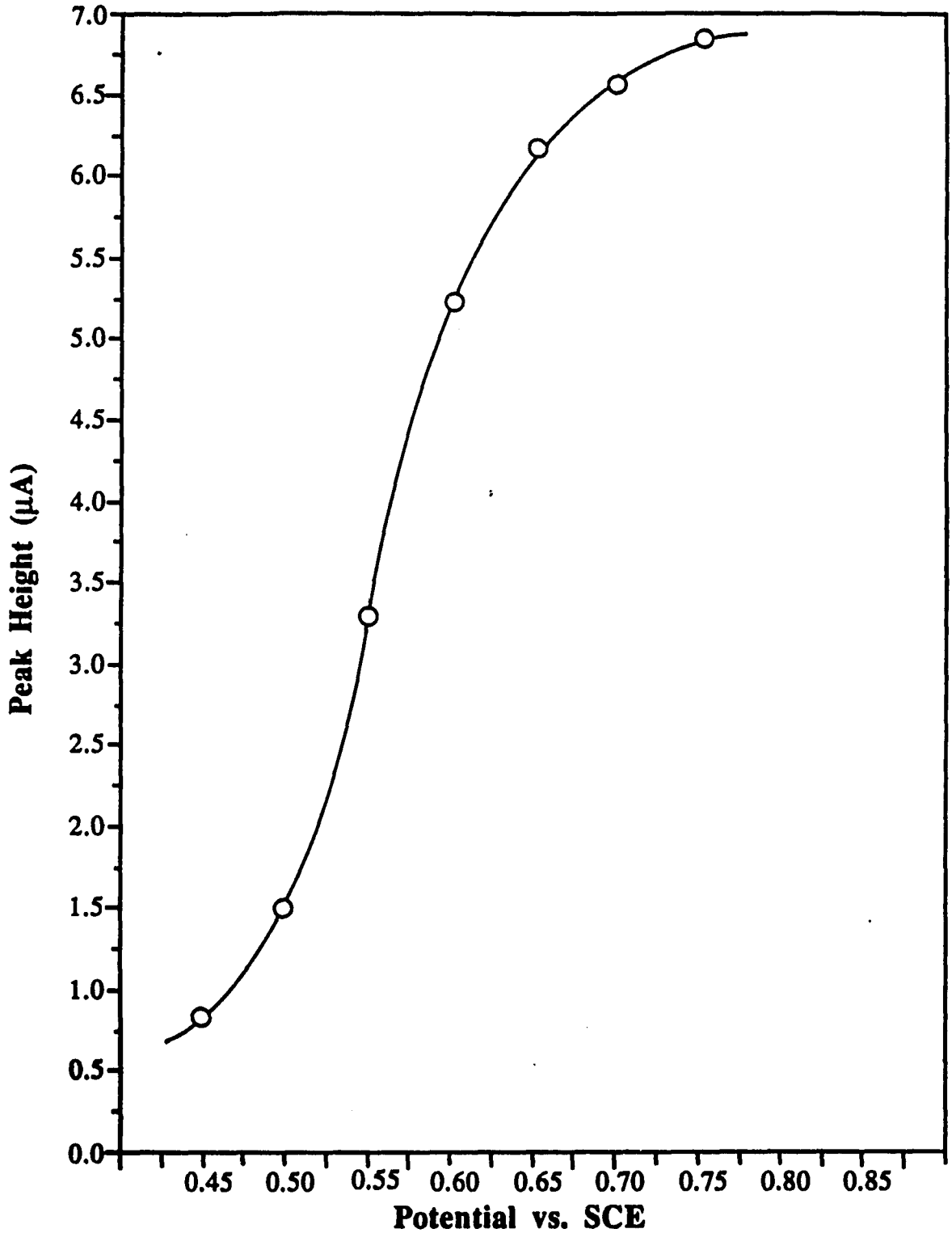

Figure 1. Hydrodynamic voltammogram of menadione on silver cathode. Chromatographic conditions: column, 150 x 3.9 mm I.D. μ-Bondapak C-18 (10 μm); mobile phase, acetonitrile-aq 0.025 M $NaClO_4$ (90+10, v/v); flow rate, 2 mL/min; sample size, 6.7 μg menadione per 20 μL acetonitrile injected at each potential setting.

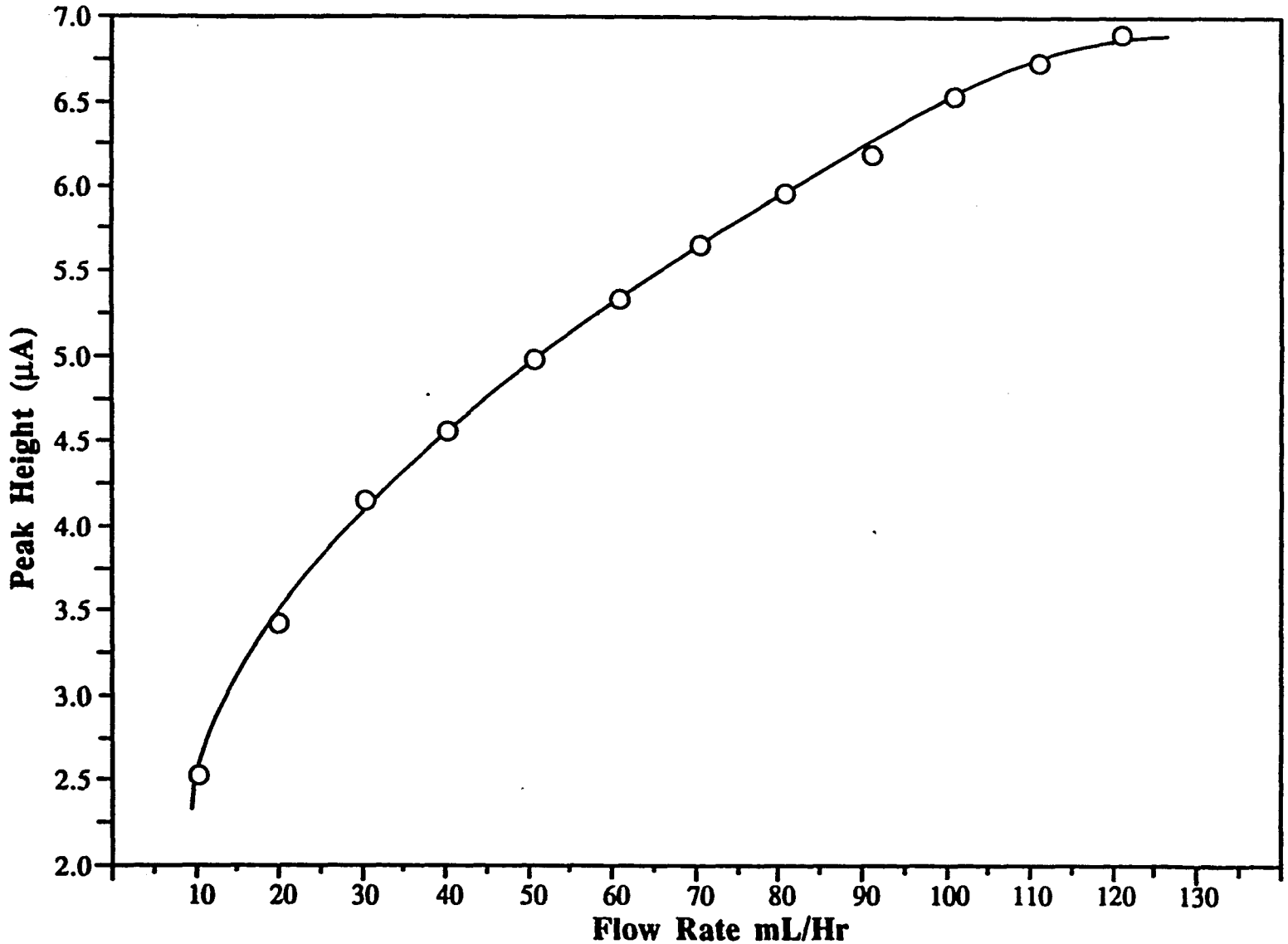

Figure 2. Variation of peak current with eluent flow rate. Chromatographic conditions: column, 150 x 39 mm I.D. µBondapak C-18; mobile phase, acetonitrile-aq 0.025 M $NaClO_4$ (90+10, v/v); Ag electrode potential, - 0.75 V *vs* SCE; Sample size, 6.7 µg menadione per 20 µL acetonitrile injected.

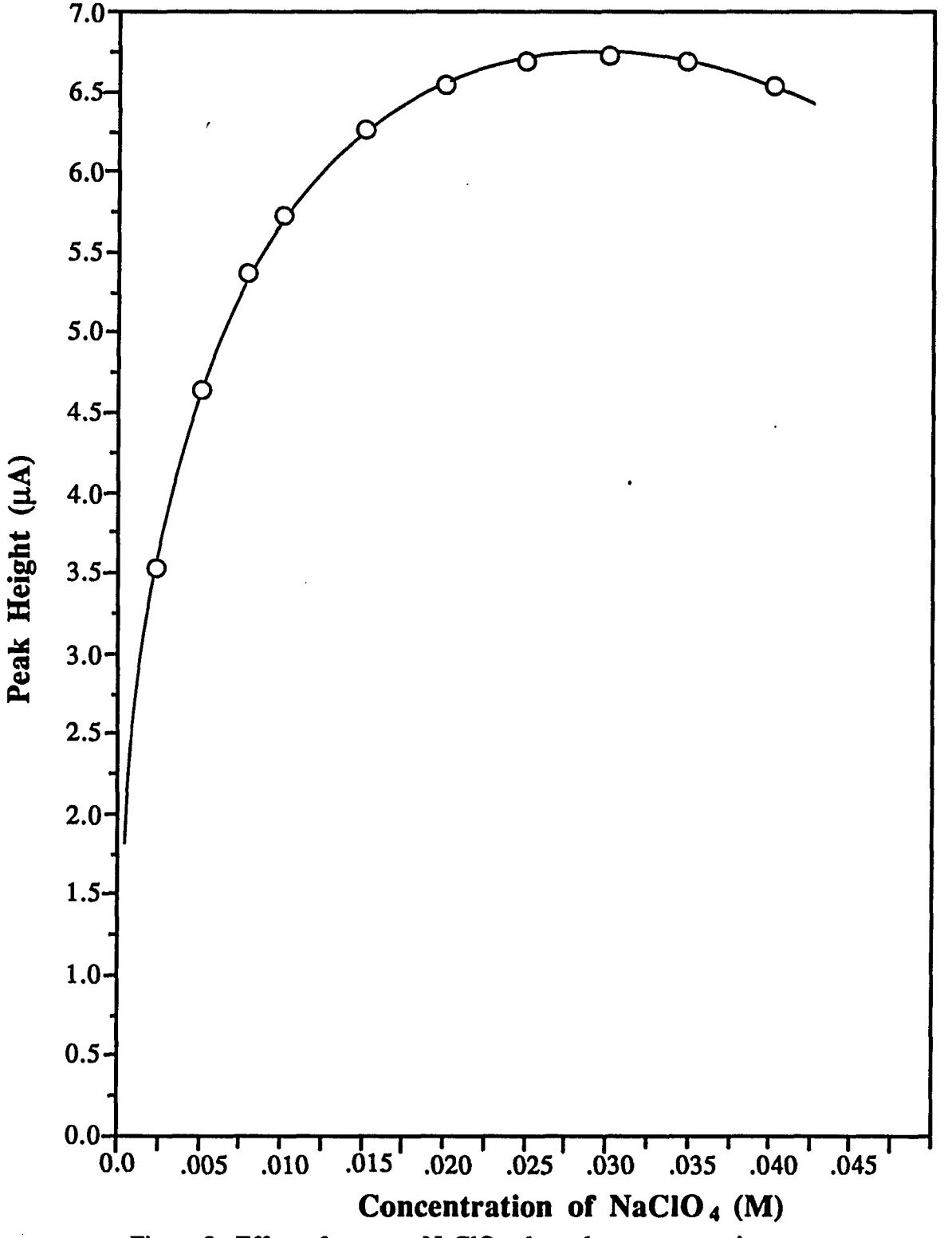

Figure 3. Effect of aqueous $NaClO_4$ electrolyte concentration on response. Chromatographic conditions: column, 150 x 3.9 mm I.D. μ-Bondapak C-18 (10 μm); stock mobile phase composition, acetonitrile-water (90+10, v/v); flow rate, 2.0 mL/min; silver electrode potential, - 0.75 V vs SCE; sample size, 6.7 μg menadione per 20 μL acetonitrile injected at each mobile phase composition.

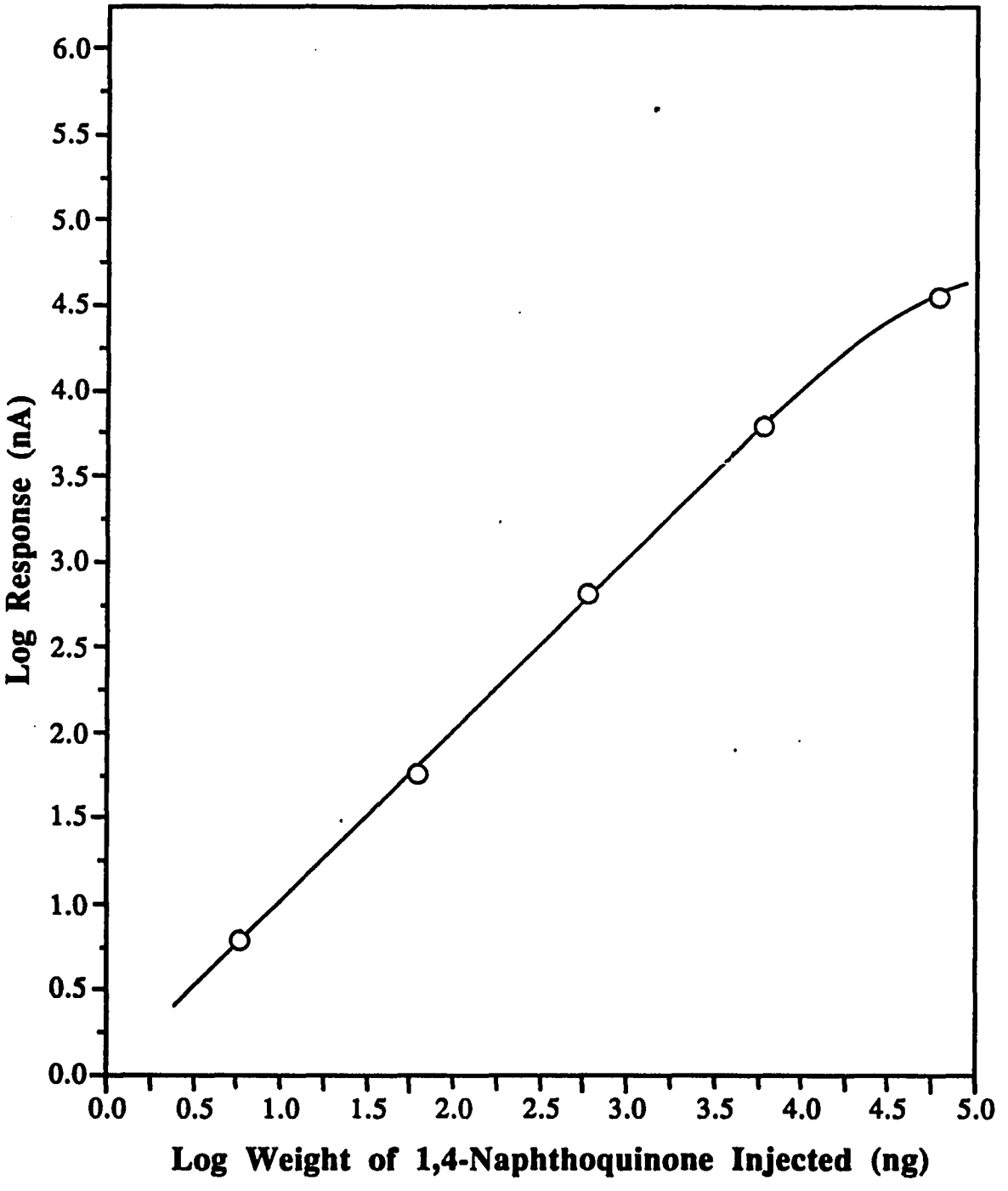

Figure 4. Linearity of silver-based detector response to amounts of 1,4 naphthoquinone in 20 µL samples. Column, 150 x 3.9 mm I.D. µ-Bondapak C-18 (10 µm). Mobile phase, 90/10 (v/v) acetonitrile-aqueous 0.025 M $NaClO_4$. Flow rate, 2.0 mL/min. Silver electrode potential, -0.75 V *vs* SCE.

It should be noted that this MDQ refers to the ECD, not the overall method (see next section, below).

SFE Efficiency

In preliminary experiments the extraction of 1,4-naphthoquinone, a compound with SFE behaviour identical to that of menadione (2-methyl-1,4-naphthaquinone) from filter paper was studied. As indicated in Tables 1 and 2, 90 % extraction of quantities added to a 2 cm. filter paper circle was achieved by extraction for 20 min at 8000 psi and 60^{0}C. The same conditions were used for the SFE of the rat chow spiked with menadione at various levels. The results are given in Table 3. There was a certain low unextractable level of menadione that remained adsorbed on some component of feed matrix. This caused the relative recovery to suffer at levels below 0.2 mg/g of feed. To determine this unextractable level, six 0.5-g feed samples were spiked with 0.5 to 1.0 mg menadione in 0.1-mg increments. Each was extracted using the SFE procedure. As shown in Figure 5, the plot of peak currents of the resulting HPLC-ECD peaks versus milligrams of menadione added was a straight line. Extrapolation to zero peak current gave the nonextractable quantity, 10 µg menadione (i.e., 20 µg/gm of feed). From a practical standpoint, 20 µg/g could be applied as a blank correction for actual samples containing menadione at levels below 0.2 mg/g. However, the addition of polar modifiers such as methanol to the extraction chamber to displace the unextracted menadione warrants future study.

Analytical Precision

To evaluate the precision of the method, menadione was added to triplicate 0.5-g feed samples at the 0.02 mg to 1.5 mg range, extracted, and determined by HPLC-ECD. As shown in Table 3, the coefficient of variation ranged from 0.4 % to 4.6%, generally increased as the level of menadione decreased. The day-to-day precision was assessed by repetitive extractions of a feed sample spiked with 1.0 mg menadione/g of feed each day for five days. The average recovery was 90.5 % with a coefficient of 2.2 %.

Confirmation of HPLC peak identity

Figure 6 shows a typical HPLC-ECD chromatogram of an SFE extract of a rat chow spiked at 1 mg/g level. Only one peak was observed, which allowed the use of a strong mobile phase to shorten the retention time. Confirmation of peak identity was

Table 1. Effect of SFE Pressure on Extraction of 1,4-Naphthoquinone from Filter Paper.

CO_2 Pressure (psi)*	Average Recovery (%)	RSD (n=3)
5000	51'	3.1
6000	60	2.5
7000	85	2.3
8000	91	2.2

* 20 min equilibration, 60 ^{0}C

Table 2. Effect of SFE Equilibration Time on Extraction of 1,4-Naphthoquinone from Filter Paper.

Equilibration time (min)*	Average Recovery (%)	RSD (n=3)
5	49	2.6
10	71	2.8
15	88	2.1
20	90	2.5

* 8000 psi CO_2, 60 ^{0}C

Table 3. SFE of Menadione from Rat Chow*

Menadione Added (mg)	Average Recovery (%)	Relative Standard Deviation (%)
1.5	96	0.42
1.0	94	0.49
0.5	92	2.2
0.1	80	0.44
0.05	65	3.5
0.02	43	4.7

*Triplicate 0.5-g samples of rat chow spiked with menadione, extracted at 8000 psi CO_2, 60 ^{0}C, 20 min equilibration time.

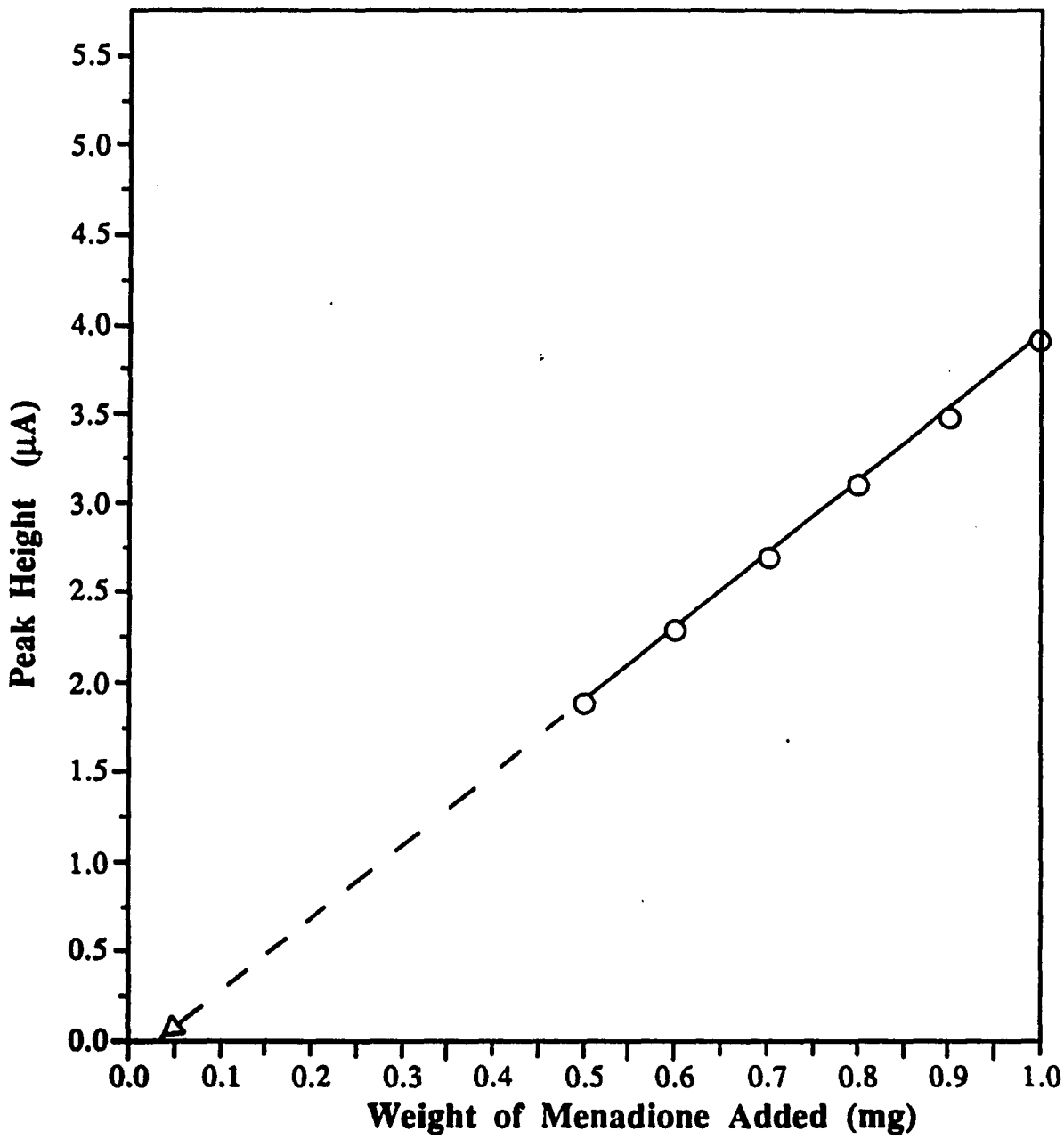

Figure 5. Effect of spiking level on the recovery of menadione from fortified animal chow. Chromatographic conditions: column, 150 x 3.9 mm I.D. μ-Bondapak C-18 (10 μm); mobile phase, 90/10 (v/v) acetonitrile-aqueous 0.025 M $NaClO_4$; flow rate, 2.0 mL/min; silver electrode potential, -0.75 V *vs* SCE; sample size, a 500 mg aliquot of feed spiked with the denoted weight of menadione prior to SFE sample preparation. Preparation conditions: SFE at 8000 psi CO_2, 60° C, 20 min.

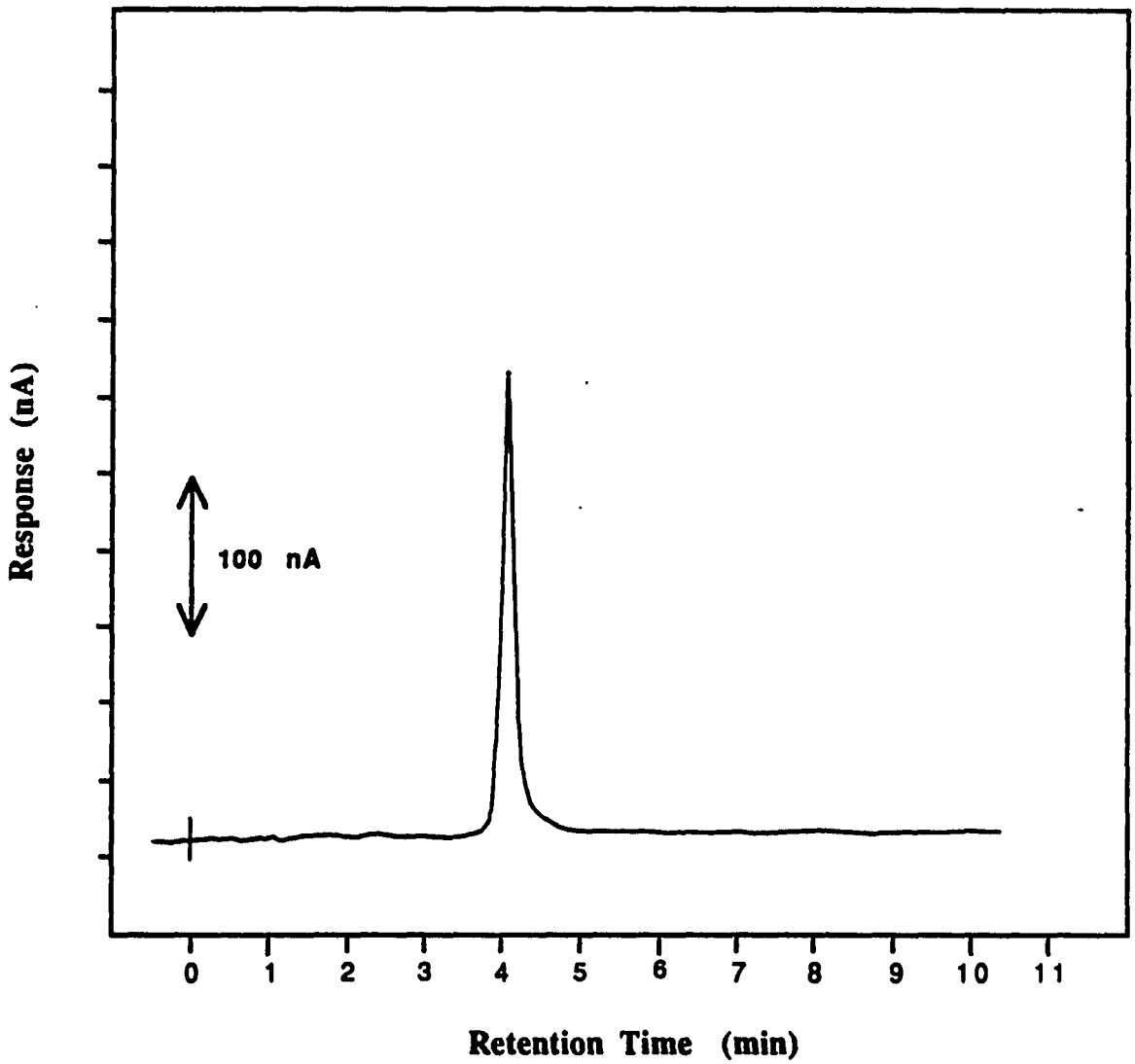

Figure 6. HPLC-ECD chromatogram of a supercritical fluid extract of menadione fortified rat chow. Chromatographic conditions: column, 150 x 3.9 mm I.D. μ-Bondapak C-18 (10 μm); mobile phase, 90/10 (v/v) acetonitrile -aqueous 0.025 M $NaClO_4$; flow rate, 2.0 mL/min; silver electrode potential, -0.75 V *vs* SCE; sample size, a 500 mg aliquot of rat chow spiked with 1 μg menadione/g of feed. SFE at 8000 psi CO_2, 60^0 C, 20 min.

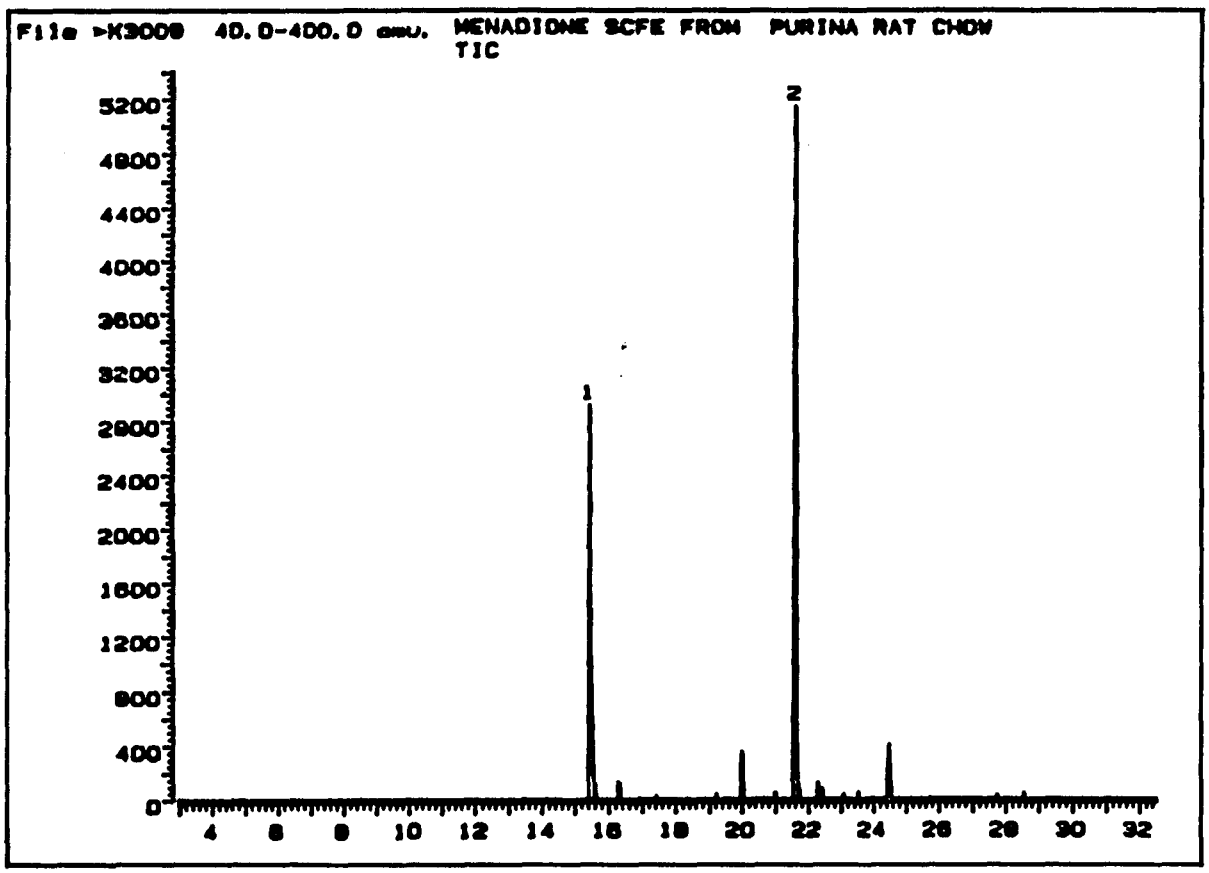

Figure 7. GC/MS total ion chromatogram of supercritical fluid extract of menadione spiked rat chow. Peak identities as follows: 1, menadione; 2, dibutylphthalate. Rat chow spiked with 1.5 mg menadione/g of feed. SFE at 8000 psi, 60°C, 20 min. GC conditions: 30 m x 0.025 mm I.D. DB-5 fused-silica capillary column; temperature, 150°C for 2 min, then temperature programmed at 10°C/min to 250° C; Carrier gas, He, 1 mL/min.

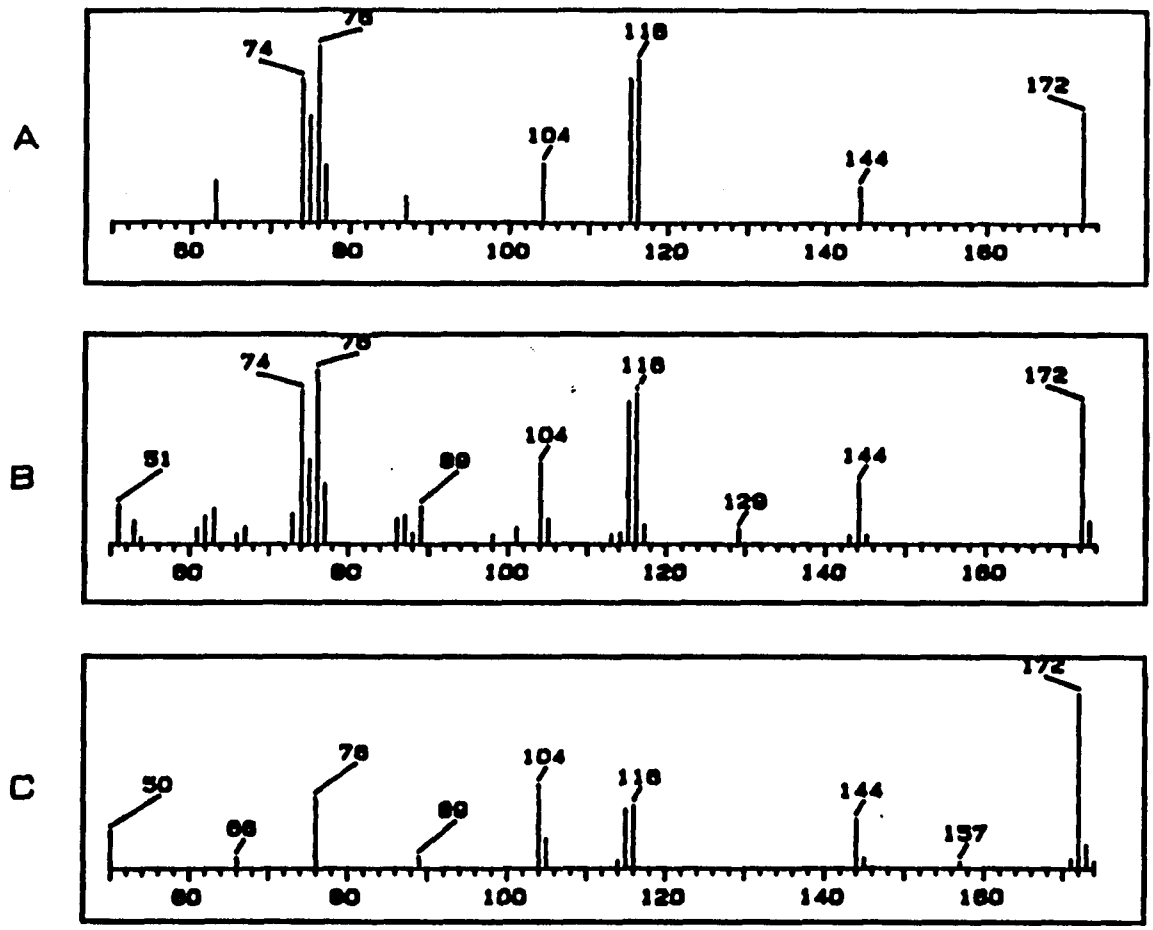

Figure 8. Comparison of mass spectra of recovered menadione with that of the library standard spectra. A = GC/MS of supercritical fluid extract of rat chow spiked with 1.5 mg menadione/g feed; B = GC/MS of menadione standard solution; C= NBS-Wiley condensed mass spectral library mass spectrum of menadione. SFE at 8000 psi, 60^{0}C, 20 min. GC conditions: 30 m x 0.025 mm I.D. DB-5 fused-silica capillary column; temperature, 150^{0}C for 2 min, then temperature programmed at 10^{0}C/min to 250^{0}C; Carrier gas, He, 1 mL/min.

accomplished in three ways. First, HPLC-ECD of an SFE of an unspiked feed sample produced no peaks at all. Second, addition of an increment of menadione to an extract produced a proportional increase in peak height with no increase in peak width. Third, the HPLC peak was collected and analyzed by GC-MS. Because the concentration in the collected peak was low, the use of selected ion monitoring MS mode (SIMS) was required. The SIMS chromatograms at six characteristic ions showed peaks at the same retention time as that of a menadione standard with the same relative peak heights as the corresponding ions in the mass spectrum. Figure 7 shows a total ion GC/MS chromatogram of an SCF extract of rat chow spiked with 1.5 mg menadione/g of feed. The simplicity of the chromatogram is somewhat surprising and probably indicates the cleanness of the SCF extraction. The identity of peak 1 was confirmed by comparison of its mass spectrum with that of a standard. In Figure 8, A is the mass spectrum of peak 1, B is the National Bureau of Standards-Wiley condensed mass spectral library mass spectrum of the compound.

Conclusions

A simple, rapid method for the determination of Vitamin K_3 in spiked animal chow by HPLC has been developed. The method utilizes supercritical fluid carbon dioxide at 8000 psi and 60^{0}C to facilitate sample preparation. Quantitative extraction requires only 20 min and does not suffer from problems such as matrix interaction or emulsion formation which are typically encountered in conventional solvent extraction of lipophilic materials from animal feeds. Quantitation of the extracts with an electrochemical detector offers enhanced sensitivity and selectivity which simplifies the chromatography by eliminating the normal phase clean-up procedure found in most reported procedures. Sufficient precision was obtained without the addition of an internal standard which further reduces the possibility of interactions. Using this method, it is possible to determine vitamin K_3 levels to as low as 20 μg/g in 1 gram of feed. The analytical procedure developed should be useful in assaying feeds for other analytes not described in the literature.

Part III chapter 6

Simultaneous Determination of Vitamins A and K_1 in Infant Food Formula

Introduction

Governmental intervention has necessitated the development of simple, rapid, and sensitive methods for the analysis of vitamin A and K_1 in infant formulas (1, 2). The interdependencies between these fat soluble vitamins, found at microgram levels, and the infant formula matrix make their simultaneous determination a formidable challenge. Previously used methods for these compounds have included various bioassays (3, 4), as well as photometric (5), thin-layer reflectance densitometric (6), and voltammetric techniques (7-13). These methods, while useful, have certain limitations in that they lack specificity, display poor internal precision, require large sample quantities, and/or are time-consuming and expensive.

In recent years, several HPLC methods based on UV absorbance detection have been developed for the measurement of fat-soluble vitamins as standards (14-17), in raw materials, premixes, concentrates, pharmaceutical preparations and milk products (18-25). While many of these methods (23-33) are suitable for sample preparation and quantitation of multiple fat-soluble vitamins present at the dosage level, few have been employed for formulations fortified at the microgram level. Of these, only an HPLC method devised by Barnett et al. (24) has received much attention. In this method, enzymatic hydrolysis using lipase is employed to degrade lipids in infant formula samples, followed by separation of vitamin A and K_1 from other fat soluble components by reversed-phase HPLC with UV detection. Several difficulties were encountered during collaborative testing. First, from a quality control view point, a chromatographic analysis time of nearly an hour is much too long. Second, resolution and retention time were highly dependent on mobile phase composition and even on the brand of bonded support employed. A change of only 3% methanol content in a mobile phase system comprised of acetonitrile-methanol-tetrahydrofuran-water (39 + 39 + 16 + 16, v/v) resulted in poor resolution and peak shape. Separation of these vitamins achieved on a Zorbax ODS column could not be duplicated under the same chromatographic conditions on a μ-Bondapak column C-18 column of similar length. Finally, dissolution of the extract in a solvent not containing a high proportion of ethyl acetate resulted in several negative peaks for each vitamin. Although multicomponent separation methods combined with extensive fractionation schemes have contributed significantly to the characterization of these samples, high detection limits and complicated procedural detail have limited their use for quality control testing.

Electrochemical detection in combination with LC has played a prominent role in the rapidly expanding applicability of HPLC to the needs of modern chemical analysis. Recent advances and applications have been reviewed (36). The chief advantages of the electrochemical system are increased sensitivity and selectivity that can be obtained compared to UV detection methods. In addition, a recent innovation has been the introduction of detectors employing two working electrodes. Dual-electrode detectors can be used in a variety of configurations, of which the series, parallel-adjacent, and parallel opposed are most popular (37-45). Each of these configurations has been shown to increase the selectivity and extend the versatility of electrochemical detection for use with complex systems (37-40).

The adjacent-parallel configuration can be readily used for the simultaneous analysis of oxidizable and reducible compounds. In this configuration, the chromatographic effluent is split between two independent electrodes poised at potentials of different polarities. By judicious choice of each working electrode potential, components having different electrochemical characteristics can be quantified when the resolution controlled by the phase system prohibits adequate separation. Several aspects of HPLC method development can be improved. First, chromatographic conditions can be greatly simplified and analysis time can be subsequently reduced. Second, less restrictive sample preparation procedures can be incorporated.

Previously reported work from our laboratory (46, pp. 181-201) has briefly described an unique approach to the quantitation of trace levels of vitamin K_1 in baby food formulas which involves the sequential performance of supercritical fluid extraction (SFE) and HPLC with electrochemical detection. As an extension of this work, the use of a dual electrode thin-layer cell for the simultaneous determination of vitamins A and K_1 is described. This mode of detection was implemented by incorporating silver and carbon working electrodes with a gasket containing an enlarged cross shaped slot into a thin-layer sandwich cell. After the LC separation, the eluate passes over the silver and glassy carbon electrodes which are poised appropriately to effect the reduction and oxidation of vitamins A and K_1, respectively. While similar in philosophy to a dual-wavelength absorbance detector, the proposed configuration is superior in terms of detection limits and cost, and its dead volume is ideally suited for high-speed LC separations.

In this chapter we evaluate the suitability of this detection configuration for vitamins A and K_1. Its applicability to the measurement of these compounds in infant formula will be demonstrated.

EXPERIMENTAL

Chemicals

Vitamin A palmitate and ergocalciferol (vitamin D_2) were purchased from Sigma Chemicals (St. Louis, MO). Vitamin K_1 was obtained from ICN Biomedicals (Costa Mesa, CA). HPLC-grade acetonitrile, isopropanol, methylene chloride, and methanol were obtained from Baker (Phillipsburg, NJ). In-house distilled water was used throughout this study. All buffer salts were reagent grade or better and used without further purification.

Stock Solution Preparation

A stock solution was prepared by dissolving 17.5 mg of vitamin A palmitate and 20.0 mg of vitamin K_1 separately in two 50 mL volumetric flasks and diluted to volume with methylene chloride to form stock solutions.

Chromatographic Standards

A reference standard containing 35.0 µg/mL of vitamin A palmitate was prepared by diluting 10 mL of the vitamin A stock solution to 100 mL with isopropanol in a volumetric flask. Ten working solutions covering the range of 3.5 to 35 µg/mL were prepared by serial dilution with isopropanol-acetonitrile (50/50, v/v) in 10 mL flasks. Similarly, a reference standard containing 4.0 µg/mL of vitamin K_1 was prepared by diluting 1.0 mL of the vitamin K_1 stock solution to 100 mL with acetonitrile in a volumetric flask. For quantitation, ten working solutions covering the range of 0.4 to 4.0 µg/mL were prepared by serial dilution with isopropanol-acetonitrile (50/50, v/v) in 10 mL volumetric flasks. In addition, a single mixed vitamin standard solution containing 10.0 µg/mL each of vitamin A palmitate and 1.0 µg/ml of vitamin K_1 was prepared in acetonitrile-isopropanol (50/50, v/v).

Apparatus

The HPLC employed, consisting of a Varian 8500 syringe-pump and a six port Rheodyne 1725 rotary valve equipped with a pneumatic loading device has been thoroughly described elsewhere (47, pp. 16-36). All separations were performed on an Altex or an Alltech 150 mm x 4.6 mm I.D. octyl column with 10 μm particles.

Dual-electrode LCEC studies were carried out using a potentiostat assembled in our laboratory (pp. 25-33) from quality operational amplifier modules (52K, Analog Devices, Norwood, MA) according to the standard adder-controller configuration (48,49). A second current-to-voltage (C-V) module based on the design of Blank (50) was included to provide the operating potential and to measure the generated current at the second working electrode. In this case, the C-V circuit was not grounded but offset by a voltage above ground equal to the difference (V_{E1}-V_{E2}). Prior to being recorded, the output current due to this offset voltage was compensated for. Each detector output was interfaced in parallel to a peak detector (51,52) and to a chart recorder with a 1.0 V f.s.d. and a chart speed of 1.0 cm/min. Technical details and schematics for the potentiostat have been reported elsewhere (pp. 27-32).

The dual-electrode flow cell was a modification of a single thin-layer design used in previous studies (47). The body of the cell consisted of two 1.0 in. x 1.0 in. blocks which were 1/2 in. thick for good rigidity. In the bottom half of the cell, made of Kel-F (AIN Plastics, Mt Vernon, NY), a silver disc (Hardy and Harmon) and a glassy carbon disc (Tokai Mfg., grade GC-30, Tokyo, Japan), each 1/8 in. in diameter, were symmetrically spaced along the center line 0.020 in. apart. A matching stainless steel top half, containing solution inlet and outlet ports, served as the auxiliary electrode and was separated from both working electrodes underneath by a 0.005 in. thick Teflon spacer. A rectangular cross section which defined a 0.125 in. x 0.5 in. flow channel was cut out from this gasket. The slot in the spacer extended from the inlet hole to the outlet hole and resulted in a working volume of only about 8-μL. The entire assembly was then clamped together with four 4-40 screws. The detector cell and column were connected by a 3.5 in. length of 1/16 in. O.D. x 0.005 I.D. in. stainless steel tubing with a 30^0 tapered 10-32 plastic Kel-F fitting (Upchurch). The calomel reference electrode was positioned in a removable plastic housing, threaded to mate with a plastic tee union which screwed into the cell outlet. The housing was filled with 3.0 M NaCl and sealed by a rubber septum through which a ceramic frit was inserted to

make electrical contact with the flowing stream. The reference electrode potential was checked daily versus a commercial SCE filled with 3.0 M KCl and was found to be 20-40 mV more positive. For adequate control at both detector electrodes it is necessary to minimize ohmic losses by positioning the auxiliary electrode across the thin-layer channel from the working electrodes. The merits of this cell design have been described elsewhere (53) for single electrode transducers.

Procedures

Mobile phase

Distilled-in-glass methanol and acetonitrile were mixed 1 to 1 on a volume basis to form a stock nonaqueous solution. To prepare the mobile phase, 450 mL of this solution was mixed with enough distilled water containing 0.1M $NaClO_4$ to make 500 mL of solution, which was then filtered through a 0.45 μm membrane filter (Gelman). This mobile phase was capped at all times to prevent evaporation.

Degassing Procedures

The exclusion of dissolved oxygen from the chromatographic system followed the procedure of Bratin and Kissinger (54), with the exception that the eluant reservoir was not heated. After a few minutes of intense helium purging, a gentle flow of helium was maintained for about 10 min, before the pump was filled. In order to prevent oxygen from re-entering the LC system during the chromatographic work, all Teflon tubing originally installed between the reservoir and pump was replaced by 1/8 in. O.D. stainless steel tubing.

For samples requiring a high sensitivity setting, deoxygenation prior to injection was necessary. Deoxygenation was achieved in a Reacti-Vial equipped with a pneumatic degassing cap detailed elsewhere (pp. 36-37). In the injection valve's load position, a stream of helium passes through the vial and exits up through the center port of the cap. After 2-3 min, the vial is sealed and pressurized by compressed helium from a solenoid valve which pumps deoxygenated sample through the loop as the valve stem is quickly toggled between the fill and load positions. The fill-up rate was adjusted by means of a needle valve, constructed from Kel-F.

Extraction Procedure

Commercial infant formulas were obtained from local stores. A gram sample, accurately weighed, was transferred to a 3/8 in. O.D. x 1/4 in. I.D. x 6 in. long stainless steel tube. If needed, samples were fortified at this point by the addition of 1 mL aliquots of standard solutions containing both vitamins dissolved in methanol. The chamber was tightened and sealed with two endfittings packed with glass wool and then carefully inserted into a lab-constructed high-pressure manifold (47, pp. 124-125). Initially, the extraction chamber was heated to 60^{0}C and gently purged with a stream of low pressure carbon dioxide for a few seconds to remove traces of oxygen. Following equlibration, the back-pressure regulator was closed and the system pressure was increased to an operating pressure of 8000 psi. After 15 min, the back-pressure regulator was opened reducing the density of carbon dioxide to such an extent that the vitamins were no longer soluble in the carbon dioxide stream, thereby facilitating their accumulation on a trap packed with C-18 bonded silica (Porasil, Waters Assoc., Milford, MA). In subdued light, the contents of the trap were emptied into a syringe fitted with an in-line filter (Gelman). The vitamins on the adsorbent were washed with 20 mL of methylene chloride-acetone (50/50, v/v), filtered and then collected in a clean dry round bottom flask. The extract was evaporated to dryness in a rotary evaporator maintained at 50^{0}C and reconstituted in 1 mL of acetonitrile-methanol (50/50, v/v) prior to HPLC determination.

HPLC Determination

20-μL aliquots of the extract were injected onto the HPLC column operated at ambient temperature with a flow rate of 2.0 mL/min. The vitamin peaks were tentatively identified on the basis of retention time. The vitamins were quantitated by comparison with peak heights obtained from vitamin standards of appropiate concentration.

Results and Discussion

Chromatography

Initial studies were conducted to determine the optimum mobile phase composition to separate vitamin K_1 and vitamin A from each other and from other possible electroactive contaminants such as vitamins D and E. A good separation of the two primary vitamins was achieved on an Altex C-8 column with an isocratic eluant comprised of acetonitrile-isopropanol-water (45/45/10, v/v). Figure 1 illustrates a

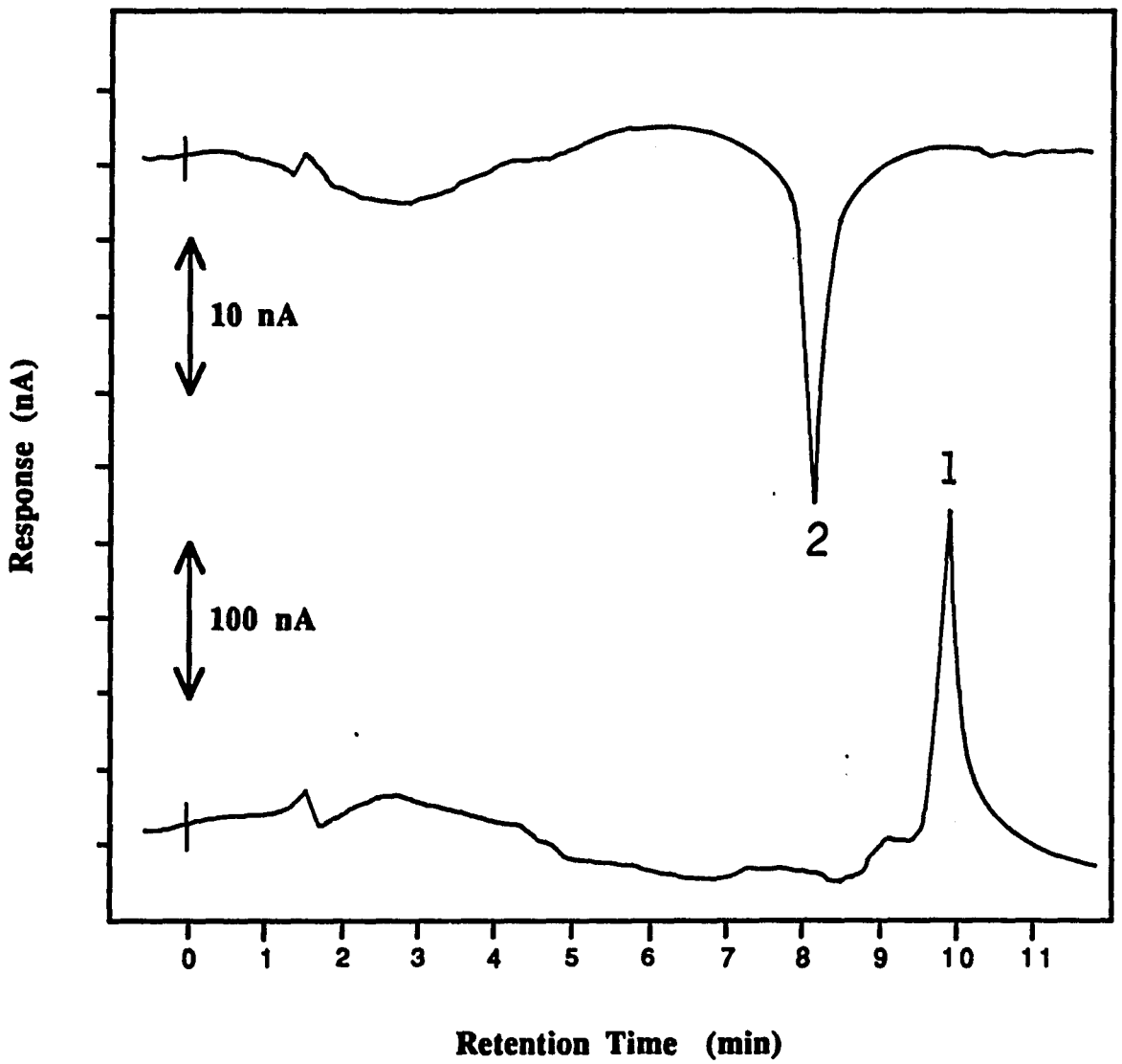

Figure 1. Chromatogram of a standard mixture of vitamins A and K-1 on a C-8 reversed-phase column, using acetonitrile-isopropanol-aq 0.025 M $NaClO_4$ (45+45+10,v/v) at a flow rate of 2 mL/min. Silver and carbon electrodes were poised at -1.0 V and 1.2 V *vs* SCE, respectively. Peak identities as follows: Peak 1, vitamin A palmitate (200 ng); 2, vitamin K-1 (20 ng).

chromatogram obtained from a standard mixture containing vitamins K_1 and A. Under the proposed chromatographic conditions, the two vitamins of interest showed satisfactory peak shapes and are well resolved within 10.5 min. Retention times of the two vitamins of interest were 8.0 min for vitamin K_1 and 10 min for vitamin A palmitate. Slight variation in retention times were noted on a day-to-day basis. The average retention times from replicate standard injections completed each day ranged from 7.8-8.3 min for vitamin K_1 and from 9.9-10.3 min for vitamin A palmitate. A small peak eluting prior to vitamin A palmitate was due to an unknown contaminant in the sample.

Performance of Dual-Cell Detector

The efficiency of a dual detector operated in the parallel-adjacent configuration can be evaluated from the shape of the hydrodynamic voltammogram produced at each electrode. Figures 2 and 3 show hydrodynamic voltammograms of vitamin K_1 and vitamin A palmitate at silver and carbon, respectively. In comparison to the electrochemical behavior previously observed for vitamin A palmitate in a conventional carbon based thin-layer cell (pp. 211-212), the shape of the oxidative wave shown in Figure 2 is very broad, lacking fine structure, and its limiting current is reached at a substantial over-potential. This behavior is presumably caused in part by electronic cross-talk from the reductively poised silver electrode. In contrast, the reduction of vitamin K_1 at the silver electrode located in the dual cell exhibited a similar over-potential and response as compared with its behavior observed in a single thin-layer cell (55-57). The applied potentials used to obtain the response data for the reduction and oxidation of vitamins K_1 and A were -1.1 and +1.2 V versus SCE, respectively.

Quantitation of Vitamins A and K_1

Using the chromatographic system described, an excellent linear relationship, as indicated by a correlation coefficient near 1, was observed in the range of 5.5 μg to 550 pg for 20-μL imjections of vitamins K_1 and A. Calibration curves of peak current (nA) against amount of each depolarizer (ng) in the injected samples were rectilinear with an intercept near zero over the range of 0.4 to 4.0 μg/mL and 3.5 to 35 μg/mL for vitamins K_1 and A, respectively. Using linear regression analysis, a slope of 1.065

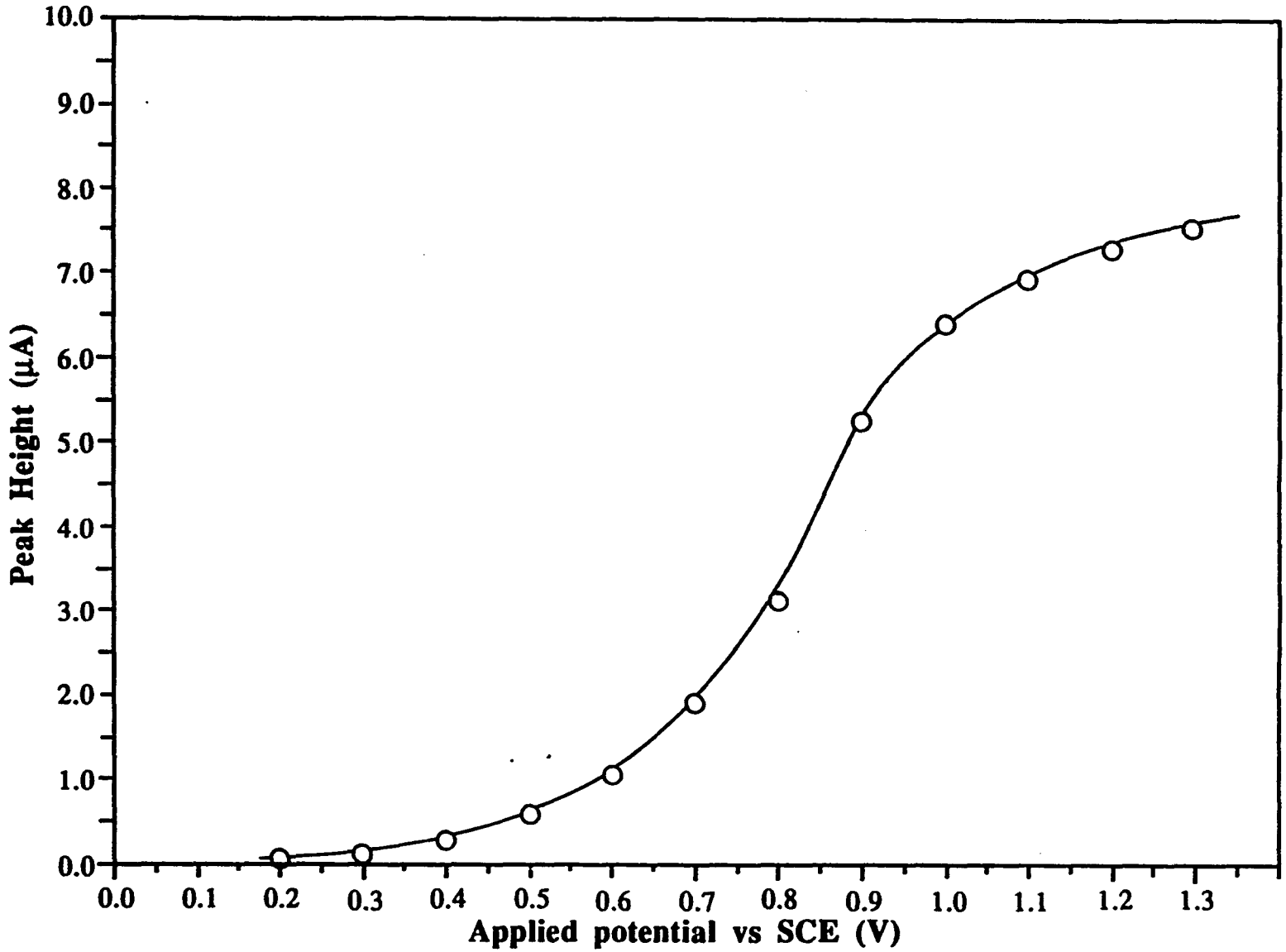

Figure 2. Hydrodynamic voltammogram of vitamin K-1 on silver electrode in the dual-electrode cell. Conditions: mobile phase, acetonitrile-isopropanol-aq 0.05 M $NaClO_4$ (45+45+10, v/v); flow rate, 2.0 mL/min; sample size, 20 µL aliquot of a 400 µg/mL vitamin K-1standard solution injected at each potential setting.

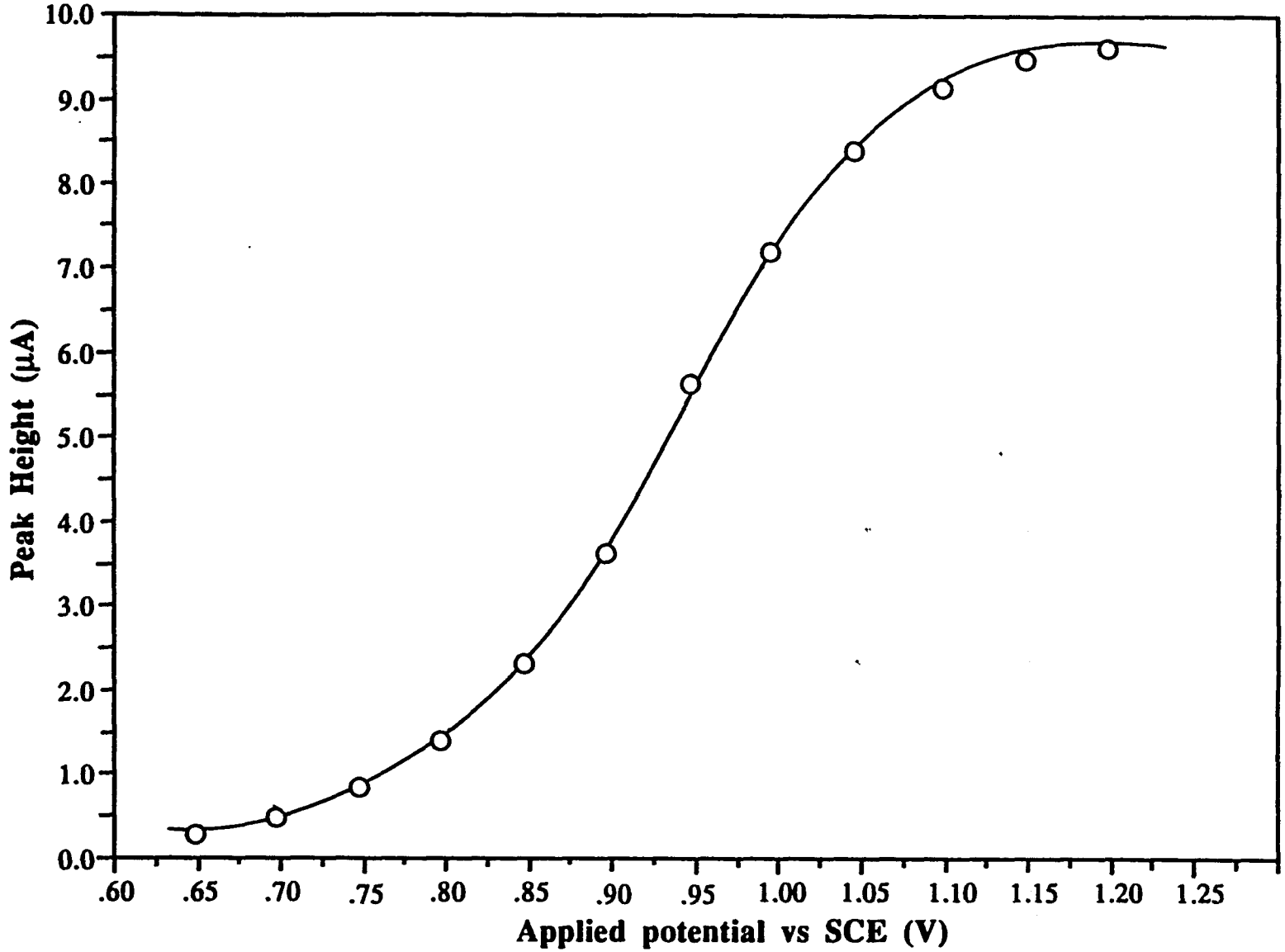

Figure 3. Hydrodynamic voltammogram of vitamin A palmitate on glassy carbon electrode in the dual-electrode cell. Conditions: Mobile phase, acetonitrile-isopropanol-aq 0.05 M $NaClO_4$ (45+45+10, v/v); flow rate, 2.0 mL/min; sample size, 20 µL aliquot of a 350 µg/mL vitamin A standard solution injected at each potential setting.

nA/ng with a correlation coefficient of 0.996 and 1.150 nA/ng with a correlation coefficient of 0.995 was obtained for vitamins K_1 and A, respectively. The detection limit, defined as the amount producing a peak amplitude thrice that of the noise level, was 275 pg for vitamin A palmitate and 80 pg for vitamin K_1. This amount of vitamin K_1 could not be detected by a conventional UV photometer operated at 0.005 aufs. After about 20 injections of vitamin A palmitate solutions in excess of 200 μg/mL, adsorption effects were observed at the glassy carbon electrode in the dual-cell. Subsequently, the surface was renewed by cycling the potential between cathodic and anodic limits until the original characteristics were restored. For these purposes, the working electrode was first potentiostated at -0.2 V for 5 min at a current sensitivity of 10 μA/V and then at +1.4 V for 5 min in a flowing stream of mobile phase. The potential at the glassy carbon electrode was then restored to +1.3 V and the peak heights obtained for vitamin A palmitate were identical to those obtained initially.

Extraction

The extraction conditions used, 8000 psi and 60°C for 15 min, were established during SFE studies (pp. 187 and 219) involving the recovery of both vitamins added individually to simple adsorbent matrices. The reliability of these same conditions for mixtures of these vitamins at the trace level in a more complex matrix was investigated by spiking unfortified milk powder with each vitamin in the range of 1 to 20 μg/g. Using supercritical carbon dioxide under these conditions, both vitamins were simultaneously isolated and quantitated with the dual electrochemical detector described. The recoveries of both vitamins following SFE and reconstitution in mobile phase are summarized in Table 1. As shown in Table 1, the mean recovery for 5 samples was 95.4% and 92.1% for vitamins A and K_1, respectively. In both cases, a single step SFE procedure afforded recoveries in excess of 90% for both vitamins within 15 min. More important, the proposed procedure maintained the integrity of each vitamin and did not introduce substances that interfered with the chromatographic separation. For the sake of comparison, these results are comparable to those reported by Thompson and Maxwell (21), in which case the sample preparation procedure must be performed on duplicate aliquots for samples which contain multiple vitamins, and to those reported by Barnett et al. (24) for an enzymolysis procedure.

Linearity of SFE Procedure

The linearity of the SFE preparation procedure was confirmed in the range of 0.5 to 50

Table 1. Extractability of Vitamins A and K_1 from Spiked Unfortified Milk Powder Using The Outlined SFE Procedure.

Vitamin A	Vitamin K_1	Percentage Recovery	
Added, µg/g	Added, µg/g	Vitamin A	Vitamin K_1
1.0	1.0	92.3	94.8
5.0	1.0	86.3	94.2
10.0	1.0	94.3	90.9
15.0	2.0	102.6	89.6
20.0	2.5	101.4	91.2
Average		95.4	92.1
RSD (n=5)		7.1 %	2.4 %

μg/g from regression analysis for milk samples fortified with both vitamins. A large tail-off in recovery was observed, particularly for vitamin A, in samples containing much less than 0.5 μg/g of either vitamin. However, this limitation is of litttle concern in the analysis of commercial formulas which are typically fortified in excess of 1.0 μg/g. On the other hand, fortification levels in excess of 50 μg/g were not examined due to some minor passivation problems encountered at the carbon electrode.

Precision

The precision of the method was examined by analyzing a sample of milk powder spiked with 1.0 μg/g of each vitamin, 5 times by 2 analysts on 3 different days. The results are shown in Table 2. Using the sample preparation and determination procedure outlined, the day-to-day relative standard for 4 replicates of the milk sample was ± 5.8 % for vitamin K_1 and ± 8.0 % for vitamin A. For within-run precision, the mean relative standard deviation for both vitamins was 5.0 % at the 1.0 μg/g level.

Application to Commercial Infant Formulations

Typical soy and milk-based infant formulas available in the U.S. were assayed for vitamin A and K content using the combination of SFE and LC with dual electrochemical detection. Figures 4 and 5 illustrate typical chromatograms for a soy-based and milk-based formula, respectively. Scrutiny of these chromatograms indicates that SFE provides an effective tool for the isolation of vitamins A and K_1, which can then be resolved in the potential domain during quantitation using the dual electrochemical detector. The results from 3 formulas are presented in Table 3. In general, the proposed method gave results which were higher than those declared for vitamins A and K_1 by an average of about 14 % and 30 %, respectively.

Standard Addition Analysis

Following analysis, standard addition-recovery studies were performed by adding known amounts of each vitamin at 0.5 to 15.0 μg/g level to duplicate samples of 3 infant formulas. Results are shown in Table 4. Recoveries of vitamin A and vitamin K_1 from spiked samples of infant formulas by this LC method ranged from 86.8 to 101.2 % and 85.0 to 103.2 %, respectively. Figures 6 and 7 are chromatograms of the same soy and milk products shown in Figures 4 and 5, respectively, which have now been spiked at 1.0 μg/g level for each vitamin prior to SFE preparation. The absence of interfering peaks for vitamins A and K_1 is evident.

Table 2. Reproducibity Results for a Milk Sample Fortified at the 1.0 μg/g Level with Vitamins A and K_1.

			Analytical Results, μg/g	
Run	Analyst	Day	Vitamin K_1	Vitamin A
1	1	1	0.92	1.22
2	1	2	1.05	1.09
3	2	2	0.98	0.99
4	2	2	0.96	1.07
5	2	3	0.91	1.03
Mean			0.96	1.08
RSD (Between-day)			5.8 %	9.0 %
RSD (Within-day)			4.9 %	5.0 %

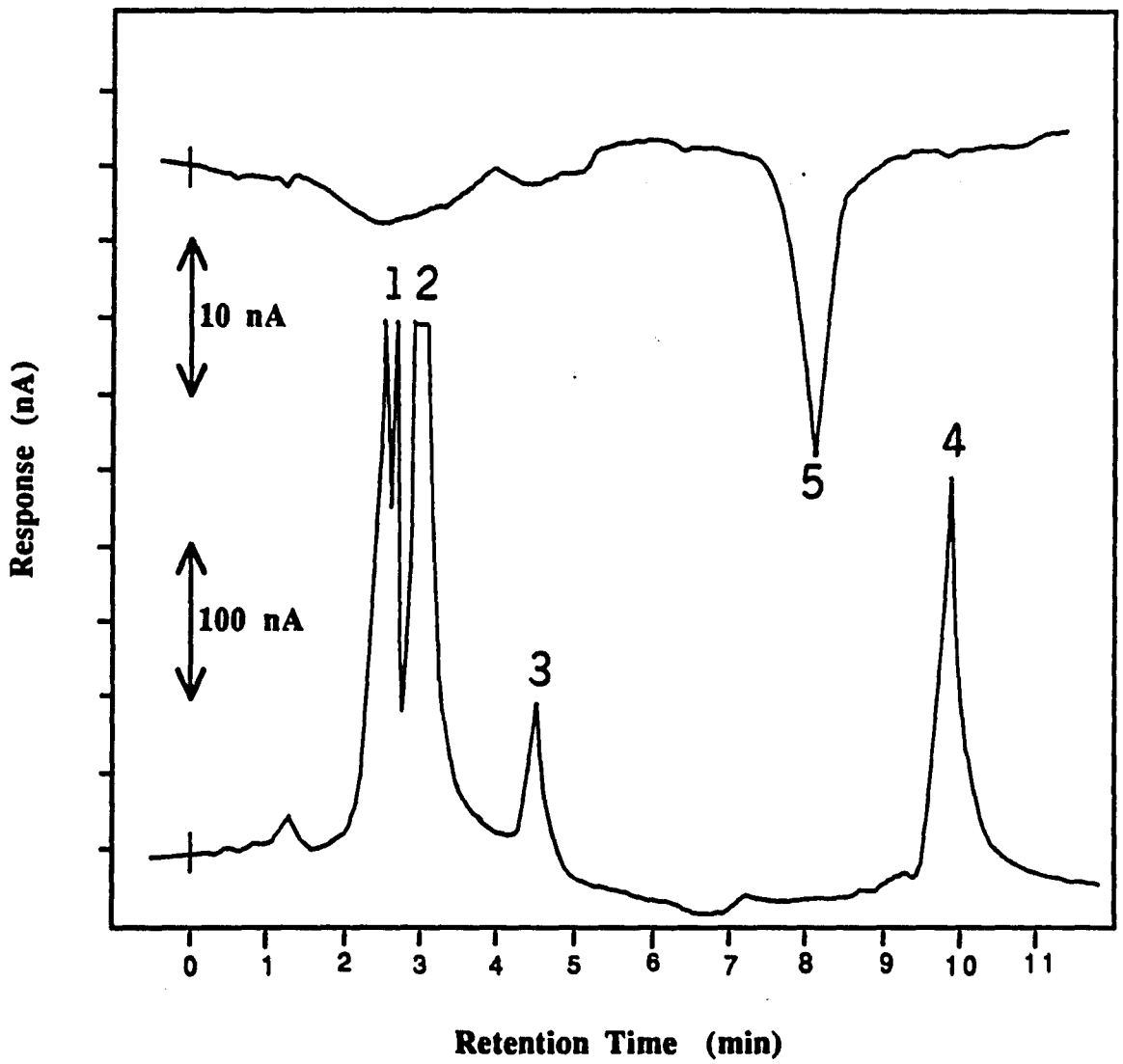

Figure 4. Dual LCEC chromatogram of a supercritical fluid extract of vitamins A and K-1 obtained from a milk-based infant formula using the described procedure. Chromatographic conditions: column, 150 x 4.6 mm I.D. Alltech C-8 (10 µm), with acetonitrile-isopropanol-aq $NaClO_4$ (45+45+10, v/v) eluant. Extraction conditions: SFE at 8000 psi CO_2,65^{0}C, 20 min. Peak identities as follows: Peak 1, BHT; 2, impurity; 3, impurity; 4, vitamin A palmitate; 5, vitamin K-1.

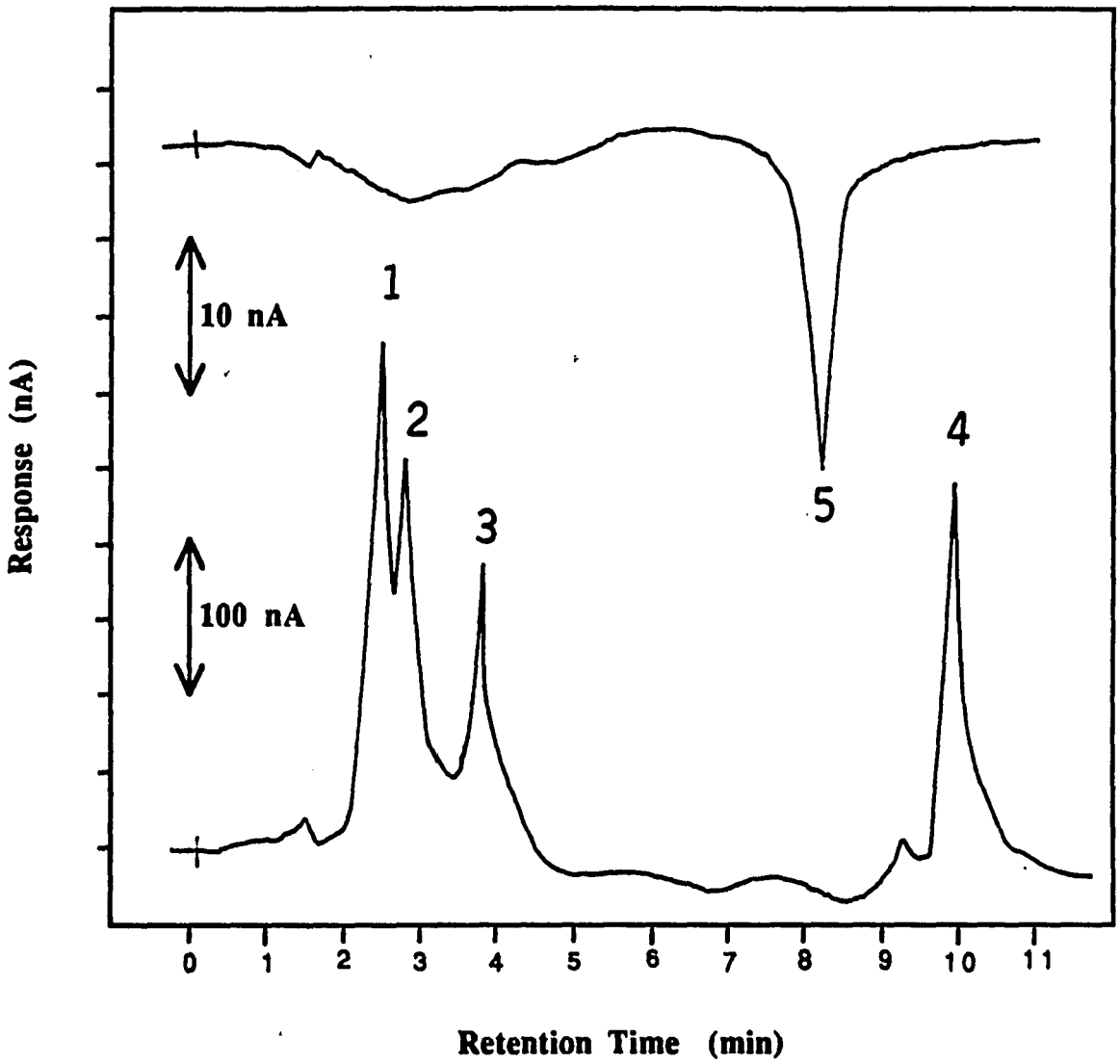

Figure 5. Dual LCEC chromatogram of a supercritical fluid extract of vitamins A and K-1 obtained from a soy-based infant formula. Chromatographic conditions: column, 150 x 4.6 mm I.D. Alltech C-8 (10 μm), with acetonitrile-isopropanol-aq $NaClO_4$ (45+45+10, v/v) eluant. Extraction conditions: SFE at 8000 psi CO_2, 65°C, 20 min. Peak identities as follows: Peak 1, BHT; 2, impurity; 3, impurity; 4, vitamin A palmitate; 5, vitamin K-1.

Table 3. Determination of Vitamin A and K_1 Content in Commercial Infant Formulas Using HPLC with ECD After SFE Fractionation.

Formula Base	Declared Value [1]		Analytical Result [2]	
	Vitamin K_1, µg/g	Vitamin A, IU/g	Vitamin K_1, µg/g	Vitamin A, IU/g
Soy	0.83	16.4	0.93	21.6
Milk	0.80	16.4	0.96	20.7
Milk	0.80	16.4	0.87	21.6
Mean (for the three different bases)			0.92	21.3
RSD (n=3)			4.9 %	2.4 %

[1] For retinyl palmitate, 1.82 IU corresponds to 1 µg.

[2] Mean of triplicate extractions and determinations.

Table 4. Recovery of Vitamins A and K_1 Added to Commercial Infant Formulas.

Formula Base	Fortification Level, µg/g		Percentage Recovery[1]	
	Vitamin K_1	Vitamin A	Vitamin K_1	Vitamin A
Soy	1.0	1.0	94.0	91.3
Soy	5.0	1.0	89.7	92.8
Milk	0.5	0.5	87.5	103
Milk	10.0	0.5	87.5	103
Milk	2.0	2.0	101	93.4
Milk	15.0	1.5	86.8	91.6

[1] Mean of triplicate extractions.

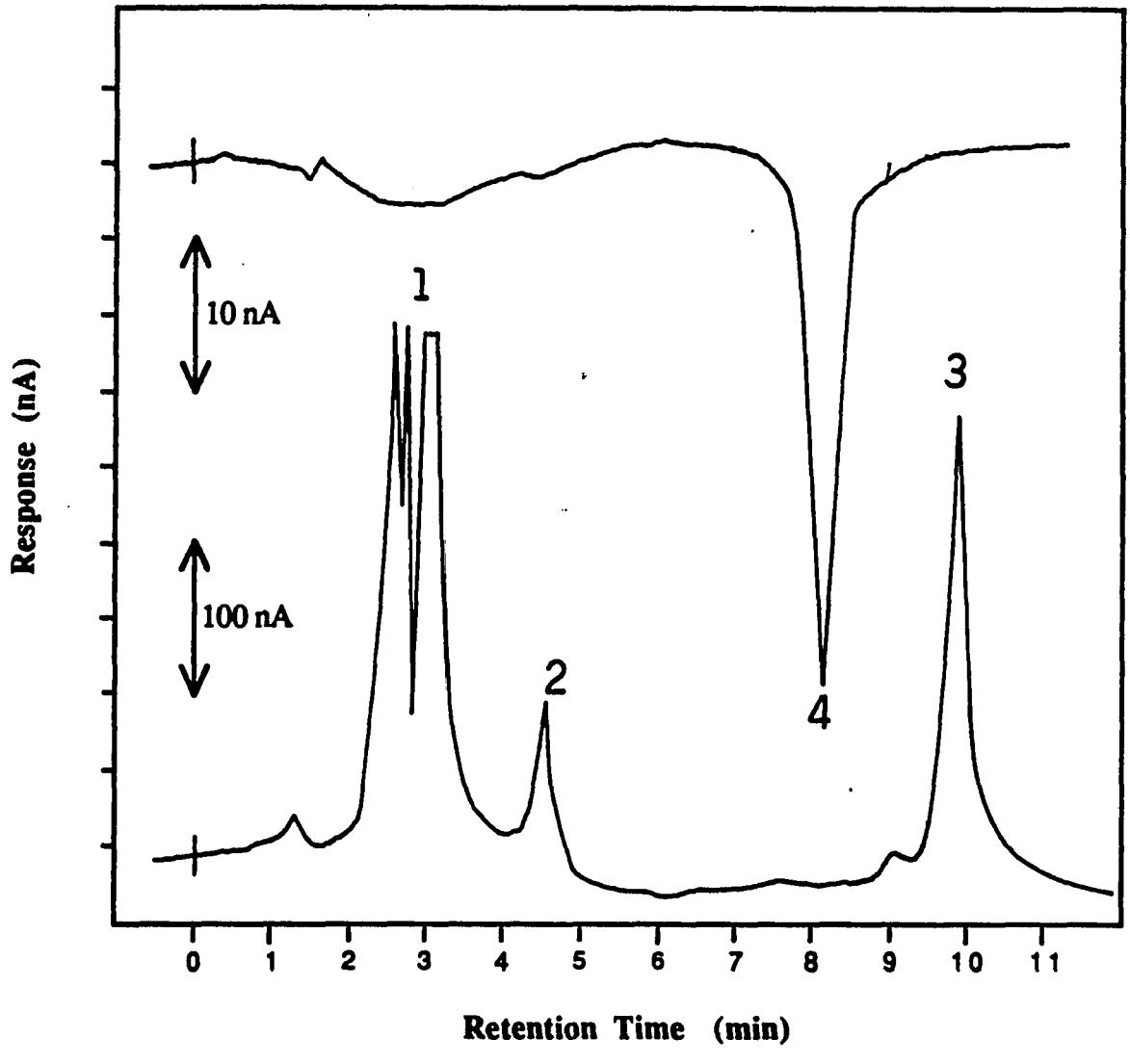

Figure 6. Dual LCEC chromatogram of vitamin fraction from milk-based powder fortified with vitamins A palmitate and K-1 prior to SFE sample preparation. Chromatographic conditions: column, 150 x 4.6 mm I.D. Alltech C-8 (10 µm), with acetonitrile-isopropanol-aq $NaClO_4$ (45+45+10, v/v) eluant. Extraction conditions: SFE at 8000 psi CO_2, 65^0 C, 20 min. Sample, a gram aliquot of a commercially available infant formula spiked with 1.0 µg of each vitamin per gram formula. Peak identities as follows: Peak 1, BHT; 2, impurity; 3, vitamin A palmitate; 4, vitamin K-1.

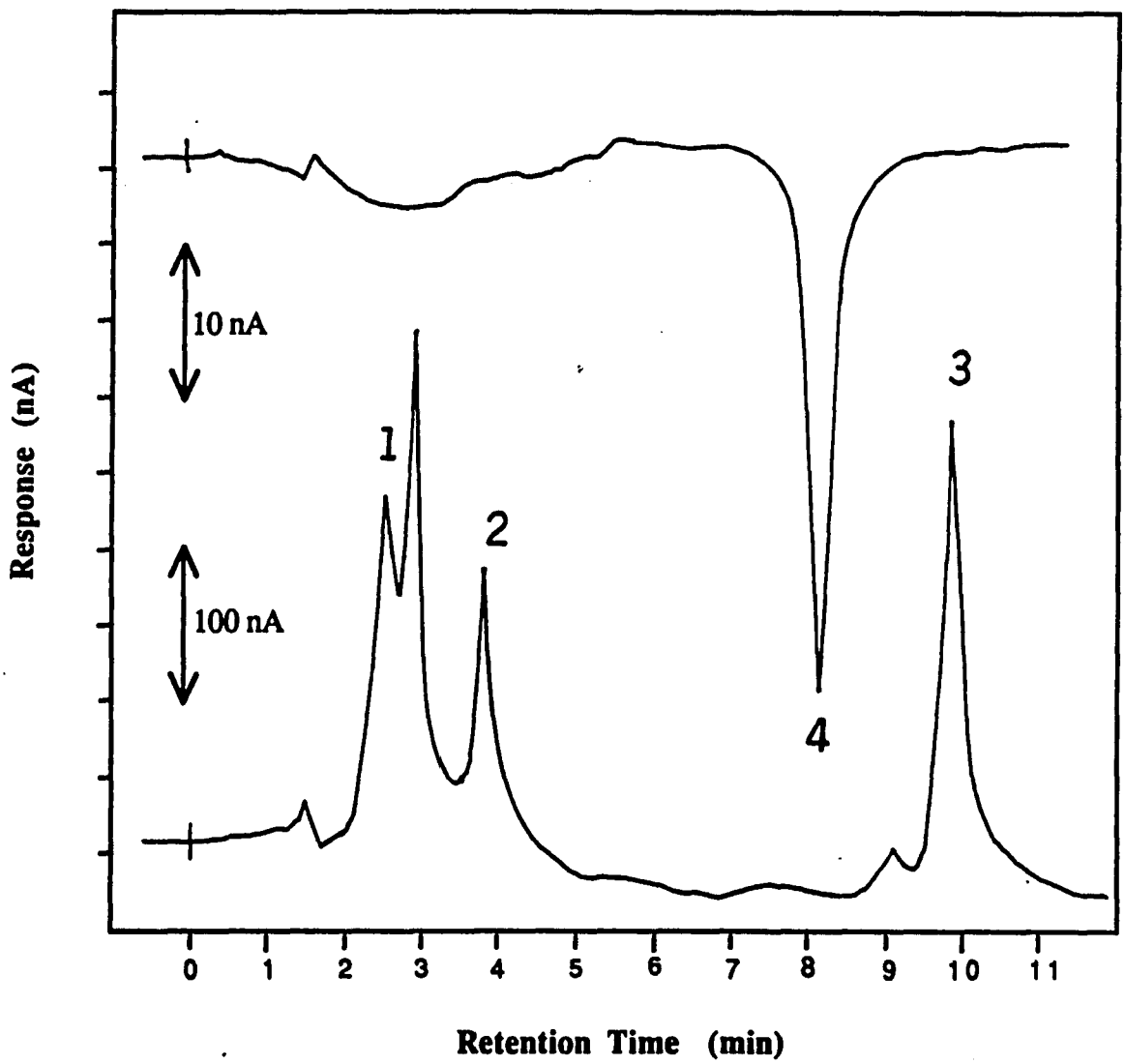

Figure 7. Dual LCEC chromatogram of vitamin fraction from soy-based powder fortified with vitamins A palmitate and K-1 prior to SFE sample preparation. Chromatographic conditions: column, 150 x 4.6 mm I.D. Alltech C-8 (10 µm), with acetonitrile-isopropanol-aq $NaClO_4$ (45+45+10, v/v) eluant. Extraction conditions: SFE at 8000 psi CO_2 ,65^0 C, 20 min. Sample, a gram aliquot of a commercially available infant formula spiked with 1.0 µg of each vitamin per gram formula. Peak identities as follows: Peak 1, BHT; 2, impurity; 3,vitamin A palmitate; 4, vitamin K-1.

Conclusions

In conclusion, a simple, economical, rapid, and relatively precise LC method which requires minimal handling time, little operator involvement and incorporates a single-step preparation procedure has been developed for the simultaneous quantification of vitamins K_1 and A in commercial infant formulas. The method is based on an initial fractionation using SFE, followed by simultaneous quantitation with a dual electrochemical detector. Using this procedure, it is possible to determine accurately and precisely both vitamins at levels as low as 0.5 μg per gram of formula. Typically a technician could be expected to analyze 8 samples per day. Because of the inherent efficiency and speed of SFE, in combination with the sensitivity and selectivity of this mode of detection, this hyphenated technique should lend itself well to many other applications involving trace determinations of other fat-soluble vitamins in various foodstuffs.

Part III Chapter 7

Potential Applications of Supercritical Fluid Extraction in a Quality Control Laboratory.

Introduction

Production of pharmaceuticals requires several levels of testing before release of finished products. Specifications for pharmaceuticals always include identity and total assay, quantitative measure of strength and potency of the active ingredients along with requirements for limits on decomposition products and other impurities, dosage uniformity among units, dissolution of solid dosage forms and other properties affecting quality. Specification and tests are developed for control of product components, packaging and labeling and critical in-process manufacturing steps. Additional methods may be necessary for monitoring physical and chemical stability of the product.

Productivity in the HPLC analyses of pharmaceutical formulations has been improved by automated sample injectors and computational data handling, but sample preparation still remains the major bottleneck for reliable chemical analysis. In addition to being the most labor intensive and time-consuming steps in the analytical process, other associated sample preparation problems include matrix interferences and component stability. The predominant method of sample preparation used in quality control laboratories involves liquid-liquid (L-L) extraction, which typically suffers from low drug recovery, non-reproducible results, incomplete removal of interfering sample components, long preparation times and the need for large volumes of solvent and subsequent concentration steps.

In pharmaceutical work, as elsewhere, the application of solid phase extraction is becoming increasingly preferred because of its ease of use, low sample elution volume, good recoveries and commercial availability of prepacked column and cartridge assemblies. These methods have been used successfully to address many of these concerns especially as regards handling time, however, these cartridges tend to become blocked easily by a porous matrix. In addition, traditional liquid-solid procedures do not eliminate the evaporation step of the elution solvent, which is often a cause of loss of the analyte of interest. Finally, significant manual intervention is still necessary.

Obsessed with the desire to cut labor costs, many elegant systems designed around a robotic arm for sample preparation in stability and dissolution programs have been described (1, 2). These systems run unattended and provide reliable analytical data at

less cost per sample than manual means. However, these systems are primarily designed around liquid-liquid or solid-liquid assemblies and as a consequence require multiple pipetting, dilutions, and concentration steps which are prone to error compounding. More importantly, these systems are not directly compatible with information-rich chromatography detectors such as a mass-spectrometer.

This chapter describes an alternative method of sample preparation of pharmaceutical formulations for subsequent batch HPLC analysis. Diazepam (7-chloro-1,3-dihydro -1-methyl-5-phenyl-2H-1,4-benzodiazepin-2-one) was chosen as a representative model substance since it is widely prescribed for a multiple of symptoms (3) such as anxiety, tension, agitation, irritability, and skeltal muscle spasms. In addition, it is widely manufactured by several generic pharmaceutical firms.

Early methods for the determination of Diazepam and other benzodiazepines in pharmaceutical formulations and body fluids concentrated extensively on GC-ECD (electron capture detector) (4,5). This methodology has been reviewed (6,7), most recently by deSilva and co-workers (8), Mehta (9), and Schultz (3). Despite the potential sensitivity and specificity of the electron capture detector, elaborate and somewhat lengthy cleanup procedures are necessary and in some cases the high temperature employed in GC may cause the decomposition of metabolites (10,11). Moreover, derivatization or acid hydrolysis to the more volatile benzophenones may also be required (12). For these reasons and because of the low temperatures used, HPLC would appear to the method of choice for the determination of benzodiazepines and their metabolites. The separation of Diazepam and its metabolites by HPLC was first reported by Scott and Bommer (13) using adsorption chromatography for the measurement of Diazepam in dog urine. Again using the adsorption chromatography on silica columns, Weber (14), Bugge (15), Rodgers (16), and Macek and Rehak (17) separated and quantified Diazepam and some other 1,4-benzodiazepines in standard mixtures and pharmaceutical preparations. In contrast, Bordie et al. (18) and Ratnaraj et al. (19) have used reversed-phase HPLC for the analysis of Diazepam and its metabolites from various biological matrices. Similarly, the Official Compendia, NFXV and USPXXI (20), also details a reversed-phase HPLC method utilizing a C-18 column and an aqueous methanolic mobile phase with UV detection at 254 nm for the evaluation of Diazepam in tablet, capsule and injectable form. These and other LC methods have been reviewed by Schwartz (21).

As a result of the loss of Hoffmann-La Roche's patent on Valium®, increased production of generic Diazepam has prompted the re-evaluation, optimization, and modification of the existing LC methods especially with regard to modern sample preparation (22-24) and detection considerations (25).

Most of the published work on the LC analysis of benzodiazepines has employed UV absorbance detection. However, nearly all of these compounds are electrochemically reducible at practical electrode potentials and their electrochemical behavior has been extensively studied (26-28).

In principle, HPLC with ECD detection offers certain advantages over UV detection in terms of selectivity, sensitivity, and cost. Also, the construction of a simple flow-through cell and precision potentiostat with low level current measuring capabilities requires minimal time and cost.

Despite these advantages, the widespread use of reductive mode electrochemical detectors for the analysis of Diazepam has been hindered, undoubtedly, by a few operating difficulties: first the need to exclude dissolved oxygen from the mobile phase and sample or discriminate against its effects; and second, the lack of a rugged, dependable and reproducible working electrode which has a wide cathodic range.

Kissinger and co-workers (29) have made major contributions to overcoming these problems and to the renaissance of the reductive mode amperometry. They developed efficient procedures in conjunction with simple devices such as a degassing syringe for the elimination of the effects of oxygen. In addition, various solid electrodes such as amalgam films, carbon composites, and glassy carbon were systematically investigated for reductive use. Various electrochemical modes such as differential and dual electrode configurations which discriminate against oxygen and its effect on the background signal were proposed. Following these guidelines, Lund (30) applied a flow-through electrochemical detector containing a glassy carbon electrode in a wall jet cell to the HPLC analysis of several benzodiazepines. Satisfactory detection limits were obtained, although applications to real samples were not reported. Subsequently, Hackman and Brooks (31) evaluated a reductive detector employing a dropping mercury electrode which was operated in the differential mode. A substantial

improvement in the signal to noise ratio was obtained due to discrimination against the effects of dissolved oxygen.

Recently, Lloyd (25) detailed an elegant, extremely versatile LCEC procedure for common 1,4 benzodiazepines which included an initial extraction on a micro scale solid-phase cartridge with microlitre volumes of aqueous acetonitrile. Using a reductive amperometric detection at a pendent mercury electrode, detection limits in the 80-200 pg range were obtained for all common benzodiazepines containing the azomethine moeity.

In our laboratory none of the problems once associated with reductive electrochemical detectors remain of significance, and reductive mode detection employing a silver based thin-layer cell is a routinely applied technique. The electrode response characteristics are highly sensitive and reproducible (from one week to the next), and the technique is as easily used as any offering parts per billion sensitivity.

The potential offered by SFE for sample preparation of various pharmaceutical samples, has attracted our interest. From this viewpoint, various levels of testing in the manufacture of Diazepam such as tablet dosage potency and content uniformity are being examined. The manipulation is straight forward and can greatly reduce the time required for sample isolation, analyte collection, and concentration steps. In fact the time required for sample preparation time can be made comparable to the chromatographic run-time. Since time for sample preparation and handling steps would be minimized, the potential for loss and degradation of the analyte species should be reduced. When an electrochemical flow-through detector is employed for extract quantitation, a tool having power beyond the scope of either technique used separately in terms of sensitivity, selectivity, speed and cost, is formed.

In this chapter, the technical aspects of an HPLC method utilizing SFE for sample preparation prior to electrochemical detection is detailed and its use is illustrated in analysis of Valium. Guidelines are given for the selection of parameters which can effect the efficiency of the extraction and chromatographic components of the over-all procedure. In addition, the performance figures of merit for the method including linearity, sensitivity, selectivity, and reproducibility are discussed.

EXPERIMENTAL

Chemicals

The benzodiazepine reference standards were obtained by donation. Commercial tablets were obtained from local distributers. HPLC-grade acetonitrile was purchased from J. T. Baker (Phillipsburg, NJ). In-house glass distilled water was used throughout the study. Buffer salts were of reagent grade or better.

Preparation of stock solution

Approximately 100 mg of USP Diazepam, accurately weighed to ± 0.1 mg, was transferred into a 100 mL volumetric flask and diluted to volume with acetontrile to ca 1 mg/mL.

Tablet Preparation

The average weight per tablet was determined and 4 tablets were ground to pass through a no. 60 mesh sieve. An accurately weighed portion of the composite containing 1 mg of Diazepam was transferred to the extraction chamber. The chamber was sealed with two endfittings packed with glass wool and the sample was subjected immediately to the proposed procedure.

Standard Benzodiazepine Mixture

A 1.0 mL aliquot of the stock solution was pipetted into a 10 mL volumetric flask containing 1.0 mg of Chlorodiazepoxide (Librium®), and diluted to volume with acetonitrile.

Preparation of Working solutions

By serial dilution of the stock solution, 10 working solutions were prepared in acetonitrile covering the range of 0 to 0.2 mg/mL in 0.02 mg/mL increments.

Apparatus

The HPLC system was designed around a Varian Model 8500 syringe-pump and Rheodyne (Cotati, CA) 7125 rotary injector. The separation was carried out with a 150 mm x 3.9 mm I.D. μ-Bondapak C-18 (10 μm) column (Waters Assoc., Milford, MA). The analytical column was protected by a guard column (50 mm x 4.6 mm) obtained from Supelco (Bellefonte, PA) and dry-packed with pellicular C-18 bonded silica (40 μm).

Compounds were eluted with a mobile phase composed of acetonitrile and aqueous phosphate buffer, pH 6.8. The mobile phase was filtered through a 0.45 μm Millipore filter (Bedford, MA) and degassed with helium for 5 min before use. The amperometric detector incorporating a silver working electrode has been described previously (pp. 14-18). Prior to use, the lower silver block was removed from the cell and sequentially polished with 800 grit silicon carbide, 0.45 μm alumina slurry, and then rinsed in distilled water. The detector cell was then reassembled and eluent was pumped through the cell until a stable baseline potential was attained. After about 15 injections, a 10 sec cleansing pulse of -200 mV was applied to the working electrode. Failure to apply the cleansing pulse resulted in a gradual decline in detector response. All chromatograms were recorded on a Linear model 1200 (Linear Instruments, Irvine, CA) chart recorder with a f.s.d of 1.0 V and a chart speed of 1 cm/min.

Extraction

The chamber with its contents was inserted into a high-pressure manifold (pp. 124-125) and heated slowly, while the system is purged of oxygen with low pressure carbon dioxide. When the oven temperature reached 60^0C, the back-pressure regulator was closed and the system was pressurized to 8000 psi. After 15 min, the back-pressure regulator was slowly opened and the extract was collected on a guard column packed with pellicular C-18 bonded silica. The trap and the interconnecting tubing was washed with methanol-acetonitrile (50/50, v/v), filtered through a 0.45 μm filter (Gelman) and transferred to a 25 mL volumetric flask. The solution was diluted to the mark with acetonitrile and subjected to HPLC analysis with EC detection.

Determination

A 20-μL aliquot of the degassed extract was injected onto the HPLC column using the chromatographic apparatus and parameters described. The benzodiazepine peaks were tentatively identified on the basis of retention time. Quantitation was based on peak height which was measured with a laboratory-constructed peak detector (pp. 30-32) Response factors for each compound were computed daily from standard curves.

Results and Discussion

Electrochemical Characteristics of Diazepam

The reduction of Diazepam in aqueous solutions is well documented (32-34). However, no data was available for the particular medium used here, namely acetonitrile-aqueous phosphate buffer (60/40, v/v), pH 6.8. As a result, hydrodynamic voltammetry was used to study the reduction characteristics in this media. In this technique, multiple injection responses of a single sample are plotted as a function of applied potential. From the HDV shown in Figure 1, the irreversible nature of the wave at silver is evident. These results are consistent with the original reports of Oelschager et al. (32), who suggested that this single wave is probably due to a 2 electron reduction of the 4,5 azomethine bond. For Diazepam, a value of -1.2 V *versus* SCE was chosen as a compromise between sensitivity and background signal and loss of selectivity.

Influence of pH on Response

The effect of pH on EC response of diazepam was studied by recording the plateau response currents at different pH values. In these trials, the pH was adjusted with acetic acid and ammonia solutions. The dependence of pH on the signal to noise ratio is illustrated in Figure 2. Although adequate peak shapes for Diazepam can be achieved at pH 4, such a buffer affords relatively poor sensitivity, due most likely to increased background currents. It was found that by increasing the pH of the buffer to 7, the sensitivity as well as peak shape can be optimized. At the same time, only very small changes in the half wave potential for diazepam in this pH range were noticed. In addition, the μ-Bondapak packing of the column is unstable at pH values much above 7.5.

Dependence on Flow Rate

As expected, the peak height response increased with flow rate over the range of 10 to 120 mL/hr. The profile is shown in Figure 3. When the data are replotted on a log-log scale, a linear curve is obtained with a slope of 0.39. This value is in good agreement with the theoretical characterization of a thin-layer cell, for which a value of 0.33 is expected for convective diffusion limited currents (35).

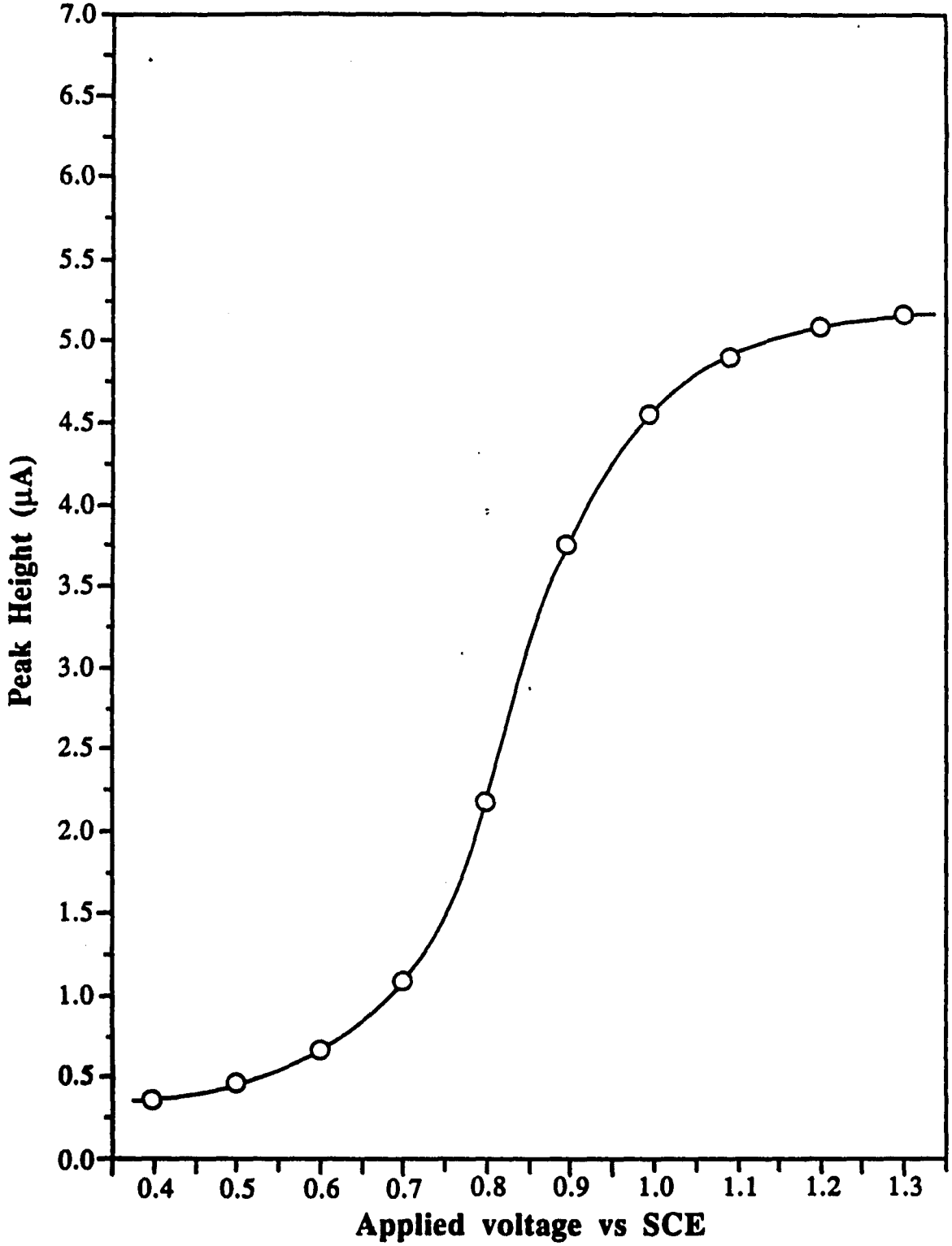

Figure 1. Hydrodynamic voltammogram of Diazepam on silver cathode. Chromatographic conditions: column, 150 x 3.9 mm I.D. μ-Bondapak C-18 (10 μm); mobile phase, acetonitrile-aq 0.05M phosphate buffer, pH 6.8 (60+40, v/v); flow rate, 2.0 mL/min; sample size, 5.0 μg Diazepam in 20 μL mobile phase injected at each potential setting.

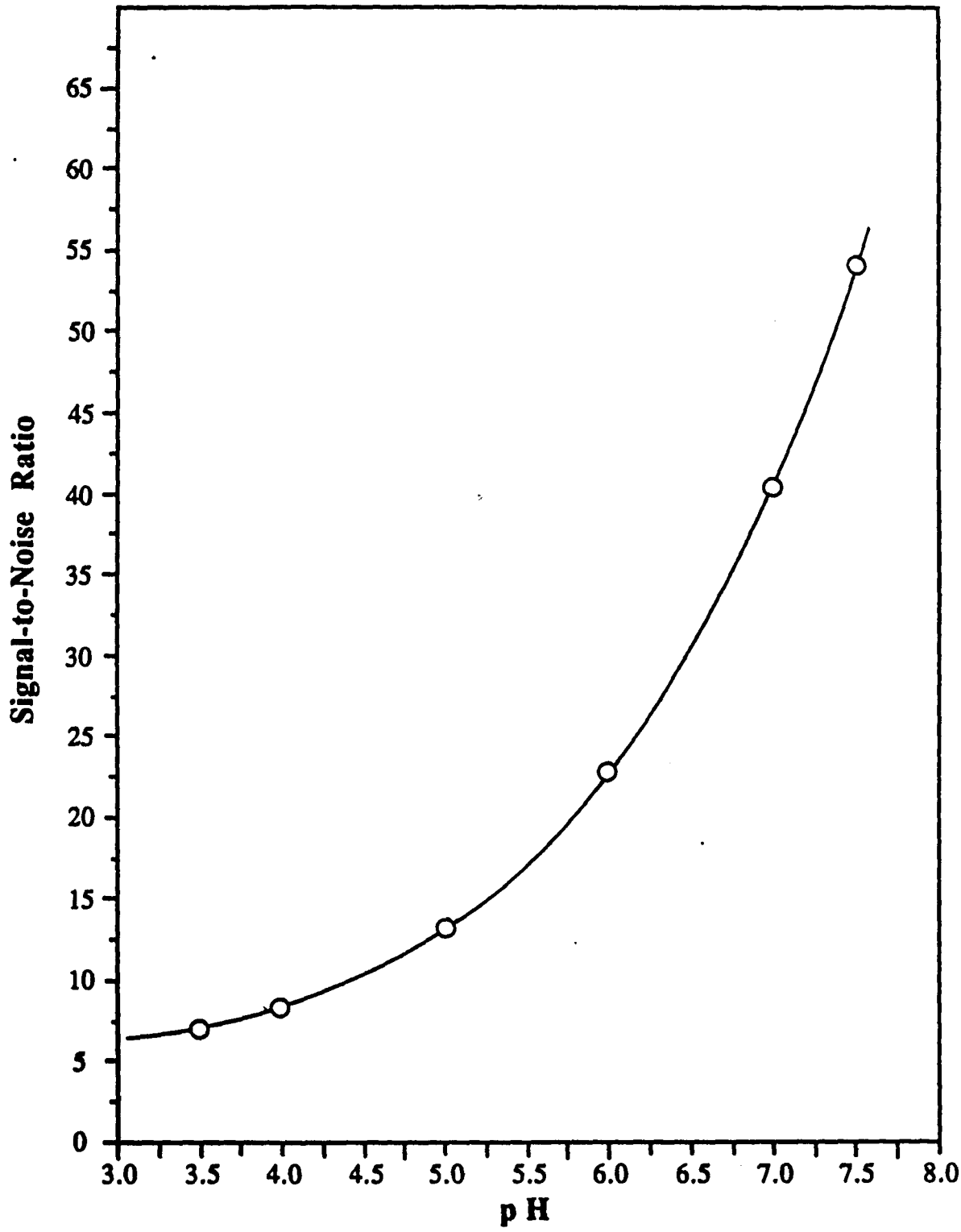

Figure 2. Influence of pH on signal-to-noise ratio in the detection of Diazepam. Chromatographic conditions: column, 150 x 3.9 mm I.D. μ-Bondapak C-18 (10 μm); mobile phase, acetonitrile-aq 0.05 M phosphate buffer, pH 6.8 (60+40, v/v); flow rate, 2.0 mL/min; applied potential, -1.1 V *vs* SCE; sample size, 5.0 μg Diazepam in 20 μL mobile phase injected at each pH value.

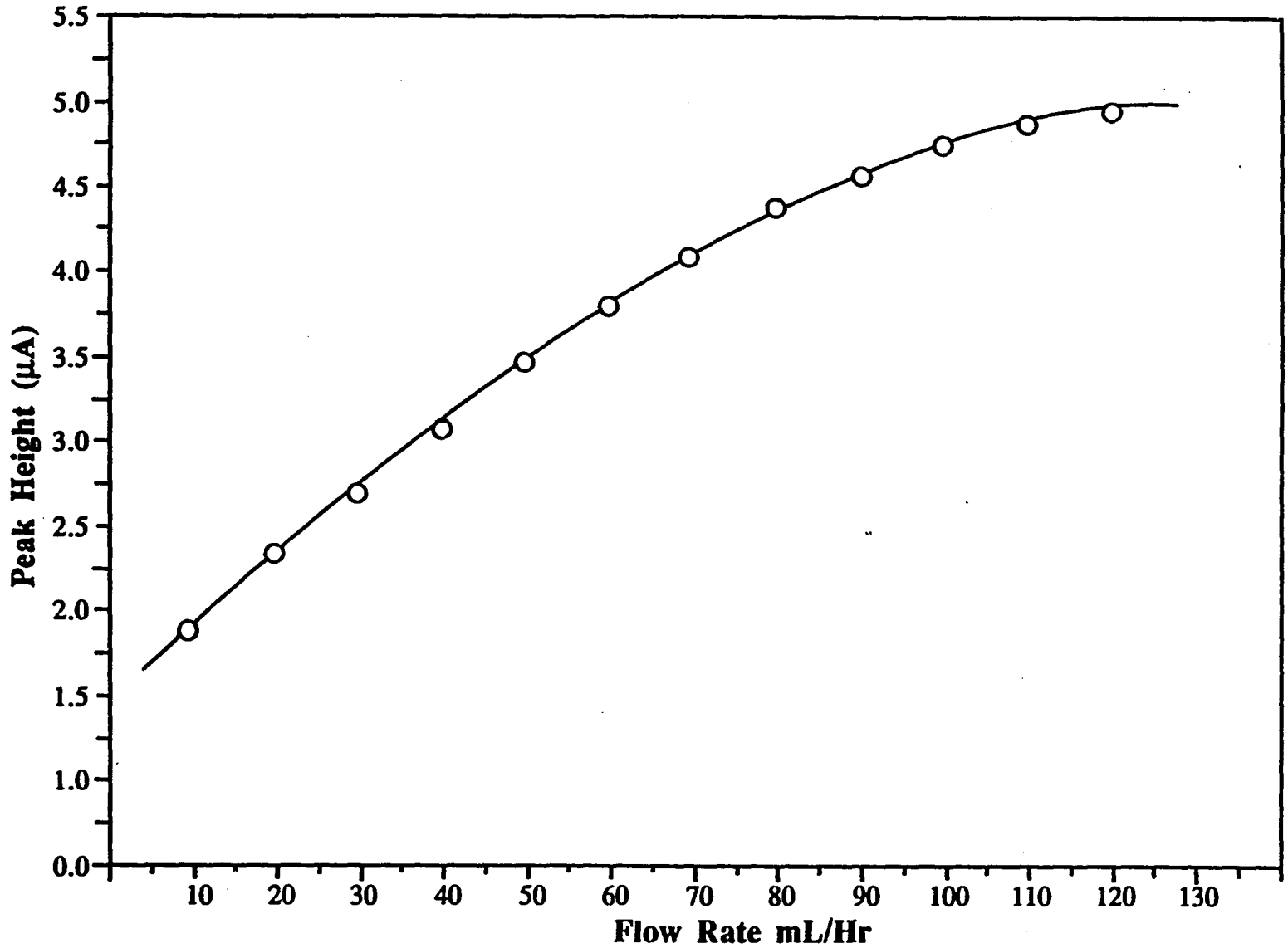

Figure 3. Dependence of response on flow rate. Conditions: column, 150 x 3.9 mm I.D. µBondapak C-18; mobile phase, acetonitrile-aq 0.05 M phosphate buffer, pH 6.8 (60+40, v/v); Ag electrode potential, -1.1 V vs SCE; sample size, 5 µg Diazepam per 20 µL mobile phase injected at each flow rate setting.

Linearity and Calibration of EC Detector

The linearity of the EC system for Diazepam was found to extend over 3 orders of magnitude from 0.2 mg/mL to 0.2 μg/mL, with a correlation coefficient of 0.995. Samples containing Diazepam were determined from a calibration curve by measuring peak heights. The calibration graph shown in Figure 4 was constructed from a set of ten standards covering the range of 0.02 to 0.2 mg/mL. Each standard was injected twice and the equation of the best fit line, computed by linear regression analysis, was y (μA) = 5.01x (mg/mL) + 0.002 with a correlation coefficient of 0.996.

Detection Limit and Sensitivity

The sensitivity of the LCEC approach depends on the chromatographic conditions, electrochemical behavior of the species in question and the magnitude of the background current at the chosen electrode. The detection limit for Diazepam at silver, based on a signal to noise ratio of 3, was found to be 750 pg. The routinely observed blank reading varied between 200 and 250 nA. The sensitivity for Diazepam at silver, defined as the slope of the peak height versus concentration curve is 5.01 μA-mL/μg.

Chromatography

The chromatographic system was primarily designed to offer short run-times and durability particularly for Diazepam at the expense of resolution of the entire class of benzodiazepines. The relationship between the solvent strength (% acetonitrile) and retention (capacity factor k') of Diazepam is shown in Figure 5. In agreement with Harzer and Barchet (36), an isocratic eluent containing 60 % (v/v) acetonitrile along with 35 % (v/v) aqueous 0.05 M phosphate buffer, pH 6.8 was found suitable for the separation from excipients. Figure 6 shows a representative chromatogram of a synthetic mixture composed of Diazepam (Valium®) and Chlorodiazepoxide (Librium®). It can be seen that Librium and Valium show satisfactory peak shapes with retention times of 5.2 and 6.5 min, respectively. An advantage of using this mobile phase in routine QC situations involves the limited dependence of retention time on slight changes in mobile phase composition. A change of 5 % vol acetonitrile content resulted in only a 0.2 min change in the retention time for Diazepam.

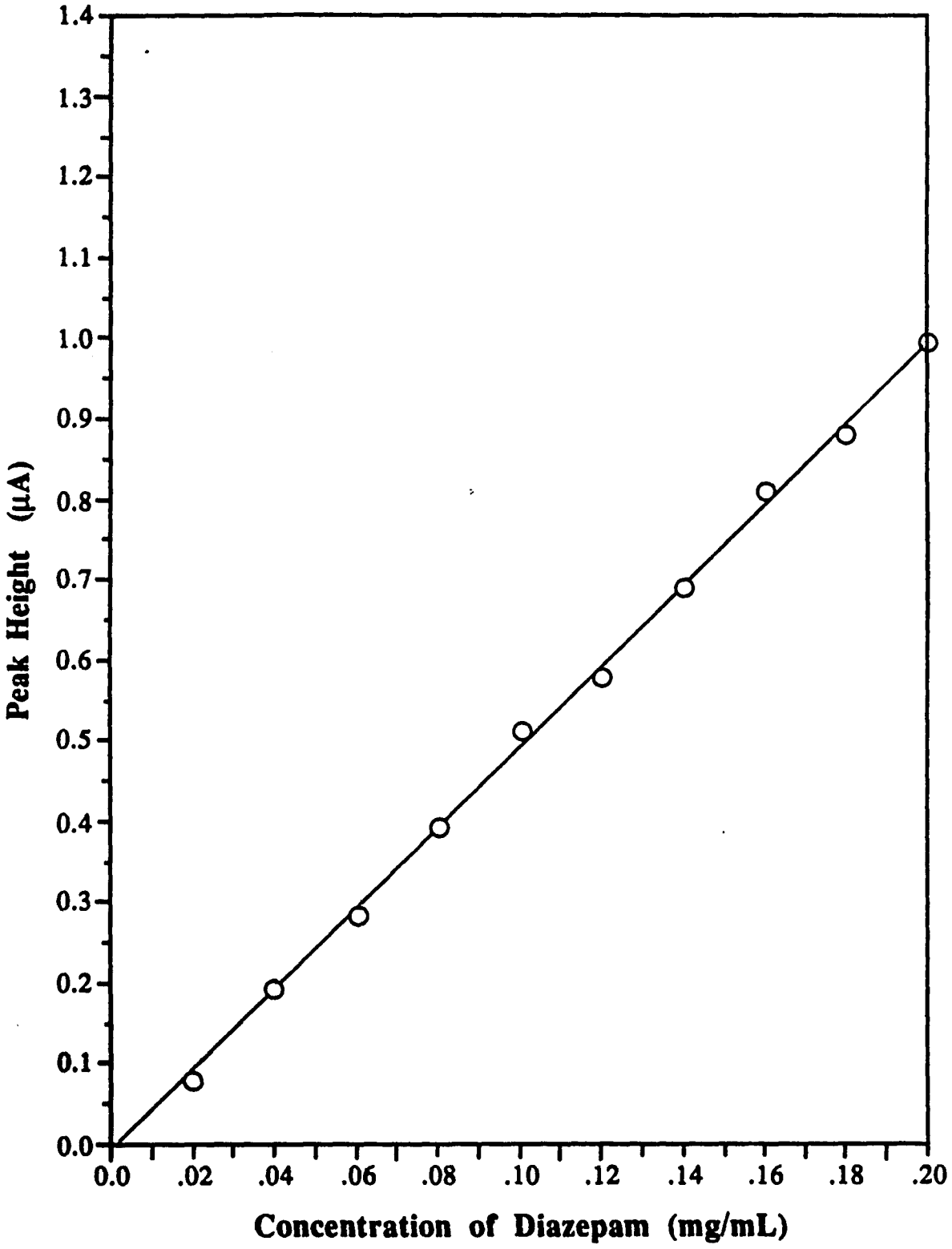

Figure 4. Calibration curve for Diazepam obtained from 20 μL injections onto a 150 x 3.9 mm I.D. μ-Bondapak column with an acetonitrile-phosphate buffer, pH 6.8 (60+40, v/v) mobile phase at a flow rate of 2.0 mL/min. Potential of silver working electrode was -1.2 V vs SCE.

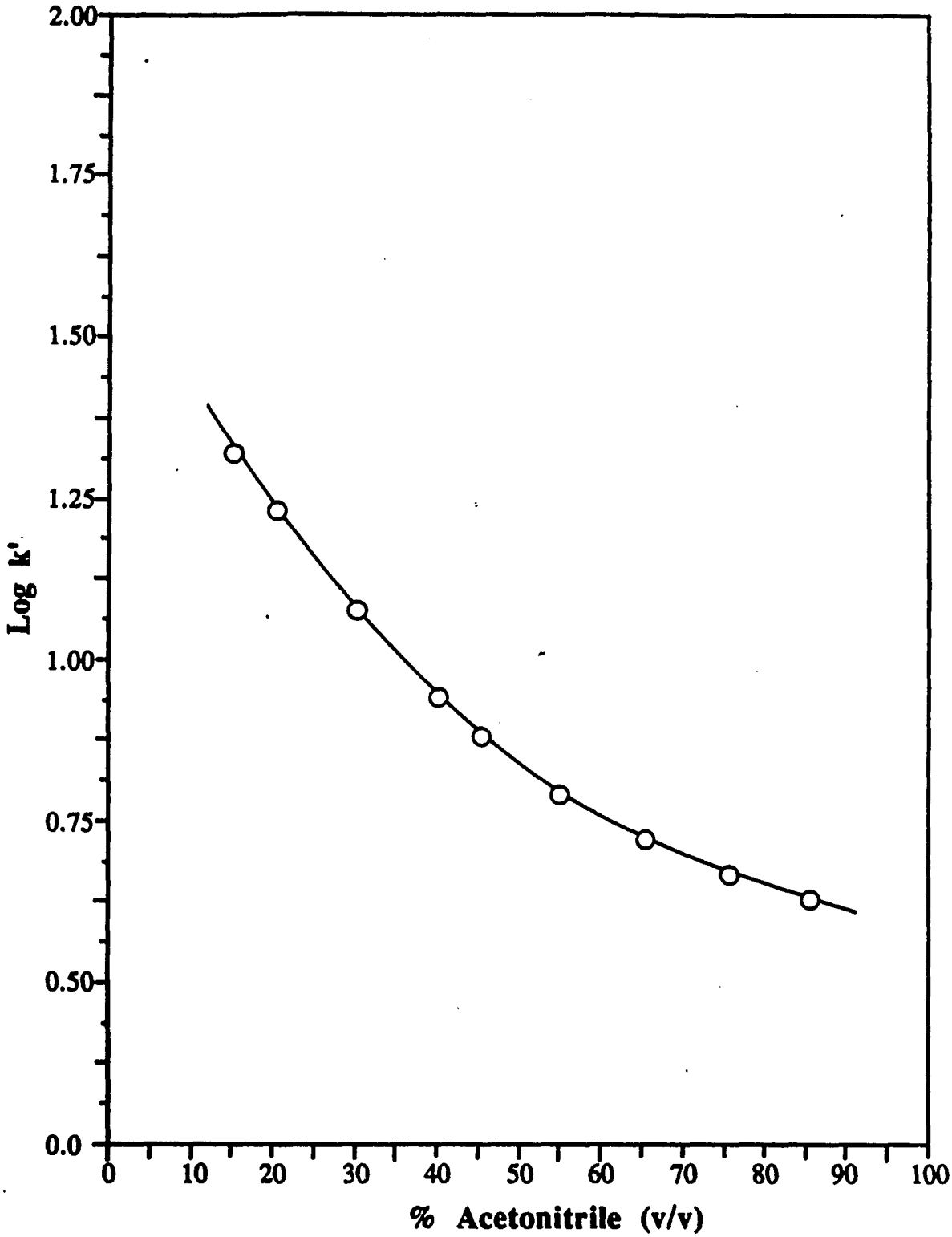

Figure 5. Effect of solvent strength on the retention of Diazepam. Chromatographic conditions: column, 150 x 3.9 mm I.D. μ-Bondapak C-18 (10 μm); mobile phase, prepared from appropiate volumes of acetonitrile and a stock aqueous phosphate (pH 6.8) buffer; flow rate, 2 mL/min; test sample, 5.0 μg Diazepam per 20 μL mobile phase injected at each mobile phase composition.

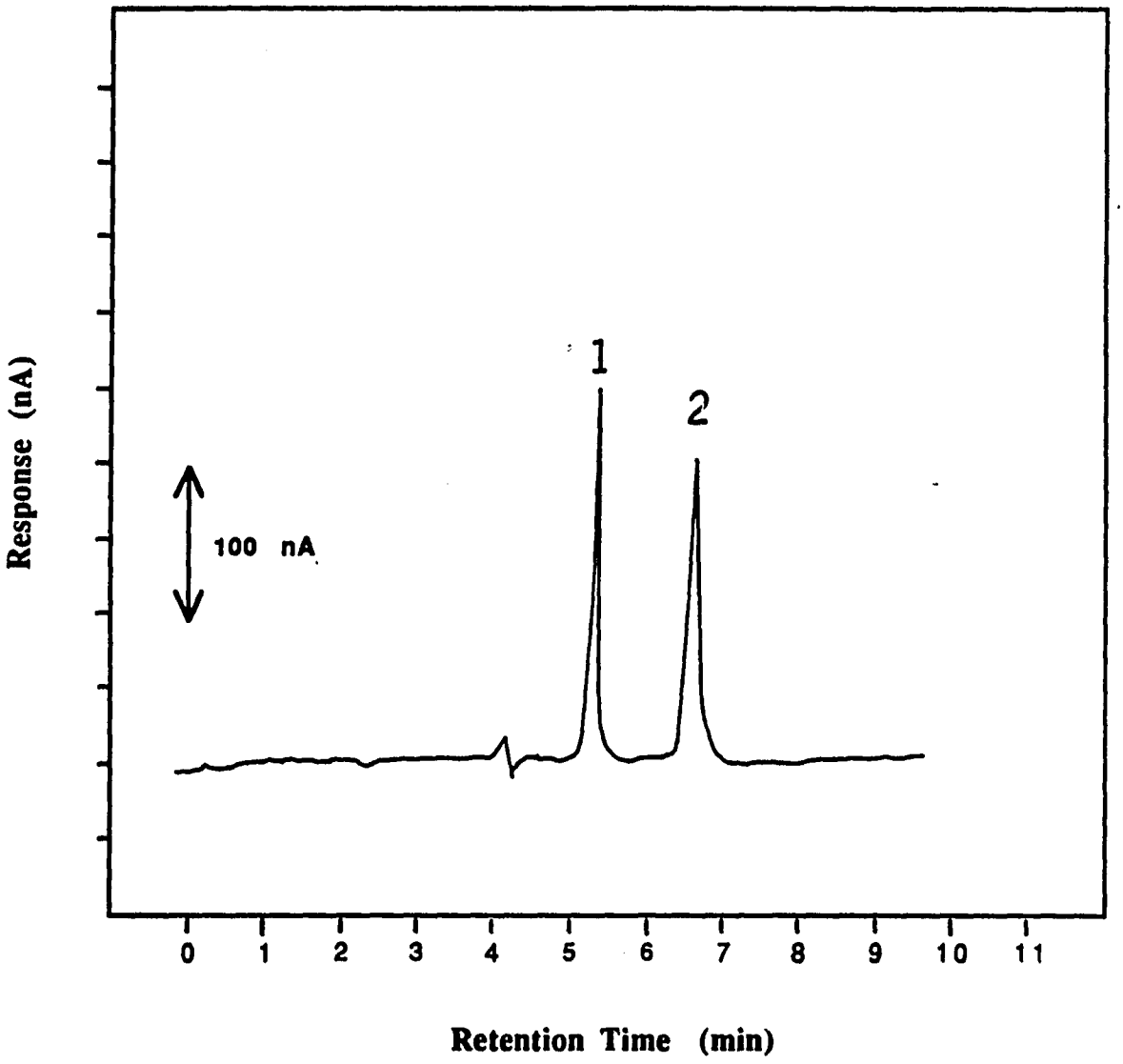

Figure 6. Chromatogram of the separation of benzodiazepines on a μBondapak C-18 (10 μm) column by isocratic elution. Chromatographic conditions: mobile phase, acetonitrile-phosphate buffer, pH 6.8 (60+40, v/v); flow rate, 2.0 mL/min; detector potential, -1.2 V vs SCE; detector sensitivity, 100 nA/V. Peak identities as follows: 1, Chlorodiazepoxide; 2, Diazepam.

Extraction Conditions

The extractability of Diazepam was characterized by performing repetitive extractions on similar samples using two supercritical fluids at several pressures. Figure 7 illustrates the dependence of percentage recovery on pressure for Diazepam using CO_2 and N_2O. From the curve obtained by using CO_2, it can clearly be seen that recovery is not quantitative for an equilibration time of 15 min. On the other hand, quantitative recovery is obtained for N_2O at 8000 psi and 65^{0}C within 15 min and these conditions were used for all further work. The increased solubility of Diazepam in N_2O is due presumably to the increased polarity of the extractant, although the exact mechanism of interaction has not yet been been determined.

Collector

The nature of the trap used to accumulate the precipitated Diazepam plays an important role in determining the over-all limit of extraction as well as the compatibility with various detectors. The relative ease of precipitating Diazepam onto a solid support enabled the use of a very short (40 mm x 4.2 mm) column packed with C-18 Corasil (Waters Assoc., Milford, MA). With a short column, the desorption volume can be made compatible with modern separation instrumentation. Figure 8 shows a desorption profile for this particular C-18 trap as a function of acetonitrile-methanol (50/50, v/v) volume. It is seen that the first 5 mL removed 75 % of the Diazepam from the trap, and an additional 5 mL of eluent was sufficient to achieve greater than 93 %.

Extraction Efficiency

The efficiency of the described sample preparation procedure was examined by adding known amounts of Diazepam dissolved in methanol to C-18 cartridges. After the methanol evaporated, the Diazepam was recovered by the SFE procedure described earlier. The recoveries of the Diazepam standards were then measured in triplicate using the EC detector following reversed-phase separation. The results are summarized in Table 1. The recoveries of Diazepam are linear over the concentration range of 1.0 mg/mL to 500 ng/mL The mean absolute recovery and CV of Diazepam over this range for the 8 samples is 90.7 ± 4.4 % (n=8). This value compares favorably with that obtained by liquid-liquid extraction of 91 ± 3 % (37). Using the procedure described, the practical limit of extraction for Diazepam was 500 ng/mL.

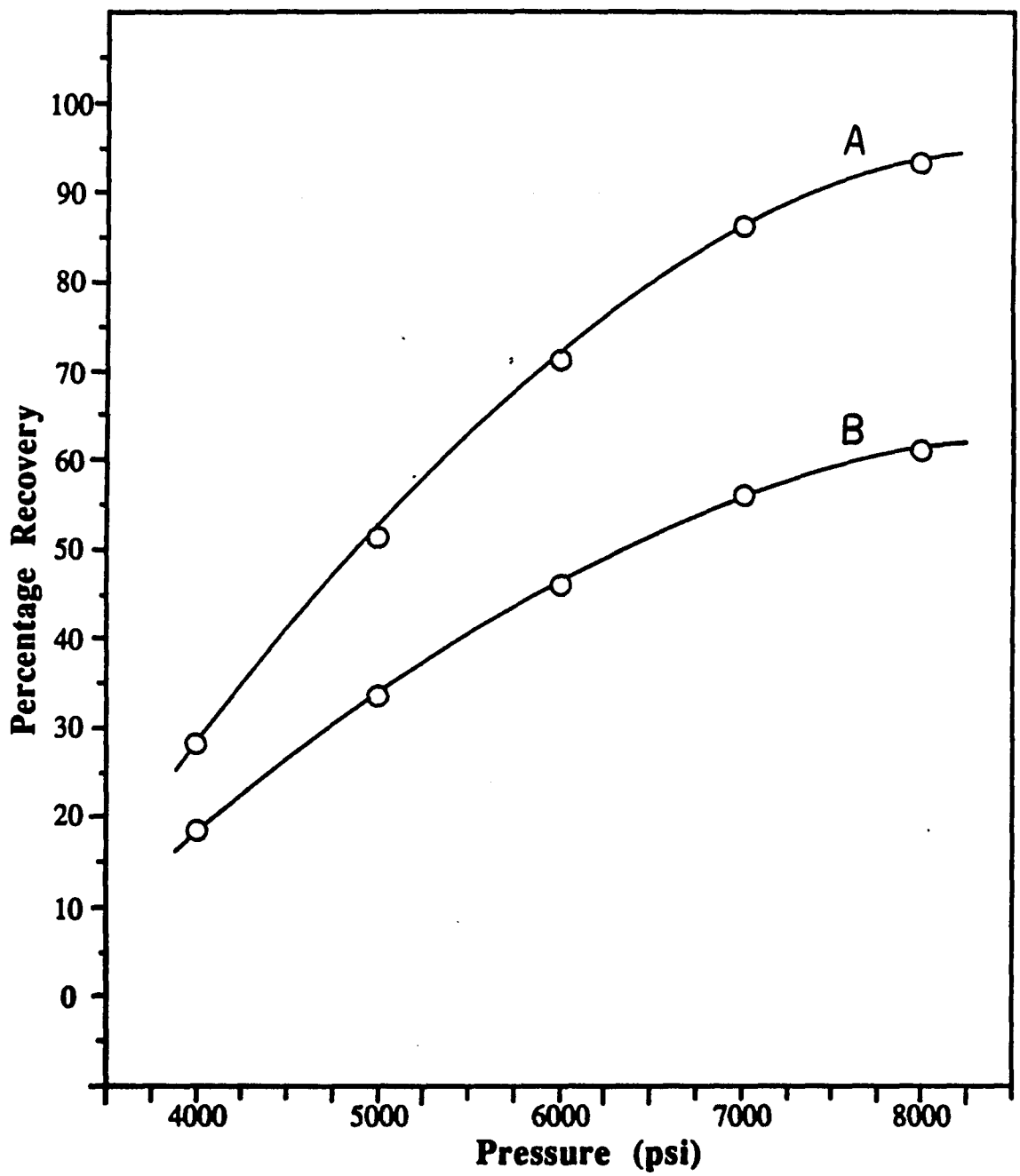

Figure 7. Effect of pressure on efficiency of SFE procedure for Diazepam using (A) CO_2 and (B) N_2O at 65^0 C for 20 min. At each pressure, one gram samples of Chromosorb W fortified with 100 µg of Diazepam were subjected to the outlined procedure. Chromatographic conditions: column, 150 x 3.9 mm I.D. µ-Bondapak C-18 (10 µm); mobile phase, acetonitrile-aq 0.05M phosphate buffer, pH 6.8 (60+40, v/v); flow rate, 2.0 mL/min; applied potential, -1.1 V *vs* SCE.

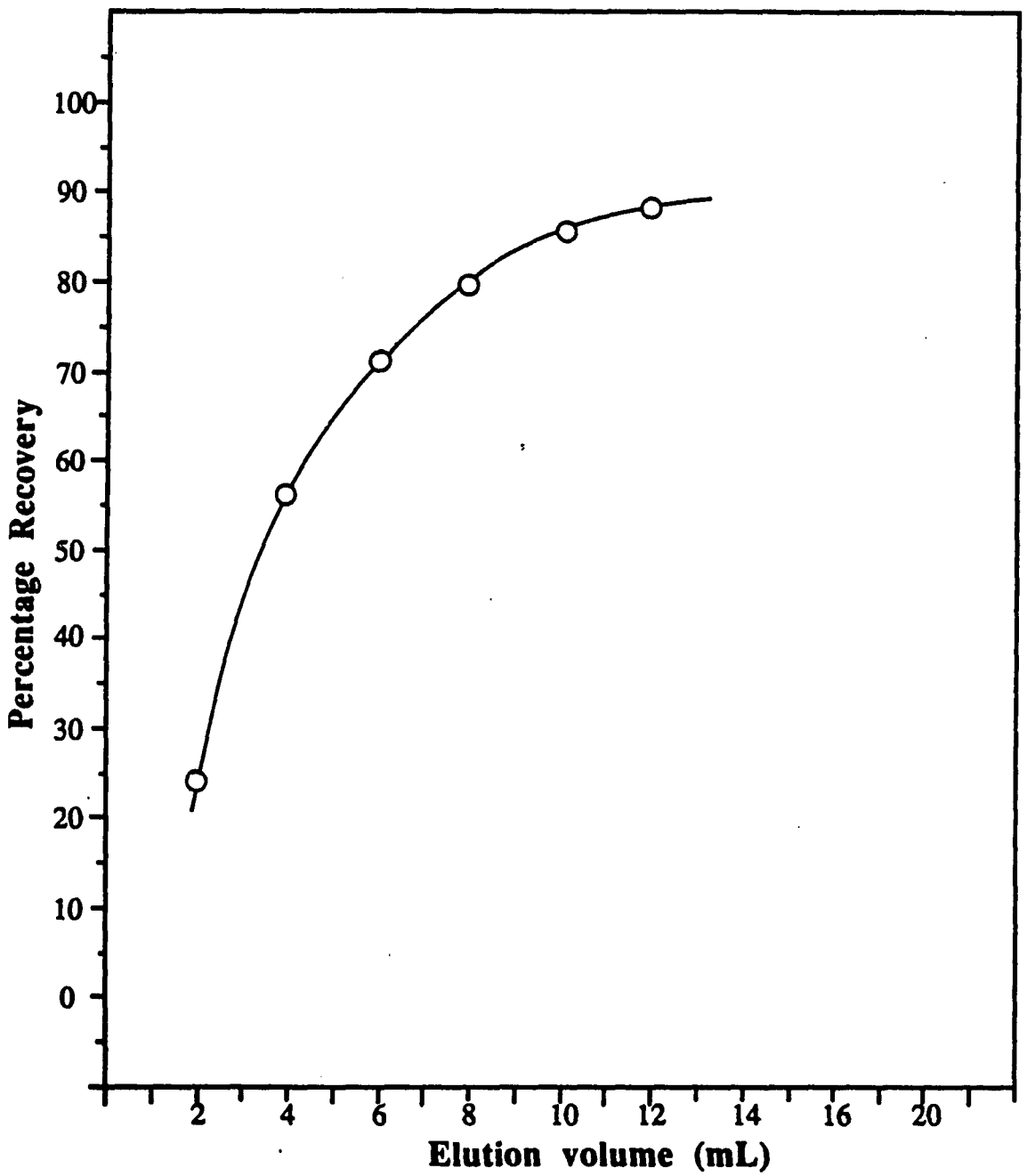

Figure 8. Recovery of Diazepam from C-18 cartridge as a function of eluent volume. Desorption conditions: eluent, methanol - acetonitrile (50+50, v/v). Sample size: cartridge spiked with 100 µg diazepam per gram of C-18 stationary phase. Chromatographic analysis conditions: column, 150 x 3.9 mm I.D. µ-Bondapak C-18 (10 µm); mobile phase, acetonitrile-aq 0.05M phosphate buffer (pH 6.8); flow rate, 2.0 mL/min; detector potential, -1.2 V vs SCE; current sensitivity, 100 nA/V.

Table 1. Recovery of Diazepam From Fortified C-18 Cartridges Using SFE approach described.

Sample No.	Fortification Level, µg/mL	Recovery, %
1	1000	91.3
2	500	92.6
3	100	94.1
4	50	93.0
5	10	88.2
6	5	93.4
7	1	90.7
8	0.5	81.9
Range	1000 - 0.5	81.9 - 94.1
Average		90.7
RSD (n=8)		4.4 %

SFE conditions: 8000 psi N_2O, 65^{0}C for 15 min.
C-18 trap, eluted with methanol-acetonitrile (50/50, v/v).

Influence of Matrix

The effect of matrix type on the efficiency of the described procedure was briefly investigated by spiking one gram samples of animal feed (Ralston-Purina Co., Type 5010-C) and C-18 (Corasil, Waters Assoc.) support with 500 μg of Diazepam prior to the SFE procedure. The recoveries were 92.3 % and 93.6 % from the feed and C-18 substrates, respectively. Based on these results and earlier studies (pg. 248), the efficiency of the described preparation and determination procedure is relatively independent of matrix interactions for the spiking levels studied. Figures 9 and 10 show chromatograms of the recovered Diazepam from C-18 and animal feed, respectively. It can be seen that resolution of Diazepam from excipients is satisfactory in both cases. The small peak eluting prior to Diazepam in the chromatogram obtained for the animal feed was presumably due to an unknown contaminant in the sample or system. No such peak was observed in other chromatograms from standards or samples taken through the entire procedure.

Application to Generic Formulations

Diazepam tablets available from 3 generic manufacturers were analyzed for drug content, content uniformity and reproducibility by the proposed method. Assay results for commercial 5.0 mg tablets are given in Table 2. As illustrated in Table 2, the method gave results that ranged from 94.7 to 103.9 % of the 5 mg value declared.

Content Uniformity

Results of individual tablets taken through the procedure are shown in Table 3. For the Durimed brand of 5 mg Diazepam tablets, individual tablets were found to contain on the average of 100.4 % of the 5.0 mg label claim in comparison to a composite assay of 101.6 %.

Reproducibility

The precision of the method was evaluated by performing 4 replicate analyses on a composite sample equivalent to 1/5 of one tablet. As shown in Table 4, the within-day coefficient of variation for Diazepam was 1.1 %. The between-day precision in the same range was 4.6 %.

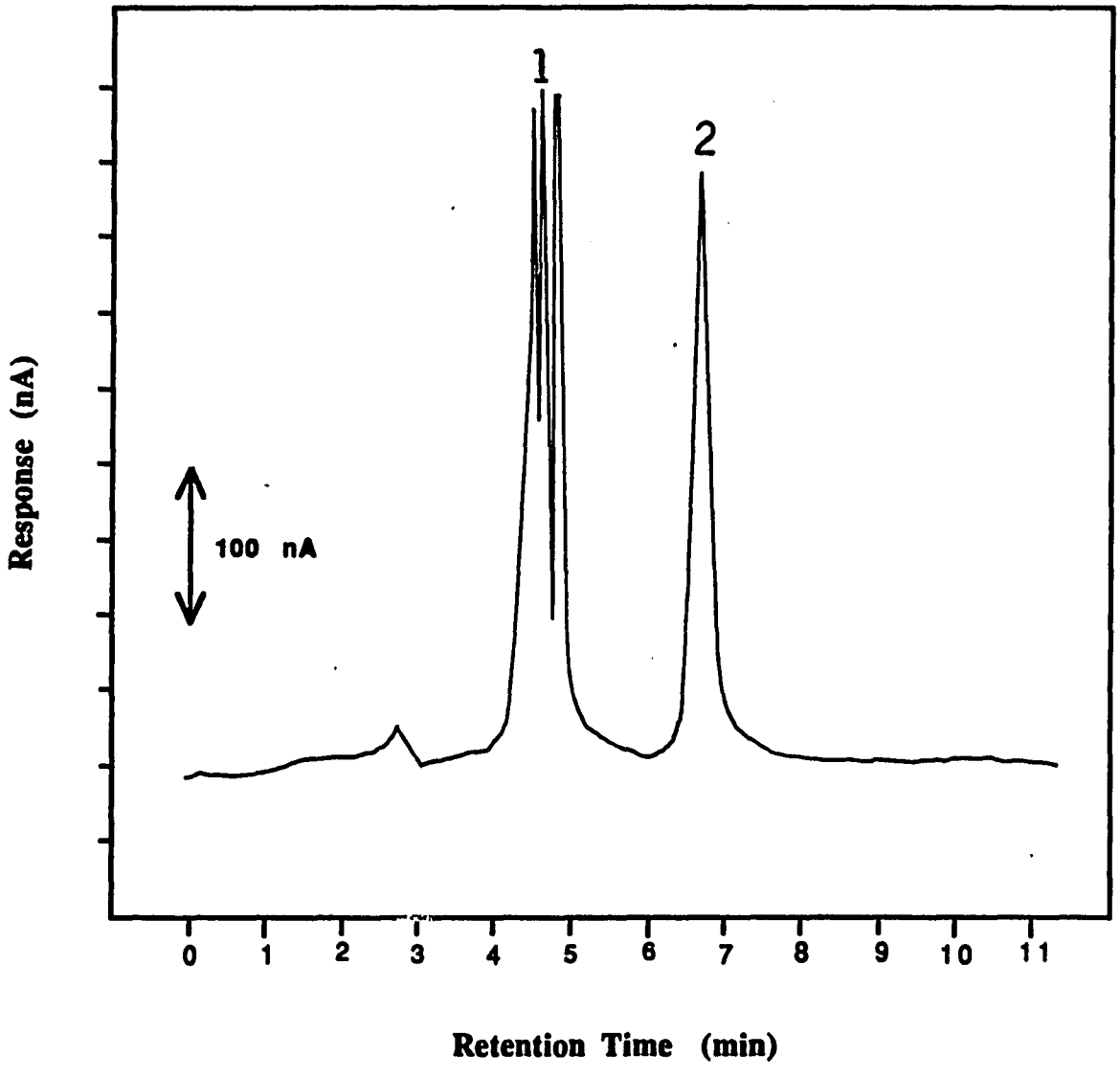

Figure 9. LCEC chromatogram of a supercritical fluid extract of Diazepam drug substance desorbed from C-18 stationary phase. Chromatographic conditions: column, 150 x 3.9 mm I.D. μ-Bondapak C-18 (10 μm); mobile phase, acetonitrile-aq 0.05 M phosphate buffer (pH 6.8); flow rate, 2.0 mL/min; detector potential, -1.2 V vs SCE; current sensitivity, 100 nA/V. Adsorbent cartridge spiked with 100 μg per gram of C-18 packing. Peak identities as follows: 1, impurities; 2, Diazepam.

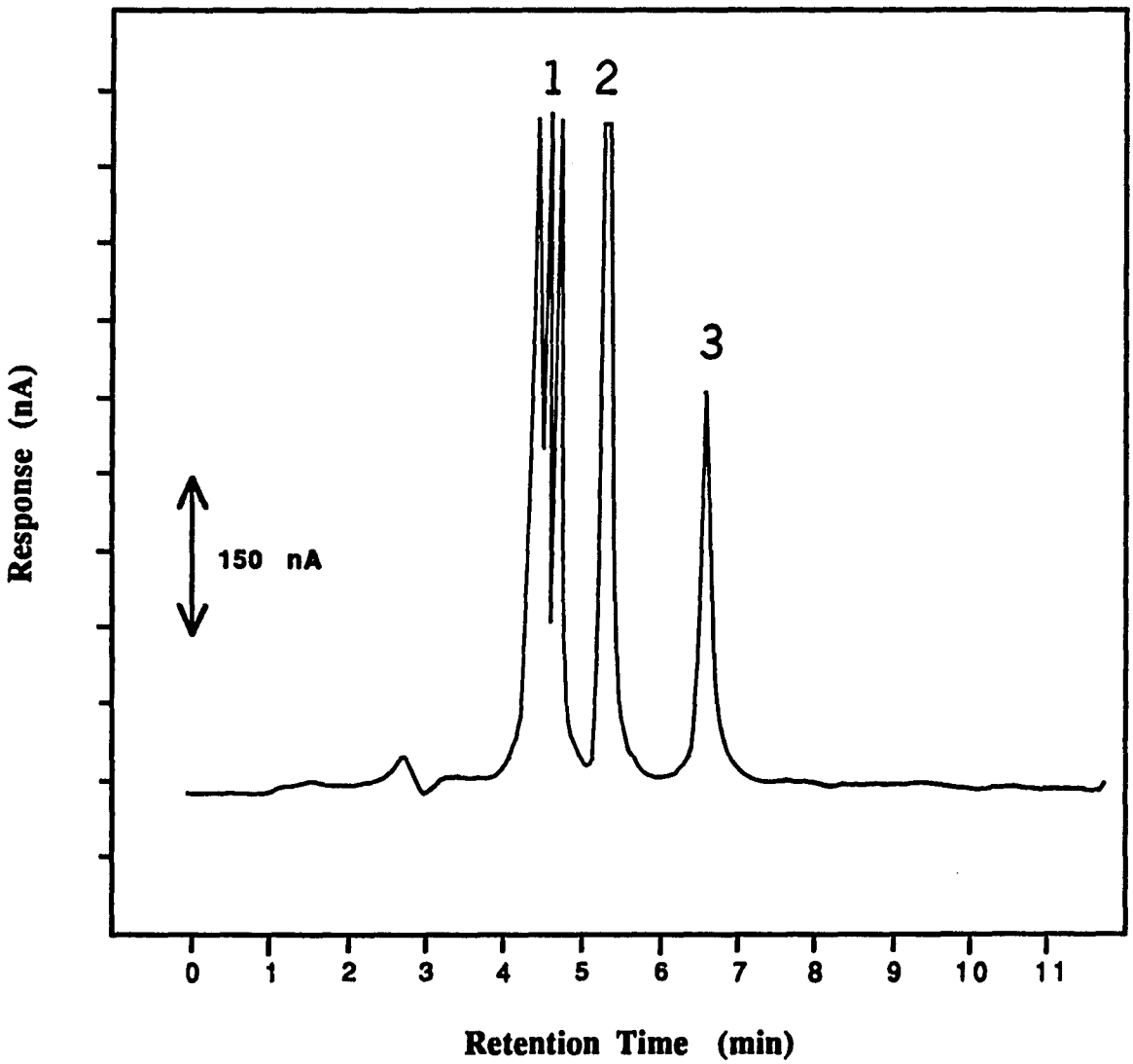

Figure 10. LCEC chromatogram of a supercritical fluid extract of a Diazepam spiked feed sample. Chromatographic conditions: column, 150 x 3.9 mm I.D. μ-Bondapak C-18 (10 μm); mobile phase, acetonitrile-aq 0.05M phosphate buffer (pH 6.8); flow rate, 2.0 mL/min; detector potential, -1.2 V vs SCE; current sensitivity, 100 nA/V. Feed sample spiked with 100 μg per gram of chow. Peak identities as follows: 1, impurities; 2, impurity; 3, Diazepam.

Table 2. Results of LC Analysis of Commercial 5 mg Diazepam Tablets following SFE Tablet Preparation.

	Found, Percentage of Declared		
Manufacturer	Run 1	Run 2	Average
Hoffmann-LaRoche	95.4	93.9	94.7
Durimed	105.1	102.6	103.9
Barr	93.4	96.6	95.0
Average			90.7
RSD (n=2)			5.2 %

SFE conditions: 8000 psi N_2O, 65^{0}C for 15 min.
C-18 trap, eluted with methanol-acetonitrile (50/50, v/v).
Diazepam determined by HPLC-ECD using following conditions: column, 150 mm x 3.9 I.D. mm μ-Bondapak C-18, mobile phase, acetonitrile-aq 0.05 M phosphate buffer, pH 6.8 (60+40, v/v); flow rate, 2.0 mL/min; applied potential, -1.1 V *vs* SCE.

Table 3. Content Uniformity Assay Results for the Durimed Brand of 5.0 mg Diazepam Tablets.

Tablet	Found, mg/Tablet	Found, % of declared
1	5.05	101.0
2	5.22	104.4
3	4.94	98.8
4	4.87	97.4
Average	5.02	100.4
RSD (n=4)		3 %

*Composite assay 5.08 mg (Average of duplicate assays on a composite sample of tablets from the same batch).

Table 4. Replicate Analyses of Diazepam Tablets by HPLC Following SFE Tablet Preparation.

Sample No.	Diazepam Found, mg	Percentage Claim*
1	5.08	101.6
2	5.14	102.8
3	5.05	101.0
4	5.15	103.0
Average	5.11	103.2
RSD (n=4)	1.1 %	

* Claim is 5.0 mg/Tablet of Diazepam.

SFE conditions: 8000 psi N_2O, 65^{0}C for 15 min.
C-18 trap, eluted with methanol-acetonitrile (50+50, v/v).

Diazepam determined by HPLC/ECD using following conditions: column, 150 mm x 3.9 I.D. mm μ-Bondapak C-18, mobile phase, acetonitrile-aq 0.05 M phosphate buffer, pH 6.8 (60+40, v/v); flow rate, 2.0 mL/min; applied potential, -1.1 V *vs* SCE.

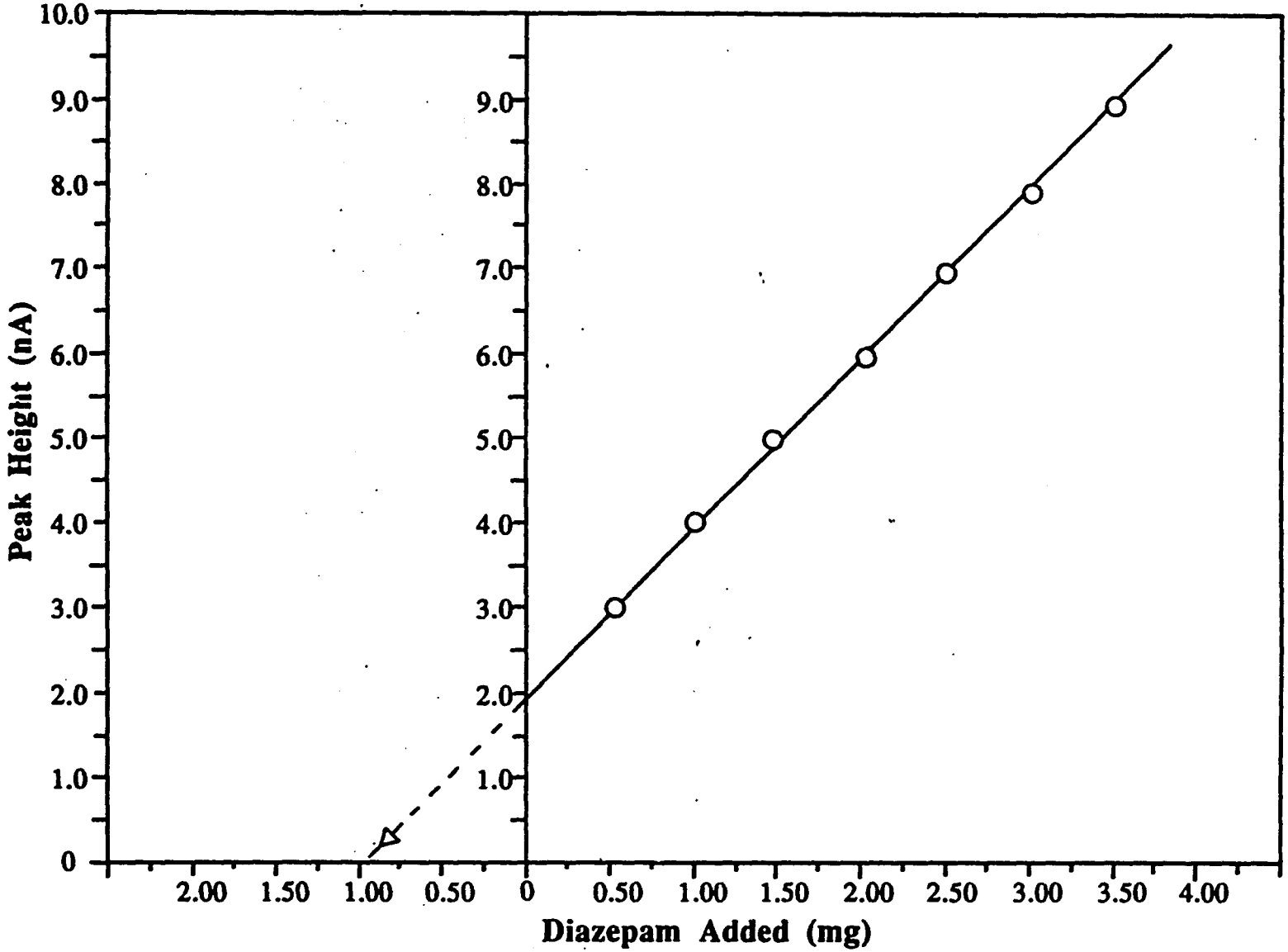

Figure 11. Standard addition curve used in the quantitation of Diazepam tablets. Chromatographic analysis conditions as in Figure 6. Each composite sample, equivalent to 1/5 label declaration, is spiked with standard Diazepam at increasing increments of 0.5 mg prior to SFE sample preparation.

Standard Addition

The performance of the proposed method for the quantitation of Diazepam formulations was further tested by standard additions of 1 to 4 mg of Diazepam in four equal intervals to a composite Diazepam sample. A typical standard addition curve for a composite sample containing 1/5 of a Diazepam tablet is shown in Figure 11. For this sample, the average Diazepam content was 5.07 mg and the recovery over this range was 98.4 %. On a single day, the relative standard deviation (RSD) for the spiked samples remained well below 2.5 % in a well equilibrated system.

Conclusions

A rapid, accurate, reproducible and relatively simple method for the determination of Diazepam tablets was developed. The method incorporates many desirable aspects of previously reported HPLC assays, but significantly reduces the complexity of the sample preparation step by eliminating many manipulation steps, including multiple extractions, transfers, and solvent evaporation. By using SFE as a quantitative sampling tool, Diazepam can be rapidly prepared for subsequent quantitation with an EC detector. A particularly attractive potential feature of this hyphenated procedure involves its utility with extremely complex matrices such as biological specimens.

Part III Chapter 8

Determination of 1-Nitropyrene in Diesel Particulate Emissions

Introduction

1-Nitropyrene (1-NP) is of interest both as a specific compound and as a member of an important class of compounds found in emissions from diesel engines. 1-NP and its isomers are reported to account for as much as 40% of the Ames assay mutagenic activity of diesel exhaust (1, 2). As one of the predominant nitroarenes in diesel emissions (3, 4), 1-NP serves as a marker for the class of nitro-aromatics in these samples. The complexity of diesel particulate matter renders difficult the identification and determination of any specific compound or even groups of compounds, especially those present at relatively low levels. Consequently, following solvent extraction of organics from diesel particulate matter, a cleanup step is required to isolate the nitroarene fraction. Various chromatographic methods have been applied to the determination of specific nitro-compounds in this fraction.

In recent work, the procedure for the extraction of 1-NP from diesel samples is usually a 8-24 hour Soxhlet extraction with methylene chloride; the somewhat faster ultrasonic extraction has also been used (5,6,7) but recovery of 1-NP from spiked diesel particulates was only 30% at the 1 ppm level and 80 % for 10 ppm (7); recovery data were not given by Robbat et al. (5) or Nelsen (6). Cleanup is commonly accomplished by using a silica column with a solvent gradient (8), or a Waters Sep-Pak (4,5,9,10). Nitrated polycyclic aromatic hydrocarbons (PAH) have been determined using gas chromatography (GC) with flame ionization (FID) (5,6,11-13), electron capture (4, 11), or thermoionic ionization detectors (NPD) (6,9,11,12,14). Campbell and Lee (15) chemically reduced the nitro groups to amino, formed pentafluoropropylamide derivatives, and determined these by capillary GC with electron capture, NPD, FID, and GC/mass spectrometry (MS). Nitrated PAHs in diesel exhaust have also been determined using GC with a chemiluminescence detector (Thermo Electron Analyzer), which is highly sensitive and selective (5,7,16). Detailed studies of nitro compounds extracted from diesel exhaust particulate matter have often used capillary GC with on-line MS (9,13,14,17-20), negative ion chemical ionization MS (11,17), high resolution MS (17,19), MS/MS (19,21), and MIKES (19) have also been used, as has GC/FTIR (17). Karasek et al. (13,18) have cautioned that 1-NP can partially decompose to 1-aminopyrene during GC/MS analysis, both on and after the column. They developed a compensation technique using deuterium-labelled 1-NP-d_9, enabling quantitative work to be done. High performance liquid chromatography (HPLC) has

also been applied to nitroarene determination in both normal and reversed phase modes. Silica columns (6), as well as a specially synthesized pyrene-butyric acid amide-bonded phase microbore column (22) have been used with UV detection. The latter column was used with a C_{18} reversed phase column with column switching to isolate and quantitate 1-NP. Post column conversion of nitro compounds to amino analogs followed by fluorescence detection (9,20) has also been used. Reductive mode electrochemical detection (ECD) of nitroarenes has been applied with glassy carbon electrodes (GCE) (10,23) and gold amalgam electrodes (20), following reversed-phase HPLC separation. The linear range of GCE is reported to be about 10^3, with a sensitivity of 10-100 pg (10). Hydrodynamic voltammograms (HDVs) can be an aid to qualitative identification of nitro compounds (10). The ECD is sensitive to quinones, and anthraquinone and 1,4-naphthoquinone which were detected in diesel exhaust particulate matter.

We have developed a rapid procedure for 1-NP based on the supercritical fluid extraction (SFE) of the compound followed by HPLC with a reductive mode ECD using a silver electrode. In this method, the extract, which is obtained in 20 min, is trapped by depressurization of the SCF CO_2 solvent across a short silica-packed tube, and eluted from that with a small volume of methylene chloride-acetone (50/50, v/v). The solvent is evaporated, the residue is taken up in the HPLC eluent, and the 1-NP is separated from other electrochemically reducible species on a C-18 column in 5.5 min prior to detection with a reductive mode electrochemical detector.

Experimental

Reagents

1-Nitropyrene (Gold label grade) was purchased from Aldrich Chemical Co., (Milwaukee, WI). HPLC grade acetonitrile, acetone, methylene were obtained from J. T. Baker (Phillipsburg, NJ). In-house glass distilled water was used throughout the study.

Apparatus

The HPLC chromatograph was built from components. A Varian 8500 syringe pump provided pulse free flow of eluents. Samples were injected with a Rheodyne 7125 sampling valve. Sample solutions were placed in a 4 mL Reacti-Vial, degassed with a stream of helium or nitrogen, and pneumetically flushed through the 20-µL

sample loop to avoid any exposure to air. Oxygen is detected by reductive mode ECD at voltages more negative than -0.2 V vs SCE. The column was a 150 mm x 3.9 mm I.D. 10 μm μ-Bondapak C-18, (Waters Associates, Milford, MA). The mobile phase conditions, 60/40 (v/v) acetonitrile/0.025 M aq. $NaClO_4$ at 2 mL per min, were established experimentally to separate the 1-NP peak cleanly from the other peaks detected, and to minimize analysis time. Eluent was degassed by rapid bubbling of He or N_2 through a porous steel diffuser for 15 min. ECD detection was accomplished with a laboratory constructed silver based thin-layer cell (pp. 16-18).

GC/MS

GC peak identities were confirmed using a Hewlett-Packard Model 5988A GC/ quadrupole MS with Hewlett-Packard 1000 data system. A 30 m x 0.25 mm I.D. bonded phase fused silica capillary column, J & W DB-5 (J &W Scientific, Folsom, CA) was used. An initial, 5 min temperature of 150^0C was followed by a 100^0C/min temperature program to 280^0C, with a 40 min final hold at 280^0C.

Procedure

About 100 mg, accurately weighed, of diesel samples (NBS, SRM 1650) were loaded into a 6 in. x 3/8 in. extraction chamber and held in place with glass wool plugs. The extraction chamber was assembled into the extraction manifold (pp. 124-125), brought to system temperature, and the system flushed for a minute with low pressure CO_2. The exit valve was then closed and the system pressurized to the extraction pressure. After a 15 or 20 min equilibration, the exit valve was carefully and partially opened to allow the extract to be collected. The depressurization occurs across a 6 in. x 1/8 in. O.D. ss tube packed with silica gel attached directly to the exit valve. The solubility of the extract in sub-critical pressure CO_2 is essentially zero; the silica acts probably as much as a physical filter as an adsorbent. The silica was removed and washed with methylene chloride-acetone (50/50, v/v); the extraction chamber and exit valve were rinsed with the same. The combined volume of eluate and rinsings was 30 mL. The solution was evaporated nearly to dryness in a rotary evaporator and remaining solvent evaporated in a stream of N_2. The residue was taken up in 10 mL mobile phase for HPLC. For GC and GC/MS, 2-μL aliquots were removed from the rotary evaporator flask before final evaporation.

RESULTS AND DISCUSSION

Response of electrochemical detector to 1-Nitropyrene (1-NP)

In order to optimize the sensitivity of the electrochemical detector towards 1-nitropyrene, the current obtained from 20-μL injections of a 77 μg/mL stock standard injected into the flowing mobile phase was measured as a function of a stepwise change in applied potential. Figure 1 shows the resulting hydrodynamic voltammogram (HDV). From this curve, the plateau voltage of -1.1 V vs SCE was selected for HPLC quantitation. Furthermore, the ($E_{3/4}$-$E_{1/4}$) value, 130 mV, indicates the 2-electron reduction is irreversible (24).

The linearity of the LCEC system was assessed from 6 injections of 1-NP over the range of 38 ng/mL - 0.4 mg/mL. A log-log plot of the detector response as a function of amount injected is illustrated in Figure 2. The response is linear to at least 7.6 μg 1-NP injected, i.e. over at least a range of 4 x 10^4; the upper bound is limited by solubility of 1-NP in the partially aqueous mobile phase. A least squares treatment of these data yielded an equation of y (nA) = 1.43x (nA/ng) + 0.016 with a correlation coefficient of 0.993. The detection limit, defined as that weight of 1-NP producing a peak height 3 times the noise level, is 197 pg for a detector noise level of 75 pA.

Extraction Efficiency

In order to establish the optimum conditions of extraction for 1-NP, a 2.5 g sample of 100/120 mesh Chromsorb W was spiked with 2 μg of 1-NP and extracted at four pressures in the range of 5000 to 8000 psi at both 45^{0}C and 65^{0}C for 20 min. The influence of pressure on percentage recovery at 45^{0}C and 65^{0}C is shown in Figure 3. As can be seen, recoveries increase with increase in pressure at both temperatures but the effect is more pronounced at 65^{0}C. Figure 4 shows that percentage recovery of 1-NP reaches the maximum level within 20 min, after which no significant changes in percentage recoveries were observed. For all further work, extractions were performed at 8000 psi and 65^{0}C for a period of 20 min. To test the efficacy of these conditions, supercritical fluid extractions were carried out on four samples of Chromosorb W spiked at four different concentration levels. The results are summarized in Table 1. Under these conditions, the average percentage recovery was 94 % ± 3.3 % (n=3).

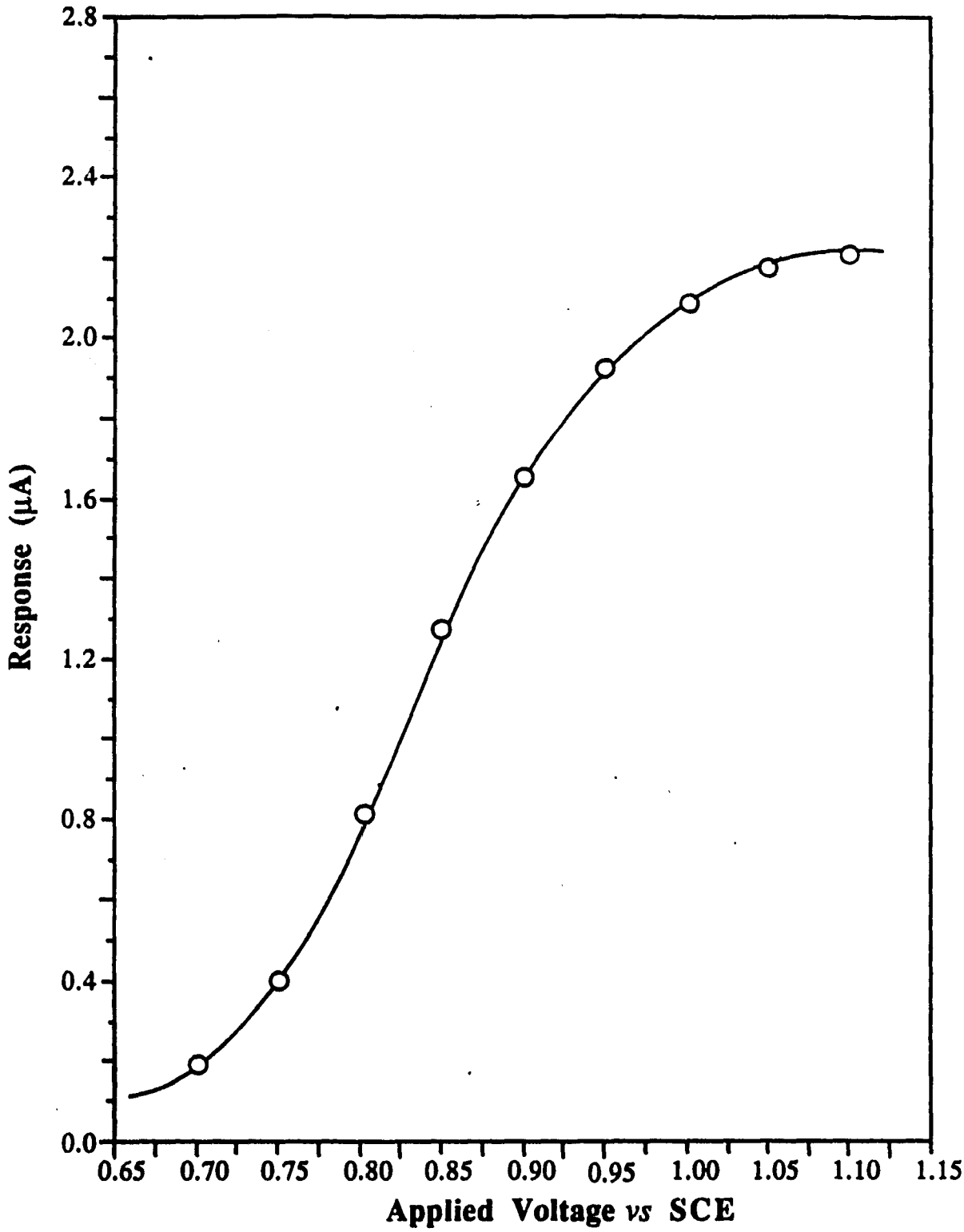

Figure 1. Hydrodynamic voltammogram of 1-nitropyrene on silver electrode vs. SCE. Chromatographic conditions: column, 150 x 3.9 mm I.D. μ-Bondapak C-18 (10 μm); mobile phase composition, 60/40 (v/v) acetonitrile-aqueous .025 M $NaClO_4$; flow rate, 2.0 mL/min; sample size, 1.54 μg 1-nitropyrene per 20 μl mobile phase injected at each potential setting.

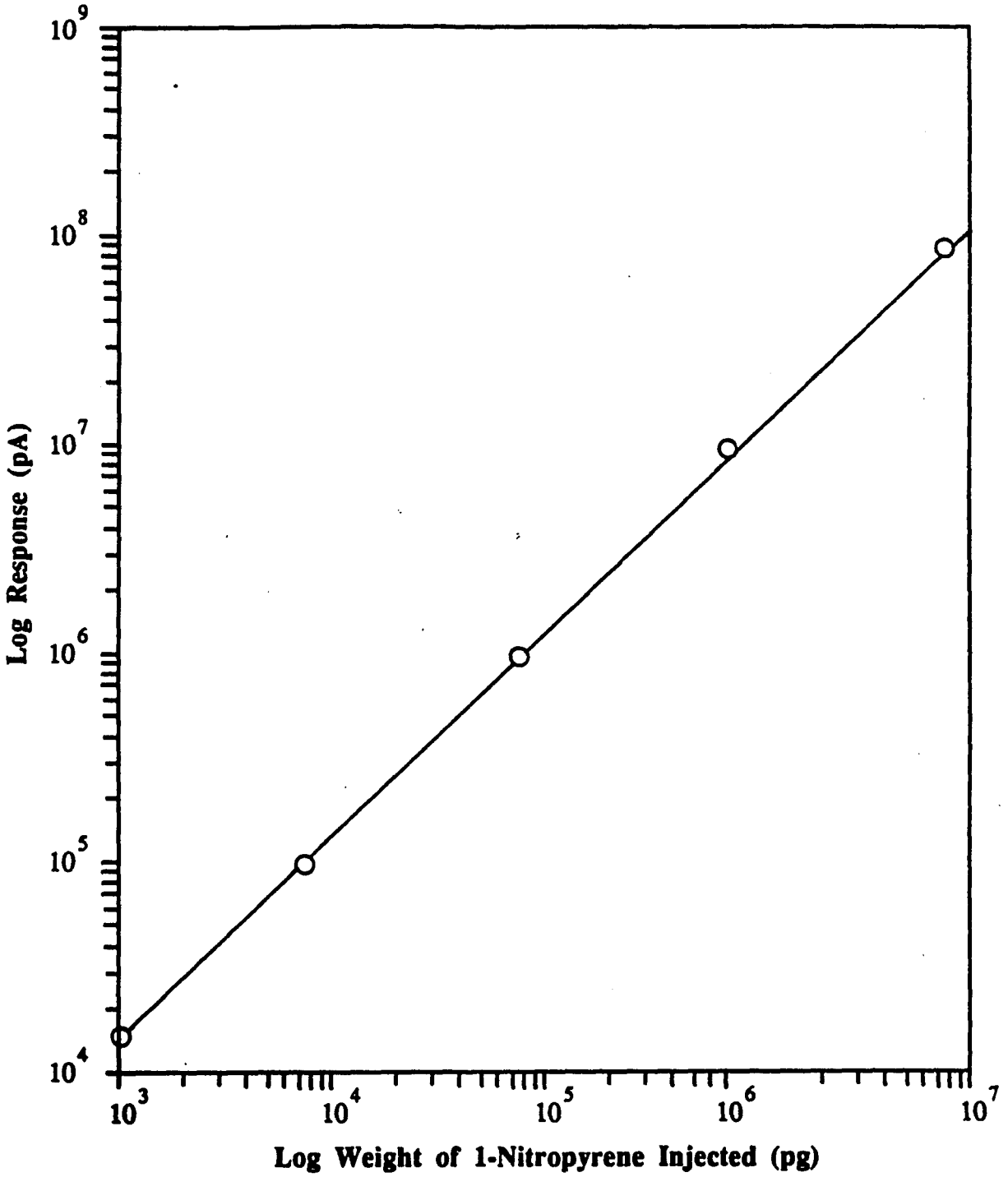

Figure 2. Detector response toward 1-nitropyrene. Chromatographic conditions: column, 150 x 3.9 mm I.D. μ-Bondapak C-18 (10 μm); mobile phase composition, 60/40 (v/v) acetonitrile-aqueous 0.025 M $NaClO_4$; flow rate, 2.0 mL/min; applied potential, -1.1 V *vs* SCE.

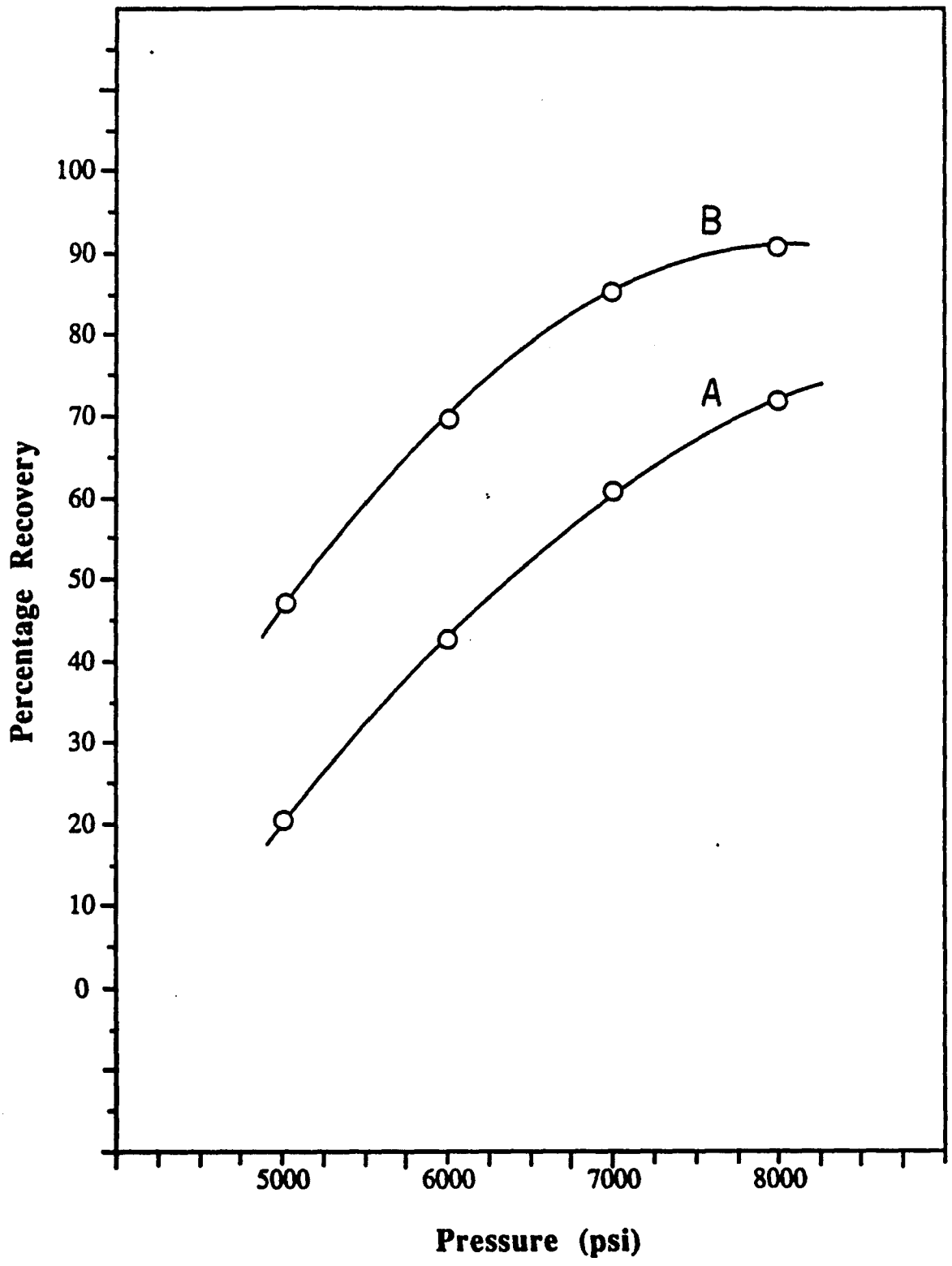

Figure 3. Influence of pressure on efficiency of extraction procedure for 1-nitropyrene at (A) 45^{0}C and (B) 65^{0}C. An equilibration period of 20 min used for each extraction. HPLC analysis conditions as in Figure 1.

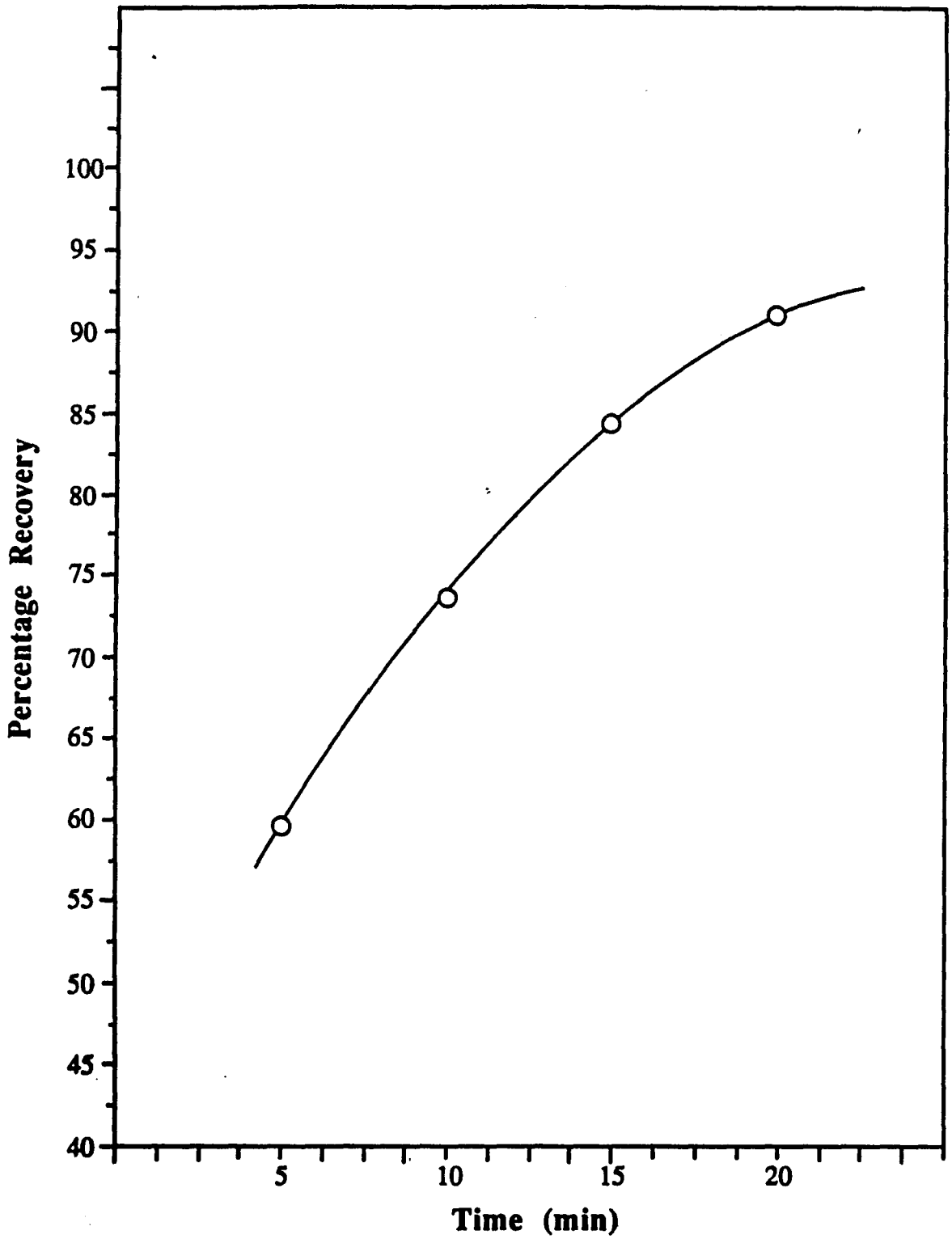

Figure 4. Effect of equilibration time on recovery of 1-nitropyrene. Pressure and temperature for each extraction maintained at 8000 psi and 65°C, respectively. HPLC analysis conditions as in Figure 1.

Table 1. Recovery of 1-Nitropyrene (1-NP) from Chromosorb W.

Spiking Level, μg/g	Recovery ± RSD, % [1]
75	96.0 ± 2.5
50	94.5 ± 2.8
25	95.0 ± 3.3
1	91.0 ± 4.5
Average	93.6 ± 3.3

[1] Based on triplicate determinations at each level.

[2] SFE conditions: 8000 psi CO_2, 65°C for 20 min. Silica trap, eluted with methylene chloride-acetone (50+50, v/v).

[3] 1-Nitropyrene determined by HPLC/ECD using following conditions: column, 150 x 3.9 mm I.D. μ-Bondapak C-18; mobile phase, acetonitrile-0.025 M aq $NaClO_4$ (60+40, v/v); flow rate, 2 mL/min; silver applied potential, -1.1 vs SCE.

Application to diesel samples

To test the overall method, we analyzed the NBS SRM 1650 for 1-NP using the extraction and determination method described in the experimental section. A typical chromatogram of an extract obtained by SCFE is shown in Figure 5. Quantitation of the 1-NP peak in Figure 5 was carried out by comparison of the peak height with a linear calibration plot obtained by injecting standard solutions of 1-NP dissolved in mobile phase into the LC. Our result based on HPLC-ECD is 19.9 μg 1-NP/g of the diesel particulate sample, in excellent agreement with the NBS certified value, 19 ± 2 μg/g. Quantitation by GC/MS was not attemped because of the thermal breakdown problems noted by Karasek et al. (13,18). The deuterated standard was not available to us.

Confirmation of the identity was carried out in several ways. First, the HPLC peak was collected and analyzed by GC/MS in the selected ion monitoring mode (SIMS) at m/z=247 (molecular ion, M), 217 (M-NO), 201 (M-NO_2), and 189 (M-CNO_2) (19). The GC retention time matched that of pure 1-NP, and the distribution of the ions monitored was similar to those in the mass spectrum of the known 1-NP peak.

Second, the SRM 1650 was spiked with 1 μg/g of 1-NP, extracted with supercritical fluid carbon dioxide, and the extract analyzed. A typical chromatogram of an extract of a spiked diesel sample is shown in Figure 6. The LC peak retained its original width and increased in height. The GC/MS in SIMS mode found a peak at the retention time of 1-NP in higher intensity and with the same ion distribution as the unspiked sample.

The third method involved step-wise SFE at two different pressures. This is one of the advantages of SCFE, ability to use SFE at one pressure as clean-up step and at a second pressure to extract the compound of interest. The results are given Figures 7A and B. The lower pressure SFE of the SRM 1650 sample at 5000 psi, 65^{0}C, and 20 min produced an extract with a GC-total mass spectral ion current (TIC) chromatogram shown in Figure 7A. A clean silica trap was installed and the extraction pressure raised to 8000 psi and held for 20 min at 65^{0}C. The resulting GC/TIC chromatogram is shown in Figure 7B. The paraffin hump seen in Figure 7A, characteristic of oil-derived samples, has been completely removed in the chromatogram of the high pressure extract. It should be emphasized that no clean-up procedure has been used except the two pressure level SFE; the chromatograms are of the total extract

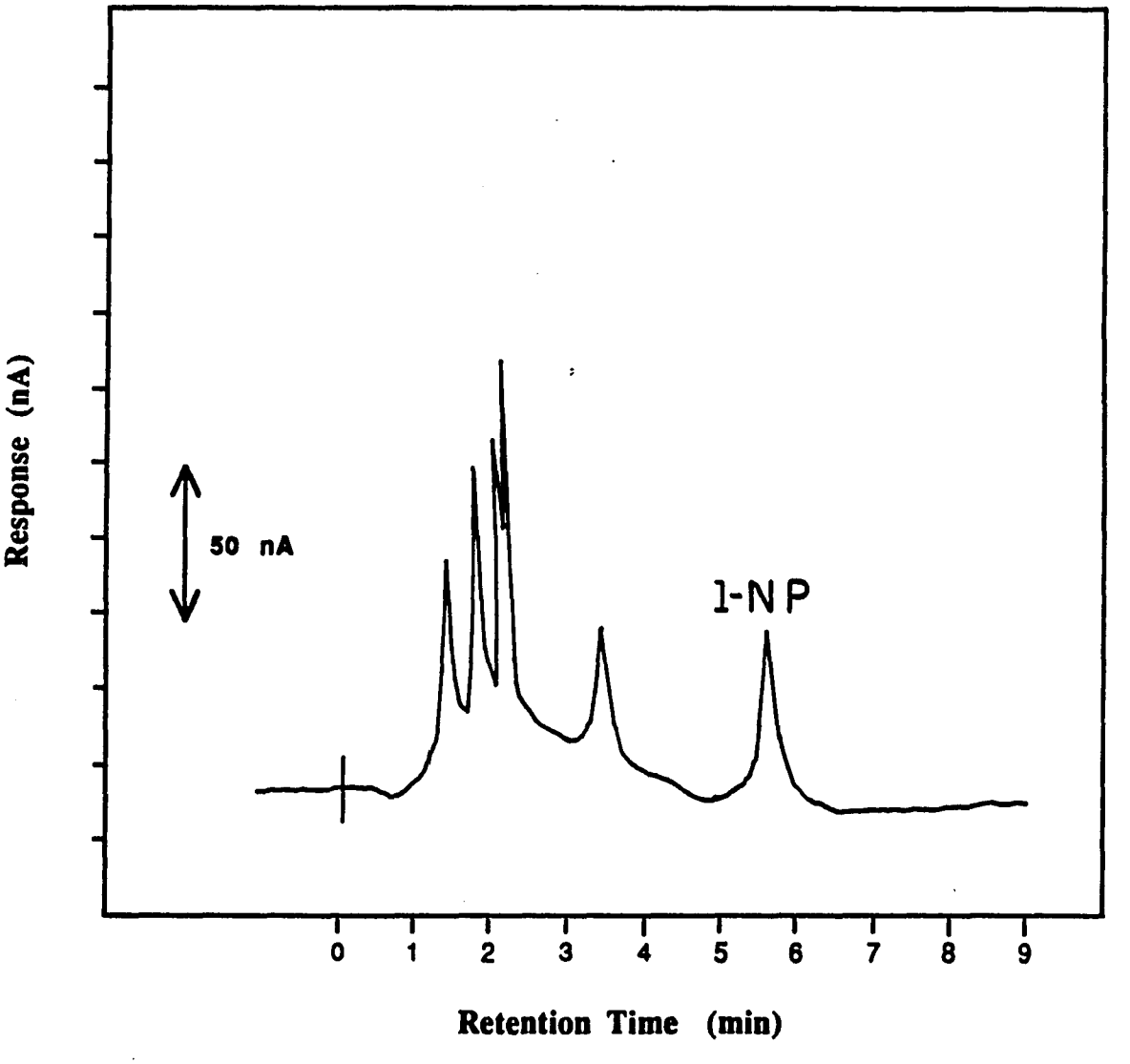

Figure 5. LCEC chromatogram of a high pressure supercritical fluid extract of NBS SRM 1650 on a 150 x 3.9 I.D. mm μ-Bondapak column using a mobile phase comprised of 60/40 (v/v) acetonitrile / 0.025 M aq $NaClO_4$ at a flow rate of 2.0 mL/min. Extraction conditions: SFE with 8000 psi CO_2, 65^0C, 20 min.

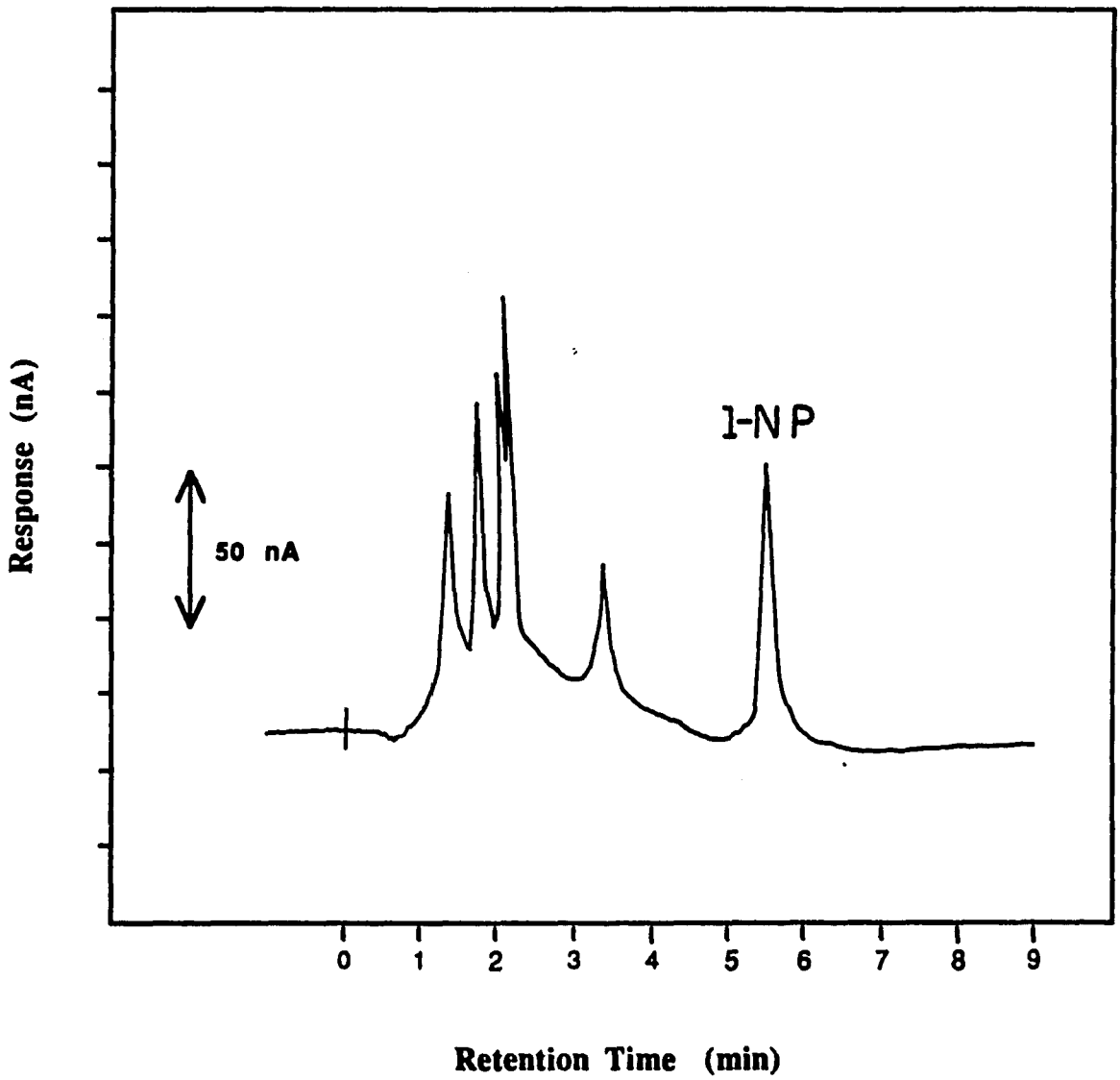

Figure 6. LCEC chromatogram of a high pressure supercritical fluid extract of NBS SRM 1650 fortified with 1.15 μg of 1-nitropyrene prior to sample preparation and chromatographic analysis. Chromatographic analysis conditions: column, 150 x 3.9 I.D. mm μ-Bondapak (10 μm); mobile phase, acetonitrile-0.025 M aq $NaClO_4$(60+40, v/v); flow rate, 2.0 mL/min. Extraction conditions: SFE with 8000 psi CO_2, 65^0 C, 20 min.

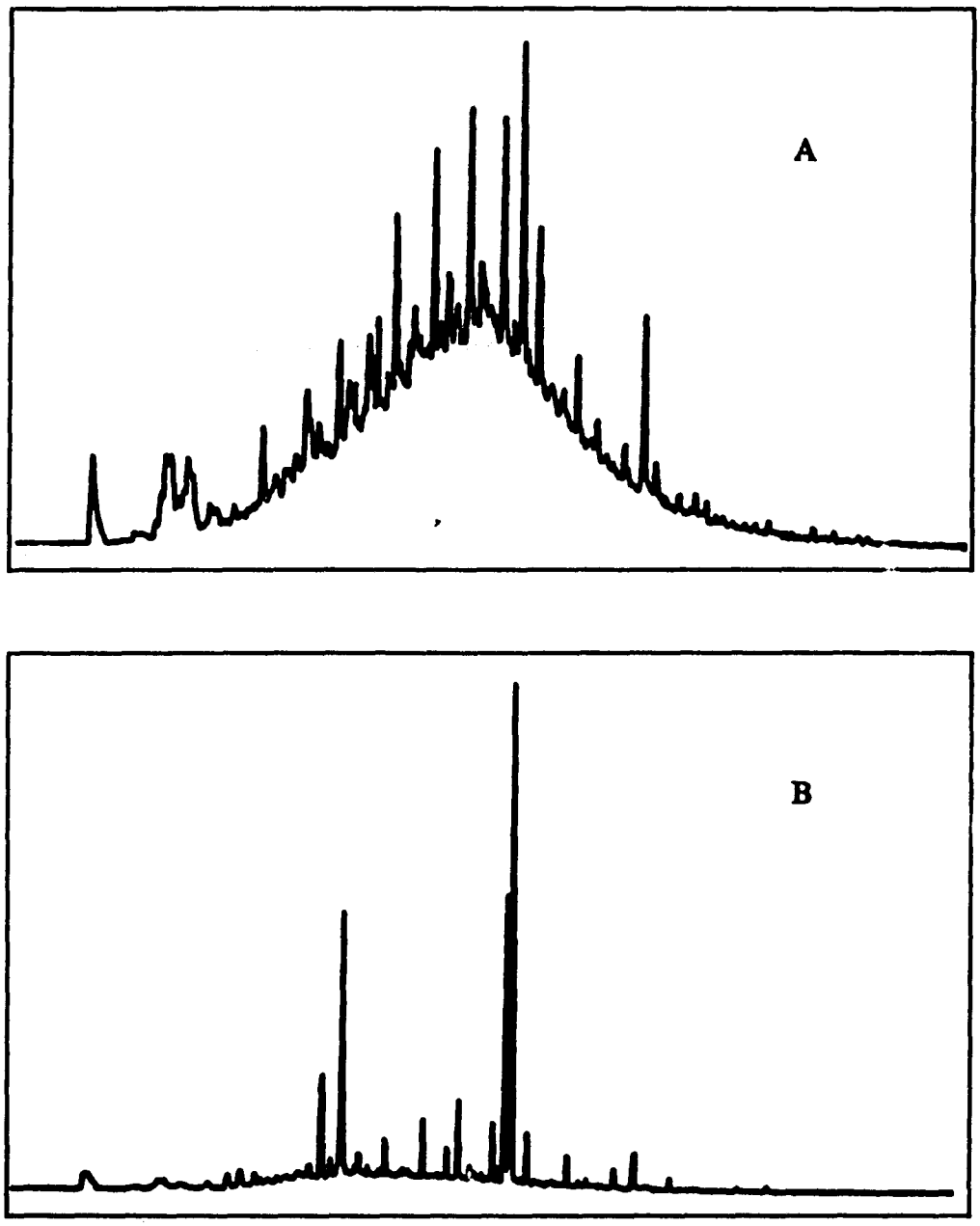

Figure 7. GC/MS total ion chromatograms of (A) low pressure and (B) high pressure supercritical fluid extracts of NBS SRM 1650. SFE at 5000 psi and 8000 psi for low and high pressure extracts, respectively. A temperature of 60^{0}C and an equilibration time of 20 min used in both extractions. GC conditions: 30 m x 0.025 mm I.D. DB-5 fused-silica capillary column; temperature, 150^{0}C for 2 min, then temperature programmed at 10^{0}C/min to 250^{0}C; Carrier gas, He, 1 mL/min.

obtained in each case. SIMS was employed to confirm the presence of 1-NP in each extract. In Figures 8 and 9 are the SIMS results at the four ions characteristic of 1-NP; it is clear that no 1-NP is extracted at 5000 psi. However, the compound is clearly present in the 8000 psi extract. Identification of the other peaks in Figure 9 has not been made; the peak just preceding 1-NP could be an isomer of 1-NP. A clean-up procedure will be required to characterize the nitro-and oxy-PAHs other than 1-NP in present in the sample extract.

The HPLC/ECD analysis of the high and low-pressure SFEs further substantiates the presence of 1-NP in the higher pressure and absence in the lower pressure extracts. The lower (C) and middle (B) chromatograms in Figure 10 are the HPLC/ECDs at -1.1 V vs SCE of the lower pressure and higher pressure extracts, respectively. No electroactive compound whatsoever is observed in low pressure extract. The early-eluting peak in the higher pressure extract may be a quinone. The short retention time is consistent with the compound's being polar; nitro compounds elute later, e.g. 1-NP. Earlier SCFE work (pp. 133-135) has shown that recoveries of quinones are low at 5000 psi but essentially quantitative at 8000 psi. The upper chromatogram in Figure 10, of the higher pressure extract run with the ECD Ag electrode potential set at -0.5 V vs SCE, has only a single peak. The 1-NP peak disappeared, because the foot of its HDV occurs at about -0.65 V. The compound is not 9-fluorenone, another compound certified by the NBS in SRM 1650; the HDV for 9-fluorenone has a foot at -1.1V (pg. 77), and so would not be detected at -0.5 V. 9-Fluorenone is, however, tentatively identified by the coincidence of GC retention times of a peak in the extract and that of a standard. The mass spectrum intensity is too low to allow reliable identification.

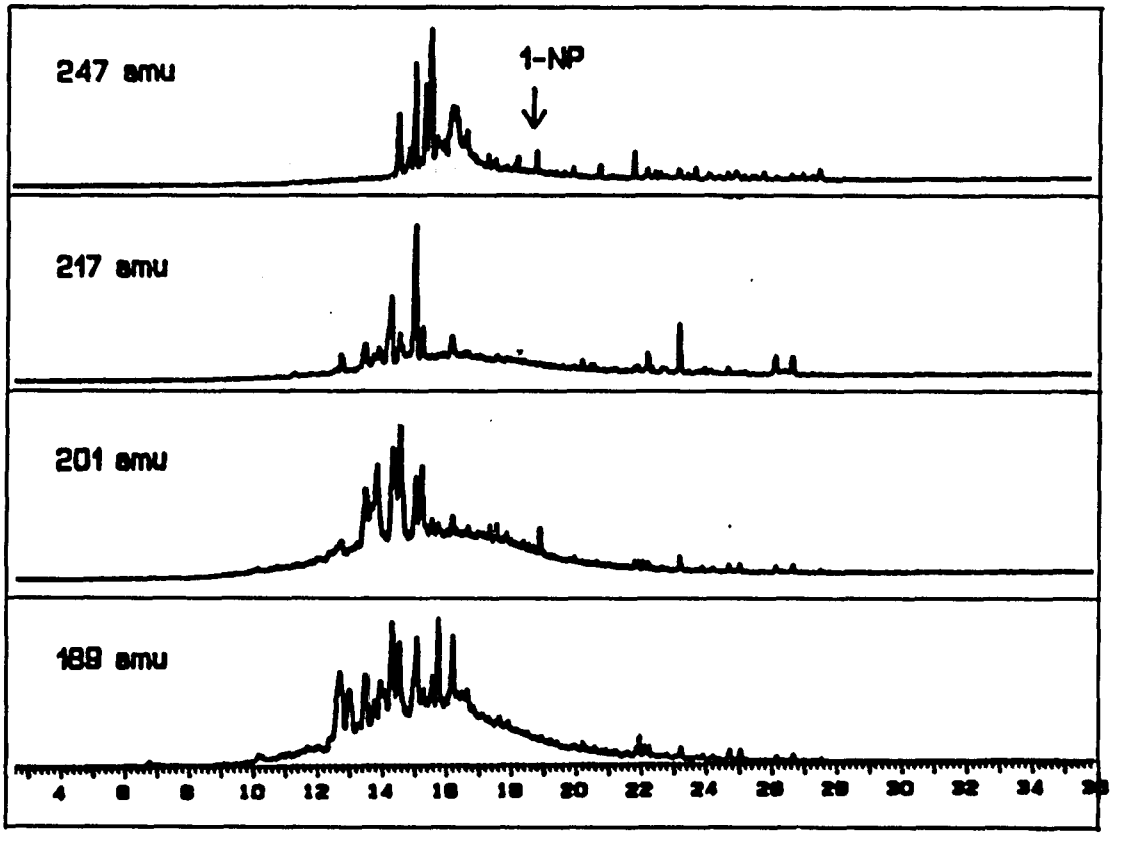

Figure 8. SIMS chromatograms of lower pressure supercritical fluid extract of NBS SRM 1650. SFE at 5000 psi, 60^{0}C, 20 min. GC conditions: 30 m x 0.025 mm I.D. DB-5 fused-silica capillary column; temperature, 150^{0}C for 2 min, then temperature programmed at 10^{0}C/min to 250^{0}C; Carrier gas, He, 1 mL/min. The arrow indicates the retention time of 1-nitropyrene (1-NP).

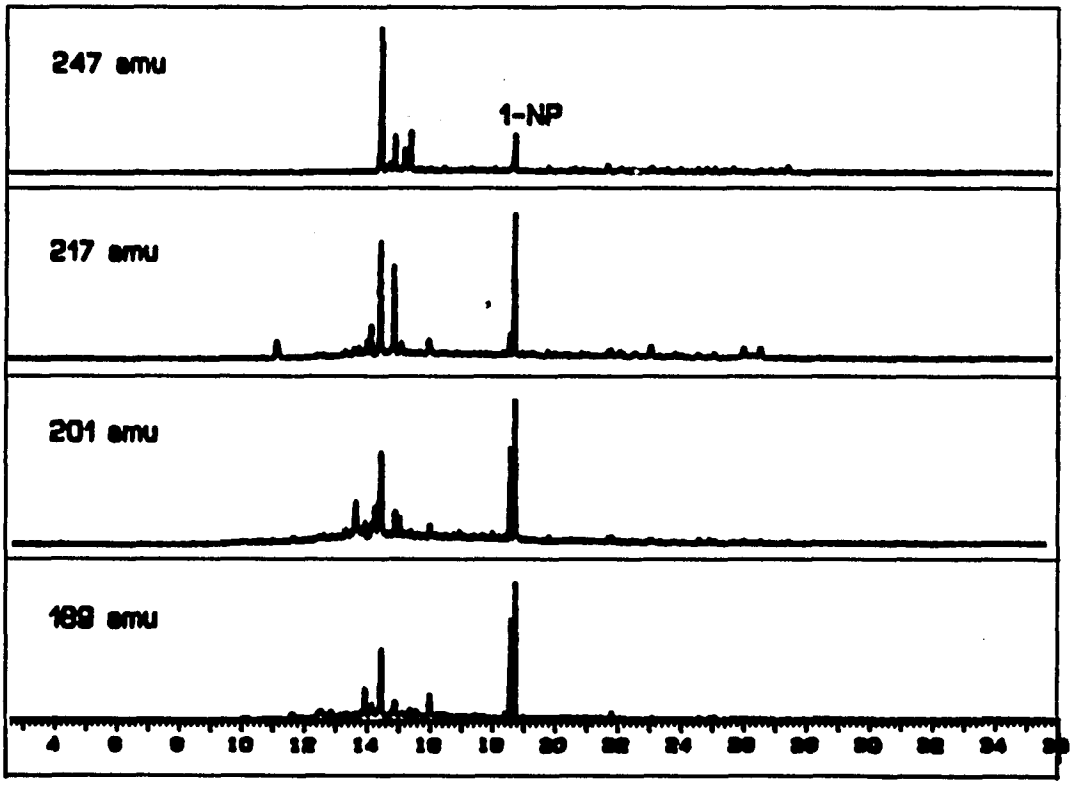

Figure 9. SIMS chromatograms of higher pressure supercritical fluid extract of two-step SFE of NBS SRM 1650. SFE at 5000 psi, 60^{0}C, 20 min. GC conditions: 30 m x 0.025 mm I.D. DB-5 fused-silica capillary column; temperature, 150^{0}C for 2 min, then temperature programmed at 10^{0}C/min to 250^{0}C; Carrier gas, He, 1 mL/min. The arrow indicates the retention time of 1-nitropyrene (1-NP).

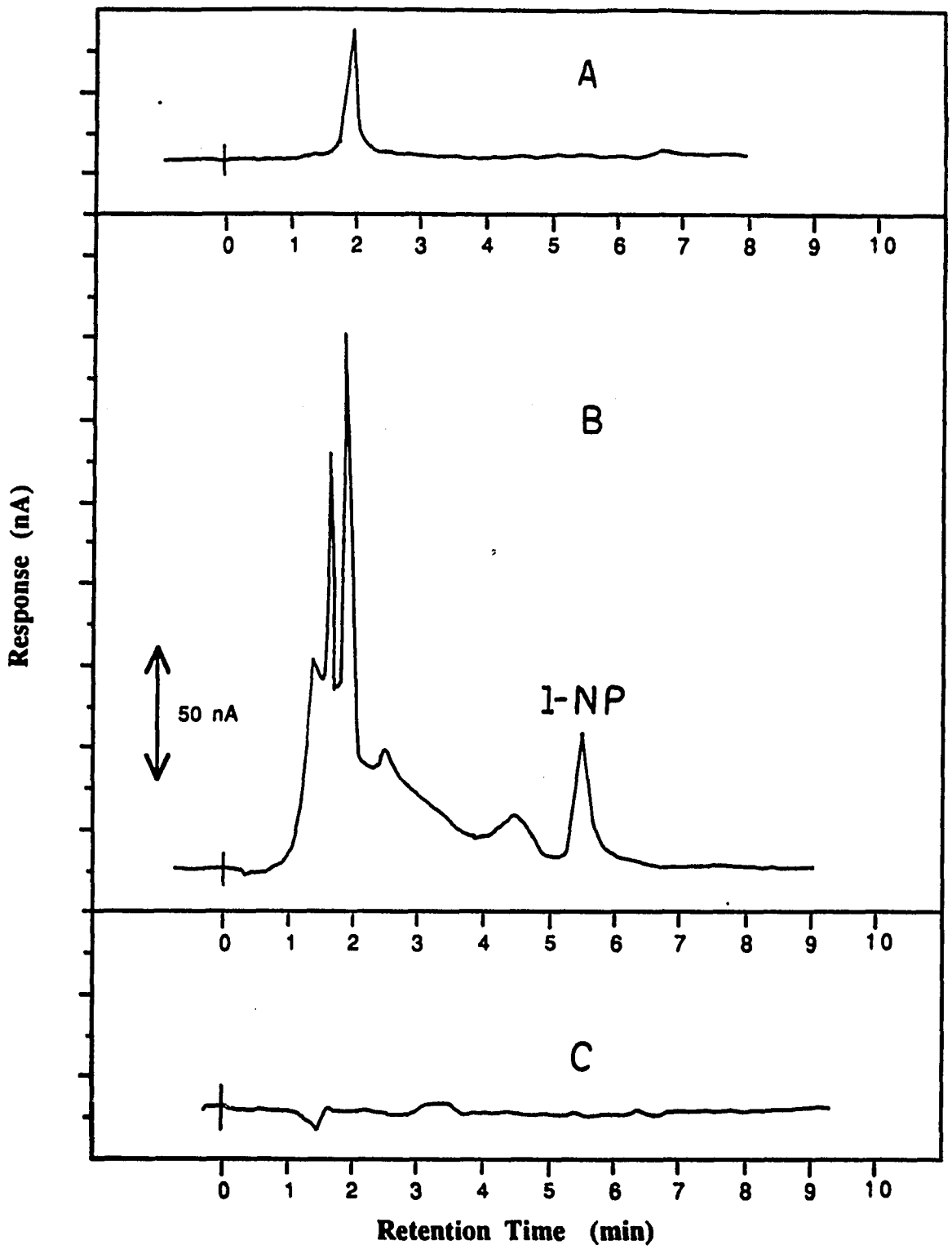

Figure 10. Chromatograms of various supercritical fluid extracts obtained by changing the pressure used in the extraction or the potential used in the detection. A. HPLC/ECD of 8000 psi extract of two-step SCFE of NBS SRM 1650. Ag electrode potential, -0.5 V vs. calomel. B. HPLC/ECD of 8000 psi extract of two-step SCFE. Ag electrode potential, -1.1 V vs. calomel. C. HPLC/ECD of 5000 psi extract of two-step SCFE procedure. Ag electrode potential, -1.1 V vs. calomel.

Conclusions

Preliminary results suggest that analytical scale extraction with supercritical carbon dioxide can provide quantitative as well as qualitative information about a complex matrix such as diesel exhaust particulate matter. Carbon dioxide at 8000 psi and 65^{0}C can be used as a sample preparation tool to quantitatively extract 1-nitropyrene (1-NP) from particulate diesel emissions within 20 min. Excellent quantitative agreement is obtained between the results of this method and the National Bureau of Standards-certified value for 1-NP in Standard Reference Material 1650. Furthermore, the outlined extraction procedure was also performed in a stepwise configuration by adjusting the pressure to fractionate the complex sample on the basis of molecular dimensions and thereby provide an extract more suitable for gas chromatography/mass spectrometry. Used in this way, a pre-extraction performed at 5000 psi removes most of the extraneous PAH interferences and simplifies the interpretation of the total ion chromatogram of a subsequent extract obtained at 8000 psi.

The electrochemical detector provides high sensitivity (i.e. minimum detectable quantity (signal/noise=3) of 1-NP is 200 pg, and response is linear over at least 4 orders of magnitude), and good selectivity (solvent front peaks only) and, in tandem with LC analysis, provides a rapid method for the quantitation of 1-NP without derivatization, without preconcentration or further sample clean-up.

Part III Chapter 9

Determination of Parathion Residues in Foodstuffs of High Fat-Content

Introduction

Organophosphate pesticides such as parathion are frequently applied as protectants to stored commodities such as cereals, legumes, and oil seeds (1). Since the decay of parathion is dependent upon temperature, relative humidity, and time (2), there is a need to ascertain that on the one hand the commodity is not consumed when residue level is still high and, on the other, that the risk of infestation by insects is not overly increased when the level becomes too low.

The main problem encountered in the analytical determination of parathion in such commodities is the presence of large amounts of fats, proteins, and sterols. As a result, extracts obtained with general procedures (3-6) will invariably contain considerable amounts of co-extractives. In such cases, direct analysis by GC or HPLC is impractical, since the traces of fat can quickly lead to serious losses in column efficiency and detector performance. A secondary problem associated with the processing of such samples arises from the thermal-lability of parathion and its tendency to hydrolyze into nitrophenol in solution (2). Because of these demanding requirements, a mild and rapid sample preparation technique followed by a selective chromatographic approach is desirable.

Progress in the field of sample preparation for organophosphorus pesticides has lagged far behind the methods for their quantitation (6). Indeed, the lack of attention is manifested by the limited number of publications in this specific area.

Current compendial methodologies available for processing these commodities are based on multiple solvent extractions followed by fat removal using separatory funnel partition (3-6). The initial isolation of the lipid soluble pesticide from the bulk matrix, as adopted by both the Food and Drug Administration's PAM (3), and the AOAC (6) involves a serial extraction of the ground sample with petroleum ether followed by an additional extraction with diethyl ether-petroleum ether (1+1) in the presence of ethanol. This approach has been popular since relatively large samples can be handled, most analysts are familiar with the procedure and most laboratories have the necessary glassware and equipment on-hand. However, the process is labor intensive and slow. It requires large volumes of pure and expensive solvents. Furthermore, numerous solvent transfer steps and the possibility of emulsion formation can result in sample loss. Finally and most importantly, a secondary cleanup is invariably necessary

to remove residual traces of fat.

Previously, the method of choice for fat cleanup involved separatory funnel partition between an immiscible solvent pair such as acetonitrile-hexane (4). In this method, the crude extract is dissolved in hexane, the solution is shaken with acetonitrile, and the acetonitrile phase is separated and shaken with water. The resultant one-phase system is extracted with hexane, and the aqueous phase is discarded. Presumably, most of the fat has been removed in the initial hexane phase and the pesticide residue is contained in the second hexane phase.

Although valuable, separatory funnel techniques are not practical for routine sampling because they are labor intensive, very costly, and not amenable to automation. They require back transfer into a low boiling, low polarity solvent and consequently much glassware. Furthermore to a large degree, the accuracy of the procedure is dependent on the manipulative skills of the analyst. Finally, they are suitable for use only on high potency samples. Other existing cleanup methods are based on a wide range of techniques including gel permeation chromatography (7-10), solubilization in sulfuric acid (11), metal precipitation (12), sweep-codistillation (13), and solid-phase extraction (14-17). Among these, solid-phase extraction (SPE) is receiving increased attention as ready-to-use cartridges have become available.

SPE offers a number of advantages over liquid partition for extract cleanup. Most importantly, the method is faster because it has fewer operational steps, avoids formation of emulsions and offers superior selectivity towards the compounds of interest. It has lower solvent and apparatus cost. Furthermore, it is compatible with automated elution manifolds. Finally, it prolongs the analytical column lifetime because particulate matter and strongly retained compounds can be removed prior to injection.

The extensive utilization of SPE with viscous extracts from foodstuffs has been hampered by the large sample volume requirements and by the problems encountered during the loading of the sample onto the cartridge. In fact, quantitative transfer of viscous extracts by manual intervention may require more solvent than that needed for the break-through of the solute of interest. In such cases, problems encountered during charging, such as clogging, lack of sufficient equilibration, or exceeding the

break-through volume before the cartridge is eluted with another solvent, may result in low recoveries and complete loss of selectivity. For lipidic extracts, there is undoubtedly increasing need for a rapid, simple and inexpensive tool which can uniformally deposit such samples directly on SPE cartridges with minimal solvent volume and operator involvement.

Quantitation of parathion residues has most frequently involved GC analysis, although thermal-lability problems can often result in poor reproducibility (18). As suggested in review articles (19-21), HPLC offers a nearly ideal system of determination of parathions due in part to the gentleness of the conditions under which separations are accomplished. However, a search of the literature reveals few systematic studies describing the development of HPLC methods for the trace level determination of parathions in the complex matrices. Such a situation can be attributed to the fact that optical HPLC detectors often lack the sensitivity and selectivity required for trace work.

Electrochemical detection has become a frequently employed alternative to optical detectors. Such detection schemes offer excellent sensitivity, selectivity toward electroactive analytes, wide linear ranges, and low costs. General articles have covered the basics of technique (22), and the large volume of recent literature is well covered in reviews (23) and a bibliography of over 100 references (24).

Amperometric detection was first proposed for parathion in adulterated lettuce extracts by Kohen and Huber (25). In this study several experimental problems, most notably caused by dissolved oxygen and electrode clogging, resulted in high detection limits and poor precision. Indeed, several workers have avoided the use of electrochemical detectors on these grounds. Kissinger (26) refined this approach for parathion in run-off waters by employing a mercury film on a gold substrate contained in a thin-layer flow cell. In addition, specific degassing procedures and electrode pretreatment protocols were routinely followed. As a result, improved detection limits compared to those reported by Kohen (25) were obtained. Clark and Goodin (27) inserted a UV detector in series with a reductive amperometric detector equipped with a glassy carbon working electrode. With this arrangement, improved qualitative and quantitative measurements were obtained for green vegetables contaminated with parathion. Ding and Krull (28) explored the possibilty of quantitatively converting

parathion into a readily oxidizable species with UV light prior to electrochemical detection in order to enhance selectivity and detection limits. To date, comprehensive studies describing the various aspects of this detection approach for parathion have not appeared.

Our experience with supercritical fluid extraction (SFE) for sample preparation has promped us to investigate its use in a scheme which can yield relatively fat-free parathion extracts from fat-laden matrices. The scheme incorporates a solid phase column packed with alumina in series with the extraction chamber. In this manner, the upstream supercritical fluid extractor serves as an unique means of introducing the lipidic extract directly onto the sorbent bed. Subsequently, the column is disconnected and back flushed prior to LC separation with an electrochemical detection. In exploiting the principles of both SPE and SFE, the proposed single step procedure is compatible with large sample quantities, requires small elution volumes, and has a low lipid carry-over. The resulting extracts are directly amenable to chromatographic analysis.

We have examined the capabilities of this approach in detail as it pertains to the analysis of parathion in commodities such as oil seeds, cereals, and legumes. In addition, we will present the performance characteristics of this procedure with regard to sensitivity, linearity, and reproducibility as well as its applicability to several fortified crops.

EXPERIMENTAL

Chemicals

Methyl parathion and ethyl parathion of Anal R grade were obtained from Chem Services (Chester, PA). Nitrophenol was obtained from Aldrich. HPLC-grade methanol, acetonitrile, hexane were purchased from J. T. Baker. Buffer salts were acquired from Fisher and used without further purification. In-house glass distilled water was used in all studies.

Apparatus

The design and construction of the supercritical fluid extractor incorporating a solid-phase collector has been thoroughly detailed elsewhere (29, pp. 124-125). The syringe pump based LCEC system employing a silver working electrode has also been

described (28). Voltage for electrochemical detector was provided from a lab-constructed dual potentiostat (29). The output of its current to voltage (C-V) circuit was fed, in parallel to a Linear model 1200 strip chart recorder (Linear Instruments, Irvine, CA) and a peak detector based on the circuit described by Strohl and Curran (30), which was used for acquisition of peak height measurement.

Preparation of standards

Stock solutions of parathions were prepared by transferring 125 mg, accurately weighed, to a 100 mL volumetric flask and diluting to the mark with acetonitrile. Working solutions ranging from 12.5 µg/mL to 12.5 ng/mL were prepared by diluting the stock solution with acetonitrile or methanol.

Extraction Procedure

Cereals, legumes, and oilseeds were obtained in area retail markets. The weighed samples were ground with sufficient glass-bead powder to form a homogeneous coarse powder. At this time, the samples were spiked with 1 mL of the pesticide in methanol and the solvent allowed to evaporate at room temperature. Next, the sample was transferred to the extraction chamber and extracted for a period of 15 min, at 8000 psi and 45^0C. After this period, the back-pressure regulator was carefully cracked open allowing the crude extract to be uniformly deposited onto the sorbent collector. Subsequently, the cartridge was disconnected and back flushed along with the exit valve and interconnecting tubing with 20 mL of acetonitrile from a 50 mL glass syringe fitted with a luer to female 10-32 adaptor. The eluate was evaporated in a rotary evaporator to dryness, reconstituted in 1 mL of mobile phase and then subjected to HPLC analysis.

HPLC determination

The mobile phase was prepared from NaH_2PO_4 (Fisher Scientific Co.), H_3PO_4 (Mallinckrodt) and HPLC grade acetonitrile (Baker). After a study of the effect of the concentrations of the various mobile phase constituents on retention times, a mobile phase consisting of 50 % (v/v) acetonitrile and 50 % (v/v) aq 0.025 M NaH_2PO_4 with sufficient H_3PO_4 to give a pH of 6.8 was selected.

After the acetonitrile and aqueous buffer were mixed in the proper proportions, the mobile phase was degassed with nitrogen for 15 min to assure removal of oxygen. The mobile phase was then loaded into the syringe pump cylinder without exposure to air by proper positioning of the valves on the liquid chromatograph manifold. Following the equilibration of the baseline at a flow rate of 2 mL/min, 1 mL aliquots of the sample were gently bubbled with mobile phase saturated with nitrogen for one min, and 20 µL introduced into the HPLC using the chromatograpic apparatus and parameters described. The parathion peak was identified on the basis of retention time and quantitated by comparision with a calibration curve.

RESULTS AND DISCUSSION

Electrochemical characteristics of parathion

The electrochemical characteristics of methyl and ethyl parathion have been investigated by Bowen and Edwards (31) prior to the development of thin-layer flow cells. To ascertain the optimal electrochemical conditions applicable in a thin-layer flow cell equipped with a silver working electrode, an HDV was generated by repeated injection of a mixture containing 12.5 µg/mL each of ethyl and methyl parathion at 18 different applied potentials ranging from -0.2 to -1.0 V with respect to the SCE electrode. An HDV for both methyl and ethyl parathion is shown in Figure 1. On the basis of these measurements an applied potential of -0.85 V was selected for both methyl and ethyl parathion as the minimum applied potential at which the current reaches the limiting-current plateau of these analytes. The use of a less negative potential resulted in loss of sensitivity, whereas more negative potentials led to detector drift and increased background noise. The electrochemical response to p-nitrophenol, a major degradation product of parathion was briefly examined and was found to reach only 75 % of its maximum sensitivity under the chosen conditions.

Effect of pH

The optimum response is also dependent the pH of the eluant. As the pH is increased at a constant potential, the absolute sensitivity for each parathion decreases, however, the background at silver decreases even more rapidly. The dependence of the signal-to-noise ratio on pH is illustrated in Figure 2. It may be concluded from this Figure that the optimum S/N ratio is achieved with buffers of pH 5 to 7. In buffers with pH values greater than 9, hydrolysis of parathion into nitrophenol leads to a

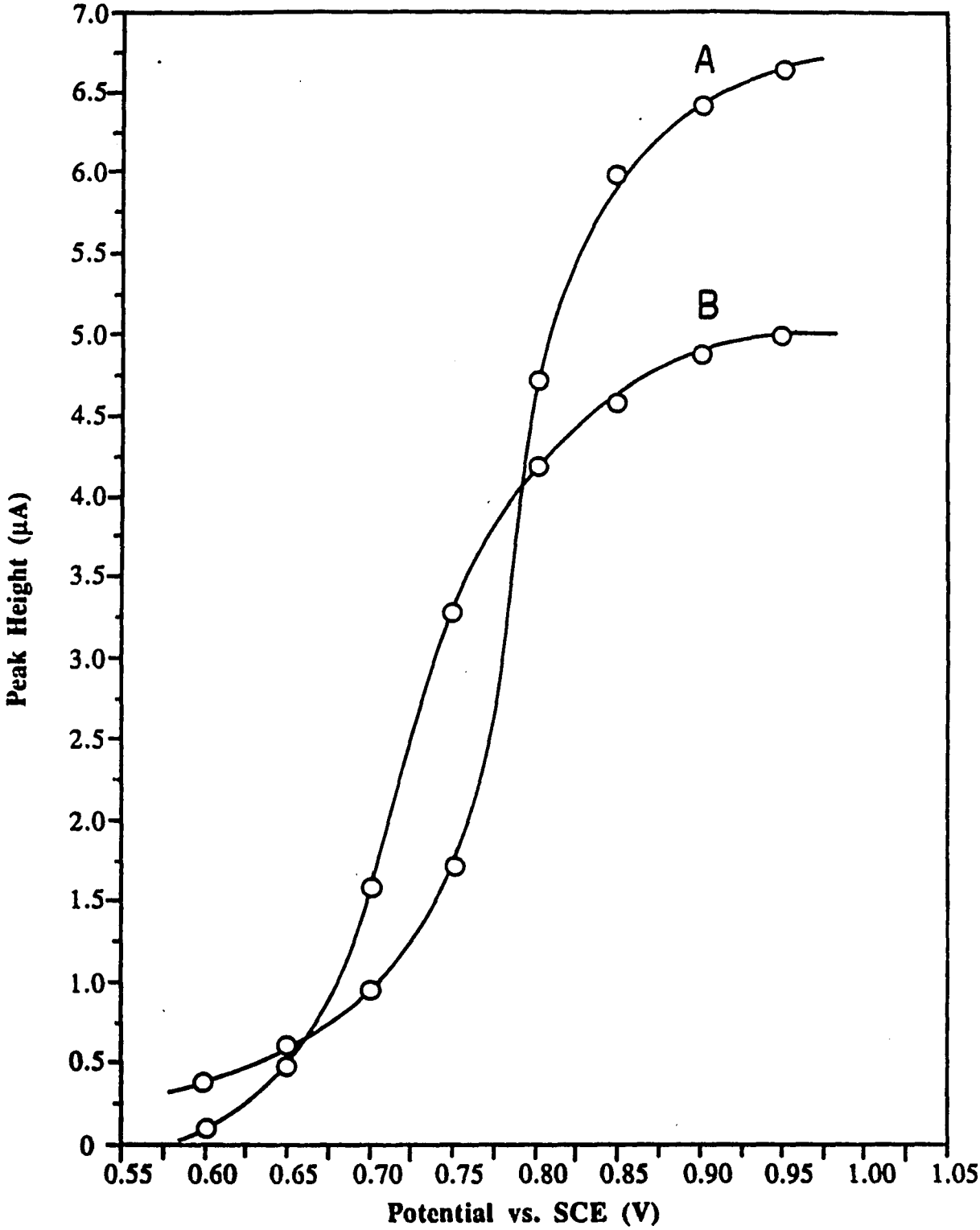

Figure 1. Hydrodynamic voltammogram of (A) methyl and (B) ethyl parathion on silver cathode *vs* SCE. Chromatographic conditions: column, 150 x 3.9 I.D. mm μ-Bondapak C-18 (10 μm); mobile phase, acetonitrile -0.025 M aq phosphate buffer, pH 6.8 (50+50, v/v); flow rate, 2.0 mL/min; sample size, 0.250 μg of each parathion per 20 μL mobile phase injected at each potential setting.

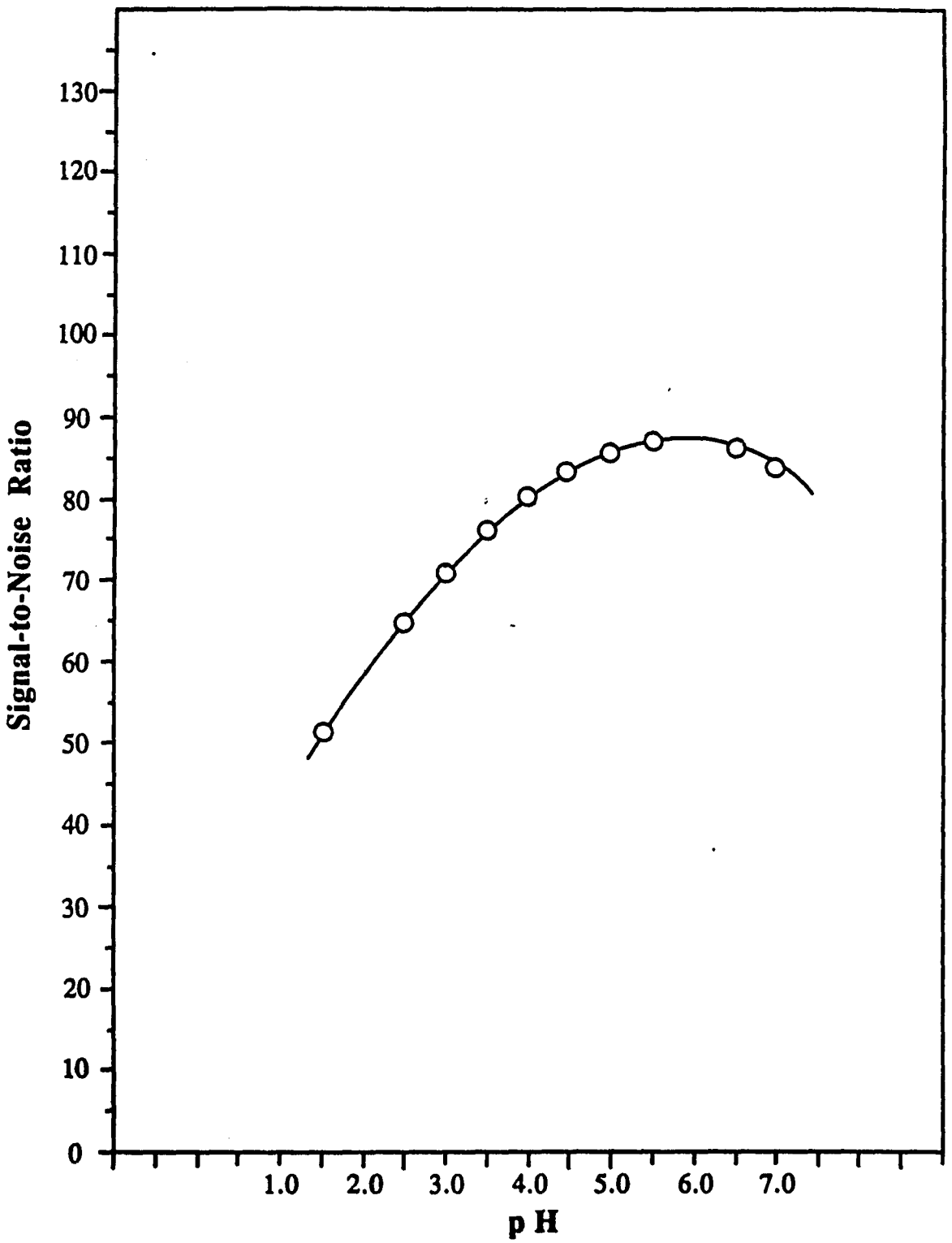

Figure 2. Influence of pH on signal-to-noise ratio for methyl parathion. Chromatographic conditions: column, 150 x 3.9 I.D. mm μ-Bondapak C-18 (10 μm); mobile phase, acetonitrile-0.025 M aq phosphate buffer, pH 6.8 (50+50, v/v); flow rate, 2.0 mL/min; applied potential, -0.85 *vs* SCE; sample size, 20 μg of ethyl parathion per 20 μL mobile phase injected at each pH value.

dercrease in the signal-to-noise ratio for parathion.

Detector Response

The response characteristics of the detector for the parathions were studied using a series of dilute solutions, each containing parathion in acetonitrile and covering the range of 12.5 ppb to 125 ppm. For each concentration 3 replicate injections were made and log-log plots of peak height against concentration were constructed. The calibration curve for ethyl parathion, illustrated in Figure 3, exhibits a linear dynamic range of at least 3 orders of magnitude. The equation of the best fit line, computed using linear regression analysis for ethyl and methyl parathion were y (nA) = 2.8x (ng)+0.009 and y (nA) = 2.0x (ng)+ 0.015, respectively. In principle the response factors for both parathions should be equal in magnitude, however, in practice the purity factors for each parathion differs from unity. The lower limit of detection for both parathions was approximately 200 ng per 20 μL injection, allowing for a signal to noise ratio of 3 to 1. This detection limit compares well with the value reported by Clark et al. (27) for amperometric detection at glassy carbon, and represents a 10-fold improvement over the detection limit obtained by Paschal et al. (32) using a UV detector operated at 270 nm. Upper concentration limits were held at 12.5 ppm to minimize the possibility of electrode fouling. When the cell lost sensitivity abruptly after a few days of continuous use, electrochemical cleaning with a series of short pulses between 0 and -1.5 V returned the cell to its original sensitivity. Peak heights measured for repetitive injections of the extract were highly reproducible, typically with relative standard deviations of less than 1.5 %. Comparable reproducibilities were observed from one day to the next, with chromatograph and potentiostat shut down overnight.

Chromatography

Separation of methyl and ethyl parathion from interfering degradation products was pursued by reversed-phase chromatography on a μ-Bondapak RP C_{18} column with an acetonitrile-aqueous phosphate mobile phase. In initial studies, capacity factors (k') for ethyl parathion, methyl parathion, and nitrophenol were measured at different mobile phase compositions, thereby allowing the selection of an optimal mobile phase. The influence of acetonitrile content on retention time is shown in Figure 4. An acetonitrile content of 50% appears to offer a good compromise between run-time and selectivity.

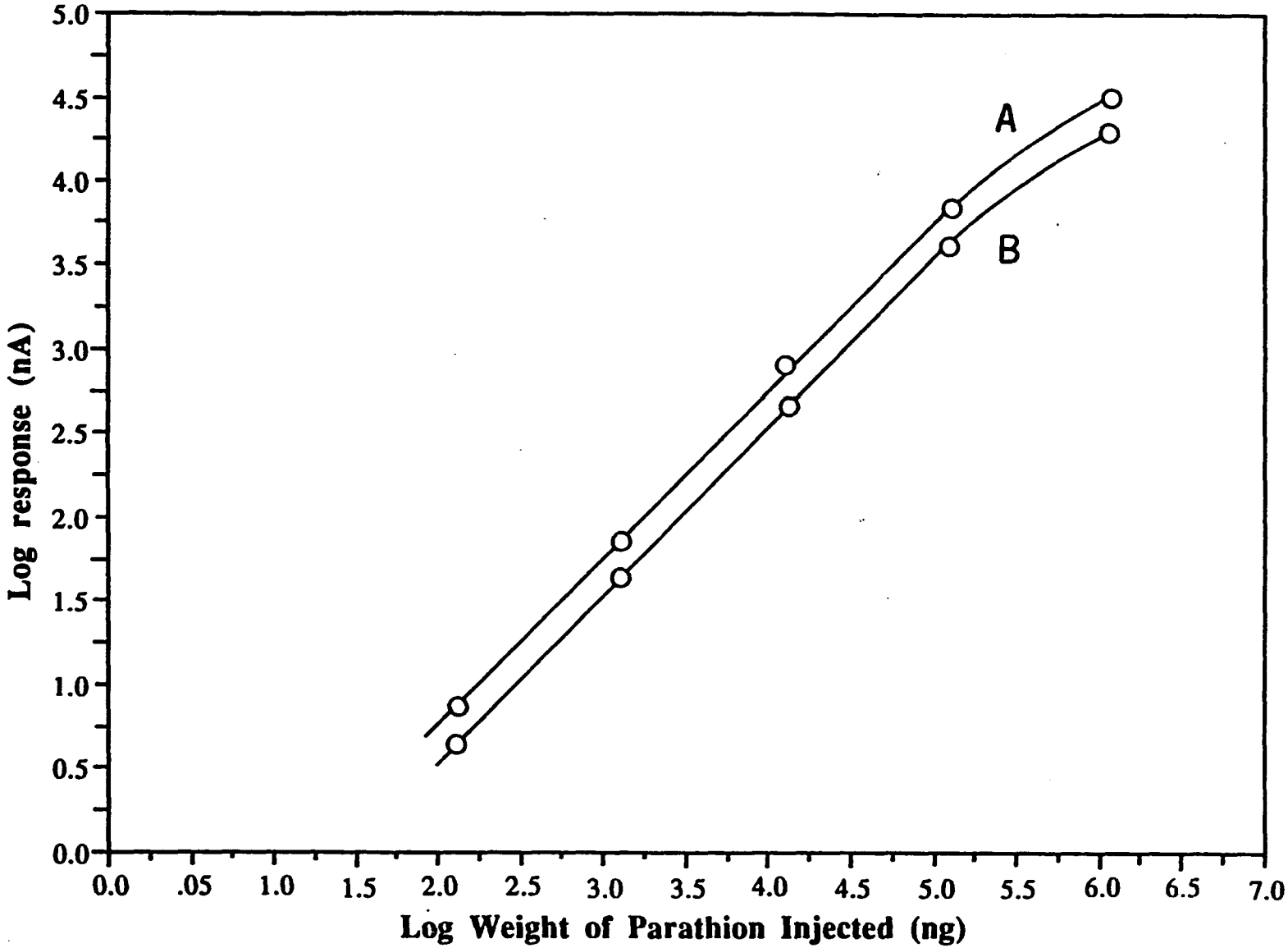

Figure 3. Linearity of detector response to amounts of (A) methyl and (B) ethyl parathion in 20 µL samples. Column, 150 x 3.9 I.D. mm µ-Bondapak C-18. Eluent, acetonitrile-aq phosphate buffer, pH 6.8 (50+50, v/v). Flow rate, 2.0 mL/min. Potential of working electrode, -1.2 V *vs.* SCE.

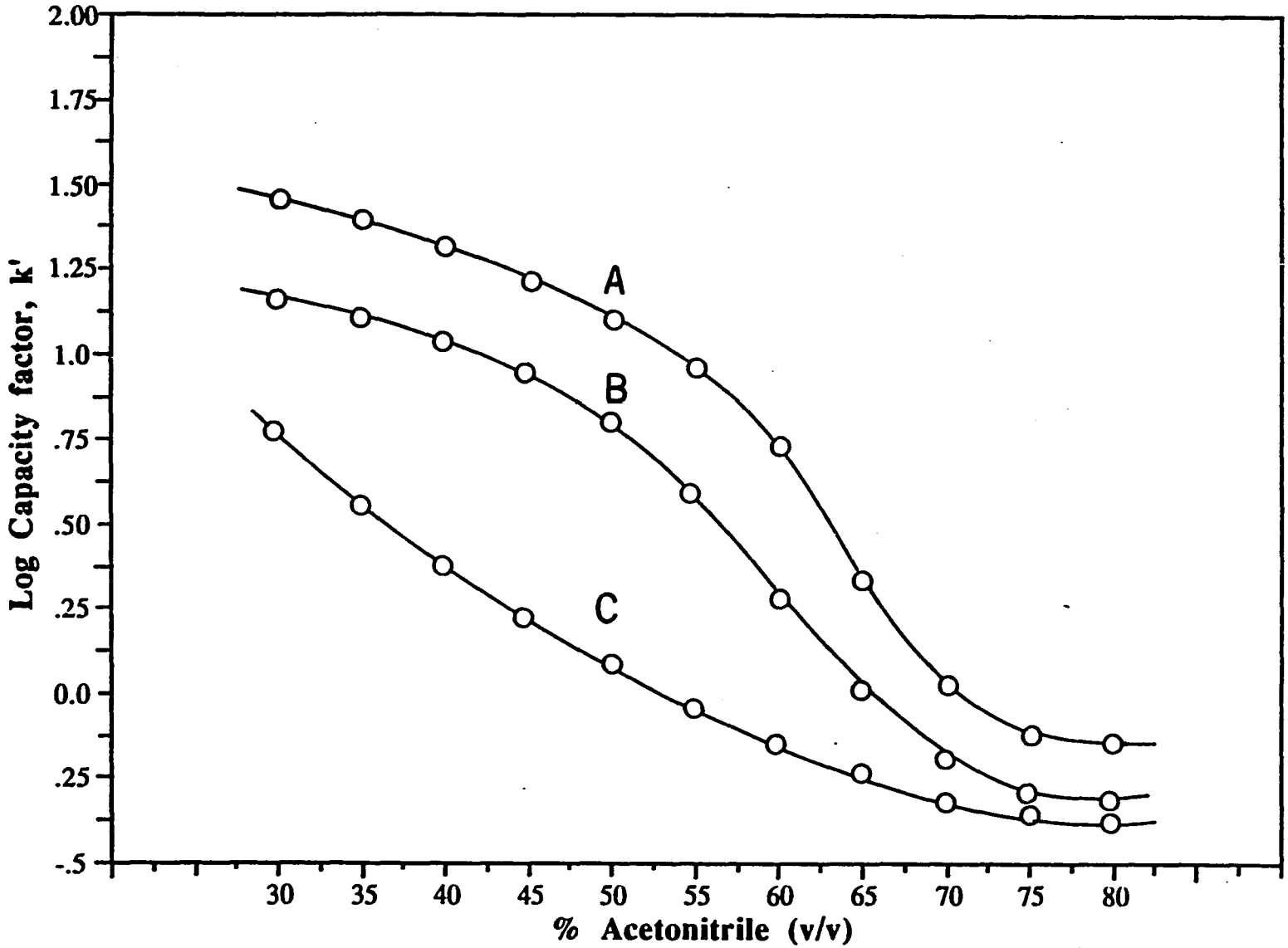

Figure 4. Dependency of capacity factor of (A) methyl parathion, (B) ethyl parathion and (C) nitrophenol on acetonitrile content of mobile phase. Column: 150 x 3.9 mm I.D. μ-Bondapak C-18 (10 μm). Flow rate: 2.0 mL/min. Silver electrode potential: -0.85 V *vs* SCE.

The pH of the potassium phosphate buffer used in the mobile phase was crucial to the peak symmetry of the three components. In particular, the effect of pH on the peak shape of nitrophenol is dramatic. Peak tailing and a decrease in capacity factor was observed when pH exceeded 7.5. In some cases, even multiple peaks were obtained for a standard solution of nitrophenol chromatographed with such buffers. Considering this problem and the stability of the column packing, the pH was maintained at 6.8 for all studies.

A typical electrochemical chromatogram for a synthetic mixture of methyl parathion, ethyl parathion, and nitrophenol is shown in Figure 5. With the chosen mobile phase consisting of acetonitrile-0.025 M aq phosphate buffer, pH 6.8, (50/50, v/v), the chromatographic peaks for the parathions were sharp and well separated from each other and from nitrophenol such that the retention times for nitrophenol, methyl parathion, and ethyl parathion were 4.0, 5.8, and 7.0 min., respectively. The run-time was only 8 min.

Optimization of sample preparation technique

During the development of the method just described, it was necessary to select the extraction conditions that would offer the best compromise between recovery and time. The dependence of percentage recovery on pressure in the range of 5000 to 8000 psi for parathion deposited at the 12.5 μg level on two gram samples of Chromosorb W is illustrated for 45 and 60^{0}C in Figure 6. Each extraction was performed in triplicate for a period of 15 min. As can be seen, the percentage recovery increased with pressure at both temperatures until a limiting value suitable for quantitation was reached near 7000 psi; the effect was more dramatic at 45^{0}C. This is not the unexpected since the density of supercritical carbon dioxide is greater at lower temperature. In fact at 6000 psi, a reversal in recovery is seen and the recovery obtained beyond 6000 psi at 45^{0}C is slightly greater than at 60^{0}C. A similar cross-over effect has been observed in case of aldrin and other volatile compounds (33). Considering the thermal lability of the compounds involved, an extraction temperature of 45 ^{0}C and a pressure of 7000 psi was used throughout the study. Under these conditions, recoveries of standard methyl and ethyl parathion at the 12.5 μg level extracted from Chromosorb W averaged 95 %.

Additional studies were conducted to evaluate the effect of equilibration time. Figure 7 shows the influence of equilibration time on recovery of methyl parathion at a constant

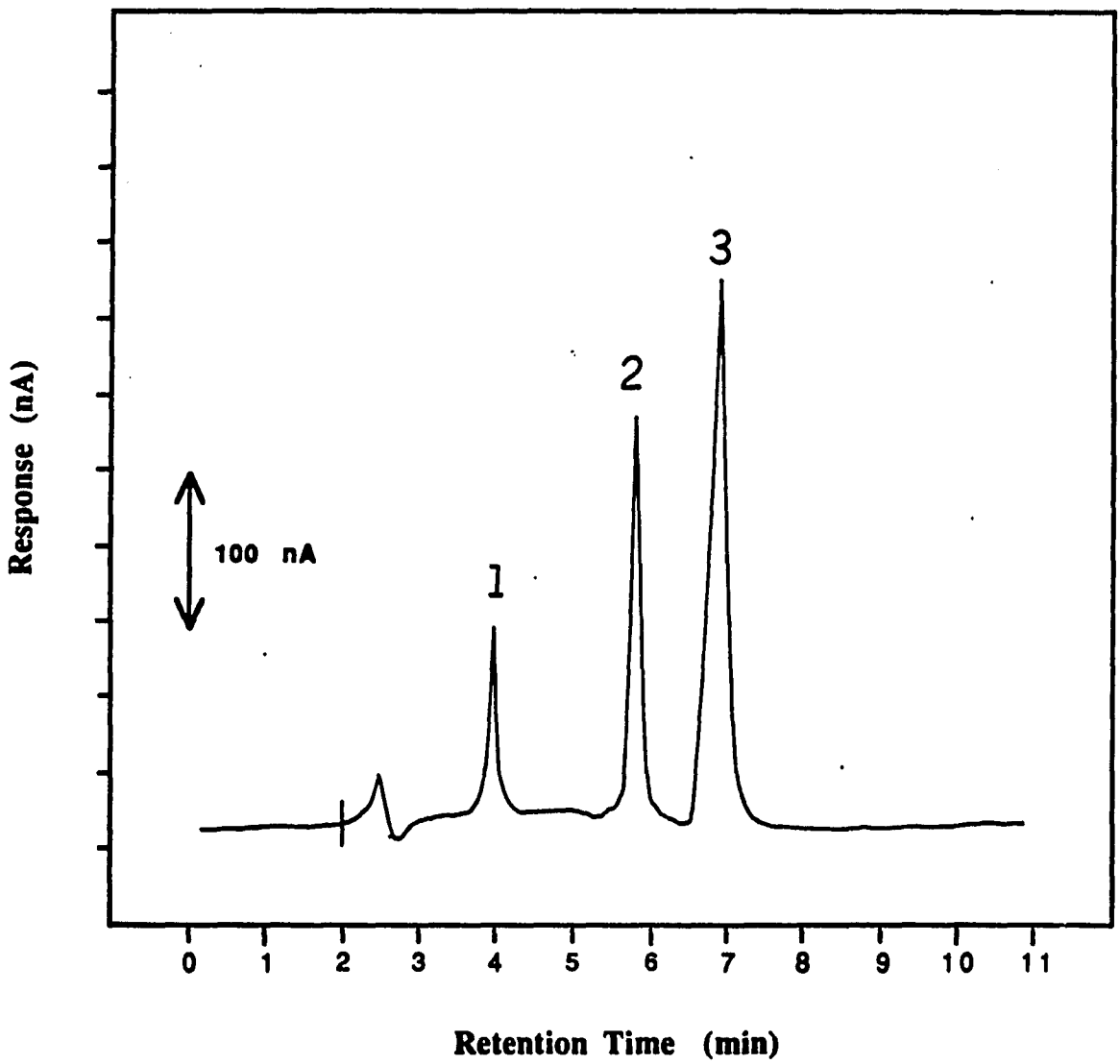

Figure 5. Chromatogram of the separation of ethyl parathion, methyl parathion and nitrophenol on a μ-Bondapak C-18 (10 μm) column by isocratic elution. Chromatographic conditions: mobile phase, acetonitrile-aq phosphate buffer, pH 6.8 (50/50, v/v); flow rate, 2.0 mL/min; detector potential, -0.85 V *vs* SCE; detector sensitivity, 100 nA/V. Peak identities as follows: 1, nitrophenol; 2, methyl parathion; 3, ethyl parathion.

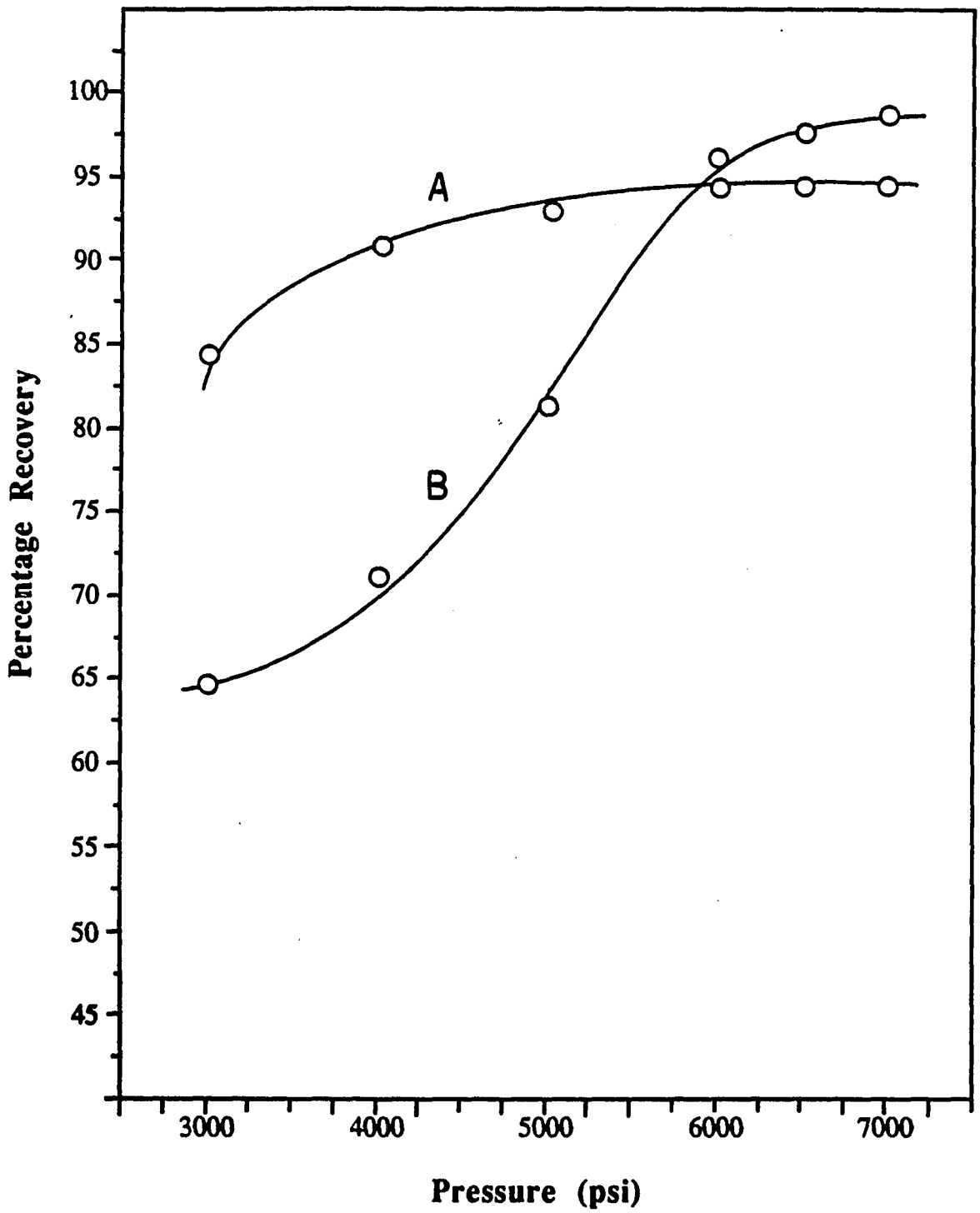

Figure 6. Effect of pressure on efficiency of SFE procedure for ethyl parathion at (A) 65^{0}C and (B) 45^{0}C. In each case equilibration time was 20 min. A 2 gram cartridge of Chromosorb W fortified with 12.5 µg of ethyl parathion was extracted at each pressure. HPLC analysis conditions as in Figure 5.

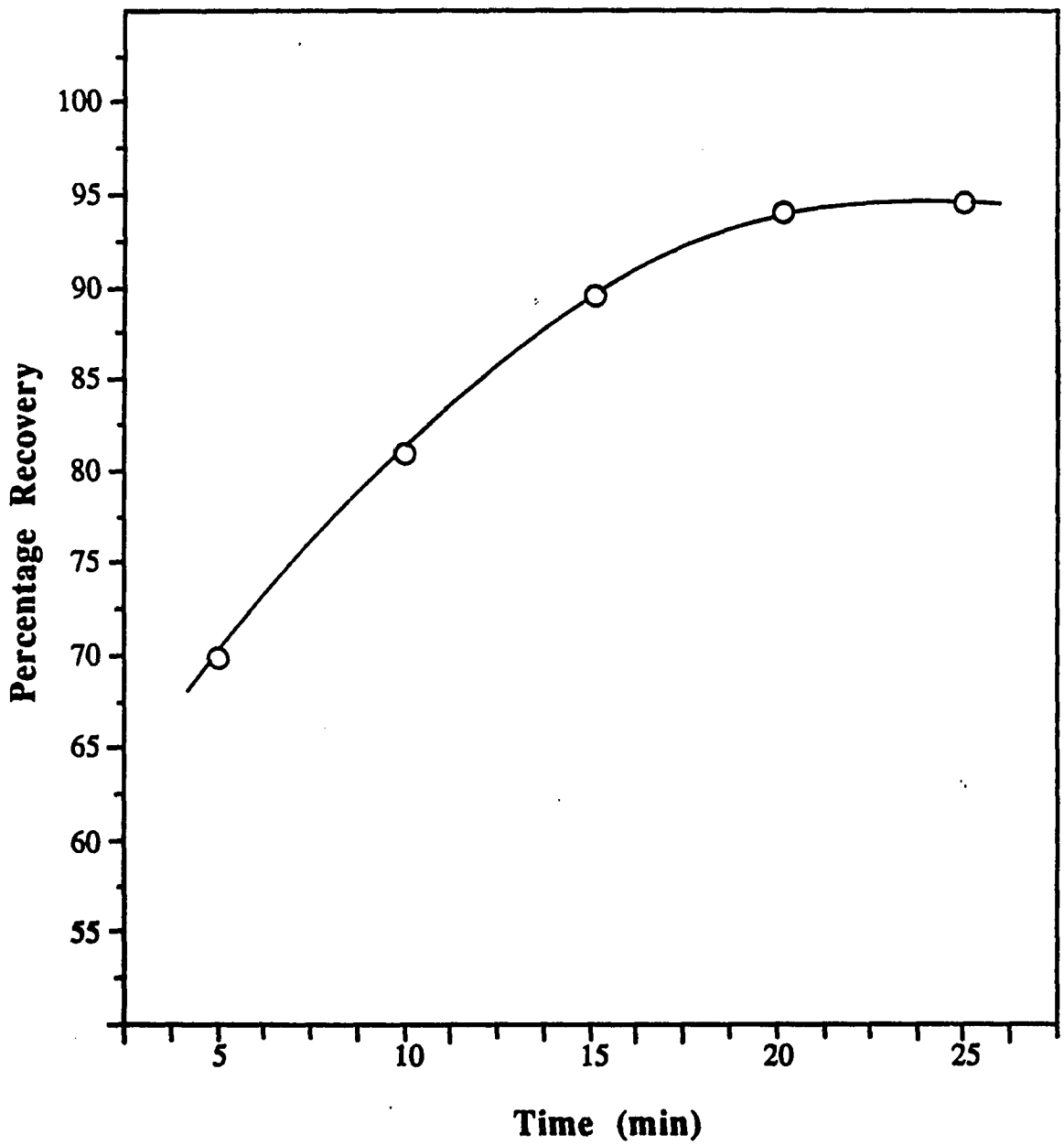

Figure 7. Effect of time on the efficiency of SFE procedure for methyl parathion using 8000 psi CO_2 at 45 °C. HPLC chromatographic analysis conditions as in Figure 5.

temperature and pressure of 45^{0}C and 7000 psi, respectively. As can be seen, an equilibration time of 15 min is sufficient for quantitative recovery, after which no change is observed up to at least 30 min.

Linearity of over-all procedure

The linearity of extraction/clean-up step in the range of 125 ng/g to 12.5 μg/g for parathion was confirmed by carrying out the described procedure on fortified rice samples. The lower limit of extraction was 50 ng/g, which in this case approaches the detection limit of the ECD for parathion.

Effect of lipid load

In order to investigate the effect of the lipid load on extraction efficiency, four samples of soybean oils representing oil loads of 25, 50, 75, and 100 mg were adsorbed on two gram samples of Chromosorb W and fortified with parathion at three spiking levels. The samples were then extracted according to the optimum conditions specified above. Table 1 shows the percentage recovery of parathion as a function of initial lipid load. As shown in Table 1, recoveries were always 80 % or better, approaching complete recovery in most cases and were not related to either the spiking level or to the lipid load in the ranges tested.

Comparison with Pipet Loading

To examine the advantages of loading solid phase cartridges by SFE dissolution/ precipitation over conventional means, a one mL aliquot of a hexane extract containing parathion was manually loaded onto a cartridge packed with 1.5 g of alumina (Fisher Scientific, Pittsburgh, PA) which was pre-conditioned by heating in a drying oven at 215^{0}C. The glassware and the implements used to transfer the extract were washed and these rinsings, amounting to 2.0 mL, were also transferred to the cartridge. The excess eluate was collected and the column was further eluted with three 1 mL portions of acetonitrile. Fractions were collected at 0.5 mL intervals in Reacti-Vials already containing 0.5 mL of methanol. A plot of response as a function of eluant volume is shown in Figure 8. As can be seen, parathion breaks through at a volume of 2.5 mL on a cartridge which has a dead volume of 2.3 mL. Moreover, the collected fractions remained oily in nature, indicating excessive lipid carry-over. The loss of selectivity and efficiency of the SPE cartridge for parathion was attributed to the lack of efficient equilibration with the packing due to clogging and the need for excessive washings

Table 1. Recovery of Parathion Added to Soybean Oil.

Oil Load, mg	Mean Percentage Recovery [1]		
	Concentration of Added Parathion (ppm)		
	12.5	1.25	0.125
25	93	87	89
50	85	101	92
75	96	91	84
100	88	80	82

[1] Each recovery value represents an average of 3 extractions and determinations.

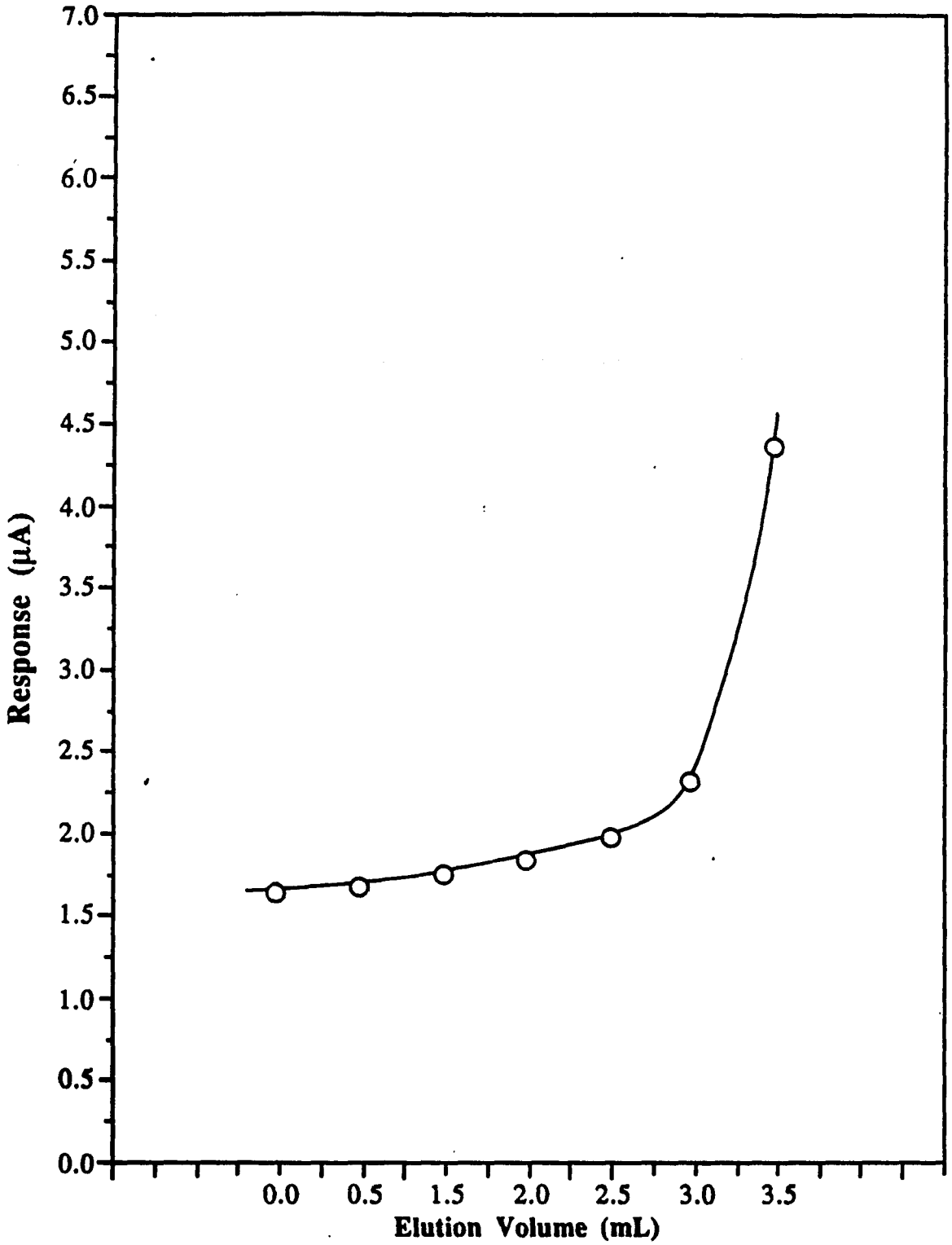

Figure 8. Desorption profile of parathion from alumina cartridge as a function of elution volume. Desorption conditions: eluent, 100 % acetonitrile. Sample size: a 1.5 g of alumina cartridge spiked with 500 μg ethyl parathion per mL of hexane. Chromatographic analysis conditions: column, 150 x 3.9 I.D. mm μ-Bondapak C-18 (10 μm); mobile phase, acetonitrile-aq 0.025 M phosphate buffer, pH 6.8 (50+50, v/v); flow rate, 2.0 mL/min; detector potential, -0.85 V *vs* SCE; current sensitivity, 100 nA/V.

with hexane. In contrast in the proposed method, lipidic extracts are deposited directly onto the packing material promoting the efficient partitioning of the pesticide between the packing and the acetonitrile eluent. Minimal lipid release also enables extracts to be further concentrated.

Application to Crop Analysis

To illustrate the analytical utility of this precipitation procedure in HPLC methods for residual pesticides, various crops fortified with parathion and which are notoriously high in lipid content were analyzed. Representative chromatograms of treated peanuts and corn samples after supercritical fluid extraction and HPLC with electrochemical detection are shown in Figures 9 and 10, respectively. There is excellent separation between methyl parathion and ethyl parathion with near baseline resolution. The virtual absence of interferences allows detection limits of less than 50 ng/g to be achieved. For the sake of comparision, the same extract used in Figure 9 was re-examined with a UV detector at 270 nm and its chromatogram is shown in Figure 11. From this chromatogram, the lack of selectivity of UV detector for extracts containing extraneous materials is evident. The quantitative results for the four different crops at three spiking levels are summarized in Table 2. Mean percentage recoveries obtained from these crop substrates, fortified at levels from 1.25 μg/g to 12.5 ng/g, were typically greater than 88 % and ranged from 68 to 97 %.

The completeness of extraction was verified by exhaustive Soxhlet extraction of the remaining pulp with methylene chloride for 24 h. Re-extraction, in the case of a rice sample fortified at 1.25 μg/g, gave no additional recovery of parathion.

Reproducibility

The within-day precision was ascertained by analyzing, in triplicate, several samples of rice fortified with methyl and ethyl parathion at three different spiking levels. The results are shown in Table 3. The coefficent of variation for both parathions carried through the entire procedure over this thousandth-fold fortification level ranged from 1.9 to 4.8 % (n=3).

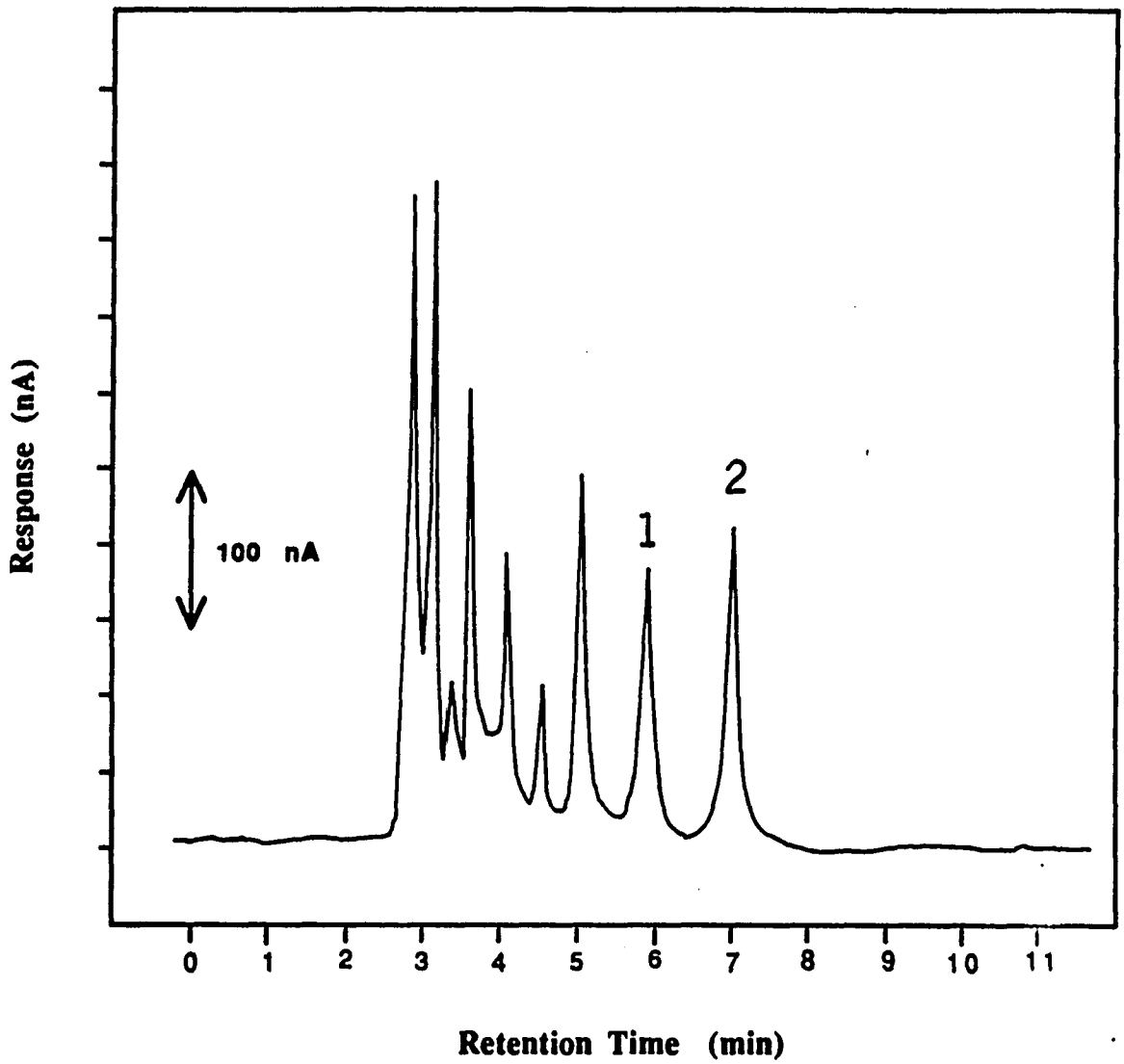

Figure 9. LCEC chromatogram of a supercritical fluid extract of a peanut sample treated with ethyl parathion and methyl parathion. Extraction conditions: SFE with 8000 psi CO_2, 65°C, 20 min. A gram aliquot of a dried peanut sample spiked with 150 µg of ethyl parathion and methyl parathion per gram of peanuts was subjected to the outlined procedure. HPLC-ECD conditions as in Figure 5. Peak identities as follows: 1, methyl parathion; 2, ethyl parathion.

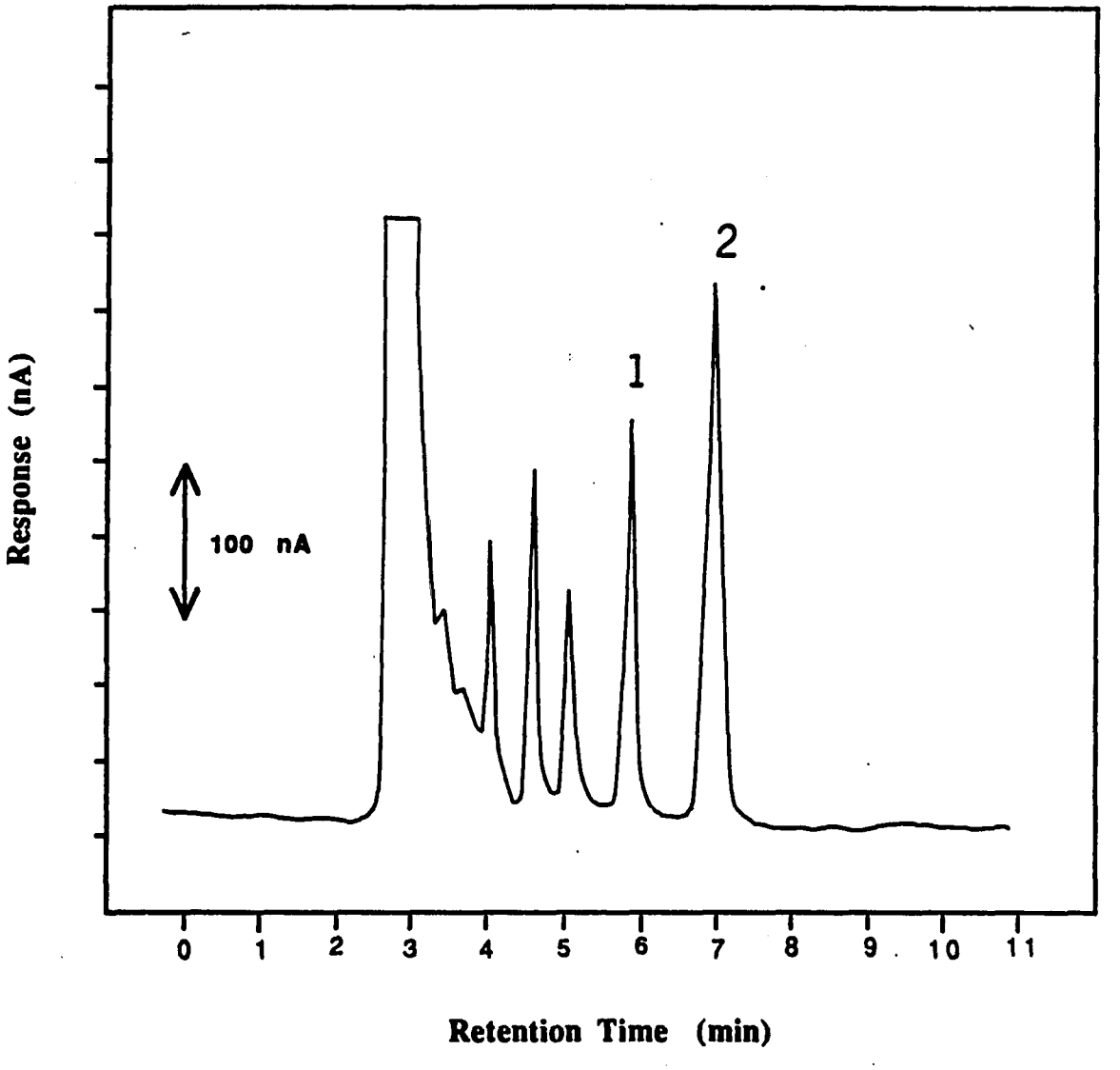

Figure 10. LCEC chromatogram of a supercritical fluid extract of a corn sample treated with ethyl parathion and methyl parathion. Extraction conditions: SFE with 8000 psi CO_2, 65 ^{0}C, 20 min. A gram aliquot of a dried corn sample spiked with 150 µg each of ethyl parathion and methyl parathion per gram of corn was subjected to the outlined procedure. HPLC-ECD conditions as in Figure 5. Peak identities as follows: 1, methyl parathion; 2, ethyl parathion.

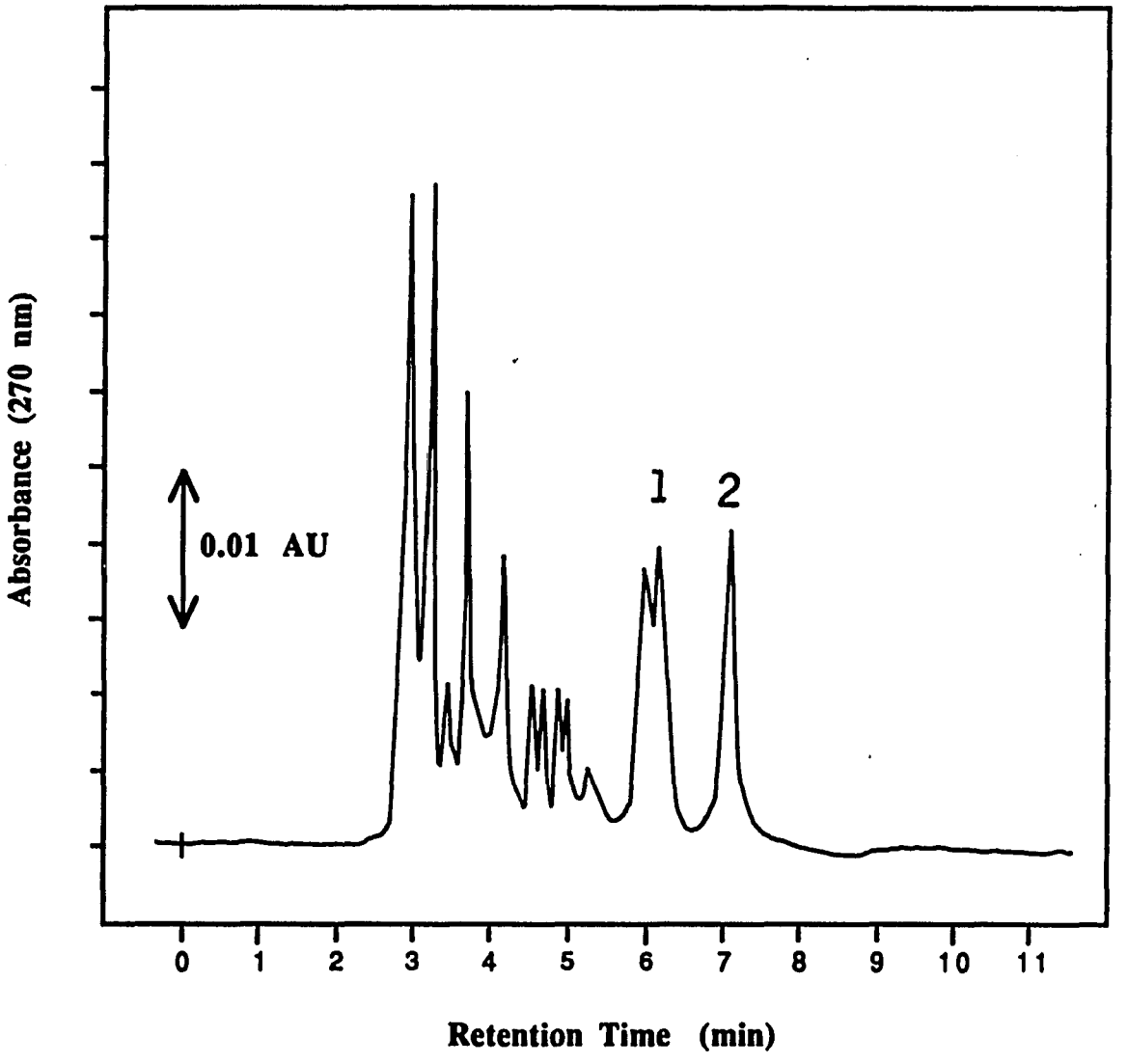

Figure 11. Liquid chromatogram with UV detection of a supercritical fluid extract of a peanut sample spiked with 150 µg each of methyl parathion and ethyl parathion. Column: 150 mm x 4.6 mm I.D. Supelcosil C-18 (10 µm). Mobile phase: acetonitrile-aq phosphate buffer, pH 6.8 (50+50, v/v). Flow rate was 2.0 mL/min. Detector: Perkin-Elmer 4000 LC system equipped with UV detector at 270 nm. Sensitivity, 0.10 AUFS. Peak identities as follows: 1., methyl parathion; 2., ethyl parathion. Extraction conditions: 8000 psi CO_2 at 45°C, for 20 min.

Table 2. Recovery of Parathion from Fortified Oil Seeds and Cereals.

Substrate	Added, µg/g	Recovery, %	RSD (n=3), %
Rice	1.25	97	1.9
	0.125	88	3.5
	0.0125	75	7.0
Corn	1.25	91	2.4
	0.125	87	3.0
	0.0125	69	5.5
Peanut	1.25	95	2.9
	0.125	91	3.1
	0.0125	74	4.9
Sunflower seed	1.25	93	2.1
	0.125	89	3.6
	0.0125	68	7.5

Table 3. Reproducibility of SFE and HPLC-ECD Method For Methyl and Ethyl Parathion.

Amount fortified, µg/g	Amount recovered, µg/g	RSD (n=3), %
	Methyl Parathion	
25	23.8	3.8
2.5	2.3	1.9
0.3	0.23	4.8
	Ethyl Parathion	
25	25.5	4.1
2.5	2.2	2.1
0.3	0.25	3.9

Conclusions

The results of these studies demonstrate the efficiency, speed, and the simplicty of the proposed sample preparation procedure for the use in the HPLC analysis of parathion residues. The method is based on the unique ability of supercritical carbon dioxide to concentrate parathion in the supercritical phase before the solid-phase cartridge. This is accomplished by maintaining the system density above that which is needed for dissolution of parathion. The density is then decreased rapidly through the cartridge resulting in the precipitation of parathion on the top of the cartridge. The performance of the method is characterized by high recovery, good reproducibility, and low lipid carry-over. More importantly, the extracts provided by this method are completely soluble in acetonitrile and hence, are suitable for direct introduction into an HPLC system. Accordingly, as many as 50 samples can be analyzed without changing the analytical column.

The procedure is expected to offer a viable alternative to the bottleneck problems of manually charging solid phase cartridges and is readily adaptable to laboratory automation. In addition, the enhanced selectivity of the reductive amperometric detector relative to the UV detector makes it most suitable for the primary screening of treated samples.

References

Part I

1. R. P. W. Scott," Liquid Chromatography Detectors"; Elsevier: Amsterdam, 1977.

2. B. Dhingra, Ph.D. Dissertation, City University of N.Y., 1983; Dissertation Abstracts International, 44 (10), 3071-B (1984).

3. H. Poppe, in "Instrumentation for HPLC"; J. F. K. Huber (Ed.), Elsevier: Amsterdam, 1978; pg. 131.

4. R. E. Majors, H. G. Barth, and C. H. Lochmüller, Anal. Chem., 54, 323R-363R (1982).

5. K. Stulik and V. Pacakova, CRC Crit. Rev. Anal. Chem., 14, 297-351 (1983).

6. D. A. Roston, R. E. Shoup, and P. T. Kissinger, Anal. Chem., 54, 1417A-1434A (1982).

7. K. Toth, G. Nagy, Z. Feher, G. Horvai, and E. Pungor, Anal. Chim. Acta, 114, 45-48 (1980).

8. M. D. Ryan and G. S. Wilson, Anal. Chem., 54, 20R-27R (1982).

9. R. J. Rucki, Talanta, 27, 147-156 (1980).

10. K. Brunt, Pharm. Weebl., 113 (29), 689-698 (1978); Chem. Abstracts, 89, 91448d (1978).

11. K. Stulik and V. Pacakova, J. Electroanal. Chem., 129, 1-24 (1981).

12. W. A. MacCrehan, R. A. Durst, and J. M. Bellame, In "Trace Organic Analysis: A New Frontier in Analytical Chemistry"; Proceedings of the

4 th Materials Research Symposium; NBS: Gaithersburg, MD, 1978; pp. 57-63.

13. R. E. Shoup (Ed.), "Recent Reports on Liquid Chromatography / Electrochemistry"; Bioanalytical Systems Press: West Lafayette, IN, 1982.

14. D. C. Johnson, A. M. Bond, R. M. Wightman, R. E. Shoup, and I. S. Krull, Anal. Chim. Acta, 180, 187-250 (1986).

15. S. G. Weber and W. C. Purdy, Anal. Chim. Acta, 100, 531-544 (1978).

16. R. E. Shoup, C. S. Bruntlett, W. A. Jacobs, and P. T. Kissinger, Am. Lab., 13 (3), 144-153 (1981).

17. "Electrochemical Detectors-Fundamental Aspects and Analytical Applications"; T. H. Ryan (Ed.), Plenum Press: New York, 1984, and references cited therein.

18. P. T. Kissinger, In "Laboratory Techniques in Electroanalytical Chemistry"; P. T. Kissinger and W. R. Heineman (Eds.), Marcel Dekker: New York, 1984; Chapter 22, pp. 616-635 and references cited therein.

19. "Principles and Applications of Liquid Chromatography/Electrochemistry"; Bioanalytical Systems Press: West Lafayette, IN, 1984, and references cited therein.

20. J. Ruzicka and E. H. Hansen, "Flow Injection Analysis"; Wiley: New York, 1981.

21. P. Kissinger and K. Bratin, "Recent Developments in the Reductive LCEC of Organic Compounds using Mercury Film and Glassy Carbon Electrodes"; presented at the Eastern Analytical Symposium, New York, Sept. 21, 1980; Paper No. 137.

22. P. T. Kissinger, K. Bratin, W. King, and J. R. Rice, In "Pesticide Analytical

Methodology"; J. Harvey and G. Zweig (Eds.), American Chemical Society: Washington, D.C., 1981; ACS Symposium Series No. 136, pp. 57-88 (1981).

23. W. MacCrehan and R. Durst, "Optimizing Reductive Electrochemical Detection in Liquid Chromatography"; ACS/CSJ Chemical Congress, Honolulu, HA, April 5, 1979; Abstract No. 207.

24. P. T. Kissinger, C. S. Bruntlett, K. Bratin, and J. R. Rice, "Trace Organic Analysis: A New Frontier in Analytical Chemistry"; S. N. Chesler and H. S. Hertz (Eds.), 1979; NBS Special Publication Number 519, pp. 705-711.

25. K. Brunt, C. H. P. Bruins, and D. A. Doornbos, Anal. Chim. Acta, 125, 85-91 (1981).

26. D. J. Miner and R. J. Bopp, "The Reproducibility of Measurements by LCEC"; presented at the LCEC Symposium on Environmental and Industrial Applications of LCEC and Voltammetry, Indianapolis, IN, May 17-19, 1981; Abstract No. 25.

27. R. M. Wightman, E. C. Paik, S. Borman, and M. A. Dayton, Anal. Chem., 50, 1410-1414 (1978).

28. K. Bratin and P. T. Kissinger, Talanta, 29, 365-370 (1982).

29. R. E. Shoup, C. S. Bruntlett, and W. A. Jacobs, "Installation/Operations Manual for LC-4A Amperometric Controller"; Bioanalytical Systems Press: West Lafayette, IN, 1981.

30. "Degasser: ERC-300 Series"; Erma Inc., Scientific Instruments Department, Tokyo, Japan.

31. K. Bratin and P. T. Kissinger, "The LCEC Symposium on Environmental and Industrial Applications of LCEC and Voltammetry"; Indianapolis, IN, May 17-19, 1981; Abstract No. 5.

32. K. Bratin and P. T. Kissinger, J. Liq. Chromatogr., 3, 321-357 (1981).

33. F. Senftleber, D. Bowling, and M. S. Stahr, Anal. Chem., 55, 807-812 (1983).

34. H. Gunasingham, B. T. Tay, K. P. Ang, and L. L. Koh, J. Chromatogr., 285, 103-108 (1984).

35. A. Trojanek and K. Holub, Anal. Chim. Acta, 121, 23-28 (1980).

36. J. W. Bixler and A. M. Bond, Anal. Chem., 58, 2859-2863 (1986).

37. A. M. Bond, H. A. Hudson, and P. A. van den Bosch, Anal. Chim. Acta, 127, 121-133 (1981).

38. R. E. Relm, Anal. Chem., 55, 1188-1191 (1983).

39. M. E. Rollie, C. Ho, and I. M. Warner, Anal. Chem., 55, 2445-2448 (1983).

40. W. A. MacCrehan and W. E. May, Anal. Chem., 56, 635-628 (1984).

41. W. A. MacCrehan and W. E. May, Anal. Chem., 60, 194-199 (1988).

42. Technical Publication for Model 5100A Coulochem Electrochemical Detector, Environmental Sciences Associates (ESA), Bedford, MA, 1981.

43. Y. Haroon, C. A. W. Schubert, and T. V. Hauschka, J. Chromatogr. Sci., 22, 89-93 (1984).

44. W. A. MacCrehan and R. A. Durst, Anal. Chem., 50, 2108-2112 (1978).

45. A. Maitoza and D. C. Johnson, Anal. Chim. Acta, 118, 233-241 (1980).

46. K. Stulik and V. Pacakova, J. Chromatogr., 208, 269-278 (1981).

47. K. Bratin and P. T. Kissinger, J. Liq. Chromatogr., 4 (2), 321-357 (1981).

48. K. Bratin, P. T. Kissinger, and C. S. Bruntlett, J. Liq. Chromatogr., 4, 1777-1795 (1981).

49. H. B. Hanekamp, P. Bos, and R. W. Frei, J. Chromatogr., 186, 489-496 (1979).

50. H. B. Hanekamp, W. H. Voogt, P. Bos, and R. W. Frei, J. Chromatogr., 3, 1205-1217 (1980).

51. W. Kutner, J. Debowski, and W. Kemula, J. Chromatogr., 191, 47-60 (1980).

52. R. Beauchamp, P. Boinay, J. Fombome, J. J. Fombon, and J. Tacussel, J. Chromatogr., 204, 123-130 (1981).

53. J. G. Koen, J. F. K. Huber, H. Poppe, and G. den Boef, J. Chromatogr. Sci., 8, 192-197 (1970).

54. J. G. Koen and J. F. K. Huber, Anal. Chim. Acta, 51, 303-307 (1970).

55. H. A. Moye, J. Chromatogr. Sci., 13, 268-272 (1975).

56. C. Bollet, P. Oilva, and M. Caude, J. Chromatogr., 149, 625-630 (1977).

57. R. C. Buchta and L. J. Papa, J. Chromatogr. Sci., 14, 213-219 (1976).

58. K. Hasebe and J. G. Osteryoung, Anal. Chem., 47, 2412-2418 (1981).

59. R. Samuelsson, J. O'Dea, and J. G. Osteryoung, Anal. Chem., 52, 2215-2216 (1980).

60. M. R. Symth and J. G. Osteryoung, Anal. Chim. Acta, 96, 335-344 (1978).

61. G. J. Clark, R. R. Goodin, and J. W. Smiley, Anal. Chem., 57, 2223-2228 (1985).

62. K. Bratin and R. C. Briner, Curr. Sep., 2, 1 (1980).

63. D. J. Miner and P. T. Kissinger, J. Pharm. Sci., 68, 96-99 (1979).

64. W. Kemula, B. K. Glod, and W. Kutner, J. Liq. Chromatogr., 6, 1823-1835 (1983).

65. P. Kissinger, K. Bratin, G. David, and L. Pachla, J. Chromatogr. Sci., 17, 137-146 (1979).

66. K. Bratin, P. T. Kissinger, R. C. Briner, and C. S. Bruntlett, Anal. Chim. Acta, 130, 295-311 (1981).

67. S. M. Rappaport, Z. L. Jin, and X. B. Xu, J. Chromatogr., 240, 145-154 (1982).

68. H. B. Hanekamp, P. Bos, and R. W. Frei, TRAC, Trends in Anal. Chem., 1, 135-140 (1982).

69. H. B. Hanekamp, W. H. Voogt, P. Bos, and R. W. Frei, Anal. Lett., 12 (A2), 175-189 (1979).

70. A. Trojanek and L. Krestan, J. Liq. Chromatogr., 6 (10), 1759-1776 (1983).

71. S. Ikenoya, T. Tsuda, Y. Yamano, Y. Yamanishi, K. Yamatsu, M. Ohmae, K. Kawabe, H. Nishino, and T. Kurashihi, Chem. Pharm. Bull., 26, 35-30 (1978).

72. S. Ikenoya, K. Abe, T. Tsuda, Y. Yamano, O. Hiroshima, and M. Ohmae, Chem. Pharm. Bull., 27, 1237-1245 (1979).

73. S. Ikenoya, M. Takada, T. Yuzuriha, K. Abe, and K. Katayama, Chem. Pharm. Bull., 29, 158-164 (1981).

74. A. W. Andrews, S. Schubert, J. Morrison, E. W. Zirik, and W. R. Matsun, Am. Lab., 14 (5), 140-155 (1982).

75. W. Buchberger and K. Winsaer, Mikrochim. Acta, 2, 257-262 (1980).

76. W. A. MacCrehan, Anal. Chem., 53, 74-77 (1981).

77. W. A. MacCrehan, R. A. Durst, and J. M. Bellame, Anal. Lett., 10, 1175-1188 (1977).

78. M. O. Funk, M. B. Keller, and B. Levison, Anal. Chem., 52, 773-774 (1980).

79. D. Chou and D. C. Locke, J. Assoc. Off. Anal. Chem., 67, 913-915 (1984).

80. A. M. Bond, I. D. Heritage, G. G. Wallace, and M. J. McCormick, Anal. Chem., 54, 582-585 (1982).

81. G. A. Sherwood and D. C. Johnson, Anal. Chim. Acta, 129, 101-111 (1981).

82. S. K. Vohra and G. W. Harrington, J. Chromatogr. Sci., 18, 379-383 (1980).

83. S. K. Vohra, "The Use of the LC Polarography Detector in the Analysis of N-Nitrosoamines"; Presented at the Pittsburgh Conference on Anal. Chem. and Appl. Spectroscopy, 1980; Abstract No. 582.

84. R. Samuelsson and J. Osteryoung, Anal. Chim. Acta, 123, 97-105 (1981).

84. M. Righezza, J. Chromatogr., 410, 145-155 (1987).

85. M. R. Hackman and M. A. Brooks, J. Chromatogr., 222, 197 (1981).

86. W. F. Smyth (Ed.), "Polarography of Molecules of Biological Significance"; Academic Press: London, 1979.

87. W. F. Smyth and M. R. Smyth, Pure and Appl. Chem., 59 (2), 245-256 (1987).

88. A. Ivaska and W. F. Smyth, Anal. Chim. Acta, 114, 283-291 (1980).

89. I. M. Kolthoff and J. J. Lingane "Polarography"; 2nd ed., Interscience: New York, 1952.

90. B. Drake, Acta Chem. Scand., 4, 554 (1950); Chem. Abstracts, 44, 8408g (1950).

91. W. Kemula, Roczniki Chem., 26, 281 (1952); Chem. Abstracts, 47, 7344d (1953).

92. J. Blaedel and J. W. Todd, Anal. Chem., 30, 1821-1825 (1958).

93. B. Fleet and C. Little, J. Chromatogr. Sci., 12, 747-752 (1974).

94. H. B. Hanekamp, W. H. Voogt, P. Bos, and R. W. Frei, Anal. Chim. Acta, 118, 81-86 (1980).

95. H. B. Hanekamp, W. H. Voogt, P. Bos, and R. W. Frei, Anal. Chim. Acta, 118, 73-79 (1980).

96. C. K. Mann, Anal. Chem., 29, 1385-1386 (1957).

97. O. H. Muller, J. Amer. Chem. Soc., 69, 2992-2997 (1947).

98. L. D. Wilson and R. J. Smith, Anal. Chem., 25, 218-220 (1953).

99. J. A. Lewis and K. C. Overton, Analyst, 79, 293-296 (1954).

100. G. J. Alkire, K. Koyama, K. J. Hahn, and C. E. Michelson, Anal. Chem., 30, 1912-1915 (1958).

101. R. L. Rebertus, R. J. Cappell, and G. W. Bond, Anal. Chem., 30, 1825-1827 (1958).

102. S. J. Lyle and I. M. Saleh, Talanta, 28, 251-254 (1981).

103. V. G. Levich, "Physiochemical Hydrodynamics"; Prentice-Hall: Englewood Cliffs, NJ, 1962.

104. W. Kemula, Pure and Appl. Chem., 21, 449-460 (1970).

105. W. Kutner, J. Debroski, and W. Kemula, J. Chromatogr., 191, 47-60, (1980).

106. W. Kutner, J. Debroski, and W. Kemula, J. Chromatogr., 218, 45-50 (1980).

107. P. L. Meschi and D. C. Johnson, Anal. Chem., 52, 1304-1307 (1980).

108. R. Tamamushi, S. Momiyama, and N. Tanaka, Anal. Chim. Acta, 23, 585-589 (1963).

109. W. J. Blaedel and J. H. Strohl, Anal. Chem., 33, 205-207 (1962).

110. K. Dusczyki, W. Kutner, D. Sybiska, and W. Kemula, J. Chromatogr., 241, 141-146 (1982).

111. C. P. Tyler and J. H. Karchner, Anal. Chem., 31, 499-502 (1959).

112. I. Smoler, Chem. Listy, 47, 1667-1669 (1953); Chem. Abstracts, 48, 4333d (1954).

113. T. M. Florence, J. Electroanal. Chem., 27, 273-281 (1970).

114. E. Scarno, M. G. Bonicelli, and M. Florino, Anal. Chem., 42, 1470-1472 (1970).

115. T. Wasa and S. Musha, Bull. Chem. Soc. Japan, 48 (7), 2176-2181 (1975).

116. R. Stillman and T. S. Ma, Microchim. Acta, 32, 641-648 (1974).

117. H. Hartmann and G. Budan, Chem. Ztg., 74, 606-607 (1950); Chem. Abstracts, 45, 1879b (1951).

118. S. G. Mairanovski and N. B. Neiman, Doklady Akad. Nauk SSSR, 82, 93-96 (1952); Chem. Abstracts, 46, 8476e (1952).

119. L. Michel and A. Zalka, Anal. Chim. Acta, 105, 109-117 (1979).

120. P.A.R. Model 310 Polarographic Detector, Princeton Applied Research, (EG & G Brookdeal Electronics), Princeton, NJ, 1980.

121. Metrohm Model E-611 Electrochemical Detector, Brinkmann Instruments, Westbury, NY.

122. D. L. Rabenstein and R. Saetre, Anal. Chem., 49, 1036 -1039 (1977).

123. R. Saetre and D. L. Rabenstein, Anal. Chem., 50, 276-280 (1978).

124. D. L. Rabenstein and R. Saetre, Clin. Chem., 24, 1140-1143 (1980).

125. H. M. A. Killa and D. L. Rabenstein, Anal. Chem., 60, 2283-2287 (1988).

126. A. Trojanek, J. Chromatogr., 323, 406-409 (1985).

127. A. M. Bond and R. D. Jones, Anal. Chim. Acta, 121, 1-11 (1980).

128. K. Stulik and V. Pacakova, J. Chromatogr., 208, 269-278 (1981).

129. K. Stulik, V. Pacakova, and B. Starkova, J. Chromatogr., 213, 41-46 (1981).

130. M. Stulikova and K. Stulik, Chem. Listy, 68, 800-803 (1974); Chem. Abstracts, 80, 43691v (1974).

131. W. M. Petersen, Am. Lab., 11 (12), 69 (1979).

132. H. W. Nurnberg, Anal. Chim. Acta, 164, 1-6, (1984).

133. T. M. Florence, J. Electroanal. Chem., 168, 207-218 (1984).

134. T. E. Edmonds, Anal. Chim. Acta, 116, 323-327 (1980).

135. T. E. Edmonds and G. Coutts, Anal. Chem., 54, 2105-2107 (1982).

136. Z. Feher and E. Pungor, Anal. Chim. Acta, 71, 425-432 (1974).

137. P. W. Alexander and S. H. Quereshi, J. Electroanal. Chem., 71, 235-240 (1976).

138. J. B. Lloyd, Anal. Chim. Acta, 154, 121-131 (1983).

139. W. A. MacCrehan and R. A. Durst, Anal. Chem., 50, 2108-2112 (1978).

140. W. A. MacCrehan and R. A. Durst, Anal. Chem., 53, 1700-17004 (1981).

141. R. E. Shoup, C. S. Bruntlett, P. T. Kissinger, and W. A. Jacobs, Industrial Research and Development, May, 1981; pg. 148.

142. C. E. Lunte, P. T. Kissinger, and R. E. Shoup, Anal. Chem., 57, 1541-1546 (1985).

143. C. E. Lunte, T. H. Ridgusy, and W. R. Heineman, Anal. Chem., 59, 761-766 (1987).

144. L. A. Allison and R. E. Shoup, Anal. Chem., 55, 8-12 (1983).

145. C. E. Lunte and P. T. Kissinger, Anal. Chem., 55, 1458-1462 (1983).

146. R. E. Shoup, C. S. Bruntlett, W. A. Jacobs, and P. T. Kissinger, Am. Lab., 13 (10), 144 (1981).

147. F. Vydra, K. Stulik, and E. Julakova, "Electrochemical Stripping Analysis"; Wiley: New York, 1976.

148. J. Wang and M. Ariel, Anal. Chim. Acta, 128, 147-153 (1981).

149. J. A. Cox and T. Zbignien, Anal. Chem., 52, 1503-1505 (1980).

150. K. E. Haaporka and J. J. Kankare, Anal. Chim. Acta, 117, 367-370 (1981).

151. H. Matusiewicz, J. Fish, and T. Malinski, Anal. Chem., 59, 2264-2269 (1987).

152. J. Wang, "Stripping Analysis: Principles, Instumentation and Applications"; VCH Publishers: Deerfield Beach, FL, 1985.

153. J. Wang, Am. Lab., 7, 14 (1983).

154. J. Wang, H. D. Dewald, and B. Greene, Anal. Chim. Acta, 146, 45-48 (1983).

155. J. Wang and H. D. Dewald, Anal. Chem., 55, 933-936 (1983).

156. M. Fleishmann, K. Korinek, and D. Pletcher, J. Electroanal. Chem., 37, 39-49 (1971).

157. E. S. Brandt, Anal. Chem., 57, 1276-1280 (1985).

158. S. Pons and M. Fleischmann, Anal. Chem., 59, 1391A-1399A (1987).

159. D. L. Jeanmaire and R. P. Van Duyne, J. Electroanal. Chem., 84, 1-20 (1977).

160. R. P. Van Duyne In "Chemical and Biochemical Applications of Lasers"; C. B. Moore (Ed.), Academic Press: New York, 1979; Vol. 4.

161. M. L. Meyer, T. P. De Angelis, and W. R. Heineman, Anal. Chem., 49, 602-606 (1977).

162. W. R. Heineman, Anal. Chem., 50, 390A-400A (1978).

163. M. Bos, J. H. H. Wiligen, and W. E. van der Linden, Anal. Chim. Acta, 156, 71-76 (1984).

164. P. W. Alexander and U. Akapongkul, Anal. Chim. Acta, 148, 103-109 (1983).

165. P. W. Alexander and U. Akapongkul, Anal. Chim. Acta, 166, 119-127 (1984).

166. W. J. Blaedel and J. H. Strohl, Anal. Chem., 37, 64-67 (1965).

167. H. Gunasingham, B. T. Tay, and K. P. Ang, Anal. Chem., 59, 262-266 (1987).

168. M. J. Brand and B. Fleet, Analyst, 93, 498-506 (1968).

169. M. Donten, Z. Stojek, and Z. Kublik, J. Electroanal. Chem., 163, 11-21 (1984).

170. M. Donten and Z. Kublik, Electroanal. Chem., 196, 275-290 (1985).

171. G. Bontempelli, B. Corain, and F. Magno, Anal. Chem., 49, 1005-1008 (1977).

172. Z. Stojek and Z. Kublik, J. Electroanal. Chem., 60, 349-358 (1975).

173. Z. Stojek and Z. Kublik, J. Electroanal. Chem., 77, 205-224 (1977).

174. P. Ostapczuk and Z. Kublik, J. Electroanal. Chem., 93, 195-212 (1978).

175. K. Wikel and Z. Kublik, J. Electroanal. Chem., 161, 269-281 (1984).

176. R. Eggli and R. Asper, Anal. Chim. Acta, 101, 253-259 (1978).

177. R. E. Meyer and P. M. Luntz, J. Electroanal. Chem., 61, 155-163 (1975).

178. J. Golas and J. Osteryoung, Anal. Chem., 59, 389-392 (1987).

179. J. R. Poulsen and J. W. Birks, Anal. Chem., 61, 2267-2276 (1989).

180. B. L. Trumpower (Ed.), "Function of Quinones in Energy Conserving Systems"; Academic Press: New York, 1982.

181. R. M. Wightman, Anal. Chem., 53, 1125A-1134A (1981).

182. M. Fleischmann, S. Pons, D. R. Rolison, and P. P. Schmidt, "Ultramicroelectrodes"; Datatech Systems, Inc., Science Publishers: Morganton, NC, 1987.

183. K. R. Wehmeyer, M. R. Deaken, and R. M. Wightman, Anal. Chem., 57, 1913-1916 (1985).

184. N. A. Hampson, D. Larkin, and J. R. Morley, Electrochem. Soc., 114 (8), 817-818 (1967).

185. N. A. Hampson and J. B. Lee, J. Electroanal. Chem., 45, 149-151 (1973).

186. N. A. Hampson, J. B. Lee, J. R. Morley, and B. Scanlon, Can. J. Chem., 47, 3729-3736 (1969).

187. J. P. G. Farr and N. A. Hampson, J. Electroanal. Chem., 13, 433-441 (1967).

188. S. L. Petersen and D. E. Tallman, Anal. Chem., 60, 82-86 (1988).

189. D. A. Fine and M. H. Miles, Anal. Chim. Acta, 153, 141-147 (1983).

190. M. H. Miles and D. A. Fine, J. Electroanal. Chem., 127, 143-155 (1981).

191. R. D. Rocklin and E. L. Johnson, Anal. Chem., 55, 4-7 (1983).

192. B. Philar and L. Kosta, Anal. Chim. Acta, 114, 275 (1980).

193. B. Philar, L. Kosta, and B. Hiristovski, Talanta, 26, 805-810 (1979).

194. B. Fleet, A.Y.W. Ho, and J. Tenygl, Analyst, 97, 321-327 (1972).

195. B. Fleet, A.Y.W. Ho, and J. Tenygl, Anal. Chem., 44, 2156-2161 (1972).

196. G. Kokkindis and K. Jüttner, Electrochim. Acta, 26, 971-974 (1981).

197. C. Nishihara and H. Shindo, J. Electroanal. Chem., 202, 231-239 (1986).

198. R. Hirasora, T. Mukaibo, H. Hagegasa, N. Odan, and T. Murayama, J. Phys. Chem., 72, 2541-2547 (1968).

199. J. Ruzicka and E. H. Hansen, Anal. Chim. Acta, 99, 37-76 (1978).

200. C. Amatore, J. M. Saveant, and D. J. Tessier, J. Electroanal. Chem., 147, 39-51 (1983).

201. G. Dryhurst and D. L. McAllister In "Laboratory Techniques in

Electroanalytical Chemistry"; P. T. Kissinger and W. R. Heineman (Eds.), Marcel Dekker: New York, 1984; pp. 294-301.

202. L. A. Knecht, E. J. Guthrie, and J. W. Jorgensen, Anal. Chem., 56, 479-482 (1984).

203. J. L. Anderson and R. E. Sioda, Talanta, 30, 627-629 (1983).

204. L. Anderson, D. Jagner, and M. Josefson, Anal. Chem., 54, 1371-1376 (1982).

205. D. L. Jeanmaire and R. P. Van Duyne, J. Electroanal. Chem., 84, 1-20 (1977).

206. D. Jagner and K. Aren, Anal. Chim. Acta, 100, 375-388 (1978).

207. D. Jagner, Anal. Chem., 50, 1924-1928 (1978).

208. D. Jagner, Anal. Chem., 51, 342-345 (1979).

209. J. A. Wang, Anal. Chim. Acta, 128, 147-153 (1981).

210. J. E. Anderson and D. E. Tallman, Anal. Chem., 48, 209-212 (1976).

211. D. E. Weisshaar, D. E. Tallman, and J. L. Anderson, Anal. Chem., 53, 1809-1813 (1981).

212. D. N. Armentrout, J. D. McLean, and M. W. Long, Anal. Chem., 51, 1039-1045 (1979).

213. J. L. Anderson and D. J. Chesney, Anal. Chem., 52, 2156-2161 (1980).

214. D. J. Chesney, J. L. Anderson, E. E. Weisshaar, and D. E. Tallman, Anal. Chim. Acta, 124, 321-331 (1981).

215. J. L. Anderson, K. K. Whiten, J. D. Brewster, T. Ou, and W. K. Nonidez, Anal. Chem., 57, 1366-1373 (1985).

216. D. E. Tallman and D. E. Weisshaar, J. Liq. Chromatogr., 6, 2157-2172 (1983).

217. D. E. Weisshaar, D. E. Tallman, and J. L. Anderson, Anal. Chem., 53, 593-598 (1981).

218. J. E. Anderson, D. E. Tallman, D. J. Chesney, and J. L. Anderson, Anal. Chem., 50, 1051-1056 (1978).

219. J. L. Anderson, D. E. Weisshaar, and D. E. Tallman, Anal. Chem., 53, 906-908 (1981).

220. W. L. Caudill, A. G. Ewing, S. Jones, and R. M. Wightman, Anal. Chem., 55, 1877-1881 (1983).

221. W. L. Caudill, J. O. Howell, and R. M. Wightman, Anal. Chem., 54, 2532-2535 (1982).

222. W. L. Caudill and R. M. Wightman, Anal. Chim. Acta, 141, 269-278 (1982).

223. A. G. Ewing, N. A. Dayton, and R. M. Wightman, Anal. Chem., 53, 1842-1847 (1981).

224. M. A. Dayton, J. C. Brown, K. J. Stutts, and R. M. Wightman, Anal. Chem., 52, 946-950 (1980).

225. M. A. Dayton, A. G. Ewing, and R. M. Wightman, Anal. Chem., 52, 2392-2396 (1980).

226. L. N. Klatt, D. R. Connel, R. E. Adams, I. L. Honigberg, and J. C. Price, Anal. Chem., 47, 2470-2472 (1975).

227. E. B. Buchanan and J. R. Bacon, Anal. Chem., 39, 615-620 (1967).

228. I. A. Fowlis and R. P. W. Scott, J. Chromatogr., 11, 1-10 (1963).

229. P. T. Kissinger, C. Refshauge, R. Dreiling, and R. N. Adams, Anal Lett., 6, 465-477 (1973).

230. G. C. Davis, P. T. Kissinger, and R. E. Shoup, Anal. Chem., 53, 156-159 (1981).

231. D. A. Roston and P. T. Kissinger, Anal. Chem., 53, 1695-1699 (1981).

232. K. Stulik and V. Pacakova, J. Chromatogr., 208, 269-278 (1981).

233. K. Stulik and V. Pacakova, J. Chromatogr., 192, 135-141 (1980).

234. K. Brunt and L. H. Bruins, J. Chromatogr., 161, 310-314 (1978).

235. K. Brunt and L. H. Bruins, J. Chromatogr., 172, 37-47 (1979).

236. K. Brunt, Trace Anal., 1, 47-52 (1981).

237. H. Gunasingham and B. Fleet, Analyst, 107, 896-902 (1982).

238. H. Gunasingham and B. Fleet, Analyst, 108, 316-321 (1982).

239. W. Lund and L. N. Ophen, Anal. Chim. Acta, 88, 275-279 (1977).

240. W. Lund, M. Hannisdal, and T. Greibrokk, J. Chromatogr., 173, 249-261 (1979).

241. W. Kemula, D. Sybilska, and K. Diszczyk, Microchem. J., 11, 296-305 (1966).

242. J. A. Wang, Anal. Chim. Acta, 128, 147-153 (1981).

243. M. H. Shah and I. L. Honigberg, Anal Lett., 16 (A15), 1149-1163 (1983).

244. W. J. Blaedel and J. Wang, Anal. Chem., 51, 799-802 (1979).

245. A. Trojanek, J. Chromatogr., 323, 406-409 (1985).

246. D. G. Swartzfarger, Anal. Chem., 48, 2189-2192 (1976).

247. M. W. White, J. Chromatogr., 178, 229-240 (1979).

248. Y. Hirata, P. T. Lin, M. Novotny, and R. M. Wightman, J. Chromatogr., 181, 287-294 (1980).

249. D. C. Johnson and J. Larochelle, Talanta, 20, 959-971 (1973).

250. W. J. Blaedel and G. S. Schieffer, J. Electroanal. Chem., 80, 259-271 (1977).

251. J. Wang and M. Ariel, Anal. Chim. Acta, 99, 89-98 (1978).

252. J. Wang and M. Ariel, Anal. Chim. Acta, 101, 1-8 (1978).

253. B. Miller, J. Electrochem. Soc., 116, 1117-1121 (1969).

254. L. B. Andersen and C. N. Reilley, J. Electroanal. Chem., 10, 295-305 (1965).

255. L. B. Andersen and C. N. Reilley, J. Electroanal. Chem., 10, 538-543 (1965).

256. J. L. Anderson and J. R. Kincaid, Appl. Spectrosc., 32, 356-361 (1978).

257. M. Krejci, K. Slais, D. Kourilova, and M. Vespalcova, J. Pharm. Biomed. Anal., 2, 197-205 (1984).

258. R. J. Fenn, S. Siggia, and D. J. Curran, Anal. Chem., 50, 1067-1073 (1978).

259. C. L. Blank, J. Chromatogr., 117, 35-46 (1976).

260. S. A. McClintock and W. C. Purdy, Anal. Lett., 14 (B10), 791-798 (1981).

261. S. G. Weber, Ph.D. Thesis, McGill University, Montreal (1979); Dissertation Abstracts International, 40 (6), 2640-B (1979).

263. J. G. Graene, G. E. Tobey, and L. D. Huelsman, "Operational Amplifiers, Design and Applications"; McGraw-Hill: New York, 1971; Chapter 8.

264. D. E. Johnson and J. L. Hilburn, "Rapid Practical Designs of Active Filters"; Wiley: New York, 1975.

265. J. K. Roberge, "Operational Amplifiers"; John Wiley and Sons, Inc.: NY, 1975.

266. L. M. Faulkenberry, "An Introduction to Operational Amplifiers"; John Wiley and Sons, Inc.: NY, 1982.

267. P. Horowitz and W. Hill, "The Art of Electronics"; Cambridge University Press: Cambridge, 1980; pg. 158.

268. W. L. Underkufler and Shain, In "Symposium on Operational Amplifiers", Anal. Chem., 35, 1770-1833 (1963).

269. J. Lankelma and H. Poppe, J. Chromatogr., 125, 375-388 (1976).

270. J. Lankelma and H. Poppe, J. Chromatogr. Sci., 14, 310-315 (1976).

271. D. T. Napp, D. C. Johnson, and S. Bruckenstein, Anal. Chem., 39, 481-485 (1967).

272. R. E. Shoup and P. T. Kissinger, Chem. Instru., 7, 171-177 (1976).

273. A. N. Strohl and D. J. Curran, Anal. Chem., 51, 1045-1049 (1979).

274. W. E. Bauer, A. P. Wade, and S. R. Crouch, Anal. Chem., 60, 287-288 (1988).

275. J. B. F. Lloyd, J. Chromatogr, 256, 323-325 (1983).

276. Technical Note No.1, Rheodyne, Cotati, CA, September (1979).

277. S. G. Weber, "The Signal-to-Noise Ratio Problem in Electrochemical Detectors used in Liquid Chromatography"; Presented at FACSS, Philadelphia, PA, 1982; Abstract No. 257.

278. D. J. Miner, Anal. Chim. Acta, 134, 101-109 (1982).

279. H. B. Hanekamp and H. G. de Jung, Anal. Chim. Acta, 135, 351-354 (1982).

280. B. R. Helper, S. G. Weber, and W. C. Purdy, Anal. Chim. Acta, 102, 41-59 (1978).

281. X.-K. Xing and D. Scherson, J. Electroanal. Chem., 196, 439-442 (1985).

282. R. C. Baetzold, J. Chem. Phys., 55 (9), 4363-4370 (1971).

283. D. Roy and T. E. Furtak, J. Electroanal. Chem., 228, 229-250 (1987).

284. T. Katan, S. Szpak, and D. N. Bennion, J. Electrochem. Soc., 122 (8), 1063-1071 (1974).

285. T. M. Devine, T. E. Furtak, and S. H. Macomber, J. Electroanal. Chem., 164, 299-303 (1984).

286. J. E. Pemberton and M. M. Grand, J. Electroanal. Chem., 217, 79-92 (1987).

287. M. Janik-Czachor, J. Electrochem. Soc., 128 (12), 513C-519C (1981).

288. J. F. Evans, M. G. Albercht, D. M. Ullevig, and R. M. Hexter, J. Electroanal. Chem., 106, 209-234 (1980).

289. D. D. Tuschel, T. E. Pemberton, and J. E. Cooke, Langmuir, 2 (4), 380-388 (1986); Chem. Abstracts, 105, 5670a (1986).

290. R. Schumacher, J. G. Gordon, and O. Melroy, Electroanal. Chem., 216, 127-135 (1987).

291. U. Stimming and F. W. Schultze, Electrochem. Acta, 24, 859-862 (1975).

292. B. Eremias and M. Prazak, Collect. Czech. Chem. Commun., 39 (11), 3192-3199 (1974); Chem. Abstracts, 82, 89018a (1974).

293. E. J. Calvo and D. J. Schiffing, J. Electroanal. Chem., 163, 257-275 (1989).

294. J. M. Droog and F. Huisman, J. Electroanal. Chem., 115, 211-224 (1980).

295. H. Gerischer and W. Mehl, Z. Electrochem., 59, 1049-1059 (1955); Chem. Abstracts, 50, 4681a (1956).

296. N. Furuga and S. Motoo, J. Electroanal. Chem., 78, 243-256 (1977).

297. N. Furuga and S. Motoo, J. Electroanal. Chem., 72, 165-175 (1976).

298. D. Larken, K. L. Guyer, J. T. Hupp, and M. J. Weaver, J. Electroanal. Chem., 138, 401-423 (1982).

299. J. Lindquist, J. Electroanal. Chem., 52, 37-46 (1974).

300. J. Lindquist, Anal. Chem., 45, 1006-1008 (1973).

301. K. Jüttner, H. J. Lorenz, G. Staikov, and E. Budevski, Electrochim. Acta, 23 (8), 741-748 (1978); Chem. Abstracts, 90, 111983a (1979).

302. J. Tomes, Collect. Czech. Chem. Commun., 9, 81-103 (1937); Chem. Abstracts, 31, 4905 (1937).

303. K. J. Vetter, Z. Electrochem., 56, 797-806 (1952); Chem. Abstracts, 47, 3723e (1953).

304. A. M. Abd. El-Halim, K. Jüttner, and W. J. Lorenz, J. Electroanal. Chem., 106, 193-207 (1980).

305. R. R. Adzic, D. N. Simic, D. M. Drazic, and A. R. Despic, J. Electroanal. Chem., 61, 117-120 (1975).

306. L. Young in "Anodic Oxide Films"; Academic Press: London, 1961; pg. 302.

307. N. A. Hampson, J. B. Lee, K. I. MacDonald, and M. J. Shaw, J. Chem. Soc. B, 1766-1769 (1970).

308. G. T. Burstein and R. C. Newman, Electrochim. Acta, 26 (8), 1143-1145 (1981).

309. H. Bort, K. Jüttner, W. J. Lorenz, and E. Schmidt, J. Electroanal. Chem., 90, 413-424 (1978).

310. E. Schmidt, M. Christen, and P. Beyeler, J. Electroanal. Chem., 42, 275-289 (1973).

311. H. Siegenthaler and K. Jüttner, Electrochim. Acta, 24 (1), 109-111 (1979); Chem. Abstracts, 91, 63145a (1979).

312. S. G. Weber, J. Electroanal. Chem., 145, 1-7 (1983).

313. S. G. Weber and W. C. Purdy, J. Electroanal. Chem., 115, 175-187 (1980).

314. J. M. Elbicki, D. M. Morgan, and S. G. Weber, Anal. Chem., 56, 978-985 (1984).

315. S. Prabhu and J. L. Anderson, Anal. Chem., 59, 157-163 (1987).

316. D. M. Morgan and S. G. Weber, Anal. Chem., 56, 2560-2567 (1984).

317. B. Haginhara, J. Chromatogr., 281, 59-71 (1983).

318. S. G. Weber and W. C. Purdy, Ind. Eng. Chem. Prod. Res. Dev., 20, 593-598 (1981).

319. H. B. Hanekamp and H. J. van Nieuwkerk, Anal. Chim. Acta, 121, 13-22 (1980).

320. S. Moldoveanu and J. L. Anderson, J. Electroanal. Chem., 239-252 (1985).

321. J. L. Anderson, T. Y. Ou, and S. Moldoveanu, J. Electroanal. Chem., 196, 213-226 (1985).

322. S. Moldoveanu and J. L. Anderson, J. Electroanal. Chem., 197, 67-79 (1984).

323. S. B. Khoo, H. Gunasingham, K. P. Ang, and B. T. Tay, J. Electroanal. Chem., 216, 115-126 (1987).

324. A. Caprani, C. Deslouis, S. Robin, and B. Tribollet, J. Electroanal. Chem., 238, 67-91 (1987).

325. T. Gueshi, K. Tokuda, and H. Matsuda, J. Electroanal. Chem., 238, 67-91 (1987).

326. T. Gueshi, K. Tokuda, and H. Matsuda, J. Electroanal. Chem., 89, 247-260 (1978).

327. W. R. Kenneth, M. R. Deakin, and R. M. Wightman, Anal. Chem., 57, 1913-1916 (1985).

328. P. M. Kovach, W. L. Caudill, and R. M. Wightman, J. Electroanal. Chem., 185, 285-295 (1985).

329. K. Tokuda, T. Gueshi, and H. Matsuda, J. Electroanal. Chem., 102, 47-48 (1979).

330. K. Aoki, K. Honda, K. Tokuda, and H. Matsuda, J. Electroanal. Chem., 182, 267-279 (1985).

331. M. Ohsawa, H. Matsuda, and W. Suëtaka, Chem. Phys. Lett., 84 (1), 163-166 (1981).

332. J. C. Rubim, I. G. Gutz, and O. Sala, J. Mol. Struct., 101(1-2), 1-6 (1983); Chem. Abstracts, 99, 87547z (1983).

333. M. M. Musiani, G. Mengoli, M. Fleischmann, and R. B. Lowry, J. Electroanal. Chem., 217, 187-202 (1987).

334. G. L. Woodroffe and J. D. Munro, Analyst (London), 95, 153-157 (1970).

335. S. Dilli and E. Patsalides, J. Chromatogr., 280, 59-68 (1983).

336. S. Harrison and G. L. Woodroffe, Analyst, 90, 44-49 (1965).

Part II

1. L. G. Randall, Sep. Sci. Technol., 17 (1), 1-118 (1982).

2. F. R. Groves, Jr., B. Brady, and F. C. Knopf, Crit. Rev. Environ. Control, 15, 237-274 (1985).

3. M. A. McHugh and V. J. Krukonis, "Supercritical Fluid Extraction, Principles and Practice"; Butterworths: Boston, MA (1986).

4. G. M. Schneider, E. Stahl, and G. Wilke (Eds.), "Extractions with Supercritical Gases"; Verlag-Chemie: Deerfield Beach, FL (1980).

5. K. P. Johnston, D. H. Zieger, and C. A. Eckert, Ind. Eng. Chem. Fundam., 21, 191-197 (1982).

6. M. E. Paulaitis, V. G. Krukonis, R. T. Kurnik, and R. C. Reid, Rev. Chem. Eng., 1(2), 179-250 (1983); Chem. Abstracts, 99, 177999c (1983).

7. E. Stahl, E. Schutz, and H. K. Mangold, J. Agric. Food Chem., 28, 1153-1157 (1980).

8. R. T. Kurnik, S. J. Holla, and R. C. Reid, J. Chem. Eng. Data, 26, 47-50 (1981).

9. E. Stahl and E. Willig, Microchim. Acta, 2, 465-469 (1980).

10. D. F. Williams, Chem. Eng. Sci., 36, 1769 (1981).

11. M. A. McHugh and M. E. Paulaitis, J. Chem. Eng. Data, 25, 326-329 (1980).

12. J. Chrastil, J. Phys. Chem., 86, 3016-3019 (1982).

13. M. E. Mackay and M. E. Paulaitis, Ind. Eng. Chem. Fundam., 18, 149-153 (1979).

14. R. A. Van Leer and M. E. Paulaitis, J. Chem. Eng. Data, 25, 257-264 (1980).

15. B. W. Wright, C. W. Wright, R. W. Gale, and R. D. Smith, Anal. Chem., 59, 38-44 (1987).

16. S. B. Hawthorne and D. J. Miller, Anal. Chem., 59, 1705-1708 (1987).

17. J. H. Raymer and E. D. Pellizzari, Anal. Chem., 59, 1043-1048 (1987).

18. M. E. P. McNally and J. R. Wheeler, J. Chromatogr., 447, 53-63 (1988).

19. E. Stahl, J. Chromatogr., 142, 15-21 (1979).

20. K. K. Unger and P. Roumeliotis, J. Chromatogr., 282, 519-526 (1983).

21. K. Sugiyama and M. Saito, J. Chromatogr., 332, 107-116 (1985).

22. M. E. P. McNally and J. R. Wheeler, J. Chromatogr., 435, 63-71 (1988).

23. H. T. Kalinoski, H. R. Udseth, B. W. Wright, and R. D. Smith, Anal. Chem., 58, 2421-2425 (1985).

24. B. W. Wright, S. R. Frye, D. G. McMinn, and R. D. Smith, Anal. Chem., 59, 640-644 (1987).

25. S. B. Hawthorne, M. S. Krieger, and D. J. Miller, Anal. Chem., 60, 472-477 (1988).

26. S. B. Hawthorne and D. J. Miller, J. Chromatogr., 403, 63-76 (1988).

27. S. B. Hawthorne, D. J. Miller, and M. S. Krieger, Fresenius Z. Anal. Chem., 330, 211-215 (1988).

28. S. B. Hawthorne and D. J. Miller, J. Chromatogr. Sci., 24, 258-264 (1986).

29. S. B. Hawthorne and D. J. Miller, Anal. Chem., 61, 736-740 (1989).

30. I. L. Davies, M. W. Raynor, J. P. Kithinji, K. D. Bartle, R. T. Williams, and G. E. Andrews, Anal. Chem., 60, 683A-699A (1988).

31. J. C. Scott, Ph.D. Dissertation, City University of New York, 1984; Dissertation Abstracts International, 45, 174-B (1984).

Part III

Chapter 1

1. H. H. Holton and F. L. Chapman, Tappi, 60 (11), 121-125, (1977).

2. J. O. Bröenstad, B. Dahl, and K. H. Schroeder, J. Chromatogr., 206, 392-395 (1981).

3. N. Kiba, M. Takamatsu, and M. Furusawa, J. Chromatogr., 328, 309-315 (1985).

4. B. I. Fleming, F. J. Kubes, J. M. Macleod, and H. I. Bolker, Tappi, 63 (11), 73-77 (1980).

5. J. O. Bröenstad, K. H. Schroeder, and H. O. Friestad, Anal. Chim. Acta, 119, 243-249 (1980).

6. I. Gourang, R. Cassidy, and C. W. Dence, Tappi, 62 (7), 43-47 (1979).

7. J. E. Currah, Tappi, 62 (8), 73-76 (1979).

8. K. H. Nelson and D. J. Cietek, J. Chromatogr., 281, 237-244 (1983).

9. P. Delahay, "New Instrumental Methods in Electrochemistry"; John Wiley-Interscience: New York, 1954; pg. 220.

10. S. G. Weber, J. Electroanal. Chem., 145, 1-11 (1983).

Chapter 2

1. P. N. Magee, R. Montesano, and R. Presussman, In "Chemical Carcinogens"; ACS Monograph 173, C. E. Searle (Ed.), American Chemical Society, Washington, D.C., 1976; pg. 491.

2. W. Lijinsky and S. Epstein, Nature, 21, 225-227 (1970).

3. P. N. Magee and J. M. Barnes, Brit. J. Cancer, 10, 114-122 (1956).

4. G. A. Digenis and C. H. Issiderides, Bioorg. Chem., 8, 97-137 (1979).

5. E. J. Olajos, Ecotoxicol. Environ. Safety, 1, 175-196 (1977).

6. A. L. Fridman, F. M. Mukhametshin, and S. S. Novikov, Russ. Chem. Rev., 40, 34-50 (1971); Chem. Abstracts, 74, 87247k (1971).

7. H. Fevier, "The Chemistry of Nitro and Nitroso Groups"; Part 2, John Wiley-Interscience: New York, NY (1970).

8. L. K. Keefer and P. R. Roller, Science, 181, 1245 (1973).

9. A. I. Vogel in "A Textbook of Practical Organic Chemistry"; Longmans, Green and Company: New York, NY, Third Edition, 1956; pg. 426.

10. J. H. Boyer in "Chemistry of Nitroso Groups"; Part I, H. Fever (Ed.), John Wiley-Interscience: New York, NY, 1969; Chapter 5.

11. R. A. Scalan, CRC Critical Reviews in Food Sci. Technicology, 5, 357-402 (1975).

12. N. P. Sen, "Safety of Foods"; 2nd ed., H. D. Graham (Ed.), AVI Publishing Co., Inc.: Westpoint CT, 1980; pp. 319-349.

13. B. Spiegelhalder, G. Eisenbrand, and R. Preussmann, Presented at the Sixth International Meeting on Analysis and Formation of N-nitrosoamine Compounds, Budapest, Hungary, Oct. 16-19 (1979).

14. N. P. Sen, L. A. Schwighawer, B. A. Donaldson, and W. F. Miles, J. Agric. Food Chem., 29, 1280-1287 (1979).

15. N. P. Sen and S. Seaman, J. Assoc. Off. Anal. Chem., 64, 1238-1242 (1981).

16. D. C. Harvey, J. H. Hotchkiss, and T. Fazio, J. Dairy Sci., 65, 182-185 (1981).

17. L. M. Libbey, R. A. Scalan, and J. F. Barbour, Food Cosmet. Toxicol., 18, 459-461 (1980).

18. L. Lakritz and J. W. Pensabene, J. Dairy Sci., 64, 371-374 (1981).

19. N. P. Sen," Multidetection Methods for Determining Volatile Nitrosoamines in Foods"; in N-Nitroso Compounds Analysis and Formation, P. Bogorski, R. Preussmann, and E. A. Walker (Eds.), International Agency for Research on Cancer, Sci. Publ. No. 3, Lyon, France (1978), pg. 25.

20. G. Eisenbrand "Determination of volatile nitrosoamines at low levels in food by acid-catalyzed denitrosation and formation of derivatives from resulting amines"; in N-Nitroso Compounds Analysis and Formation, P. Bogovski, R. Preussman, and E. A. Walker (Eds.), International Agency for Research on Cancer, Sci. Publ. No. 3, Lyon, France (1978), pg. 64.

21. T. Kawabata, J. Vibu, H. Ohshima, M. Matsui, and M. Hamano, In N-Nitroso Compounds Analysis, Formation and Occurrence, E. A. Walker, M. Casteynaro, L. Griccute, and M. Borzonyi (Eds.), International Agency for Research on Cancer, Sci. Publ., No. 3, Lyon, France (1978), pg. 481.

22. N. P. Sen, S. Seaman, and W. F. Miles, Food Cosmet. Toxicol., 14, 167-170 (1976).

23. K. Goodhead and T. A. Gough, Food Cosmet. Toxicol., 13, 307-312 (1975).

24. D. C. Harvey, T. Fazio, and J. W. Howard, J. Assoc. Off. Anal. Chem., 61, 1374-1378 (1978).

25. J. H. Hotchkiss, L. M. Libbey, and R. A. Scalan, J. Assoc. Off. Anal. Chem., 63, 74-79 (1980).

26. D. H. Fine, D. Lieb, and F. Rufeh, J. Chromatogr., 107, 351-357 (1975).

27. Ch. Ruhl and J. Reush, J. Chromatogr., 328, 326-366 (1985).

28. S. K. Vohra and G. W. Harrington, Food Cosmet. Toxicol., 19, 485-487 (1981).

29. S. K. Vohra and G. W. Harrington, J. Chromatogr. Sci., 18, 379-383 (1980).

30. E. G. and G Princeton Applied Research, Princeton, NJ, Application Note C-4 (1980).

31. M. A. Schneiderman, A. K. Sharma, and D. C. Locke, J. Chromatogr., 409, 343-353 (1987).

32. L. G. Randall, Sep. Sci. Technol., 17 (1), 1-118 (1982).

33. D. C. Locke, M. A. Schneiderman, A. K. Sharma, J. Cai, E. Wolfe, and K. R. R. Mahamama, Abstract of Papers, 40th Pittsburgh Conference and Exposition on Analytical Chemistry and Applied Spectroscopy, Atlanta, GA, 1989; paper 395.

34. K. Sugiyama, M. Saito, T. Hondo, and M. Senda, J. Chromatogr., 332, 107-116 (1985).

35. E. Lundanes and T. Greibrokk, J. Chromatogr., 349, 439-446 (1985).

36. R. D. Smith and H. R. Udseth, Sep. Sci. Technol., 18, 245-252 (1983).

37. M. M. Schantz and S. N. Chesler, J. Chromatogr., 363, 397-401 (1986).

38. S. B. Hawthorne and D. J. Miller, J. Chromatogr. Sci., 24, 228-264 (1986).

39. S. B. Hawthorne and D. J. Miller, Anal. Chem., 59, 1705-1708 (1987).

40. B. W. Wright, C. W. Wright, R. W. Gale, and R. D. Smith, Anal. Chem., 59, 38-44 (1987).

41. B. W. Wright, H. T. Kalinoski, and R. D. Smith, Anal. Chem. 57, 258-264 (1985).

42. P. T. Kissinger, Anal. Chem., 49, 447A-456A (1977).

43. W. E. Bauer, A. P. Wade, and S. R. Crouch, Anal. Chem., 60, 287-288 (1988).

44. R. Samuelson and J. Osteryoung, Anal. Chim. Acta, 123, 97-105 (1981).

45. K. Hasebe and J. Osteryoung, Anal. Chem., 47, 2412-2418 (1975).

46. F. Pulidori, G. Burghesani, C. Bijhi, and R. Pedriali, J. Electroanal. Chem., 27(3), 385-396 (1970).

47. S. K. Chang and G. H. Harrington, Anal. Chem., 47, 1857-1860 (1975).

48. N. P. Sen and S. Seaman, J. Assoc. Off. Anal. Chem., 64, 933-938 (1981).

Chapter 3

1. Code of Federal Regulations (1987) CFR 21 Part 107, U.S. Government Printing Office, Washington, DC; pp. 73-79.

2. H. F. DeLucey, "Handbook of Lipid Research-The Fat-Soluble Vitamins"; Vol. 2, Plenum Press: New York, NY, 1978; Chapter 4.

3. W. H. Sebrell and R. S. Harris, "The Vitamins"; Vol. 2, 2nd ed., Academic Press: New York, NY; Chapter 9.

4. H. J. Almquist, "Biological Symposia Volume XII"; J. Cattel (Ed.), The Jaques Cattel Press: Lancaster, PA, 1947; pp. 508-523.

5. R. M. Seifert, J. Agric. Food Chem., 27, 1301-1304 (1979).

6. D. A. Libby, A. R. Prosser, and A. J. Sheppard, J. Assoc., 50, 806-809 (1967).

7. J. D. Manes, H. B. Fluckiger, and D. L. Schneider, J. Agric. Food Chem., 20, 1130-1132 (1972).

8. R. J. Nowak, H. B. Mark, J. C. Vire, and G. J. Patriarche, Anal. Chem., 49, 1343-1346 (1977).

9. L. Krivankova and V. Dadak, Anal. Biochem., 75, 305-307 (1976).

10. J. J. Aaron, J. E. Villafranca, V. R. White, and J. M. Fitzgerald, Appl. Spec., 30, 159-162 (1976).

11. J. P. Hart and A. Catterall, Anal. Chim. Acta, 128, 245-250 (1981).

12. K. Takamura, M. Sakamoto, and Y. Hayakawa, Anal. Chim. Acta, 106, 261-269 (1979).

13. J. Linquist and S. M. Farroha, Analyst, 100, 377-385 (1975).

14. Y. Haroon, M. J. Shearer, S. Rahim, W. G. Gunn, G. McEnery, and P. Barkhan, J. Nutr., 112, 1105-1117 (1982).

15. S. A. Barnett, L. W. Frick, and H. M. Baine, Anal. Chem., 52, 610-614 (1980).

16. M. P. Bueno and M. C. Villalobos, J. Assoc. Off. Anal. Chem., 66, 1063-1066 (1983).

17. S. M. Hwang, J. Assoc. Off. Anal. Chem., 68, 684-689 (1985).

18. J. N. Thompson, G. Hatina, and W. B. Maxwell in "Application of HPLC Methods for Determination of Fat-Soluble Vitamins A, D, E, and K in Foods and Pharmaceuticals"; Symposium Proceedings, Association of Vitamin Chemists, Chicago, IL; pp. 84-102.

19. Y. Haroon, C. A. Schubert, and P. V. Hauschka, J. Chromatogr. Sci., 22, 89-93 (1984).

20. T. Ueno and J. W. Suttie, Anal. Biochem., 133, 62-67 (1983).

21. S. Ikenoya, K. Abe, T. Tsuda, Y. Yamano, O. Hiroshima, M. Ohmae, and K. Kawabe, Chem. Pharm. Bull., 27, 1237-1244 (1979).

22. J. P. Langenberg and U. R. Tjaden, J. Chromatogr., 305, 61-72 (1984).

23. O. Hiroshima, S. Ikenoya, M. Ohmae, and K. Kawabe, Chem. Pharm. Bull., 29, 451-455 (1981).

24. Association of Official Analytical Chemists. Official Methods of Analysis, 14th ed., Arlington, VA, 1984; Sec. 43.007, pg. 831.

25. L. F. Fieser and R. B. Turner, J. Am. Chem. Soc., 69, 2335-2340 (1947).

26. G. J. Patriarche and J. J. Lingane, Anal. Chim. Acta, 49, 241-250 (1970).

27. P. H. Rieger, "Electrochemistry"; Prentice-Hall: Englewood Cliffs, NJ, 1987; pg. 303.

28. S. G. Weber, J. Electroanal. Chem., 145, 1-11 (1983).

Chapter 4

1. D. B. Parrish, C.R.C. Crit. Rev. Food Sci. Nutr., 9, 375-394 (1970).

2. D. B. Parrish, R. A. Moffitt, R. J. Noel, and J. N. Tompson, "Vitamin A"; in Methods of Vitamin Assay, 4th ed., J. Augustin, B. P. Klein, D. Becker, and P. B.Venugopal (Eds.), John Wiley and Sons: New York, NY, 1985; pp. 153-184.

3. J. N. Thompson, "Trace Analysis of Vitamins by Liquid Chromatography"; in Trace Analysis, Vol. 2, J. F. Lawrence (Ed.), Academic Press: New York, NY, 1982.

4. Association of Official Analytical Chemists. Official Methods of Analysis, 14th ed., Arlington, VA, 1984; Secs. 43.008-43.013, pp. 832-834.

5. J. N. Thompson, J. Assoc. Off. Anal. Chem., 69, 727-738 (1986).

6. S. A. Barnett, L. W. Frick, and H. M. Baine, Anal. Chem., 52, 610-614 (1980).

7. R. V. Vivilecchia, B. G. Lightbody, N. Z. Thimot, and H. M. Quinn, J. Chromatogr. Sci., 15, 424-433 (1977).

8. A. Krishen, J. Chromatogr. Sci., 15, 434-439 (1977).

9. M. Holasova and J. Blattna, J. Chromatogr., 123, 225-230 (1976).

10. W. O. Landen and R. R. Eitenmiller, J. Assoc. Off. Anal. Chem., 62, 283-289 (1979).

11. W. O. Landen, J. Assoc. Off. Anal. Chem., 63, 131-136 (1980).

12. J. M. Brown-Thomas, A. A. Moustafa, S. A. Wise, and W. E. May, Anal. Chem., 60, 1929-1933 (1988).

13. Association of Official Analytical Chemists. Official Methods of Analysis, 14th ed., Arlington, VA, 1984; Sec. 43.008, pg. 832.

14. J. B. Neeld and W. N. Pearson, J. Nutr., 70, 454-456 (1963).

15. R. E. Dugan, N. A. Frigerio, and J. M. Siebert, Anal. Chem., 36, 114-116 (1964).

16. H. Sobotka, S. Kann, and J. Lowenstein, J. Am. Chem. Soc., 65, 1959-1961 (1943).

17. J. W. Erdman, S. F. Hou, and A. La Chance, J. Food Sci., 38, 447-449 (1973).

18 P. Gregory and W. N. Pearson (Eds.), "The Vitamins"; 2nd ed., Vol. 6, Academic Press: New York, NY; pp. 158-164.

19. J. N. Thompson and W. B. Maxwell, J. Assoc. Off. Anal. Chem., 60, 766-771 (1977).

20. S. K. Henderson and L. A. McLean, J. Assoc. Off. Anal. Chem., 62, 1358-1360 (1979).

21. D. C. Egberg, J. C. Heroff, and R. H. Potter, J. Agric. Food Chem., 25, 1127-1132 (1977).

22. H. Cohen and M. Lapointe, J. Agric. Food Chem., 26, 1210-1214 (1978).

23. A. Mankel, Dtsch. Lebensm. Rundsch., 75(3), 77-85 (1979); Chem. Abstracts, 90, 202291q (1979).

24. S. H. Ashoor and M. J. Knox, J. Chromatogr., 409, 419-425 (1987).

25. D. B. Dennison and J. R. Kirk, J. Food Sci., 42, 1376-1379 (1977).

26. M. Head and E. Gibbs, J. Food Sci., 42, 395-398 (1977).

27. J. N. Thompson, G. Hatina, and W. B. Maxwell, J. Assoc. Off. Anal. Chem., 63, 894-898 (1980).

28. W. A. Widicus and J. R. Kirk, J. Assoc. Off. Anal. Chem., 62, 637-644 (1979).

29. D. B. Dennison and J. R. Kirk, J. Food Sci., 42, 1376-1379 (1977).

30. N. A. Parris, J. Chromatogr., 147, 615-624 (1978).

31. W. O. Landen and R. R. Eitenmiller, J. Assoc. Off. Anal. Chem., 62, 283-289 (1979).

32. W. O. Landen, J. Assoc. Off. Anal. Chem., 65, 810-816 (1982).

33. S. S. Atuma, J. Lindquist, and K. Lundstrom, Analyst, 99, 683-689 (1975).

34. S. S. Atuma, K. Lundstrom, and J. Lindquist, Analyst, 100, 827-834 (1975).

35. M. L. Huang, G. J. Burchart, and R. Venkatarmanan, J. Chromatogr., 380, 331-338 (1986).

36. K. Bratin and P. T. Kissinger, Talanta, 29, 365-370 (1982).

37. S. G. Weber, J. Electroanal. Chem., 145, 1-11 (1983).

Chapter 5

1. J. D. Wilson, "Vitamin Deficiency and Excess"; in Harrison's Principles of Internal Medicine, 11th ed., E. Braunwald, K. J. Isselbacher, R. G. Petersdorf, J. D. Wilson, J. B. Martin, and A. S. Fauci (Eds.), McGraw-Hill: New York, 1987; Chapter 76.

2. J. W. Suttie, "Vitamin K Metabolism and Vitamin K-Dependent Proteins"; University Park Press: Baltimore, MD, 1980.

3. C. F. Bourgeois, S. H. Hel, J. P. Belliot, P. R. George, and C. A. Slomianny, J. Assoc. Off. Anal. Chem., 68, 1121-1125 (1985).

4. Association of Official Analytical Chemists. Official Methods of Analysis, 14th ed., Arlington, VA, 1984; Sec. 43.132-33.

5. S. M. Hassan, J. Assoc. Off. Anal. Chem., 64, 611-615 (1981).

6. A. J. Sheppard and W. D. Hubbard, Methods Enzymol., 18 C, 46-69 (1971).

7. M. J. Schearer, Adv. Chromatogr., 21, 2432-301 (1983).

8. L. F. Fieser and M. Fieser, J. Am. Chem. Soc., 57, 491-94 (1935).

9. T. Ueno and J. W. Suttie, Anal. Biochem., 133, 62-67 (1963).

10. Y. Haroon, C. A. W. Schubert, and P. V. Hauscha, J. Chromatogr. Sci., 22, 89-93 (1984).

11. S. Ikenoya, K. Abe, T. Tsuda, Y. Yamano, O. Hiroshima, M. Ohmae, and K. Kawabe, Chem. Pharm. Bull., 27, 1237-1244 (1977).

12. J. P. Langenberg and U. R. Tjaden, J. Chromatogr., 305, 61-72 (1984).

13. R. H. Rieger, "Electrochemistry"; Prentice-Hall: Englewood Cliffs, NJ, 1987; pg. 303.

14. S. G. Weber, J. Electroanal. Chem., 145, 1-11 (1983).

Chapter 6

1. Code of Federal Regulations, Title 21, Part 105.65, U. S. Government Printing Office, Washington DC (1981).

2. Infant Formula Act of 1980, Public Law 96-359.

3. H. F. Deluca, "Handbook of Lipid Research - The Fat-Soluble Vitamins"; Vol. 2, Plenum Press: New York, 1978; Chapter 4.

4. W. H. Sebrell, Jr and R. S. Harris, "The Vitamins"; Vol. 2, Academic Press: New York, 1954; Chapter 9.

5. F. H. Carr and E. A. Price, Biochem. J., 20, 497-501 (1926).

6. J. D. Manes, H. B. Fluckiger, and D. L. Schneider, J. Agric. Food Chem., 20, 1130-1132 (1972).

7. Y. Haroon, C. Schubert, and P. V. Harschka, J. Chromatogr. Sci., 22, 89-93 (1984).

8. S. Ikenoya, K. Abe, T. Tsuda, Y. Yamano, O. Hiroshima, M. Ohmae, and K. Kawabe, Chem. Pharm. Bull., 27, 1237-1244 (1979).

9. S. Ikenoya, M. Takada, T. Yuzuriha, K. Abe, and K. Katayama, Chem. Pharm. Bull., 29, 158-164 (1981).

10. T. Ueno and J. W. Suttie, Anal Biochem., 133, 62-67 (1983).

11. J. P. Langenberg and U. R. Tjaden, J. Chromatogr., 305, 61-72 (1984).

12. S. S. Atuma, J. Lindquist, and K. Lundstrom, Analyst, 100, 827-834 (1975).

13. S. S. Atuma, J. Lindquist, and K. Lundstrom, Analyst, 99, 683-689 (1974).

14. R. C. Williams, J. A. Schmitt, and R. A. Henry, J. Chromatogr., 10, 494-501 (1972).

15. D. F. Tomkins and R. J. Tscherne, Anal. Chem., 46, 1602-1604 (1974).

16. A. C. Ray, J. N. Dwyer, and J. C. Reagor, J. Assoc. Off. Anal. Chem., 60, 1296-1301 (1977).

17. H. Hofsass, A. Grant, N. J. Alicino, and S. B. Grunbaum, J. Assoc. Off. Anal. Chem., 59, 251-260 (1976).

18. J. W. Dolan, J. R. Grant, N. Tanaka, R. W. Giese, and B. L. Krager, J. Chromatogr. Sci., 16, 616-622 (1978).

19. J. N. Thompson, W. B. Maxwell, and M. L'Abbe, J. Assoc. Off. Anal. Chem., 60, 998-1009 (1977).

20. J. N. Thompson and G. Hatina, J. Liq. Chromatogr., 2, 327-344 (1979).

21. J. N. Thompson and W. B. Maxwell, J. Assoc. Off. Anal. Chem., 60, 766-771 (1977).

22. D. C. Edberg, J. C. Heroff, and R. H. Potter, J. Agric. Food Chem., 25, 1127-1132 (1977).

23. G. J. Krol, C. A. Mannon, F. Q. Genmill, G. E. Kicks, and B. T. Kho, J. Chromatogr., 74, 43-49 (1972).

24. S. A. Barnett, L. W. Frick, and H. M. Baine, Anal. Chem., 52, 610-614 (1980).

25. C. Mackay, J. Tillman, and D. T. Burns, Analyst, 104, 626-635 (1979).

26. J. Vermont, M. Deleuil, A. J. De Vries, and C. L. Guillemin, Anal. Chem., 47, 1329-1337 (1975).

27. E. J. De Vris, J. Zeeman, R. J. E. Esser, B. Borsje, and F. J. Mullers, J. Assoc. Off. Anal. Chem., 62, 129-135 (1979).

28. K. J. Bombaugh, J. Chromatogr., 107, 201-206 (1975).

29. H. Steverle, J. Chromatogr., 115, 447-453 (1975).

30. M. Osatca and M. Araujo, J. Assoc. Off. Anal. Chem., 60, 993-997 (1977).

31. D. W. Niereenberg and D. Lester, J. Chromatogr., 341, 275-284 (1985).

32. A. T. Rhys Williams, J. Chromatogr., 341, 198-201 (1985).

33. M. L. Huang, G. J. Burckart, and B. R. Vekataramanan, J. Chromatogr., 380, 331-338 (1986).

34. H. C. Furr, D. A. Cooper, and J. A. Olson, J. Chromatogr., 378, 45-53 (1986).

35. R. Shoup (Ed.), "Bibliography of Recent Reports on Electrochemical Detection"; Bioanalytical Systems Press: West Lafayette, IN (1982).

36. D. A. Roston, R. E. Shoup, and P. T. Kissinger, Anal. Chem., 54, 1417A-1434A (1982).

37. S. M. Lunte and P. T. Kissinger, J. Chromatogr., 317, 579-584 (1984).

38. G. A. Mayer and R. E. Shoup, J. Chromatogr., 255, 533-544 (1983).

39. L. A. Allison and R. E. Shoup, Anal. Chem. 55, 8-12 (1983).

40. D. A. Roston and P. T. Kissinger, Anal. Chem., 54, 429-434 (1982).

41. L. Blank, J. Chromatogr., 117, 35-46 (1976).

42. W. A. MacCrehan and R. A. Durst, Anal. Chem., 53, 1700-1704 (1981).

43. C. E. Lunte and P. T. Kissinger, Anal. Chem., 54, 1458-1462 (1983).

44. S. G. Weber and W. C. Purdy, Anal. Chem., 54, 1757-1760 (1982).

45. M. Goto, G. Zou, and D. Ishi, J. Chromatogr., 275, 271-284 (1983).

46. M. A. Schneiderman, S. K. Sharma, and D. C. Locke, J. Assoc. Off. Anal. Chem., 71, 815-817 (1988).

47. M. A. Schneiderman, A. K. Sharma, and D. C. Locke, J. Chromatogr., 409, 343-353 (1987).

48. W. L. Underkufler and B. Shain, Anal. Chem., 35, 1778-1786 (1963).

49. J. L. Anderson and J. R. Kincaid, Appl. Spectrosc., 32, 356-361 (1978).

50. W. E. Bauer, A. P. Wade, and S. R. Crouch, Anal. Chem., 60, 1045-1049 (1988).

51. A. N. Strohl and D. J. Curran, Anal. Chem., 51, 1045-1049 (1979).

52. P. T. Kissinger, Anal. Chem, 49, 449A-456A (1977).

53. K. Bratin and P. T. Kissinger, Talanta, 29, 365-370 (1982).

54. M. Krejci, K. Slais, D. Kourilova, and M. Vespalcova, J. Pharm. Biomed. Anal., 2, 197-205 (1984).

55. S. Ikenoya, K. Abe, T. Tsuda, Y. Yamano, O. Hiroshima, M. Ohmae, and K. Kawabe, Chem. Pharm. Bull., 27, 1237-1244 (1979).

56. Y. Haroon, C. A. Schubert, and P. V. Hauschka, J. Chromatogr. Sci., 22, 89-93 (1984).

Chapter 7

1. D. J. Higgs and J. T. Vanderslice, In "Advances in Laboratory Automation-Robotics"; G. L. Hawk and J. R. Strimaitis (Eds.), Zymark Corp., Hopkinton, MA, 1985; pp. 95-207.

2. D. J. Higgs and J. T. Vanderslice, J. Chromatogr. Sci., 25, 187-197 (1987).

3. H. Schutz, "Benzodiazepines"; Springer-Verlag: Berlin (1982).

4. J. A. F. deSilva, M. A. Schwartz, V. Stefanovic, J. Kaplan, and L. d'Arconte, Anal. Chem., 36, 2099-2104 (1964).

5. J. A. F. deSilva, I. Bekersky, C. V. Puglisi, M. A. Brooks, and R. E. Winfield, Anal. Chem., 48, 10-19 (1976).

6. D. M. Hailey, J. Chromatogr., 98, 527-568 (1974).

7 J. M. Clifford and W. F. Smyth, Analyst, 99, 241-272 (1974).

8. J. A. F. deSilva, in "Pharmacology of Benzodiazepines"; E. Usdin, P. Skolnick, J. F. Tallman Jr., D. Greenblatt, and S. M. Paul (Eds.), Macmillan: London, 1982; pg. 239.

9. A. C. Mahta, Talanta, 31, 1-8 (1984).

10. J. A. F. deSilva, C. V. Puglisi, and N. Munno, J. Pharm. Sci., 63(4), 520-527 (1974).

11. J. A. F. deSilva, I. Berkersky, and C. V. Puglisi, J. Chromatogr. Sci., 11, 547-554 (1970).

12. J. M. F. Douse, J. Chromatogr., 301, 137-154 (1984).

13. C. G. Scott and P. Bommer, J. Chromatog. Sci., 8, 446-448 (1970).

14. D. J. Weber, J. Pharm. Sci., 61(11), 1797-800 (1972).

15. A. Bugge, J. Chromatogr., 128, 111-116 (1976).

16. D. H. Rogers, J. Chromatogr. Sci., 12, 742-746 (1974).

17. K. Macek and V. J. Rehak, J. Chromatogr., 105, 182-185 (1975).

18. R. R. Brodie, L. F. Chasseaud, and T. Taylor, J. Chromatogr., 150, 361-366 (1978).

19. N. Ratnaraj, V. D. Goldberg, A. Elyas, and P. T. Lascelles, Analyst, 106, 1001-1004 (1981).

20. United States Pharmacopeia (XX1) and National Formularly (XV1), U.S. Pharmacopoeial Convention, Inc., Rockville, MD, 1985; pp. 306-308.

21. M. A. Schwartz, in "The Benzodiazepines"; S. Garatlini, E. Mussini, and L. Randall (Eds.), Raven Press: New York, 1973.

22. T. J. Good and J. S. Andrews, J. Chromatgr. Sci., 19, 562-566 (1981).

23. S. Cottler, C. V. Puglisi, and J. H. Gostatson, J. Chromatogr., 222, 95-98 (1981).

24. N. Rao, A. K. Dhar, H. Kutt, and M. Okamoto, J. Chromatogr., 231, 341-347 (1982).

25. J. B. F. Lloyd and D. A. Parry, J. Chromatogr., 449, 281-297 (1988).

26. M. A. Brooks and J. A. F. deSilva, Talanta, 22, 849-859 (1975).

27. M. A. Brooks, J. J. Bel Bruno, J. A. F. deSilva, and M. R. Hackman, Anal. Chim. Acta, 74, 367-385 (1975).

28. W. F. Smyth, M. R. Smyth, J. A. Groves, and S. B. Tan, Analyst, 103, 497-508 (1978).

29. K. Bratin and P. T. Kissinger, Talanta, 32, 365-370 (1982).

30. W. Lund, M. Hannisdal, and T. Greibrokk, J. Chromatogr., 173, 249-261 (1981).

31. M. R. Hackman and M. A. Brooks, J. Chromatogr., 222, 179-190 (1981).

32. H. Oelschläger, J. Volke, and H. Hoffmann, Collect. Czech. Chem., 31(3), 1264-1272 (1966); Chem. Abstracts, 61, 10536h (1966).

33. B. Z. Senkowiski, M. S. Levin, J. R. Urbigkit, and E. G. Wollish, Anal. Chem., 36, 1991-1994 (1964).

34. E. Jacobsen and T. V. Jacobsen, Anal. Chim. Acta, 55, 293-301 (1971).

35. S. G. Weber, J. Electroanal. Chem., 145, 1-11 (1983).

36. K. Harzer and R. Barchet, J. Chromatogr., 132, 83-90 (1977).

37. N. Stronjny, C. V. Puglisi, and J. A. F. deSilva, Anal. Lett., B 11, 135-60 (1978).

Chapter 8

1. H. Tokiwa, R. Nakagawa, K. Horikawa, and A. Ohkube, Environ. Health Perspectives, 73, 191-199 (1987).

2. D. Scheutzle, Environ. Health Perspectives, 47, 65-80 (1983).

3. M. L. Yu and R. A. Hites, Anal. Chem., 53, 951-954 (1983).

4. D. L. Lacourse and T. E. Jensen, Anal. Chem., 58, 1894-1895 (1986).

5. A. Robbat, Jr., N. P. Corso, P. A. Doherty, and M. H. Wolfe, Anal. Chem., 58, 2078-2084 (1986).

6. T. Nielsen, Anal. Chem., 55, 286-290 (1983).

7. B. A. Tomkins, R. S. Brazeli, M. E. Roth, and V. H. Ostrum, Anal. Chem., 56, 781-786 (1984).

8. D. Schuetzle, F. S. C. Lee, T. J. Prater, and S. B. Tejada, Intl. J. Environ. Anal. Chem., 9, 93-144 (1981).

9. A. Hartung, J. Kraft, J. Schulze, H. Kiess, and K. H. Lies, Chromatographia, 19, 269-273 (1984).

10. S. M. Rappaport, Z. L. Jin, and X. B. Xu, J. Chromatogr., 240, 145-154 (1982).

11. M. Oehme, S. Mano, and H. Stray, J. High Res. Chromatogr. Commun., 5, 417-423 (1982).

12. C. M. White, A. Robbat, Jr., and R. M. Hoes, Anal. Chem., 56, 232-236 (1984).

13. H. Y. Tong, J. A. Sweetman, and F. W. Karasek, J. Chromatogr., 264, 231-239 (1983).

14. M. C. Paputa-Peck, R.S. Marano, D. Schuetzle, T. L. Riley, C.V. Hempton, T. J. Prater, L. M. Skewes, T. E. Jensen, P. H. Reuhle, L. C. Bosch, and W. P. Duncan, Anal. Chem., 55, 1946-1954 (1983).

15. R. M. Campbell and M. L. Lee, Anal. Chem., 56, 1026-1030 (1984).

16. W. C. Yu, D. H. Fine, K. S. Ciu, and K. Biemann, Anal. Chem., 56, 1158-1162 (1984).

17. D. L. Newton, M. D. Erickson, K. B. Tower, E. D. Pellizzari, P. Gentry, and R. B. Zweidinger, Environ. Sci. Technol., 16, 206-213 (1982).

18. J. A. Sweetman, F. W. Karasek, and D. Schuetzle, J. Chromatogr., 247, 245-254 (1982).

19. D. Schuetzle, T. L. Riley, T. J. Prater, T. M. Harvey, and D. F. Hunt, Anal. Chem., 54, 265-271 (1982).

20. W. A. MacCrehan and W. E. May, In "Polynuclear Aromatic Hydrocarbons"; M. Cooke and A. J. Dennis (Eds.), Battelle, Press: Columbus, OH, 1985; pg. 857.

21. T. R. Henderson, J. D. Sun, R. E. Royer, C. R. Clark, A. P. Li, T. M. Harvey, D. H. Hunt, J. E. Fulford, A. M. Lovette, and W. R. Davidson, Environ. Sci. Technol., 17, 443-353 (1983).

22. W. Linder, W. Bosch, O. S. Wolfbeis, and P. Tritthart, Chromatographia, 20, 213-218 (1985).

23. Z. L. Jin and S. M. Rappaport, Anal. Chem., 55, 1778-1781 (1983).

24. R. H. Rieger, "Electrochemistry"; Prentice-Hall: Englewood Cliffs, NJ, 1987; pg. 303.

Chapter 9

1. J. T. Snelson, "Grain Protectants"; Aust Gov Publ Serv: Canberra, Australia (1987).

2. M. Eto, "Organophosphorus Insecticides, Organic and Biological Chemistry"; CRC Press: Cleveland, Ohio, 1974; pg. 241.

3. Food and Drug Administration. Pesticide Analytical Manual, Washington, DC, Vol. 1, 1985; Secs. 231 and 232.

4. Association of Official Analytical Chemists. Official Methods of Analysis, 14th ed., Arlington, VA, 1984; Secs. 29001-29015 and 29053-29057.

5. P. Bottomley and P. G. Baker, Analyst, 109, 85-90 (1984).

6. L. D. Sawyer, J. Assoc. Off. Anal. Chem., 65, 1122-1128 (1982).

7. L. D. Johnson, R. H. Waltz, J. P. Ussary, and F. E. Keiser, J. Assoc. Off. Anal. Chem., 59, 174-187 (1976).

8. J. A. Ault, C. M. Schofield, L. D. Johnson, and R. H.Waltz, J. Agric. Food Chem., 27, 825-828 (1979).

9. W. Specht and M. Tilkes, Fresenius Z. Anal. Chem., 301, 300-307 (1980).

10. J. Pflugmacher and W. Ebing, Fresenius Z. Anal. Chem., 263, 120-127 (1975).

11. D. Veievov and N. Abaronson, J. Assoc. Off. Anal. Chem., 63, 202-207 (1980).

12. K. Adachi, N. Ohokuni, and T. Mitsubashi, J. Assoc. Off. Anal. Chem., 67, 798-804 (1984).

13. R. W. Storheer, E. J. Murray, I. Klein, and L. A. Rosenberg, J. Assoc. Off. Anal. Chem., 50, 605-608 (1967).

14. T. C. Chiang, W. Liao, and L. R. Williams, J. Assoc. Off. Anal. Chem., 70, 100-102 (1987).

15. A. D. Muccio, A. M. Cirero, I. Camoni, D. Pontenecorvo, and R. Dommarrco, J. Assoc. Off. Anal. Chem., 70, 106-108 (1987).

16. K. C. Van Horne, "Sorbent Extraction"; in Sample Preparation Technology, Zymark Corporation, Hopkinton, MA, 1985; pp. 1-39.

17. C. F. Bourgeois and N. Ciba, J. Assoc. Off. Anal. Chem., 71, 12-15 (1988).

18. R. R. Watts (Ed.),"Manual of Analytical Methods for the Analysis of Pesticides in Human and Environmental Samples"; U. S. Environmental Protection Agency, Research Triangle Park, NC, 1980; EPA-600/8-8-038.

19. H. A. Moye, J. Chromatogr. Sci., 13, 268-279 (1975).

20. J. F. Lawrence and D. Turton, J. Chromatogr., 159, 207-226 (1978).

21. A. R. Hawks and B. M. Colvin, In "Pesticide Analysis"; K. G. Das (Ed.), Marcel Dekker: New York, 1981; pp. 99-174.

22. P. T. Kissinger, Anal. Chem., 49, 447A-456A (1977).

23. D. A. Roston, R. E. Shoup, and P. T. Kissinger, Anal. Chem., 54, 1417A-1434A (1982).

24. "Recent Reports on Liquid Chromatography/ Electrochemistry"; Bioanalytical Systems Press: West Lafayette, IN (1982).

25. J. G. Kohen and J. F. K. Huber, Anal. Chim. Acta, 51, 303-308 (1970).

26. K. Bratin, P. T. Kissinger, and C. S. Bruntlett, J . Liq. Chromatogr., 4, 1777-1795 (1981).

27. G. J. Clark, R. R. Goodin, and J. W. Smiley, Anal. Chem., 57, 2223-2228 (1985).

28. X. Ding and I. S. Krull, J. Agric. Food Chem., 32, 622-628 (1984).

29. M. A. Schneiderman, A. K. Sharma, and D. C. Locke, J. Chromatogr., 409, 343-353 (1987).

30. A. N. Strohl and D. J. Curran, Anal. Chem., 51, 1045-1049 (1979).

31. C. V. Bowen and F. I. Edwards, Anal. Chem., 22, 706-708 (1950).

32. D. C. Paschal, R. Bicknell, and D. Desbach, Anal. Chem., 49, 1551-1554 (1977).

33. E. H. Chimowitz and K. J. Rennis, AIChE J., 34, 1740-1742 (1988).